Structure spatiale à multi-échelles de la biodiversité benthique des monts sous-marins et pentes insulaires à partir de l'analyse d'images : approches méthodologiques et rôle de l'habitat

Mélissa Hanafi-Portier

THESE DE DOCTORAT DE

L'UNIVERSITE
DE BRETAGNE OCCIDENTALE

ECOLE DOCTORALE N° 598
Sciences de la Mer et du littoral
Spécialité : « *Ecologie Marine* »

Par

Mélissa HANAFI-PORTIER

Structure spatiale à multi-échelles de la biodiversité benthique des monts sous-marins et pentes insulaires à partir de l'analyse d'images : approches méthodologiques et rôle de l'habitat

Thèse présentée et soutenue à Plouzané, le vendredi 21 octobre 2022
Unité de recherche :
UMR Biologie et Ecologie des Ecosystèmes Marins Profonds (BEEP) (Ifremer, Plouzané)
UMR 7205 ISYEB, Équipe "Explorations, Espèces et Spéciations" (MNHN, Paris)

Rapporteurs avant soutenance :

Éric THIEBAUT
Professeur, Sorbonne Université, CNRS

Vianney DENIS
Associate Professor, Institute of Oceanography, National Taiwan University

Composition du Jury :

Éric THIEBAUT (Rapporteur)
Professeur, Sorbonne Université, CNRS
Vianney DENIS (Rapporteur)
Associate Professor, Institute of Oceanography, National Taiwan University
Gauthier SCHAAL (Examinateur)
Maître de Conférences, Université de Bretagne Occidental
Didier JOLLIVET (Président du jury)
Directeur de recherche CNRS, UMR Adaptation et Diversité en Milieu Marin Unité de recherche UMR7144
Karine OLU (Directrice de thèse)
Cadre de recherche, UMR BEEP, Ifremer
Sarah SAMADI (Co-directrice de thèse)
Professeure, UMR 7205 ISYEB, MNHN

Invité(s) :

Christophe FONTFREYDE Directeur du Parc naturel marin de Mayotte, Office français de la biodiversité
Patrick BALDONI-ANDREY Chef de Service Environnement Développement Durable, TotalEnergies

قس ق لا بـ ن الاعـ ز . بـ دراً فـ صار الـ هلال سار قدرا ما شـ ئت اذا سافـ ر

"Voyage, si tu ambitionnes une valeur certaine.
C'est en parcourant les cieux que le croissant devient pleine lune."

Ibn Qalakis (1137-1172)
Calligraphie d'Hassan Massoudy

Remerciements

Voici presque quatre années de thèse qui se clôturent, et non sans émotions…

Ces années en doctorat auront effectivement été un ascenseur émotionnel, une grande période riche intellectuellement et en rencontres professionnelles et personnelles.

Je souhaite exprimer mes remerciements et ma reconnaissance envers les nombreuses personnes rencontrées sur le chemin menant à l'aboutissement de mon projet.

Mes premiers remerciements vont à **Karine Olu** et **Sarah Samadi** mes deux directrices de thèse. Merci pour votre soutien, votre bienveillance, votre disponibilité, pour m'avoir fait confiance et pour avoir été à l'écoute, tout au long de ce cheminement pour devenir chercheure. J'ai beaucoup appris à vos côtés, de votre expérience et de votre intégrité. J'ai eu un immense plaisir à travailler avec vous et je ne vous remercierai jamais assez pour la belle opportunité que vous m'avez offert de réaliser cette thèse. Grâce à vous, j'ai pu participer à une campagne océanographique au large de la Nouvelle-Calédonie, découvrir Taïwan, ou encore présenter mes travaux à divers colloques. Ce fut une belle rencontre et une belle aventure.

Je souhaiterais remercier mes laboratoires d'accueil au sein du Laboratoire Environnement Profond (LEP) et de l'Institut de Systématique, Évolution, Biodiversité (YSIEB) respectivement. En particulier, je remercie **Pierre-Marie Sarradin** d'avoir facilité l'optimisation de mon bureau dans les moments critiques de mal de dos, ce qui m'a permis de continuer à travailler.

Je remercie les responsables du projet PAMELA, **Jean-Francois Bourillet**, **Philippe Bourges**, **Jean-Noël Ferry**, et **Jean-Philippe Mathieu** ; ainsi que les correspondants TotalEnergies, **Patrick Baldoni-Andrey** et **Anne Bassères**. En particulier, je souhaite remercier Jean-François Bourillet pour avoir rendu possible la prolongation de mon contrat, me permettant de mener à bien mon projet malgré une pandémie mondiale et des problèmes de dos.

J'adresse également mes remerciements à mes deux rapporteurs **Éric Thiébaut** et **Vianney Denis** et aux membres examinateurs et invités du jury ; **Gauthier Schaal**, **Didier Jollivet**, **Christophe Fontfreyde, Patrick Baldoni-Andrey** ; pour avoir accepté d'évaluer ce travail.

Je remercie mon comité de suivi individuel de thèse pour son temps dédié à nos réunions annuelles, pour sa bienveillance, ses retours constructifs et ses conseils qui ont contribué au bon avancement de mon projet : **Boris Leroy**, **Lénaick Menot**, **Thomas Saucède**, **Laure Corbari** et **Olivier Gauthier**.

Je souhaiterais aussi remercier tous.tes mes collaborateur.rice.s et co-auteur.rice.s, pour le temps dédié à la relecture de manuscrits, pour vos retours critiques, et vos conseils, qui ont contribué à l'avancement certain de mon projet et à la publication de mon premier article scientifique. Je remercie notamment l'ensemble des taxonomistes avec qui j'ai eu la chance de travailler et auprès de qui j'ai appris à découvrir cette belle discipline scientifique que sont la description, classification et dénomination du vivant : **Enrique MacPherson**, **Daniela Pica**, **Paco Cardenas**, **Nicolas Puillandre**, **Magalie Castelin**, **Éric Pante**, **Nadia Ameziane**, **Mao-Ying Lee**, **Marcelo Kitahara**, **Jhen-Nien Chen**, **Christopher Mah**, **Paul Giannasi**, **Cécile Debitus**, **Philipe Maestrati**, **Tim O'Hara**. Plus particulièrement, je remercie **Thomas Saucède**, **Tin-Yam Chan** et **Wei-Jen Chen** pour votre enthousiasme et votre implication dans le développement des clés d'identification. *Also, thank you Tin-Yam and Wei-Jen for hosting me in your labs in Taiwan which was a great PhD first year experience for me.* Un merci spécialement adressé à **Laure Corbari**, pour son encadrement et son accompagnement pendant mon stage de master 2, qui a abouti à une belle première publication de thèse.

Merci à **Thibault Napoléon** pour nos diverses collaborations qui m'ont permis d'obtenir de précieuses données sur les substrats, mais surtout qui m'ont introduite au domaine très intéressant de l'apprentissage automatique.

En lien avec mon voyage à Taïwan, *I would like to thank **Siu-Chi Chang** for introducing me to the Taiwanese culture, for our long walks and discussions in Keelung which helped me to feel comfortable there. Also, I would like to thank **all the members of the NTU and Keelung laboratories and the students** for your involvement in helping me in the identification of the decapods and fishes on the images, but also for your welcome and your kindness.*

Je souhaite également remercier tous.tes les technicien.ne.s et ingénieur.e.s avec qui j'ai travaillé et qui ont participé à l'obtention de mes données ou qui m'ont aidée lorsque j'en avais besoin. En particulier, je remercie **Julie Tourolle**, **Catherine Borremans**, **Olivier Soubigou** et **Christophe Brandily** pour leurs aides précieuses afin de dépasser certaines difficultés avec le SIG, BIIGLE, pour l'annotation d'images ou encore avec des données CTD récalcitrantes. Je remercie **Eve-Julie Pernet** pour le tri des échantillons de la campagne BIOMAGLO, et pour nos quelques discussions très appréciées en Nouvelle-Calédonie, et notre longue… très longue balade – où l'on s'est perdues une heure au Parc de la Rivière Bleue, ce qui restera un très bon souvenir.

Merci à **tous.tes mes collègues du LEP**. Les périodes « covidesques » et longs mois de télétravail, accentués par mon besoin de rester en télétravail en fin de thèse, à mon caractère très discret et réservé, ont fait que nous n'avons pas échangé énormément. Je tenais donc à vous remercier pour votre gentillesse et pour tous ces instants de rire à la pause du midi ou à la porte du bureau, qui ont été des moments très appréciés et essentiels à mon bien-être au laboratoire. Je remercie **tous les membres de l'équipe 3E**, pour leur accueil chaleureux lors de mes visites dans mon second laboratoire à l'YSIEB.

Comment ne pas remercier mes collègues et ami.e.s doctorant.e.s, d'abord **Joan**, mentor du bureau des thésards, et parti le premier, pour tes conseils avisés et tes encouragements ; **Loïc,** le petit dernier, pour ta bienveillance, ton enthousiasme communicatif en toute circonstance, et pour être toujours prêt à aider même quand tu étais toi-même en difficulté ; **Claire**, ma camarade de projet PAMELA, merci pour les piques-niques du midi improvisés et pour le soutien mutuel. Enfin, **Julien**, merci d'avoir si souvent fait tomber tes stylos à terre, ils n'auront cessé de me faire rire, pour nos longues discussions de bureau et à Glasgow. Un merci particulier à toi et à **Sarah**, pour nos fous rires, vos conseils, ces moments de détentes à l'escalade, et pour les prochains qui nous attendent.

Merci **Alicia** et **Adriana** pour vos encouragements et je vous souhaite à mon tour beaucoup de courage pour concrétiser vos projets respectifs (et à toi aussi Loïc !).

Une pensée pour les post-doctorant.e.s rencontré.e.s au fil des années, notamment **Fanny**, **Mauricio**, **Mark**, **Vera** et **Sam**, pour avoir partagé vos expériences en tant qu'anciens doctorants et vos parcours post-thèse, ainsi que nos discussions toujours appréciées. Je remercie particulièrement **Elda Miramontes**, pour avoir été présente et disponible lors de mes premiers mois de thèse, pour m'avoir aidée à prendre en main les données du projet PAMELA. Merci pour ta bonne humeur et nos moments de rires.

Je remercie les étudiants que j'ai encadrés, **Simon Gourdon** et **Annaëlle Saint-Germain** qui m'ont aidée dans le labeur de l'annotation d'image en salle vidéo qui plus est dans le noir ! Merci pour votre implication dans l'obtention de ces données, qui n'aurait pas été possible sans vous. Je vous souhaite une belle poursuite dans vos études.

Je remercie également mes maraîchers, **Medhi** et **Jean-François**, pour m'avoir nourrie de vos bons produits ces derniers mois où j'avais besoin de couleur dans l'assiette, pour vos encouragements et votre bonne humeur chaque dimanche matin.

Enfin, plus personnellement je voudrais remercier mes familles.
D'abord ma maman **Corinne** et mon papa **Mérouane**, sans qui je ne serais pas là à écrire ces remerciements. Merci maman pour ton courage, pour les valeurs que tu nous as transmises d'intégrité, d'honnêteté et de persévérance, et d'avoir toujours fait en sorte que nous puissions mener à bien nos études. Merci papa pour ta créativité, ton optimisme en toutes circonstances et ton soutien dans mes choix professionnels et personnels. Merci à mon frère **Ben**, que je ne vois pas souvent mais à qui je tiens énormément et que j'estime profondément. Merci **Rati**, pour ta douceur, ton écoute, et ton soutien qui sont des qualités très importantes à mes yeux. Merci à mes sœurs **Feyrouz** et **Maia-Ourida**, pour les bons moments passés et tous ceux à venir. Une pensée particulière pour **mes familles élargies** qui je sais sont derrière moi, à me soutenir aux quatre coins de la France, par-delà la Méditerranée, la mer des Caraïbes ou dans les Cieux. Merci à **Houria** et **Lorenna**, pour vos encouragements et votre amour sincère depuis l'enfance.

Puis, je remercie **Fani** et **Paul**, pour votre soutien tellement immense que le mot immense ne suffit pas à le caractériser. Votre rencontre sur mon chemin a été une bulle d'air salvatrice dans des moments difficiles de ma vie. Merci pour tous ces moments ensemble que je n'oublie pas. Je suis heureuse d'avoir rencontré sur ce chemin **Simon**, merci pour nos discussions qui vont « diguer » en profondeur et retourner l'esprit, et pour tes musiques qui m'ont accompagnées pendant ma thèse. Merci **Sam** pour ta douceur, ton esprit libre, et ton rire communicatif. Merci **Marie-Anne**, **Pierre** et **Pascal** pour l'affection que vous me portez et qui est réciproque. Enfin, je remercie **Mamou** et sa maison accueillante où j'ai passé des moments doux et reposants entre deux lignes de rédaction, ainsi que **Joëlle** pour ses pensées affectueuses.

Merci **Ghislaine** pour ton regard aiguisé de relectrice sur mon introduction et conclusion de manuscrit.

A tous.tes mes ami.e.s, je dis merci pour vos encouragements, pour nos moments de rires, pour votre présence. Pour beaucoup, l'éloignement géographique a fait que nous ne nous voyons pas souvent, mais sachez que notre amitié est précieuse. Donc merci à **Yoann**, **Mae**, **Clem**, **Coco**, **Laura**, **Cyrielle**, **Cath**, **Nono**, **Maca**, **Nico**, **Pierre Esox**, **Ben**, **Ferdi**, **Szymczak**, **Quentin**, **Linda**, **Marine**, **Anaïs** et **Marine**, **Xavier** et **Lucie**, **Clairette de St Malo, Pierre** et **Chloé**. En particulier, une pensée à mes trois camarades et amies, **Alex**, **Léa** et **Camillus** qui ont débuté l'aventure de la thèse en même temps que moi, et que j'aime profondément ; ainsi qu'aux amitiés naissantes **Garance** et **Léo** pour ces moments qui ont contribué à égayer ces derniers mois.

Enfin un remerciement infini, tout spécialement à mon amoureux, **Félix**, pour son soutien immense, ses encouragements, et son implication active à me secourir dans les moments difficiles de ma thèse, comme la mise en forme de mon manuscrit qui fut épique... Merci pour nos fous rires salvateurs pendant les moments critiques et de fatigue, merci pour ta douceur, pour ton amour et d'être toi…

A tous.tes celles et ceux que j'ai oublié.e.s, je m'excuse sincèrement et vous adresse mes remerciements chaleureux.

A Brest, le 11/09/2022,

Mélissa

Cette thèse est cofinancée par TotalEnergies et Ifremer dans le cadre du projet scientifique PAMELA (Passive Margin Exploration Laboratories).
"Le programme de recherche PAMELA (PAssive Margins Exploration LAboratories) fait l'objet d'un partenariat depuis 2013 entre TOTAL, l'IFREMER, l'IFPEN, le CNRS et des universités françaises de Bretagne Occidentale, Rennes 1 et Paris VI, visant à améliorer nos connaissances sur les marges continentales passives". https://doi.org/10.18142/236

TABLE DES MATIERES

Liste des figures

Liste des tables

Liste des matériels supplémentaires

Introduction générale

Enjeux écologiques

L'océan profond – généralement défini comme la zone au-delà de 200 m sous le niveau de la mer, au niveau de la rupture de la pente continentale et où la lumière ne pénètre plus pour réaliser de la photosynthèse (Thistle, 2003) – recouvre environ 65 % de la surface de la terre (Danovaro et al., 2017). Il abrite de nombreux paysages marins, tels que des sources froides, cheminées hydrothermales, fosses océaniques, canyons ou monts sous-marins, abritant eux-mêmes toute une diversité de formes de vie (Ramirez-Llodra et al., 2011). Il fournit également de nombreux services écosystémiques (ex : séquestration du dioxyde de carbone, cycle des nutriments, ressources alimentaires et énergétiques, bioprospection ou service culturel) (Thurber et al., 2014).

Tandis que les dernières années sont caractérisées par l'émergence d'une économie bleue, suscitant un fort intérêt pour l'exploitation des ressources marines (minières et énergétiques, câbles sous-marins, pêcheries en haute mer, etc.) (Glover et al., 2018), l'océan profond reste encore largement sous-exploré (~ 1 %) (Feng et al., 2022). Ceci en raison de son accessibilité difficile en comparaison de sa vaste étendue et de l'hétérogénéité des habitats qu'il abrite (Ramirez-Llodra et al., 2011). Acquérir des connaissances sur les compartiments profonds de l'océan représente un coût important (Bell et al., 2022), et requiert, d'une part, d'étendre la couverture spatiale de l'exploration, encore faible, générant des biais de représentation des habitats profonds et des paradigmes mal établis sur le fonctionnement des écosystèmes profonds car fondés sur des cas d'études particuliers (McClain et Schlacher, 2015). D'autre part, notre compréhension du fonctionnement de ces écosystèmes repose en partie sur les avancées technologiques qui limitent notamment l'exploration de certaines régions profondes situées dans les Zones Économiques Exclusives (ZEE) des nations en voie de développement (Howell et al., 2020). Les menaces passées et émergentes mènent ainsi à un besoin urgent de développer nos connaissances sur la biodiversité et le fonctionnement des écosystèmes marins profonds ; requis nécessaire pour la mise en place de stratégie de restauration et de protection des habitats profonds (Da Ros et al., 2019).

La célèbre campagne HMS *Challenger* (1872-1876) a ouvert la voie à une série d'autres campagnes d'exploration de l'océan profond dans les années 1950-1960, considérées comme l'âge d'or de ces explorations pionnières (Ramirez-Llodra et al., 2011 ; Tyler et al., 2016). Depuis cette ère, l'échantillonnage physique des compartiments profonds de l'océan au moyen par exemple de dragues, chaluts, ou de traîneau épibenthique (Clark et al., 2016), a apporté et continue d'apporter des connaissances essentielles sur la biodiversité vivant à ces profondeurs, permettant la description d'espèces nouvelles pour la science ainsi que la documentation de la distribution géographique des espèces.

Le développement des technologies d'exploration sous-marine, et notamment des techniques acoustiques et d'imagerie dans les années 1970-1980 (ex : caméras tractées et submersibles tels que des ROV – Remotely Operated Vehicle – ou AUV – Autonomous Automated Vehicle) a permis des avancées considérables sur la connaissance de l'hétérogénéité de l'habitat, son rôle dans la structure et le maintien de la biodiversité, ainsi que sur la compréhension du fonctionnement des écosystèmes profonds (Danovaro et al., 2014 ; Levin et Sibuet, 2012 ; Ramirez-Llodra et al., 2011).

Parmi ces écosystèmes profonds, les monts sous-marins constituent un des biomes majeurs de l'océan global (Rogers, 2018). Ces structures sont des montagnes sous-marines répandues et nombreuses dans les fonds marins ; elles ont généralement une origine tectonique volcanique (Staudigel et Clague, 2010). Ces structures se forment principalement aux abords des dorsales médio-océaniques, et moins souvent au niveau de points chauds intraplaques ou des arrière-arcs insulaires situés dans des zones de subduction (Staudigel et Clague, 2010). Selon leur hauteur au-dessus du fond marin, les définitions au sens large distinguent les monts sous-marins à proprement parler (> 1000 m du fond), les guyots ("knolls") (> 500 m du fond) et les monticules ("hills") (< 500 m du fond) (Rogers, 2018 ; Yesson et al., 2011). Les estimations en décomptent de plus de 150 000 à 25 millions au niveau mondial selon les catégories de hauteur des monts et les méthodes d'estimation (**Figure 0.1**, d'après la revue bibliographique de Rogers, 2018). Les îles volcaniques correspondent à une phase émergée des monts sous-marins, soumise à l'érosion des sols et à la formation d'eaux souterraines et relarguant du matériel particulaire et des sédiments des terres vers les eaux et écosystèmes marins alentour, pouvant affecter les communautés profondes (Staudigel et Clague, 2010).

Pour cette raison, les îles volcaniques sont généralement distinguées des monts sous-marins d'un point de vue écologique (Rogers, 2018).

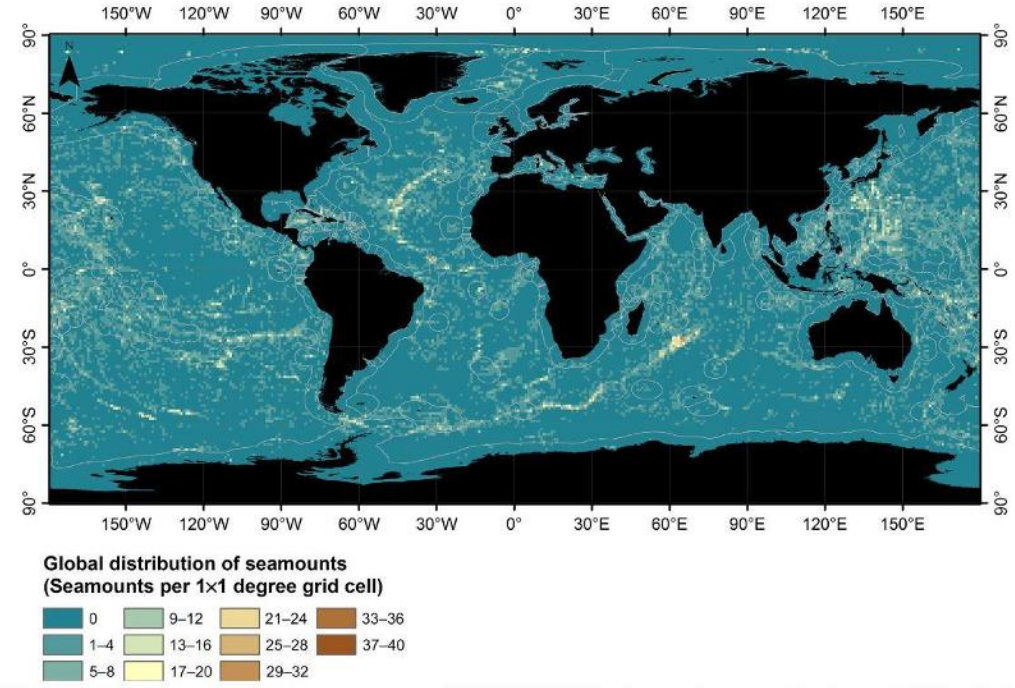

Figure 0.1 : Carte de distribution des monts sous-marins (> 1000 m) d'après la revue bibliographique de Rogers, 2018 (carte préparée à partir de la base de données OCTOPUS – Ocean Tool for Public Understanding and Science – basée sur l'étude de Yesson et al., 2011)

Les pêcheurs, marchands et explorateurs les découvrent indirectement depuis le XV^{e} siècle via l'observation d'agrégations de poissons et de courants accélérés au voisinage des monts sous-marins ; puis à la fin du XIX^{e} siècle (1869), l'exploration du banc Joséphine est rapportée dans la littérature scientifique (Brewin et al., 2007) ; enfin, les vingt-cinq dernières années, du fait notamment de la pression pour l'exploitation des ressources biologiques, ont marqué un intérêt scientifique et des avancées importantes dans la compréhension du fonctionnement de cet écosystème (Rogers, 2018).

Les monts sous-marins se caractérisent par une forte hétérogénéité des conditions environnementales à différentes échelles spatiales en termes de substrat, géomorphologie, gradient bathymétrique et caractéristiques des masses d'eau ; et de couplage entre ces facteurs (Probert et al., 2007). Leur élévation par rapport au plancher océanique génère notamment de fortes interactions à l'origine de courants forts (accélération et rectification des courants, cône de Taylor, ondes internes, etc.) (Lavelle et Mohn, 2010) (**Figure 0.2**).

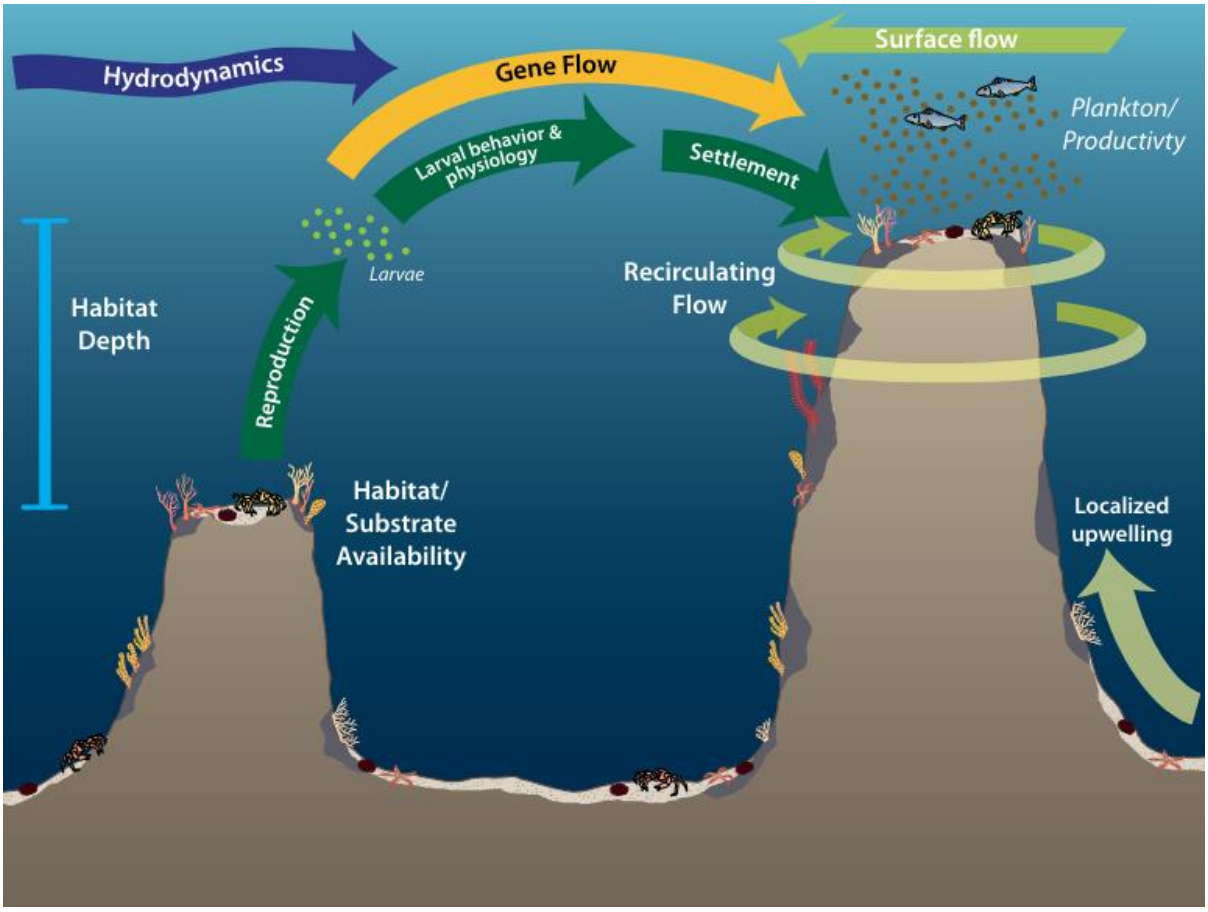

Figure 0.2 : Illustration d'après Shank, (2010) de l'hétérogénéité des conditions environnementales présentes au sein d'un mont et entre différents monts sous-marins (ex : profondeur d'immersion, hydrodynamisme et cellules de circulation, hauteur des monts, habitats biogéniques), couplé aux traits d'histoire de vie des espèces (comportement larvaire, capacité de dispersion, etc.) ; expliquant le degré de flux de gènes entre les monts, et donc la variabilité en composition faunistique entre les monts et au sein d'un mont

La nature des fonds est par conséquent composée principalement de substrats durs, notamment au niveau des sommets et hauts de pente balayés par les courants. Ainsi les communautés biologiques les plus communément observées sur les monts explorés à ce jour sont constituées d'organismes sessiles épi-benthiques (ex : scléractiniaires, antipathaires, alcyonaires, éponges, pour les monts sous-marins en zone bathyale) qui peuvent parfois correspondre à des biomasses élevées (ex : Auscavitch et al., 2020b ; Dijkstra et al., 2021 ; Ramiro-Sánchez et al., 2019 ; Rogers, 2018). Par exemple, de fortes biomasses de scléractiniaires *Solenosmilia variabilis* ou *d'Enallospammia rostrata*, pouvant former de larges récifs, ont été documentées au large de la Nouvelle-Zélande (Goode et al., 2021), au large de la côte Sud-Est de l'Australie (Thresher et al., 2014, 2011), ou encore au large du Royaume-Uni (Atlantique Nord-Est) (Davies et al., 2015) (**Table 0.1**).

Table 0.1 : Liste non exhaustive d'études réalisées depuis 2009 sur la structure de la faune méga-benthique constructrice d'habitats biogéniques ; illustrant les assemblages rencontrés dans les différentes régions océaniques, les méthodes d'échantillonnage mises en œuvre et les échelles d'études considérées. Pour plus de détails, se référer à la revue de Rogers, 2018 (Table 1 et 2). ***Régionale = comparaison inter-monts, locale = étude ciblée sur un mont, intégrative = régionale et locale. HOV = Human Occupied Vehicle, ROV = Remotely Operated Vehicle, AUV = Autonomous Underwater Vehicle*

Océan	Région	Faune dominante	Méthode d'échantillonnage	Échelle de l'étude**	Auteurs
Pacifique Sud	ZEE Nouvelle-Zélande	**Alcyonacea**, **Demospongiae, Hexactinellida, Hydrozoa** (Stylasteridae spp.), **Scleractinia** *(Solenosmilia variabilis, Enallopsammia rostrata)*	Caméra tractée	Intégrative (2 monts)	(Goode et al., 2021)
Pacifique Sud	ZEE Nouvelle-Zélande	**Actiniaria**, **Alcyonacea** (Primnoidae/Isididae), **Hexactinellida**, **Hydrozoa** (Stylasteridae), **Scleractinia** (branching), **Xenophyophoroidea**	Caméra tractée	Intégrative (3 monts)	(Boschen et al., 2015)
Pacifique Sud	ZEE Chili	**Algues rouges encroûtantes, Actiniaria** (anémones), **Ceriantharia**, **Pennatulacea**, **Hydrozoa** (*Stylaster* sp.)	ROV + échantillonnage physique (chalut)	Intégrative (7 monts et pentes supérieures d'îles)	(Tapia-Guerra et al., 2021)
Pacifique Sud-Est	Mer de Tasmanie, au large de la côte Est de l'Australie	**Cnidaria**, **Porifera**	Traîneau épibenthique, chalut	Régionale (5 sites)	(Williams et al., 2011)
Pacifique Sud-Est	Mer de Tasmanie, au large de la côte Sud-Est de l'Australie	**Actiniaria** (Hormatiidae), **Alcyonacea** (gorgones, Isididae *: Keratoisis, Isidella),* **Scleractinia** (*Solenosmilia variabilis, Enallopsammia rostrata)*	Caméra tractée + ROV + échantillonnage physique (via le ROV)	Régionale	(Thresher et al., 2011)
Pacifique Sud-Est	Mer de Tasmanie, au large de la côte Sud de l'Australie	**Actiniaria**, **Alcyonacea** (Isididae), **Scleractinia** (récifs à *Enallopsammia rostrata*, *Solenosmilia variabilis*)	Caméra tractée + échantillonnage physique (traîneau épibenthique)	Régionale (7 monts et 3 habitats à fond dur)	(Thresher et al., 2014)

(Suite Table 0.1)

Océan	Région	Faune dominante	Méthode d'échantillonnage	Échelle de l'étude**	Auteurs
Pacifique Sud-Ouest	Au large de la Nouvelle-Zélande et de l'Australie	**Alcyonacea** (Primnoidae : *Narella*, Coralliidae : *Corallium),* **Scleractinia** (récifs à *Solenosmilia variabilis*, *Enallopsammia rostrata)*	Caméra tractée + échantillonnage physique (traîneau épibenthique)	Régionale (20 monts)	(Rowden et al., 2010b)
Pacifique Nord -Ouest	Est de la mer des Philippines (Magellan Seamount Chain)	**Alcyonacea** (Primnoidae), **Porifera** (**Hexactinellida** : *Tetrapleura*)	HOV/ROV + échantillonnage physique (via le ROV)	Locale (1 mont)	(Shen et al., 2021)
Pacifique Nord-Est	Au large de la Californie (USA)	**Alcyonacea** (gorgones), **Antipatharia** (*Lillipathes* cf. *lillei, Bathypahes),* **Corallines encroûtantes** (Algue rouge), **Demospongiae** (*Halichondria panicea*), **Hexactinellida**, **Hydrozoa** (*Stylaster* spp.), **Macroalgue** (Algue brune : *Desmarestia viridis)*	ROV + AUV	Locale (1 mont)	(Du Preez et al., 2016)
Pacifique Nord	Au Nord-Ouest des îles Hawaïennes	**Alcyonacea, Actiniaria, Antipatharia, Ceriantharia, Corallimorpharia, Pennatulacea, Porifera, Scleractinia**	AUV	Locale (1 mont)	(Morgan et al., 2019)
Pacifique Nord	Au Nord-Ouest des îles Hawaïennes, Ride de Necker	**Alcyonacea** (Isididae, Chrysogorgiidae), **Ascidiacea, Demospongiae, Hexactinellida** (Euplectellidae)	HOV + échantillonnage physique	Régionale (5 monts)	(Morgan et al., 2015)

(Suite Table 0.1)

Océan	Région	Faune dominante	Méthode d'échantillonnage	Échelle de l'étude**	Auteurs
Pacifique Nord (central)	Hawaiian Seamount Chain	**Actiniaria**, **Alcyonacea** (*Corallium* sp., Gorgonian, Primnoidae), **Antipatharia** (*Stichopathes, Antipathes*), **Hexactinellida, Pennatulacea**	ROV + HOV	Intégrative (27 monts, bancs et îles océaniques)	(Schlacher et al., 2014)
Pacifique Nord	Au large de la Californie (USA)	**Alcyonacea, gorgones, Antipatharia, Pennatulacea, Porifera (Hexactinellida** : *Chonelasma* sp., *Farrea* sp., *Heterochone* sp., *Staurocalyptus* sp.), **Scleractinia, Zoantharia**	ROV + échantillonnage physique (via le ROV)	Intégrative (3 monts)	(Lundsten et al., 2009)
Pacifique Nord-Est	Au large de la Californie (USA) (Taney Seamount Chain)	**Cnidaria, Porifera**	ROV + échantillonnage physique (via le ROV)	Intégrative (3 monts)	(McClain et Lundsten, 2015)
Pacifique Nord-Est	Au large de la Californie (USA)	**Actiniaria, Alcyonacea** (gorgones, *Anthomastus ritteri, Acanella* sp., *Chrysogorgia monticola),* **Antipatharia** (*Lillipathes*, *Umbellapathes*), **Demospongiae, Hexactinellida**	ROV + échantillonnage physique (via le ROV)	Locale (1 mont)	(McClain et al., 2010)
Atlantique Nord-Ouest	Proximité de la dorsale médio-atlantique (New England and Corner Rise Seamount Chains)	**Actiniaria, Alcyonacea** (Isidiae, Primnoidae, Corallidae, Chrysogorgiidae), **Antipatharia** (*Bathypathes, Paranthipathes, Teleopathes*), **Ceriantharia, Pennatulacea**	HOV + ROV + échantillonnage physique (via le ROV)	Intégrative (15 monts)	(Lapointe et al., 2020)

(Suite Table 0.1)

Océan	Région	Faune dominante	Méthode d'échantillonnage	Échelle de l'étude**	Auteurs
Atlantique Nord-Est	ZEE Espagne, Ouest de la côte Nord-Ouest espagnole (Galicia Bank)	**Alcyonacea** (*Acanella arbuscula,* gorgones *: Anthothela grandiflora),* **Antipatharia,** **Demospongiae** (*Thenea muricata),* **Hexactinellida** (ex : *Aphrocallistes beatrix,* Geodiidae indet., *Asconema setubalense)*, **Pennatulacea** (*Umbellula*), **Scleractinia** (**recifs** à *Lophelia pertusa* et *Madrepora oculata),* **solitaire** *: Desmophyllum dianthus, Flabellum chunii*)	Échantillonnage physique (chaluts)	Locale (1 mont)	(Serrano et al., 2017)
Atlantique Nord-Est	Ouest du Royaume-Uni (Écosse) (Fosse de Rockall, Hebrides Terrace Seamount)	**Alcyonacea** (Isididae : *Isidella*), **Antipatharia** *(Stichopathes cf. abyssicola),* **Demospongiae** (*Hexadella dedritifera),* **Hexactinellida** (*Aprocallistes beatrix*), **Scleractinia** (récifs à *Solenosmilia variabilis*), **Xenophyophoroidea** (*Syringammina fragilissima*)	ROV	Locale (1 mont)	(Henry et al., 2015)
Atlantique Nord-Est	ZEE Portugal	**Alcyonacea** (gorgones, Plexauridae, Elliselidae), **Antipatharia** (*Antipathella*), **Ascidiacea** (colonial), **Corallines encroûtantes** (Algues rouges), **Demospongiae,** **Macroalgue brune,** **Scleractinia** (*Dendrophyllia cornigera*)	ROV	Locale (1 mont)	(Ramos et al., 2016)

(Suite Table 0.1)

Océan	Région	Faune dominante	Méthode d'échantillonnage	Échelle de l'étude**	Auteurs
Atlantique Nord-Est	ZEE Royaume-Uni	**Actiniaria,** **Alcyonacea,** **Antipatharia,** **Ceriantharia,** **Demospongiae,** **Hexactinellida** *(Aphrocallistes* sp.*, Pheronema carpenteri*), **Hydrozoa** (Stylasteridae spp.), **Scleractinia** (recifs à *Lophelia pertusa* et *Madrepora oculata*), **Xenophyophoroidea** (*Syringammina fragilissima*)	Caméra tractée	Locale (1 mont)	(Narayanaswamy et al., 2013)
Atlantique Nord-Est	Ouest de l'Écosse (Fosse de Rockall, Anton Dohrn Seamount)	**Alcyonacea (gorgones),** **Antipatharia,** **Ceriantharia,** **Scleractinia** (récifs à *Lophelia pertusa, Solenosmilia variabilis;* Caryophylliidae), **Zoantharia (récifs),** **Xenophyophoroidea** (*Syringammina fragilissima*)	Caméra tractée	Locale (1 mont)	(Davies et al., 2015)
Atlantique Équatorial (Est)	Sud du Cap-Vert (Grimaldi Bathymetrists Seamount Chain)	**Actiniaria** (Hormathiidae, *Liponema*), **Alcyonacea** (Chrysogorgiidae, *Acanella* sp., *Corallium* sp., Isididae, *Clavularia)*, **Antipatharia** *(Parantipathes* sp.*, Bathypathes* sp.*, Leiopathes* sp.*),* **Ceriantharia,** **Hydrozoa** (Stylasteridae), **Pennatulacea,** **Scleractinia** (récifs à *Solenosmilia variabilis*)	ROV	Locale (1 mont)	(Victorero et al., 2018)

(Suite Table 0.1)

Océan	Région	Faune dominante	Méthode d'échantillonnage	Échelle de l'étude**	Auteurs
Atlantique Sud	ZEE des îles Ascension, Saint Helena et Tristan da Cunha (Au sein de la dorsale médio-atlantique et de Guinea Seamount Chain)	**Actiniaria** (Hormathiidae), **Hydrozoa** (Stylasteridae), **Porifera** (formes encroûtantes et érigées), **Scleractinia** (Caryophyllidae : *Caryophyllia)*	Caméra tractée	Integrative (13 monts et îles océaniques)	(Bridges et al., 2021)
Mer Méditerranée Sud-Ouest	~ 10 km de la côte Sud espagnole	**Alcyonacea** (*Alcyonium palmatum, Chironephthya mediterranea,* gorgones, Isididae) **Antipatharia** **Pennatulacea,** **Porifera/Hexactinellida** (*Asconema*), **Rhodophytes-maërl,** **Scleractinia** (récifs à *Madrepora oculata ;* Caryophyllidae : *Caryophyllia)*	ROV	Locale (1 mont)	(de la Torriente et al., 2018)
Mer Méditerranée	Nord-Ouest de la Sardaigne (Mer Tyrrhénienne)	**Alcyonacea** (*Alcyonium coralloides*, *Paralcyonium spinulosum*, **gorgones** : *Eunicella cavolinii, Paramuricea clavata),* **Ascidiacea** (colonial : *Diazona violacea*), **Corallines encroûtantes** (Algues rouges), **Demospongiae** (*Axinella*), **Macroalgue brune** (*Laminaria rodriguezii*), **Porifera** (formes encroûtantes)	ROV + échantillonnage physique	Locale (1 mont)	(Bo et al., 2011)

(Suite Table 0.1)

Océan	Région	Faune dominante	Méthode d'échantillonnage	Échelle de l'étude**	Auteurs
Mer Méditerranée	Nord de la Corse (Mer Ligurienne)	**Alcyonacea** (Isididae : *Chelidonis aurantiaca)* **Antipatharia** (*Parantipathes, Antipathes dichotoma*), **Demospongiae** (Tetractinellida), **Hexactinellida** (*Farrea cf. bowerbanki),* **Scleractinia** (récifs morts : *Lophelia pertusa ; Desmophyllum dianthus*), Thanatocénose de cnidaires	ROV + échantillonnage physique via le ROV ciblé (pour le groupe Isididae)	Locale (1 mont)	(Bo et al., 2020)
Océan Austral	Mer Ross (au large de l'Antarctique) (Scott Island Seamount Chain)	**Actiniaria,** **Ascidiacea,** **Hexactinellida,** **Pennatulacea** *(Umbellula pallida),* **Scleractinia** (Caryophyllidae : *Caryphilla)*	Caméra tractée + échantillonnage physique (traîneau épibenthique)	Intégrative (5 monts)	(Clark et Bowden, 2015)
Océan Indien Nord-Est	Mer Adaman, plateau Indien	**Alcyonacea (gorgones),** **Antipatharia,** **Hexactinellida** (*Pheronema* sp., *Euplectella* sp.)	Caméra tractée + échantillonnage physique (quelques spécimens) via un bras hydraulique	Intégrative (2 monts et un bassin d'arrière-arc)	(Sautya et al., 2011)

Certains de ces organismes sessiles épi-benthiques peuvent former de denses habitats biogéniques (Bo et al., 2020 ; Ramos et al., 2016 ; Salinas-de-León et al., 2020) abritant au sein de leurs larges architectures tridimensionnelles une faune de plus petite taille (**Figure 0.3**), contribuant à une forte diversité de faune associée (de la Torriente et al., 2020 ; Tapia-Guerra et al., 2021). Les communautés des monts sous-marins comprennent également des invertébrés benthiques de plus grande taille (ex : ophiures, holothuries, crinoïdes, astérides, brachiopodes) (Clark et Bowden, 2015 ; Du Preez et al., 2016) et des poissons souvent observés en fortes agrégations (ex : l'hoplostète orange, le béryx, la légine australe ; requins, thons et autres grands prédateurs pélagiques), bénéficiant des monts comme zone de migration transitoire, nurserie, reproduction ou d'alimentation (Morato et Clark, 2007). L'histoire géologique propre à chaque mont génère également une diversité de paysages topographiques (fracture, cratère, escarpement, etc.), associée à différentes natures de substrats (ex : lobe de lave, dalle de carbonate, sédiments, graviers). Au sein de cuvettes ou dans des zones protégées des courants, notamment au niveau de la base des monts sous-marins, l'accumulation de sédiments meubles crée des habitats propices à des communautés dominant dans les sédiments fins telles que des pagures (Goode et al., 2021), des anémones, des cérianthes, des pennatules (Tapia-Guerra et al., 2021), ou des holothuries (McClain et al., 2010).

De plus, en raison de leur profondeur d'immersion variable, certains monts sous-marins atteignent la zone photique/mésophotique, générant, par exemple, des communautés composées de macroalgues et de corallines (algues rouges) encroûtantes (Du Preez et al., 2016 ; Ramos et al., 2016 ; Tapia-Guerra et al., 2021).

En raison de ces caractéristiques particulières et de leur positionnement isolé dans une vaste étendue d'océan autrement composé principalement de sédiments meubles, plusieurs paradigmes écologiques ont longtemps supposé que les monts sous-marins se comportaient comme des environnements insulaires ; caractérisés par de faibles niveaux de connectivité (Hubbs, 1959), des taux de spéciation et d'endémicité élevés (Hubbs, 1959 ; Richer de Forges et al., 2000 ; Wilson et Kaufmann, 1987), et qu'ils constituaient des points chauds de biodiversité (Richer de Forges et al., 2000), et de biomasse (Genin et al., 1986 ; Hubbs, 1959). Cependant, ces hypothèses reposaient sur un petit nombre de données récoltées, principalement à partir de cas d'études dans des régions productives, ou pour des monts à

forte biomasse. Ces hypothèses reflètent donc plutôt des biais en termes d'effort d'échantillonnage et de couverture spatiale sur les monts (limités aux sommets principalement), ainsi que de couverture géographique.

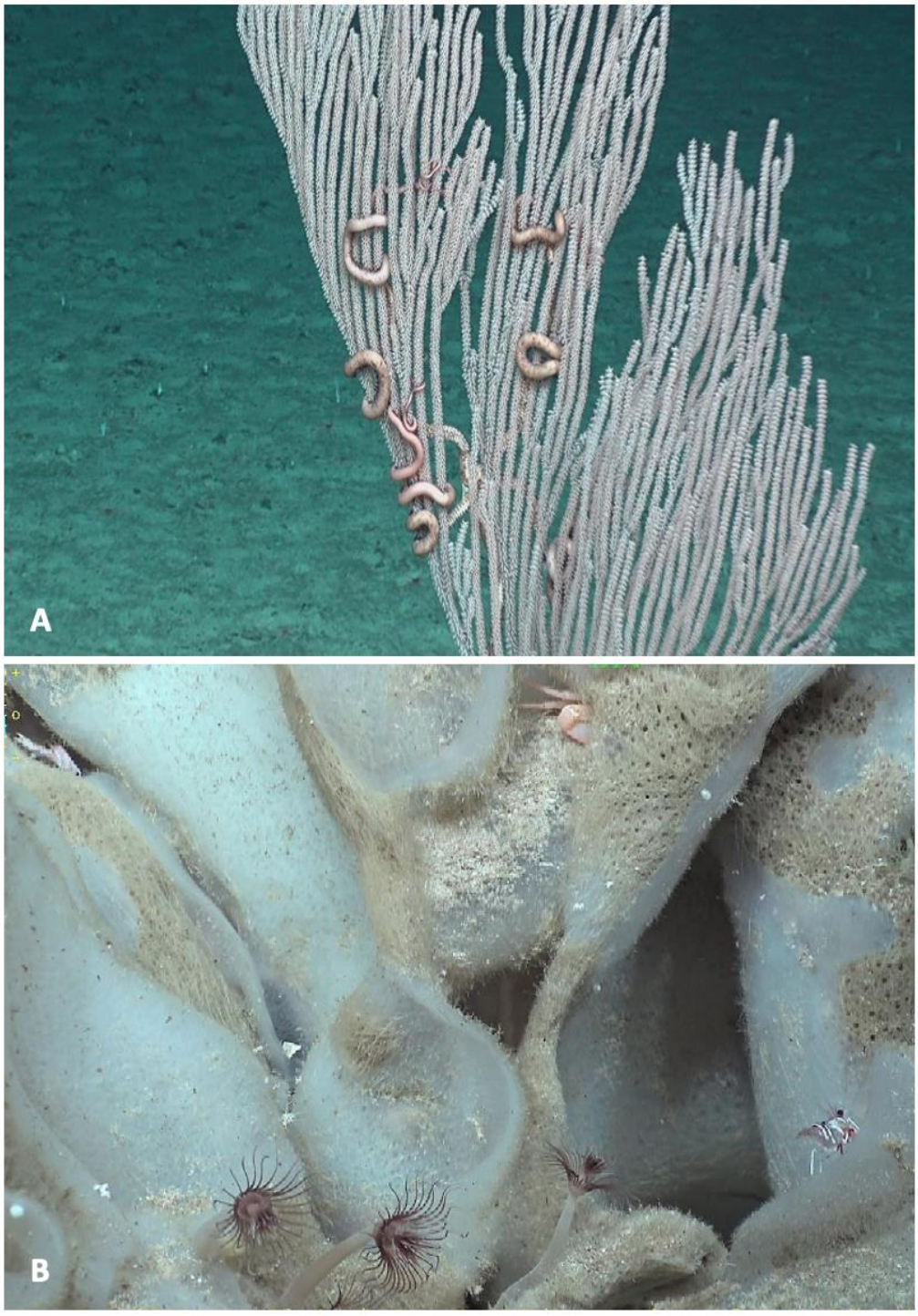

Figure 0.3 : Illustrations de la mégafaune et macrofaune benthique habitant au sein des cnidaires et éponges. **(A)** Ophiures agrippées à un large cnidaire arborescent (Primnoidae). **(B)** Zoom sur une éponge (Hexactinellida), abritant dans ses loges des petits hydrozoaires en bas à gauche, un décapode en bas à droite, un crabe en haut au milieu et une galathée en haut à droite de l'image. Crédit : campagne KANADEEP 2 (Samadi et Olu, 2019)

À ce jour, seulement 0,4 % à 4 % de monts ont été explorés (Kvile et al., 2014), et des données sur l'écologie des communautés ont été principalement acquises dans les régions Atlantique Nord (près de la dorsale médio-Atlantique, au large du Royaume-Uni et Açores) et Pacifique Sud (ZEE de Nouvelle-Zélande, Australie) ou Pacifique Nord (au large de la Californie et de l'archipel Hawaïen) (**Table 0.1**, **Figure 0.4**). Au vu de la diversité des monts sous-marins, qui diffèrent en taille (hauteur, largeur), en forme (ex : plateforme, conique ou irrégulière), en profondeur d'immersion, en localisation géographique (latitude), et en contexte/âge géologique (Rowden et al., 2005), les communautés qu'ils abritent sont affectées par des conditions environnementales variables, rendant les généralisations et développement de théories et modèles prédictifs difficiles.

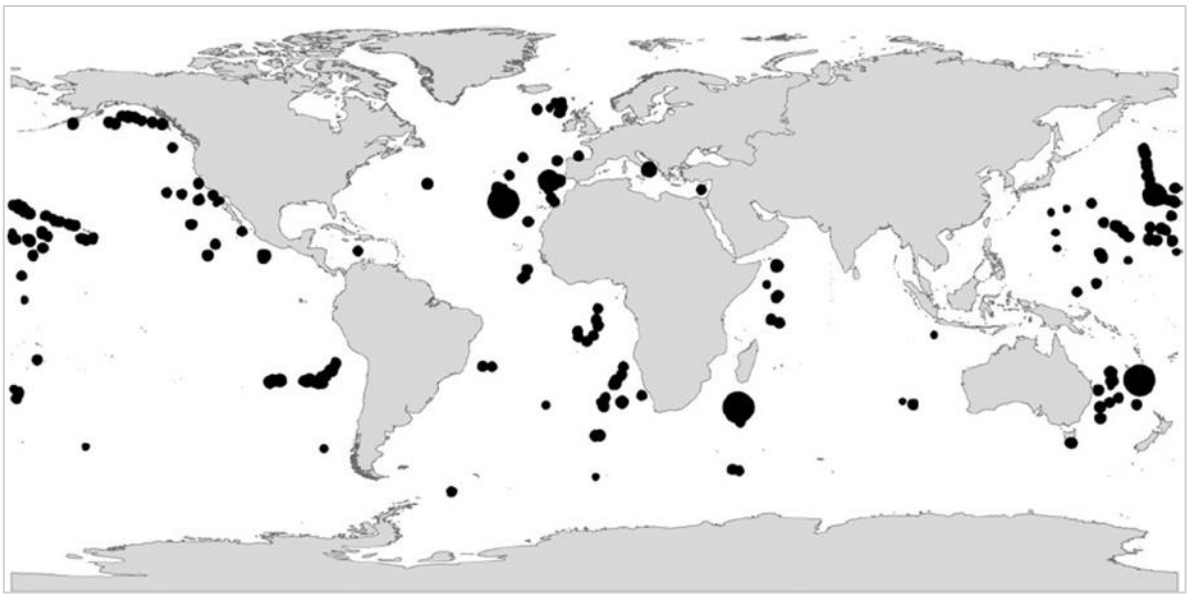

Figure 0.4 : Carte de distribution des monts sous-marins à l'échelle mondiale pour lesquels des données d'occurrences d'espèces ont été enregistrées (enregistrement datant de 2010). Carte d'après la revue bibliographique de Clark et al., (2010) ; et données issues de la base de données SeamountOnline. La taille des cercles est proportionnelle au nombre d'espèces enregistrées sur ces monts, reflétant l'effort d'échantillonnage porté dans les différentes régions

Un programme de recherche CENSEAM (''A Global Census of Marine Life on Seamounts") lancé en 2005 dans le cadre du projet Census of Marine Life (Stocks et al., 2012) a permis de concentrer les recherches sur différents volets, pour confirmer ou réfuter ces hypothèses.

À la suite du programme CENSEAM, une revue bibliographique de Rowden et al. (2010a) a permis de faire l'état des paradigmes écologiques précédemment énoncés, au vu des études menées et des données compilées dans le cadre de ce programme.

Certaines études ont ainsi pu montrer que les monts sous-marins ne sont pas des structures topographiques si isolées que le suggérait la théorie insulaire, avec pour certains taxons des niveaux d'endémicité plutôt plus faibles comparés aux pentes continentales adjacentes ou d'autres habitats profonds (Hall-Spencer et al., 2007 ; Howell et al., 2010 ; McClain et al., 2009 ; O'Hara, 2007 ; Samadi et al., 2006). Cependant, pour d'autres taxons, des niveaux plus élevés d'endémicité ont été mis en évidence dans les mêmes régions avec par exemple jusqu'à 39 % pour le genre *Chrysogorgia* sur les monts sous-marins de la ZEE de Nouvelle-Calédonie (Pante et al., 2015). D'autres hypothèses restent plausibles, telle que l'hypothèse d'oasis d'abondance, suggérant que les monts sous-marins supportent, dans certains cas, des abondances/biomasses d'individus plus conséquentes que d'autres habitats profonds, probablement en raison d'une productivité et concentration en nutriments accrues au niveau de leurs sommets. Cependant, les conditions dans lesquelles ce phénomène d'oasis est observé doivent encore être analysées, notamment en étudiant et comparant les situations connues avec des monts sous-marins dans des régions océaniques moins productives et/ou pour des monts sous-marins moins productifs. De même, l'hypothèse de points chauds de biodiversité reste discutée car les résultats ne sont pas consensuels : certains résultats suggèrent des niveaux de diversités plus élevés sur les monts comparés à d'autres habitats (ex : Morato et al., 2010), et d'autres ne montrent aucune différence (Howell et al., 2010 ; O'Hara, 2007). D'autres enfin suggèrent des compositions faunistiques peu différentes entre les monts sous-marins et d'autres habitats profonds (ex : pentes continentales adjacentes, bancs), mais une structure (abondances absolues et/ou relatives) différente, à même profondeur (Howell et al., 2010 ; McClain et al., 2009). Cependant, les études comparatives quantitatives avec d'autres habitats profonds sont encore trop rares pour généraliser ces observations.

Des recommandations ont été faites au terme du programme CENSEAM, notamment d'augmenter l'effort d'échantillonnage et de concentrer les efforts d'exploration aux régions encore largement sous-explorées, telles que le sud de l'océan Atlantique, le Pacifique central et le sud de l'océan Indien (Clark et al., 2012 ; Kvile et al., 2014), et dans des conditions environnementales (par exemple de productivité primaire) variables ; avec un effort d'échantillonnage plus conséquent (Clark et al., 2012), afin d'obtenir une vue plus complète de la biodiversité des monts sous-marins et des facteurs qui la structurent.

Les dernières années ont vu émerger des études qui ont fait l'effort d'intégrer aux données d'identification des patrons de biodiversité, des données environnementales et quantitatives notamment sur la nature du substrat, ou sur l'hétérogénéité des fonds (par exemple à partir d'indices topographiques), mais elles restent peu nombreuses (Bridges et al., 2021 ; Clark et Bowden, 2015 ; Goode et al., 2021 ; Morgan et al., 2019, 2015 ; Schlacher et al., 2014 ; Shen et al., 2021 ; Victorero et al., 2018).

Les récentes études s'intéressant à évaluer le rôle de l'hétérogénéité de l'habitat sur la structure des communautés ont mis en évidence une structure spatiale des communautés qui est très hétérogène, aussi bien au sein d'un mont (ex : Du Preez et al., 2016 ; Morgan et al., 2019 ; Serrano et al., 2017 ; Shen et al., 2021 ; Victorero et al., 2018) qu'entre différents monts sous-marins d'une région, par exemple au sein d'une chaîne de monts sous-marins au large de l'archipel de Hawaï (Schlacher et al., 2014), le long de la ride de Necker (Pacifique Nord) (Morgan et al., 2015) ou le long de la ride de Norfolk et de Lord Howe Rise (Pacifique Sud-Ouest) (Williams et al., 2011).

À l'échelle régionale (comparaison inter-monts), les facteurs structurant ces communautés mis en évidence sont la productivité primaire de surface (Clark et Bowden, 2015), influant notamment sur la richesse spécifique (Bridges et al., 2022), le gradient latitudinal (Morgan et al., 2015 ; Williams et al., 2011), qui structure également la richesse spécifique (Bridges et al., 2022) et la composition des assemblages (Bridges et al., 2021), mais aussi le gradient longitudinal (Lapointe et al., 2020). De plus, les caractéristiques hydrologiques de la colonne d'eau (température, oxygène et flux de carbone organique particulaire) (O'Hara et al., 2010 ; Turnewitsch et al., 2016), la distance des monts à la côte – reflétant des différences de composition des assemblages (O'Hara et al., 2010) – et le gradient bathymétrique (Boschen et al., 2015 ; Clark et Bowden, 2015 ; Lapointe et al., 2020 ; Schlacher et al., 2014 ; Williams et al., 2011) – en lien avec les différentes masses d'eau parcourues par les monts (Auscavitch et al., 2020a ; Bridges et al., 2022 ; Lapointe et al., 2020) et générant différents patrons de diversité bêta (différenciation spatiale des communautés) (McClain et Lundsten, 2015) – ont également été relevés comme des facteurs structurant les communautés entre différents monts sous-marins.

Quelques études ont également mis en évidence l'influence de l'hétérogénéité de la géomorphologie des monts sur les différences d'abondance des communautés benthiques

(Sautya et al., 2011), ainsi que de la différence de composition en substrat entre les monts sur la structure des assemblages benthiques (Boschen et al., 2015 ; Sautya et al., 2011), bien que moins significatif à une échelle régionale chez Lapointe et al. (2020) et Morgan et al. (2015). La topographie propre à chaque mont aurait également un rôle structurant (Boschen et al., 2015), du moins certains auteurs en font l'hypothèse (Clark et Bowden, 2015). De plus, la présence ou non de croûte riche en cobalt à la surface des monts jouerait un rôle sur la composition et l'abondance relative des espèces (Schlacher et al., 2014) ainsi que la présence de magnétisme – proxy de l'activité hydrothermal – pour les monts actifs (Boschen et al., 2015).

Très peu d'études ont testé l'influence de l'hydrodynamisme et bien que ce facteur n'ait pas été démontré significativement structurant à une échelle régionale, la dynamique des courants joue probablement un rôle sur la composition et l'abondance des communautés d'invertébrés benthiques (Clark et Bowden, 2015). Cependant, plus localement, au sein d'un mont, l'influence des courants de surface a été mise en évidence, et explique des différences de composition des assemblages faunistiques selon les flancs explorés (Morgan et al., 2019).

Localement, à l'échelle d'un mont, les facteurs structurants mis en évidence sont le gradient bathymétrique en lien avec des paramètres corrélés (ex : température, masse d'eau, lumière), générant une zonation verticale de composition des communautés ("turnover"), aussi bien sur un large gradient bathymétrique (Du Preez et al., 2016 ; McClain et al., 2010 ; Ramos et al., 2016 ; Victorero et al., 2018) que sur une gamme plus étroite (Long et Baco, 2014 ; Morgan et al., 2019). Cependant, cette zonation verticale n'est pas toujours graduelle (Shen et al., 2021).

Les masses d'eau ont également un rôle structurant, par exemple, sur la différenciation de richesse spécifique des communautés soit le long d'un gradient de profondeur (Victorero et al., 2018) ; ou à l'interface entre deux masses d'eau (Henry et al., 2015). De plus, bien que très peu testé, le flux de carbone organique particulaire semble jouer également un rôle sur l'abondance des assemblages d'invertébrés benthiques à l'échelle d'un mont (Morgan et al., 2019).

D'autres facteurs structurants ont été mis en évidence, tel que la complexité du terrain (microtopographie et rugosité), en lien avec la géomorphologie du mont, et ses différents

éléments topographiques (ex : sommet, pente, orientation des pentes) (Clark et Bowden, 2015 ; Du Preez et al., 2016 ; Goode et al., 2021 ; Long et Baco, 2014 ; Morgan et al., 2019 ; Sautya et al., 2011 ; Shen et al., 2021 ; Victorero et al., 2018). L'hétérogénéité du substrat (Morgan et al., 2019) et sa composition (ex : Bridges et al., 2021 ; Goode et al., 2021 ; Sautya et al., 2011 ; Shen et al., 2021) ont également un rôle structurant, notamment sur la différence d'abondance et le turnover/remplacement des espèces (Victorero et al., 2018).

Enfin, la présence d'habitats biogéniques le long des monts, générés par des taxons tels que des cnidaires, éponges, macro-algues ou corallines encroûtantes, joue un rôle sur la distribution spatiale et la diversité d'espèces associées à ces habitats (de la Torriente et al., 2020, 2018 ; Du Preez et al., 2016).

Néanmoins, à ce jour, les efforts de recherche concernent soit des études ayant ciblé un seul mont sous-marin, généralement sur un large gradient bathymétrique (de la Torriente et al., 2018 ; Du Preez et al., 2016 ; Henry et al., 2015 ; Hoff et Stevens, 2005 ; McClain et al., 2010 ; Serrano et al., 2017 ; Shen et al., 2021 ; Victorero et al., 2018), mais aussi sur une gamme de profondeur plus étroite (Bo et al., 2020, 2011 ; Long et Baco, 2014 ; Morgan et al., 2019) ; ou bien des études à une échelle régionale (comparaison inter-monts) (Auscavitch et al., 2020a ; Bridges et al., 2022 ; McClain et al., 2010 ; Morgan et al., 2015 ; O'Hara et Tittensor, 2010 ; Thresher et al., 2014, 2011 ; Williams et al., 2011).

Des études plus intégratives ont évalué aussi bien la structure spatiale des communautés à une échelle régionale que localement au sein d'un mont (ex : Boschen et al., 2015 ; Bridges et al., 2021 ; Clark et Bowden, 2015 ; Goode et al., 2021 ; Lapointe et al., 2020 ; Lundsten et al., 2009 ; McClain et Lundsten, 2015 ; Sautya et al., 2011 ; Schlacher et al., 2014 ; Tapia-Guerra et al., 2021).

Cependant, toutes ces études ne considèrent qu'un sous-ensemble des multiples variables environnementales identifiées comme structurantes ou dont l'hypothèse est qu'elles sont structurantes. Les données quantifiées, notamment sur la complexité du terrain, sont généralement issues de modèles bathymétriques faiblement résolus (grille > 25 m). De plus, il existe encore peu de données quantitatives sur la nature du substrat et son hétérogénéité, et rares sont les études considérant des données sur les courants et la productivité primaire.

Enfin, à ce jour, encore peu d'études sur les monts sous-marins concernent des régions où la productivité est plus faible, avec seulement quelques cas dans la région Sud-Atlantique (Bridges et al., 2022, 2021) et l'océan Indien Nord-Est (Sautya et al., 2011), ce qui fournit une compréhension partielle de cet écosystème.

Pour mieux comprendre les facteurs structurant les peuplements benthiques des monts sous-marins, des études intégratives et quantitatives, tenant compte de ces multiples échelles spatiales – études ciblées sur un mont et comparant différentes structures d'une région afin de considérer l'hétérogénéité entre les monts –, sont nécessaires. De plus, ces études doivent considérer les multiples facteurs environnementaux – identifiés comme structurants, ou dont l'hypothèse est qu'ils sont structurants (ex : courant, productivité primaire) – allant de forçage hydrodynamique, hydrologique (productivité primaire de surface et masses d'eau) au rôle de l'hétérogénéité et de la composition du substrat et des microtopographies à petite échelle. L'intégration de ces différents facteurs permettrait également de quantifier et comprendre leurs effets combinés (par exemple, la relation courant/topographie) sur la structure des communautés.

En parallèle, cet écosystème est sujet à de nombreuses menaces (ex : exploitation minière, chalutages en eaux profondes, pollutions d'origine anthropique) (Rogers, 2019). L'intérêt économique que suscitent les monts sous-marins amène à un besoin de conservation et régulation des activités de pêche industrielle et d'exploitation minière des croûtes de ferromanganèse, riches en cobalt (métal rare), qui se forment en surface de ces structures (Petersen et al., 2016). Ces activités ont pour conséquence la fragilisation et la destruction des habitats benthiques des monts sous-marins (Clark et al., 2019 ; Gollner et al., 2017 ; Williams et al., 2020b), dont les potentiels de restauration sont peu connus car encore peu étudiés (Da Ros et al., 2019). Les habitats des monts sous-marins sont principalement formés par des espèces vulnérables, c'est-à-dire des organismes faiblement résilients à ces pressions anthropiques de par leur trait d'histoire de vie (reproduction tardive, croissance lente, longue durée de vie) (Watling et Auster, 2021). De plus, l'impact des changements globaux (ex : réchauffement des eaux et stratification et acidification des océans, désoxygénation) sur ces communautés benthiques (Sweetman et al., 2017) est une préoccupation majeure à prendre en considération. Ces différentes menaces accélèrent le besoin d'acquérir des connaissances sur la structure à multi-échelle de la biodiversité des monts sous-marins, des facteurs

environnementaux structurants, et des échelles de structuration spatiale afin de modéliser la distribution des habitats et de la biodiversité. Ces modélisations prédictives sont nécessaires au vu du nombre conséquent de mont sous-marins à l'échelle mondiale, qu'il serait impossible à tous échantillonner (Clark et al., 2012). De telles modélisations nécessitent dans un premier temps d'acquérir des données sur le système (Woodstock et Zhang, 2022).

L'acquisition de données biologiques sur les monts sous-marins repose, en partie, sur l'échantillonnage physique de la faune, qui permet d'obtenir des données qualitatives sur les espèces, et de répondre à des questions relatives à l'endémisme, la connectivité entre les monts sous-marins et pour définir des bio-régions, à large échelle. Cependant, l'échantillonnage physique à lui seul ne permet pas d'appréhender des questions relatives à la structuration spatiale des communautés à petite échelle, et du rôle structurant de l'hétérogénéité de l'habitat à cette échelle. Seule l'acquisition d'images des fonds marins au moyen de caméras tractées ou autres submersibles peut fournir ces données quantitatives essentielles, afin de replacer les espèces dans leur contexte écologique et expliquer leur distribution spatiale.

Cependant, l'imagerie installe des nouvelles problématiques en termes de caractérisation des communautés biologiques, notamment dans ces environnements profonds où le compartiment biologique est mal connu, en particulier pour des régions encore peu explorées et très diversifiées.

Une première problématique de ce projet de thèse est de répondre aux enjeux scientifiques et de conservation des monts sous-marins. Celle-ci en amène une seconde qui est de réussir à intégrer des données taxonomiques sur les communautés biologiques avec des rangs d'identification finement résolus, combinées à des données environnementales de haute résolution et à multi-échelle.

Or, la question de l'identification d'organismes à partir d'images, dans des régions très diversifiées et peu explorées, est un réel défi scientifique, qui limite nos connaissances et notre compréhension sur la structure des communautés benthiques.

Défis méthodologiques

L'avènement des submersibles et des techniques d'imagerie a permis d'observer de manière directe et de cartographier les habitats benthiques et la mégafaune – faune visible à partir d'images (~ > 2 cm) (Grassle et al., 1975) –, révélant une hétérogénéité d'habitats insoupçonnée (Ramirez-Llodra et al., 2011). Les outils d'imagerie (ex : ROV, caméra tractée, AUV, etc.) permettent de répondre à divers objectifs (ex : exploration, cartographie des habitats, étude de suivi, échantillonnage ciblé de la faune visible et caractérisation *in situ* des biotopes). Ces engins permettent d'obtenir à partir d'images ou de vidéos des données quantitatives biologiques (ex : densité, abondance, pourcentage de recouvrement et données sur les comportements) ou sur la caractérisation de l'habitat (ex : pourcentage de recouvrement et diversité du substrat), à l'échelle du kilomètre au millimètre, qui soient répétables spatialement et temporellement, et à moindre impact sur les communautés biologiques (Bowden et al., 2020 ; Henry et Roberts, 2014).

Cependant, le passage d'une image brute à une information qualitative sur l'identité des taxons qui la composent n'est pas si trivial. Une première étape consiste à détecter les organismes observés sur les images, et à les identifier en lien avec un référentiel taxonomique.

La taxonomie est une discipline scientifique qui consiste à identifier, classer et nommer la biodiversité (Thomson et al., 2018). Afin de classer des organismes nouveaux pour la science, cette discipline repose sur l'évaluation de caractères (ex : morphologiques, génétiques) qui nécessitent une analyse détaillée des organismes en main (ex : analyse des tissus, morphométrie) et une comparaison avec l'état des connaissances existantes (à travers la littérature et les collections d'histoire naturelle).

À partir d'images, cette analyse détaillée n'est pas possible car les caractères diagnostiques d'une espèce utilisée en taxonomie ne sont pas tous évaluables et applicables à l'étude de photos d'organisme *in situ*, ce qui nécessite de trouver d'autres outils diagnostiques, qui soient applicables aux images. Il paraît évident qu'une simple image ne permet pas de réaliser des analyses génétiques/moléculaires ou des coupes et des analyses morphométriques précises. De plus, de nombreux freins s'ajoutent à l'identification taxonomique d'organismes sur images, tels que la résolution de l'image, l'angle de vue et la taille de l'organisme, son niveau de visibilité (Beisiegel et al., 2017 ; Durden et al., 2016b ; Williams et al., 2015), et

surtout, le degré de connaissance initial que nous avons de la faune dans la région étudiée (Beisiegel et al., 2017). En effet, la connaissance taxonomique et la prise en compte de ce cadre de référence sont un requis indispensable au préalable d'une étude s'intéressant à décrire et comprendre la structure de la biodiversité, sans quoi les conclusions sur l'écologie/structure spatiale des communautés étudiées et le fonctionnement de l'écosystème seraient erronées (Barberousse et Bary, 2019).

Dans ce contexte, et en l'absence de caractères diagnostiques d'identification applicables sur des images, de nombreuses études écologiques basées sur l'imagerie caractérisent les communautés benthiques à partir d'une approche fondée sur les caractères visibles en définissant des morphotypes considérés comme des entités taxonomiques opérationnelles (OTU pour Operational Taxonomic Unit) et utilisées comme des proxies pour les espèces. Sur les images, cette approche est le plus souvent para-taxonomique car les caractères utilisés sont ceux identifiables sur les images sans référence aux caractères considérés comme pertinents (diagnostiques) dans la littérature taxonomique (Krell, 2004). De plus, les critères de regroupement ne sont généralement pas explicités au cours des études et sont subjectifs d'un observateur à l'autre (Durden et al., 2016a). Enfin, les noms de morphotypes attribués ne sont pas standardisés selon un vocabulaire commun, et ne sont donc pas comparables d'une étude à l'autre. Ces problématiques ont amené, par exemple, le développement de catalogue standard d'annotation de la faune à partir d'images – proposant un format hybride qui mixe à la fois une identification taxonomique (noms linnéens conventionnels) de haut rang avec des classes morphologiques (Althaus et al., 2015). Ce catalogue a l'avantage de permettre l'annotation standard de tout organisme visible sur une image, notamment lorsque ceux-ci ne peuvent être identifiés taxonomiquement. Cependant, ce schéma d'annotation reste imprécis car il permet principalement d'annoter des morphotypes sans prendre en compte clairement un cadre taxonomique de référence.

Pour prendre en compte de façon rigoureuse ce cadre taxonomique, il est nécessaire d'associer des collectes physiques d'organismes aux données d'imagerie, afin d'obtenir un catalogue et une base de données de référence des taxons présents dans la zone d'étude (Howell et al., 2020). Cette approche permet de construire des clés d'identification utilisables en imagerie en permettant de définir des jeux de caractères diagnostiques applicables aux images dans un contexte donné. Cette association est d'autant plus importante dans des

régions encore peu explorées où l'inventaire de la faune est largement incomplet et rend donc difficile l'attribution des organismes à des formes connues. Les dernières années marquent un intérêt scientifique sur la nécessité de formaliser et standardiser l'identification de la mégafaune profonde à partir d'images (Bowden et al., 2020 ; Henry et Roberts, 2014), notamment dans le cadre des principes FAIR (Findable, Accessible, Interoperable, Reusable) (Schoening et al., 2022 ; Wilkinson et al., 2016).

Récemment, un groupe de travail (SMARTAR-ID) a proposé une trame de travail afin de développer des catalogues standards d'identification des morpho-espèces pour différentes régions océaniques. Cette étude soulève également le besoin d'un effort international pour développer des clés d'identification adaptées aux images et à l'état des connaissances des localités explorées (Howell et al., 2019). Horton et al. (2021) ont par ailleurs proposé pour la première fois des recommandations afin de standardiser les nomenclatures ouvertes pour l'identification de taxons à partir d'images qui permettent d'expliciter l'état incertain de l'identification d'un organisme sur une image (Sigovini et al., 2016).

Les spécificités d'identification de chaque taxon font que certains présentent plus de facilité à être identifiés à partir d'images. Il est nécessaire de définir quels sont les taxons identifiables à partir d'images, et à quel niveau de la classification il est raisonnable de les identifier dans des analyses écologiques afin d'en augmenter la fiabilité et la reproductibilité.

Certains organismes, comme les éponges et cnidaires sont difficilement identifiables sur les images car les critères d'identification utilisés sont principalement microscopiques (Barnes et Bell, 2002 ; Łukowiak, 2020 ; Pante et al., 2012b), donc non accessibles à partir d'images du fond. Cependant, leur multiples rôles fonctionnels au sein des écosystèmes marins (ex : refuges, nurseries, sources de nourriture, cycles biogéochimiques) (Bell, 2008 ; Buhl-Mortensen et al., 2016 ; Cárdenas et al., 2012 ; Pierrejean et al., 2020) et leur faible résilience aux perturbations anthropiques (Baco et al., 2020 ; Du Preez et al., 2020) soulèvent aussi bien des enjeux de conservation de ces communautés que des questions plus fondamentales sur la caractérisation de leur rôle structurant et leurs réponses aux contraintes de l'environnement.

Ce dernier point constitue une dernière problématique, qui est de réussir à caractériser et quantifier au mieux les communautés d'éponges et de cnidaires à partir d'images, dans le cas où leur identification taxonomique est limitante.

À défaut de pouvoir être caractérisée par des traits taxonomiques, la diversité de ces taxons – pouvant former des habitats biogéniques – peut également être appréhendée sous un angle fonctionnel. En effet, la forte plasticité morphologique de ces organismes mais aussi la convergence morphologique (DeBiasse et Hellberg, 2015 ; Elliott, 2016 ; Todd, 2008) rendent difficile et peu fiable leur identification à partir d'images, même à haut rang d'identification (ex : ordre). Cependant, il est intéressant de caractériser cette diversité morphologique de ces communautés d'organismes constructeurs pour évaluer à la fois comment elle répond aux facteurs de l'environnement (Schönberg, 2021), mais aussi comment elle structure la diversité des organismes pour lesquels ces organismes constructeurs forment potentiellement des habitats (Buhl-Mortensen et al., 2010, 2016 ; de la Torriente et al., 2020).

Objectifs de la thèse

Dans ce contexte, les trois grands objectifs de ce projet de thèse sont de :

(1) Décrire et comparer les patrons de structuration des communautés de mégafaune benthique (composition des assemblages, densité, diversités α et β) des monts sous-marins et pentes insulaires de Mayotte et Bassas da India, dans une zone géographique peu explorée, au sein du canal du Mozambique

- **a.** À une échelle locale (étude ciblée sur un mont ou une pente insulaire)
- **b.** À une échelle régionale (comparaison des patrons de structuration inter-monts et pentes insulaires).

(2) Identifier les facteurs environnementaux mesurés à différentes échelles spatiales, liés à la géologie, à l'hydrodynamique et l'hydrologie, à la géographie (latitude, distance à la côte), qui structurent les communautés aux échelles régionale (le long du canal) et locale, à l'échelle d'un mont ou d'une pente insulaire, et quantifier leurs contributions relatives et combinées. Les pentes insulaires de Mayotte et Bassas da India ont par ailleurs fait l'objet d'une analyse ciblée afin d'évaluer les échelles des structures spatiales des communautés le long d'une pente, et leurs interrelations avec les facteurs abiotiques.

(3) Développer une méthodologie intégrée pour améliorer l'identification de la mégafaune benthique sur les images afin d'estimer de façon plus robuste la structure de la biodiversité des peuplements de mégafaune benthique.

Afin de répondre à ces objectifs, le plan de manuscrit de thèse se découpera en trois chapitres, sous la forme d'articles scientifiques publiés ou en préparation.

Une partie importante de ce travail de thèse consiste à contribuer au développement d'une méthodologie d'analyse de la biodiversité à partir des images. Deux chapitres (1 et 3) y sont consacrés.

Ainsi **le premier chapitre** vise à **(1)** établir une comparaison des différentes méthodes d'échantillonnage généralement utilisées pour caractériser la mégafaune benthique (imagerie, échantillonnage physique par dragage et chalutage) et **(2)** proposer une méthodologie combinant ces différentes approches. Ce premier chapitre propose de formaliser une méthodologie d'identification de la mégafaune benthique à partir d'images, méthodologie sur laquelle repose la qualité de mon jeu de données faunistiques, sur lequel porteront les analyses spatiales des communautés benthiques.

Le deuxième chapitre porte sur l'analyse des patrons de structuration des communautés de mégafaune benthique (densité, composition, diversités α et β) aux échelles régionale (le long du canal) et locale (intra-mont/pente insulaire), et sur la caractérisation des facteurs de l'habitat structurant à ces échelles, et leurs imbrications.

Le troisième chapitre propose une approche méthodologique morpho-fonctionnelle portant sur l'analyse de la mégafaune benthique des taxons constructeurs d'habitats biogéniques (cnidaires et éponges), difficilement identifiables sur les images. L'analyse réalisée sur le même jeu de données que celui analysé dans le chapitre 2 constitue un cas d'application de la méthode proposée ainsi qu'une caractérisation de la réponse morpho-fonctionnelle de ces groupes aux contraintes de l'habitat, ainsi que leur rôle structurant pour les organismes pour lesquels ils forment potentiellement des habitats.

Avant-propos sur les données et zones d'études

D'une part, le chapitre 1 intègre des données acquises en Papouasie-Nouvelle-Guinée au cours de trois campagnes. Les campagnes BIOPAPUA (Samadi et Corbari, 2010) et PAPUANIUGINI (Payri et al., 2012), dans le cadre du programme Tropical Deep Sea Benthos et mené par le Muséum national d'Histoire naturelle (MNHN), étaient dédiées à l'exploration et l'acquisition de connaissances sur la biodiversité des habitats profonds en mer de Bismarck. Ces campagnes ont permis la découverte de nouveaux environnements, notamment une zone de suintement froid, au large de la rivière Sepik dans la Broken Bay, et une pente sédimentaire avec une zone d'accumulation de bois coulés et un canyon plus en profondeur, au niveau de l'Astrolabe Bay.

Ces environnements ont été ciblés au cours d'une autre campagne, MADEEP (Corbari et al., 2014), qui est venue compléter le jeu de données dans cette région par d'autres échantillonnages physiques de la faune, et a permis notamment d'obtenir des premières données images sur ces habitats profonds à partir de transects de caméra tractée menés le long d'une sélection de traits de dragues et de chaluts déployés au cours des deux précédentes campagnes. Pour cette étude, les habitats sélectionnés en Papouasie-Nouvelle-Guinée comprennent donc une pente continentale sédimentaire (Astrolabe Bay) avec deux transects dans une zone d'accumulation de bois coulés (entre 500-800 m), et un transect situé plus en profondeur dans un canyon (930 m), ainsi qu'un transect situé dans une zone de suintement froid au large de la rivière Sepik.

D'autre part, des données acquises lors de l'exploration des pentes externes volcaniques de l'île de Mayotte au cours de la campagne BIOMAGLO (Corbari et al., 2017) viennent constituer le jeu de données finales de cette étude. Des transects de caméra tractée suivis d'opérations d'échantillonnage physique par dragage et chalutage co-localisées ont été déployés le long de ces pentes, sur une gamme bathymétrique allant de 450 à 1180 m.

Les données du chapitre 2 et 3 de la thèse sont issues d'un projet de collaboration entre l'Institut français pour l'exploitation de la mer (Ifremer) et TotalEnergies, le projet PAMELA (Bourillet et al., 2013), qui ont lancé en 2014 une succession de campagnes océanographiques dans le canal du Mozambique, associant l'acquisition de données environnementales ainsi que des données d'imagerie des habitats et un premier échantillonnage de la faune profonde.

D’autre part, plusieurs campagnes du Muséum national d'histoire naturelle (MNHN) dans cette même zone ont fourni un échantillonnage plus complet de la faune, permettant d’obtenir les connaissances taxonomiques nécessaires à l’interprétation des images acquises. La campagne BIOMAGLO, financée par les Terres Australes et Antarctiques Françaises (TAAFs) dans le cadre de la mise en œuvre du X^{ème} FED régional « gestion durable du patrimoine naturel de Mayotte et des îles Éparses », et menée par le MNHN en collaboration avec l’Ifremer, a associé prises de vue par caméra tractée et opérations de dragage/chalutage. Cette campagne est venue compléter le jeu de données disponibles pour une approche intégrée de la structure de la biodiversité des monts sous-marins du canal du Mozambique. Les pentes externes de l’île de Mayotte ont notamment fait l’objet d’une approche détaillée et multi-échelles.

Ces campagnes ont permis d’explorer quatre monts sous-marins (terrasse des Glorieuses, Banc du Jaguar, Banc de Hall, mont Sakalaves sur la ride de Davie) et les pentes externes des îles de Mayotte et de Bassas da India, le long d’un gradient latitudinal de 10° au sein du canal du Mozambique. La profondeur minimale des structures (sommets des monts et terrasses des pentes insulaires) se situe dans une tranche bathymétrique relativement étroite (370-800 m) tandis que les hauts de pente ont été explorés jusqu’à 900-1180 m selon les monts.

I. Méthodologie intégrative pour l'identification de la mégafaune à partir d'images

L'imagerie est devenue un outil essentiel pour évaluer la biodiversité méga-benthiques des grands fonds, historiquement basée sur l'échantillonnage physique à l'aide d'engins de pêche. Les jeux de données images permettent des estimations quantitatives et répétables, ainsi que l'évaluation des modèles spatiaux à petite échelle et des descriptions d'habitats. Cependant, l'identification des taxons à partir d'images est difficile et repose souvent sur des morphotypes sans tenir compte d'un cadre taxonomique. L'identification des taxons est particulièrement difficile dans les régions où la faune est mal connue et/ou très diversifiée. Par ailleurs, l'efficacité de l'imagerie et de l'échantillonnage physique peut varier selon les types d'habitats.

Ici, nous avons comparé les métriques de biodiversité (diversités alpha et gamma, composition) basées sur de l'échantillonnage physique (dragage et chalutage) et des images capturées à partir d'une caméra tractée (1) le long d'une pente continentale supérieure de Papouasie-Nouvelle-Guinée (pente sédimentée avec des bois coulés, un canyon et des suintements froids), et (2) sur les pentes extérieures volcaniques de l'île de Mayotte, dominées par des fonds durs. La comparaison a été faite pour des taxons cibles (Pisces, Crustacea, Echinoidea, Asteroidea), qui sont de bons candidats pour l'identification à partir d'images. Les rangs d'identification taxonomique obtenus pour les images varient parmi ces taxons (par exemple, famille/ordre pour les poissons, genre pour les échinodermes). A ces rangs, l'imagerie a permis d'évaluer une plus grande richesse taxonomique dans les habitats à fonds durs et hétérogènes, ce qui s'explique en partie par la faible performance du chalutage sur ces fonds accidentés. Pour la même raison, la diversité gamma des Poissons et des Crustacés était également plus élevée à partir des images, mais aucune différence n'a été observée pour les échinodermes. Dans les fonds meubles, l'échantillonnage physique a permis d'évaluer une plus grande diversité alpha et gamma pour les poissons et les crustacés, mais ces différences ont eu tendance à diminuer pour les crustacés identifiés au niveau

spécifique/morpho-spécifique à partir des images. L'échantillonnage physique et l'imagerie étaient sélectifs vis-à-vis de certains taxons (par exemple en fonction de la taille ou du mode de vie), donnant ainsi accès à différentes facettes de la biodiversité. De plus, les spécimens collectés à une plus grande échelle ont facilité l'identification de la mégafaune à partir d'images.

Sur la base de cette approche complémentaire, nous proposons une méthodologie robuste d'identification de la faune à partir d'images reposant sur un cadre taxonomique, issu d'un travail collaboratif avec des taxonomistes. Un résultat original de ce travail collaboratif est la création de clés d'identification dédiées spécifiquement aux images *in situ* et qui tiennent compte de l'état des connaissances taxonomiques pour les sites explorés.

Mots clés : mégafaune des grands fonds, identification à partir d'images, évaluation de la biodiversité, clés d'identification, méthodologie intégrative, caméra tractée, échantillonnage physique

Cette étude fait l'objet d'une publication dans Frontiers in Marine Science (cf. Annexe) :

Hanafi-Portier M, Samadi S, Corbari L, Chan T-Y, Chen W-J, Chen J-N, Lee M-Y, Mah C, Saucède T, Borremans C and Olu K (2021) When Imagery and Physical Sampling Work Together: Toward an Integrative Methodology of Deep-Sea Image-Based Megafauna Identification. Front. Mar. Sci. 8:749078. DOI: 10.3389/fmars.2021.749078

When Imagery and Physical Sampling Work Together: Toward an Integrative Methodology of Deep-Sea Image-Based Megafauna Identification

Mélissa Hanafi-Portier[1,2*], Sarah Samadi[2†], Laure Corbari[2†], Tin-Yam Chan[3], Wei-Jen Chen[4], Jhen-Nien Chen[4], Mao-Ying Lee[5], Christopher Mah[6], Thomas Saucède[7], Catherine Borremans[1] and Karine Olu[1†]

[1] Laboratoire Environnement Profond, IFREMER, REM/EEP, Centre de Bretagne, Plouzané, France, [2] UMR 7205 ISYEB, Équipe "Explorations, Espèces et Spéciations", Muséum National d'Histoire Naturelle, Paris, France, [3] Institute of Marine Biology and Center of Excellence for the Oceans, National Taiwan Ocean University, Keelung, Taiwan, [4] Institute of Oceanography, National Taiwan University, Taipei, Taiwan, [5] Marine Fisheries Division, Fisheries Research Institute, Council of Agriculture, Keelung, Taiwan, [6] Department of Invertebrate Zoology, National Museum of Natural History, Smithsonian Institution, Washington, DC, United States, [7] Biogéosciences, UMR 6282, CNRS, Université Bourgogne Franche-Comté, Dijon, France

Edited by: *Ashley Alun Rowden, National Institute of Water and Atmospheric Research (NIWA), New Zealand*

Reviewed by: *Franziska Althaus, Commonwealth Scientific and Industrial Research Organisation (CSIRO), Australia Damianos Chatzievangelou, Jacobs University Bremen, Germany*

***Correspondence:** Mélissa Hanafi-Portier - Melissa.Hanafi.Portier@ifremer.fr hanafimelissa@gmail.com

†These authors have contributed equally to this work

Specialty section: *This article was submitted to Deep-Sea Environments and Ecology, a section of the journal Frontiers in Marine Science*

Abstract

Imagery has become a key tool for assessing deep-sea megafaunal biodiversity, historically based on physical sampling using fishing gears. Image datasets provide quantitative and repeatable estimates, small-scale spatial patterns and habitat descriptions. However, taxon identification from images is challenging and often relies on morphotypes without considering a taxonomic framework. Taxon identification is particularly challenging in regions where the fauna is poorly known and/or highly diverse. Furthermore, the efficiency of imagery and physical sampling may vary among habitat types. Here, we compared biodiversity metrics (alpha and gamma diversity, composition) based on physical sampling (dredging and trawling) and towed-camera still images (1) along the upper continental slope of Papua New Guinea (sedimented slope with wood-falls, a canyon and cold seeps), and (2) on the outer slopes of the volcanic islands of Mayotte, dominated by hard bottoms. The comparison was done on selected taxa (Pisces, Crustacea, Echinoidea, and Asteroidea), which are good candidates for identification from images. Taxonomic identification ranks obtained for the images varied among these taxa (e.g., family/order for fishes, genus for echinoderms). At these ranks, imagery provided a higher taxonomic richness for hard-bottom and complex habitats, partially explained by the poor performance of trawling on these rough substrates. For the same reason, the gamma diversity of Pisces and Crustacea was also higher from images, but no difference was observed for echinoderms. On soft bottoms, physical sampling provided higher alpha and gamma diversity for fishes and crustaceans, but these differences tended to decrease for crustaceans identified to the species/morphospecies level from images. Physical sampling and imagery were selective against some taxa (e.g., according to size or behavior), therefore providing different facets of biodiversity. In addition, specimens collected at a larger scale facilitated megafauna identification from images. Based on this complementary approach, we propose a robust methodology for image-based faunal identification relying on a taxonomic framework, from collaborative work with taxonomists. An original outcome of this collaborative work is the creation of identification keys dedicated specifically to *in situ* images and which take into account the state of the taxonomic knowledge for the explored sites.

Keywords: deep-sea megafauna, image-based identification, biodiversity assessment, identification keys, integrative methodology, towed camera, physical sampling

I.1 Introduction

The deep ocean (depths below 200 m) faces increasing threats, ranging from climate change to direct anthropogenic activities, such as fisheries, mining and physical/chemical pollution (Levin and Le Bris, 2015; Levin and Sibuet, 2012; Ramirez-Llodra et al., 2011). Continental margin habitats (e.g., upper sedimentary slopes, seeps and wood-fall-related environments, cold-water corals, canyons, seamounts) are especially at risk to be affected by human activities (Levin and Sibuet, 2012). Such habitats, especially those of the bathyal zone, often display biological or energy/mineral resources; their proximity to the coast and relatively shallow depth compared to abyssal ones, makes them vulnerable to terrestrial pollution and human activities. However, despite the acceleration of technological developments to prospect deep-sea resources through fisheries and mining, their impact on benthic communities is still poorly documented (Bowden et al., 2016). It is therefore urgent to develop conservation and restoration planning for marine biodiversity and habitats, first with an understanding of natural ecosystem variability, at regional and local scales (Da Ros et al., 2019).

Megafauna, which is usually defined as fauna of sufficient size to be seen by eyes from the images (Grassle et al., 1975) or that can be caught by fishing gears such as sledges, dredges and trawls (Clark et al., 2016), plays many key roles in deep-sea habitats. For instance, they can add structural complexity to the habitat, thereby promoting the diversity of associated fauna (Buhl-Mortensen et al., 2010) and/or, through their activity, modify the local environment of other species (Levin, 2005).

However, reliable assessment of the megafauna biodiversity in the deep sea and of the factors contributing to its spatial structuring is challenging. Historically, the megafauna from the deep sea were explored using fishing gears such as sledges, trawls, or dredges. Paradigms depicting the deep ocean as a species-poor and homogeneous environment have been progressively revised with technological developments (Tyler, 2003), revealing multiscale heterogeneity of the deep-sea floor (Danovaro et al., 2014; Ramirez-Llodra et al., 2011).

Physical sampling is indeed needed for assessing the biodiversity of the fauna because accurate taxonomic identification can only be carried out upon morphological and/or molecular examination of the collected specimens. Biodiversity surveys from image data do not need the collection of physical samples; however, taxonomic identification from images

still relies on the current state of knowledge, which is based on physical sampling. The same situation is encountered for biodiversity surveys based on environmental DNA/metabarcoding approach that also requires well-documented genetic reference libraries based on voucher specimens to be fully interpreted (Vieira et al., 2021). Studies comparing diversity metrics obtained via images and collected samples have shown that the latter provide a higher estimation of species richness (Beisiegel et al., 2017; Williams et al., 2015).

Furthermore, occurrence data derived from the identification of physical samples enable large-scale analyses of community structure and have revealed, for example, a temperate-tropical water transition of megafaunal assemblages along a uniform horizontal abiotic gradient (O'Hara et al., 2020) or significant geographical structure of coral species assemblages with longitude and along bathymetric gradients at the scale of the Azores Exclusive Economic Zone (Braga-Henriques et al., 2013). These data also help to answer phylogenetic (Kroh and Smith, 2010; Mah, 2007; O'Hara et al., 2019) and biogeographic studies (McClain et al., 2009) and subsequent conservation questions.

However, finer scale (meter) characterization of species distribution patterns, and structuring factors such as substrate heterogeneity, cannot be straightforward prospected with classical sampling, and require *in situ* habitat observation. In complex topographic habitats particularly, fishing gears alone provide mainly qualitative data and only poor quantitative estimates as reported by Williams et al. (2015) from epibenthic sled and also by Nybakken et al. (1998) in the context of soft bottoms from trawling operations. Moreover, fishing gear performance or capture efficiency can vary according to the type of organism, bottom, or fishing gear (e.g., trawl vs. dredge) and therefore also only provide estimates of true abundance. Although endofauna is well captured by trawling in soft bottoms, fishing gears have been shown to be selective against species attached to hard substrates, such as corals or sponges from an epibenthic sled (Williams et al., 2015) or against some attached soft-bottom cnidarians, such as pennatulids or cerianthids from a trawl (Nybakken et al., 1998) or from an epibenthic sledge (Rice et al., 1982). Recently, a comparative study between imagery tools (ROV and towed camera) and trawling in soft bottoms, also highlighted a selectivity of trawling against some small-sized pennatulids, as well as a higher capture efficiency of mobile fauna, due to the light avoidance of mobile forms toward camera systems (de Mendonça and Metaxas, 2021). In

addition, all these fishing gears can be less effective if their nets become clogged by sediment or biogenic debris before the end of the transect (Rice et al., 1982; Williams et al., 2015).

Since the end of the 1970s and with the advent of submersibles, the growing use of imagery has made it possible to document the biological and abiotic components of the seafloor quantitatively and *in situ* (Durden et al., 2016b). Although imagery only allows the observation of epifauna of sufficient size to be detected from images (Beisiegel et al., 2017; Nybakken et al., 1998; Rice et al., 1982; Williams et al., 2015), it has become a common scientific tool used for documenting seafloor heterogeneity, diversity and spatial patterns of benthic megafauna communities, even at submeter scales (Danovaro et al., 2014). Image-based studies in various environments have revealed that benthic communities are spatially heterogeneous, especially through the presence of habitat-building species that promote beta diversity (variation in species composition among sites, Legendre, 2014). For instance, in cold-water coral gardens (Buhl-Mortensen et al., 2010), or in deep-sea sponge grounds (Beazley et al., 2013). The spatial heterogeneity of benthic communities can also be related to substrate heterogeneity assessed at the scale of meters using sediment size characterization from images (Robert et al., 2014). In the case of marine protected areas, or vulnerable ecosystems as well as for long-term temporal monitoring—imagery is desirable as a minimal disturbance approach (Beisiegel et al., 2017). However, this study also pointed out the necessity of having good prior knowledge of the species composition in the region by collecting the organisms to be identified from images. This is particularly necessary in poorly explored environments for which knowledge of the fauna is very poor.

The examination of morphological characters that allows accurate taxonomic identification of organisms is often limited from images, especially if the aim is to identify organisms at the species level (Henry and Roberts, 2014; Howell et al., 2014). A common approach used in ecology is to delineate morphospecies (or parataxonomic units) to define community assemblages and approximate taxonomic diversity (Krell, 2004). This morphospecies delineation consists in dividing the organisms into biological units based on external morphology without assigning them to scientific names that requires the observation of diagnostic characters generally not visible from images. In poorly known environments, this morphospecies approach may be biased due to an erroneous interpretation of the significance of any morphological polymorphism (i.e., undetected sexual dimorphism, intraspecific

polymorphism, ontogenetic change, cryptic species, etc.). Therefore, this approach likely leads to a biased approximation of taxonomic diversity (Krell, 2004).

The taxonomic literature alone hardly allows the identification of organisms from images because illustrative *in situ* images of organisms are lacking and, when taxonomic-identification keys are available, the diagnostic characters used are often not observable from images. Image-based identification thus requires the use of other resources such as the often sparse literature on the species biology/ecology which give complementary information (depth range, associated species, etc.), or handbooks dedicated to some specific environments (e.g., deep-sea hydrothermal vent fauna) or online catalogs (e.g., NOAA, Atlantic Deep Sea Catalog). However, these resources do not provide taxonomic identification keys applicable for images, and accurate identification remains at relatively high taxonomic level. The construction of identification keys dedicated to image-based identification relies on having a detailed knowledge of the organisms present in the targeted areas. Such taxonomic identification guides have only been recently developed for example for the Antarctic area (Saucède et al., 2020), or for the Northwest Atlantic (Wudrick et al., 2020), two areas where the environment and fauna are well explored.

Deep-sea habitat explorations remain disparate, and have mainly been focused on the Northern Hemisphere while the Southern Hemisphere has remained underexplored (Cunha et al., 2017). Papua New Guinea and Mayotte (northern Mozambique Channel) are two southern regions where high faunal diversity has been reported (Obura, 2012; Pante et al., 2012a). However, to date, the diversity of the deep-sea fauna is still poorly documented. An exploration program, Tropical Deep Sea Benthos (TDSB), led by the French National Natural History Museum (Muséum national d'histoire naturelle ; MNHN) and the French National Research Institute for Sustainable Development (Institut de Recherche pour le Développement ; IRD) established a geographically and taxonomically non-exhaustive inventory in progress, of benthic species in these areas. In 2014, images have been acquired to provide additional information on deep-sea habitats and the structure of biodiversity at small spatial scales. The challenge is therefore to propose an integrative method relying on robust taxonomic data to analyze the structure of communities at local scales in little-known areas with high faunal diversity.

In this context, we first compared the patterns of biodiversity for the megafauna obtained from physical sampling (dredges and trawls) with those based on still images taken by a towed camera, in various bathyal environments: along the sedimentary continental slopes of Papua New Guinea including a cold-seep area and a bay with wood-falls and a canyon, as well as along the outer slopes of Mayotte dominated by a hard-bottom substrate. We addressed the following questions: **(1)** What is the lowest taxonomic rank of identification reached for different taxa from images? **(2)** What biodiversity metrics (alpha and "gamma" diversities, faunistic composition) do these two approaches provide? **(3)** How physical sampling improve image-based identification, especially in areas where the fauna is poorly known and how to use it to formalize photo-taxa identification from images?

I.2 Materials and methods

I.2.1 Study areas and field collection

I.2.1.1 Papua New Guinea: upper sedimented slopes and cold seeps

Papua New Guinea (PNG) lies in the Coral Triangle in the southwest Pacific Ocean, and shows exceptional biological diversity, especially of zooxanthellate coral, accounting for up to 76% of the species known worldwide (Veron et al., 2009). The region is characterized by geological complexity and dynamics (Tregoning et al., 2000), which have resulted in a diversity of habitats, such as vents (Collins et al., 2012; Van Dover, 2012), seeps (Tappin et al., 2001), seamounts, canyons, sedimentary plains, wood-falls and other plant remains (Pante et al., 2012a; Samadi et al., 2015).

Several expeditions, as part of the TDSB program (MNHN/IRD; 2010-2014), explored and discovered new environments in this area, down to about 1,000 m depth. Two of these expeditions [BIOPAPUA (Samadi and Corbari, 2010); PAPUA NIUGINI (Payri et al., 2012)] revealed in particular two chemosynthetic habitats linked to cold seeps off the Sepik River mouth and in the Basamuk Canyon where impact of nickel factory release was evidenced (Pante et al., 2012a; Samadi et al., 2015). High abundance of wood-falls and other plant debris in Astrolabe Bay were revealed as well from samples. The physical sampling of the benthic fauna provided a first glimpse of the species occurring in these areas.

All dredging and trawling operations undertaken respectively in Astrolabe Bay and in the Sepik area during the BIOPAPUA and PAPUA NIUGINI expeditions were integrated in this study to

help with the taxonomic identification from images by providing a baseline of species occurring in the whole Astrolabe Bay or Sepik area. These samples are referred to as surrounding area samples (called "Cl-around"). A total of 25 sites were sampled (**Table I.1**). We use the term "sedimented slopes habitats" to refer to the habitats explored in PNG area.

Table I.1 : Summary of image acquisition and physical sampling efforts with sites information for the dive, sampling along dive (cl-dive) and in the surrounding area (cl-around) in the Astrolabe Bay and Sepik River area (Papua New Guinea)

Area	Dive	Dive transect length analyzed (m)	Images total area (m^2)	Number of analyzed images	Depth (m)
Sepik/cold seeps	Dive06	1,697	2,244	490	431–581
Astrolabe/canyon	Dive13	1,649	1,951	426	931–940
Astrolabe/lower slopes	Dive16	4,187	4,538	991	795–820
Astrolabe/upper slopes	Dive18	3,780	4,534	990	546–587
Area	**Sampling along dive (CL-DIVE)**	**Corresponding dive**	**Sampling transect length (m)**	**Sampling total area (m^2)**	**Depth (m)**
Sepik/cold seeps	CP4040 CP4042	Dive06	3,497	13,989	468–779
Astrolabe/canyon	CP4022	Dive13	2,802	11,207	926–941
Astrolabe/lower sedimented slopes	CP4027	Dive16	3,629	14,514	793–820
Astrolabe/upper sedimented slopes	CP4025	Dive18	2,814	11,258	549–578
Area	**Surrounding area sampling (CL-AROUND)**	**Sampling transect length (m)**	**Sampling total area (m^2)**		
Astrolabe Bay	14 CP	49,063	196,254		
Sepik Bay	11 CP	32,996	131,984		
Total	25 CP	82,059	328,238		

Sampling operations refer to beam trawl (CP). Image acquisition was carried out in April 2014 and sampling operations in September/October 2010 (Biopapua expedition) and December 2012 (Papua Niugini expedition).

Image acquisition was undertaken during the MADEEP expedition (Corbari et al., 2014), on board the R/V Alis on 05 May 2014. Images were acquired along a selection of dredge and trawl transects carried out during past TDSB expeditions (BIOPAPUA, PAPUA NIUGINI). Two sites were visited by camera. The first site is Astrolabe Bay, covering an area of about 514 km^2, and showing topographic gradients from the upper slope (~300 m depth) down to ~1,000 m depth. The bay is divided by a canyon, which is 100-600 m deeper than the adjacent slope. A total of eight camera transects (called "Dives") were carried out in Astrolabe Bay along previous trawl or dredge transects (called "Cl-dives") and three were selected for this study: Dive18, Dive16 and Dive13 because they are representative of each habitat (upper slope, intermediate slope and canyon). Each transect was about 4 km. From image observations, Dive18 and Dive16 were mainly composed of soft sediment and wood-falls or plant debris, and Dive13 showed a mix between soft sediment and the presence of large cobbles. The second site is Broken Bay, off the Sepik River mouth, where cold-seep fauna, Bathymodiolinae mussels and Siboglinidae tubeworms had previously been sampled at 450 m depth (Samadi et

al., 2015). Here, we call this area the Sepik area. Dive06 was located along two trawl transects in this area (**Figure I.1**, **Table I.1**).

Summary of image acquisition and physical sampling efforts with sites information for the dive, sampling along dive (cl-dive) and in the surrounding area (cl-around) in the Astrolabe Bay and Sepik River area (Papua New Guinea)

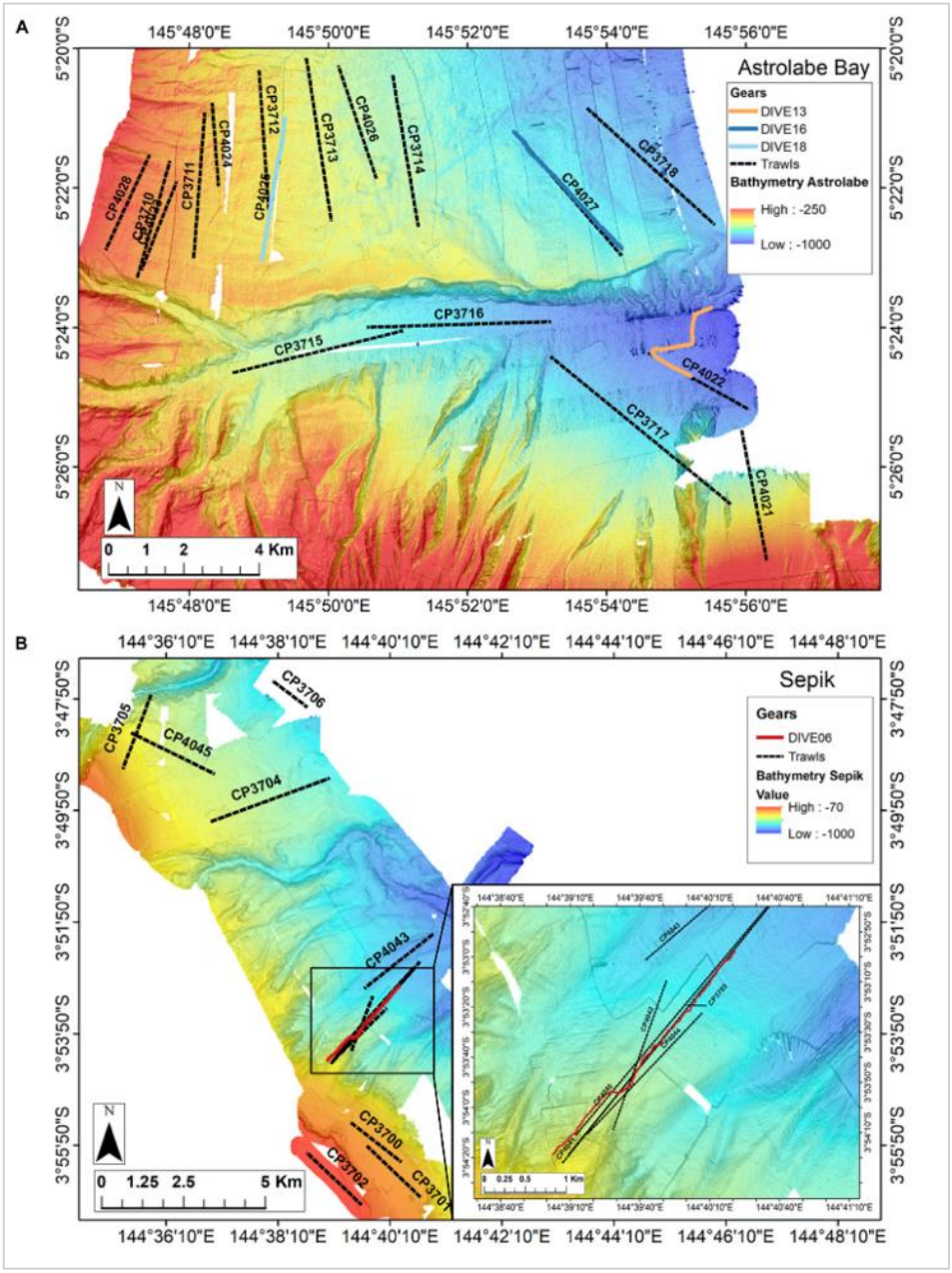

Figure I.1 : Location of the camera transects and dredge/trawl transects operations (dive, sampling along dive and in the surrounding area): Panel **(A)** in the Astrolabe Bay and panel **(B)** in the Sepik River area (Broken Water Bay). Colored lines represent camera transects, black dotted lines represent dredging (DW) and trawling (CP) operations

I.2.1.2 Mayotte: volcanic island outer slopes dominated by hard bottoms

Mayotte is located in the northern Mozambique Channel, between Madagascar and the Mozambique coast in the West Indian Ocean. It is part of the Comoros archipelago, and is surrounded by a barrier reef that hosts a large lagoon (1,100 km^2) (Audru et al., 2006), which is part of the Mayotte Marine Natural Park. Mayotte islands are crisscrossed by numerous faults, due to post-eruptive volcanic activities (Audru et al., 2006). The outer slopes range from 4 to 20° in inclination (up to 88° on some western flanks) and extend to 1,000 m depth from the barrier reef in the north and east and connect to the abyssal plain through two plateaus in the south and west. The slopes are characterized by geomorphological and substrate complexity, composed of a network of canyons surrounding the all islands, plateaus, cliffs, volcanic cones and of rugged areas (Audru et al., 2006) and provide a supplementary interesting study case for our comparison.

The northern part of the Mozambique Channel is also considered as a hotspot of biodiversity, after the Coral Triangle in the southwest Pacific Ocean, from its exceptional coral reef diversity (Obura et al., 2012). However, little is known regarding the non-reef environments, especially the deep-sea habitats.

Past expeditions of the TDSB program have provided knowledge of the species occurring in the region, with sampling carried out along the Mozambique Coast (MAINBAZA, Bouchet and Ramos, 2009), the Northwest and South Madagascar coast (MIRIKY, Bouchet, 2009) and (ATIMO VATAE, Bouchet et al., 2010) respectively. IFREMER expeditions provided additional data on the central part of the Mozambique Channel (PAMELA-MOZ01, Olu, 2014); PAMELA-MOZ04, Jouet and Deville, 2015). However, biodiversity data on the Comoros archipelago are scarce, with only one dedicated expedition in this area (BENTHEDI, Thomassin, 1977) and with sampling gears deployed down to 3,700 m. Details of the MNHN and BENTHEDI expeditions can be found on BaseExp database (Muséum national d'Histoire naturelle, 2019)[1].

Images were acquired during the BIOMAGLO expedition (Corbari et al., 2017), on board the R/V *Antea* on 21 January 2017 in the Mayotte-Glorieuses area. Three slope orientations were explored by camera: (1) the northwestern slopes characterized by a plateau at 600 m depth and covering 100 km^2 then surrounded by deeper crater-like or volcanoes network features;

[1] https://expeditions.mnhn.fr/?lang=en_US

(2) the southwestern slopes with a deeper and larger plateau at 750 m covering 250 km^2 and (3) the eastern slopes, extending continuously down to 1,000 m depth and characterized by shallower volcanic cones (Audru et al., 2006).

A total of five camera transects were carried out and three were selected for this study (Dive01, Dive03, Dive05) (**Figure I.2**), as they provide similar sampling and image acquisition effort, and include a substrate gradient from Dive01 (soft bottom) to Dive05 (hard and heterogeneous bottom), to assess the influence of bottom type.

Dive01 and Dive03 cross a relatively homogeneous bathymetric gradient around 600-700 m and 450-500 m depth, respectively, along the plateaus, and both ending at the mouth of a deeper channel (880 and 1,100 m respectively). Dive01 is mainly composed of soft substrate with sparse blocks or peaks and Dive03 shows an intermediate area of soft sediment and others with large rocky blocks (~1 m size). Dive05 presents a larger and continuous bathymetric gradient from 500 m down to 1,130 m depth, ending with a passage on a volcanic cone. The area is mainly composed of carbonate and volcanic hard bottoms and is characterized by a very heterogeneous seafloor (gravels, pebbles, cobbles, boulders, blocks, and rugged areas, etc.).

Images were acquired before undertaking co-located dredge and trawl transects (Cl-dives). Each dive included more than one co-located sampling; thus, the different dredge and trawl transects undertaken along each of the three camera transect positions were pooled for comparisons of diversity. A total of three dives and 10 dredge/trawl transects were analyzed (**Table I.2**). Each transect was about 9 km long. Similar to the PNG area, all the 73 sampling catches undertaken during the BIOMAGLO expedition (i.e., all around Mayotte area and the other explored Comoros islands including Glorieuses islands, Moheli, Geyzer Bank) were included in the comparison and referred to as surrounding area samples (Cl-around) (**Table I.2**). These samplings helped the identification from images by providing a baseline of species occurring in the area. Moreover, we also used species baseline knowledge provided by past expeditions undertaken along the Mozambique Channel to help with the identification.

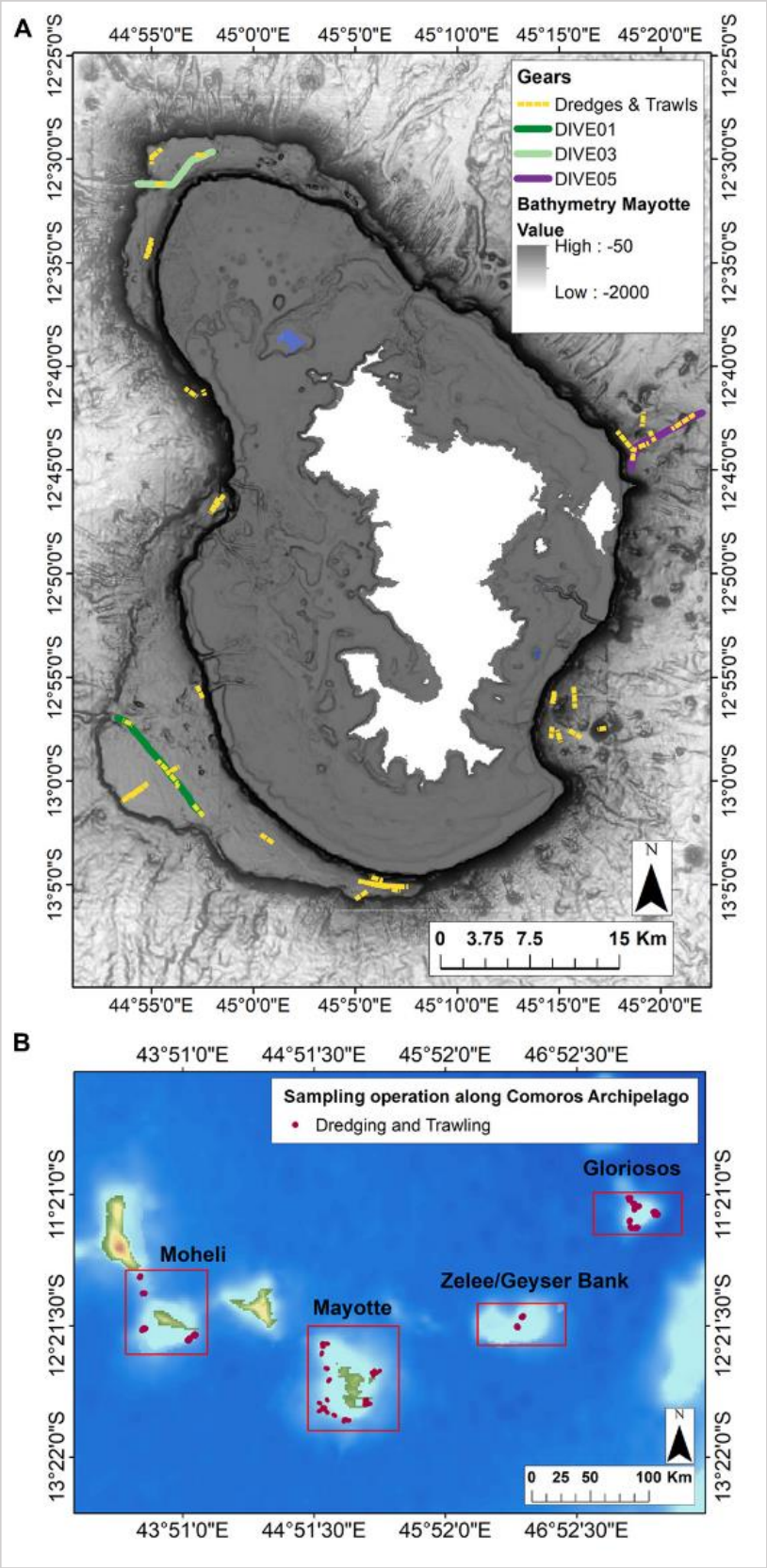

Figure I.2 : (A) Location of the camera transects and dredge/trawl transects operations (dive, sampling along dive and in the surrounding area) undertaken along the outer slopes of Mayotte. **(B)** Location of the sampling in the surrounding area undertaken in the Comores Archipelago (Moheli, Geyzer Bank, Glorieuses). Solid lines represent camera transects and yellow dotted lines represent dredging (DW) and trawling (CP) operations

Table I.2 : Summary of image acquisition and physical sampling efforts with sites information for the dive, sampling along dive (cl-dive) and in the surrounding area (cl-around) along volcanic island slopes of Mayotte

Area	Dive	Dive transect length analyzed (m)	Images total area (m^2)	Number of analyzed images	Depth (m)
Southwest slope/soft-bottom area	Dive01	10,456	4,122	900	545–900
Northwest slopes/mix substrate	Dive03	7,408	5,043	1,101	433–1,200
East slopes/hard-bottom area	Dive05	8,125	4,296	938	460–1,100
Area	**Sampling along dive (CL-DIVE)**	**Corresponding dive**	**Sampling transect length (m)**	**Sampling total area (m^2)**	**Depth (m)**
Southwest slope/soft-bottom area	**CL-DIVE01** (DW4850 CP4852 DW4851 DW4853 CP4858)	Dive01	5,063	10,495	664–864
Northwest slopes/mix substrate	**CL-DIVE03** (DW4860 DW4861)	Dive03	1,928	1,928	486–646
East slopes/hard-bottom area	**CL-DIVE05** (DW4871 DW4872 DW4873)	Dive05	4,467	4,467	486–795
Area	**Surrounding area sampling (CL-AROUND)**	**Sampling transect length (m)**	**Sampling total area (m^2)**		
Around Mayotte island	11 CP/21 DW	44,995	110,481		
Others Comoros Islands	5 CP/36 DW	54,335	88,897		

Sampling operations refer to Warén dredge (DW) and beam trawl (CP). Image and sampling acquisition were carried out in late January/early February 2017.

I.2.2 Physical sampling gears and towed camera

Physical sampling was carried out along 1-2 km transects using a Warén dredge of 1 m width with a fine 3-5 mm mesh size and a large and more robust 20-50 mm mesh size, deployed for hard substrate; and using a beam trawl of 4 m width, with a fine mesh (15-12 mm) deployed for soft sediment. On board, the sampling strategy aimed to maximize the number of taxa sampled. These two fishing gears have different selectivity for the different fauna components (for example, mobile and epibenthic fauna are generally better sampled with trawls than dredges). However, the topography does not always allow deploying both sampling gears.

Camera transects were carried out with a towed camera (SCAMPI, French Oceanographic Fleet), at 2.5-3 m above seafloor at 0.5 m/s. Images were acquired at 10 s intervals (PNG) and 30 s intervals (Mayotte) with an HD Camera (NIXON D700, focal length 18 mm, resolution 4,256 × 2,832 pixels) and geo-referenced using the ship positioning system processed with ADELIE tools (French Oceanographic Fleet) developed at IFREMER and implemented using ArcGiS software V10.3.

The detection of organisms either from the observation in images or from capture by the fishing gears, reflects the respective efficiency of the cameras and the gears rather than the exact occurrence of the organisms at a given place. Indeed, some organisms may have been

missed because the images are not overlapping. Similarly the probability of capture by the fishing gears may vary according to the topography and/or the nature of the substrate.

I.2.3 Taxonomic processing

I.2.3.1 Specimen identification

On board, all dredge and trawl catches were sorted at high taxonomic level and some taxa were photographed to record color patterns before being preserved in ethanol. Photographs were also obtained of preserved specimens stored in the MNHN collections[2]. These photos were used to build catalogs of taxa sampled in the area. Faunal samples were sent to an international network of taxonomists for processing and taxon identification. Taxon identification workshop sessions organized with taxonomists to study these collections stimulated discussions to determine the limits of identification from images for each taxonomic group.

I.2.3.2 Identifications from Images

A total of 7,674 images were analyzed and annotated (i.e., organism delineation in images and labelling of taxonomic ranks) using the web platform BIIGLE 2.0 (Benthic Image Indexing and Graphical Labelling Environment) (Langenkämper et al., 2017). BIIGLE 2.0 was chosen because it provides effective methods (1) allowing collaborative and interactive work with taxonomists who can actively contribute to the identification of organisms from images and (2) allowing easy comparisons and revisions of annotations with the LARGO tool. The platform allows the export of a database with observation records of each faunal annotation. We then summed up these observations to obtain an abundance matrix for each georeferenced image.

Megafaunal identification from images consisted of five steps divided into three main processes that involve different levels of expertise: non-expert annotation, objective identification and contextual identification, the last two performed in collaboration with taxonomists (**Figure I.3** and corresponding details on the working steps in **Supplementary material I.1**). Finally, identification keys adapted to images were produced for Decapoda, Asteroidea (**Supplementary material I.2**, **Supplementary material I.3**) and Echinoidea[3].

[2] https://science.mnhn.fr/institution/mnhn/item/search/form?expedition=BIOMAGLO&image=on&lang=en_US
[3] https://mozechinoids-deepsea-scampi.identificationkey.org

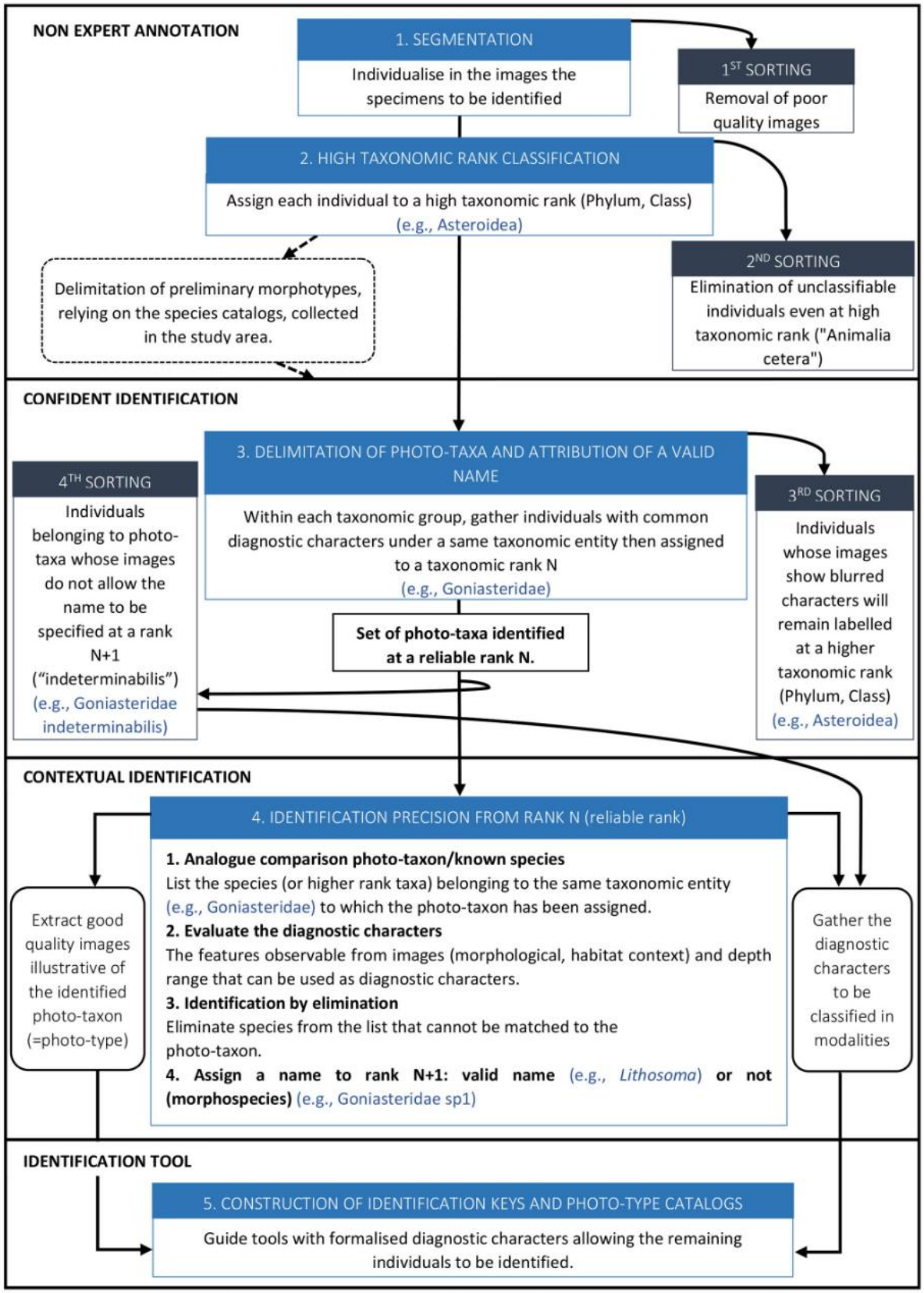

Figure I.3 : Flowchart of faunal identification steps from images. Five steps – from image annotation to construction of identification keys – divided into three main processes that involve different levels of expertise: non-expert annotation, confident identification and contextual identification

I.2.4 Final dataset processing

After exporting the matrix of specimen observations from each georeferenced image of the BIIGLE platform, hierarchical taxonomic labels were homogenized between physical sample and image datasets according to the taxonomic hierarchy provided by the Worlds Register of Marine Species (WoRMS) database. Contrary to physical sampling, images can provide abundance data. Thus, to compare biodiversity patterns between images and physical samples along dives and in the surrounding area, we transformed the abundance data from image analysis into presence/absence data for each image. For easier naming convention, we will refer to the term Pisces for Osteichthyes/Chondrichthyes groups.

Diversity metrics were used: alpha diversity corresponding to the intra-transect diversity that was analyzed at the different levels of identification reached in the images, which were generally not the species level. Thus, for images, alpha diversity generally does not represent the species diversity and is represented by taxonomic richness. Beta diversity cannot be compared between images and physical samples because we could not assess this diversity from trawls or dredges (data integrated across the whole transect). For the sedimented slopes area, the regional scale ("gamma" diversity) corresponds to the pooling of the four dives and the four co-located trawl transects, respectively, of Astrolabe Bay and the Sepik area. For the Mayotte slopes area, the "gamma" diversity corresponds to the pooling of the three dives and the 10 co-located dredge/trawl transects, respectively.

I.2.5 Statistical analyses

All analyses were performed using the R environment (V3.6.3) (R Core Team, 2020). Taxonomic richness comparison between camera transects and co-located sampling was assessed at different taxonomic levels using sample-based rarefaction curves with 999 random permutations on presence/absence data using the 'vegan' package (*specaccum()* function) (Oksanen et al., 2019).

Differences in assemblage composition between camera transects and co-located sampling were assessed using principal component analysis (PCA) on Hellinger-transformed presence/absence data with the 'ade4' package (*dudi.pca()* function) (Dray and Dufour, 2007). This transformation allows the species presence/absence dataset to be represented in a Euclidean space (Legendre and Gallagher, 2001). For crustaceans, PCA and Venn analyses were

performed at the genus rank only, to consider comparative taxonomic names between image and sampling datasets (i.e., at a specific rank of comparison, morphospecies names in the image dataset do not match the species name in the sampling dataset).

Similarities and dissimilarities in taxonomic composition between images and physical samples and according to the image acquisition and physical sampling efforts (camera transects, colocated dredge/trawl transects and surrounding area transects) were represented in Venn diagram using the 'gplots' package (*venn()* function) (Warnes et al., 2020).

I.3 Results

I.3.1 Biodiversity pattern compared between images and physical samples

I.3.1.1 Taxonomic levels and community composition

For sedimented slopes we were able to reach an identification level above class for both images and physical samples mainly for Pisces (Chordata) and Crustacea (Arthropoda). The taxonomic ranks we reached ranged from order to family for fishes, and from genus to species/morphospecies for crustaceans (**Table I.3A**). These two taxonomic groups were also well represented both in the images and physical samples along volcanic island slopes, at the same taxonomic ranks respectively (**Table I.3B**). The high proportion of Annelida (93%) and Mollusca (49%) we identified to the family level in the images of the Sepik cold-seep area reflect respectively the dominance of Siboglinidae and Bathymodiolinae. Along the volcanic island slopes, the proportion of mollusks we identified to the class level (97%) reflects the dominance of Gastropoda, abundantly observed in images. However, the small individual size did not allow us to identify them beyond the rank of class from images, whereas we identified the collected specimens to the genus rank (27%). Animalia cetera identifications, fauna observed in images that were unclassifiable into phyla, represent 17% (1669 ind.) of the total fauna in the PNG area and 5% (783 ind.) in Mayotte.

On the sedimented slopes, we abundantly observed cnidarians (mainly composed of actinids, cerianthids and pennatulids) in images; however, our identifications remained limited to the class level (40%) and never exceeded the order (39%). In the physical samples, we collected few cnidarian individuals, mainly identified as pennatulids. In the time of this study, we were only able to identify them to the order (**Table I.3A**).

Table I.3 : Percentages of individuals identified by taxonomic rank and by method (images = dive, sampling along dive = cl-dive), **(A)** along sedimented slopes (PNG) and **(B)** along volcanic island slopes dominated by hard bottom (Mayotte) with **(C)** a focus on echinoids and asteroids

(A) Sedimented slopes (PNG)

TAXA	ANNELIDA		ARTHROPODA		CHORDATA		CNIDARIA		ECHINODERMATA		MOLLUSCA	
Taxonomic rank	DIVE	CL-DIVE	DIVE	CL-DIVE	DIVE	CL-DIVE	DIVE	CL-DIVE	DIVE	CL-DIVE	DIVE	CL-DIVE
Phylum	7	–	–	–	2	–	21	–	–	–	2	–
Class	–	–	70	1	32	–	40	–	86	–	41	–
Order	–	–	7	–	18	–	39	100	14	–	8	–
Family	93	70	2	10	48	3	–	–	–	–	49	10
Genus	–	30	20	15	–	27	–	–	–	–	–	76
Species	–	–	1	74	–	70	–	–	–	–	–	14
Morphospecies	20	–	12	–	–	3	–	–	–	–	–	–
Total individuals (n)	289	471	4,677	242	432	30	677	8	2,417	–	925	351

(B) Volcanic island slopes (Mayotte)

TAXA	ARTHROPODA		CHORDATA		CNIDARIA		ECHINODERMATA		MOLLUSCA		PORIFERA	
Taxonomic rank	DIVE	CL-DIVE	DIVE	CL-DIVE	DIVE	CL-DIVE	DIVE	CL-DIVE	DIVE	CL-DIVE	DIVE	CL-DIVE
Phylum	–	–	–	13	34	–	–	–	–	–	51	59
Class	5	11	52	–	–	4	38	7	97	–	39	8
Order	49	5	24	6	45	–	14	–	–	–	–	–
Family	18	33	19	–	13	36	7	7	3	71	1	–
Genus	23	14	4	50	7	52	41	37	–	27	2	25
Species	5	37	1	31	1	8	<<1	49	–	2	7	8
Morphospecies	13	–	13	6	–	–	4	–	2	–	1	–
Total individuals (n)	535	116	688	16	6,004	25	1,070	57	3,501	59	2,773	12

(C) Volcanic island slopes (focus on echinoderms)

ECHINODERMATA	ECHINOIDEA		ASTEROIDEA	
Taxonomic rank	DIVE	CL-DIVE	DIVE	CL-DIVE
Class	4	10	55	–
Order	1	–	7	–
Family	7	–	18	7
Genus	88	28	17	72
Species	–	62	3	21
Morphospecies	7	–	4	
Total individuals (n)	452	40	243	14

Morphospecies proportion is not included in the total proportion summed from phylum to species as it cannot be referred to any specific level.

Along the volcanic island slopes, we observed many cnidarians and poriferans in images. However, we reached identification only to high taxonomic ranks (i.e., phylum and class for Porifera and order for Cnidaria). The diversity of these two groups was thus underestimated. For individuals sampled using dredges or trawls the specialists involved in the study generally identified them to the genus rank. Consequently, compared with images, diversity appeared higher for physical captures (**Table I.3B**). For these taxonomic groups, the morphological characters required for identification are mainly microscopic and therefore cannot be observed from images.

We observed few asteroids along the sedimented slopes habitat, and the total of 2,417 observed Echinodermata individuals reflected the dominance of only one morphotype of

semi-burying spatangoid echinoid, considering most of them were visible (**Table I.3A**). Along the volcanic island slopes, we identified a higher number of echinoderm taxa either from specimens observed in images or from specimens collected by the sampling gears. For asteroids and echinoids identification from images, we reached the genus rank for most individuals (**Table I.3C**).

For comparing the level of diversity estimated from images and from physical samples, in sedimented slopes and volcanic island slopes datasets, we selected the order and family ranks for fishes, and the genus and species/morphospecies ranks for crustaceans. We made the comparisons at the genus rank in hard-bottom environments for asteroids and echinoids, because we generally reached these levels of identification both for specimens observed in images and for specimens collected by the sampling gears. The inventory for each targeted taxon and taxonomic level, in the images and physical samples, are listed in **Supplementary material I.4** and raw databases used for analyses are available in **Supplementary material I.5** (PNG) and **Supplementary material I.6** (Mayotte). For each percentage of individuals in **Table I.3**, the corresponding number of taxa identified at each taxonomic rank are available in **Supplementary material I.7**.

I.3.1.2 Pisces

We evaluated the richness of Pisces orders in the sedimented slopes habitats of PNG, as two-fold higher in images than in physical samples while we estimated it as equivalent at the family level (**Figure I.4A**). Conversely, for the canyon site (Dive13), we estimated that the richness of orders and families was lower from images than from physical samples.

In volcanic island habitats of Mayotte, we estimated the Pisces order richness at least two-fold higher in images than in physical samples for both families and orders levels (**Figure I.4B**). In the sedimented slopes habitats, we found the compositions of fish families in the physical samples and in the images similar for two sites (Dive06, Dive16), but unalike for the two others (**Figure I.5A**), with some families only sampled by trawls within the canyon and sedimented slope sites (Cl-dive13, Cl-dive18).

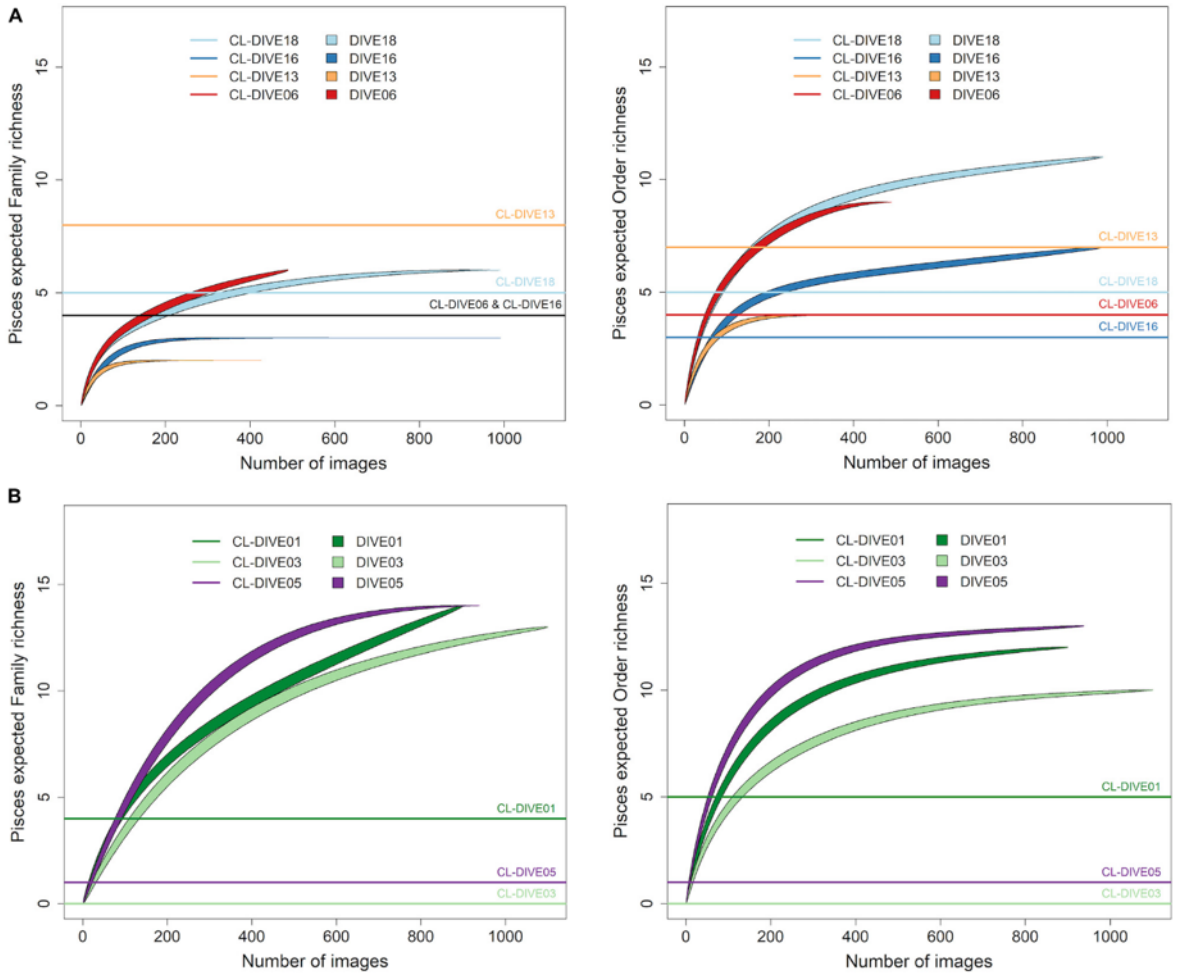

Figure I.4 : Expected richness from rarefaction curves for Pisces at order and family ranks (exact method, n = 999 permutations), along **(A)** sedimented slope habitats (PNG) and **(B)** volcanic island slopes (Mayotte). Comparison between imagery (dive) and sampling along dive (cl-dive)

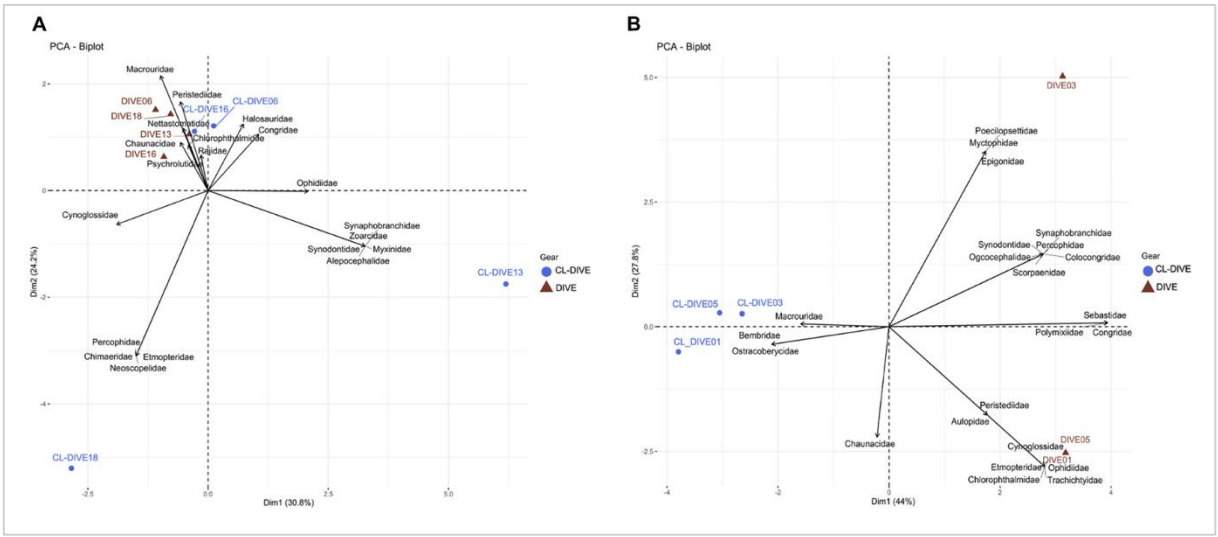

Figure I.5 : Comparison of fish assemblages between imagery (dive) and sampling along dive (cl-dive) along **(A)** sedimented slope habitats (PNG) (55% of variance on first two PCs) and **(B)** volcanic island slopes (Mayotte) (71.8% of variance on first two PCs). Principal Component Analysis (PCA) of Hellinger-transformed presence/absence fish data at family rank

On the contrary, in volcanic island areas, the dredges and trawls sampled a few families not, or poorly observed in images (Macrouridae) (**Figure I.5B**). In the case of Bembridae and Ostracoberycidae (Perciformes), identification of specimens observed in images was possible only to the order level. However, images allowed us to observe many families that were not sampled by the fishing gears.

In sedimented slopes habitats, by pooling the four camera transects (dives) and the four trawl transects (cl-dives) respectively, we confirmed that the estimated diversity of fish families was higher from physical sampling than from observation in images (**Figure I.6A**). Moreover, taking into account the surrounding area samples (cl-around) we considerably increased the family richness, and also added a few orders. These samples helped us to identify one additional order and two families from the images, which were not collected in the co-located samples. Inversely, on volcanic island slopes, the family diversity and the order diversity, estimated from the observations in images pooled from the camera transects was higher than from the pool of specimens from the trawl transects (**Figure I.6B**). The benefit of the surrounding area samples for taxon identification using images was more pronounced on volcanic island slopes, with 13 additional families and 6 additional orders identified from images (**Figure I.6B**).

I.3.1.3 Crustacea

In the sedimented slopes habitats of PNG, we estimated the genus richness of crustaceans higher in physical sampling than in images (Dive18, Dive13) or equivalent (Dive06, Dive16). At the species level (including morphospecies), we estimated the same richness patterns except for two sites (Dive18, Dive06), where we estimated the richness higher from images than sampling (**Figure I.7A**). In volcanic island habitats of Mayotte, we estimated the genus richness as higher in the physical sampling than in the images and the species richness as equivalent, in the soft-bottom-dominated site (Dive01). Inversely, in the two hard-bottom-dominated sites (Dive03, dive05) and at both taxonomic levels, we estimated the richness higher from images (**Figure I.7B**).

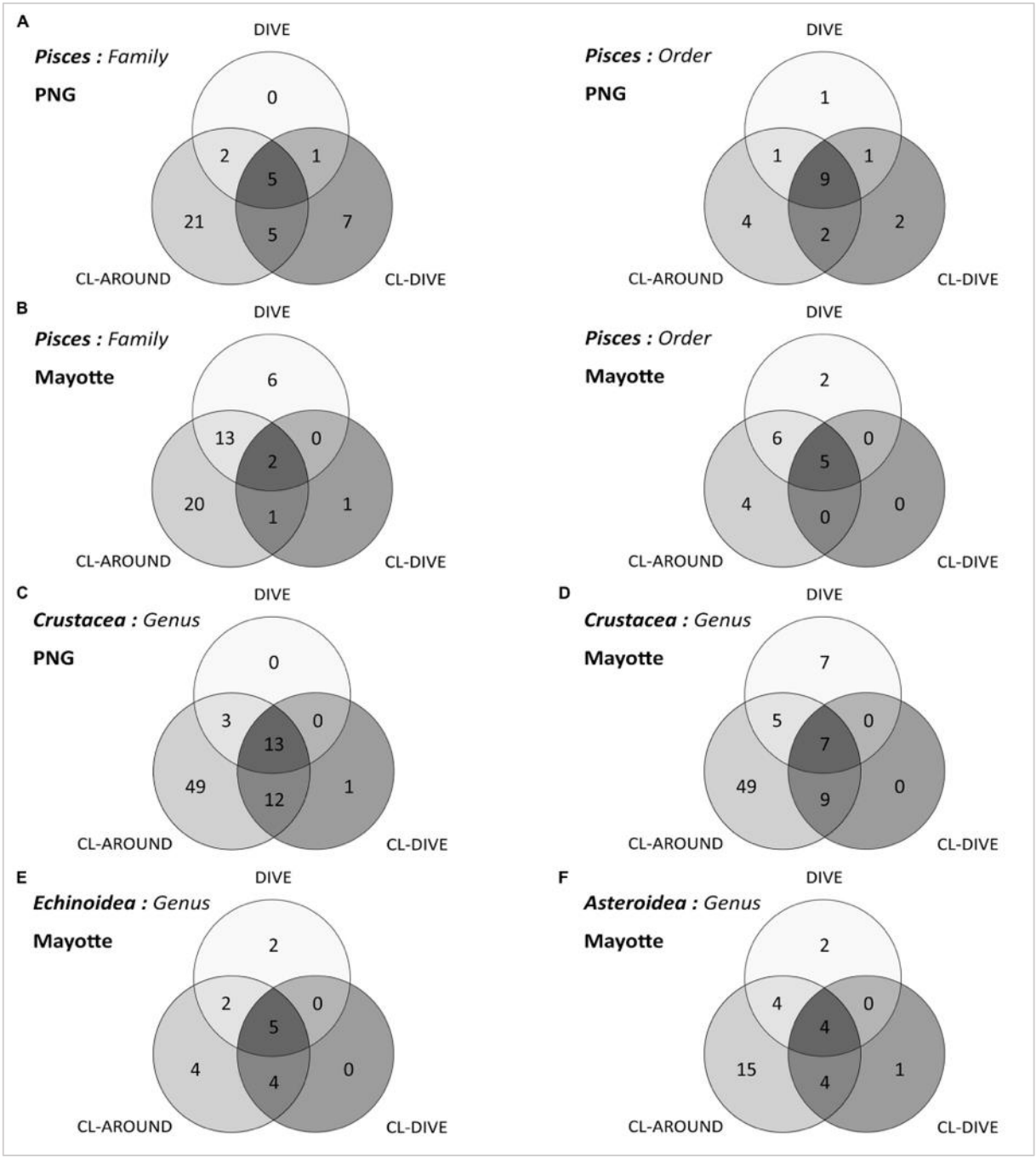

Figure I.6 : Venn diagrams of taxonomic richness captured and identified from images (dive), sampling along dive (cl-dive) and in the surrounding area (cl-around): **(A)** Pisces at order and family ranks along sedimented slope habitats (PNG) and **(B)** along volcanic island slopes (Mayotte); **(C)** Crustacea at genus rank in PNG and **(D)** in Mayotte; **(E)** Echinoidea at genus rank in Mayotte; **(F)** Asteroidea at genus rank in Mayotte. In each circle the sum of numbers represents a taxonomic rank captured (e.g., number of order or family, etc.)

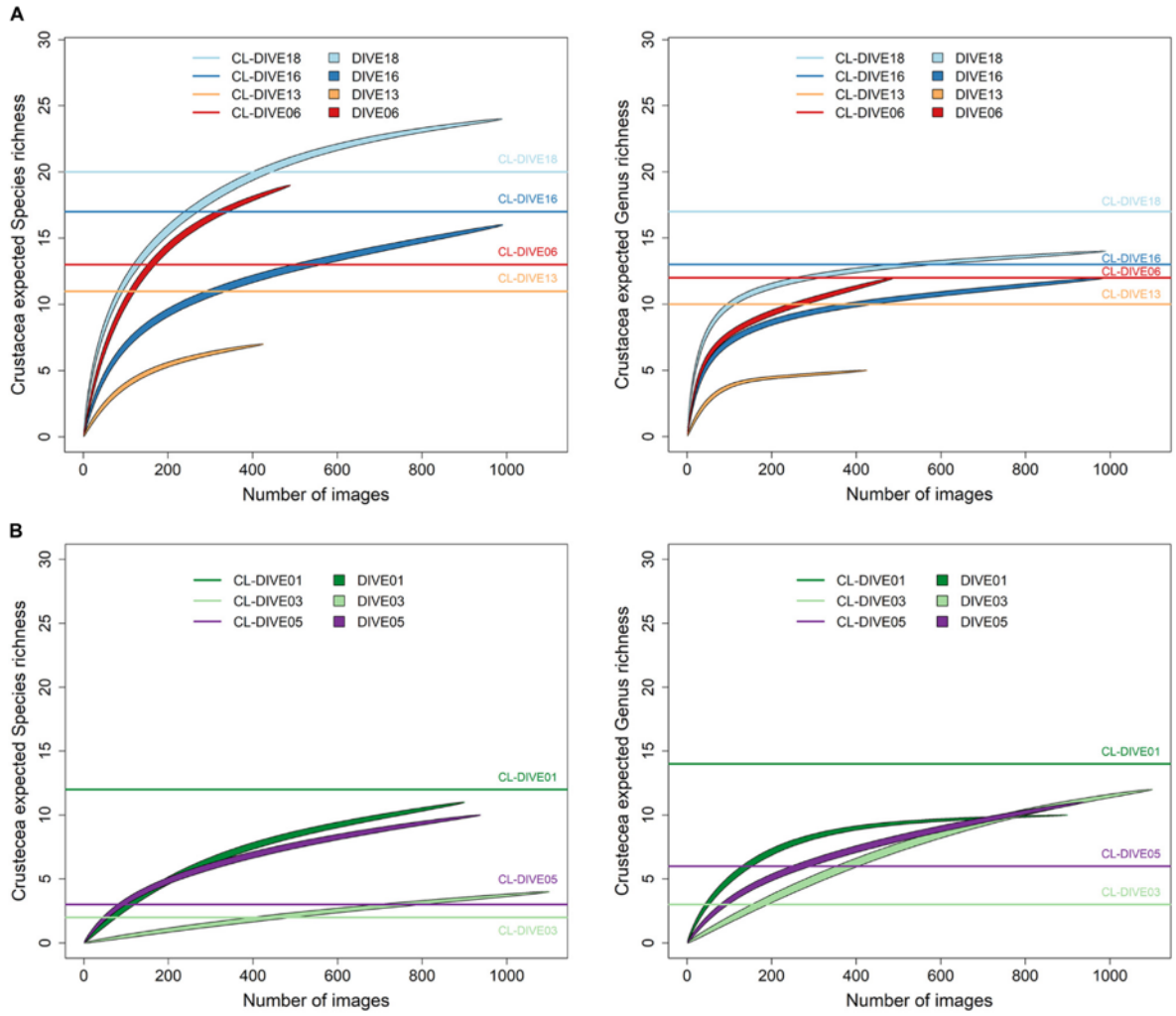

Figure I.7 : Expected richness from rarefaction curves on Crustacea at genus and species ranks (exact method, n = 999 permutations), along **(A)** sedimented slope habitats (PNG) and **(B)** volcanic island slopes (Mayotte). Comparison between imagery (dive) and sampling along dive (cl-dive)

Small-sized and endogenous crustacean genera were captured more easily with trawls than observed in images (e.g., *Ethusa, Lepas*, *Bathycheles*, *Stereomastis*) along the sedimented slopes of PNG (**Figure I.8A**). Inversely, we repeatedly observed four genera in images that were poorly sampled with trawls (e.g., *Xylocheles*, *Haliporoides*, *Agononida*, *Galacantha*) (**Figure I.8A**). We observed common genera in images (*Nematocarcinus*, *Glyphocrangon*, *Haliporoides*, *Hymenopenaeus*), whereas we identified a higher diversity of genera from trawl samples. Selectivity appeared more pronounced between the camera and trawl transects along the volcanic island slopes of Mayotte (**Figure I.8B**). We identified galatheids of small-size or associated with biogenic habitat and woods exclusively from specimens captured by trawls (*Uroptychus*, *Munidopsis*, *Paramunida*), whereas we identified large-sized crabs (*Brachyura*) exclusively from observation of the images from the Dive03 (e.g., *Beuroisia*,

Cyrtomaia, *Gornodopsis*). The images allowed us to identify more genera while dredge/trawl transects showed more similar genus compositions (**Figure I.8B**). Therefore, we estimated a higher gamma diversity of crustacean genera from physical samples than from observation in images on sedimented slopes habitats, and conversely in hard-bottom habitats.

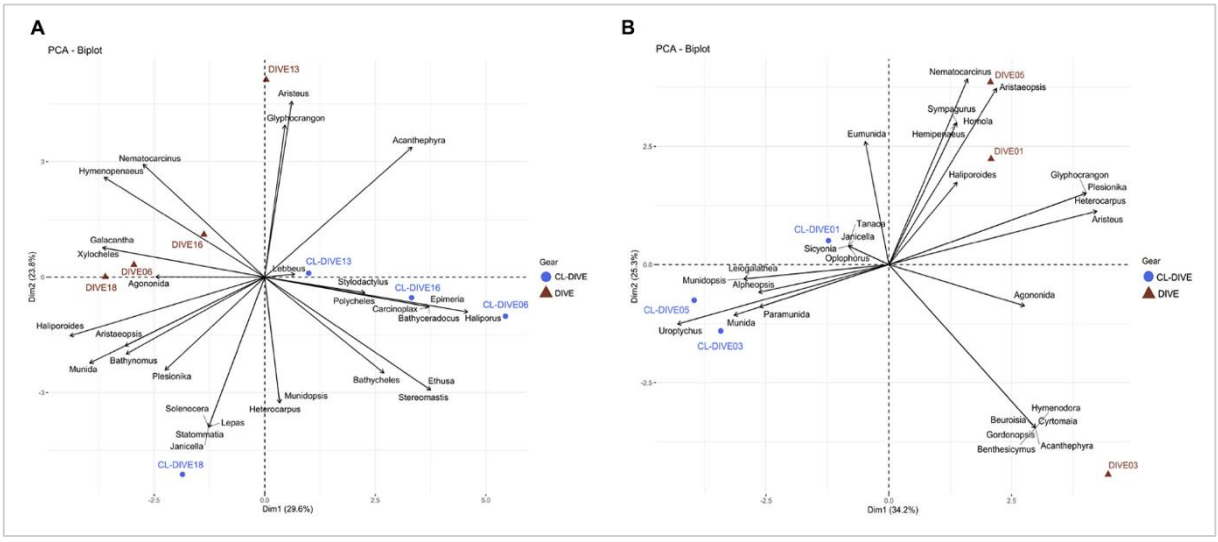

Figure I.8 : Comparison of crustacean assemblages between imagery (dive) and sampling along dive (cl-dive) along **(A)** sedimented slope habitats (PNG) (53.4% of variance on first two PCs) and **(B)** volcanic island slopes (Mayotte) (59.5% of variance on first two PCs). Principal Component Analysis (PCA) of Hellinger-transformed presence/absence crustacean data at genus rank

The sampling from the surrounding area (cl-around) allowed us to identify 49 additional genera in both habitats (**Figure I.6C-D**); supplementing the regional diversity inventory, insufficiently described with the camera transect and co-located sampling. These surrounding samples enabled the identification of three and five additional crustacean genera in images respectively on soft sediment slopes and volcanic island slopes.

I.3.1.4 Echinoidea

We estimated the Echinoid genus richness (from rarefaction curves not shown) as equivalent from images and physical sampling in the soft-bottom-dominated site (Dive01) but higher from images than from physical sampling in the two hard-bottom-dominated sites (Dive03, Dive05).

Some genera were well sampled in physical samples, particularly the small-sized echinoids (*Echinocyamus* and *Podocidaris*) and some cidarid genera (*Stereocidaris*, *Goniocidaris*, *Histocidaris*). In contrast, we better observed and identified from images spatangoid echinoids (*Spatangus* and *Echinolampas*) and the very fragile, regular echinoid *Aspidodiadema*. We

estimated a higher diversity of Cidaridae genera from physical sampling than from observation in images (**Figure I.9**), but we observed the genera *Stereocidaris* and *Stylocidaris* (Cidaridae) only from images. From the pooled camera transect (dives) and the pooled co-located sampling (cl-dives), respectively, we observed equal values of genus diversity between the two methods (9 genera) (**Figure I.6E**). The surrounding area sampling allowed us to identify four additional genera (**Figure I.6E**) that in turn allowed the identification of two additional genera from images (*Stylocidaris*, *Aspidodiadema*).

I.3.1.5 Asteroidea

As for echinoids, we estimated (from rarefaction curves not shown) a higher richness of asteroid genera from physical sampling than from observation in images in the soft-bottom-dominated site (Dive01) and conversely in the two hard-bottom-dominated sites. Besides, no asteroid was recovered from the sampling operations along the Dive03.

Asteroids genus composition between images and physical samples were different. We identified six genera exclusively from observation in images (*Lithosoma*, *Paranepanthia*, *Tremaster*, *Anthenoides*, *Sphaeriodiscus*, *Astroceramus*), and five genera exclusively in the physical samples (*Allostichaster*, *Tamaria*, *Mediaster*, *Persephonaster* and *Tritonaster*). However, we observed a more similar genus composition between images and physical samples in the soft-bottom-dominated slope (Dive01) (i.e., *Plinthaster*, *Henricia*, *Cheiraster*) than for the other two hard-bottom-dominated volcanic slopes (**Figure I.10**). Furthermore, we also observed *Henricia* and *Cheiraster* in images of the Dive03 and Dive05, but these genera were not captured in their co-located sampling operations (Cl-dive03 and Cl-dive05).

When pooling respectively camera transects (dives) and dredge/trawls transects (cl-dives), we estimated an equivalent diversity at the genus rank from observation in images and from identification of specimens from physical samples (**Figure I.6F**). However, we identified two families only from images (Myxasteridae and Solastereidae), but because of the lack of diagnostic characters visible in images we were not able to identify them at the genus level. Consequently, we underestimated the genus diversity from images. The surrounding area sampling (cl-around) allowed us to identify 15 supplementary genera, that in turn allowed the identification of four additional genera from images.

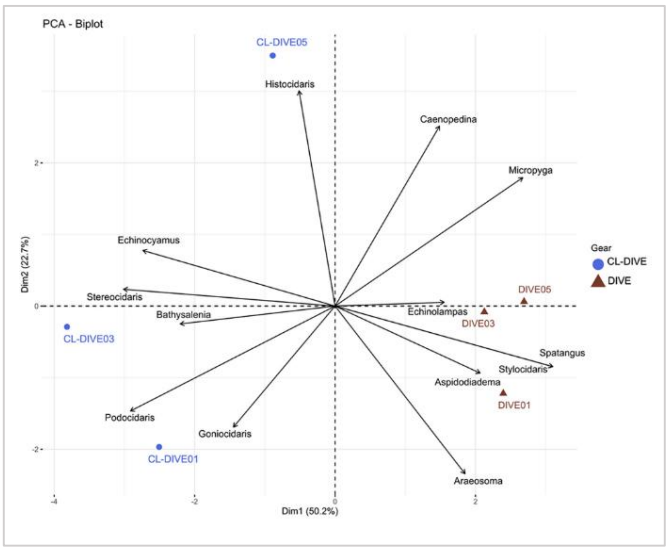

Figure I.9 : Comparison of echinoid assemblages between imagery (dive) and sampling along dive (cl-dive) along volcanic island slopes (Mayotte) (72.9% of variance on first two PCs). Principal Component Analysis (PCA) of Hellinger-transformed presence/absence echinoid data at genus rank

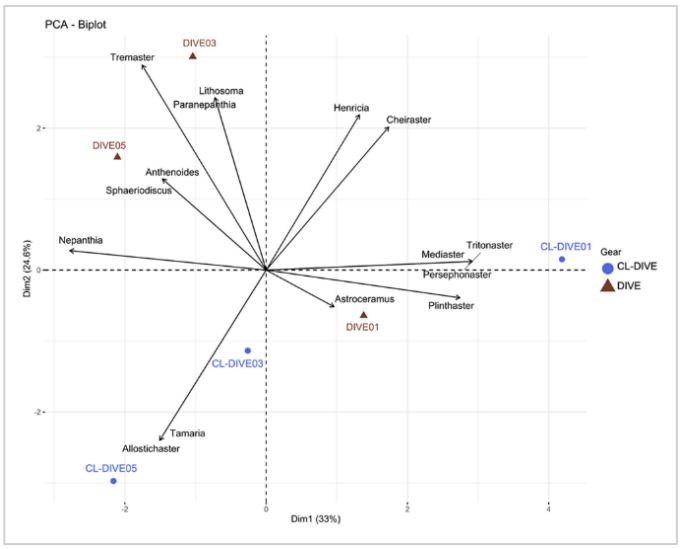

Figure I.10 : Comparison of asteroid assemblages between imagery (dive) and sampling along dive (cl-dive) along volcanic island slopes (Mayotte) (57.6% of variance on first two PCs). Principal Component Analysis (PCA) of Hellinger-transformed presence/absence asteroid data at genus rank

I.3.2 Illustration of the proposed integrative methodology for the photo-taxa identification of crustaceans (Caridea and Galatheoidea): construction of photo-type catalogs and identification keys

Specimens collected in the co-located sampling and in the surrounding area in Astrolabe Bay and the Sepik area (PNG), and in the Comoros archipelago (for Mayotte), provide additional knowledge of the species occurring in these areas, and directly aid the identification of photo-taxa. Here we use the Caridea, observed on three dives along Mayotte volcanic island slopes, to illustrate our method of identification from images. This example illustrates the identification steps, from the phototaxon identification to the construction of the identification key. We provide another illustration of the methodology in **Supplementary material I.8** for galatheid identification at the morphospecies level along the four PNG sedimented slopes.

We considered four groups of Caridea specimens observed in images as belonging to different genera and thus delimited them into four different photo-taxa attributed to a reliable genus

rank. We identified these four genera primarily based on observable morphological characters from images. In the physical samples (data from the BIOMAGLO expeditions as well as from previous expeditions), we identified species attributed to these four genera that thus constitute a pool of species potentially present in the analyzed images (**Table I.4**). For each of these four genera, we compared the morphological characters observable on the photo-taxa by using the characters of potential species. From this comparison, we were able to determine the individuals to the species or morphospecies ranks, whereas for some photo-taxa, identification did not go beyond the genus rank.

Table I.4 : Examples of Caridea photo-taxa identified from images in relation with Caridea species collected either from sampling along dive, or from sampling in the surrounding area from Mayotte, Moheli, Geyzer Bank and Glorieuses (BIOMAGLO expedition), or from regional sampling from past expeditions undertaken along the Mozambique Channel

Photo-taxon (identified at a reliable rank N)	Dive	Sampled species belonging to the rank attributed to the photo-taxon	Spatial scale of sampling	Photo-taxon (contextual identification)
Heterocarpus	DIVE01 DIVE03 DIVE05	*Heterocarpus laevigatus* Bate, 1888	Along dive /Around	*Heterocarpus laevigatus*
		Heterocarpus ensifer A. Milne-Edwards, 1881	Around/Regional	*Heterocarpus* indeterminabilis
		Heterocarpus lepidus de Man, 1917	Along dive /Around/Regional	
		Heterocarpus dorsalis Bate, 1888	Around	
		Heterocarpus calmani Crosnier, 1988 *Heterocarpus gibbosus* Bate, 1888	Regional	
Plesionika	DIVE01 DIVE03 DIVE05	*Plesionika semilaevis Bate, 1888*	Along dive/Around/Regional	*Plesionika* indeterminabilis
		Plesionika ensis (A. Milne-Edwards, 1881) *Plesionika crosnieri* Chan & Yu, 1991 *Plesionika spinensis* Chace, 1985 *Plesionika martia* (A. Milne-Edwards, 1883) *Plesionika bifurca* Alcock & Anderson, 1894	Around	
		Plesionika neon Komai & Chan, 2010 *Plesionika alcocki* (Anderson, 1896)	Regional	
		Plesionika nesisi (Burukovsky, 1986) *Plesionika spinidorsalis* (Rathbun, 1906) *Plesionika edwardsii* (Brandt, 1851) *Plesionika crosnieri* Chan & Yu, 1991 *Plesionika indica* de Man, 1917	Around/Regional	
Nematocarcinus	DIVE01 DIVE05	*Nematocarcinus parvus* Burukovsky, 2000	Around/Regional	*Nematocarcinus* sp1 *Nematocarcinus* sp2
		Nematocarcinus tenuirostris Bate, 1888 *Nematocarcinus productus* Bate, 1888 *Nematocarcinus nudirostris* Burukovsky, 1991 *Nematocarcinus tenuipes* Bate, 1888	Regional	
Glyphocrangon	DIVE01 DIVE03 DIVE05	*Glyphocrangon amblytes* Komai, 2004 *Glyphocrangon pulchra* Komai & Chan, 2003 *Glyphocrangon ferox* Komai, 2004 *Glyphocrangon brevis* Komai, 2006 *Glyphocrangon dentata* Komai, 2004 *Glyphocrangon indonesiensis* Komai, 2004 *Glyphocrangon musorstomia* Komai, 2006	Regional	*Glyphocrangon amblytes*
		Glyphocrangon crosnieri Komai, 2004	Along dive /Around/Regional	*Glyphocrangon crosnieri*

For the photo-taxon assigned to the genus *Heterocarpus*, comparisons made it possible to differentiate individuals belonging to this photo-taxon with morphological characters attributed to the species *Heterocapus laevigatus* (i.e., dorsal rostrum without tooth in most

length, no dorsal spine on the abdomen, with a body red to orange, with red vertical stripes on abdomen between somites). Thus, for these individuals, we delimited a new photo-taxon assigned to the species *H. laevigatus*. For the other *Heterocarpus* individuals, the quality of the images was insufficient to establish a difference at the species rank. Thus, these individuals remained assigned to the genus *Heterocarpus* with the qualifier status “indeterminabilis”.

For the photo-taxon assigned to the genus *Plesionika*, although several potential species corresponding to this genus were collected and are known in the study area, the quality of the images and the observable characters were insufficient to differentiate several subsets at the species level. Many of these observable characters (e.g., white spots on the abdomen) are shared between several species, or highly variable within species (e.g., specimens color variation according to the background substrates). Therefore, we limited our identification to the genus level with the qualifier status “indeterminabilis”.

For the photo-taxon assigned to the genus *Nematocarcinus*, five species are known in the area (Burukovsky, 2011). However, the characters observable from images were not sufficient to identify them at the species rank with a valid species name. Nevertheless, we were able to differentiate two groups of individuals within this photo-taxon: individuals with a banded abdomen and individuals with homogeneous orange abdomen. These two patterns indubitably correspond to at least two different species, as the eight species of *Nematocarcinus* have their colorations illustrated in Burukovsky (2013), all lacking bands on the abdomen. We thus assigned them to two distinct morphospecies.

Finally, for the photo-taxon assigned to the genus *Glyphocrangon*, we distinguished two potential species on a distinct morphological character (i.e., post-antennal spines widely directed outward or not from the front carapace). Using the list of the eight *Glyphocrangon* species present in the region, the state of this observable character from images allowed us to assign each of these two groups of individuals respectively to *Glyphocrangon amblytes* or *Glyphocrangon crosnieri* [also according to their white body coloration with black eyes and orange bands on the abdomen amongst the species reported in the region (Komai and Chan, 2013)].

After having delimited Caridea photo-taxa and attributed each one to at least a genus rank (taxonomic rank illustrated for this example), we selected the best-quality images to compile

the photo-type catalogs for use in identifying the remaining photo-taxa. We then compiled all the diagnostic characters we identified as relevant for the identification of these photo-taxa.

Therefore, resulting from this methodology of identification, we developed identification keys for three target taxa based respectively on the expertise of Pr. Tin-Yam Chan and Dr. Laure Corbari for Crustacea (mainly Dendrobranchiata and Caridea), Dr. Thomas Saucède for Echinoidea and Dr. Christopher Mah for Asteroidea. The keys for shrimps and asteroids are dichotomous while the key for echinoids is an online multiple-entry interactive key. We built these keys based on the identification of specimens observed in the images from the Mayotte volcanic island slopes, and from other seamounts in the Mozambique Channel. The taxonomic rank reached in these keys represents the identification rank achieved from the images. Therefore, these keys are yet incomplete. First, for some taxonomic group the characters needed to differentiate the taxa at lower level might be not observable in images. Second, we do not have images of all the species known in the Mozambique Channel. These keys must thus be completed with additional data.

I.4 Discussion

I.4.1 Efficiency of images and physical samples in different habitat types

I.4.1.1 Taxonomic coverage and resolution

We reached a level of identification lower than the class level for Pisces (order/family), Asteroidea and Echinoidea (down to genus) and Crustacea (down to species/morphospecies). Assignment to these taxonomic ranks reflects both their recurrence on the images, the available literature and the involvement and availability of taxonomy experts in the identification of specimens both from images and from collected samples. Furthermore, for these groups, a sufficient number of diagnostic characters can be examined from images (e.g., test shape and spine thickness for echinoids, antennular length and color or rostral teeth for shrimps).

Identification of other phyla in images is of lower resolution, from phyla/class for Porifera, order for Cnidaria, and class to family for Mollusca. It is worth noting that the mollusks, as well as the annelids identified at the family level were specialized fauna associated with cold seeps where the low diversity and the large size of individuals (e.g., Sibuet and Olu, 1998) make the identification of these groups easier. On the contrary, in other habitats, annelids and bivalves

are usually of small-size and inconspicuous (i.e., buried in the sediments or hidden in habitat-forming organisms such as corals or sponges). For instance, we observed a high proportion of gastropods along the Mayotte island volcanic slopes but whose identification from images of the shells only never exceeded the class rank. We expected such limitation, which was previously observed on hard bottoms (Beisiegel et al., 2017; Williams et al., 2015).

We also obtained incomplete identification from physical samples for mollusks and annelids and for other groups as well (e.g., actinians and echinoderms from the upper PNG sedimented slopes area). This reflects the time-consuming practice of taxonomy (e.g., fieldwork, species delimitation, description and naming, curation of collections, etc.). Moreover, this scientific field suffers from poor funding, decreasing numbers of experts and lack of employment opportunities (Agnarsson and Kuntner, 2007). These hindrances further increase the time between the discovery and the description of new species (Fontaine et al., 2012). Furthermore, in areas where the fauna is poorly known and very diversified such as in PNG – where more than 300 new species have been described by the TDSB Program—and in the north Mozambique Channel—with 85 species described from one expedition (Benthedi)—the identification effort needed from taxonomists is all the more important.

Lastly, from images, we annotated many cnidarians and poriferans, whose identification beyond the class or order ranks was difficult and uncertain. These taxonomic groups have complex taxonomy and show high morphological plasticity or convergence from the high to intraspecific levels (Barnes and Bell, 2002; Todd, 2008). Moreover, diagnostic characters required for identification at the species rank are mainly microscopic or internal (e.g., *Chrysogorgia* species) (Pante and Watling, 2012), and thus cannot be observed from images. In addition, we observed that the erect 3D structure of these habitat-forming species was not efficiently captured in dredges and trawls on the hard bottoms of the Mayotte volcanic island slopes; similarly for pennatulids and actinians which have been observed only in images along sedimented slopes of PNG. This fishing gear selectivity has already been mentioned for hard bottoms (Williams et al., 2015) and for soft bottoms (e.g., pennatulids, actinians) (de Mendonça and Metaxas, 2021; Nybakken et al., 1998; Rice et al., 1982). However, cnidarians and poriferans represent key groups in the benthic ecosystem functioning, because they can host a large diversity of associated fauna (Beazley et al., 2013; Buhl-Mortensen et al., 2010). They are also highly vulnerable to anthropogenic impacts due to their low resilience (Schlacher

et al., 2010) and thus provide a good vulnerable marine ecosystem (VME) indicator (FAO, 2009). For these groups, the use of ROVs can help identification by coupling high-resolution imagery with the collection of targeted specimens and establish a robust baseline catalog. However, the cost by using ROVs is much higher than using the towed cameras, and have still their limitation to survey the whole diversity. This underlines the necessity for developing alternative approaches to assess the diversity of habitat-forming taxa, which is an ongoing work of M. Hanafi-Portier' Ph.D. by developing a classification of observable characters based on their morphology and their function (e.g., size, 3D structure) independently of their taxonomy. Such characters have been reported to be good proxies for the role of these habitat-forming species on associated fauna and how they could respond to abiotic constraints (Denis et al., 2017; Schönberg, 2021; Schönberg and Fromont, 2014; Zawada et al., 2019b).

Our study underlines the need to put the research efforts on targeted taxonomic groups that fulfill at least three conditions: (1) an extensive record of both physical specimens and identifications in collections, (2) the ability to identify diagnostic morphological characters from images and (3) the availability and active involvement of taxonomists to identify them from images. For those unidentifiable from images and/or not efficiently collected, biodiversity quantification must then be assessed using other approaches (e.g., morpho-functional).

I.4.1.2 Biodiversity metrics for the targeted taxonomic groups

For each targeted taxonomic group, we have compared the diversity and composition metrics at the taxonomic rank reached for images. For a given sampling area, these metrics differ when estimated based on physical samples or from observations made in images.

In areas dominated by hard bottoms or showing high habitat heterogeneity such as cold seeps, we observed higher taxonomic richness in images than in physical samples, for all the targeted taxa in this study, and at variable taxonomic ranks of comparison. This reflects mainly the difficulties for the dredges in these environments, with for example, large boulders (~1 m in size) along the Mayotte slopes. In the cold-seep area, abundant large siboglinid tubeworm bushes and mussel beds clogging the trawl nets seems to have limited the sampling of other taxa.

In areas dominated by soft sediment, including the sedimented slopes of Astrolabe Bay in PNG and the soft-bottom areas of the Mayotte island slopes (Dive01), we expected a better sampling efficiency than in hard bottoms. However, at the transect scale we did not detect consistent differences in taxonomic richness estimated from observation from images and from identification of physical samples. This low richness of the very mobile fauna in fishing gears—as observed for Pisces—highlight the need to widen the sampling area. The physical sampling alone captured only part of the faunal diversity, probably because of gear selectivity and insufficient sampling effort with respect to the diversity of the different groups in the studied regions. Assessment by environmental DNA/metabarcoding approach could be an interesting complement to improve the biodiversity exploration at the local scale. However, this approach requires DNA-barcoding reference databases which are yet far from completed for the deep-sea fauna. Crustaceans are better sampled by fishing gears if comparing the metrics at the genus rank. However, when considering the identification of morphospecies in images and the identification of species for physical samples, we obtained similar metrics. The metrics estimated at the species level for images might have overestimated the real richness. Indeed, several morphospecies can represent a single species with intraspecific polymorphism. Such issues can be solved only when DNA barcoding analysis is conducted on the collected specimens. Nevertheless, underestimation of diversity is also possible, because one morphospecies can potentially gather several species (Williams et al., 2015). This could explain the lower richness observed in images compared to physical samples in this study (190 species identified from sleds vs. 57 photo-taxa) which contrasts with our results. The use of taxonomic levels, or thresholds, defined for each taxonomic group, could be a more cautious and robust way to assess the biodiversity from image datasets, even if these levels are heterogeneous.

Images alone give a partial estimation of the diversity notably due to identification limitations, particularly for the mobile species that appeared blurry in images (e.g., Malacostraca indeterminabilis dominated in the canyon site) or for small-sized taxa (e.g., genus *Echinocyamus* for echinoids, genus *Lepas* for crustaceans). In soft bottoms, endogenous fauna cannot be detected in images (Rice et al., 1982); this also applies to some crustacean genera (e.g., *Stereomastis*) and burrowing fish families which camouflage themselves (Synodontidae, Myxinidae). Also, some diagnostic characters cannot be observed in images for some taxa

(e.g., the Myxasteridae family for Asteroidea, the Perciformes order for Pisces). For echinoids the diversity of some families was better represented from sampling (e.g., Cidaridae) mainly due to the difficulty in identifying characters from images. Thus, imagery tends to smooth the gamma diversity for this family.

Nevertheless, selectivity of fishing gears was also deduced from this comparison, especially in complex seabed habitats for very mobile taxa, but also due to the living habits or fragility of some species. For instance, the fragile genus *Aspidodiadema* (Echinoidea), which lives with its test raised above the seafloor by its long spines, was not collected. Interestingly, images revealed the occurrence of this genus in hard-bottom areas making evident the misconceptions about the soft-bottom living habits of the genus. Similarly, the half-buried spatangoid genera and the burrowing ones (e.g., *Eupatagus*) were identified in images but not in samples, likely because of their fragility.

In summary, we conclude that neither imagery nor physical sampling at the transect scale can give a complete view of megafauna diversity and composition. Imagery is advantageous in hard-bottom and heterogeneous habitats, where the topography and the nature of the substrate limit the efficiency of fishing gears. In contrast, in soft-bottom habitats, the benefit of physical sampling is more pronounced, because endogenous and small-sized fauna cannot be detected in images. Gamma diversity is better estimated from sampling in soft-bottom habitats. The use of imagery in these environments can provide complementary information on habitats (e.g., wood distribution, cold seeps) at the transect scale, or among transects, revealing their potential role in structuring megafauna biodiversity. In hard-bottom environments, due to sampling difficulties, sampling effort should cover a larger spatial scale to catch the regional species pool and allow identification from images.

I.4.2 Increase the robustness of photo-taxa identification by an integrative methodology

The sampling undertaken in the surrounding areas (up to 400 km) contributed to a significant increase in the knowledge of species occurring in the area. In return, this knowledge helped the identification of individuals from images. For Pisces, the contribution of the knowledge of the surrounding fauna is the highest for the volcanic island slopes, with an increase up to nine-fold of family richness. For echinoids, specimens sampled in the surrounding areas increased the genus richness to a lesser extent than for the very mobile fauna (~1.7 ×), probably because

of a higher probability of capture and a lower gamma diversity, leading to capture much of the diversity from the "local" samples along the dives. It seems that the contribution increases with fauna mobility and with gamma diversity.

The case study of decapods illustrates the methodological approach we developed based on a taxonomic framework. It shows in particular that photo-taxon identification relies on observation of morphological characters relative to one or several potential analogous species/taxa collected in the area. If morphological characters cannot be sufficiently differentiated between or within one photo-taxon to proceed to a lower identification level, we suggest identification at the lowest robustly determined taxonomic rank.

Although morphological characters cannot be sufficiently observed to assign a species name to a specimen in images, we suggest morphospecies delimitation from knowledge of the taxa occurring in the area at regional and also local scales (specimens exclusively sampled along dive). This approach can be applied to any rank higher than genus (e.g., morphospecies delimited at the family level) according to the lowest resolved identification level. However, when the distinction between morphological characters does not allow the clear delimitation between individuals, identification remains at the lowest robustly resolved taxonomic rank designated with an identification status qualifier "indeterminabilis" (e.g., *Plesionika* indeterminabilis).

In some cases, species-level identification is possible, as illustrated with *H. laevigatus*, because this species was the only one of the *Heterocarpus* genus collected in the surrounding area that showed diagnostic characters corresponding to those observed in the photo-taxon.

We also tried to supplement and enhance the robustness in identification with an integrative approach, by also considering the species habitat, feeding preferences, substrate, living habits or position relative to seafloor. Habitat context was not an informative diagnostic character for the identification of decapods, because most specimens observed in images belonged to genera characteristic of soft- or mixed-bottom types and with a wide depth range. However, for some other taxa, habitat provided useful information. For instance, the knowledge of the preference of some *Munidopsis* species for sunken wood (Hoyoux et al., 2012) that were sampled in the area was a helping criterion to increase confidence in the identification of this genus from images. Similarly, the knowledge of feeding preference of some asteroid species

belonging to the genus *Henricia*, that predate on sponges (Mah, 2020), increased confidence in image-based identification of this genus. At the species/morphospecies rank of identification, to weight potentially diagnostic features and increase confidence in the distinction among the potential species, it may be useful to add additional criteria relative to the environment, as discussed above for genus-level identification.

Finally, we developed photo-type catalogs to help in the identification of the remaining photo-taxa to be identified. However, catalogs alone are subject to interpretation according to observers and can lead to erroneous identifications or variable identifications between observers (Durden et al., 2016a; Henry and Roberts, 2014; Howell et al., 2014). Therefore, catalogs of marine taxa need to be fed by formalized diagnostic criteria required for consistent and robust identification.

I.4.3 Formalization of image-based taxonomic identification from keys adapted for imagery

We observed that images and physical samples provide differential and complementary views of the structure of the benthic megafauna, and uncovered the need for and the contribution of physical sampling at local scales and beyond to help in the identification of photo-taxa. Our formalization of the process of identification of the organisms observed in images gives a taxonomic framework to photo-taxon identification, to refine the taxonomic rank of determination, and for morphospecies delimitation.

From this complementarity, and for three target taxa (Echinoidea, Asteroidea, Decapoda), the diagnostic characters observed in images, the satisfactory level of identification, the collaboration and involvement of taxonomists all enabled the development of identification keys adapted to the images acquired from the Mayotte slopes, and by extension adapted to the Mozambique Channel area. This is a first step for these keys, which can be adapted to other areas in the future (Indo-West Pacific area).

We tested the identification keys for asteroid and decapod identification on a set of four naive observers, as recommended in Walter and Winterton (2007). Results indicated some limitations for the two dichotomous keys, including misinterpretation or low image resolution leading to inefficient or inadequate observation of diagnostic characters. Obviously, the identification of photo-taxa using keys is easier for specialists than for non-experts. We then integrated photo-type images and illustrations of characters to make the keys more user-

friendly. However, inherent to their structure, dichotomous keys can be difficult to use due to pathway problems. Misinterpretation or unanswerable couplets of characters can lead to a dead-end, and thus require going back to the starting entry points (Hagedorn et al., 2010; Walter and Winterton, 2007). Unanswerable couplets can be particularly limiting in the case of image analyses (characters not visible from image), leading us to focus on the development of a multiple-access key such that the user can choose any character according its availability (observable from images) or familiarity (doubt regarding some characters), and also recommended by Howell et al. (2019) in the case of image-based identification.

This type of key is available for echinoid identification at the genus rank. It can be easily updated and quickly provides the information sought to end-users on a web platform. It also facilitates the documentation of environmental settings and of main abiotic and biotic elements of habitats along with their implementation in datasets (e.g., taxon depth range, substrate type, associated living communities, etc.).

The development of image-based keys for fish identification holds promise, but the limited image resolution and top-view acquisition were not suitable to build such keys. Indeed, the morphological characters observable in the images, especially when images were taken with a towed camera, are poorly informative for taxonomic identification. We consequently recommend to systematically supplement top views with a profile view, especially for the identification of Pisces (e.g., number of dorsal fins, profile shape, etc.) and Decapoda (e.g., rostrum shape and armature, abdominal armature etc.), or to use stereo cameras which can provide 3D views. Video sequences can provide informative supplementary diagnostic characters, allowing observation of behavior, flexibility and movement. Advances in biomimicking robotics such as fish-like robots could help encompassing such limitations by offering side-view observations and the exploration of behaviors (Katzschmann et al., 2018; Laschi and Calisti, 2021).

Furthermore, from a non-expert point of view, we noticed different complex methodological choices and questions in terms of photo-taxon identification and morphospecies delimitation. For instance, regarding the choice of whether or not to delimit different morphospecies for a given photo-taxon, the confidence we placed in the species identification level or the choice to maintain the taxon at an indeterminabilis level of identification. We combined these questions in an integrative scheme, considering in particular new recommendations for a

standardized, open nomenclature for image-based identification (Horton et al., 2021; **Figure I.11**).

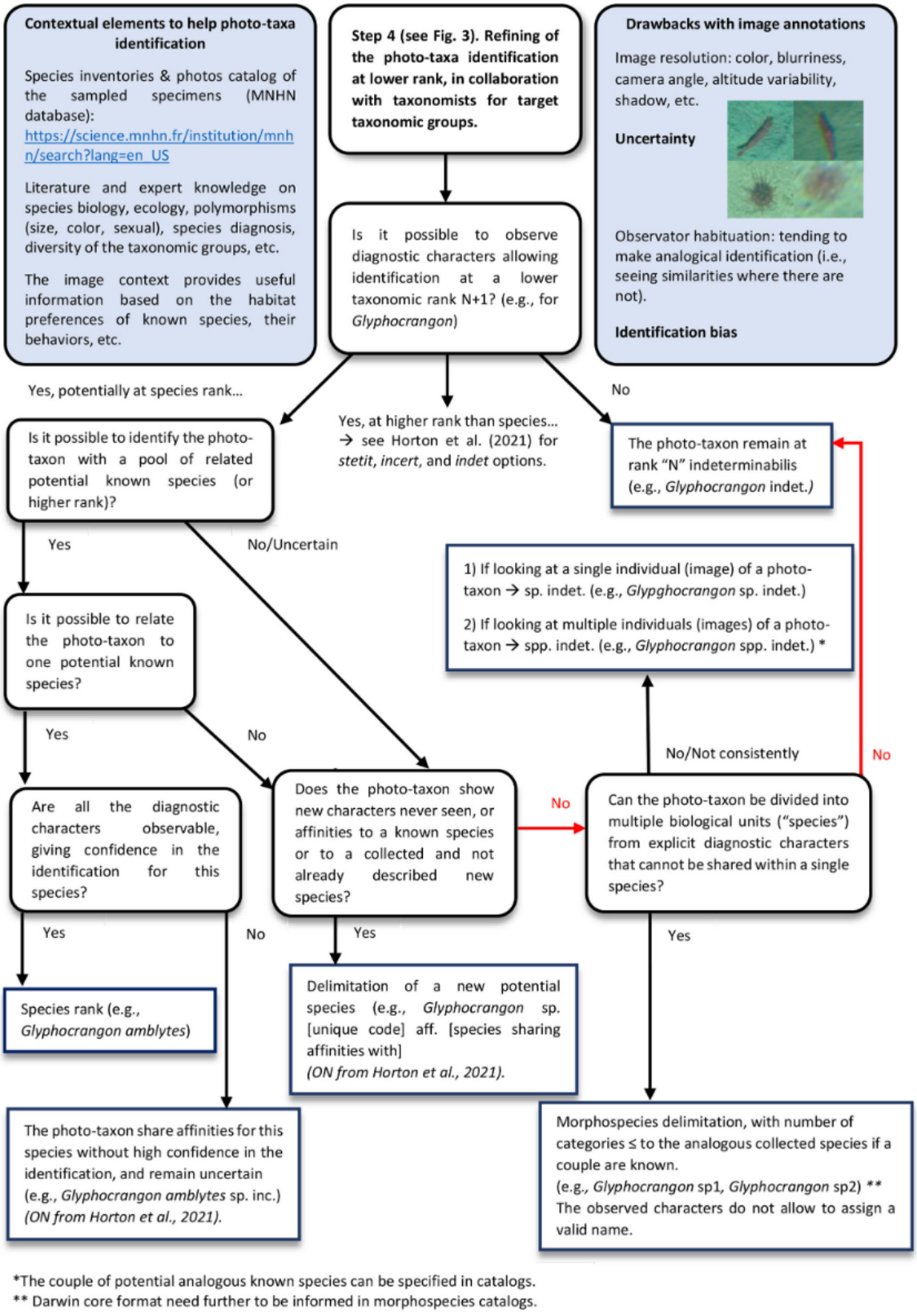

Figure I.11 : Integrative scheme for photo-taxa identification and nomenclature from images

Open nomenclature (ON) provides a set of terms and their abbreviation (signs) to inform on the provisional uncertainty status of an identification (Sigovini et al., 2016).

However, the use of Sigovini et al. (2016) ON adapted to physical specimens, as recommended by Horton et al. (2021), for image identifications, requires the sampling of the specimens observed in images, which is possible using ROV but not using a towed camera. We can only make hypotheses of known analogous species to link the photo-taxa observed from images with the pool of species collected in the area and sharing similar diagnostic morphological or other characters. Although systematic collection by ROV of specimens observed in images is hardly feasible in highly diverse areas, and onerous, targeted sampling appears to be an efficient option to calibrate photo-taxa identification from images.

Furthermore, as mentioned by Horton et al. (2021), the choice of which ON signs to use will depend on the intended application (analyses, taxon catalogs, etc.) and in the case of community matrix/ecological analyses, that a taxonomic roll-up (merge taxa to higher taxonomic rank) to the most confident identification should be processed. We therefore recommend setting, for each taxonomic group to be analyzed, a threshold taxonomic identification rank enabling to avoid the use of “incertae” ON signs. Using such threshold for the identification rank, the community structure analyses can be robustly conducted. The robustness of this community analysis will rest on the consistency of the taxonomic rank reached within a given taxonomic group. The selection of this threshold depends on the taxonomic group considered, the level of knowledge of the taxa occurring in the area and on the morphological criteria detectable from images. The morphospecies rank can be considered in these analyses if they are confidently delimited and validated by a taxonomy expert.

However, in some cases, we determined the photo-taxa to the species rank, and based on affinities to collected specimens, we assigned them to a species name using “cf” or “aff” ON signs for the analogous species. We corrected the use of these ON signs for “sp incertae” following recommendation of Horton et al. (2021). For analysis, the lack of distinction between uncertainty in the identifications at a given rank and uncertainty of the species name at the species rank can lead to a loss of information if roll-up every photo-taxon assigned to “incertae” ON sign. Therefore, these species, despite uncertain identification, can be included in species rank analyses.

Finally, the keys help mainly for identification at the family or the genus levels. Sometimes morphospecies level delimitations are suggested or, at least, a set of observable morphological characters of the morphospecies are listed in the key. Such indications should help the delimitation of morphospecies in future studies. However, the naming convention for certain morphospecies in this study will certainly not be the same in another study. There is a need for future studies to develop identification keys in other oceanic regions, systematically accompanied by a morphospecies catalog—if morphospecies are delimited—and by listing the corresponding, potentially analogous known species in the area. The identification keys and the morphospecies catalog should both relied on the standardized database of marine taxa image catalog developed by Howell et al. (2019) in the Atlantic region, and using a Darwin Core format.

I.5 Conclusion

Imagery and physical sampling have benefits and biases that influence the estimated patterns of biodiversity. The taxonomic level of identification, the studied taxonomic groups and habitat type are important elements to be considered. Each of these choices needs to be carefully considered according to the questions addressed by the study but also by the costs and the environmental issues.

In poorly explored areas with poorly known fauna, processing taxon identification from images is very difficult and could lead to potential important misidentifications. Our study shows that deploying imagery-based studies require prior extensive physical sampling to establish a baseline knowledge of the species occurrences in the area. To assess the pattern of benthic megafauna communities, in homogeneous or soft-bottom habitats, dredges and trawls seem to be more suitable options than towed camera. In such environments, image acquisition is a supplementary approach to check for the absence of more complex structures formed by engineer species. In more heterogeneous habitats, such as cold seeps or hard-substrate environments composed of fragile biotic habitats (corals, sponges), imagery should be favored and supplemented with limited physical sampling effort. Ideally, targeted sampling by ROV should be preferred, including new robotic hands or “needle-biopsy” samplers for a minimally invasive sampling (Pomponi, 2016), but this recommendation cannot be generalized due to its implementation cost.

Imagery and physical sampling are complementary methods and using both together will improve assessments of benthic megafauna community patterns. These elements are important to consider for establishing policy management in environments increasingly threatened by anthropic activities, such as Astrolabe Bay, where the Ramu refinery activity could lead to potentially destructive impacts (Samadi et al., 2015) or in the context of the Mayotte Natural Marine Park. From these complementary methods, we propose an integrative methodological approach to process faunal identification from images, based on contextual tools and supported by a taxonomical framework.

Above all, the difficulty of carrying out identification from images raises the necessity of collaborative work with taxonomists. Their expertise is essential for assessing the quality and the validity of the identification, at the lowest taxonomic level possible. This complexity reveals the need to focus on specific taxonomic groups that present observable morphological characters from images and the need to set a reasonable and robust level of identification. Such considerations require the involvement in the study of taxonomists to identify collected specimens and photo-taxa (specimens in images). This methodology has led to the development of identification keys adapted for imagery data, for target taxonomic groups (echinoids, asteroids and shrimps). Improvement of image resolution and different camera angles could offer interesting perspective to improve megafauna' identification from images, and for instance, to develop identification keys for fish. The combination of image acquisition with targeted sampling is also a crucial way for the calibration of the identification. Finally, these identification keys were developed from the Mozambique Channel seamount fauna dataset and could be extended to other areas of the Indo-West Pacific region, through further international collaborative effort.

DATA AVAILABILITY STATEMENT

The original contributions presented in the study are included in the article/Supplementary Material, further inquiries can be directed to the corresponding author/s.

AUTHOR CONTRIBUTIONS

KO, LC, and SS designed the sampling and led the data acquisition. MH-P, KO, and LC analyzed the data. MH-P, KO, and CB processed the images. T-YC, LC, TS, W-JC, M-YL, J-NC, CM, and MH-P identified taxa in the images and constructed the identification keys. MH-P, KO, and SS

wrote the manuscript. KO, SS, LC, T-YC, TS, W-JC, and M-YL contributed to the critical revision of the manuscript. KO and SS are Ph.D. supervisors. All authors contributed to the article and approved the submitted version.

FUNDING

The BIOMAGLO cruise and project was supported by funding from the Xth European Development Fund (Fonds Européen de Développement ; FED) “sustainable management of the natural heritage of Mayotte and the Eparses Islands” program led by the French Southern and Antarctic Lands (Terres australes et antarctiques françaises ; TAAF) with the support of the Mayotte Departmental Council (Conseil Départemental de Mayotte), the French Development Agency (Agence Française de Développement ; AFD) and the European Union. Collaboration with Taiwan was supported by funding from the Ministry of Science and Technology, Taiwan (MOST 102-2923-B-002-001-MY3, MOST 107-2611-M-002-007and MOST 108-2611-M-002-012-MY2 to W-JC) and the French National Research Agency (ANR 12-ISV7-000501 to SS) and the Center of Excellence for the Oceans, National Taiwan Ocean University to T-YC. The thesis of MH-P is co-funded by TotalEnergies and IFREMER as part of the PAMELA (Passive Margin Exploration Laboratories) scientific project.

ACKNOWLEDGMENTS

We would like to thank the officers and crews of RV’s ANTEA and ALIS as well as the SCAMPI towed-camera team for their contribution and assistance with data acquisition. We are grateful to the chief scientists of the MADEEP, BIOMAGLO, BIOPAPUA, and PAPUA NIUGINI cruises as well as the entire scientific team. Moreover, we would like to thank J. Tourolle for the helping and assisting in the analysis of GIS data, EJ. Pernet for the processing of the fauna samples, L. Keszler for the primary annotation of the BIOMAGLO campaign images. We are grateful to T. Nattkemper and D. Langenkämper for allowing the loading of the image data and their annotation with BIIGLE 2.0 and for their technical support. We are particularly grateful to all the taxonomists who have contributed to the identification of the fauna in the images and in the collections: N. Puillandre (gastropods), P. Maestrati (bivalves), E. Pante and D. Pica (cnidarians), P. Cardenas and C. Debitus (poriferans), P. Giannassi (fishes), E. Macpherson (galatheids). This paper has been professionally edited for the English language

by C. Engel-Gautier (CHRYSALIDE). Finally, we would like to thank the two reviewers for their critical comments that have contributed to improve the manuscript quality.

I.6 References

Agnarsson, I., Kuntner, M., 2007. Taxonomy in a Changing World: Seeking Solutions for a Science in Crisis. Systematic Biology 56, 531–539. https://doi.org/10.1080/10635150701424546

Audru, J.-C., Guennoc, P., Thinon, I., Abellard, O., 2006. Bathymay : la structure sous-marine de Mayotte révélée par l'imagerie multifaisceaux. Comptes Rendus Geoscience 338, 1240–1249. https://doi.org/10.1016/j.crte.2006.07.010

Barnes, D.K.A., Bell, J.J., 2002. Coastal sponge communities of the West Indian Ocean: morphological richness and diversity. African J Ecol 40, 350–359. https://doi.org/10.1046/j.1365-2028.2002.00388.x

Beazley, L.I., Kenchington, E.L., Murillo, F.J., Sacau, M. del M., 2013. Deep-sea sponge grounds enhance diversity and abundance of epibenthic megafauna in the Northwest Atlantic. ICES Journal of Marine Science 70, 1471–1490. https://doi.org/10.1093/icesjms/fst124

Beisiegel, K., Darr, A., Gogina, M., Zettler, M.L., 2017. Benefits and shortcomings of non-destructive benthic imagery for monitoring hard-bottom habitats. Marine Pollution Bulletin 121, 5–15. https://doi.org/10.1016/j.marpolbul.2017.04.009

Bouchet, P., 2009. MIRIKY Cruise, RV MIRIKY [WWW Document]. URL https://expeditions.mnhn.fr/campaign/miriky?lang=en_US

Bouchet, P., Perez, T., Le Gall, L., 2010. ATIMO VATAE cruise, RV Antea. https://doi.org/10.17600/10110040

Bouchet, P., Ramos, A., 2009. MAINBAZA Cruise, RV Vizcondede Eza [WWW Document]. URL https://expeditions.mnhn.fr/campaign/mainbaza?lang=en_US

Bowden, D.A., Rowden, A.A., Leduc, D., Beaumont, J., Clark, M.R., 2016. Deep-sea seabed habitats: Do they support distinct mega-epifaunal communities that have different vulnerabilities to anthropogenic disturbance? Deep Sea Research Part I: Oceanographic Research Papers 107, 31–47. https://doi.org/10.1016/j.dsr.2015.10.011

Braga-Henriques, A., Porteiro, F.M., Ribeiro, P.A., de Matos, V., Sampaio, I., Ocaña, O., Santos, R.S., 2013. Diversity, distribution and spatial structure of the cold-water coral fauna of the Azores (NE Atlantic). Biogeosciences 10, 4009–4036. https://doi.org/10.5194/bg-10-4009-2013

Buhl-Mortensen, L., Vanreusel, A., Gooday, A.J., Levin, L.A., Priede, I.G., Buhl-Mortensen, P., Gheerardyn, H., King, N.J., Raes, M., 2010. Biological structures as a source of habitat heterogeneity and biodiversity on the deep ocean margins: Biological structures and biodiversity. Marine Ecology 31, 21–50. https://doi.org/10.1111/j.1439-0485.2010.00359.x

Burukovsky, R.N., 2013. Shrimps of the family Nematocarcinidae Smith, 1884 (Crustacea, Decapoda, Caridea) from Taiwan and the Philippines collected by the TAIWAN, PANGLAO 2005 and AURORA expeditions in the western Pacific, in: Ahyong, S.T., Chan, T.-Y., Corbari, L., P. K. L., N. (Eds.), Tropical Deep-Sea Benthos 27 Mémoires Du Muséum National d'Histoire Naturelle (1993). pp. 154–189.

Burukovsky, R.N., 2011. Geographic distribution of nematocarcinidae shrimps (Crustacea, Decapoda). Zoologicheskii Zhurnal 90, 293–301.

Clark, M.R., Consalvey, M., Rowden, A.A. (Eds.), 2016. Biological Sampling in the Deep Sea, Wiley-Blackwell. ed.

Collins, P., Kennedy, R., Van Dover, C., 2012. A biological survey method applied to seafloor massive sulphides (SMS) with contagiously distributed hydrothermal-vent fauna. Mar. Ecol. Prog. Ser. 452, 89–107. https://doi.org/10.3354/meps09646

Corbari, L., Olu, K., Samadi, S., 2014. MADEEP cruise, RV Alis. https://doi.org/10.17600/14004000

Corbari, L., Samadi, S., Olu, K., 2017. BIOMAGLO cruise, RV Antea. https://doi.org/10.17600/17004000

Cunha, M.R., Hilário, A., Santos, R.S., 2017. Advances in deep-sea biology: biodiversity, ecosystem functioning and conservation. An introduction and overview. Deep Sea Research Part II: Topical Studies in Oceanography 137, 1–5. https://doi.org/10.1016/j.dsr2.2017.02.003

Da Ros, Z., Dell'Anno, A., Morato, T., Sweetman, A.K., Carreiro-Silva, M., Smith, C.J., Papadopoulou, N., Corinaldesi, C., Bianchelli, S., Gambi, C., Cimino, R., Snelgrove, P., Van Dover, C.L., Danovaro, R., 2019. The deep sea: The new frontier for ecological restoration. Marine Policy 108, 103642. https://doi.org/10.1016/j.marpol.2019.103642

Danovaro, R., Snelgrove, P.V.R., Tyler, P., 2014. Challenging the paradigms of deep-sea ecology. Trends in Ecology & Evolution 29, 465–475. https://doi.org/10.1016/j.tree.2014.06.002

de Mendonça, S.N., Metaxas, A., 2021. Comparing the Performance of a Remotely Operated Vehicle, a Drop Camera, and a Trawl in Capturing Deep-Sea Epifaunal Abundance and Diversity. Front. Mar. Sci. 8, 631354. https://doi.org/10.3389/fmars.2021.631354

Denis, V., Ribas-Deulofeu, L., Sturaro, N., Kuo, C.-Y., Chen, C.A., 2017. A functional approach to the structural complexity of coral assemblages based on colony morphological features. Scientific Reports 7. https://doi.org/10.1038/s41598-017-10334-w

Dray, S., Dufour, A.-B., 2007. The ade4 Package: Implementing the Duality Diagram for Ecologists. J. Stat. Soft. 22. https://doi.org/10.18637/jss.v022.i04

Durden, J.M., Bett, B., Schoening, T., Morris, K., Nattkemper, T., Ruhl, H., 2016a. Comparison of image annotation data generated by multiple investigators for benthic ecology. Marine Ecology Progress Series 552, 61–70. https://doi.org/10.3354/meps11775

Durden, J.M., Schoening, T., Althaus, F., Friedman, A., Garcia, R., Glover, A.G., Greinert, J., Jacobsen-Stout, N., Jones, D.O.B., Jordt, A., Kaeli, J., Koser, K., Kuhnz, L., Lindsay, D., Morris, K., Nattkemper, T.W., Osterloff, J., Ruhl, H., Singh, H., Tran, M., Bett, B.J., 2016b. Perspectives in visual imaging for marine biology and ecology: from acquisition to understanding. Oceanography and Marine Biology An Annual Review, Oceanography and Marine Biology - An Annual Review 54, 1–72. https://doi.org/10.1201/9781315368597

FAO (Ed.), 2009. International guidelines for the management of deep-sea fisheries in the high seas: = Directives internationales sur la gestion de la pêche profonde en haute mer. Food and Agriculture Organization of the United Nations, Rome.

Fontaine, B., Perrard, A., Bouchet, P., 2012. 21 years of shelf life between discovery and description of new species. Current Biology 22, R943–R944. https://doi.org/10.1016/j.cub.2012.10.029

Grassle, J.F., Sanders, H.L., Hessler, R.R., Rowe, G.T., McLellan, T., 1975. Pattern and zonation: a study of the bathyal megafauna using the research submersible Alvin. Deep Sea Research and Oceanographic Abstracts 22, 457–481. https://doi.org/10.1016/0011-7471(75)90020-0

Hagedorn, G., Rambold, G., Martellos, S., 2010. Types of identification keys 6.

Henry, L.-A., Roberts, J.M., 2014. Recommendations for best practice in deep-sea habitat classification: Bullimore et al. as a case study. ICES Journal of Marine Science 71, 895–898. https://doi.org/10.1093/icesjms/fst175

Howell, K.L., Bullimore, R.D., Foster, N.L., 2014. Quality assurance in the identification of deep-sea taxa from video and image analysis: response to Henry and Roberts. ICES Journal of Marine Science 71, 899–906. https://doi.org/10.1093/icesjms/fsu052

Howell, K.L., Davies, J.S., Allcock, A.L., Braga-Henriques, A., Buhl-Mortensen, P., Carreiro-Silva, M., Dominguez-Carrió, C., Durden, J.M., Foster, N.L., Game, C.A., Hitchin, B., Horton, T., Hosking, B., Jones, D.O.B., Mah, C., Laguionie Marchais, C., Menot, L., Morato, T., Pearman, T.R.R., Piechaud, N., Ross, R.E., Ruhl, H.A., Saeedi, H., Stefanoudis, P.V., Taranto, G.H., Thompson, M.B., Taylor, J.R., Tyler, P., Vad, J., Victorero, L., Vieira, R.P., Woodall, L.C., Xavier, J.R., Wagner, D., 2019. A framework for the development of a global standardised marine taxon reference image database (SMarTaR-ID) to support image-based analyses. PLOS ONE 14, e0218904. https://doi.org/10.1371/journal.pone.0218904

Hoyoux, C., Zbinden, M., Samadi, S., Gaill, F., Compère, P., 2012. Diet and gut microorganisms of Munidopsis squat lobsters associated with natural woods and mesh-enclosed substrates in the deep South Pacific. Marine Biology Research 8, 28–47. https://doi.org/10.1080/17451000.2011.605144

Jouet, G., Deville, E., 2015. PAMELA-MOZ04 cruise, RV Pourquoi pas ?,. https://doi.org/10.17600/15000700

Katzschmann, R.K., DelPreto, J., MacCurdy, R., Rus, D., 2018. Exploration of underwater life with an acoustically controlled soft robotic fish. Sci. Robot. 3, eaar3449. https://doi.org/10.1126/scirobotics.aar3449

Komai, T., Chan, T.-Y., 2013. New records of Glyphocrangon A. Milne-Edwards, 1881 (Crustacea, Decapoda, Caridea, Glyphocrangonidae) from recent French expeditions off the Mozambique Channel and Papua New Guinea, with description of one new species. Mémoires du Muséum national d'Histoire naturelle (1993).

Krell, F.-T., 2004. Parataxonomy vs. taxonomy in biodiversity studies – pitfalls and applicability of 'morphospecies' sorting. Biodiversity and Conservation 13, 795–812. https://doi.org/10.1023/B:BIOC.0000011727.53780.63

Kroh, A., Smith, A.B., 2010. The phylogeny and classification of post-Palaeozoic echinoids. Journal of Systematic Palaeontology 8, 147–212. https://doi.org/10.1080/14772011003603556

Langenkämper, D., Zurowietz, M., Schoening, T., Nattkemper, T.W., 2017. BIIGLE 2.0 - Browsing and Annotating Large Marine Image Collections. Frontiers in Marine Science 4. https://doi.org/10.3389/fmars.2017.00083

Laschi, C., Calisti, M., 2021. Soft robot reached the deepest part of the ocean. Nature 591, 35–36. https://doi.org/10.1038/d41586-021-00297-4

Legendre, P., 2014. Interpreting the replacement and richness difference components of beta diversity: Replacement and richness difference components. Global Ecology and Biogeography 23, 1324–1334. https://doi.org/10.1111/geb.12207

Legendre, P., Gallagher, E.D., 2001. Ecologically meaningful transformations for ordination of species data. Oecologia 129, 271–280. https://doi.org/10.1007/s004420100716

Levin, L.A., 2005. Ecology of cold seep sediments: interactions of fauna with flow, chemistry and microbes 46.

Levin, L.A., Le Bris, N., 2015. The deep ocean under climate change. Science 350, 766–768. https://doi.org/10.1126/science.aad0126

Levin, L.A., Sibuet, M., 2012. Understanding Continental Margin Biodiversity: A New Imperative. Annual Review of Marine Science 4, 79–112. https://doi.org/10.1146/annurev-marine-120709-142714

Mah, C., 2007. Phylogeny of the Zoroasteridae (Zorocallina; Forcipulatida): evolutionary events in deep-sea Asteroidea displaying Palaeozoic features. Zoological Journal of the Linnean Society 150, 177–210. https://doi.org/10.1111/j.1096-3642.2007.00291.x

Mah, C.L., 2020. New species, occurrence records and observations of predation by deep-sea Asteroidea (Echinodermata) from the North Atlantic by NOAA ship Okeanos Explorer. Zootaxa 4766, 201–260. https://doi.org/10.11646/zootaxa.4766.2.1

McClain, C.R., Lundsten, L., Ream, M., Barry, J., DeVogelaere, A., 2009. Endemicity, Biogeography, Composition, and Community Structure On a Northeast Pacific Seamount. PLoS ONE 4, e4141. https://doi.org/10.1371/journal.pone.0004141

Nybakken, J., Craig, S., Smith-Beasley, L., Moreno, G., Summers, A., Weetman, L., 1998. Distribution density and relative abundance of benthic invertebrate megafauna from three sites at the base of the continental slope off central California as determined by camera sled and beam trawl. Deep Sea Research Part II: Topical Studies in Oceanography 45, 1753–1780. https://doi.org/10.1016/S0967-0645(98)80016-7

Obura, D., 2012. The Diversity and Biogeography of Western Indian Ocean Reef-Building Corals. PLoS ONE 7, e45013. https://doi.org/10.1371/journal.pone.0045013

Obura, D., Church, J., Gabrié, C., Macharia, D., 2012. Assessing Marine World Heritage from an Ecosystem Perspective: The Western Indian Ocean 125.

O'Hara, T.D., Hugall, G., Andrew F., Woolley, S.N.C., Bribiesca-Contreras, G., Bax, N.J., 2019. Contrasting processes drive ophiuroid phylodiversity across shallow and deep seafloors 18.

O'Hara, T.D., Williams, A., Woolley, S.N.C., Nau, A.W., Bax, N.J., 2020. Deep-sea temperate-tropical faunal transition across uniform environmental gradients. Deep Sea Research Part I: Oceanographic Research Papers 161, 103283. https://doi.org/10.1016/j.dsr.2020.103283

Oksanen, J., Blanchet, F.G., Friendly, M.K., Legendre, P., McGlinn, D., 2019. vegan: Community Ecology Package. R package version 2.5-6.

Olu, K., 2014. PAMELA-MOZ01 cruise, RV L'Atalante. https://doi.org/10.17600/14001000

Pante, E., Corbari, L., Thubaut, J., Chan, T.-Y., Mana, R., Boisselier, M.-C., Bouchet, P., Samadi, S., 2012. Exploration of the Deep-Sea Fauna of Papua New Guinea. Oceanography 25. https://doi.org/10.5670/oceanog.2012.65

Pante, E., Watling, L., 2012. Chrysogorgia from the New England and Corner Seamounts: Atlantic–Pacific connections. Journal of the Marine Biological Association of the United Kingdom 92, 911–927. https://doi.org/10.1017/S0025315411001354

Payri, C., Archambault, P., Samadi, S., 2012. MADANG 2012 cruise, RV Alis. https://doi.org/10.17600/18000841

Pomponi, S.A., 2016. Emerging Technologies for Biological Sampling in the Ocean. National Ocean Exploration Forum 2016.

R Core Team, 2020. R: A language and environment for statistical computing. Vienna: R Foundation for Statistical Computing.

Ramirez-Llodra, E., Tyler, P.A., Baker, M.C., Bergstad, O.A., Clark, M.R., Escobar, E., Levin, L.A., Menot, L., Rowden, A.A., Smith, C.R., Van Dover, C.L., 2011. Man and the Last Great Wilderness: Human Impact on the Deep Sea. PLoS ONE 6, e22588. https://doi.org/10.1371/journal.pone.0022588

Rice, A., Aldred, R., Darlington, E., Wild, R., 1982. The quantitative estimation of the deep-sea megabenthos - a new approach to an old problem. Oceanologica Acta 5, 63–72.

Robert, K., Jones, D., Huvenne, V., 2014. Megafaunal distribution and biodiversity in a heterogeneous landscape: the iceberg-scoured Rockall Bank, NE Atlantic. Marine Ecology Progress Series 501, 67–88. https://doi.org/10.3354/meps10677

Samadi, S., Corbari, L., 2010. BIOPAPUA cruise, RV Alis. https://doi.org/10.17600/10100040

Samadi, S., Puillandre, N., Pante, E., Boisselier, M.-C., Corbari, L., Chen, W.-J., Maestrati, P., Mana, R., Thubaut, J., Zuccon, D., Hourdez, S., 2015. Patchiness of deep-sea communities in Papua New Guinea and potential susceptibility to anthropogenic disturbances illustrated by seep organisms. Marine Ecology 36, 109–132. https://doi.org/10.1111/maec.12204

Saucède, T., Eléaume, M., Jossart, Q., Moreau, C., Downey, R., Bax, N., Sands, C., Mercado, B., Gallut, C., Vignes-Lebbe, R., 2020. Taxonomy 2.0: computer-aided identification tools to assist Antarctic biologists in the field and in the laboratory. Antarctic Science 1–13. https://doi.org/10.1017/S0954102020000462

Schlacher, T.A., Williams, A., Althaus, F., Schlacher-Hoenlinger, M.A., 2010. High-resolution seabed imagery as a tool for biodiversity conservation planning on continental margins: Submarine canyon megabenthos and conservation planning. Marine Ecology 31, 200–221. https://doi.org/10.1111/j.1439-0485.2009.00286.x

Schönberg, C.H.L., 2021. No taxonomy needed: Sponge functional morphologies inform about environmental conditions. Ecological Indicators 129. https://doi.org/https:DDdoi.orgD10.101BDj.ecolind.2021.107A0B

Schönberg, C.H.L., Fromont, J., 2014. (PDF) Sponge functional growth forms as a means for classifying sponges without taxonomy [WWW Document]. ResearchGate. URL https://www.researchgate.net/publication/278627643_Sponge_functional_growth_forms_as_a_means_for_classifying_sponges_without_taxonomy (accessed 6.22.20).

Sibuet, M., Olu, K., 1998. Biogeography, biodiversity and fluid dependence of deep-sea cold-seep communities at active and passive margins. Deep Sea Research Part II: Topical Studies in Oceanography 45, 517–567. https://doi.org/10.1016/S0967-0645(97)00074-X

Sigovini, M., Keppel, E., Tagliapietra, D., 2016. Open Nomenclature in the biodiversity era. Methods Ecol Evol 7, 1217–1225. https://doi.org/10.1111/2041-210X.12594

Tappin, D.R., Watts, P., McMurtry, G.M., Lafoy, Y., Matsumoto, T., 2001. The Sissano, Papua New Guinea tsunami of July 1998 – offshore evidence on the source mechanism. Marine Geology 23.

Thomassin, B., 1977. BENTHEDI I cruise, RV Le Suroît. https://doi.org/10.17600/77003111

Todd, P.A., 2008. Morphological plasticity in scleractinian corals. Biological Reviews 83, 315–337. https://doi.org/10.1111/j.1469-185X.2008.00045.x

Tregoning, P., McQueen, H., Lambeck, K., Jackson, R., Little, R., Saunders, S., Rosa, R., 2000. Present-day crustal motion in Papua New Guinea. Earth Planet Sp 52, 727–730. https://doi.org/10.1186/BF03352272

Tyler, P.A. (Ed.), 2003. Ecosystems of the Deep Oceans. Elsevier.

Van Dover, C., 2012. Hydrothermal Vent Ecosystems and Conservation. oceanog 25, 313–316. https://doi.org/10.5670/oceanog.2012.36

Veron, J.E.N., Devantier, L.M., Turak, E., Green, A.L., Kininmonth, S., Stafford-Smith, M., Peterson, N., 2009. Delineating the Coral Triangle. Galaxea, Journal of Coral Reef Studies 11, 91–100. https://doi.org/10.3755/galaxea.11.91

Vieira, P.E., Lavrador, A.S., Parente, M.I., Parretti, P., Costa, A.C., Costa, F.O., Duarte, S., 2021. Gaps in DNA sequence libraries for Macaronesian marine macroinvertebrates imply decades till completion and robust monitoring. Divers Distrib 27, 2003–2015. https://doi.org/10.1111/ddi.13305

Walter, D.E., Winterton, S., 2007. Keys and the Crisis in Taxonomy: Extinction or Reinvention? Annual Review of Entomology 52, 193–208. https://doi.org/10.1146/annurev.ento.51.110104.151054

Warnes, R.G., Bolker, B., Bonebakker, L., Gentleman, R., Huber, Liaw, A., 2020. gplots: Various R Programming Tools for Plotting Data. R package version 3.1.0.

Williams, A., Althaus, F., Schlacher, T.A., 2015. Towed camera imagery and benthic sled catches provide different views of seamount benthic diversity: Gear selectivity for seamount benthos. Limnology and Oceanography: Methods 13, e10007. https://doi.org/10.1002/lom3.10007

Wudrick, A., Beazley, L., Culwick, T., Goodwin, C., Cárdenas, P., Xavier, J., Kenchington, E., 2020. A pictorial guide to the epibenthic megafauna of Orphan Knoll (northwest Atlantic) identified from in situ benthic video footage 161.

Zawada, K.J.A., Madin, J.S., Baird, A.H., Bridge, T.C.L., Dornelas, M., 2019. Morphological traits can track coral reef responses to the Anthropocene. Functional Ecology. https://doi.org/10.1111/1365-2435.13358

I.7 Supplementary materials

The Supplementary Materials for this article can be found online at:

https://www.frontiersin.org/articles/10.3389/fmars.2021.749078/full#supplementary-material

Supplementary material I.1 : Details of the working steps followed in the process of fauna identification from images

1. Non-expert annotation processing

First, we delimited each faunal observation as an individual to be identified within images (segmentation). In the context of biodiversity metrics comparison between physical sampling and imagery, we conserved all images annotated for analyses, even some poor-quality images (i.e., too dark or light, too low or high relative to the sea bottom) to compare all the taxonomic groups and identification ranks accessible from images compare to samples. In PNG area, the pool of poor-quality images represents 1.6% of the dataset while in Mayotte, it represents 7%.
Second, each individual was assigned a label corresponding to a high taxonomic classification rank from phylum to class. These classifications and identifications relied on objective observations of morphological features that are diagnostic of each high-ranking taxonomic group and do not require advanced taxonomic skills. Non-recognizable individuals, even at a phylum rank were dismissed and attributed an “Animalia cetera” label.
To facilitate more precise identifications in collaboration with taxonomists, we delimited preliminary morphotypes for some taxonomic groups based on observations of similar morphological features between individuals to be identified from images and photos of collected specimens.

2. Objective identification processing

In step three, in collaboration with taxonomists, we evaluated the morphotypes/high-rank taxonomic groups on the basis of objective morphological characters that can be observed in images. These characters correspond to diagnostic characters (i.e., characters differentiating taxa), allowing the identification of individuals at a taxonomic rank N with certainty. Therefore, each set of individuals sharing the same diagnostic characters was defined as a photo-taxon (i.e., a set of individuals classified into the same taxonomic entity) and then assigned to a taxonomic rank N (e.g., genus rank).
The photo-taxon concept was originally proposed to divide organisms in images into operational taxonomic units (OTU) (used by Williams et al. (2015) and defined in Althaus et al. (2009)). Like morphospecies, these OTUs may be difficult to associate with a valid name, particularly at the species level. The photo-taxa are thus associated with different taxonomic ranks.
Individual organisms whose images showed blurred characters that did not allow an assessment of their morphological characters remained labelled at a high taxonomic rank only (e.g., phylum, class).
In order to specify the identification of a photo-taxon at a lower rank, some poor-quality images (blurriness, view angle, missing characters) had to been set aside. In this case, we added the qualifier “indeterminabilis” to the rank assigned to the photo-taxon, which is consistent with open nomenclature proposed by Sigovini et al. (2016) and more recently adapted by Horton et al. (2021) for image-based identification. The remaining good quality images of the photo-taxon were used to precise its identification rank.

3. Contextual identification processing

In step four, we proceeded with a contextual identification, meaning that photo-taxa assigned to a reliable taxonomic rank N in images were specified at a lower taxonomic rank (N+1) from contextual elements. These elements are based on the knowledge of taxa collected in the study area and potentially similar to the specimens to be identified in images. They reflect the experts' knowledge and data from the literature, and consider: (1) the morphological characters of collected species/taxa that we can compare with individuals to be identified in images; (2) the ecology of the species/taxa in the study area (depth range, suitable substrate, preferred prey, species association, position relative to substrate, etc.); (3) character variability (intraspecific polymorphism, interspecific convergence of characters) and (4) species distribution and diversity level (e.g., number of known species within a genus, number of known genus within a family, etc.).
For each photo-taxon identified at a given taxonomic rank N, we computed the list of the known taxa attributed to this name (e.g., if the photo-taxon is attributed to a genus name, then we listed all the species belonging to this genus, in the physical samples analyzed in this study and from physical sampling undertaken during previous cruises in the region). For each photo-taxon, the set of identified physical specimens allowed us to evaluate the characters that might be used on the images to refine the identification of the photo-taxon. This step resulted in defining a sequence of suitable diagnostic characters for image-based identification. Potential species whose diagnostic characters did not match those in the images of the photo-taxon to be identified were eliminated from the list.
By elimination, we were able to refine the identification of photo-taxa to lower taxonomic levels. Either photo-taxa were assigned to a valid name of rank N+1 (corresponding to the name of the most likely taxon) or it was not possible to assign a valid species name or morphospecies. We delimited morphospecies when, for a photo-taxon identified at a reliable rank N, the observation among individuals belonging to this photo-taxon allowed the differentiation of two or more subsets, based on the observation of characters that are known to be not shared within a single species. However, most often, observable characters were not sufficient to attribute a valid name to these species.

4. Identification key construction

We selected good-quality images that were illustrative of the identified photo-taxon at rank N or N+1 (when finer identification was possible). This set of identified images was considered as a reference in the identification process and is referred to as photo-types. The catalog of photo-types could be easily built with the Annotation catalog option proposed by BIIGLE 2.0 allowing a mosaic view of the different photo-taxa for each taxonomic entity (label).
Lastly, we compiled the diagnostic characters used to identify photo-taxa, and classified them into distinct modalities to construct identification keys. Based on photo-types and the knowledge of diagnostic characters, it was possible to identify the remaining photo-taxa.

Supplementary material I.2 : Decapoda identification key adapted for deep-sea images

Shrimps, prawns and lobsters in the Mozambique Channel: image-based identification key.

(0a) Body laterally compressed. Antennal flagella thin and thread-like. Telson posteriorly pointed. Mostly swimming in the water column, pleopods very long and extending laterally. Antennal scale very broad and elongate, often extended laterally (i.e., "V" shape quite visible).

Dendrobranchiata* (1)

*Third pereiopod with chela, second abdominal pleuron overlapping first abdominal pleuron, never carrying eggs.

(0b) Body generally laterally compressed. Antennal flagella thin and thread-like. Telson posteriorly pointed. Mostly walk near or on the bottom. Antennal scale and pleopods not extending laterally.

Pleocyemata (Caridea) (10)

***Third pereiopod without chela, second abdominal pleuron not overlapping first abdominal pleuron, carrying eggs after spawning.**

(0c) Body dorsoventrally compressed. Antennae thick and whip-like. Telson posteriorly truncated. Mostly walk near or on the bottom. Thick, strong cylindrical carapace covered with many spines/granules. Moderate to large body size. Absence of prominent rostrum. Pereiopods simple, without claws (end with a simple curved dactyl). Eyes protected by two strong frontal horns (frontal projections of the carapace).

Achelata (Palinuridae) (21)

(1a) Always black eyes (be careful, sometimes with golden reflection from underwater lighting for photography), rostrum long.

2

(1b) Eyes black or white, rostrum short (shorter than eyes, with only one or two, occasionally three, rostral/postrostral teeth), shell soft, thin. Body orange to red and with no distinct banding, upper antennular flagella long.

Benthesycimidae (*Benthesycimus*)

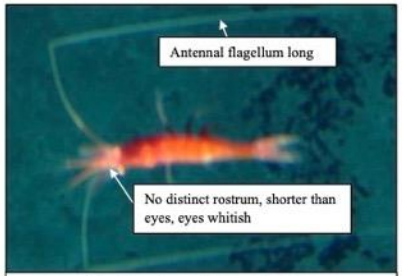

Benthesycimus indeterminabilis

(2a) Upper antennular flagella short, cervical groove often not to upper carapace. Body and antennal flagella always red/orange.

Aristeidae (3)

(3b) Upper antennular flagella long, cervical groove (can be difficult to see from images) long and extending to or near to upper carapace. Body pink to pale orange, antennal flagella white.

8

(3a) Body yellow/light orange. Presence of one elongated overhanging spine on third abdominal somite.

Hemipenaeus

Hemipenaeus indeterminabilis

2

(3b) Body red to orange, abdominal somites with posterior spines but never with elongated overhanging spine on third somite.

4

(4a) Body moderately robust, red to pale pink and often banded, sometimes with distinct purple color. Occurred in 300-1200 m depth.

***Aristeus* (6)**

Aristeus indeterminabilis

(4b) Body very robust, dark red and deep red color, no banding on the abdomen.

5

3

Supplementary Material

(5a) Carinae and grooves on carapace long and very distinct. Abdomen only with small posterior spines. Exopod of second maxilliped fringed by double row of long setae which give it a feathery characteristic.

Aristaeopsis edwardsiana

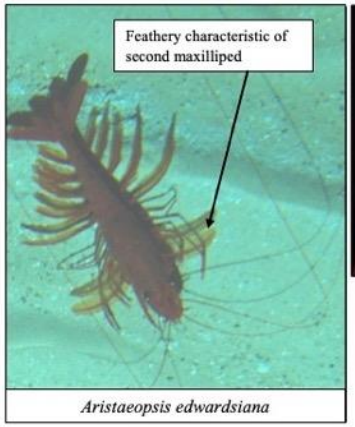

Aristaeopsis edwardsiana

* Only species of the genus *Aristaeopsis*, depth range 500m-1500m.

(5b) Carapace without long distinct grooves and carinae. Abdomen with three large posterior spines.

Cerataspis monstrosus

4

(6a) Purple/pink bands color pattern, unique character of the species.

Aristeus mabahissae

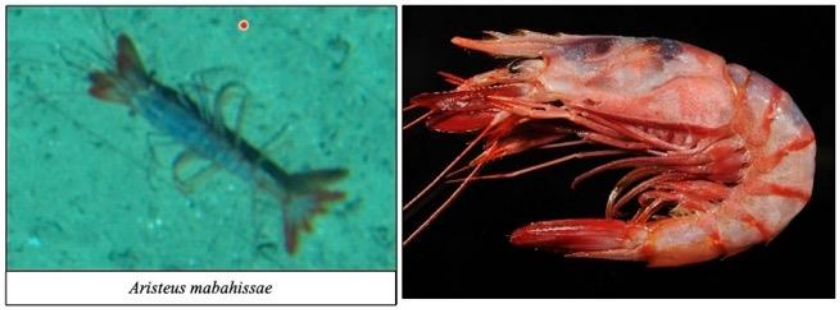

Aristeus mabahissae

(6b) Body red to orange, sometimes with banding but never with purple color.

7

(7a) Body hairy with rough-looking cuticle.

Aristeus virilis

5

(7b) Body smooth and shiny.

Aristeus antennatus

(8a) Cervical groove reaching dorsal carapace. Rostrum broad and crest-like.

Solenoceridae (*Haliporoides*) (9)

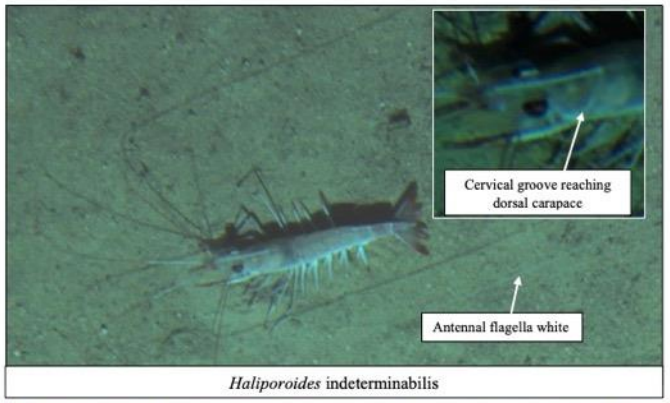

Haliporoides indeterminabilis

*Four species in the *Haliporoides* genus that correspond to subspecies with specific geographic range, and only two are restrictive to the Mozambique Channel/Madagascar area.

(8b) Cervical groove not reaching dorsal carapace. Rostrum thin and not crest-like.

Penaeidae (*Penaeopsis*)

Penaeopsis indeterminabilis

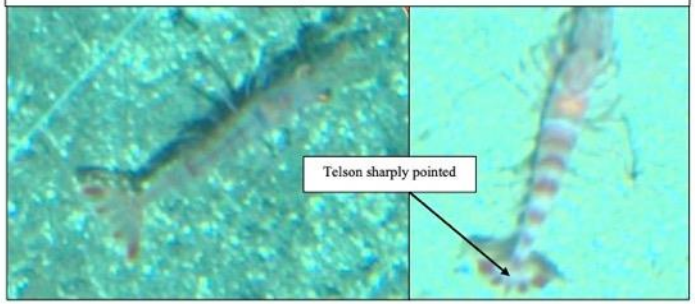

6

Penaeopsis balssi

Four species of *Penaeopsis* in this area: *P. balssi, P. eduardoi, P. jerryi* and *P. rectacuta*. These species are very similar (mainly differences in the petasma and thelycum) and only *P. balssi* differs from the other three in the rostrum distinctly convex and curving downwards, others more or less straight.

(9a) Curved and thinner rostrum (lateral view needed). White dot at tip of uropods.

Haliporoides sibogae

(9b) Rostrum thicker and less curved, no white dots at tip of uropods.

Haliporoides trihartrus

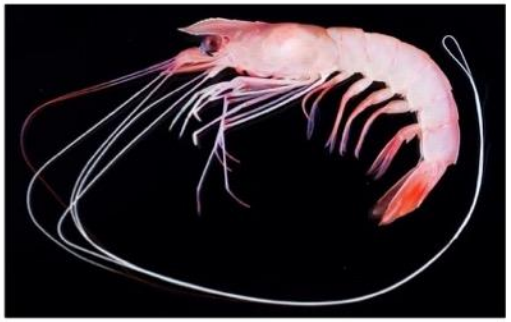

(10a) Body dorsoventrally depressed, abdomen sculptured. Postantennal spines large and expanded. Rostrum thick on top view.

Glyphocrangonidae (*Glyphocrangon*)* (11)

*Potentially two groups: large black eyes one (potentially yellow eyes resulting from reflection effect of the underwater image but high light reflection effect can indicate presence of big black eyes) and small white eyes one. Various color pattern, band abdomen or not. Only one genus: *Glyphocrangon*.

(10b) Body more laterally compressed, abdomen not sculptured. Postantennal spines absent or minute.

12

(11a) Postantennal spines more or less parallel, not distinctly directly outwards.

Glyphocrangon crosnieri*

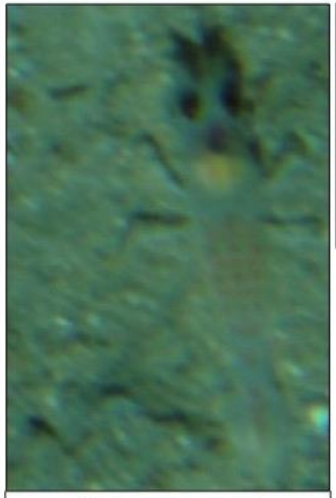

Glyphocrangon crosnieri

(11b) Postantennal spines widely directed outwards (extended spine quite visible on each side of the carapace frontal part).

Glyphocrangon amblytes*

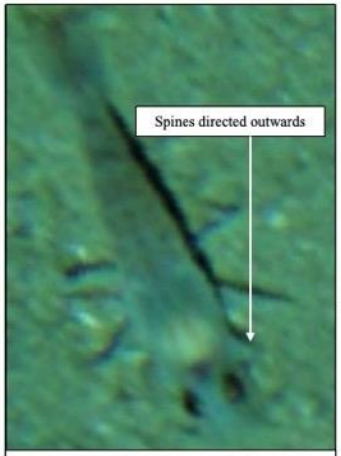

Glyphocrangon amblytes

* Orange band pattern on the abdomen for both species.

(12a) Body strongly laterally compressed, all red body color pattern, no banding, potentially white eyes or black eyes, often swimming (pleopods not so long and distinct, do not confuse with dendrobranchiata red shrimp families).

Acanthephyridae (13)

(12b) Body not strongly laterally compressed, various color pattern and sometimes banding, eyes always black. Walking on the bottom.

15

(13a) Always black eyes.

***Acanthephyra* (14)**

(13b) White eyes, very short rostrum, no long pleopods, red body, bentho-pelagic, similar to Benthesycimidae. No clear image of this photo-taxon.

Hymenodora

(14a) Only one ventral rostral tooth.

Acanthephyra armata

(14b) Three to eight ventral rostral teeth.

Acanthephyra eximia

(15a) Pereiopods not extremely long, rostrum often very long, well developed (but sometimes short), often sabre-like, slightly to strongly curved upwards, with ventral and dorsal rostral teeth.

Pandalidae* (16)

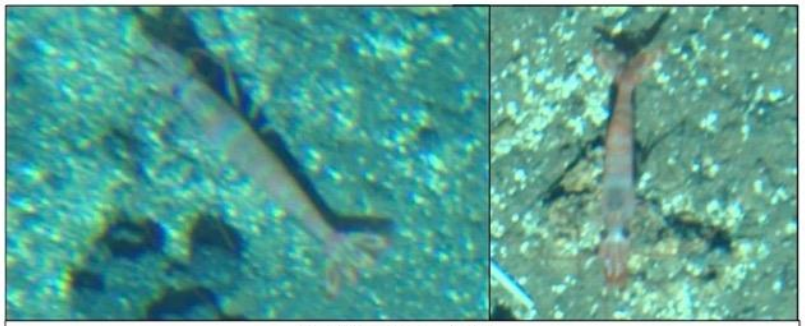

Pandalidae indeterminabilis

*Blue eggs sometimes visible, characteristic of the family. Observed sometimes with red rostrum tip.

(15b) Pereiopods extremely long and extending from both sides, spider-like, rostrum usually short (more or less as long as antennular peduncle).

Nematocarcinidae (*Nematocarcinus) (20)**

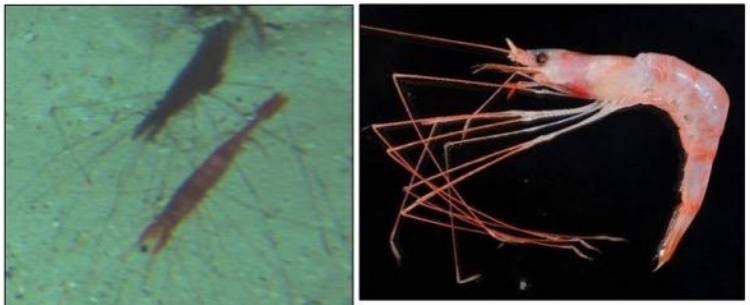

Nematocarcinus indeterminabilis

*Only single genus *Nematocarcinus* distributed in 500-2000 m depth. Band pattern, some are pink, some are red. Potentially five species in the area of the Mozambique Channel with grey/orange/light purple body color pattern (discriminant species character). Presence of band or not. Rostrum short or long (discriminant species pattern). Image observation show them with the sixth abdominal segment very compressed, and uropods with a rectangular shape.

(16a) Body robust, eyes always rounded, carapace with distinct lateral carinae (varies from two-three), some species with large spines on the abdomen. Body never with distinct white dots.

***Heterocarpus* (17)**

(16b) Body often elongate, eye sometimes elongate (kidney-shaped) and extended laterally, carapace without lateral carina, abdomen never with large spines. Body sometimes with distinct white dots/lines. Large to small specimens.

***Plesionika* (19)**

Plesionika indeterminabilis

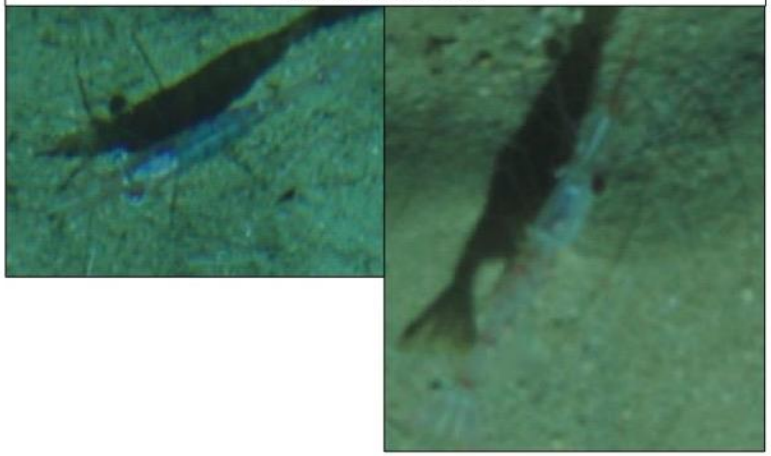

(17a) Body pink to light orange

Heterocarpus Lepidus*

Heterocarpus lepidus

* With dorsal rostral teeth throughout, shallower species (Depth: 300-700m).

(17b) Body red to light orange.

(18a) Dorsal margin of rostrum toothed at base only. Body red to orange, with red vertical stripes on the abdomen between somites. Occur in 500-1000 m depth.

Heterocarpus laevigatus

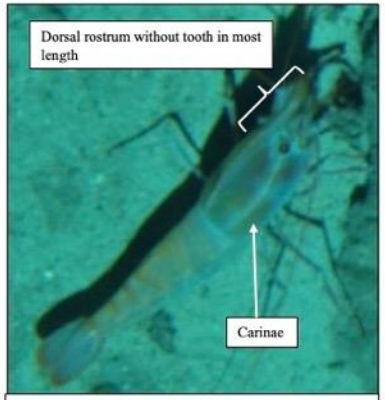

Heterocarpus laevigatus

(18b) With dorsal teeth on rostrum. Body reddish. Occur from more than 1000 m depth (deeper species).
Photo-taxon not identified

Heterocarpus tricarinatus

(19a) Body more or less banded.

Plesionika semilaevis*

*Eyes kidney-shaped. Depth range: 100-700m.

(19b) Body not banded.

Plesionika martia*

*Eyes kidney-shaped. Depth range: 100-700m.

(20a) Five white/red band color pattern on the abdomen.

***Nematocarcinus* sp1**

Nematocarcinus sp1

(20b) Abdomen not banded. Orange body color pattern.

***Nematocarcinus* sp2**

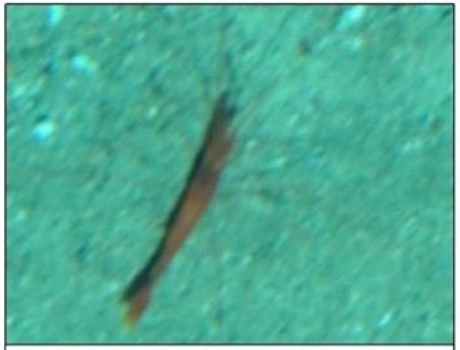

Nematocarcinus sp2

****All the above are soft bottom species.**

(21) Carapace with median ridge bearing large spines behind cervical groove. Abdomen with complex sculpture. Pleura terminating ventrally in two strong teeth (observable from images, giving laterally on the abdomen white spiny appearance at the end of each abdomen segment). Posterior half of the tail fan soft and flexible.

***Puerulus** (22)**

*Occurs mainly from 200 to 700 m deep in the Indo-West Pacific: Western Indian Ocean: Zanzibar, Mozambique, Natal (South Africa), Madagascar, Saya de Malha Bank.

(22a) Sparsely pubescent and with some darker surface granules. Pereiopods whitish. Abdomen mostly orange-pink with sunken areas pale pink/whitish. Eyes black/brown and antennal flagella uniformly orange/pink. Base of antennular peduncle with distinct white spots. Two large and sharp supraorbital horns (frontal horns) distant far apart from each other (followed by two small teeth difficult to observe from images). Tips, posterior bases of frontal horns as well as median area between frontal horns are whitish. Three distinct white dots on median ridge behind cervical groove.

Puerulus carinatus*

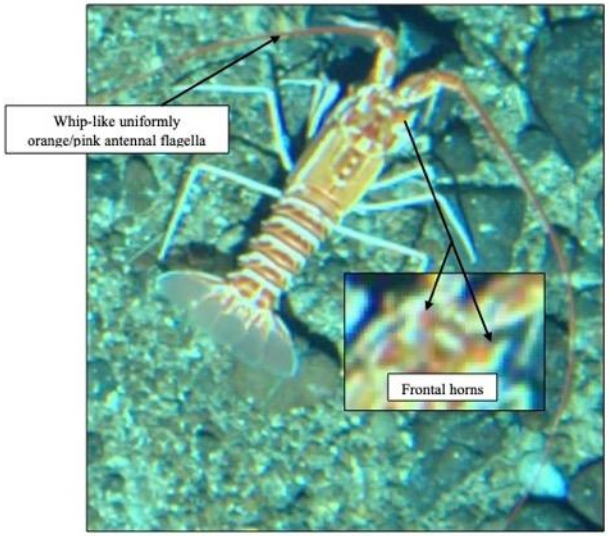

(22b) Moderately pubescent with distinct granules. Pereiopods, antennular flagella and the soft part of tail fan are pale pink to light orange. Body with a red/white mosaic color pattern. Eyes black/brown and antennal flagella banded red/white. Frontal horns short followed by three teeth (difficult to observe from images).

Puerulus gibbosus*

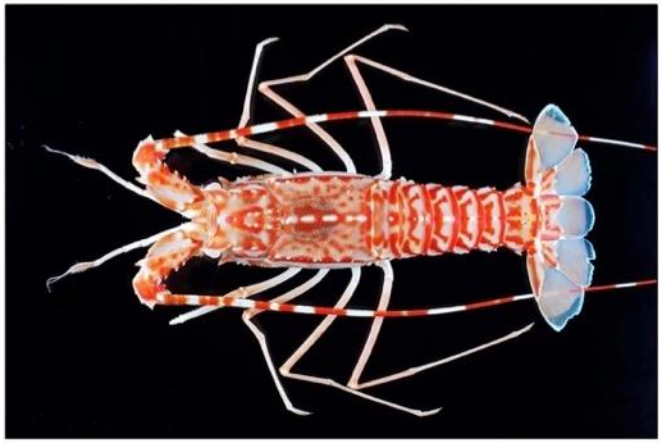

* Only *P. carinatus* and *P. gibbosus* are found in the southwestern Indian Ocean. *P.carinatus* is less common. Both species can be distinguished from their coloration: *P. carinatus* is mainly with reddish/orange body color and homogeneous antennal flagella while *P. gibbosus* has a red/white mosaic color pattern and the antennal flagella banded.

Supplementary material I.3 : Asteroidea identification key adapted for deep-sea images

Asteroids in the Mozambique Channel: image-based identification key.

Vocabulary: R = length from disk center to armtip / r = length from disk center to edge of the disk

(0) Arms 6 or more, extremely elongate (R/r =>10) when observed in situ often extended into water current (not frequently observed on substrate). Spines present along sides of arm. Disk small, arms discontinuous.

(1)

(0') Arms 5. Disk small or large, continuous with arms distinct or indistinct. Body variably stellate (i.e., arms triangular, distinct from disk) to pentagonal in shape (i.e., arms indistinct from disk).

(8)

(1) Arms moderately long, distinct, moderately thick, fleshy and elongate but R/r (ratio) less than 10, numbering 6 to 18. Lateral spines absent or present, if present not elongate but forming a rough outline along arm's ventrolateral edge in some taxa (e.g., Solasteridae). Disk small or large.

(4)

(1') Arms extremely elongate, tapering, R/r > 15.0, numbering 6 to 20. In some instances, diameter of complete organism ranges between 30 to 60 cm (1 to 2 feet). Prominent, elongate spines present extending along lateral side of arm forming serial series. When viewed in situ, arms in most observations, extended into water currents, or lifted above the surface, although arms are sometimes lying on substrate. Disk very small.

Brisingida (Brisingidae (two types) and Freyellidae) (2)

(2) Lateral spines club-shaped, prominent, but not needle-like. Papulae present on disk and arm surface. Color rich orange/red with white plates or pure orange. Arms always 12 or more. Present primarily 100-600 m settings. Difficult to identify family level without close evaluation of the specimen. Look similar to Crinoids, but for the Brisingids, the mouth face down.

Brisingaster* or *Novodinia

Brisingida indeterminabilis

(2') Lateral spines needle-like, elongate. No papulae evident. Color orange, yellow to white. Arms 6 or more, sometimes at great length (up to 60 cm). Occurring to 6000 m depths.

Freyellidae or Brisingidae (3)

(3) Arm surface covered by distinct ribs along arms.

Brisingidae

(3') Arm surface covered by flattened plates along arms, disk. In some cases, spines present along lateral surface but also abactinal surface. Color orange but also completely white in some species. One genus, *Freyastera*, consistently displays six rays (= arms).

Freyellidae

(4) Opening (= osculum, "hole") present directly center on disk. Arms 6 to 11. Surface covered by widely spaced, tissue covered paxillae/spines appearing club-shaped in. These club-shaped spines convey a "fuzzy" appearance to the surface. Skeleton with window-like spaces. Body appears thick with tapering arms. Primarily observed below 1000 m.

Myxasteridae (*Asthenactis* or *Myxaster*)

Myxasteridae indeterminabilis

(4') Osculum absent. No spines forming "fuzzy" surface. Skeleton without window-like spaces (= fenestrate).
(5)

(5) Surface covered by sharp spines, each bearing a prominent tuft of pedicellariae. These spines are arranged in regular rows along arms. Arms number 6 to 12 (8 to 10 in most Pacific species), arms either splayed out or jumbled into a big pile. Some individuals up to 25 cm diameter.

Asteriidae (*Coronaster*)

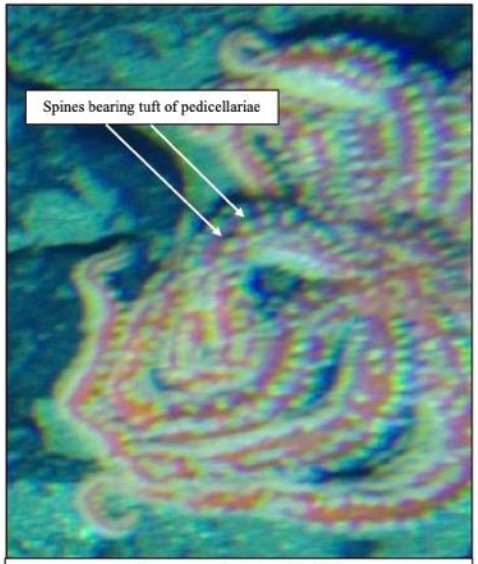

Coronaster indeterminabilis

(5') Surface with no prominent spines, although smaller present in some. Arms number 6 to 12. Body shape variable.
(6)

(6) Disk large (i.e., about 20% or more of arm length from center to arm tip), arms and body thick. Surface rough in appearance with some genera (e.g., *Crossaster*) having prominent paxillae on surface. Paxillae present around marginal periphery in some species, edge around arms is rough and appears serrated in some taxa. Arms 6 to 15, variably short to moderate in length. Predatory on sea cucumbers, sea stars and other megafauna.

Solasteridae

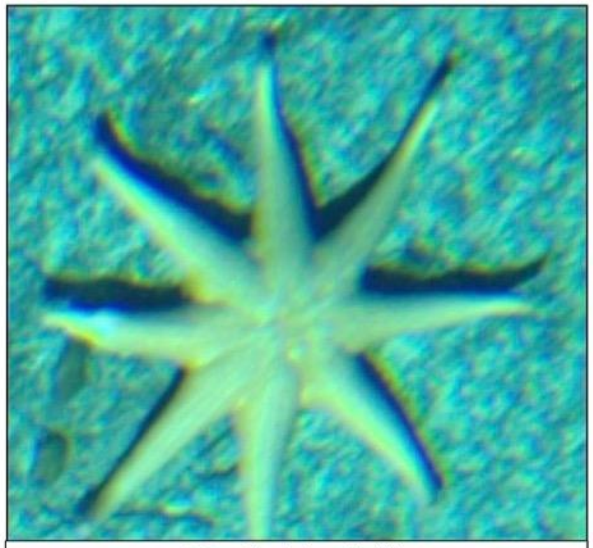

Solasteridae indeterminabilis

(6') Disk small, surface composed of smooth plates or soft surface. Arms number 6* to 8.

*5 arms possible (e.g., *Nepanthia*)

(7)

(7) Surface composed of overlapping or imbricate plates (rugged appearance, weakly visible depending on images quality). If more than 6 arms present, they are regrowing, following asexual fissiparity. Disk small, arms moderately elongated. Present at shallower depths (< 300 m). Arm tips curved, round-like, cylindrical.

Asterinidae (*Nepanthia*)

Nepanthia indeterminabilis

(7') Surface appears soft, thin body membrane. Weakly developed spines along radius present in some taxa. Disk small, arms long but narrow, elongate in one taxon. No spines around periphery. Similar to some shallow water Asteriidae. Six armed forms in abyssal deep-sea settings, seven or eight armed forms in Southern Ocean waters.

Pedicellasteridae or Paulasteriidae

No photo-taxa identified.

(8) Body form pentagonal or nearly so (R/r < 2.0). Arms weakly expressed, continuous with disk. Interradial arcs tend to be weakly curved to straight.

(9)

(8') Body form with distinct arms (R/r > 3.0), triangular to rounded, extending well away from disk. Interradial arcs curved, varying from wide to acute.

(11)

(9) Osculum (hole in disk center) absent. Body surface not appearing as such. Plates articulated, forming body surface. Peripheral (= marginal) plates present. Body shape flattened, dome-shaped or pentagonal.

(10)

(9') Osculum present, body often appears inflated or swollen due to supradorsal membrane. Surface varies from appearing rough to pillow-like or transparent. Disk and arms thick. Body shape varies from pentagonal to weakly stellate. Marginal plates not evident. No apparent plates composing body surface. Color in life varies from white to bright red or purple.

Pterasteridae ("look fat")

(Commonly encountered genera include ***Pteraster**** and ***Hymenaster****, but many more are known)

****Pteraster***: look more textured and thicker.
****Hymenaster***: softer surface, look fleshier than *Pteraster*.

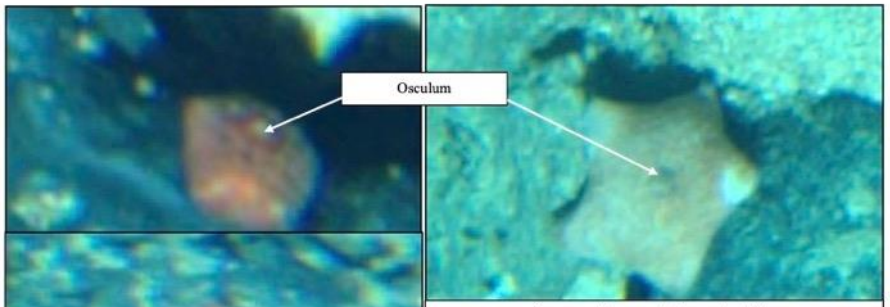

Pterasteridae sp. indeterminabilis

Pterasteridae, potentially *Pteraster* Gen. inc. sp. indet.

(10-1) Body bowl or dome-shaped, high aspect, with rim around edge. Surface composed of imbricate (overlapping) plates with 5 distinct openings on disk center. Marginal plates indistinct. In situ observations show them flush on hard substrates, variably orange to white and orange.

Asterinidae (*Tremaster mirabilis*)

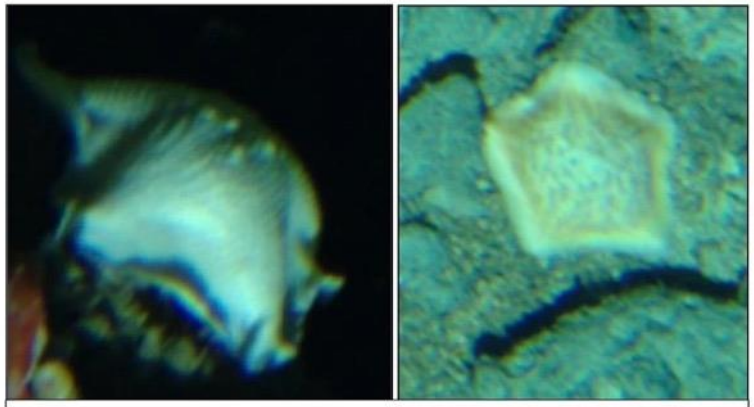

Tremaster mirabilis

(10-2) Body is flattened, sometimes extremely so, ranging from paper-thin to simply flat and thick, but with interradial arc flush with the surface (bottom).

Asterinidae (*Anseropoda or *Paranepanthia***)**

****Anseropoda:*** 5 or more short arms. Body extremely thin. Narrow mid radial bands thickened (thick bands visible in the middle of the arms). Margins straight to slightly curved.
Photo-taxon not identified.

** ***Paranepanthia**:* Arms 5, medium length, wide basally and pointed or rounded distally. Disk flat actinally and rays (arms) elevated to low. In situ observations show them flush on hard substrates.

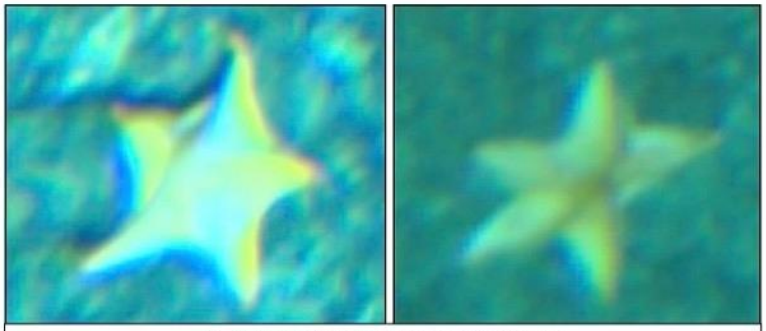

Asterinidae, potentially *Paranepanthia* Gen. inc.

(10-3) Body pentagonal or weakly stellate in shape with distinct, prominent peripheral edge. Body appears "cookie" or biscuit-shaped. Body composed of distinct plates which vary in size but are large enough to be counted from imagery in some species (e.g., *Sphaeriodiscus*). When observed alive, disk varies from flat to swollen.

Goniasteridae

("cookies" such as *Sphaeriodiscus*[1], *Plinthaster*[2], *Ceramaster, Apollonaster*, some *Astroceramus* species, etc.)

[1]***Sphaeriodiscus**:* Specimens from the South Indian Ocean observed with a color pattern of light red to dark orange interradial bands. Three species in the area*: S. biomaglo, S. ganae,* and *S. mirabilis.*

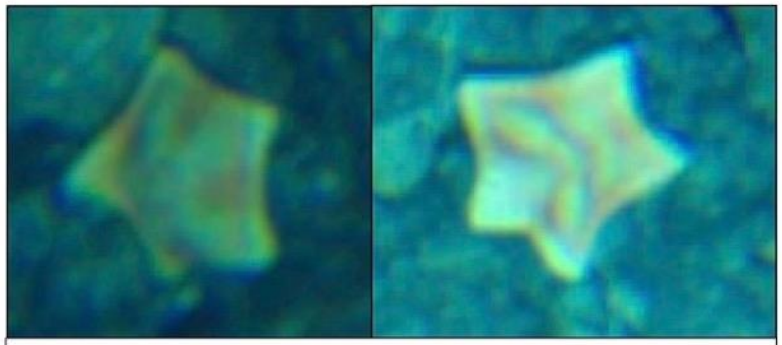

Sphaeriodiscus indeterminabilis

[2]***Plinthaster***: Disk very large, pentagonal and arms very short. Interradial arc straight. Marginal plates relatively few per interadius (6 to 8). Orange color pattern.
Nb: pentagonal-shaped or small-sized *Astroceramus* can look similar to *Plinthaster*. Small-sized *Sibogaster* can look similar to very stellate *Plinthaster.*

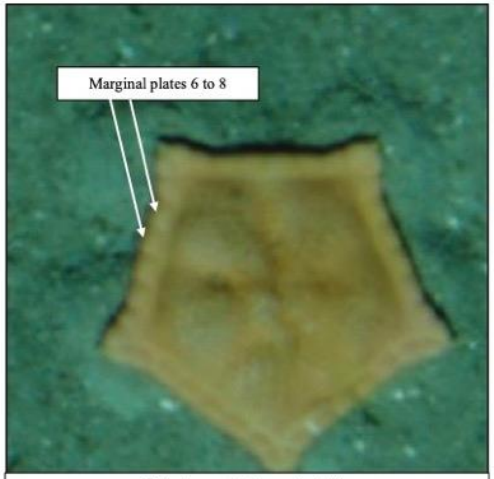

Plinthaster indeterminabilis

(11) Marginal plates indistinct, not evident from immediate viewing. Disk small with elongate arms in most taxa (R/r = 5.0 to 10.0), which are round or triangular in shape.

(14)

(11') Body with distinct peripheral frame or border (the marginal plates) present around edge of body. The marginal plates can be strongly expressed from the surface or facing laterally. Prominent spines present on marginals and/or abactinal surface in some taxa but others are bare or covered in other accessories, such as tubercles, etc. Disk large or small, arms variable in length and size.

(12)

(12) Arms not strap-like, disk thick and large. Marginal plates distinctly observed forming peripheral edge. Abactinal surface and marginal plate surfaces variably covered by spines, tubercles, granules or by no accessories. Skeleton is well-developed and many taxa display plates in distinct and ordered patterns. The most diverse group within the Asteroidea, demonstrating a wide range of habitats, from deposit feeding to predation on corals.

Goniasteridae

("stellate" shape: such as *Calliderma emma* [1], *Circeaster, Anthenoides marleyi*[2], *Lithosoma*[3], *Mediaster*[4], *Wallastra)*

[1]***Calliderma emma:*** Disk flat, arms triangular and tapering abruptly to tip.
Arm tips upturned (shadow visible under the arms). Interradial arc weakly curved to straight. Abactinal surface covered with spines over radial area and absent interradially (image observation show white stellate pattern on the abactinal surface, where the spines are located). Documented distribution in the Mozambique Channel and Pacific. Ranging around 138 to 407 m depth.

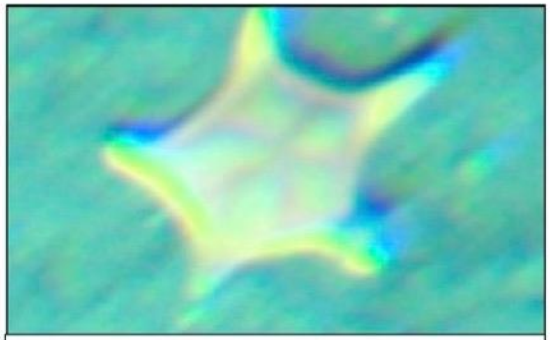

Calliderma emma sp. inc.

[2]***Anthenoides marleyi:*** Arms triangular, wide basally, pointed distally, and upturned. Interradial arcs broadly curved. Large granules button-like present on abactinal and marginal plate surfaces, giving a white stellate pattern on abactinal surface visible in the images. From images, pattern similar to *Calliderma emma*. Occurrence in South Africa, off the coast of Natal Zanzibar channel, Reunion Island, Mascarene Islands, Madagascar, north of Mayotte Island. Depth range around 183–490 m.

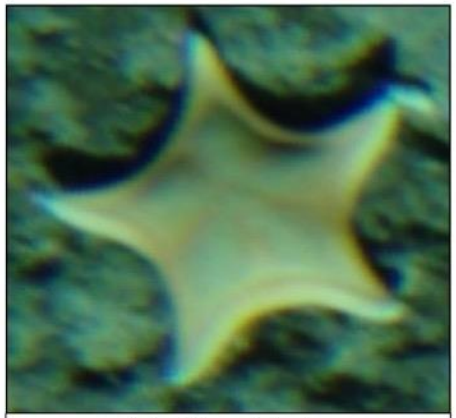

Anthenoides marleyi sp. inc.

[3]***Lithosoma:*** Body strongly stellate and flat, arms very elongate, triangular and tapering distally. Interradial arc curved. Abactinal surface with smooth/bare appearance, with no surficial accessories. Superomarginal plates abutted over midline on arms (2 series organised) along arms. Documented distribution in the Indo-Pacific Ocean regions.

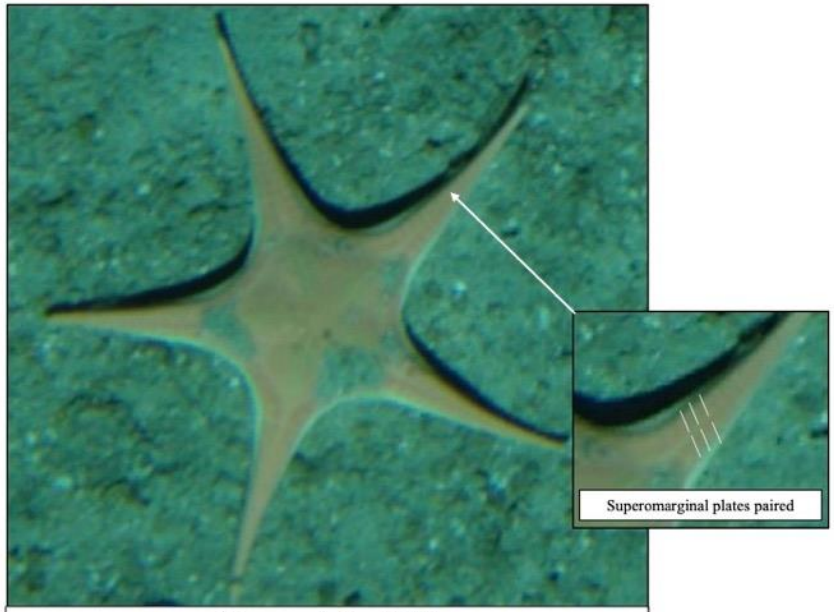

Lithosoma sp. indeterminabilis

[4]***Mediaster:*** Arms elongate with upturned or attenuated tips. Interradial arcs weakly curved to straight. Five swollen radial areas (giving five interradial marks on the abactinal surface). Abactinal, marginal, actinal surface covered by granules (Mah, 2018) (but difficult to observe from images).

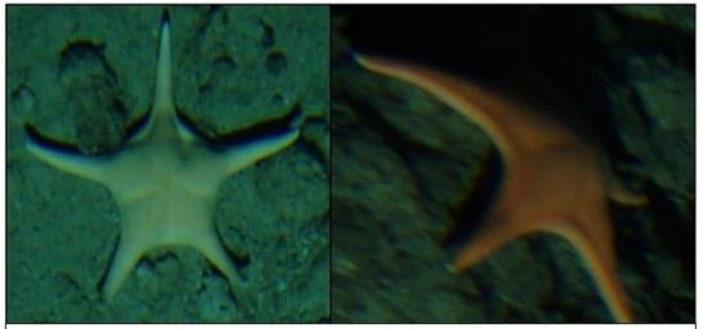

Goniasteridae indeterminabilis (*Mediaster* Gen. inc.)

Nb: Goniasteridae morphospecies identified in the area:

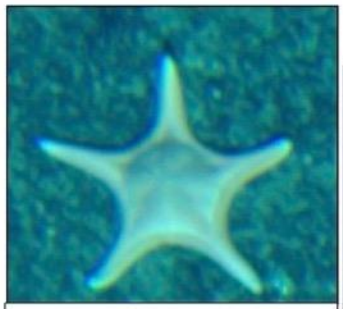

Goniasteridae sp1 (*Circeaster* Gen. inc.)

Goniasteridae sp2 (*Hippasteria* Gen. inc.)

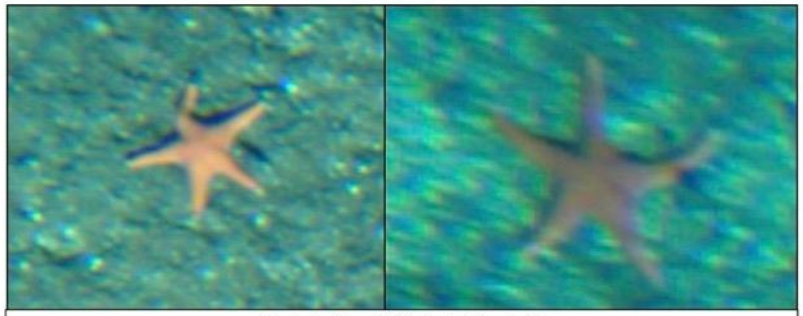

Goniasteridae sp3 (*Mediaster* Gen. inc.)

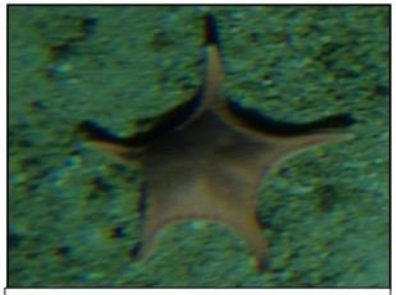

Goniasteridae sp4 (potentially *Wallastra elenderae* sp. inc.)

Goniasteridae sp5 (Gen. indeterminabilis)

Goniasteridae sp1: Body large, arms slender, interradial arcs straight. Possibly *Circeaster*. Possibly a porcellanasterid but too shallow, and lying on the wrong substrate. Large disk, thick, body shape flat, distinct marginal frame/border (= marginal plates), bared.

Goniasteridae sp2: Whitish, swollen, big morphology.

Goniasteridae sp3: Affinity with *Mediaster* as we observe radial areas swollen on the disk. Less likely would be *Nepanthia*, but here Goniasteridae sp3 has a larger disk.

Goniasteridae sp4: Distinct marginal frame bared with dark separations, ordered. Body and disk large. Shape elevated from seabed (shadow visible under the body).

Goniasteridae sp5: Disk large, marginal plates form clear (light) periphery.

(12') Arms triangular in shape, flattened and strap-like and tapering. Interradial arcs narrow and acute. Plates on disk do not form ordered patterns. Paxillae present or not. Buried or not.

(13)

(13) Spines present or absent. Spines not observed on disk or arm surface, but spines present or absent on some taxa. When moving tube feet are prominent with pointed tips and animal is moving over sediment (could not be observed from still images). These taxa are often encountered buried under top layer of sediment.

Astropectinidae (and other Paxillosida)

Astropectinidae indeterminabilis

(13') Sharp spines abundant on abactinal surface, marginal plates. Arms elongate, not buried in sediment. Tube feet not prominent. Not buried in sediment*.

Benthopectinidae

**Cheiraster* sometimes observed lying on soft sediment/coarse gravels.

Cheiraster indeterminabilis

(14) Surface covered by paxillae, arms short. Peripheral edge with prominent marginal paxillae (tree-like structures) forming lateral edge (but difficult to see from images, rather with a rugged appearance, buttons-like). Body skeleton reticulate forming widely meshed net on body surface. Predatory on crinoids and other invertebrates.

Solasteridae (*Lophaster*)

No photo-taxa identified.

(14') Surface not covered by paxillae, arms elongate. Body skeleton not reticulate.

(15)

(15) Body covered by spines, along surface of arm and along lateral sides and or along mid radial series. Arms triangular or round in cross section.

(16)

(15') No spines on body surface. Arms elongate, cylindrical in cross section.

(17)

(16-1) Sharp, needle-like spines covering the body surface (difficult to see from images), with prominent series along radius of arms and along lateral surface near oral surface. Spines not present in all members but most. *Zoroaster* found in star-shaped depression in sediment. Plates on body in ordered rows. Arms very elongate and tapering, disk very small. Can often reach large size (approaching 20 cm). Color from white to reddish orange.
Zoroasteridae (*Zoroaster*)

(16-2) Short, blunt spines evenly present on body surface, in ordered rows. Arms short, disk small.
Stichasteridae

No photo-taxa identified.

(16-3) Spines along radial ridge and along sides enlarged, prominent with enlarged tufts or bushes of pedicellariae. Arms short, disk small.
Asteriidae (e.g., *Sclerasterias*)

No photo-taxa identified.

(17) Body rigid, arms cylindrical. Plates ordered with many taxa displaying plates and papulae in ordered series arranged in regular order. Tubercles or other round features present on arm and disk surface. Armtips round. Surface appears granular. Occur in shallower water.
Ophidiasteridae

No photo-taxa identified.

(17') Body showing more net-like, or reticular plate pattern, not in serial arrangement. Surface almost entirely featureless otherwise. Arms elongate but many with curled armtips. In situ color white. Predatory on sponges.
Echinasteridae (*Henricia*)

Henricia indeterminabilis

Henricia indeterminabilis in predation on a sponge

17

Supplementary material I.4 : Inventory of photo-taxa identified from images (dive) and of species collected along dive according to the target taxa and taxonomic rank: **(A)** along the PNG sedimented slopes and **(B)** along Mayotte volcanic outer slopes

Available online at:

https://www.frontiersin.org/articles/10.3389/fmars.2021.749078/full#supplementary-material

Supplementary material I.5 : Datasets of sampled (from fishing gears) versus observed (from images) specimens in Papua New Guinea areas

Available online at:

https://www.frontiersin.org/articles/10.3389/fmars.2021.749078/full#supplementary-material

Supplementary material I.6 : Datasets of sampled (from fishing gears) versus observed (from images) specimens in Mayotte areas

Available online at:

https://www.frontiersin.org/articles/10.3389/fmars.2021.749078/full#supplementary-material

Supplementary material I.7 : Number of distinct taxa remained identified at each taxonomic rank according to the method (images = dive, sampling along dive = cl-dive), (A) along sedimented slopes (PNG) and (B) along volcanic island slopes dominated by hard bottom (Mayotte) with (C) a focus on echinoids and asteroids

(A) Sedimented slopes (PNG)

TAXA	ANNELIDA		ARTHROPODA		CHORDATA		CNIDARIA		ECHINODERMATA		MOLLUSCA	
Taxonomic rank	DIVE	CL-DIVE	DIVE	CL-DIVE	DIVE	CL-DIVE	DIVE	CL-DIVE	DIVE	CL-DIVE	DIVE	CL-DIVE
Phylum	-	-	-	-	-	-	-	-	-	-	-	-
Class	-	-	1	1	3	-	2	-	4	-	4	-
Order	-	-	2	-	10	-	3	2	2	-	1	-
Family	4	6	9	4	8	1	-	-	-	-	4	11
Genus	-	7	10	6	-	5	-	-	-	-	-	22
Species	-	-	3	34	-	16	-	-	-	-	-	5
Morphospecies	2	-	27	-	-	1	-	-	-	-	-	-
Total individuals (n)	289	471	4677	242	432	30	677	8	2417	-	925	351

(B) Volcanic island slopes (Mayotte)

TAXA	ARTHROPODA		CHORDATA		CNIDARIA		ECHINODERMATA		MOLLUSCA		PORIFERA	
Taxonomic rank	DIVE	CL-DIVE	DIVE	CL-DIVE	DIVE	CL-DIVE	DIVE	CL-DIVE	DIVE	CL-DIVE	DIVE	CL-DIVE
Phylum	-	-	-	-	-	-	-	-	-	-	-	-
Class	1	1	2	-	-	-	5	1	3	-	2	1
Order	2	2	11	1	7	-	4	-	-	-	-	-
Family	12	9	17	-	5	2	10	4	4	16	2	-
Genus	17	6	7	1	6	8	17	11	1	6	3	2
Species	9	14	1	3	1	2	2	12	2	1	1	1
Morphospecies	10	-	24	1	-	-	6	-	9	-	2	-
Total individuals (n)	535	116	688	16	6004	25	1070	57	3501	59	2773	12

(C) Volcanic island slopes (focus on echinoderms)

ECHINODERMATA	ECHINOIDEA		ASTEROIDEA	
Taxonomic rank	DIVE	CL-DIVE	DIVE	CL-DIVE
Class	-	-	-	-
Order	2	-	1	-
Family	4	-	6	1
Genus	9	4	8	7
Species	-	10	2	2
Morphospecies	2	-	4	-
Total individuals (n)	452	40	243	14

Data accessibility:
Sampling datasets used for the analyses are available in supplementary materials 5 and 6 and databases of the physical samples are available in the Muséum National d'Histoire Naturelle (Paris) databases, at the following open access address: https://science.mnhn.fr
Image datasets are available in supplementary materials 5 and 6, and the raw annotations data from the Biigle 2.0 web platform, on request at the following address: Karine.Olu@ifremer.fr

Supplementary material I.8 : Illustration of the integrative methodology for the galatheids identification from images at morphospecies rank, along the upper sedimented slopes of the Papua New Guinea

Six groups of galatheids specimens observed in the images were considered to be different species and thus were delimited in 6 different morphospecies and one species was identified both from the images and collected in the surrounding area (Astrolabe Bay and Sepik area). Each of these 6 morphospecies were first assigned to one of the three following genera (*Agononida, Munidopsis* and *Munida*). We identified *Agononida* and *Munida* based primilarly on identifiable morphological characters in the images while *Munidopsis* identification was combined with habitat context from the frequently image observations of a *Munidospis*/wood association). These three genera were also identified in the trawls, and each of the three genera gather respectively a pool of potential species sampled and identified in the sampling undertaken along dives or at larger scale (**Table S8**). The morphospecies corresponding to each of these three genera were delimited from morphological differences observable in the images. In the methodological approach applied to our study, a morphological criterion specific to the species must be visible in the images in order to be able to assign a name to the species present in the area. The limits of the observable characteristics did not allow this identification except for the species *Galacantha subspinosa*, Macpherson, 2007. Each morphospecies is therefore associated with a degree of confidence of belonging to a group of potential species because they have been sampled and identified in the area (locally and/or at a larger scale (Astrolabe Bay and Sepik area).

Table S8. Galatheids morphospecies identified from images in relation to galatheids species trawled either along dive, or in the surrounding area in the Astrolabe Bay and Sepik area.

Morphospecies	Dive	Sampled species potentially analogous	Spatial scale of sampling
***Agononida* sp1**	18	*Agononida isabelensis* Cabezas, Macpherson & Machordom, 2009	Around
		Agononida rubrizonata Macpherson & Baba 2009	Around
		Agononida similis (Baba, 1988)	Around
***Munida* sp1**	18 06	*Munida compacta* Macpherson, 1997	Along dive/ Around
		Munida curvirostris Henderson, 1885	Around
		Munida striola Macpherson & Baba 1993	Around
***Munidopsis* sp1 (*similior* group)**	18 16 06	*Munidopsis andamanica* MacGilchrist 1905	Along dive/ Around
		Munidopsis cylindrophthalma Alcock 1894	Along dive/ Around
***Munidopsis* sp2 (*andamanica* group)**	18 06	*Munidopsis formosa* Wu & Chan 2000	Along dive
		Munidopsis hirsutissima Balss 1913	Transect
Munidopsis sp3	18 16	*Munidopsis latimana* Miyake & Baba 1966	Around
		Munidopsis nitida A Milne Edwards 1880	Along dive/ Around
***Munidopsis* sp4**	06	*Munidopsis* sp. nov.	Around
		Munidopsis similior Baba 1988	Along dive/ Around
		Munidopsis sinclairi MacArdle 1901	Along dive/ Around
		Munidopsis subchelata Balss 1913	Along dive/ Around
***Galacantha subspinosa* Macpherson 2007**	16 18 06	*Galacantha subspinosa* Macpherson 2007	Around

II. Patrons spatiaux à multi-échelles des communautés méga-benthiques des monts sous-marins et pentes insulaires, et facteurs environnementaux structurants

Les monts sous-marins abritent une biodiversité probablement en partie structurée par l'hétérogénéité de l'habitat à diverses échelles spatiales. Peu d'études ont examiné les patrons spatiaux des assemblages de mégafaune benthique des monts sous-marins, avec une approche multi-échelle, en considérant divers facteurs environnementaux et en quantifiant l'hétérogénéité de l'habitat à une échelle fine. Par ailleurs, une seule étude portant sur les communautés de la mégafaune des monts sous-marins dans l'océan Indien a été publiée jusqu'à présent.

Le canal du Mozambique se compose de plusieurs systèmes carbonatés, formant les îles Eparses, et de monts sous-marins, correspondant à des plateformes submergées affectées par des processus tectoniques et du volcanisme, et conduisant à des géomorphologies complexes à sommet plat. Dans cette étude, nous avons analysé des images issues d'une caméra tractée et des données environnementales à multi-échelles sur quatre monts sous-marins, et sur les pentes insulaires de Bassas da India et de Mayotte. Les sites sont répartis le long de 10° de latitude et dans un gradient de profondeur de 370 à 1180 mètres. Les images ont été analysées pour caractériser et quantifier la mégafaune dans des unités d'échantillonnage standardisées, ainsi que pour valider les classes géomorphologiques (échelle du km) identifiées à partir des données de rétrodiffusion et bathymétrique du sondeur multifaisceaux. Ces images ont également servi à entraîner un algorithme d'apprentissage automatique pour classer le substrat à une échelle plus fine (échelle d'une 10^{aine} de mètre). D'autres paramètres quantitatifs sur la complexité du terrain ont été traités à partir de la bathymétrie à haute résolution. Des variables océanographiques, dont la vitesse du courant, ont également été

traitées à différentes échelles spatiales. A partir de cet ensemble de données, nous avons cherché à décrire les patrons spatiaux des assemblages de mégafaune benthique (densité, composition, diversités alpha et bêta) et à explorer les facteurs environnementaux à multi-échelles de ces assemblages, au sein et entre les monts sous-marins et les pentes insulaires étudiées.

Les patrons de richesse, de densité et de diversité bêta diffèrent entre les monts sous-marins (jusqu'à un facteur 10 pour la densité) et entre les pentes d'une même île, sous l'effet des différences de dureté, de nature et de diversité du substrat, ainsi que de la productivité primaire de surface et de la vitesse du courant.

Une forte diversité bêta caractérise tous les monts sous-marins et les pentes insulaires malgré la faible gamme de profondeur explorée (< 500 m), à l'exception de la plateforme de de l'archipel des Glorieuses (dalle carbonatée). La diversité bêta est principalement due au remplacement ("turnover") des taxons, avec une forte contribution des spongiaires et des cnidaires – potentiellement constructeurs d'habitats biogéniques – ainsi que de quelques taxons mobiles.

A partir d'une analyse de réseaux biogéographiques, nous avons identifié 12 assemblages dominants, caractérisés par quelques taxons très abondants et présentant une distribution inégale, avec une variabilité de la composition à la fois entre et au sein des monts sous-marins et des pentes insulaires. Les différences d'assemblages entre les monts sous-marins ont été expliquées par 19 variables environnementales agissant à différentes échelles. Le partitionnement des variations a permis d'évaluer que l'hydrologie (courants et productivité primaire) explique ~15% de la structure spatiale des communautés méga-benthiques le long du canal du Mozambique, tandis que la géomorphologie (échelle kilométrique), la topographie (échelle de 60 à 500 m) et le substrat (unités de 60 m) expliquent ensemble 24% des patrons spatiaux de la faune. L'évaluation des échelles spatiales au sein des pentes insulaires – à partir d'analyses de cartes de vecteurs propres de Moran basées sur la distance (dbMEM) – révèle des structures de communautés méga-benthiques de moyenne (~1 km) à grande échelle (~2-6 km) liées à divers facteurs comprenant la topographie, le substrat, la profondeur, la pente et l'hydrologie ; tandis qu'un modèle spatial à petite échelle, bien que observable le long d'une pente, était difficilement expliqué par l'environnement, en raison de

la très grande hétérogénéité de l'habitat, et des faibles densités de faune qui est cependant très diversifiée.

Malgré les limites de l'identification taxonomique dans cette zone peu échantillonnée, cette étude a mis en évidence une grande hétérogénéité des assemblages méga-benthiques à plusieurs échelles, en réponse à l'hydrographie et à la géologie complexes de la zone. Une caractérisation plus poussée des facteurs environnementaux à l'échelle locale et régionale est donc nécessaire pour améliorer la prédiction d'habitats favorables aux écosystèmes marins vulnérables. La contribution élevée des taxons constructeurs d'habitats biogéniques – identifiés au rang taxonomique de la classe ou de l'ordre – est remarquable, ainsi que le bénéfice de l'effort taxonomique pour améliorer l'identification sur les images pour certains taxons mobiles, qui contribuent également aux patrons spatiaux des communautés aux différentes échelles.

Mots clés : monts sous-marins, pentes insulaires, assemblages méga-benthiques, diversité bêta, facteurs abiotiques multi-échelles, analyses spatiales, analyses d'images, domaine bathyal, canal du Mozambique

Ce manuscrit est en cours de préparation pour une soumission avec les auteurs suivants :

Mélissa Hanafi-Portier, Sarah Samadi, Marion Boulard, Laure Corbari, Simon Courgeon, Stephan Jorry, Louise Keszler, Boris Leroy, Elda Miramontes, Thibault Napoléon, Pierrick Penven, Karine Olu

Multiscale spatial patterns and environmental drivers of seamount and island slope megafaunal assemblages along the Mozambique Channel

Abstract

Seamounts support biodiversity, likely partly structured by habitat heterogeneity at various spatial scales. Few studies have investigated patterns of their benthic megafaunal assemblages with a multiscale approach, by considering various environmental drivers and quantifying fine scale habitat heterogeneity. Moreover, only one study focusing on seamount megafauna communities in the Indian Ocean has been published so far.

The Mozambique Channel is characterized by several carbonate systems forming the Eparses islands, and flat top seamounts corresponding to drowned platforms affected by tectonic processes and volcanism, leading to complex flat-topped geomorphologies. Here, we analyzed towed-camera still images transects and multiscale environmental data from four seamounts, and from Bassas da India and Mayotte island slopes. The sites are distributed along 10°-latitude and within a 370-1180 meter depth gradient. Images were analyzed to characterize and quantify megafauna in standardized sampling units, as well as to groundthruth geomorphological classes identified from backscatter (km scale) and to train a machine learning algorithm for substrate classes at finer scale (10s m scale). Other quantitative terrain parameters processed from high resolution bathymetry as well as oceanographic variables including current speed were processed at different spatial scales. From this dataset, we aimed to describe spatial patterns of benthic megafaunal assemblages (density, composition, alpha and beta diversities) as well as explore the multiscale environmental drivers of these assemblages, within and between seamounts and island slopes.

Patterns of richness, density and beta diversity differ between seamounts (of a factor 10 for density) and between slopes of the same island, driven by differences in substrate hardness, nature and diversity, as well as in surface primary productivity and current speed.

High beta diversity characterized all seamounts and island slopes despite the limited depth range explored (< 500 m), except the carbonate-slab platform of the Glorieuses archipelago. Beta diversity is mainly due to taxa turnover, with high contribution of the habitat-forming sponges and cnidarians, together with a few mobile taxa.

From biogeographic network analyses, we identified 12 dominant assemblages, characterized by few highly abundant taxa and displaying patchy distribution, with variability in composition both between and within seamount(s)/island slope(s). Assemblage differences between seamounts were explained by 19 environmental variables acting at various scales. Variation partitioning assessed that hydrology (currents and primary productivity) explained ~15% of the megabenthic structure along the Mozambique Channel, while geomorphology (km scale), topography (60-500 m scale) and substrate (60 m units) explain together 24% of the faunal spatial patterns. Assessment of spatial scales within island slopes using distance-based Moran eigenvector map (dbMEM) analyses reveals medium (~1 km) to large scale (~2-6 km) megabenthic community structures related to various drivers comprising topography, substrate, depth, slope and hydrology; while small scale spatial pattern though observable along a slope was hardly explained by the environment, attributed to very high habitat heterogeneity, low faunal densities but high diversity.

Despite limitations in taxonomic identification in this poorly sampled area, this study highlighted high heterogeneity of megabenthic assemblages at multiple scales, in response to the complex hydrography and geology of the area. Further characterisation of environmental drivers at both local and regional scales are therefore needed to improve prediction of suitable habitats of vulnerable marine ecosystems. High contribution of habitat-forming taxa identified at the class or order level is noteworthy, as well as the benefit of taxonomic effort to improve identification on images for some mobile taxa, which also contribute to community patterns at the different scales.

Keywords: seamounts, island slopes, megabenthic assemblages, beta-diversity, multiscale abiotic factors, spatial analyses, image analyses, bathyal domain, Mozambique Channel

II.1 Introduction

Seamounts are isolated topographic features of geological origin that rise at least 1000 m above seafloor (Rogers, 2018). When emerging above the sea surface, these topographies are defined as oceanic islands, whose nearshore features are more subject to nutrient input and terrigenous runoff from the land (Staudigel and Clague, 2010).

Interaction of seamounts with oceanic circulation generates eddies formation and other circulation cells such as internal waves and Taylor column formation (i.e., doming structure above the seamount) (Clark et al., 2010). These rectified flows potentially enhance particulate mixing, and in addition to the trap of vertically migrating zooplankton, would contribute to support a highly productive system, especially of dense aggregation of benthopelagic and demersal fish (Clark et al., 2010; Morato et al., 2008). For this reason, seamounts are targeted by commercial fisheries (Morato and Clark, 2007). In addition, some of these structures are covered by ferromanganese surface deposits which are of potential economic interest for seabed mining of highly concentrated rare metals found in these deposits (e.g., cobalt) (Hein et al., 2010).

Increased hydrodynamic flow, prevalence of hard substrata and concentration of nutrients and preys, foster the settlement of epibenthic suspension feeders (Genin et al., 1986). These megabenthic animals (i.e., benthic megafauna; animals of sufficient size to be observable from images, ~2 cm; (Grassle et al., 1975) are commonly observed over seamounts (e.g., Porifera, Actiniaria, Octocorallia, Brachiopoda, Crinoidea) (Rogers, 2018). Some of these organisms can form more or less dense biological aggregates (e.g., cnidarians, sponges) - that can host a diversified associated fauna composed mainly of small benthic invertebrates (e.g., crinoids, brittle stars, squat lobsters and other small decapods, molluscs, etc.) (Buhl-Mortensen et al., 2010). These large habitat-forming invertebrates are long-lived and slow-growing, and threatened by deep-sea trawling (Althaus et al., 2009; Baco et al., 2020). Their ecological importance associated with their poor resilience contribute to the vulnerability of benthic populations on seamounts.

Although estimates of the number of these underwater structures range from 150,000 to 25 million worldwide depending on seamount definition (sensus stricto > 1000 m or sensus lato >100 m) and the method used to make the estimation (Rogers, 2018), fewer than 0.4%-4%

have been sampled to date (Kvile et al., 2014), mainly in the Atlantic and Pacific regions (Clark et al., 2010; Rowden et al., 2010a). Given the emerging threats to this ecosystem, there is an urgent need for protection and management measures. However, our knowledge on the patterns of seamount benthic communities structure and these driving factors is still limited, especially due to a lack of spatial sampling coverage.

Seamounts occur across a wide variety of latitude, depth range, and have diverse morphologies, therefore are affected by temporal and spatial variation of oceanographic processes affecting the benthic communities, making generalization difficult (Clark et al., 2010; Kvile et al., 2014; Rowden et al., 2005; White et al., 2007).

Megabenthic assemblages on seamounts vary from patchy distribution along a mosaic of habitats within a single seamount to overall change among seamounts over geographic distance (Clark et al., 2010; Rogers, 2018). The controlling factors of this spatial heterogeneity have been explored in several case studies, focused on one or a few seamounts, in different regions of the world oceans.

In the different studied regions, the benthic megafauna communities of the set of surveyed seamounts were shown to be structured by surface primary productivity (Bridges et al., 2022; Clark and Bowden, 2015), temperature and oxygen concentration, and particulate organic carbon (POC) concentration (Morgan et al., 2019; Turnewitsch et al., 2016), hydrodynamics (Morgan et al., 2019), latitudinal gradient (Williams et al., 2011), distance from the coast (O'Hara et al., 2010) but also by water mass characteristics linked to bathymetric gradients (Lapointe et al., 2020). Some studies explored in more detail the factors acting at a local scale. For example, some studies showed that at the scale of one seamount, depth-related factors (Long and Baco, 2014) but also water masses (Victorero et al., 2018) structured the distribution of the benthic megafauna.

The geomorphology of the different seamounts, resulting from their own geological history, generates a variety of landforms (ripples, flanks, summits) and substrates (lava lobe, massive boulders, bedrock, small pebbles, etc.) displaying seafloor heterogeneity over different spatial scales as well as different microtopography. These seafloor parameters also appear in different studies as structuring the communities both at the seamount scale and among

seamounts (de la Torriente et al., 2018; Sautya et al., 2011; Shen et al., 2021; Victorero et al., 2018).

An important source of heterogeneity in the communities comes from the presence of biogenic habitats, including corals and sponges. Many studies underlined the heterogeneity in the distribution of the habitat-forming organisms with areas presenting scattered animals to dense plurispecific aggregates (Auscavitch et al., 2020b; Baco et al., 2020; Morgan et al., 2015) Some studies showed that the densities can moreover change through time (Bo et al., 2020).

In summary, previous studies revealed that multiple controlling factors, both physical and biological, operate at various spatial scales to drive the heterogeneity in benthic communities. Most of these studies have either focused on a single seamount (usually using remotely operated vehicle – ROV – and imagery data), or integrated several seamounts of a given region, based on imagery or dredge/trawl data. However, these various studies rarely integrated the same set of environmental factors at the regional and at the local scales. Integrating the same set of physical and biological factors at multiple spatial scales is required to better understand their respective influences on the distribution of benthic megafaunal communities.

Considering the available background knowledge, we first hypothesize that the differences in overall richness and density between seamounts would be influenced by hydrodynamics and surface productivity which may depend on geographical factors such as distance from the coast and latitude. In addition, the geological history of the seamounts and therefore the nature of the dominant substrate and their heterogeneous geomorphology would also explain the differences in the assemblage structure between seamounts. Moreover, these features cross different bathymetric ranges, thus different water masses, along which oxygen concentration, temperature and salinity vary, and would also be potentially structuring.

Secondly, within a seamount or along an island slope, we hypothesize that geomorphology, topography and slope orientation relative to the current, as well as substrate heterogeneity and microtopography would explain the local spatial structure of megafaunal assemblages.

To address these hypotheses, it is necessary to consider different spatial scales (different seamounts, and the whole set of environmental parameters under hypotheses) with biological data obtained from the same data acquisition methods.

On the one hand, studies based on physical sampling (dredges, trawls) provide accurate taxonomic data and allow a qualitative description of large-scale biodiversity patterns (bioregions), connectivity and endemism on seamounts. However, these data neither allow the quantification and description of community structure at fine spatial scales – which is only possible from image data acquisition – nor allow the integration of fine resolution environmental data to explain the observed distribution patterns and contribute to predictive models based on habitat data.

On the other hand, most studies of seamount megabenthic communities relying on images are conducted with a morphospecific (morphotype) approach, for which taxonomic data are not very robust and not comparable between studies. Our challenges here were to navigate between these two aspects and to find a compromise between taxonomic resolution and environmental data resolution. Moreover, there are still few integrative image-based studies considering multiscale (regional to local) environmental forcing.

The Mozambique Channel lies within the western Indian Ocean, between the African Mozambique margin and Madagascar Island. The region is characterized by a unique and highly turbulent hydrographic system with intense mesoscale eddies activities (Marsac et al., 2014), and low sea surface chlorophyll a concentration (< 0.2 mg/m^3), constituting an oligotrophic region (Malauene et al., 2014). The northern part of the channel is a second hotspot of tropical marine biodiversity after the coral triangle in the Pacific and displays a high diversity of reef corals (Obura et al., 2012). The exploration of the deep-sea habitats of this region is recent. For example one of the main sources of taxonomic knowledge for the northern part of the channel is the sampling provided by the BENTHEDI campaign conducted by Thomassin (1977). In 2017, Castelin et al. (2017), counted 85 species described from this sampling. Since this count, at least three additional species have been described (d'Hondt and d'Hondt, 2019; Rubio and Rolán, 2022; Taylor and Glover, 2018).

We explored for the first time in 2014 and 2015 four seamounts (a bank in the Glorieuses archipelago, the Jaguar and Hall banks in the southern part of the channel, the Sakalaves platform on the Davie Ridge) and a slope of Bassas da India Island, along a 10° latitudinal gradient within the Mozambique Channel, by a towed camera. Three terraces on the outer slopes of Mayotte Island, located in the same depth range as seamount summits, were then explored in 2017. The seamounts and island slopes explored show a diversity of morphologies

and substrates, inherited from their volcanic origin and their complex geological evolution (Audru et al., 2006; Courgeon et al., 2017, 2016). Mayotte Island and Glorieuses archipelago are both part of marine protected areas, the former under the management of the French Biodiversity Office (Office français de la biodiversité ; OFB), and the latter under the management of the French Southern and Antarctic Territories (Terres Australes et Antarctiques Françaises ; TAAF).

Explorations focused on the seamount summits, island slope terraces and upper slopes in a bathymetric range located in the bathyal domain (370-1180 m). This dataset allows a multiscale analysis, from regional with eight seamounts and island slopes separated by a few tens of km to ~1400 km, to local analysis on summits or terraces and upper slopes (few tens of km). It also allows us to compare patterns between seamounts and island outer slopes. We therefore propose to test several hypotheses on the structure of benthic megafauna communities at these different scales.

Considering the eight seamounts and island slopes explored along the Mozambique Channel, we aimed to: **(1)** Assess community metrics (density, alpha and beta diversities) and their environmental drivers between seamounts and island slopes. **(2)** Assess the pattern of spatial distribution of megabenthic communities between seamounts and island slopes and identify and quantify the respective influence of environmental factors on these communities at multiscale (~1400 km-60 m). **(3)** Finally, the scales of spatial structures and their interrelationships with abiotic factors have been particularly studied along the Mayotte and Bassas Da India Island slopes.

II.2 Materials and methods

II.2.1 Study area

The Mozambique Channel is located in the western Indian Ocean, between the African Mozambique margin and the island of Madagascar, over a width of 400 to 900 km and a length between latitude S10 and S25 of about 1700 km. The region is characterized by a unique and complex hydrographic system, rich in mesoscale eddies, up to 300 km in diameter. These eddies are generated north of the channel as dipoles (cyclonic and anticyclonic eddy pairs) at a frequency of 6-8 per year and flow southwards at a speed of ~4.5 km per day (de Ruijter et al., 2004). These eddies, in contact with the continental shelves of the Mozambique and

Madagascar margins, affect the variability of primary productivity, which is increased at their center, and can reach the ocean floor to a depth of 1000 m (Marsac et al., 2014). The presence of coastal upwelling, particularly along the Madagascar coast, is also a source of particulate input to the open sea (Marsac et al., 2014). The north of the channel is dominated by a strong westerly current (North East Madagascar Current, NEMC) which splits into two branches, once where it meets the Davie Ridge, and again where it meets the East African coast, and branches off in a South-East and South-West direction respectively (Collins et al., 2016). Between the surface and 1500 m depth, the Mozambique Channel consists of five main water masses. From the north, the NEMC transports salty tropical surface water (TSW), subtropical surface water (STSW) and South Indian Central Water (SICW) to a depth of about 600 m. The latter water mass is the main constituent of the permanent thermocline. In the intermediate water, oxygen-poor Red Sea water (RSW) (~900 to 1200 m) enters the channel from the north along the East African coast, and circulates southwards, notably carried into the core of mesoscale eddies. To the south of the channel, intermediate Antarctic water (AAIW) (800-1500 m), is transported northwards by the Mozambique undercurrent along the Mozambique coast (Charles et al., 2020; Collins et al., 2016; de Ruijter et al., 2004).

The region also exhibits seasonal variation in chlorophyll a concentration (Chla), with higher levels in winter than in other seasons, due to wind regimes and mesoscale eddies that cross the channel. Chla concentrations do not exceed 1 mg/m^3 in deep water in the channel, with an average concentration of 0.15 mg/m^3 (Tew-Kai and Marsac, 2009). Primary production rates are twice as high in the south of the channel in winter compared to the north. The main differences in physical forcing between the northern, central and southern parts of the channel are due to the intense mesoscale eddies in the central and southern parts incorporating a non-seasonal signal, while in the north the circulation is predominantly monsoonal (Ângelo Adolfo Langa, 2021).

The Mozambique Channel hosts various seamounts and carbonate platforms, resulting from intense volcanic and tectonic activities originating from the emergence of the channel 180 million years ago, during the drift of the supercontinent Gondwana, and the separation of Madagascar from the African continent. From these volcanic and tectonic activities the Davie Ridge was formed, which extends from the East African margin to Madagascar (9°S-23°S) and consists of various seamounts, notably Sakalaves platform at 17-19°S (Courgeon et al., 2018).

The southern part of the channel hosts two guyots (Hall and Jaguar banks) as well as a modern atoll (Bassas da India) which consists of a 12 km wide terrace (Courgeon et al., 2017). To the north, the channel hosts the Comoros archipelago, comprising from west to east the Grand Comoros Islands, Moheli, Anjouan and Mayotte. Further north, a carbonate platform lies off the Glorieuses Islands. These reliefs, formed by volcanic activity, were colonized by shallow reefs, before subsiding at depth. For some features (Jaguar, Hall Bank, Bassas da India), a reactivation of volcanism was accompanied by tectonic deformations. The result is a highly heterogeneous substrate, ranging from more or less fractured volcanic outcrops and lava flow fields to large areas of sandy dunes. For others (Glorieuses), the geological evolution has resulted in the formation of carbonate terraces covered with sandy deposits from the island (Courgeon et al., 2017, 2016).

The island of Mayotte is composed of a barrier reef that hosts a lagoon (1100 km^2), which is an integral part of the Mayotte Natural Marine Park. The outer slopes of the island are characterized by a complexity of geomorphology and substrate, and are composed of a network of canyons, vast plateaus/terraces, cliffs, volcanic cones and rugged areas (Audru et al., 2006).

II.2.2 Data acquisition

II.2.2.1 Image data

The data were obtained from the cruises PAMELA-MOZ01 (Olu, 2014) onboard the research vessel (R/V) *L'Atalante* and PAMELA-MOZ04 (Jouet and Deville, 2015) onboard the R/V *Le Pourquoi Pas?*. These cruises are part of the PAMELA project (Bourillet et al., 2013) and explored four seamounts along the Mozambique Channel, from North to South: a carbonate platform in the Glorieuses Archipelago, the Sakalaves mounds along the Davie Ridge, and the Jaguar, and Hall Bank, as well as a terrace in Bassas da India closely located to the later (**Figure II.1**).

The BIOMAGLO cruise (Corbari et al., 2017), onboard the R/V *L'Antea*, completed the image dataset with an exploration of the outer slopes of Mayotte Island. Three slope orientations were selected for the study – North, East and West – (**Figure II.1C**). The western and northern slopes are characterized by the presence of terraces located at depths similar to the seamount summits.

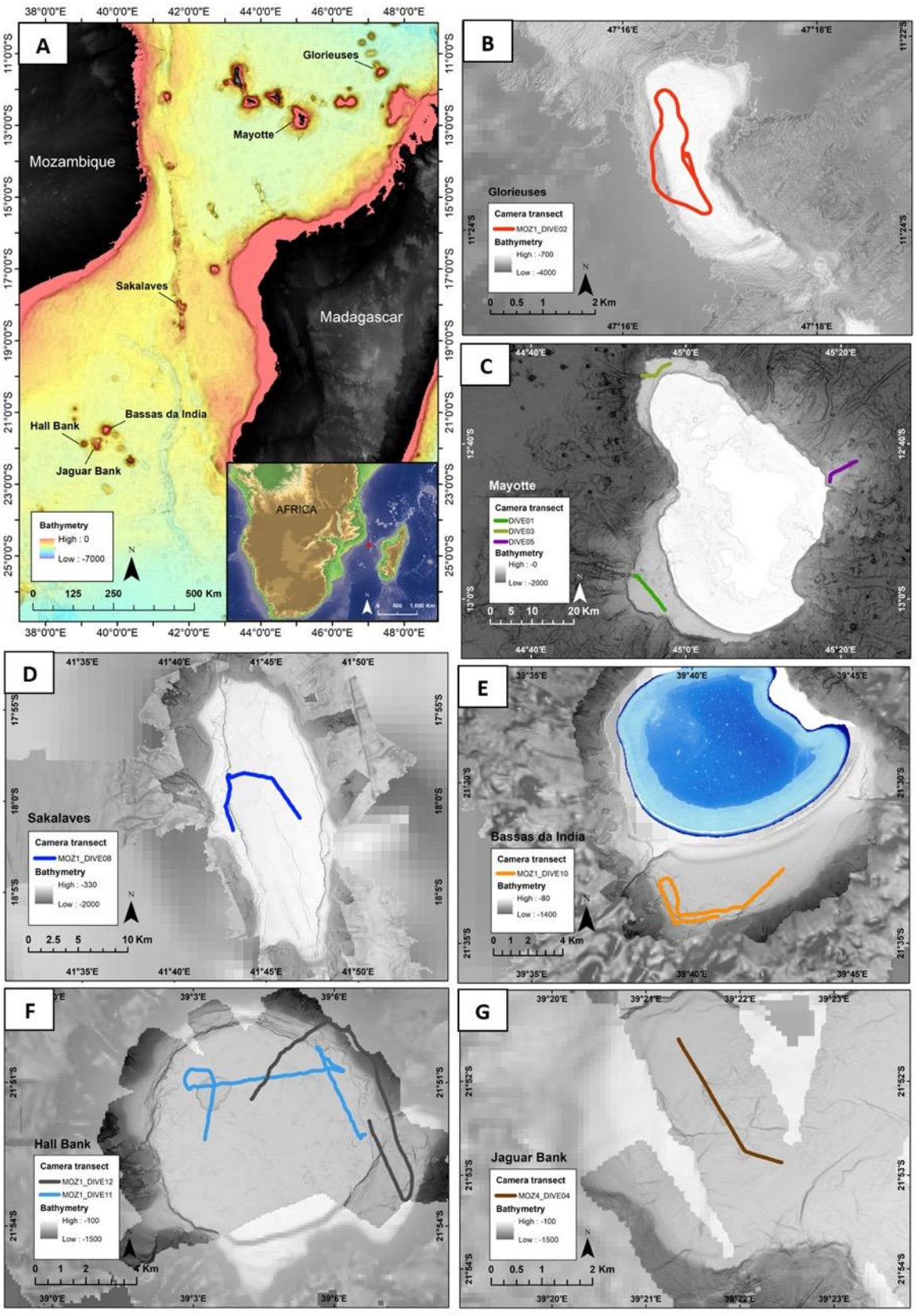

Figure II.1 : (A) Map of the Mozambique Channel locating the different seamounts and islands explored, and specific maps of each towed camera transect on seamounts and island slopes: **(B)** Glorieuses, **(C)** Mayotte Island slopes, **(D)** Sakalaves platform, **(E)** Bassas da India, **(F)** Hall Bank, **(G)** Jaguar Bank

Images were captured on each of these structures, with a towed camera (SCAMPI, French Oceanographic Fleet), on the seamount summits and upper slopes (exploration by towed camera does not allow exploration of very steep slopes), as well as on an island terraces and upper slope of Bassas da India. On Mayotte, images were captured: (1) on the northern slope characterized by a terrace at ~600 m depth surrounded by deeper features resembling craters or volcano networks at ~1000 m depth; (2) on the western slope consisting of a deeper and wider plateau at 750 m covering 250 km^2 and a shallow bathymetric gradient, (3) and finally the eastern slope which covers a broad bathymetric and continuous gradient from a small relatively flat area ("spur") to ~1100 m depth, characterized by shallow volcanic cones (Audru et al., 2006).

The images were captured in a vertical position, at a speed of about 0.5 m/s, at intervals of 30 seconds (except for Glorieuses: about 15s), and at an average of 2.5-3 m above the bottom, with an HD camera (NIKON D700, focal length 18 mm, resolution 4 256 × 2 832 pixels). The images were then georeferenced using the vessel positioning system processed with the ADELIE application (French oceanographic fleet) developed at IFREMER and implemented using ArcGiS V10.3 software. A total of nine camera transects were processed for this study. Except for the island slopes (Bassas, Mayotte); we will refer to the term seamount for all the remaining topographic features studied (seamounts, atolls or terraces, guyot and carbonate platforms). Indeed, they are all originally submarine volcanoes colonized in shallow waters and then eroded during their subsidence, and some of them have subsequently undergone different phases of volcanism and tectonic deformation. Volcanic islands have the same origin, and the terraces explored along their slopes can be compared to seamount summits, as hypothesized to have been eroded during aerial phases before subsidence (Audru et al., 2006).

The sampling effort for this study is summarized in **Table II.1**.

II.2.2.2 Environmental data

For the Mayotte island slopes we used bathymetry and acoustic reflectivity data acquired by the BATHYMAY cruise (Audru et al., 2006). For other sites (seamounts and Bassas island) multibeam data were acquired during the PTOLEMEE (Jorry, 2014) and PAMELA-MOZ01 cruises with a multibeam echosounder (Kongsberg EM122 for the deepest areas and EM710 for the shallowest areas) (Courgeon et al., 2016). CTD (temperature, salinity, pressure) and

oxygen data were acquired during the Scampi dives from CTD SBE19 and optode (microcat) sensors mounted on the camera frame. The temperature sensor did not work for the northern slope of Mayotte, nor did the oxygen sensor for the dive on the Sakalaves platform.

Table II.1 : Summary of sampling effort, location and depth for the nine towed camera transects

Cruise	Sites	Morphology	Camera transect	Depth (m) (min-max)	Number of images	Transect length (km)	Latitude (start-end transect)	Longitude (start-end transect)	Samples (200 m² polygon)
Biomaglo	Mayotte, West slope	Island slope (terrace)	DIVE01	654-888	900	11	-13.02/-12.95	44.95/44.89	191
	Mayotte, North slope	Island slope (terrace)	DIVE03	449-1183	1101	8	-12.49/-12.52	44.97/44.90	121
	Mayotte, East slope	Island slope	DIVE05	492-1117	938	8.5	-12.75/-12.70	45.30/45.37	149
Pamela moz01	Glorieuses	Carbonate platform	MOZ1 DIVE02	724-883	1155	6	-11.39/-11.38	47.28/42.28	106
	Sakalaves	Platform and escarpment	MOZ1 DIVE08	368-482	1251	15	-18.02/-18.01	41.72/41.78	268
	Bassas da India	Island slope (terrace and upper slope)	MOZ1 DIVE10	453-623	1123	14	-21.54/-21.57	39.71/39.68	248
	Hall (summit)	Bank summit	MOZ1 DIVE11	456-540	1170	16	-21.87/-21.85	39.05/39.07	279
	Hall (summit-slope)	Bank summit, terrace upper slope	MOZ1 DIVE12	480-903	1050	16	-21.86/-21.86	39.11/39.07	256
Pamela moz04	Jaguar	Bank summit	MOZ4 DIVE04	456-549	926	3	-21.88/-21.86	39.37/39.36	58

II.2.3 Taxonomic data processing from images

We annotated 9614 images using the web-based image annotation platform BIIGLE 2.0 (Langenkämper et al., 2017). This software facilitates the annotation of taxa on images, their classification, identification and revision, in collaboration with the taxonomists invited to the platform. For this work, crustaceans were identified by Dr. Laure Corbari and Pr. Tin-Yam Chan, fish by Pr. Wei-Jen Chen, Dr. Jhen-Nien Chen and Dr. Mao-Yin Lee, echinoids by Dr. Thomas Saucède, and asteroids by Dr. Christopher Mah. Details of the method for identifying taxa in images are described in Hanafi-Portier et al. (2021). This method consists in considering the knowledge of the species collected in the region, to identify the taxa at the lowest possible identification rank on the images. The identification is based on objective identification criteria (morphological characters of the taxon) and contextual criteria (knowledge of similar species collected in the region and their habitat). The characters that can be observed on images are not equally informative among the taxonomic groups.

We thus selected, for each taxon, the lowest identification ranks achieved on the images, while we avoided nesting the levels for the same taxonomic group. Thus, different

identification ranks were achieved in the dataset; with final taxonomic ranks (genus, morphospecies/species) for echinoids, decapods, asteroids, some fishes; and higher ranks (phylum, class, order) for other groups (e.g., brachiopods, gastropods, annelids, poriferans, cnidarians, fishes). By avoiding nested taxonomic identification, we did not consider the individuals in the dataset that are identifiable only at high rank (e.g., Actinopterygii, Porifera, Cnidaria, Asteroidea).

The annotations were then exported from the BIIGLE platform, in the form of a 'taxon observation matrix per image'. Before formatting the matrix in a 'taxon abundance per image' format, we compiled the identification data at the taxonomic identification ranks selected for the dataset (list of the taxonomic composition available in **Supplementary material II.1**).

To obtain robust ecological signals and given the low faunal count per image in our study area, we aggregated the abundance/image data into 200 m² (~60 m linear) sample units defined spatially from the navigation of the camera and its speed, using the ADELIE software (internal dev. IFREMER; ArcGIS 10.7 plugin). We tested sampling units of 100 and 150 m², but 200 m² was an optimum surface area enabling us to obtain at least three images per sampling unit, while having a compromise between fauna density and habitat heterogeneity. The slightly variable speed of the towed camera, and the removal of poor-quality images from the dataset, meant that we could observe a variable number of images per polygon, varying on average from four to eight images per polygon. We therefore weighted the summed abundances in each polygon by the number of images in the polygon, and then standardized the densities by the area of the polygon. We deleted all polygons with a number of images < 1 and kept only polygons with an area between 170 and 200 m^2. Thus, out of a total of 9614 images, we kept 8430 and out of a total of 1767 polygons, we kept 1676 for the analyses (**Table II.1**).

II.2.4 Environmental data processing

Average current velocity and variability (standard deviation) data were obtained for three bathymetric layers (0-50 m, 50-200 m, 300-650 m), from daily outputs over 1993-2014, at a resolution of 4.4 km x 4.4 km.

We exported from the AquaMODIS database, the monthly satellite data of daily mean surface chlorophyll a concentration (Chla), at a resolution of 4 km x 4 km. We considered seven years of integration for the Hall, Bassas, Sakalaves sites (2007 to 2014), eight years for Jaguar (2007

to 2015) and ten years for Mayotte and Glorieuses (2007 to 2017) depending on the dates of data acquisition for the cruises at the different sites. We calculated the winter and summer climatologies, to consider the difference in primary productivity of the region; contrasted in winter and summer (Tew-Kai and Marsac, 2009) as well as the minimum, maximum and average Chla integrated over these seven to ten years of monitoring, and the average intra-annual and inter-annual variability.

CTD (temperature, salinity) and oxygen data from SCAMPI dives were georeferenced in GIS to calibrate the time step of acquisition at each frame/image (CTD profile in **Supplementary material II.2**).

High resolution bathymetry (Digital Terrain Model – DTM) and acoustic imagery were processed from multibeam echosounder data. DTM resolution is 10 m for the PAMELA project data (Charline Guérin, IFREMER Marine Geosciences lab). For Mayotte, the resolution of the DTM is 20 m on the explored areas (Audru et al., 2006; SHOM data).

We quantified the variability of the terrain using bathymetric derived indices with the Benthic Terrain Modeler (BTM) plugin in ArcGIS V10.7 (Shaun Walbridge et al., 2018). The scale of the measured indexes is therefore dependent on the DTM resolution. We considered the explanatory seafloor variables considered relevant in the literature for understanding the structure of megabenthic communities (Wilson et al., 2007).

The BPI (Bottom Position Index), measures the average differences in bottom elevation relative to a reference point successively within a moving window. It was calculated at fine (30, 60, 90 m) and large (120, 250, 500 m) scales to capture the smallest structures (faults, ripples) to the largest ones (craters, slope breaks, escarpments) on the different features.

We also measured the following variables from a moving window of 3 x 3 cells, i.e., on a 30 m scale (10 m resolution x 3 cells = 30 m, except for Mayotte at 60 m): longitudinal, transverse and total curvature; aspect converted to eastness and northness (bounded between -1 and 1) from the cosine and sine of the aspect angle; bottom roughness from an Arc Chord method, to obtain a roughness value independently of the slope value (Du Preez et al., 2016), as well as the slope.

The statistics – mean, minimum, maximum and standard deviation – of the terrain variables, the Chla, the current, the oxygen and the temperature were calculated per polygon in R from

the export of the raw data from the raster layers or the georeferenced data of each variable in ArcGIS.

We defined four geomorphological classes to characterize the structures observed at a scale greater than one kilometer on each seamount and island slope: (1) a volcanic geomorphology, which is characterized by the observation of volcanic reliefs such as lava flows, lobes, boulders or blocks, as well as discontinuous reliefs, (2) a carbonate geomorphology, which is mainly characterized by relatively flat reliefs, forming slabs of rather homogeneous carbonate rock, with a few potential fractures. However, on the eastern slope of Mayotte, this geomorphology corresponds more to discontinuous carbonate reliefs, whereas on the western slope, the geomorphology is formed by large blocks of carbonate rock or walls, (3) a sedimentary geomorphology, composed of large sandy areas, sometimes with current ridges, particularly on Sakalaves and Bassas, (4) a mixed geomorphology, characterized by a mixture of volcanic reliefs and carbonate substratum, and a sedimentary area. Sometimes the volcanic and carbonate substrates mix in the same rock forming dykes. The classification was based on the interpretation of the bottom reflectivity (in decibels); enabling the differentiation between areas of rocky and soft substratum; as well as by overlaying slope and bathymetry data in GIS to identify areas of volcanic substratum (mainly lobe shape) from carbonate substratum (homogeneous, fractured). We then ground-truthed the classes by observing a set of at least 30 *in situ* images for each class and transect (geomorphological class catalog in **Supplementary material II.3**).

We characterized and quantified the substrate composition at the different sites from a machine learning algorithm to pre-classify the substrate type in the images (ISEN school collaboration), for each seamount and island slope. We defined five substrate facies: volcanic rock, carbonate slab, fine sediment, gravel and biogenic. Because of the high substrate heterogeneity detected in the images, the algorithm did not always detect and quantify the correct substrate depending on the image brightness. Therefore, the final classification considering the five substrate facies was checked manually, and we finally distinguished primary from secondary substrates with the threshold of < 50% image coverage. From the images that presented at least one secondary substrate, we defined 12 additional composite substrate facies. Each of these 12 composite facies is a combination of 2 to 3 of the 5 initially defined facies. We finally manually attributed all the images to these 17 facies. From the

substrate facies annotations assigned to each image, we considered a reduced substrate dataset, to obtain a more succinct number of categories to calculate (1) substrate/polygon frequencies, (2) substrate/polygon diversity (Shannon Weaver, exponential component), from the previously calculated frequencies. To obtain the simplified substrate dataset, we reduced to nine the number of substrate categories (i.e., sediment, carbonate rock, volcanic rock, gravel, biogenic, mixed rock, mixed carbonate-sediment, mixed volcanic-sediment, mixed (sediment, volcanic, carbonate)) by grouping some categories (list of substrate categories and catalog in **Supplementary material II.4**). Finally, from the entire substrate dataset (17 facies), we calculated a substrate/polygon hardness index (bounded between 1 and 6). To do this, a substrate hardness score between 1 and 6 was applied for each facies. From the frequencies (%) of each substrate, we calculated the hardness index per polygon.

Summary of the environmental variables and abbreviates is available in **Table II.2**.

II.2.5 Statistical analyses

II.2.5.1 Community structure

Statistical analyses were performed using R software (V4.1.2) (R Core Team, 2021).

For all analyses, faunal densities were processed by a quadratic root transformation to reduce the weight of taxa with extreme abundances compared to taxa with intermediate to low abundances. This transformation affects large values more strongly than small values and therefore reduces the skewness of the dataset (Legendre and Legendre, 2012). In addition, a Hellinger transformation of the data was also applied to densities ('vegan' package (Oksanen et al., 2020), *decostand()* function). This transformation is recommended for community-type datasets in ecology that usually contain many zeros, as it gives little weight to variables with low values and double absences (Legendre and Gallagher, 2001).

We assessed taxonomic richness between seamounts, using sample-based rarefaction curves (on polygons) applied to faunal presence/absence data ('vegan' package, *specaccum()* function). Interpolation of taxon richness for the smallest sampling effort (n = 58 polygons) and extrapolation of taxon richness for a sampling effort close to the asymptote of each curve (n = 400 polygons) were obtained with the 'iNEXT' package (Hsieh et al., 2020), *estimateD()* function. Rarefaction curves were also produced using a fixed taxonomic rank for each

taxonomic group. In order to maintain consistency in dataset bias, we kept the same dataset (finest taxonomic rank without rank nesting) for all analyses.

Table II.2 : Summary of the environmental variables originally used for the analyses. Variables in bold are those conserved for the analyses after removal of collinearities. All the variables were averaged in 200 m^2 polygons

Parameters	Variables	Abbreviation for the variables conserved after removal of collinearities
Current	Current velocity 0-50 m	/
	Current velocity 50-200 m	/
	Current velocity 350-650 m	**SP 350.650**
	Current variability 0-50m	**STD 0.50**
	Current variability 50-200m	/
	Current variability 350-650m	**STD 350.650**
Chlorophyll a concentration (Chla)	**Winter Chla**	**CHLA.WIN**
	Summer Chla	/
	Annual Chla	/
	Minimum Chla	/
	Maximum Chla	/
	Inter-annual Chla variability	**CHLA.y.sd**
	Intra-annual Chla variability	/
Water parameters	Temperature	/
	Salinity	/
	Oxygen	/
Spatial	**Latitude**	**LAT**
	Longitude	**LONG**
	Distance to Madagascar coast	DIST.MALG
	Distance to Mozambique coast	DIST.MOZ
	Distance to the closest shore	DIST.SHORT
Bathymetry	**Bathymetry**	**BATHY**
Seafloor variables	Bottom position index (BPI) at:	
	60 m	**BPI 60**
	90 m	/
	120 m	**BPI 120**
	250 m	/
	500 m	**BPI 500**
	Longitudinal (profile) curvature	**CURV.L**
	Transverse (plan) curvature	**CURV.T**
	Total curvature	/
	Aspect northness	**A.COS**
	Aspect eastness	**A.SIN**
	Rugosity	**RUG**
	Slope	**SLOPE**
Geomorphology	**Volcanic geomorphology**	**G.VOLCA**
	Carbonate geomorphology	**G.CARBO**
	Mixed geomorphology	**G.MIX**
	Sedimentary geomorphology	**G.SEDI**
Substrate	**Substrate diversity**	**SUB.div**
	Substrate composition (nine facies):	
	Sediment	**/**
	Gravels	**GRAV**
	Biogenic	**BIOG**
	Carbonate rock	**RC**
	Volcanic rock	**RV**
	Mixed (sediment + rock)	**MIX**
	Mixed carbonate-sediment	**MIX.RC.S**
	Mixed volcanic-sediment	**MIX.RV.S**
	Mixed rock	**MIX.R**
	Hardness	**HARD**

We quantified a total beta diversity (BD) for each transect and calculated two sub-indices: LCBD (Local Contribution to Beta Diversity) and SCBD (Species Contribution to Beta Diversity) with the 'adespatial' package (Dray et al., 2022), *beta.div()* function .

LCBD values reflect the level of uniqueness of each sampling unit, i.e., polygons with high LCBD represent sites where the community composition is unique and tends to generate variability along the transect. Significant LCBDs were tested by a permutation test ($p < 0.05$, $n = 999$). The SCBD coefficients represent the level of variation of each individual taxon in the study area considered. Thus a taxon with a high SCBD value will contribute more strongly to the BD (Legendre and De Cáceres, 2013).

We performed a partition of the BD according to the components 'replacement' and 'abundance difference', for the latter on densities following a Hellinger transformation of the data, using the % difference coefficient, from the Podani indices family ('adespatial' package, *beta.div.comp()* function). Replacement (also called turnover) characterizes the tendency for taxa to replace each other along a sufficiently long gradient, while abundance difference characterizes the fact that one community may include more abundant taxa than another (Legendre, 2014).

Density comparisons between the explored transects over seamounts/island slopes were performed using a Kruskall-Wallis test for significance of density differences ('vegan' package, *kruskal.test()* function), and a post-hoc test of pairwise comparisons between the different groups with a bonferroni correction applied for multiple testing (*pairwise.wilcox.test()* function).

We defined the megabenthic assemblages using a biogeographic network method applied on density data (Vilhena and Antonelli, 2015), with the 'biogeonetworks' package (Leroy, 2022). This recent method provides an alternative approach to traditional classification methods based on a distance matrix. It is generally applied for large-scale case studies to define bioregions, and has the advantage of preserving species identity and considering only presence data between sites. We quantified the indicator values of taxa, their specificity and fidelity within their assemblages, with the 'labdsv' package (Roberts, 2019), *indval()* function. Specificity is the relative abundance of the species in each cluster (total abundance in the cluster/total abundance). Fidelity is the relative frequency of the taxon in each cluster

(number of sites where the species is present/number of sites in the cluster). The indicator value IndVal corresponds to the product of Fidelity * Specificity and allows the identification of characteristic taxa for a group of sites (habitat or cluster) resulting from a clustering analysis (Dufrêne and Legendre, 1997; Roberts, 2019).

Graphical representations were made with the 'ggplot2' package (Wickham et al., 2016).

II.2.5.2 Role of environmental factors

Assessment of the environmental factors explaining differences in richness, density and BD between sites was carried out using simple and multiple regression models for the response variables density and beta diversity (continuous quantitative) with the *lm()* function of the 'stats' package (R Core Team, 2021). For richness (discrete quantitative), we used generalized linear regression models, following a Poisson distribution, with the *glm()* function of the 'stats' package.

To evaluate the environmental factors structuring the composition of the assemblages we carried out a redundancy analysis (RDA), with the 'vegan' package, *rda()* function. Since this analysis is sensitive to collinearities between variables, we first evaluated the collinearities between environmental variables using Spearman's pairwise correlations and removed the variables with high collinearities (Spearman's $r > 0.85$). The significance of the model, variables and axes is tested by a permutation test of the F-statistic (999 permutations, $p < 0.05$) with the *anova.cca()* function of the 'vegan' package. To obtain parsimonious RDA models, we applied forward selections of the explanatory variables with the *ordiR2step()* function ('vegan' package), and the application of the selection criterion of the best model by the adjusted R^2 of the model. This selection criterion reduces the risk of incorporating more variables than necessary into the model (Borcard et al., 2018).

Partial RDAs (pRDAs) allowed us to quantify the variance explained by a set of environmental variables while controlling and adjusting the regression model by the effect induced by co-variables. The co-variables tested were: spatial (latitude, longitude), geomorphology, depth, hydrology variables (current and chlorophyll) together and separately.

On each slope of Mayotte and Bassas da India islands, we assessed and quantified the overall spatial structure of the faunal dataset, which we decomposed into large, medium and fine spatial scale sub-models, using distance-based Moran eigenvector map (dbMEM) analyses

('adespatial' package, *dbmem()* function). First, RDAs are applied between the response variables (taxon densities) after removing the trend from the dataset, and the explanatory spatial variables (called MEM for Moran Eigenvectors Map). Then a permutation test of the RDA model is used to determine the significant axes and MEMs. The set of significant MEMs, which represent spatial structure patterns at different scales, are then grouped together according to the spatial scales they represent. New RDAs are applied separately on the community dataset according to each set of explanatory spatial variables (large, medium and fine scales) and significance of the axes are assessed. The correlation between significant axes, representing large, medium and fine scale patterns, and the environmental (explanatory) variables was examined using multiple regressions for each significant spatial axis with the environmental factors (*lm()* function). The conditions of application – normality and variance homogeneity of the residuals – were assessed to validate the regression models.

Finally, variation partitioning analysis of the fauna dataset (Hellinger-transformed density) were performed by integrating different matrices of explanatory environmental variables (geomorphology, substrate, terrain, hydrology, large, medium and fine scale spatial models) to quantify the percentages of variance explained by each set of environmental variables, and their interrelationships ('vegan' package, *varpart()* function). The fractions of variance explained by each matrix were represented using Venn diagrams. The fractions were tested via a permutation test (*anova.cca()* function, n = 999 permutations, p-value < 0.05).

II.3 Results

II.3.1 Structure of megabenthic assemblages

II.3.1.1 Density

The highest taxa density is observed on Glorieuses (779.8 ± 751.3 ind/200 m^2), which also shows the highest intra-site density variability, and a significant difference in density with all other sites (**Figure II.2**, **Table II.4**). The eastern slope of Mayotte (183.4 ± 169.3 ind/200 m^2) shows significantly different densities with all other sites except with Sakalaves and Jaguar, and more than twice those observed on the northern and western slopes of Mayotte, for which densities are comparable (80.3 ± 131.0 and 89.4 ± 240.8 ind/200 m^2 respectively). The Sakalaves and Jaguar seamounts show intermediate densities comparable to the eastern slopes of Mayotte. These two seamounts are located in the center and further south of the

channel and also do not show significant differences in density between them. In addition, the densities observed on Sakalaves are significantly higher than those observed on Hall and Bassas. These two seamounts have significantly lower densities than the other sites, except for the northern and western slopes of Mayotte. Finally, on Hall, we observe more variable densities along dive 11 (summit, 70.9 ± 170.5 ind/200 m^2) than along dive 12 (summit-slope, 81.0 ± 93.4 ind/200 m^2).

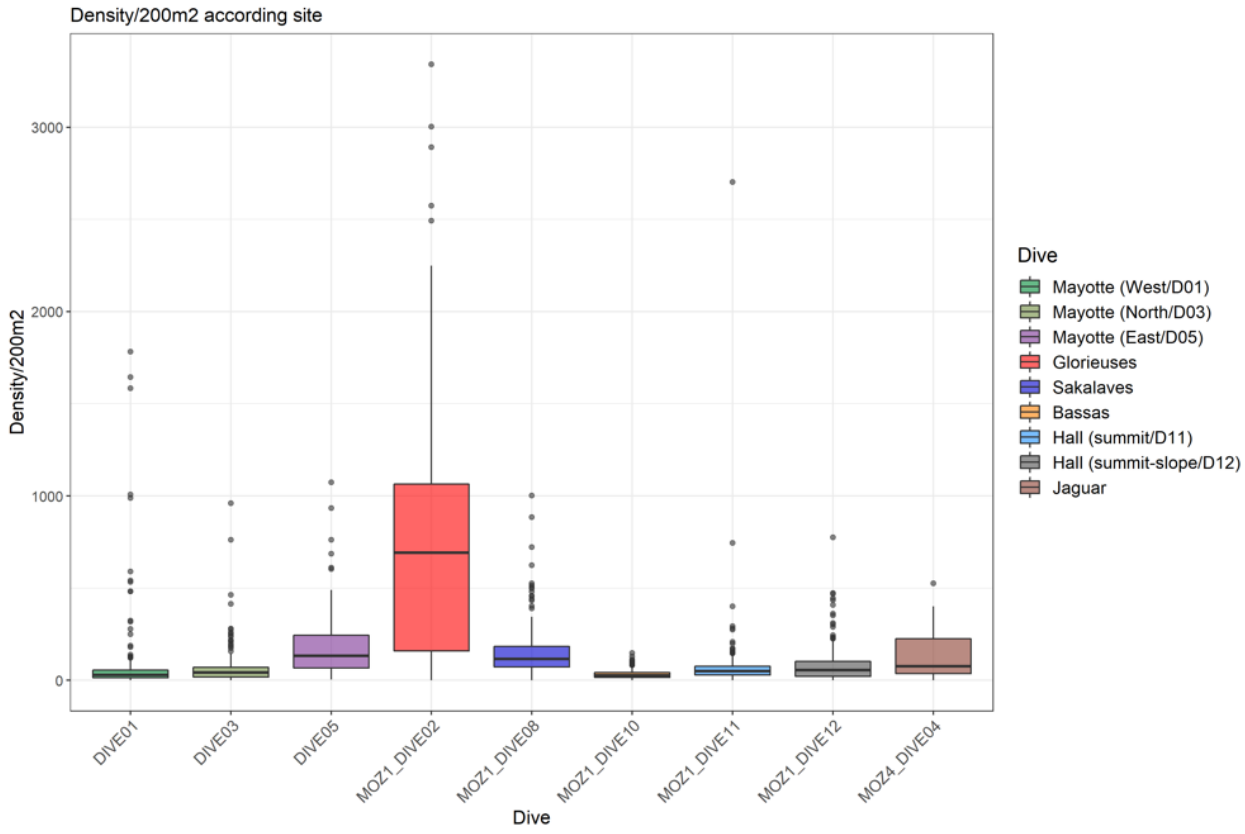

Figure II.2 : Boxplots representing the distribution of benthic megafauna density (ind/200 m^2 polygon), for the nine towed camera transects

II.3.1.2 Taxonomic richness

For the same sampling effort (n = 58 polygons), the eastern and northern slopes of Mayotte have the highest taxonomic richness (TR) compared to the other sites (TR = 54 and 52 respectively) and higher than the western slope (TR = 44). The sites in the center and south of the channel show intermediate and comparable taxonomic richness (TR between 37 and 40), while Glorieuses platform has the lowest taxonomic richness of all the sites (TR = 29) (**Figure II.3**). Extrapolated taxonomic richness (n = 400 polygons) shows that with a more consistent sampling effort, taxonomic richness on the eastern slope would be higher than on the

northern slope (TR = 83 and 73 respectively) (**Figure II.3**, **Table II.4**). However, this extrapolation does not show a significant change in the richness of each site relative to the others.

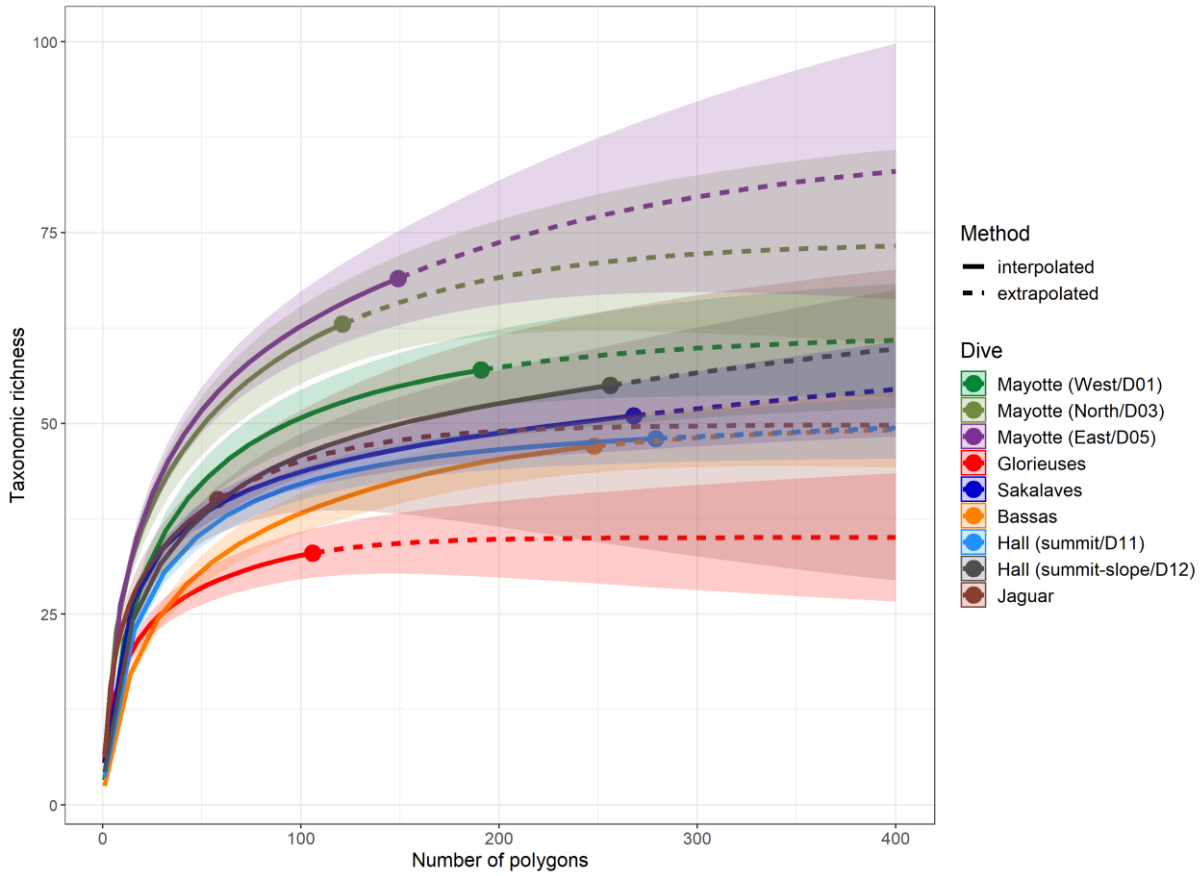

Figure II.3 : Rarefaction curves representing taxonomic richness as a function of the number of polygons (200 m^2) sampled, for each towed camera transect. Solid lines represent observed taxonomic richness while dashed lines represent extrapolated taxonomic richness for a sampling effort equal to 400 polygons, from the number of Hill (of order q = 0). The coloured areas represent the 95% confidence intervals for each transect

II.3.1.3 Taxonomic composition

A total of 99 taxa were identified (phylum to species) from the 8430 images analyzed. Some groups could only be identified to phylum (brachiopods), or class (e.g., sponges, ophiuroids, holothurians, some crinoids, gastropods). Cnidarians could be identified mainly to order and show distinct compositions and frequency between sites (relative frequency histogram of cnidarians orders in **Supplementary material II.5**). We were able to provide more detailed identifications ranging from order/family for fishes and to genus/morphospecies for decapods, urchins and asteroids.

We first compared the taxonomic composition between the seamounts and island slopes, at the higher taxonomic ranks. We observed heterogeneous site to site megabenthic composition (**Figure II.4**).

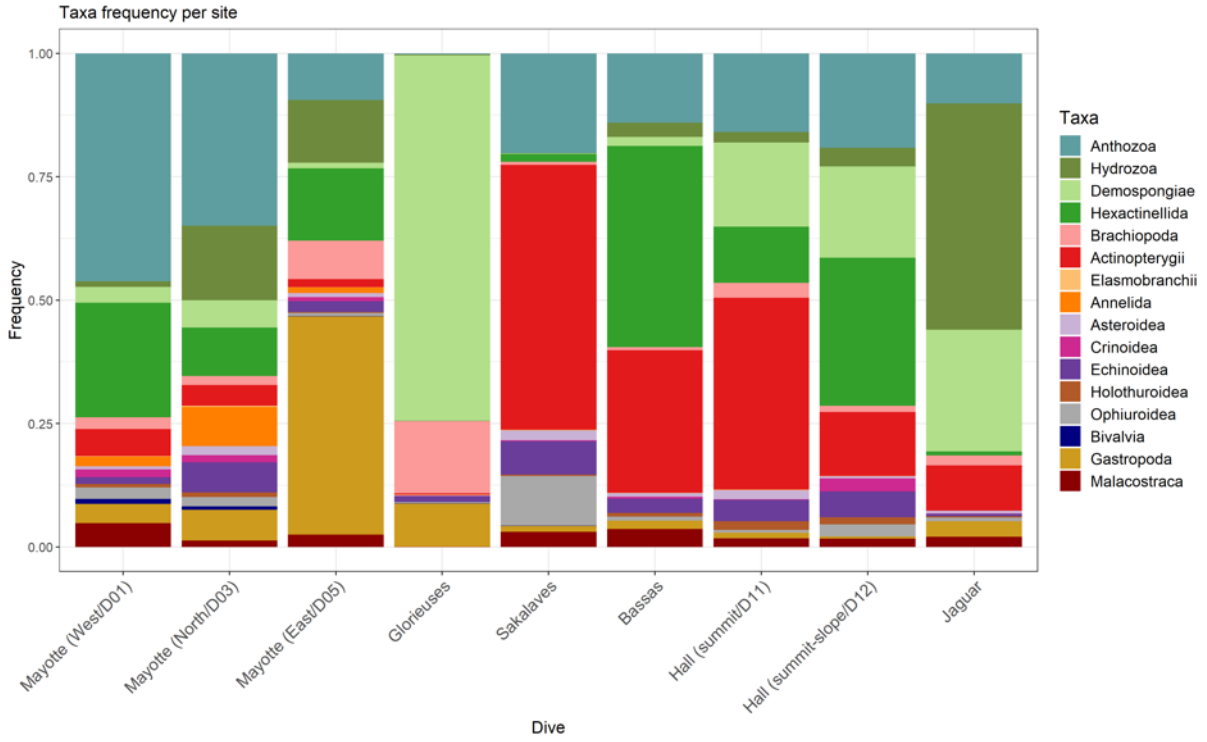

Figure II.4 : Relative frequencies of megabenthic taxa whose identification is aggregated to phylum or class rank for each transect

The relative frequency of habitat-forming taxa (cnidarians/sponges) varies between seamounts and island slopes, as for mobile taxa (**Figure II.4**, **Table II.3**).

Most of the site have higher relative frequency of habitat-forming taxa such as Glorieuses dominated by Demospongiae, the northern and western slopes of Mayotte (e.g., Anthozoa, Hexactinellida) as for Hall Bank (Anthozoa, Demospongiae, Hexactinellida), Bassas (Hexactinellida) and Jaguar (mainly Hydrozoa, i.e., Stylasteridae incertae). Among the habitat-forming taxa, we also observed relative frequency differences among sponge groups (Demospongiae, Hexactinellida) and among cnidarians (Anthozoa, Hydrozoa) between sites, as well as relative frequency differences among cnidarians and sponges in general.

Conversely, the eastern slope of Mayotte and Sakalaves display a higher relative frequency of mobile taxa such as Gastropoda on the eastern slope of Mayotte or dominance of Actinopterygii on Sakalaves and higher proportion of ophiuroids. Details of the densities of

each taxon by dive are available in **Supplementary material II.6**. Globally, fish have higher relative frequency in the central/southern sites of the channel.

Brachiopods have high relative frequencies on Glorieuses and the eastern slope of Mayotte compared to the other sites.

For the four taxa (asteroids, echinoids, fish and crustaceans) identified to lower taxonomic ranks we observed differences in composition and richness among the surveyed sites (**Figure II.5**).

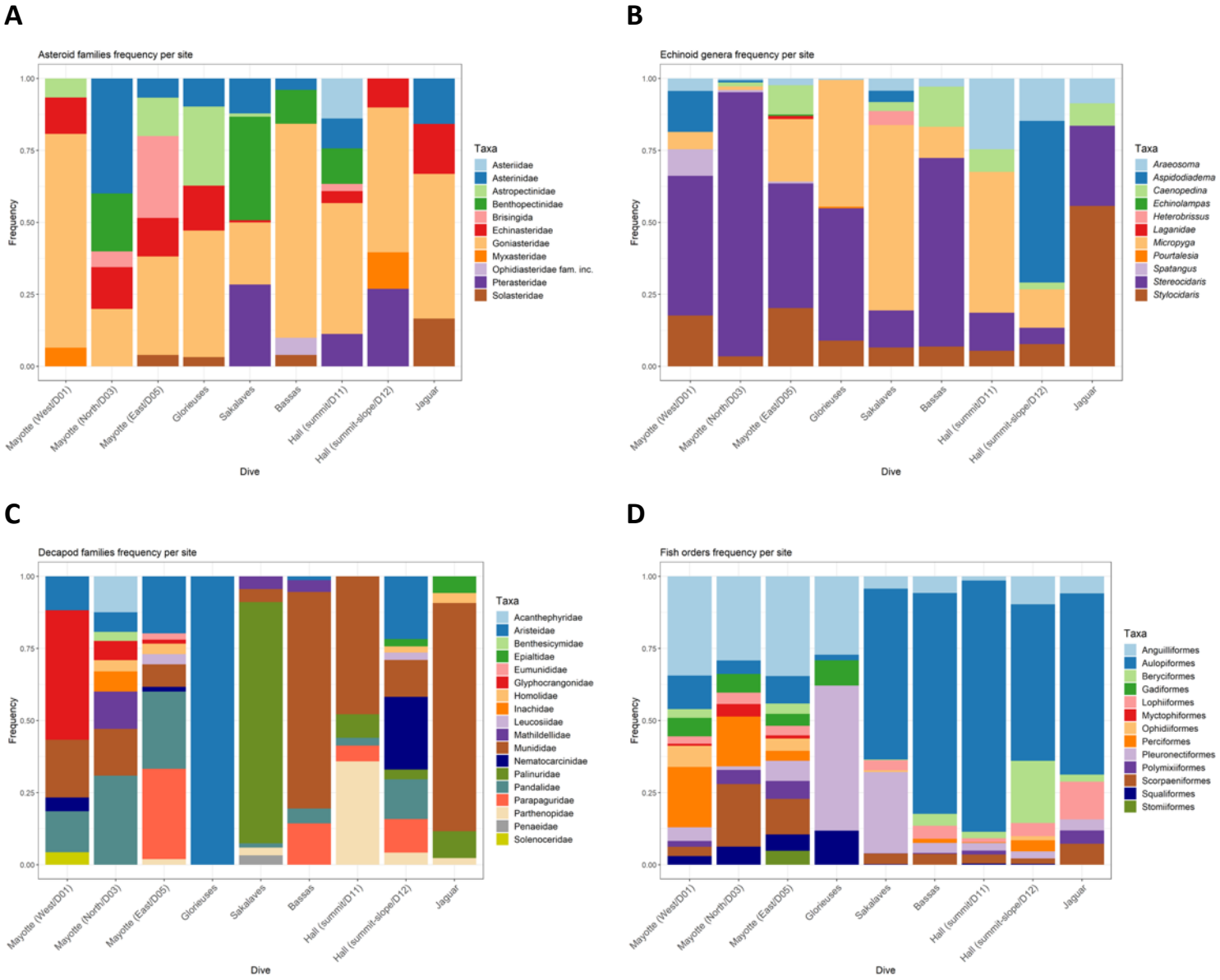

Figure II.5 : Relative frequencies of megabenthic taxa with fine identification rank for the nine transects: **(A)** asteroids aggregated to the ranks of family and order (Brisingida), **(B)** echinoids aggregated to the ranks of genus and family (Laganidae), **(C)** decapods aggregated to the rank of family, **(D)** fish aggregated to the rank of order

Some taxa show ubiquitous distributions along the Mozambique Channel. For example, the families of asteroids Goniasteridae and Echinasteridae, were present in all the sites except Bassas (**Figure II.5A**); the genera of urchins *Stereocidaris*, *Stylocidaris* and *Micropyga* were present in all the sites (**Figure II.5B**). This is also the case for the crustacean family Munididae (genera *Munida*, *Agononida*) observed at all sites except Glorieuses (**Figure II.5C**). This apparent ubiquity may however only reflect the taxonomic rank reached in the identification. Indeed, for the genus *Micropyga*, two morphospecies were identified in distinct sites, one present on Glorieuses (*Micropyga* sp2) and on Sakalaves and the second one on the summit of Hall (*Micropyga* sp1). Conversely, other taxa appear to have distributions restricted to certain sites, such as the Pterasteridae (asteroids, genus *Pteraster*), in the center and south of the channel (Sakalaves and Hall), the family Myxasteridae exclusively on the western slope of Mayotte (**Figure II.5A**), the urchin genus *Heterobrissus* on Sakalaves or *Pourtalesia* on Glorieuses (**Figure II.5B**), the crustacean family Glyphocrangonidae (genus *Glyphocrangon*), on the slopes of Mayotte (**Figure II.5C**) or the fishes Aulopiformes, which are particularly abundant in the center and south of the channel and characterize the high abundances of the genus *Chlorophthlamus* observed on Sakalaves, Bassas, Hall and Jaguar (**Figure II.5D**).

II.3.1.4 Assemblage variability

From the biogeographic network analysis, we obtained 45 distinct assemblages (clusters). The network interpretation indicates dominant clusters that are generated by a limited number of taxa, those with a very high abundance, and clusters representative of a single taxon (rare taxa in the community).

A large part of the community is composed of taxa that are found in many sites (low specificity for an assemblage) but whose abundances are variable (high fidelity for a given assemblage) (**Table II.3**). These ubiquitous taxa are generally those identified at higher ranks only. Clusters are mainly generated according to differences in abundance between sites of these ubiquitous taxa. Conversely, some taxa are present at few sites and are generally identified at a finely resolved identification rank. For these taxa specificity equal to 100% and fidelity is low reflecting the fact that they are found in very few sites of the cluster (e.g., *Tremaster mirabilis*, *Pourtalesia*, *Penaeopsis*, *Acanthephyra*, *Eumunida*, *Benthesicymus*, *Aristeus mabahissae*) (**Table II.3**).

Table II.3 : Taxonomic composition of the 12 most represented assemblages along the Mozambique Channel, and for each taxon, indication of its relative frequency of occurrence within the assemblage (Fidelity), its relative abundance (Specificity), and its indicator value of contribution to the assemblage (IndVal)

Assemblages	Taxa	Fidelity (%)	Specificity (%)	IndVal (%)
A1	**Demospongiae**	91.5	77.8	71.1
	Brachiopoda	80.9	56.4	45.6
	***Micropyga* sp2**	33.3	29.7	9.9
	Tremaster mirabilis	1.4	39.1	0.6
	Pourtalesia	0.7	100.0	0.7
A2	***Chlorophthalmus***	95.6	30.9	29.6
	Pleuronectiformes	41.6	27.2	11.3
	Anguilliformes	26.7	4.5	1.2
	Puerulus carinatus	17.1	24.4	4.2
	Poecilopsetta	15.2	41.0	6.2
	Araeosoma	8.5	16.0	1.4
	Cheiraster	5.8	16.2	0.9
	Peristediidae	8.3	22.5	1.9
	Pteraster sp.	2.5	13.3	0.3
	Penaeopsis	0.8	100.0	0.8
A3	**Hexactinellida**	99.6	15.9	15.8
	Enallopsammia	5.5	73.0	4.0
	Heterocarpus	3.4	6.3	0.2
	Acanthephyra	0.4	100.0	0.4
	Eumunida	0.4	100.0	0.4
	Benthesicymus	0.4	100.0	0.4
A4	**Gastropoda**	98.4	34.5	33.9
	Paguroidea	39.5	24.7	9.8
	Caenopedina sp.	4.8	41.5	2.0
	Stomiiformes	2.4	72.2	1.8
	Aristeus mabahissae	0.8	53.9	0.4
	Bathyalcyon	0.8	100.0	0.8
	Sympagurus sp2	0.8	100.0	0.8
	Echinolampas	0.8	100.0	0.8
A5	**Stylasteridae incertae**	100.0	63.4	63.4
	Epialtidae	2.9	100.0	2.9
A6	**Scleractinia solitary**	100.0	44.5	44.5
	Scleractinia colonial	14.9	83.5	12.4
	Heterobrissus	7.4	60.6	4.5
	Oxypleurodon	1.1	100.0	1.1
A8	**Alcyonacea**	87.9	24.5	21.6
	Comatulida	48.5	23.2	11.3
	Hydrozoa	1.5	27.9	0.4
A9	**Ophiuroidea**	100.0	75.0	75.0
A10	**Antipatharia**	80.0	37.2	29.7
	Annelida	38.3	34.8	13.4
	***Javania* sp.**	30.0	42.4	12.7
	Solasteridae	3.3	75.3	2.5
A11	***Micropyga* sp1**	77.8	32.4	25.2
	Goniasteridae	41.7	24.1	10.0
	Parthenopidae	11.1	19.6	2.2
A13	**Actiniaria**	97.1	22.2	21.6
	Squaliformes	5.7	5.5	0.3
	Synodontidae	14.3	33.4	4.8
	Myctophiformes	5.7	49.3	2.8
A14	***Stereocidaris***	91.3	37.0	33.8
	Bivalvia	30.4	22.4	6.8

Out of a total of 45 assemblages, 12 assemblages are present in at least 30 sampling units. The main indicator taxa of each of these 12 assemblages have indicator values between 20 and 75% (**Table II.3**, **Figure II.6**), except for Hexactinellida. According to the biogeographical network, Hexactinellida is the indicator taxon for assemblage 3, because although it has a low indicator value (15.8%), its fidelity within this assemblage is 99.6%, i.e., it is found in practically all the sites in this assemblage.

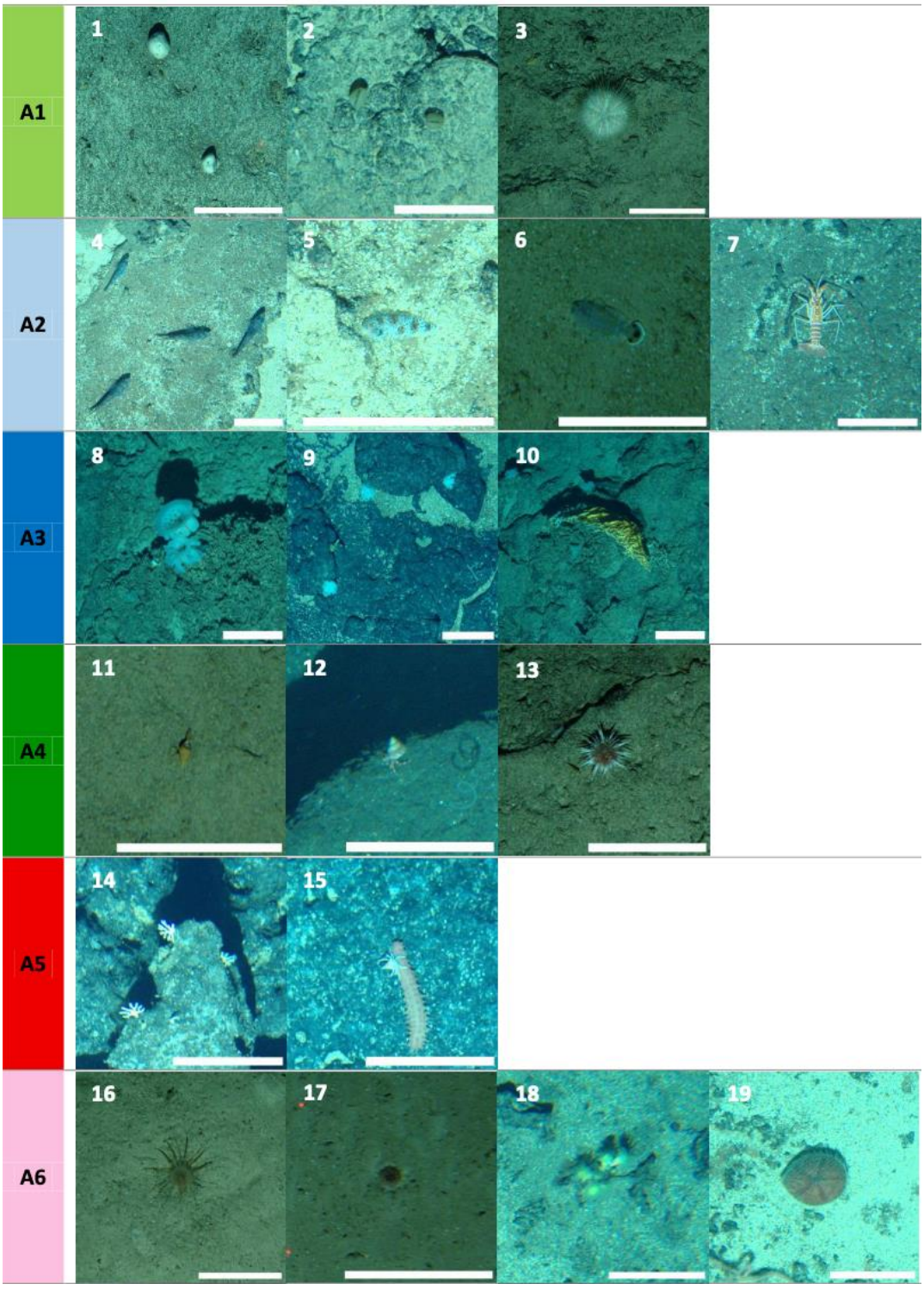

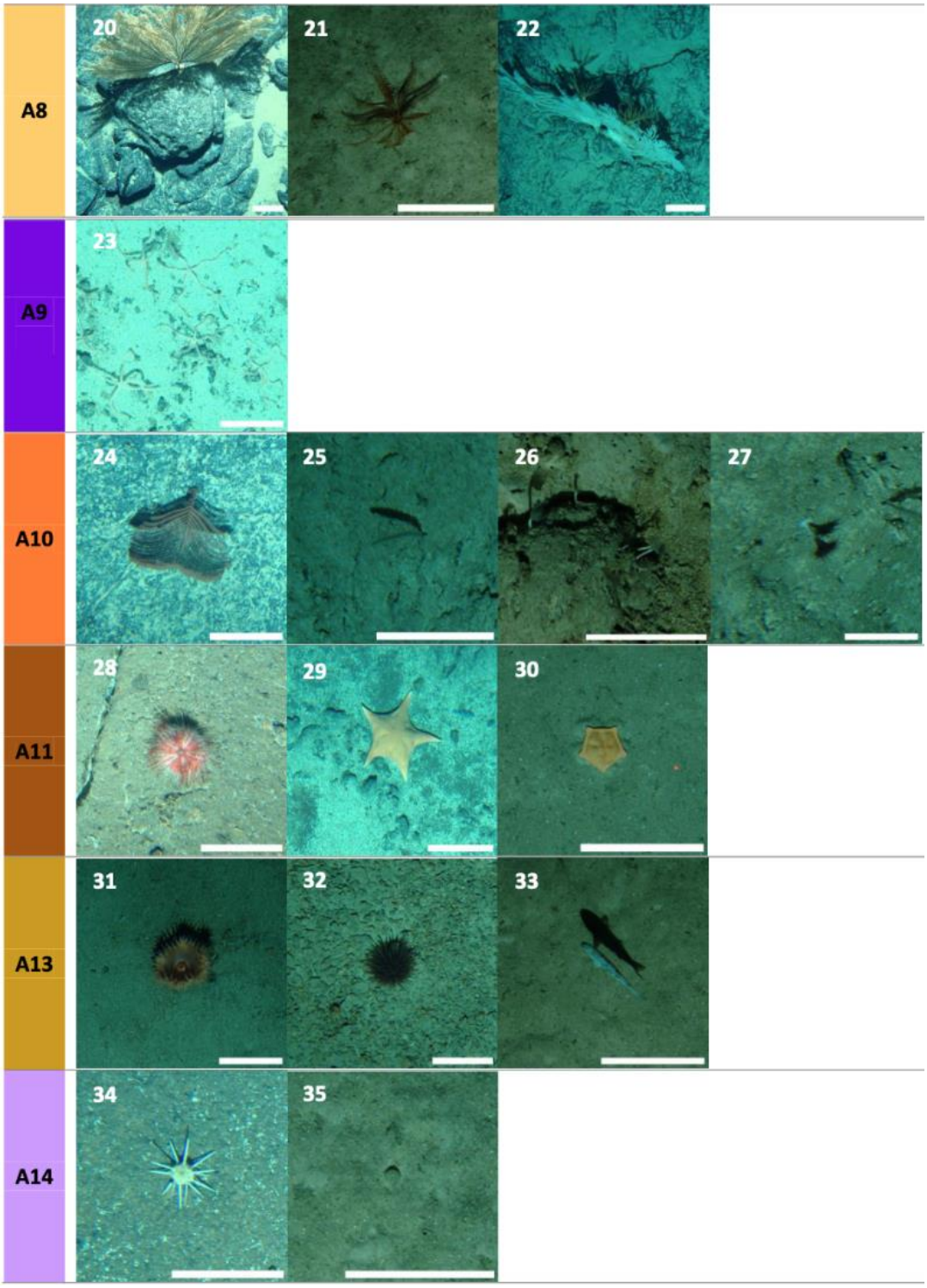

Figure II.6 : Illustrative images of the contributing taxa from the 12 assemblages observed along seamounts and island slopes. 1 – Demospongiae; 2 – Brachiopoda; 3 – *Micropyga* sp2; 4 – *Chlorophthalmus*; 5 – Pleuronectiformes; 6 – *Poecilopsetta*; 7 – *Puerulus carinatus*; 8 – *Aphrocallistes* sp.; 9 – Hexactinellida; 10 – *Enallopsammia*; 11– Gastropoda; 12 – Paguroidea; 13 – *Caenopedina* sp.; 14 – Stylasteridae incertae; 15 – Epialtidae over an Holothuroidea; 16, 17 – Scleractinia (solitary); 18 – Scleractinia (colonial); 19 – *Heterobrissus*; 20 – Alcyonacea; 21 – Comatulida; 22 – Comatulida over a large Alcyonacea coral; 23 – Ophiuroidea; 24, 25 – Antipatharia; 26 – Annelida; 27 – *Javania* sp.; 28 – *Micropyga* sp1; 29, 30 – Goniasteridae asteroids; 31, 32 – Actiniaria; 33 – Synodontidae; 34 – *Stereocidaris*; 35 – Bivalvia (Propeamussidae)

The full description of the assemblages (taxonomic composition, fidelity, specificity and indicator value) is available in **Supplementary material II.7**.

The spatial representation of these 12 assemblages within each site (transect) shows they display patchy distributions ranging from large (2 km, e.g., on Glorieuses or upper slope of Bassas) to small patch size (0.06 km; e.g., on the Northern slope of Mayotte, Hall summit-slope); i.e., representing different scales of assemblage variability (**Figure II.7**).

Assemblage dominance and spatial pattern differs also among seamounts and island slopes. (**Figure II.7**). For example, the A2 assemblage (characterized by *Chlorophthalmus* and Pleuronectiformes) occurs mainly at sites in the center and south of the channel and forms very large patches. The A4 assemblage (characterized by Gastropoda and Paguroidea) form large patches only over Glorieuses and the eastern slope of Mayotte while A5 assemblage (characterized by Stylasteridae incertae) is dominant over Jaguar, and forms larger patches than over the eastern slope of Mayotte and the other sites.

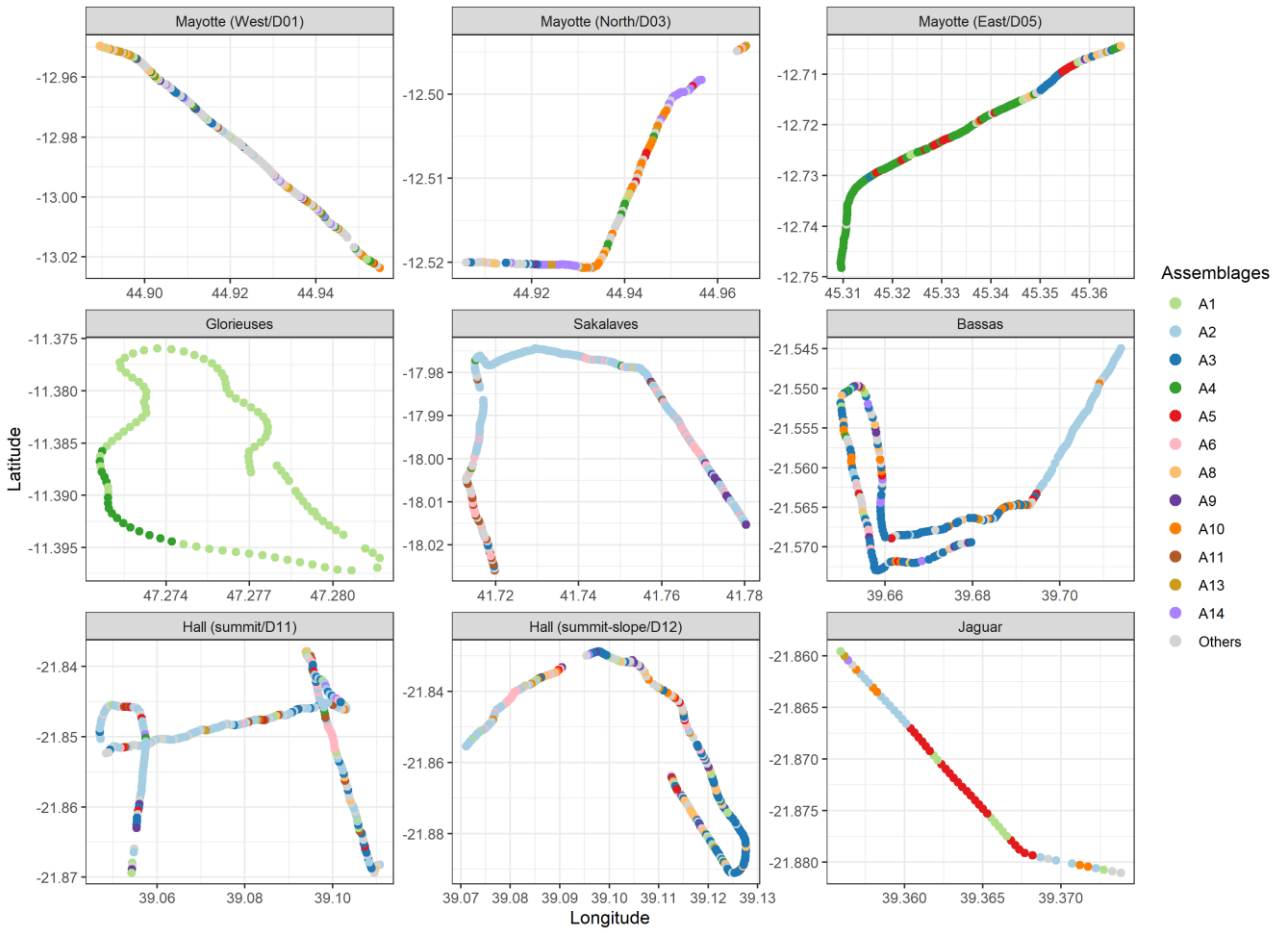

Figure II.7 : Map of the 12 most represented assemblages (each assemblage is found in at least 30 polygons) within the Mozambique Channel, obtained from a biogeographic network analysis

II.3.1.5 Beta diversity

With the exception of Glorieuses where the total beta diversity (BD) is low (BD = 0.28), the BD for all other sites is high (BD between 0.61-0.81) out of a maximum total of 1, for the Hellinger distance coefficient (**Table II.4**). The highest BDs are observed for the western and northern slopes of Mayotte. The Bassas slope and dive 12 on Hall (summit-slope) show intermediate BDs. Finally, the eastern slope of Mayotte shows a lower value (BD = 0.62) than the other two slopes of Mayotte, and a level comparable to Sakalaves at the summit of Hall and Jaguar. The decomposition of total beta diversity according to the replacement and abundance difference components shows that the replacement process is dominant at almost all sites, except for Glorieuses and Jaguar where these processes contribute equally.

Table II.4 : Summary of total mean density/polygon (200 m^2); and standard deviation, proportion of sessile fauna (comprising habitat-forming taxa and Brachiopoda) to the total mean density, interpolated taxonomic richness for n = 58 polygons (TR 58), and estimated (Hill, q = 0) for n = 400 polygons (ES 400), and total beta diversity (BD) values for the nine transects

Site	Total mean density/200 m^2	% sessile fauna	TR 58	ES 400	BD
Mayotte, West slope	89.4 ± 240.8	76.4	44	61	0.81
Mayotte, North slope	80.3 ± 131.0	67.2	52	73	0.79
Mayotte, East slope	183.4 ± 169.3	46.1	54	83	0.62
Glorieuses	779.8 ± 751.3	89.2	29	35	0.28
Sakalaves	148.3 ± 128.7	22.6	39	54	0.61
Bassas	31.5 ± 24.4	60	32	49	0.70
Hall, summit	70.9 ± 170.5	49.8	37	49	0.63
Hall, summit-slope	81.0 ± 93.4	72.8	39	60	0.69
Jaguar	139.9 ± 128.2	83.6	40	50	0.65

SCBD (Species Contribution to beta diversity) values range from 1.6% to 19.1%.

In all sites, poriferans and cnidarians, that are fixed and potentially habitat-forming taxa, have a high cumulative SCBD value, ranging from 18.7% on Glorieuses to a 45.5% on Hall's dive 12 (summit-slope) (**Figure II.8A**). These taxa comprise notably Hexactinellida, Demospongiae, Stylasteridae incertae, Antipatharia, the solitary scleractinians, Alcyonacea, Pennatulacea, Actiniaria and the scleractinian *Enallopsammia*.

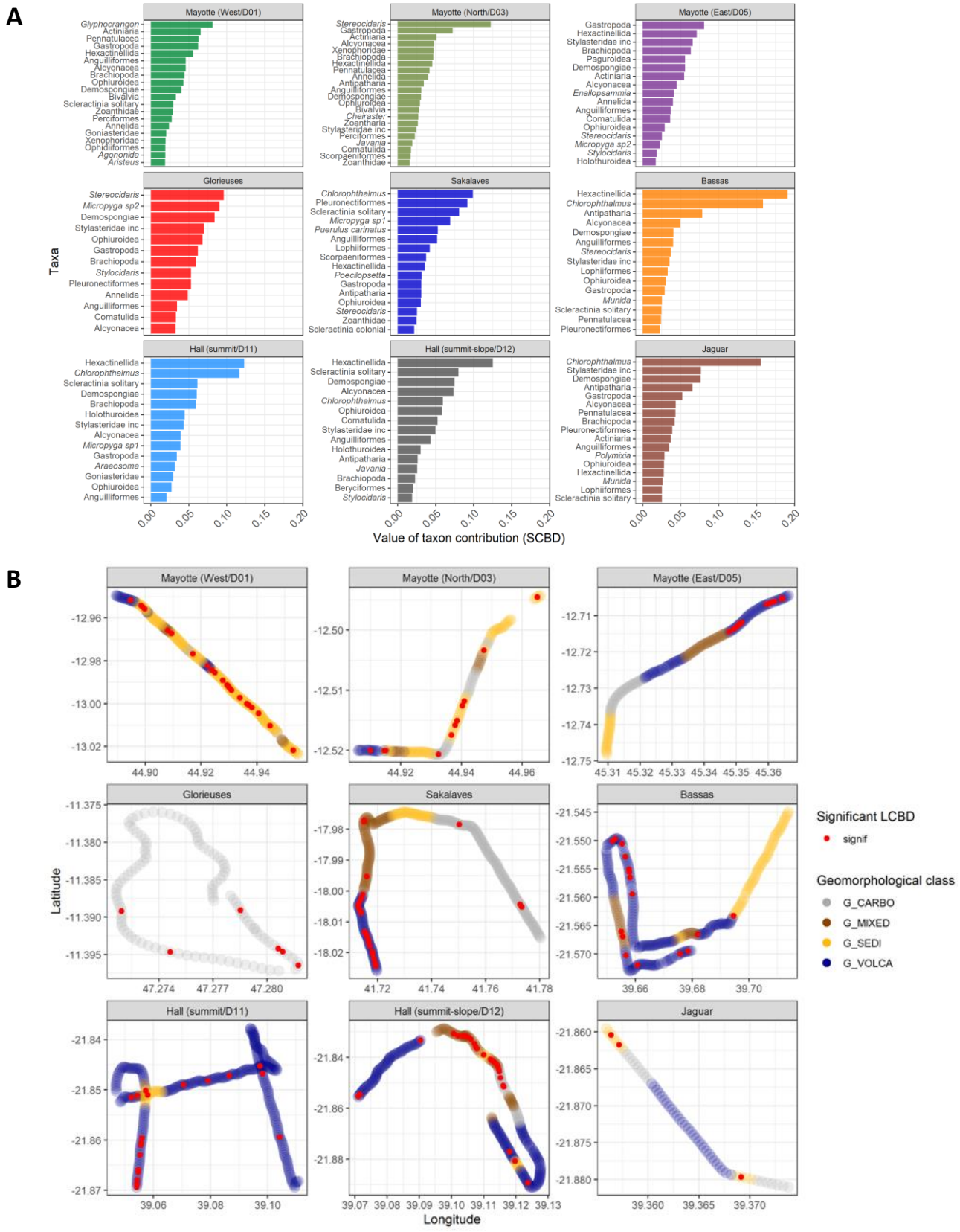

Figure II.8 : (A) Histograms representing taxa with SCBD (Species Contribution to Beta Diversity) values higher than the transect mean, for each transect. **(B)** Maps representing polygons with significant LCBD (Local Contribution to Beta Diversity) values (999 permutations, $p < 0.05$) (red dot), i.e., with a unique taxa composition, for each transect

Brachiopoda contribute to the variability along the sites as well (2-6%) except on Sakalaves and Bassas.

Mobile taxa contribute also to the total BD, with SCBD values ranging from 1.7% to 15.9%, and a cumulative contribution ranging from 28.3% on the summit-slope of Hall up to 56.3% observed on Sakalaves.

An urchin of the genus *Stereocidaris*, displays the greatest contribution on the northern slope of Mayotte (12.4%) and on Glorieuses (9.6%). Other urchins of the genus *Micropyga* have high contributions, particularly *Micropyga* sp2 (9%) on Glorieuses and *Micropyga* sp1 (6.9%) on Sakalaves. Crustaceans also contribute to the variability along transects, such as *Glyphocrangon* (8.13%) on the western slope of Mayotte or *Puerulus carinatus* (5.30%) on Sakalaves. A fish of the genus *Chlorophthalmus* is generally observed as one of the first contributing taxon on Sakalaves, Bassas, Hall and Jaguar, with contributions between 5.9% and 15.9%. Finally, the Gastropoda group is among the first contributing taxa on the slopes of Mayotte and Glorieuses (6 to 8%).

Polygons with significantly higher LCBD (Local Contribution to Beta Diversity) values are located on particular geomorphological facies or transition zones for each transect, and vary between 0.003 and 0.03 (**Figure II.8B**).

Depending on the seamount and island slope, some geomorphological facies will concentrate a great amount of polygon with significant LCBDs (i.e., polygons with unique megabenthic composition), such as sedimentary facies on the northern and western slopes of Mayotte, or volcanic facies on Sakalaves, Hall summit and Bassas, or mixed facies on a slope on Hall dive 12 (summit-slope).

Polygons with significant LCBDs can also be scarce and located at interfaces. This is the case for Jaguar, where only two significant LCBDs are located at the interface between different types of substrates (sediment-carbonate, volcanic-sediment). On Glorieuses, we also observe very few significant LCBDs, due to the low BD along this transect, however, the two LCBDs (between -11.389 latitude and 47.275 longitude) are located at the interface between the summit and the upper slope of the carbonate platform.

II.3.2 Environmental drivers of megabenthic assemblage patterns

II.3.2.1 Seamount and island slope environmental characteristics

Hydrology (current, surface primary productivity, water mass)

Varying current speeds (from 0.004 to 0.4 m/s) flow over the different seamounts and island slopes, on different bathymetric layers. Glorieuses and Sakalaves have the highest current speeds (between 0 and 650 m and between 0 and 200 m respectively) (**Table II.5**). The Hall and Jaguar seamounts and the northern and western slopes of Mayotte are traversed by intermediate velocities between 0 and 200 m while the lowest ones are estimated on the eastern slopes of Mayotte and Bassas. Further down at 350-650 m, intermediate current speeds are found in Sakalaves, Hall, Jaguar and the northern slope of Mayotte and the lowest current speeds are estimated on the western and eastern slopes of Mayotte.

Table II.5 : Summary of current variables, chlorophyll a concentrations, temperature and oxygen, substrate diversity and hardness (mean ± standard deviation). "_" = no data

Site	Winter Chla (mg/m^3)	Total Chla (mg/m^3)	Inter-annual Chla (mg/m^3)	Velocity 0-50m (m/s)	Velocity 50-200m (m/s)	Velocity 350-650m (m/s)	std velocity 0-50m (m/s)	std velocity 50-200m (m/s)	std velocity 350-650m (m/s)	Temperature (°C)	Oxygen (µmol/kg)	Substrate diversity	Hardness (1 to 6)
Mayotte, West slope	0.163 ± 0.005	0.133 ± 0.004	0.007 ± 0.001	0.106 ± 0.005	0.113 ± 0.009	0.007 ± 0.007	0.330 ± 0.008	0.265 ± 0.003	0.081 ± 0.053	8.8 ± 1.1	182.0 ± 32.0	0.19 ± 0.37	1.53 ± 1.09
Mayotte, North slope	0.162 ± 0.004	0.134 ± 0.004	0.007 ± 0.001	0.123 ± 0.004	0.102 ± 0.006	0.029 ± 0.014	0.373 ± 0.003	0.287 ± 0.004	0.078 ± 0.071	10.9 ± 1.1	206.5 ± 32.1	0.36 ± 0.41	1.96 ± 1.32
Mayotte, East slope	0.242 ± 0.083	0.203 ± 0.069	0.020 ± 0.013	0.050 ± 0.004	0.037 ± 0.003	0.004 ± 0.008	0.276 ± 0.052	0.204 ± 0.038	0.033 ± 0.042	9.1 ± 1.9	182.5 ± 43.5	0.25 ± 0.34	4.60 ± 1.97
Glorieuses	0.171 ± 0.001	0.137 ± 0.001	0.009 ± 0	0.391 ± 0.006	0.305 ± 0.001	0.140 ± 0.001	0.333 ± 0	0.265 ± 0	0.189 ± 0	7.4 ± 0.3	147.8 ± 12.9	0 ± 0	6.00 ± 0
Sakalaves	0.155 ± 0.001	0.130 ± 0	0.008 ± 0	0.196 ± 0.002	0.143 ± 0.001	0.037 ± 0.007	0.607 ± 0.005	0.450 ± 0.007	0.152 ± 0.012	14.3 ± 0.6	_	0.21 ± 0.33	5.21 ± 1.67
Bassas da India	0.166 ± 0.001	0.142 ± 0.001	0.029 ± 0	0.040 ± 0.002	0.037 ± 0.001	0.027 ± 0.003	0.417 ± 0.012	0.312 ± 0.012	0.043 ± 0.064	11.1 ± 0.5	243.3 ± 5.0	0.27 ± 0.36	4.01 ± 1.77
Hall, summit	0.158 ± 0	0.132 ± 0	0.015 ± 0.001	0.130 ± 0.002	0.100 ± 0.003	0.020 ± 0.003	0.495 ± 0.003	0.386 ± 0.004	0.174 ± 0.003	11.0 ± 0.2	243.1 ± 0.7	0.17 ± 0.29	4.47 ± 1.18
Hall summit-slope	0.159 ± 0.001	0.132 ± 0.001	0.014 ± 0.002	0.126 ± 0.003	0.096 ± 0.004	0.017 ± 0.002	0.492 ± 0.004	0.382 ± 0.005	0.171 ± 0.003	10.1 ± 0.3	220.3 ± 29.0	0.32 ± 0.38	4.94 ± 1.19
Jaguar	0.168 ± 0	0.131 ± 0	0.008 ± 0	0.119 ± 0.002	0.095 ± 0.001	0.032 ± 0.001	0.473 ± 0	0.362 ± 0	0.144 ± 0	11.2 ± 0.2	233.1 ± 2.3	0.37 ± 0.38	4.34 ± 1.92

Sakalaves also has the highest current variability between 0 and 200 m (up to 0.61 m/s) while the lowest is estimated on the slopes of Mayotte and Glorieuses (0.20 to 0.37 m/s). However, further down, at 350-650 m, the current variability is stronger on the seamounts, with a

maximum on Glorieuses (0.19 m/s) and a minimum on the slopes of Mayotte and Bassas islands (minimum 0.03 m/s).

The daily average chlorophyll a concentration integrated over seven to ten years of monitoring is the highest and the most variable on the eastern slope of Mayotte (0.20 ± 0.07 mg/m^3) while on the other sites the concentration is comparable and varies only slightly (between 0.13 and 0.14 mg/m^3), although more variable on the island slopes (Mayotte and Bassas). The concentration is higher in winter than in summer in the channel (by a factor ~1.5), with a maximum on the eastern slope of Mayotte (0.24 ± 0.08 mg/m^3) and a minimum on Sakalaves (0.15 ± 0.001 mg/m^3), except on Bassas, where the average concentration varies poorly between winter and summer.

The hydrological characteristics (temperature, oxygen) differ between the seamounts and the island slopes, depending on their depth and the different water masses encountered (summary of the environmental descriptive statistics in **Supplementary material II.8**).

Sakalaves, the shallowest site (369-482 m) is crossed by warm (14-16.6 °C) and poorly oxygenated waters (~130-160 µmol/kg) characteristic of the subtropical surface water mass (STSW), at the interface also with the beginning of the South Indian Central Water Mass (SICW).

The intermediate depth sites (Hall summit, Jaguar, Bassas) located between 453 and 623 m, are traversed by waters of intermediate temperatures (10 to 12 °C) and highly oxygenated (227-244 µmol/kg), characteristic of the SICW water mass.

The deeper areas explored on Hall Bank (> 700 m) as well as the Glorieuses site and, for the most part, the western slope of Mayotte, are located in the colder, lower oxygenated Intermediate Antarctic Water Mass (AAIW) (approximately 7-9 °C, O2 < 160 µmol/kg).

The northern and eastern slopes of Mayotte present a broad bathymetric gradient (449-1183 m, and 492-1118 m respectively), thus are traversed by a water mass gradient from SICW then AAIW until encountering the layer boundary of the Red Sea Intermediate Water Mass (RSIW), characterized by very low oxygen concentrations and temperatures (< 120 µmol/kg, 4-8 °C) in the deepest portions of the slopes. The end of the western slope of Mayotte also intersects the RSIW layer boundary.

Geomorphology and topography

The composition and proportions of each geomorphological facies (defined according to the nature of the dominant substratum and the relief) vary between the seamounts and island slopes. These facies are mapped along dive transects in **Figure II.8B**.

The surveyed area of the summit and upper slope area of Glorieuses shows that this site is composed of 100% carbonate rock, forming a homogeneous slab (mean bottom position index (BPI) close to 0.2). The explored upper slope consists in a depression of -63 m compared to the summit (BPI 500 m minimum). This is consistent with the description in Courgeon et al. (2016).

The eastern slope of Mayotte was explored along a continuous bathymetric gradient (492-1118 m) with an average slope of 12°. The upper slope is mainly composed of soft sediment (15.4%), followed by an area of carbonate geomorphology (scree and heterogeneous carbonate relief). The remaining slope is composed of mixed facies (mixture of volcanic relief, carbonate and sedimentary substrates) and volcanic facies, the composition of which varies from pure volcanic rock, forming heterogeneous reliefs, to a mixture of scree-type volcanic rock, mixed with sediment. At the end of the slope is a volcanic cone (BPI 500 m maximum = 135.2 m high).

The northern slope of Mayotte is a terrace (average depth 568 m), with a pronounced bathymetric gradient at the end of the transect forming a channel, up to 1183 m. The average slope is pronounced, equal to 10.5°. More than 50% of the slope is composed of sedimentary geomorphology. There are two main areas along the slope, consisting of boulder-forming carbonate reliefs and long walls. The end of the slope is composed of volcanic landforms (11.7% of the slope composition).

The dive on the western slope is also located on a terrace, whose average slope and depth gradient are less pronounced than the northern terrace (7.1° on average, 655-888 m). This slope is mainly composed of sedimentary geomorphology (78%) interspersed with areas of rocky relief (BPI 60 m max the highest, ~13 m difference in altitude, and above all is the most variable (sd = 2.61 m) after the eastern slope of Mayotte. The end of the dive, located along the lower edge of the terrace, is composed of volcanic reliefs (13% of the dive).

The Sakalaves platform is interspersed with faults and escarpments Courgeon et al. (2016). The summit is composed of four major geomorphologies: a carbonate slab zone (43% of the summit), a dyke zone interspersed with sedimentary substratum (mixed geomorphology, 25.7% of the transect), and an area of sedimentary ripples (Miramontes et al., 2019a) (11.6% of the transect). These three geomorphologies are separated by an escarpment of about 22° from an area of volcanic landforms (19.8% of the transect) which overhangs at ~370 m.

On Bassas da India, the average slope of the explored terrace is intermediate (7.3°), and has a low bathymetric gradient (453-622 m). The average BPI at 500 m is quite high (5.3 m). The upper slope of the explored terrace has a sedimentary geomorphology (22.6%), forming long ripples/current dunes (Miramontes et al., 2019), while the remaining part is predominantly composed of volcanic geomorphology forming irregular landforms (64.9%).

Hall is a flat-topped bank whose summit (502 m deep), consists of a 2 km diameter crater located on the center-east, filled with soft sediments. The remainder of the summit has a rather flat, volcanic geomorphology (90.0%) (average slope 2°, BPI close to 0) consisting of volcanic rock scree and sediment. Hall's Dive 12 crosses a terrace area which consists of predominantly volcanic geomorphology (60.9%) and mixed geomorphology (23.0%). The average slope is steeper (10.9°), and has a discontinuous bathymetric gradient (602 ± 102 m on average) reaching 903 m depth on the upper slope of the bank. The average BPI at 500 m is -2.7 m (i.e., depression area from the terrace and the upper slope compared to the summit).

Finally, Jaguar has a flat-topped morphology with scarp networks. The bathymetric gradient explored is low (457 to 550 m) and the average slope is also low (4.5°). Three main geomorphologies are observed on the explored summit area: a sedimentary zone at the beginning of the transect, which then reveals a carbonate slab. The middle of the dive consists of a volcanic geomorphology zone, composed of lava flow type reliefs, forming lobes, and constitutes the main geomorphology observed on this summit (52%). The last quarter of the dive is composed of carbonate slab geomorphology. The average BPI at 500 m is 2.5 m.

Substrate

Sedimentary substratum is dominant on the western and northern slopes of Mayotte (83.7% and 67.3% respectively), while rocky substratum proportions dominate on the other sites (**Figure II.9**). Soft sediment areas are however present on Bassas and Sakalaves (ripple zones).

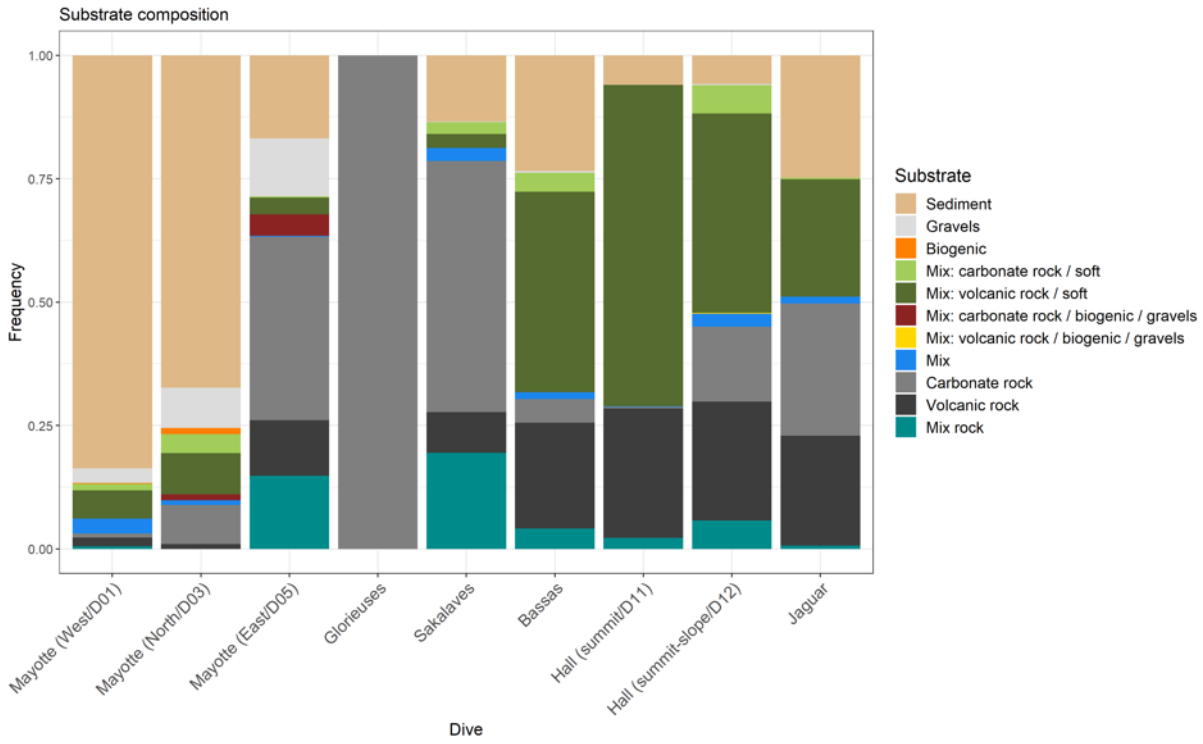

Figure II.9 : Relative frequencies of substrate categories (analyzed from all images by semi-automatic method) for each transect

The proportions of carbonate rock are high on the eastern slope of Mayotte and Sakalaves (37.1% and 50.9% respectively) and cover the whole summit/upper slope area explored on Glorieuses. Volcanic substrate proportions are higher at sites south of the channel (Hall, Jaguar and Bassas) and consist of mixed volcanic substrate with small sedimentary zones often in depression and purely volcanic substrate (21 to 26%). The eastern slope of Mayotte and Sakalaves also consist of mixed bedrock (carbonate, volcanic) (14.8% and 19.5% respectively), also present but to a lesser extent in Bassas, and Hall (2.2 to 5.9%).

Gravel proportions on the northern and eastern slopes of Mayotte are higher than at the other sites. Biogenic substrate is observed mainly on the northern slope (1.2%), and consists mainly of coral skeletal debris.

Substrate diversity and hardness indices estimated from these data are summarized in **Table II.5**. Substrate diversity is highest on Jaguar, Mayotte's northern slope and Hall's dive 12 (summit-slope). The higher hardness indices were found on Glorieuses (6) and Sakalaves (5.2) and the lowest on the western and northern slopes of Mayotte (~2). A more detailed analysis of the substrate size categories on the Mayotte slopes shows that the Eastern slope is composed of different size classes (gravels, pebbles, cobbles, boulders), as well as biogenic

substrate, and regular and irregular rocky beds. The western slope of Mayotte is mainly composed of sediments, gravels and to a lesser extent boulders, and the northern slope of sediment, carbonate blocks, biogenic debris and irregular rocky bed.

Summary of the environmental descriptive statistics is available in **Supplementary material II.8**, as well as comparative environmental condition of sites using maps of the transects (**Supplementary material II.9**).

II.3.2.2 Environmental factors influencing the structure of megabenthic communities

Environmental drivers of differences in richness, total beta diversity and mean density between seamounts and island slopes

Current velocity at 350-650 m shows a significantly positive relationship with faunal density ($p = 0.002$, adjusted $R^2 = 0.82$), negative with taxonomic richness as well as with total beta diversity ($p = 0.0015$, adjusted $R^2 = 0.75$) (**Table II.6**). Variability in current velocity at 350-650 m showed a significantly negative relationship with taxonomic richness ($p = 0.0373$). Winter Chla and mean minimum Chla also showed significant but weak positive relationships ($p = 0.0478$ and $p = 0.0197$) with richness.

The percentage cover of carbonate geomorphology shows a significantly positive relationship with mean faunal density ($p = 0.0002$, adjusted $R^2 = 0.86$), as well as a significantly negative relationship with total beta diversity ($p = 0.0002$, adjusted $R^2 = 0.73$). On the contrary, the percentage coverage of sedimentary geomorphology shows a significantly positive relationship with total beta diversity ($p = 0.0394$, adjusted $R^2 = 0.40$).

Distance to the Madagascar coast shows a significantly negative non-linear relationship with faunal density ($p = 0.0288$, adjusted $R^2 = 0.45$) while distance to the Mozambique coast shows a significantly positive relationship with faunal density ($p = 0.106$, adjusted $R^2 = 0.58$). Furthermore, the distance to the nearest coast (the islands of Mayotte and Glorieuses and the lagoon of Bassas) does not show a significant relationship with any of the metrics.

Substrate hardness shows a weak negative significant relationship with taxonomic richness ($p = 0.0478$) which is not linear and shows an optimum taxonomic richness for intermediate hardness between 4.5 and 5 out of a total of 6, being lower for lower or higher values of hardness. The relationship between hardness and BD is also significant and negative.

Table II.6 : Summary of significant explanatory variables determined from generalized linear regression model for taxonomic richness, and simple linear regression for density and beta diversity (n = 9 observations). Variables tested: depth; winter, inter-annual, total, minimum and maximum Chla; current velocity at 350-650 m, current variability at 0-50 m and 350-650 m; frequency of geomorphological classes; distances to the coast (Madagascar, Mozambique); substrate hardness and diversity. Response variables: richness (n = 58 polygons), mean density, and total beta diversity. [1]Non-significant relationship when Glorieuses was removed, [2]Non-significant relationship when Mayotte eastern slope was removed. "_" = not significant

	Richness (58 polygons)			Density			Beta diversity		
	p-value	Estimate	R^2 adj	p-value	Estimate	R^2 adj	p-value	Estimate	R^2 adj
Current: std 350-650 m	0.0373 *	-1.9129	_	_	_	_	_	_	_
Current: speed 350-650 m	0.0266 *[1]	-3.47265	_	0.000201 ***[1]	5251.23	0.86	0.001593 **[1]	-3.26806	0.75
Chla winter	0.0484 *[2]	3.6599	_	_	_	_	_	_	_
Chla total	_	_	_	_	_	_	_	_	_
Chla inter-annual	_	_	_	_	_	_	_	_	_
Chla min	0.0197 *	15.0926	_	_	_	_	_	_	_
Chla max	_	_	_	_	_	_	_	_	_
Latitude	_	_	_	_	_	_	_	_	_
Carbonate geomorphology	_	_	_	0.000192 ***	683.120	0.861	0.001985 **[1]	-0.42097	0.73
Sedimentary geomorphology	_	_	_	_	_	_	0.0394 *	0.40576	0.40
Distance to Madagascar coast	_	_	_	0.0288 *	-1.9891	0.45	_	_	_
Distance to Mozambique coast	_	_	_	0.0106 *[1]	1.441	0.58	_	_	_
Hardness	0.0478 *	-0.07229	_	_	_	_	0.009604 **	-0.08303	0.58
Substrate diversity	_	_	_	0.01658 *[1]	-1537.1	0.52	0.01975 *[1]	0.99671	0.50

Finally, substrate diversity showed a significant negative relationship with mean faunal density ($p = 0.0166$, adjusted $R^2 = 0.52$) and a significant positive relationship with total beta diversity ($p = 0.0197$, adjusted $R^2 = 0.50$).

Environmental drivers of the assemblage composition

The partial redundancy analysis applied to the assemblages shows that 16.7% of the variance is explained by the significant environmental variables after forward selection of the model variables ($p > 0.05$, 999 permutations), and that 7.9% of the variance is explained by the spatial variables (latitude, longitude) (**Figure II.10**). The adjusted R^2 of the model is equal to 0.16. Axes 1 to 9 are significant, implying that many axes explain relatively little variance.

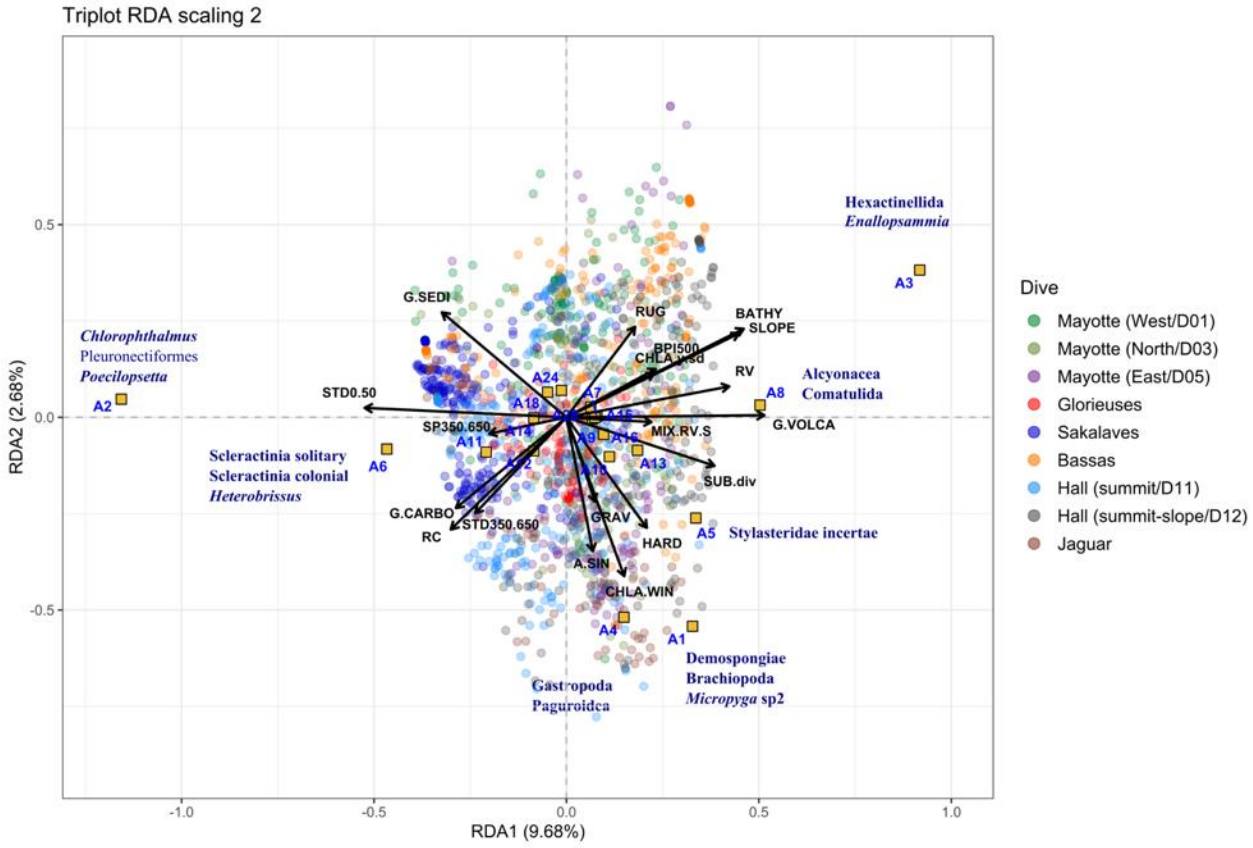

Figure II.10 : Partial Redundancy Analysis (pRDA) applied to the assemblage densities after quadratic and Hellinger transformation of the data. The conditional co-variables of the model are latitude and longitude. The significant variables of the model, obtained after a forward selection and test of the significant variables (n = 999 permutations), are shown. Refer to **Table II.3** and **Figure II.6** for the description of the assemblages

The variables volcanic geomorphology (G.VOLCA), volcanic rock (RV), depth (BATHY), slope (SLOPE), substrate diversity (SUB.div) and current variability between 0-50 m (STD0.50) and 350-650 m (STD350.650) to a lesser extent, as well as mixed volcanic rock/sediment substrate (MIX.RV.S), rather contribute to the dispersion of sites along axis 1. The triplot shows that A2 assemblage (*Chlorophthalmus*, Pleuronectiformes and other mobile fauna) and A6 assemblage (solitary and colonial Scleractinia) are mainly found in the corresponding sites at Sakalaves and Hall, strongly correlated with high current variability between 0-50 m. The A3 assemblage (Hexactinellida including *Aphrocallistes*, *Enallopsammia* for the eastern slope of Mayotte) is mainly found in the sites corresponding to Bassas, Hall (dive12, summit-slope) and on the eastern slope of Mayotte, strongly correlated to high values of depth and slope, as well as to BPI 500 m and inter-annual Chla variability. A8 assemblage (Alcyonacea, Comatulida) is strongly correlated with the presence of volcanic geomorphology, mainly on Bassas and Hall's dive 12 (top-slope). A11 assemblage (*Micropyga* sp1) appears to be slightly correlated with

high current velocities at 350-650 m and current variability at 0-50 m depth, and is found mainly at the Sakalaves and Hall sites. Finally, A13 assemblage (mainly Actiniaria) is correlated with intermediate substrate diversity values, in areas of volcanic geomorphology mainly composed of mixed volcanic/sediment substrate. Substrate hardness (HARD) and sedimentary geomorphology (G.SEDI) variables contribute equally to axis 1 and 2. A5 assemblage (Stylasteridae incertae) is correlated with substrate hardness and substrate diversity, and is found mainly at sites on the eastern and northern slopes of Mayotte, and also Jaguar and Hall. A14 assemblage (*Steredocidaris*), A18 (Pennatulacea) and A24 (*Glyphocrangon*) are poorly represented on this triplot, but appear to be slightly correlated with the presence of sedimentary geomorphology.

Finally, the variables gravel (GRAV), eastness (A.SIN) and winter Chla (CHLA.WIN) contribute rather to the dispersion of sites on axis 2, correlated with A1 (Demosponges, Brachiopoda, *Micropyga* sp2) and A4 (Gasteropoda, Paguroidea) assemblages, also correlated with substrate hardness.

The variation partitioning analysis of the megabenthic assemblage dataset shows that hydrology explains 15.3% of the variation in assemblage structure, 6.9% of which does not interact with the other variables (**Figure II.11A**). We observe an equal pure contribution from topography and substrate (1.7% each). Topography and hydrology together explained 4.7% of the variation. In total, geomorphology explains 6.5% of the variation, with the major part overlapping with substrate (3.5%). In addition, different partial RDAs (not shown) allowed us to evaluate the percentage of variance explained by currents (11.1%), primary productivity (5.8%) and bathymetry (3.4%).

The fraction of variance purely explained by space is low (0.8%), however, we observe a high overlap of variance explained by hydrology and space (2.8%) (**Figure II.11B**).

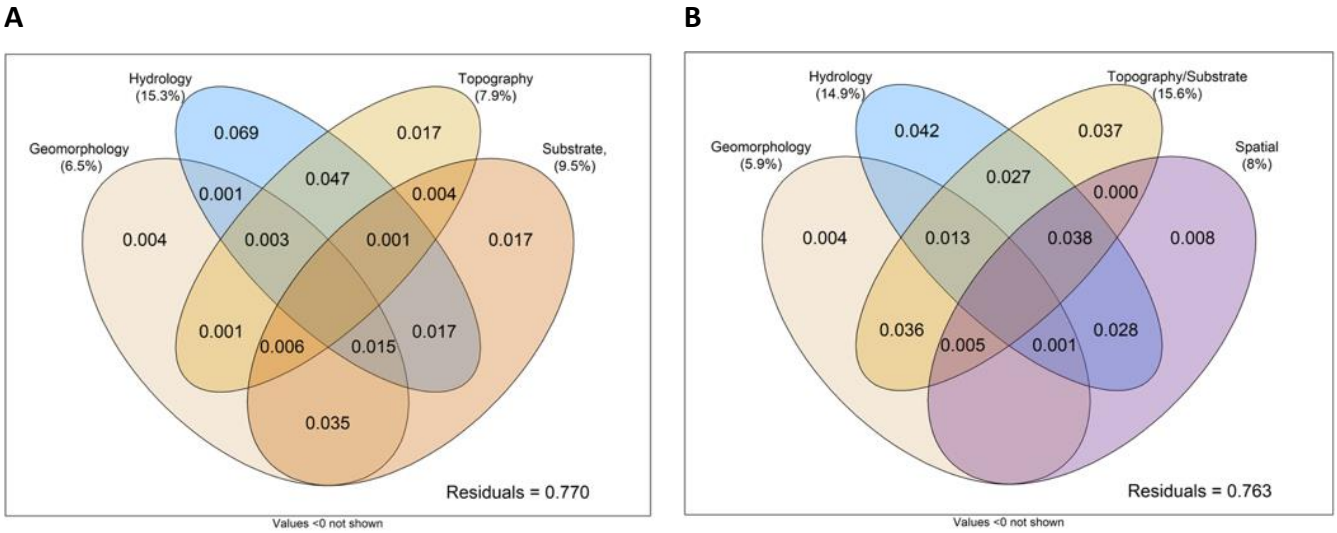

Figure II.11 : Venn diagrams representing the contributions of the different sets of explanatory variables from a variation partitioning analysis of the assemblage dataset. **(A)** Without integration of spatial variables (latitude, longitude), **(B)** With integration of spatial variables. The numbers indicate the fractions of variation explained by each set of environmental variables. Contributions < 1% are not shown

II.3.2.3 Environmental drivers of megabenthic communities spatial pattern along Mayotte and Bassas da India island slopes

Environmental factors structuring the assemblage composition along island slopes

Mayotte island slopes

On the western slope of Mayotte, the partial RDA applied to the taxon densities shows that only 5.1% of the variance is explained by the model after selection of the significant variables, and 4.4% by the spatial variables (latitude, longitude) (**Figure II.12A**). The model on the northern slope explains more variance (18.3%) with 7.3% explained by the spatial variables (**Figure II.12B**). On both slopes, substrate hardness (HARD) contributes strongly to the dispersion of sites along axis 1, with substrate diversity (SUB.div) more so on the northern slope. More or less high values of hard and diverse substrate are associated with high abundances of mainly habitat-forming taxa (e.g., Zoanthidae, Hexactinellida, Alcyonacea, Antipatharia and Demospongiae on the northern slope, Stylasteridae incertae on the western slope) together with other taxa (e.g Annelida, Comatulida). Conversely, we find taxa associated with areas of sedimentary geomorphology (e.g., Bivalvia, Pennatulacea, *Glyphocrangon* on the western slope; *Stereocidaris*, Xenophoridae on the northern slope).

The depth variable (BATHY) contributes weakly to the dispersion of sites along axis 2 on the western slope, correlated with the taxa Gastropoda, Ophiuroidea, while on the northern slope, volcanic geomorphology shows a strong contribution to the dispersion along this second axis. For these two slopes, the sites with significant LCBD are located mainly in sedimentary geomorphological zones but also in volcanic ones.

On the eastern slope of Mayotte, the RDA explains more variance than the other two slopes, (23.9%) after selection of the significant variables, with 12.8% of variance explained by the spatial variables (**Figure II.12C**). Axes 1 to 5 are significant.

The taxa Hexactinellida (including the large size *Aphrocallistes*), the scleractinian *Enallopsammia*, – and Comatulida to a lesser extent – are correlated with high values of slope, volcanic substrate and bottom elevation variability (BPI 500 m). The taxon Gastropoda is correlated with depth, and Demospongiae also, for intermediate values (but inversely correlated with slope, unlike Hexactinellida). The taxa Brachiopoda and Stylasterridae are correlated with north and east slope orientation, the former with carbonate rock, the latter with mixed bedrock (volcanic, carbonate).

Sites contributing to the BD (LCBD) are found in areas of volcanic geomorphology and associated with volcanic, carbonate, or mixed substrates, steep slopes or high BPI.

We observe a low contribution of inter-annual Chla and current variability over 0-50 m, and sedimentary geomorphology, although significant, is very poorly represented on this triplot.

Bassas da India

Finally, on the Bassas terrace, 9% of the variance is explained by the model, and 12.8% by the spatial variables (**Figure II.12D**). Axes 1 and 2 are significant. The fish *Chlorophthalmus* is correlated with the presence of sedimentary geomorphology on the upper terrace. Hexactinellida is correlated with high values of substrate hardness – a variable with a lower contribution however – and with low values of carbonate rock, curvature and current. Finally, the taxa Antipatharia and Alcyonacea are correlated with areas where BPI 500 m is high (large elevation difference, sloping area).

Sites contributing to the BD (LCBD) are found in areas of volcanic or mixed geomorphology associated with higher curvature and current variability.

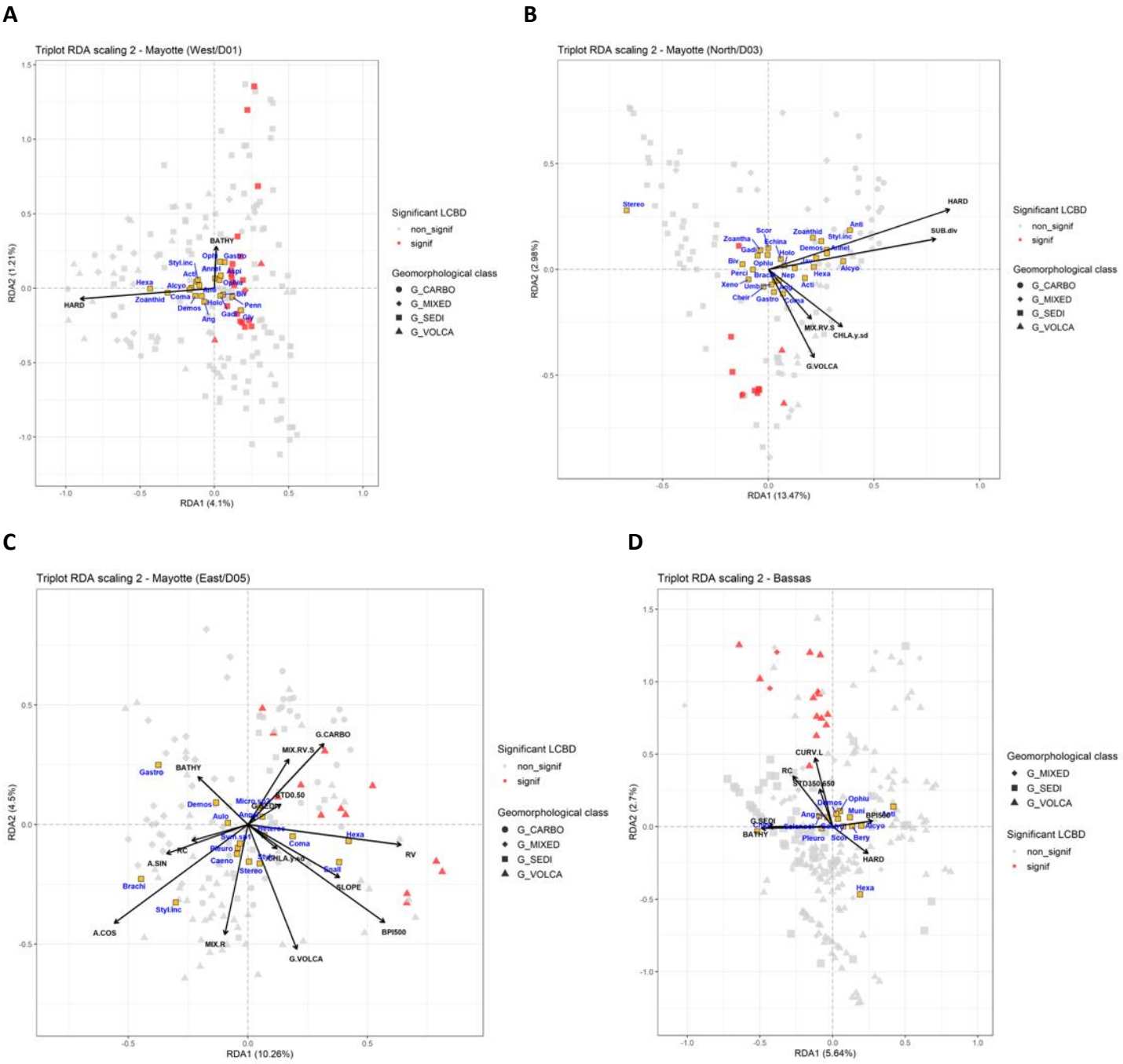

Figure II.12 : Partial Redundancy Analysis (pRDA) applied to taxon densities after quadratic and Hellinger transformation of the data. The conditional co-variables of the model are latitude and longitude. For each RDA, only the significant variables of the model are shown, obtained after a forward selection and testing of the significant variables (n = 999 permutations). **(A)** Western slope of Mayotte (D01), **(B)** Northern slope of Mayotte (D03), **(C)** Eastern slope of Mayotte (D05), **(D)** Bassas da India. Red dots indicate characteristic sites with significant LCBD values

Model of spatial scale structure along island slopes and interpretation of these structures with environmental factors

Spatial analysis (dbMEM) on the trendless community dataset shows that there are significant spatial patterns (p = 0.001) on the slopes of Mayotte and Bassas da India.

Mayotte island slopes

Along the western slope of Mayotte, four MEMs (spatial variables) show a significant positive spatial correlation but explain a small proportion (4%) of the variance of the community dataset, as the two significant axes (at most 2.1%). The spatial structure model at large (~6 km), medium (1 km) and fine (0.1 to 0.2 km) scales are significant for axis 1 ($p < 0.05$) but it is only at large scale that the multiple regression model with the environmental variables is valid. This large-scale spatial structure shows a significant relationship with winter and inter-annual Chla, as well as depth, slope, and currents (**Table II.7**). Only 7.7% of the variance is explained by the environment, of which 5.1% of the variance is explained purely by the environment (**Figure II.13A**). The spatial pure fractions are not significant.

Along the northern slope, seven MEMs are significant ($p < 0.05$), and explain 15.19% of the variance in the community dataset. The large-scale spatial model (~3 km) is significant (p = 0.012), for axis 1 (p = 0.003), but the regression with environmental variables is invalid (non-normality of residuals). The spatial pattern at medium scale (~1 km) is significant (p = 0.001), for axis 1 and 2 (p = 0.001 and 0.042 respectively) explaining 6.7% of variance. This spatial structure is significantly related to depth, BPIs, currents, sedimentary and volcanic geomorphologies, inter-annual Chla, and finally substrate diversity (**Table II.7**). The fine-scale model is insignificant (p = 0.069). The environment explains 21.3% of the variation in the community, of which 6.5% represents medium-scale structured environmental variables and 5.6% large-scale (**Figure II.13B**). The pure fine-scale fraction is insignificant, while the pure spatial structures account for a total of 3.9% and 0.7% of variance.

On the eastern slope of Mayotte, 20 MEMS are significant ($p < 0.05$) and explain 48.3% of variance. All three models are significant but only the medium-scale model can be interpreted by the environmental variables. This spatial structure, which explains 19% of the variance, is significantly related to the three types of geomorphological facies, BPIs, currents, nature, hardness and diversity of the substratum, the depth, the value and the orientation of the slope

(**Table II.7**). The environment explains 34.1% of the community variation, of which 16.2% and 7.7% is spatially structured at medium and large scales (**Figure II.13C**). At the fine scale, the pure fraction is significant and explains 1.8% of variance.

Table II.7 : Summary of significant large, medium and fine scale spatial patterns and significant environmental variables that explain these spatial structures, along the Mayotte and Bassas da India Island slopes. These spatial patterns are determined from analysis of Moran eigenvector maps based on geographic distances (dbMEM). %MIX.RC.S = % mixed substrate 'carbonate rock and sediment'; %MIX.RV.S = % mixed substrate 'volcanic rock and sediment'. "_" = not significant

	Mayotte West Slope			**Mayotte North Slope**			**Mayotte East Slope**			**Bassas da India**		
Spatial model	Large ~6 km	Medium ~1 km	Fine 0.1-0.2 km	Large ~3 km	Medium ~1 km	Fine _	Large 1-2 km	Medium 0.8-1 km	Fine 0.2 km	Large ~2 km	Medium ~1-2 km	Fine 0.5 km
Significance of the RDA model (p-value)	**0.013**	**0.001**	**0.003**	**0.012**	**0.001**	_	**0.001**	**0.001**	**0.001**	**0.001**	**0.001**	**0.002**
Significant axes	Axis 1	Axis 1	Axis 1	Axis 1	Axes 1/ 2	_	Axes 1/2/3	Axe 1/2/3/4	Axis 1	Axes 1 /2	Axis 1	Axes 1/2
Adjusted R^2 of the multiple regression model (if significant & normality of residuals)	0.85	_	_	_	0.52/0.36	_	_/_/_	0.84/0.76/0.78/0.52	_	_/0.33	_	_/_
					Explanatory variables							
Current speed: 350-650 m	***	_	_	_	_/***	_	_	_/***/_/***	_	_/**	_	_
Current variability: 0-50 m	**	_	_	_	**/_	_	_	***/***/_/***	_	_/**	_	_
Current variability: 350-650 m	**	_	_	_	_	_	_	***/***/_/***	_	_	_	_
Winter Chla	***	_	_	_	_	_	_	_	_	_/***	_	_
Inter-annual Chla	***	_	_	_	_/***	_	_	_	_	_/**	_	_
Sedimentary geomorphology	_	_	_	_	_/**	_	_	***/_/*/_	_	_	_	_
Volcanic geomorphology	_	_	_	_	_/***	_	_	***/**/***/*	_	_/*	_	_
Carbonate geomorphology	_	_	_	_	_	_	_	***/_/***/_	_	_	_	_
Mixed geomorphology	_	_	_	_	_	_	_	_	_	_	_	_
Depth	***	_	_	_	*/***	_	_	_/*/***/_	_	_	_	_
Slope	**	_	_	_	_	_	_	_/_/*/_	_	_	_	_
Longitudinal curvature	_	_	_	_	_	_	_	_	_	_	_	_
Transversal curvature	_	_	_	_	_	_	_	_	_	_	_	_
BPI 60 m	_	_	_	_	_	_	_	_	_	_	_	_
BPI 120 m	_	_	_	_	*/_	_	_	*/_/_/_	_	_	_	_
BPI 500 m	_	_	_	_	**/***	_	_	***/_/_/***	_	_/**	_	_
Northness	_	_	_	_	_	_	_	_	_	_	_	_
Eastness	_	_	_	_	_	_	_	**/**/**/_	_	_	_	_
Rugosity	_	_	_	_	_	_	_	_	_	_	_	_
Hardness	_	_	_	_	_	_	_	_/*/**/_	_	_/*	_	_
Substrate diversity	_	_	_	_	_/*	_	_	*/_/_/_	_	_	_	_
%MIX.RC.S	_	_	_	_	_	_	_	_	_	_	_	_
%MIX.RV.S	_	_	_	_	_	_	_	**/***/***/_	_	_	_	_
%Gravels	_	_	_	_	_	_	_	_	_	_	_	_
%Cabonate rock	_	_	_	_	_	_	_	_	_	_/**	_	_
%Volcanic rock	_	_	_	_	_	_	_	_/_/_/***	_	_	_	_
%Mixed	_	_	_	_	_	_	_	_	_	_	_	_
%Mixed rock	_	_	_	_	_	_	_	_/*/_/_	_	_	_	_

Bassas da India

Finally, along the Bassas terrace, 12 MEMS are significant ($p < 0.05$) and explain 35.1% of variance. A large scale (~2 km) spatial structure is significant ($p = 0.001$) for axis 1 and 2 ($p = 0.001$ and 0.003 respectively) significantly related to volcanic geomorphology, winter and inter-annual Chla, BPI at 500 m, deep current velocity and variability, substrate hardness and carbonate rock frequency. Spatial structure at medium scale (~1-2 km) and fine scale (0.5 km) are also significant ($p = 0.001$), but cannot be interpreted by regression models with the environment (non-normality of residuals) (**Table II.7**).

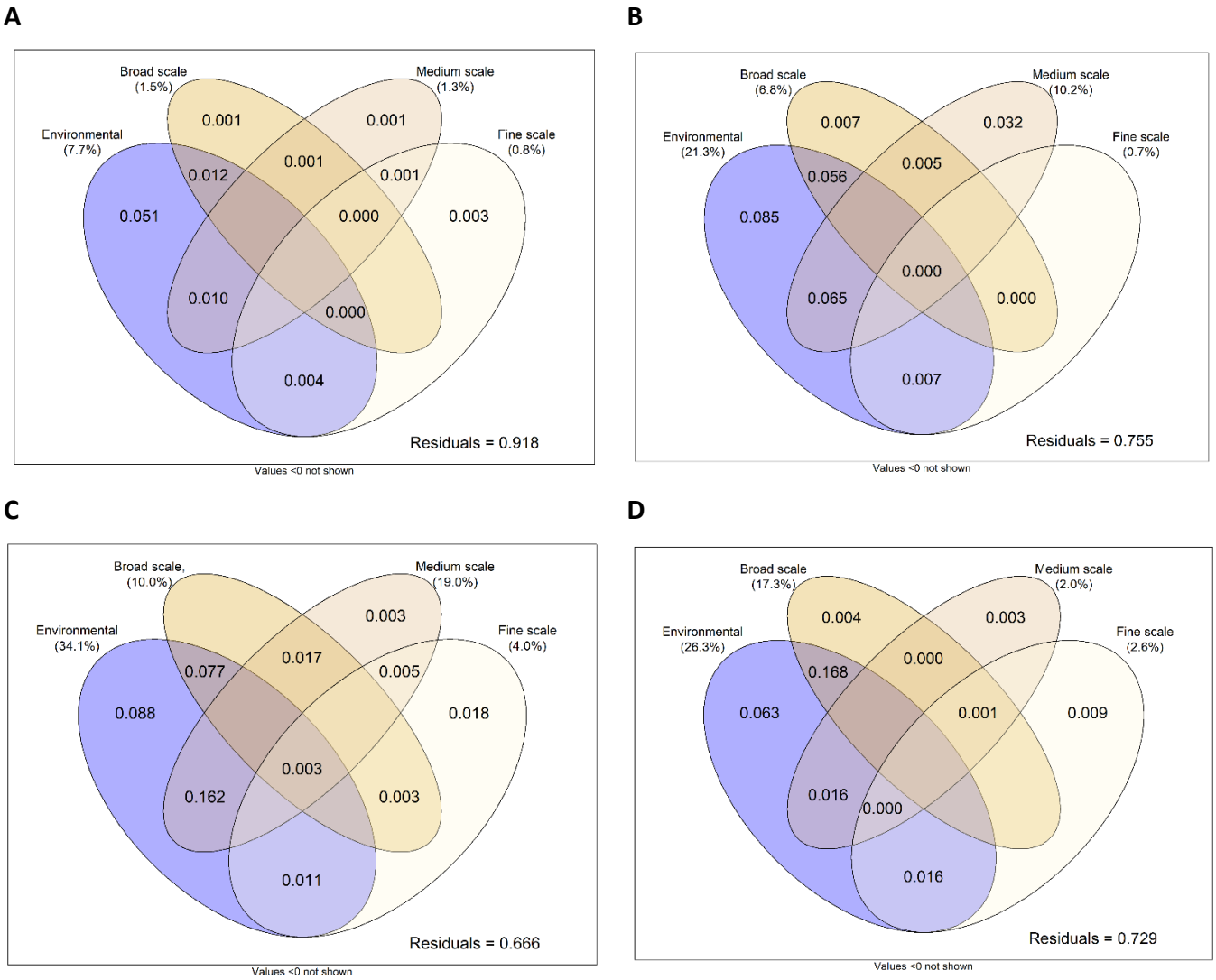

Figure II.13 : Venn diagrams representing the contributions of the different sets of explanatory variables (environment, large, medium and fine scale spatial structures), derived from a variation partitioning analysis of the community data set. The large-, medium- and fine-scale spatial structures were obtained from an analysis of Moran eigenvector maps based on geographical distances (dbMEM). **(A)** Mayotte West Slope, **(B)** Mayotte North Slope, **(C)** Mayotte East Slope, **(D)** Bassas da India

The environment explains 26.3% of the variance, of which 16.8% represents broadly structured environmental variables (**Figure II.13D**). The pure medium-scale fraction is not significant. For the large and fine scale pure spatial fractions, there is a small proportion of variance (< 1%) uncorrelated with the environment.

Maps of the significant large, medium and fine scale spatial patterns along the island slopes are available in **Supplementary material II.10**.

II.4 Discussion

II.4.1 Variability of community metrics and composition between seamounts and island slopes along the Mozambique Channel

Variability of megafaunal community characteristics at seamounts have been observed at some sites to be driven by environmental heterogeneity including currents (Morgan et al., 2019), depth and substrate (e.g., de la Torriente et al., 2018; Shen et al., 2021; Victorero et al., 2018) or surface productivity (Clark and Bowden, 2015). Such relationships need to be confirmed in other oceanic regions.

Seamount and island slopes explored in this study along the Mozambique Channel display contrasting environmental conditions with varying hydrodynamic regime and surface productivity from north to south or related to their distance to the coasts or the presence of islands. Indeed, the eastern slope of Mayotte and the Glorieuses seamount in the North showed the highest levels of Chla.

According to their minimal depth (summit or upper slope) and gradient, the explored features also encompass different water masses well characterized in the Mozambique Channel (Charles et al., 2020; Collins et al., 2016). These features also present contrasting geomorphological facies related to a complex geological history characterized from previous studies (Audru et al., 2006; Courgeon et al., 2017, 2016).

Our detailed analyses reveal that those features display variable substrate heterogeneity and hardness.

Community metric comparison revealed that densities vary between seamounts by a factor of ten with a decreasing density from north to south along the Mozambique Channel (up to ~1400 km distance among seamounts). In comparison, Sautya et al. (2011) observed density

differences up to about a factor four among two seamounts distant from ~200 km in the northeast Indian Ocean.

Island slopes densities decrease also with latitude, but also within slopes of the same island, (Mayotte) of a factor two. At the same latitude, seamounts display higher densities than along island slopes (4 to 10 fold higher in the north and 2-3 fold higher in the south). However, seamounts do not show a consistent pattern of densities difference with island slope at the scale of the channel; as observed between seamount and continental slope in Rowden et al. (2010b).

Rowden et al. (2010b) highlighted that the higher biomass estimated over seamounts compared to adjacent continental slopes in the southwest Pacific were mainly driven by the scleractinian *Solenosmilia variabilis*. Similarly, in the Mozambique Channel we observed that the highest density on seamounts are mainly due to the high proportion of sessile fauna, Demospongiae (~75-80% of the total density) on Glorieuses, and Demospongiae and Stylasteridae on Jaguar. Conversely, the high density on Sakalaves platform was mainly driven by fish.

Density differences were explained by the high current speed that crosses these sites, as well as their high coverage of carbonate slab. A relation between differential current regimes among sites and abundance of megabenthic assemblages was also described in Genin et al. (1986) and Kaufmann et al. (1989). The North East Mozambique Current (NEMC) in conjunction with the westerly flowing south equatorial current, impacts Glorieuses in the north (Collins et al., 2016). The presence of mesoscale eddies on this seamount and further along the channel, which can integrate particulate material from the surface down to 1500 meter depth (de Ruijter et al., 2002) by advection of Mozambique and Madagascar terrestrial material offshore (Tew-Kai and Marsac, 2009), may have provided favorable conditions for the establishment of dense sponge communities at Glorieuses, and of scleractinians and fish especially of genus *Chlorophthalmus* over Sakalaves platform. We therefore confirm our hypothesis in the structuring role of hydrodynamics in explaining the difference of megabenthic communities structure between seamounts.

On the slopes of Mayotte, the modelled currents are rather weak, however the eastern slope also has high faunal densities compared to the northern and eastern slope, which could be

explained by differential nutrient input. High concentrations of chlorophyll a were measured over the eastern slope of Mayotte, and although this parameter is not significant across the different sites, it was identified as a significant parameter between Antarctic seamounts (Clark and Bowden, 2015). The explored eastern slope of Mayotte is the closest to the lagoon and to the island (~2 km), while the island is composed of a dense network of rivers (Faivre et al., 2020), and would benefit from release of runoff of land materials, in addition to input from the Madagascar coast from the NEMC. Indeed, the distance of seamounts and island slopes to the Madagascar coast is significantly correlated to benthic fauna density.

The surface primary productivity showed a significant positive relationship with taxonomic richness, also observed in Bridges et al. (2022), which could be explained by a decrease in interspecific food competition. Furthermore, accurate quantification of substrates allowed us to evidence relationships between taxonomic richness and beta diversity with substrate hardness (non-linear negative relationship). A significant correlation of substrate hardness (or percentage sediment cover) was also evidenced in Shen et al. (2021) with the richness and abundance difference of beta diversity, or even if not quantified through beta diversity index, the substrate hardness was shown to have influence on the community spatial structure (Morgan et al., 2019). Victorero et al. (2018) also found a significant relation of the substrate type (qualitative data), solely on the abundance difference component of beta diversity, the richness difference being explained by water masses. In our study, beta diversity is also positively correlated to substrate diversity, including in the area both carbonate and volcanic rocks. Together with the substrate hardness, these relationships reflect the presence of a more complex bottom, composed of sedimentary, mixed and rocky substratum that would favor the installation of richer communities by providing additional habitat niches, also evidenced in Morgan et al. (2019) or in Bell et al. (2016), for intermediate value of substratum coverage (in continental margin habitat). Furthermore, these communities will also vary in space according to the spatial distribution of the substrate (Morgan et al., 2019) increasing beta diversity. This is exemplified along the western and northern slopes of Mayotte, mainly composed of sedimentary areas interspersed by discontinued rocky bottom, blocks and volcanic areas, adding complexity to the habitat and enhancing beta diversity.

As with density, taxonomic richness and beta diversity show a relationship with current speed, albeit an inverse correlation mainly driven by Glorieuses.

Depth was not identified as a driver of diversity or density differences among the studied sites. However, depth is a proxy of many covariates, such as temperature and oxygen concentration that characterized water masses and so energy flow in the system, linked to organism physiology (Thistle, 2003). Water masses would potentially influence differences in richness and beta diversity between the explored features, as for example, Mayotte island slopes encompass three different water masses (SCIW, AAIW, RSW) while Glorieuses reside mainly inside AAIW (low oxygen, low temperature). Role of water masses has been suggested as structuring parameters over depth gradient (Auscavitch et al., 2020a; Henry et al., 2015; Victorero et al., 2018) and it is likely that such gradients also promote the higher richness and beta diversity observed along Mayotte island slopes, by offering additional ecological niches. Nevertheless, the absence of a significant role of depth and latitude over the whole dataset would potentially reflect an insufficient level of taxonomic identification to establish a relationship with the richness component.

Taxonomic composition varies between the studied seamounts and island slopes, even for taxa identified at high taxonomic rank (e.g., fishes and anthozoans orders, demosponges, hexactinellids, and gastropods). Dominant fauna were composed of habitat-forming taxa such as sponges (Demospongiae, Hexactinellida) and cnidarians (Stylasteridae incertae, solitary scleractinians, Alcyonacea, Antipatharia, Actiniaria) and other sessile fauna (Brachiopoda) as well as mobile taxa (Gastropoda, Actinopterygii, Ophiuroidea, Echinoidea). Sessile fauna usually dominates but mobile fauna (dominated by fish and ophiuroids) show higher densities than sessile taxa on the Sakalaves seamount, with high proportion of soft bottoms. Similarly echinoderms dominate the summit of one of the Adaman Seamounts covered with fine sediment, while flanks and the other sites with hard bottoms are dominated by sponges (Sautya et al., 2011). In comparison, Bo et al. (2020), in the Mediterranean Basins reported scattered bathyal assemblages dominated by hexactinellids and cnidarians (Isididae); Lundsten et al. (2009), off southern and central California, reported dominance of passive suspension-feeding cnidarians over seamounts and of holothurians/echinoderms on a guyot; Tapia-Guerra et al. (2021), reported dominance of mobile fauna and predators over oceanic island and close seamounts, and dominance of sessile suspension/deposit feeder over seamounts far from islands of the Chilean Exclusive Economic Zone.

Specifically, many of the habitat-forming taxa identified in our study are shared between the seamounts and island slopes, notably due to the low identification ranks achieved. However we observe substantial frequency differences, meaning that the different seamount and island slopes are characterized by different biogenic habitats. As an example in the north of the channel, the Glorieuses terrace is dominated by Demospongiae, while cnidarians and Hexactinellida dominated along the Mayotte island slope. Between these slopes, the proportion of Anthozoa and Hydrozoa is also variable.

Identification efforts made at finer resolution for four taxa (echinoids, asteroids, decapods and fishes) enabling to observe a more specific distribution pattern. Some taxa seem ubiquitous over the channel, and with more pronounced abundances at some sites (e.g., *Stereocidaris*, *Stylocidaris*, *Munida*), while for other, there are differences in the composition of families/genera/species that seem to be restricted to a few sites such as the decapod genus *Glyphocrangon* on the slopes of Mayotte, or the sea urchin genera *Heterobrissus* on Sakalaves and *Pourtalesia* on Glorieuses. Furthermore, the fish of the genus *Chlorophthalmus* was only observed on the seamounts in the center and south of the channel. This dataset does not allow discussion of the endemism of these taxa, however, comparison of these observations with all the collection data sampled in the channel and on the Mozambique/Madagascar margins would allow further exploration of this question. Endemism has been hypothesized to occur over seamount due to its isolated characteristics that might encourage high level of speciation (Hubbs, 1959; Richer de Forges et al., 2000), however, several studies revealed no existent or low level of endemism over seamounts compared to other non-seamount habitats (continental slope, bank, oceanic island) (Hall-Spencer et al., 2007; Howell et al., 2010; McClain et al., 2009; O'Hara, 2007; Samadi et al., 2006).

II.4.2 Spatial structures within seamounts and island slopes (beta diversity)

High beta diversity has been previously reported within seamounts (e.g., 0.92 in Victorero et al. (2018); 0.83 in Shen et al. (2021)) and was generally related to the large depth gradient (respectively 2400 m and 1200 m) providing therefore more or less physico-chemical variations with depth. We also observed high beta diversity within the different seamounts and island slopes studied (from 0.61 to 0.81), except for Glorieuses, despite the low depth gradient (< 500 m) explored. These high beta diversity values reflect therefore the high habitat heterogeneity rather related to substrate and topography as well as to geomorphology

complexity of the seamounts (confirmed by regression analyses between beta diversity and substrate diversity and sedimentary geomorphology cover), over short to intermediate horizontal gradient (7 km to 16 km transects). It is not surprising to observe low levels on Glorieuses, due to the strong but stable current conditions and the presence of a carbonate slab alone, thus providing fewer niches and transition zones. Morgan et al. (2019) has also reported high beta diversity (up to 0.95) within a narrow depth range that could be attributed to the large horizontal gradient explored providing high habitat difference within the same depth layer. Shen et al. (2021) also pointed out the role of substrate and topography to explain small-scale aggregations of hexactinellids.

Furthermore, the replacement component of beta diversity is prevalent in the abundance difference of taxa (up to 65%), except for Glorieuses and Jaguar where these two ecological processes operate equally. Dominance of replacement has already been reported along seamount slopes (Goode et al., 2021; Morgan et al., 2019; Victorero et al., 2018). Victorero et al. (2018) suggests that the productive region of the study area would explain the dominance of the replacement component, as suggested from previous authors (Brault et al., 2013). Despite the oligotrophic region of the Mozambique Channel, we observe for most of the site replacement dominance over abundance difference, however, the highly water turbulent regime of the region (i.e., upwelling and mesoscale eddies) may contribute to the nutrient supply in otherwise oligotrophic environment (Lévy et al., 2001) and therefore could corroborate the hypothesis of these authors.

On each seamount and island slope, many of the taxa detected as strong contributors to total beta diversity (SCBD for Species Contribution to Beta Diversity) are attached, potentially habitat-forming taxa (cnidarians, sponges), with up to 45.5% contribution. Although their identification rank is poorly resolved, these taxa generate variability within seamounts and island slopes through their patchy distribution characterized by locally high abundance. However, at finer identification ranks, we would expect even higher levels of beta diversity along each transect, due to the observation of several potential species within each identified class and order. Mobile taxa also contribute to the BD within the studied sites, such as the fish *Chlorophthalmus*, the sea urchins *Micropyga* sp1 and *Micropyga* sp2 as well as *Stereocidaris* and *Stylocidaris*, and decapods like *Puerulus carinatus* and *Glyphocrangon*.

The taxa detected as strong contributors to total beta diversity are mainly those identified as indicator taxa of the main assemblages because they are abundant and respond well to the heterogeneity. Their distributions were localized in specific sites (LCBD for Local Contribution to Beta Diversity) of transition/interface areas that we identified as abrupt changes of substrate or topography (**Figure II.8B**).

Their preferential niches correspond to particular geomorphological facies, such as areas of volcanic relief providing favorable supports for the attachment of sessile fauna, or sloping areas to benefit from the acceleration of currents and the resuspension of particles. Furthermore, change in substratum may also impact spatial pattern of mobile fauna such as *Glyphocrangon* along the western slope of Mayotte, observed exclusively over sediment bottom; or of the sponge and corals predators cidaroids (Lawrence and Jangoux, 2020) mainly observed over hard bottom, where chance to prey sponges/corals is enhanced. However, cidaroids have flexible feeding mode and their distributional pattern appears more to be constrained by food availability than substrate type (Lawrence and Jangoux, 2020). For instance *Stereocidaris* (cidaroid) was also observed on sediment on the northern slope of Mayotte, where it can feed on bottom material or foraminiferans (Lawrence and Jangoux, 2020).

Recruitment processes may also influence the spatial pattern of some taxa, such as for cidaroids (*Stereocidaris*, *Stylocidaris*) and *Micropyga*, for which larval recruitment may occur in the same place depending on the currents regime and the nature of the substrate (personal comment, Dr. Thomas Saucède). Influence of the social pattern of *Chlorophthalmus* (indicator of A2 assemblage), observed forming schools on the images, would explain the large patches it forms. The gregarious behavior of decapods *Puerulus carinatus* (Fischer and Bianchi, 1984), may explain the high locally abundance of this species over Sakalaves rocky bottoms, where it counts among the top five contributors to beta diversity. A closely related species, *P. angulatus*, has been reported to be predator feeding on large pieces of fishes and crustaceans, and occasionally scavenging, while no sediment was found in the gut content (Sahlmann et al., 2011).

II.4.3 Environmental drivers of the assemblage spatial patterns between seamounts and island slopes at multiscale

From the 99 identified taxa, we obtained 45 faunal assemblages – but we only considered 12 clusters particularly well represented in the Mozambique Channel – using a biogeographic network analysis (Vilhena and Antonelli, 2015). This method is based on bipartite network clustering, recognized as outperforming more traditional methods using similarity indices (i.e., beta diversity) that are sensitive to sampling biases in species distribution data (Vilhena and Antonelli, 2015). It has the advantage to consider only taxa presence, and can be applied on abundance data, while conserving species identity.

Each of the 12 assemblages are represented by a limited number of taxa that are very abundant and have indicator values above 20%. The high contribution to assemblages by a small number of abundant taxa has been also mentioned in Goode et al. (2021) and observed in others previous studies on seamounts (e.g., Boschen et al., 2015; Morgan et al., 2019), and reflect the high spatial variability of megabenthic communities.

The network analysis has revealed assemblages displaying a highly patchy distribution, at varying spatial scale within seamounts and island slopes ranging from 0.06 km (60 m) (e.g., along the western and northern slope of Mayotte) to ~2.5 km (e.g., Glorieuses) as well as between sites distant from 4 km to 1400 km (**Figure II.7**). This scale of heterogeneity is highly variable between seamounts and island slopes, and within sites, according to geomorphological units (sediment and volcanic dominated areas support assemblage heterogeneity at smaller scale than carbonate dominated areas). Patchy distribution of seamounts megabenthic communities is a common pattern already observed in previous studies (Boschen et al., 2015; Clark and Bowden, 2015; de la Torriente et al., 2018; Du Preez et al., 2016; Morgan et al., 2019; Schlacher et al., 2014; Shen et al., 2021). Each assemblage is affected by a different set of environmental drivers. We have identified 19 significant environmental variables, acting at multi-scale and comprising hydrology variables (surface primary productivity and currents), substrate ones (composition, hardness, diversity), topography and terrain orientation ones (rugosity, slope, BPI 500 m, eastness), as well as depth and geomorphology.

Hydrology, including both currents at different depths and surface primary production, is identified as one of the main factors structuring the megabenthic assemblages in our study area (~15% contribution, **Figure II.11**), revealing the influence of the complex and highly turbulent hydrographic regime that characterizes the Mozambique Channel (Hancke et al., 2014). Furthermore, of these 15%, about 3% of the hydrological factors are spatially structured, revealing the difference in hydrodynamic regime between the north and central part of the Mozambique Channel. High abundance of *Chlorophthalmus* fish, Pleuronectiformes (A2 assemblage) and solitary scleractinians (A6 assemblage) were positively correlated to the high current speed that crosses Sakalaves platform and Hall bank as well.

The strong influence of the current at the Sakalaves and Hall sites probably reflects the role of the intense eddies extending over the water column and, in contact with the Mozambique coast, export particulate material down into the core of the eddies. Some fish species of the genus *Chlorophthalmus* feeds on small pelagic crustaceans (e.g., mysids, euphausiids, copepods) (Anastasopoulou and Kapiris, 2008), so it might be that these currents sustain a rich environment for the feeding of these fish.

Higher densities of ophiuroids were also observed on Sakalaves, which could be linked to high levels of organic matter over the platform. Furthermore, dense sponge and brachiopod communities (A1 assemblage) over Glorieuses may benefit from nutrient-rich conditions provided by the strong eastern current regime over the platform.

Substrate (diversity, hardness, composition) is the second set of variables displaying a high contribution in the structure of megabenthic communities (9.5%). Areas of soft substrate mainly on the northern and western slopes of Mayotte support taxa such as pennatulids, *Glyphocrangon* (decapods), and bivalves, while gravel areas support higher abundance of gastropods (A4 assemblage) such as on the eastern slope of Mayotte or accumulated in cavities on Glorieuses. Mixed substrate of volcanic and sediment was associated with the presence of actinians (A13 assemblage). Related to the substratum, its level of hardness plays a role in the anchoring of sessile fauna such as Stylasteridae incertae (A5 assemblage), observed abundantly on Jaguar. Previous studies also revealed substratum as a key driver of community structure over seamounts (Morgan et al., 2019; Sautya et al., 2011; Shen et al., 2021; Victorero et al., 2018).

Geomorphology also has a significant role in structuring the megabenthic communities (6.5%), even if its purely contribution is low (0.4%). The highest contribution is however shared with the substrate (3.5%), which reflects the strong correlation between the nature of the geomorphology and its associated substrate (e.g., relief and volcanic lava flows are scored in terms of substrate by pure volcanic rock or mixed with sediment, or areas of carbonate slab are associated with carbonate rock). However, our analysis revealed a noteworthy result, as within the rocky bottom, the volcanic reliefs are rather colonized by hexactinellids and other large habitat-forming taxa (e.g., alcyonaceans, scleractinian *Enallopsammia*), whereas on the carbonate slab areas, we observed demosponges and brachiopods as well as solitary scleractinians. Furthermore, the volcanic geomorphology zones show a slight correlation with roughness. It is likely that the specificities of these geomorphologies in term of microtopography (complexity of relief/rugosity) play a role in the preferential rock support of these taxa. For example, some demosponges have a large contact area with their attachment support and may prefer homogeneous areas, whereas hexactinellids supported by a stem or with a smaller contact area may prefer rough areas. The characterisation effort of the rocky substratum types is therefore important as one sees a structure according to the two rock types.

Topography variables (slope, BPI 500 m, eastness, rugosity) contribute for 8% of the variance of the megabenthic community and play a significant role in structuring the megabenthic communities. Several previous studies have highlighted the presence of dense communities of cnidarians and sponges preferentially located in steep or sloping areas (Bridges et al., 2021; de la Torriente et al., 2018; Du Preez et al., 2016; Hall-Spencer et al., 2007) over seamounts. We made also this observation in our study with high densities of Hexactinellida, and Alcyonacea on sloping areas such as the Hall terrace and upper slope of Bassas da India or of the scleractinian *Enallopsammia*, and hexactinellid sponges *Aphrocallistes* over an elevated volcanic cone on the eastern slope of Mayotte, while they were absent along more gentle slopes. Moreover, comatulids are associated with these biogenic structures, and would probably benefit from an elevation in the water column to enhance their intake of food particles (Buhl-Mortensen et al., 2010). Seabed orientation (i.e., eastness, northness) reflects the seafloor exposure with water movement (Wilson et al., 2007). Eastness was strongly correlated with demosponges densities on Glorieuses and Jaguar terraces, which could be

related to currents from the Madagascar coast on Glorieuses, and to currents affecting the Sakalaves terrace from North to South which interact along the escarpment (Miramontes et al., 2019b).

Contrary to previous studies (Boschen et al., 2015; de la Torriente et al., 2018; Du Preez et al., 2016; McClain et al., 2010; Morgan et al., 2019; Ramos et al., 2016; Schlacher et al., 2014; Shen et al., 2021; Victorero et al., 2018), depth does not appear as the main key drivers of the benthic seamounts communities. This discrepancy may however result from the short depth gradient considered in our study compared to others studies that covered the whole seamount slope. Along the Mayotte Eastern slope, where the depth gradient is the largest, the lower temperature and oxygen content of the AAIW water mass at depth, may, partially explain the sharp change in community composition with the presence of large size hexactinellid *Aphrocallistes* and colonial scleractinian *Enallopsammia* (A3 assemblage). These groups may also be favored by other factors (slope, BPI and Chla), as well as volcanic substrate, which have a greater contribution than depth itself along this slope. Besides hydrology and topography have a quite high shared contribution (~5%), underlining the interaction that currents and seamounts topographies have with each other and affecting the communities.

II.4.4 Structuring factors and spatial scale partitioning along island slopes

Spatial structure analyses of megabenthic communities along the island slopes of Mayotte and Bassas da India show distinct spatial patterns and controlling factors.

The outer slopes of Mayotte Island show heterogeneous spatial scales of megabenthic distribution, from small spatial scale along the western and northern slope to medium scale along the eastern slope (**Figure II.7**).

Spatial analyses (RDA and dbMEM) enable to explain a higher portion of variance along the northern and especially for the eastern slope than along the western one. From dbMEM analysis on the northern and eastern slopes we were able to explain a medium scale (~1 km) spatial structure of communities by the spatial structuration of the geomorphology, currents and depth gradient (of 500-600 m) as well as substrate heterogeneity while on the western slope, we were able to explain only a large scale spatial structure (~6 km) that explains poor variance. Although a fine-scale structure (0.1-0.2 km) was detected to be significant along the western slope, the analyses did not link this to environmental factors. The resolution of our

sampling unit (60 m linear) is probably not sufficient to capture the heterogeneity along this slope that probably occurs at finer scales, as suggested by the variability of assemblages at small scale (**Figure II.7**) and the location of polygons contributing to the beta diversity (**Figure II.8**). The location of these polygons on sedimentary areas is likely explained by the occurrence of sparse blocks of high vertical extension sparsely distributed in an almost flat sedimentary bottoms, not evidenced at the resolution of the DTM bathymetric model. It is therefore not surprising the RDA analyses detect the hardness as the main drivers of megabenthic communities along this slope, but also along the northern one. Taxa such as *Umbellula* (pennatulids), *Glyphocrangon* (decapods), bivalves, or Xenophoridae (gastropods) were observed on soft bottom while the communities on rocky areas over carbonate blocks or irregular volcanic reliefs were mainly composed of habitat-forming taxa (Hexactinellida, Alcyonacea, Zoanthidae, Demosponges, Antipatharia, Stylasteridae). Moreover, the dbMEM analyses detect only a small number of total spatial structure (4 to 7 MEM), over the western and northern slope of Mayotte.

Along the eastern slope of Mayotte, communities structure were explained by a higher number of variables (e.g., hydrology, geomorphology, topography, substrate), which suggests structuration at different scales as well as a potentially better matching between scale of variability of biological communities and environmental variables. As along the western slope, a significant unexplained fine scale spatial structure (0.2 km) was detected, but here, the pure fraction was significant, which may also reflect unmeasured processes such as the potential presence of stochastic and population dynamic processes (e.g., species association, especially with small size fauna not identified from images, competition and predation) as well as potential environmental drivers that we did not consider in this analysis, but which play a role in the communities structure at this scale (Peres-Neto and Legendre, 2010).

We observed community structures on a large scale (~2 km) along Bassas island slope, mainly related to the dichotomy of two geomorphologies, sedimentary on the upper terrace and then volcanic, whose curvature then sloping area generates potential interaction with deep currents and supports distinct communities (mainly hexactinellids and antipatharians) than on the top of the terrace (*Chlorophthalmus* fish).

Island slope of Bassas and the eastern slope of Mayotte have a greater topographic variability compared to the relative flat terrace areas of the northern and eastern slope of Mayotte,

consequently, topographic variables (BPI 500 m, curvature) and depth make a greater contribution to the structuring of communities.

It should be pointed out that the scale of the spatial structures identified depends on our smallest sampling unit and the level of taxonomic identification achieved as well. Population dynamics would probably be better characterized from fine resolution taxonomic rank; however, the low fauna densities of the study area have required gathering of data into larger sampling units, and may explain the difficulty to relate small spatial patterns.

However, even considering high identification rank, we were able to highlight a strong patchy community structure over different spatial scales (**Figure II.8**), especially for habitat-forming taxa; and which respond to various scales of environmental drivers. Sponges and cnidarians are important components of deep-sea ecosystem functioning, and may have important roles in structuring the community. Further insight on their spatial structure at finer resolution, and structuring role may be interesting using a functional angle view. To overcome the difficulties of identifying these taxa on images, a morpho-functional approach would allow a more detailed analysis of cnidarian and sponge communities (Hanafi-Portier et al., in prep.).

II.5 Conclusion

This study on seamounts and island slopes megabenthic community structure in relation to multiscale environmental drivers along the Mozambique Channel reveals:

- High density differences between seamounts (by a factor of 10), as well as density difference among Mayotte island slopes (by a factor of 2). Higher densities – correlated with strong currents and flat geomorphology – over seamounts compared to island slopes are not consistent along the channel, but are consistent considering the same latitude (north and south).

- Beta diversity differences between sites, with generally high levels (~0.60-0.80), and despite a rather low data taxonomic resolution. Only the flat carbonate terrace of the Glorieuses archipelago contrasts with a low beta diversity (0.28). High beta diversity is explained by substrate diversity.

- Habitat-forming taxa (Porifera, Cnidaria) are among the most contributors of beta diversity even if identified at low taxonomic rank (e.g., Demospongiae, Hexactinellida,

Alcyonacea, Antipatharia) in addition to mobile taxa identified at finer taxonomic resolution (e.g., *Chlorophthalmus*, *Stereocidaris*, *Puerulus carinatus*).

- Megabenthic assemblages structure differ within and among seamounts. The assemblages display a highly patchy distribution from 0.06 km (60 m) to 2 km within a single seamount to assemblage differences over seamounts distant from 4 km to 1400 km.

- Along the Mozambique Channel, various environmental drivers play a role in shaping megabenthic assemblages over different spatial scales. Hydrology (current, primary productivity) is an important driver identified in our study, with up to ~15% contribution, along with interaction with other factors having high contribution: geomorphology (> km) (6.5%), topography (60-500 m) (7.9%), as well as substrate (60 m) (9.5%) (composition, hardness, diversity). In particular, the difference of rocky nature (volcanic vs. carbonate) play a role in benthic communities spatial structuration (e.g., demosponges and brachiopods favor carbonate slab related to flat morphologies while hexactinellids favor volcanic reliefs related to ruguous areas). This highlights the importance to consider rock bottom specificity in future studies.

- Within island slopes, the partitioning of spatial scales reveals medium-scale (or even large-scale) megabenthic community structures explained by factors such as topography, substrate, depth, slope and hydrology. The assemblage variability visible at smaller scales is more difficult to explain by the environment due to the low faunal densities in our study area, and a high level of diversity. Further characterisation of environmental factors at these small scales (using high resolution bathymetric models and image analysis) is required. Increasing the resolution of hydrodynamic data and quantifying current/topography/substrate interactions would be interesting from long-term *in situ* models or measurements. Furthermore, the low taxonomic resolution does not allow to characterize the functional diversity and biological interactions present in the structuring of communities. For the latter, an approach focusing on the functional morphologies of habitat-forming taxa rather than their taxonomic entity would make it possible to assess the structuring role of biogenic habitats on the associated megafauna.

- Mayotte island slopes and Glorieuses terrace display highly contrasting community structure with striking density, richness, composition and beta diversity differences as well as scales of spatial patterns. The scale of habitat heterogeneity and differences among the two sites are important elements to consider for the management of Mayotte and Glorieuses areas, which are integral parts of marine protected areas, the former under the management of the French Biodiversity Office and the latter under the management of the French Southern and Antarctic Territories.

II.6 References

Althaus, F., Williams, A., Schlacher, T., Kloser, R., Green, M., Barker, B., Bax, N., Brodie, P., Hoenlinger-Schlacher, M., 2009. Impacts of bottom trawling on deep-coral ecosystems of seamounts are long-lasting. Marine Ecology Progress Series 397, 279–294. https://doi.org/10.3354/meps08248

Anastasopoulou, A., Kapiris, K., 2008. Feeding ecology of the shortnose greeneye Chlorophthalmus agassizi Bonaparte, 1840 (Pisces: Chlorophthalmidae) in the eastern Ionian Sea (eastern Mediterranean). J Appl Ichthyol 24, 170–179. https://doi.org/10.1111/j.1439-0426.2007.01028.x

Ângelo Adolfo Langa, A., 2021. Seasonal and Spatial Variability of Primary Production in the Mozambique Channel. WROS 10, 61. https://doi.org/10.11648/j.wros.20211003.14

Audru, J.-C., Guennoc, P., Thinon, I., Abellard, O., 2006. Bathymay : la structure sous-marine de Mayotte révélée par l'imagerie multifaisceaux. Comptes Rendus Geoscience 338, 1240–1249. https://doi.org/10.1016/j.crte.2006.07.010

Auscavitch, S.R., Deere, M.C., Keller, A.G., Rotjan, R.D., Shank, T.M., Cordes, E.E., 2020a. Oceanographic Drivers of Deep-Sea Coral Species Distribution and Community Assembly on Seamounts, Islands, Atolls, and Reefs Within the Phoenix Islands Protected Area. Front. Mar. Sci., a 7, 42. https://doi.org/10.3389/fmars.2020.00042

Auscavitch, S.R., Lunden, J.J., Barkman, A., Quattrini, A.M., Demopoulos, A.W.J., Cordes, E.E., 2020b. Distribution of deep-water scleractinian and stylasterid corals across abiotic environmental gradients on three seamounts in the Anegada Passage. PeerJ, b 8, e9523. https://doi.org/10.7717/peerj.9523

Baco, A.R., Morgan, N.B., Roark, E.B., 2020. Observations of vulnerable marine ecosystems and significant adverse impacts on high seas seamounts of the northwestern Hawaiian Ridge and Emperor Seamount Chain. Marine Policy 115, 103834. https://doi.org/10.1016/j.marpol.2020.103834

Bell, J.B., Alt, C.H.S., Jones, D.O.B., 2016. Benthic megafauna on steep slopes at the Northern Mid-Atlantic Ridge. Marine Ecology 37, 1290–1302. https://doi.org/10.1111/maec.12319

Bo, M., Coppari, M., Betti, F., Massa, F., Gay, G., Cattaneo-Vietti, R., Bavestrello, G., 2020. Unveiling the deep biodiversity of the Janua Seamount (Ligurian Sea): first Mediterranean sighting of the rare Atlantic bamboo coral Chelidonisis aurantiaca Studer, 1890. Deep Sea Research Part I: Oceanographic Research Papers 156, 103186. https://doi.org/10.1016/j.dsr.2019.103186

Borcard, D., Gillet, F., Legendre, P., 2018. Numerical Ecology with R, Use R! Springer International Publishing, Cham. https://doi.org/10.1007/978-3-319-71404-2

Boschen, R., Rowden, A., Clark, M., Barton, S., Pallentin, A., Gardner, J., 2015. Megabenthic assemblage structure on three New Zealand seamounts: implications for seafloor massive sulfide mining. Marine Ecology Progress Series 523, 1–14. https://doi.org/10.3354/meps11239

Bourillet, J.-F., Ferry, J.-N., Bourges, P., 2013. PAMELA : Passive Margins Exploration Laboratories. https://doi.org/10.18142/236

Brault, S., Stuart, C.T., Wagstaff, M.C., McClain, C.R., Allen, J.A., Rex, M.A., 2013. Contrasting patterns of α- and β-diversity in deep-sea bivalves of the eastern and western North Atlantic. Deep Sea Research Part II: Topical Studies in Oceanography 92, 157–164. https://doi.org/10.1016/j.dsr2.2013.01.018

Bridges, A.E.H., Barnes, D.K.A., Bell, J.B., Ross, R.E., Howell, K.L., 2022. Depth and latitudinal gradients of diversity in seamount benthic communities. Journal of Biogeography jbi.14355. https://doi.org/10.1111/jbi.14355

Bridges, A.E.H., Barnes, D.K.A., Bell, J.B., Ross, R.E., Howell, K.L., 2021. Benthic Assemblage Composition of South Atlantic Seamounts. Front. Mar. Sci. 8, 660648. https://doi.org/10.3389/fmars.2021.660648

Buhl-Mortensen, L., Vanreusel, A., Gooday, A.J., Levin, L.A., Priede, I.G., Buhl-Mortensen, P., Gheerardyn, H., King, N.J., Raes, M., 2010. Biological structures as a source of habitat heterogeneity and biodiversity on the deep ocean margins: Biological structures and biodiversity. Marine Ecology 31, 21–50. https://doi.org/10.1111/j.1439-0485.2010.00359.x

Castelin, M., Delavenne, J., Brisset, J., Chambart, C., Corbari, L., Keszler, L., Lozouet, P., Olu, K., Poncet, L., Puillandre, N., Samadi, S., 2017. Exploration et étude de la biodiversité benthique profonde de Mayotte et des îles éparses (Rapport final de la convention MNHN-TAAF dans le cadre du Xème FED régional « gestion durable du patrimoine naturel de Mayotte et des îles Eparses »).

Charles, C., Pelleter, E., Révillon, S., Nonnotte, P., Jorry, S.J., Kluska, J.-M., 2020. Intermediate and deep ocean current circulation in the Mozambique Channel: New insights from ferromanganese crust Nd isotopes. Marine Geology 430, 106356. https://doi.org/10.1016/j.margeo.2020.106356

Clark, M.R., Bowden, D.A., 2015. Seamount biodiversity: high variability both within and between seamounts in the Ross Sea region of Antarctica. Hydrobiologia 761, 161–180. https://doi.org/10.1007/s10750-015-2327-9

Clark, M.R., Rowden, A.A., Schlacher, T., Williams, A., Consalvey, M., Stocks, K.I., Rogers, A.D., O'Hara, T.D., White, M., Shank, T.M., Hall-Spencer, J.M., 2010. The Ecology of Seamounts: Structure, Function, and Human Impacts. Annual Review of Marine Science 2, 253–278. https://doi.org/10.1146/annurev-marine-120308-081109

Collins, C., Hermes, J.C., Roman, R.E., Reason, C.J.C., 2016. First dedicated hydrographic survey of the Comoros Basin. Journal of Geophysical Research: Oceans 121, 1291–1305. https://doi.org/10.1002/2015JC011418

Corbari, L., Samadi, S., Olu, K., 2017. BIOMAGLO cruise, RV Antea. https://doi.org/10.17600/17004000

Courgeon, S., Bachèlery, P., Jouet, G., Jorry, S.J., Bou, E., BouDagher-Fadel, M.K., Révillon, S., Camoin, G., Poli, E., 2018. The offshore east African rift system: new insights from the Sakalaves seamounts (Davie Ridge, SW Indian Ocean). Terra Nova 30, 380–388. https://doi.org/10.1111/ter.12353

Courgeon, S., Jorry, S.J., Camoin, G.F., BouDagher-Fadel, M.K., Jouet, G., Révillon, S., Bachèlery, P., Pelleter, E., Borgomano, J., Poli, E., Droxler, A.W., 2016. Growth and demise of Cenozoic isolated carbonate platforms: New insights from the Mozambique Channel seamounts (SW Indian Ocean). Marine Geology 380, 90–105. https://doi.org/10.1016/j.margeo.2016.07.006

Courgeon, S., Jorry, S.J., Jouet, G., Camoin, G., BouDagher-Fadel, M.K., Bachèlery, P., Caline, B., Boichard, R., Révillon, S., Thomas, Y., Thereau, E., Guérin, C., 2017. Impact of tectonic and volcanism on the Neogene evolution of isolated carbonate platforms (SW Indian Ocean). Sedimentary Geology 355, 114–131. https://doi.org/10.1016/j.sedgeo.2017.04.008

d'Hondt, M.J., d'Hondt, J.L., 2019. Note sur quelques espèces d'Anthomastus et autres Anthomastinae (Octocoralliaires, Alcyoniidae) ; description de Pseudoanthomastus gloriosus n. sp. Bulletin de la Société Linnéenne de Bordeaux 154(1/2), nouvelle série n°47 103–108.

de la Torriente, A., Serrano, A., Fernández-Salas, L.M., García, M., Aguilar, R., 2018. Identifying epibenthic habitats on the Seco de los Olivos Seamount: Species assemblages and environmental characteristics. Deep Sea Research Part I: Oceanographic Research Papers 135, 9–22. https://doi.org/10.1016/j.dsr.2018.03.015

de Ruijter, W.P.M., Aken, H.M. van, Beier, E.J., Lutjeharms, J.R.E., Matano, R.P., Schouten, M.W., 2004. Eddies and dipoles around South Madagascar: formation, pathways and large-scale impact. Deep Sea Research Part I: Oceanographic Research Papers 51, 383–400. https://doi.org/10.1016/j.dsr.2003.10.011

de Ruijter, W.P.M., Ridderinkhof, H., Lutjeharms, J.R.E., Schouten, M.W., Veth, C., 2002. Observations of the flow in the Mozambique Channel. Geophysical Research Letters 29, 140-1-140–3. https://doi.org/10.1029/2001GL013714

Dray, S., Bauman, D., Blanchet, F.G., Borcard, D., Clappe, S., Guenard, G., Jombart, T., Larocque, G., Legendre, P., Madi, N., Wagner, H., 2022. adespatial: Multivariate Multiscale Spatial Analysis. R package version 0.3-16.

Du Preez, C., Curtis, J.M.R., Clarke, M.E., 2016. The Structure and Distribution of Benthic Communities on a Shallow Seamount (Cobb Seamount, Northeast Pacific Ocean). PLoS ONE 11, e0165513. https://doi.org/10.1371/journal.pone.0165513

Dufrêne, M., Legendre, P., 1997. Species assemblages and indicator species: the need for a flexible asymmetrical approach. Ecological Monographs 67, 22.

Faivre, L., Teichert, N., Valade, P., Monnier, O., Couprie, S., 2020. Evaluation des conditions de référence des cours d'eau de Mayotte - Projet REZORD -MAY - Volet 1 : Caractérisation des pressions s'exerçant sur les populations de poissons et de macro- crustacés amphihalins de Mayotte. Rapport final OCE, MNHN, OFB.

Fischer, W., Bianchi, G. (Eds.), 1984. FAO Species Identification Sheets for Fishery Purposes. Western Indian Ocean (Fishing Area 51), Prepared and Printed with the Support of the Danish International Development Agency (DANIDA). ed. FAO, Rome.

Genin, A., Dayton, P.K., Lonsdale, P.F., Spiess, F.N., 1986. Corals on seamount peaks provide evidence of current acceleration over deep-sea topography. Nature 322, 59–61. https://doi.org/10.1038/322059a0

Goode, S.L., Rowden, A.A., Bowden, D.A., Clark, M.R., Stephenson, F., 2021. Fine-Scale Mapping of Mega-Epibenthic Communities and Their Patch Characteristics on Two New Zealand Seamounts. Front. Mar. Sci. 8, 765407. https://doi.org/10.3389/fmars.2021.765407

Grassle, J.F., Sanders, H.L., Hessler, R.R., Rowe, G.T., McLellan, T., 1975. Pattern and zonation: a study of the bathyal megafauna using the research submersible Alvin. Deep Sea Research and Oceanographic Abstracts 22, 457–481. https://doi.org/10.1016/0011-7471(75)90020-0

Hall-Spencer, J., Rogers, A., Davies, J., Foggo, A., 2007. Deep-sea coral distribution on seamounts, oceanic islands, and continental slopes in the Northeast Atlantic 13.

Hanafi-Portier, M., Samadi, S., Corbari, L., Chan, T.-Y., Chen, W.-J., Chen, J.-N., Lee, M.-Y., Mah, C., Saucède, T., Borremans, C., Olu, K., 2021. When Imagery and Physical Sampling Work Together: Toward an Integrative Methodology of Deep-Sea Image-Based Megafauna Identification. Front. Mar. Sci. 8, 749078. https://doi.org/10.3389/fmars.2021.749078

Hein, J.R., Conrad, T.A., Staudigel, H., 2010. Seamount mineral deposits, a source of rare metals for high-technology industries. Oceanography 23, 184–189.

Henry, L.-A., Vad, J., Findlay, H.S., Murillo, J., Milligan, R., Roberts, J.M., 2015. Environmental variability and biodiversity of megabenthos on the Hebrides Terrace Seamount (Northeast Atlantic). Scientific Reports 4. https://doi.org/10.1038/srep05589

Howell, K.L., Mowles, S.L., Foggo, A., 2010. Mounting evidence: near-slope seamounts are faunally indistinct from an adjacent bank: Seamounts are not faunally distinct. Marine Ecology 31, 52–62. https://doi.org/10.1111/j.1439-0485.2010.00368.x

Hsieh, T.C., Ma, K.H., Chao, A., 2020. iNEXT: iNterpolation and EXTrapolation for species diversity. R package version 2.0.20.

Hubbs, C.L., 1959. Initial discoveries of fish faunas on seamounts and offshore banks in the eastern Pacific. Pacific Science 12, 311–316.

Jorry, S., 2014. PTOLEMEE cruise, RV L'Atalante. https://doi.org/10.17600/14000900

Jouet, G., Deville, E., 2015. PAMELA-MOZ04 cruise, RV Pourquoi pas ?,. https://doi.org/10.17600/15000700

Kaufmann, R.S., Wakefield, W.W., Genin, A., 1989. Distribution of epibenthic megafauna and lebensspuren on two central North Pacific seamounts. Deep Sea Research Part A. Oceanographic Research Papers 36, 1863–1896. https://doi.org/10.1016/0198-0149(89)90116-7

Kvile, K.Ø., Taranto, G.H., Pitcher, T.J., Morato, T., 2014. A global assessment of seamount ecosystems knowledge using an ecosystem evaluation framework. Biological Conservation 173, 108–120. https://doi.org/10.1016/j.biocon.2013.10.002

Langenkämper, D., Zurowietz, M., Schoening, T., Nattkemper, T.W., 2017. BIIGLE 2.0 - Browsing and Annotating Large Marine Image Collections. Frontiers in Marine Science 4. https://doi.org/10.3389/fmars.2017.00083

Lapointe, A.E., Watling, L., France, S.C., Auster, P.J., 2020. Megabenthic assemblages in the lower bathyal (700–3000 m) on the New England and Corner Rise Seamounts, Northwest Atlantic. Deep Sea Research Part I: Oceanographic Research Papers 165, 103366. https://doi.org/10.1016/j.dsr.2020.103366

Lawrence, J.M., Jangoux, M., 2020. Chapter 21: Cidaroids, in: Lawrence, J.M. (Ed.), Sea Urchins: Biology and Ecology.

Legendre, P., 2014. Interpreting the replacement and richness difference components of beta diversity: Replacement and richness difference components. Global Ecology and Biogeography 23, 1324–1334. https://doi.org/10.1111/geb.12207

Legendre, P., De Cáceres, M., 2013. Beta diversity as the variance of community data: dissimilarity coefficients and partitioning. Ecology Letters 16, 951–963. https://doi.org/10.1111/ele.12141

Legendre, P., Gallagher, E.D., 2001. Ecologically meaningful transformations for ordination of species data. Oecologia 129, 271–280. https://doi.org/10.1007/s004420100716

Legendre, P., Legendre, L.F., 2012. Numerical ecology, 3rd ed. Elsevier.

Leroy, B., 2022. biogeonetworks: Biogeographical Network Manipulation And Analysis. R package version 0.1.2.

Lévy, M., Klein, P., Treguier, A.-M., 2001. Impact of sub-mesoscale physics on production and subduction of phytoplankton in an oligotrophic regime. Journal of Marine Research 59, 535–565. https://doi.org/10.1357/002224001762842181

Long, D.J., Baco, A.R., 2014. Rapid change with depth in megabenthic structure-forming communities of the Makapu'u deep-sea coral bed. Deep Sea Research Part II: Topical Studies in Oceanography 99, 158–168. https://doi.org/10.1016/j.dsr2.2013.05.032

Lundsten, L., Barry, J., Cailliet, G., Clague, D., DeVogelaere, A., Geller, J., 2009. Benthic invertebrate communities on three seamounts off southern and central California, USA. Mar. Ecol. Prog. Ser. 374, 23–32. https://doi.org/10.3354/meps07745

Malauene, B.S., Shillington, F.A., Roberts, M.J., Moloney, C.L., 2014. Cool, elevated chlorophyll-a waters off northern Mozambique. Deep Sea Research Part II: Topical Studies in Oceanography 100, 68–78. https://doi.org/10.1016/j.dsr2.2013.10.017

Marsac, F., Barlow, R., Ternon, J.F., Ménard, F., Roberts, M., 2014. Ecosystem functioning in the Mozambique Channel: Synthesis and future research. Deep Sea Research Part II: Topical Studies in Oceanography 100, 212–220. https://doi.org/10.1016/j.dsr2.2013.10.028

McClain, C.R., Lundsten, L., Barry, J., DeVogelaere, A., 2010. Assemblage structure, but not diversity or density, change with depth on a northeast Pacific seamount: Bathymetric patterns in diversity, abundance and assemblage structure. Marine Ecology 31, 14–25. https://doi.org/10.1111/j.1439-0485.2010.00367.x

McClain, C.R., Lundsten, L., Ream, M., Barry, J., DeVogelaere, A., 2009. Endemicity, Biogeography, Composition, and Community Structure On a Northeast Pacific Seamount. PLoS ONE 4, e4141. https://doi.org/10.1371/journal.pone.0004141

Miramontes, E., Jorry, S.J., Jouet, G., Counts, J.W., Courgeon, S., Le Roy, P., Guerin, C., Hernández-Molina, F.J., 2019a. Deep-water dunes on drowned isolated carbonate terraces (Mozambique Channel, south-west Indian Ocean). Sedimentology 66, 1222–1242. https://doi.org/10.1111/sed.12572

Miramontes, E., Penven, P., Fierens, R., Droz, L., Toucanne, S., Jorry, S.J., Jouet, G., Pastor, L., Silva Jacinto, R., Gaillot, A., Giraudeau, J., Raisson, F., 2019b. The influence of bottom currents on the Zambezi Valley morphology (Mozambique Channel, SW Indian Ocean): In situ current observations and hydrodynamic modelling. Marine Geology 410, 42–55. https://doi.org/10.1016/j.margeo.2019.01.002

Morato, T., Clark, M.R., 2007. Seamount fishes: ecology and life histories, in: Pitcher, T.J., Morato, T., Paul, J.B.H., Clark, M.R., Nigel, H., Ricardo, S.S. (Eds.), Seamounts: Ecology, Fisheries & Conservation. John Wiley & Sons, Ltd, pp. 170–188. https://doi.org/10.1002/9780470691953.ch9

Morato, T., Varkey, D., Damaso, C., Machete, M., Santos, M., Prieto, R., Pitcher, T., Santos, R., 2008. Evidence of a seamount effect on aggregating visitors. Mar. Ecol. Prog. Ser. 357, 23–32. https://doi.org/10.3354/meps07269

Morgan, N.B., Cairns, S., Reiswig, H., Baco, A.R., 2015. Benthic megafaunal community structure of cobalt-rich manganese crusts on Necker Ridge. Deep Sea Research Part I: Oceanographic Research Papers 104, 92–105. https://doi.org/10.1016/j.dsr.2015.07.003

Morgan, N.B., Goode, S., Roark, E.B., Baco, A.R., 2019. Fine Scale Assemblage Structure of Benthic Invertebrate Megafauna on the North Pacific Seamount Mokumanamana. Front. Mar. Sci. 6, 715. https://doi.org/10.3389/fmars.2019.00715

Obura, D., Church, J., Gabrié, C., Macharia, D., 2012. Assessing Marine World Heritage from an Ecosystem Perspective: The Western Indian Ocean 125.

O'Hara, T.D., 2007. Seamounts: centres of endemism or species richness for ophiuroids? Global Ecology and Biogeography 16, 720–732. https://doi.org/10.1111/j.1466-8238.2007.00329.x

O'Hara, T.D., Consalvey, M., Lavrado, H.P., Stocks, K.I., 2010. Environmental predictors and turnover of biota along a seamount chain: Assemblage composition along a seamount chain. Marine Ecology 31, 84–94. https://doi.org/10.1111/j.1439-0485.2010.00379.x

Oksanen, J., Blanchet, F.G., Friendly, M., Kindt, R., Legendre, P., McGlinn, D., Minchin, P.R., O'Hara, R.B., Gavin, L.S., Peter, S., H. Stevens, M. henry, Szoecs, E., Wagner, H., 2020. vegan: Community Ecology Package. R package version 2.5-7.

Olu, K., 2014. PAMELA-MOZ01 cruise, RV L'Atalante. https://doi.org/10.17600/14001000

Peres-Neto, P.R., Legendre, P., 2010. Estimating and controlling for spatial structure in the study of ecological communities. Global Ecology and Biogeography 19, 174–184. https://doi.org/10.1111/j.1466-8238.2009.00506.x

R Core Team, 2021. R: A language and environment for statistical computing. Vienna: R Foundation for Statistical Computing.

Ramos, M., Bertocci, I., Tempera, F., Calado, G., Albuquerque, M., Duarte, P., 2016. Patterns in megabenthic assemblages on a seamount summit (Ormonde Peak, Gorringe Bank, Northeast Atlantic). Marine Ecology 37, 1057–1072. https://doi.org/10.1111/maec.12353

Richer de Forges, B., Koslow, J.A., Poore, G.C.B., 2000. Diversity and endemism of the benthic seamount fauna in the southwest Pacific. Nature 405, 944–947. https://doi.org/10.1038/35016066

Roberts, D.W., 2019. labdsv: Ordination and Multivariate Analysis for Ecology. R package version 2.0-1.

Rogers, A.D., 2018. The Biology of Seamounts: 25 Years on, in: Advances in Marine Biology. Elsevier, pp. 137–224. https://doi.org/10.1016/bs.amb.2018.06.001

Rowden, A.A., Clark, M.R., Wright, I.C., 2005. Physical characterisation and a biologically focused classification of “seamounts” in the New Zealand region. New Zealand Journal of Marine and Freshwater Research 39, 1039–1059. https://doi.org/10.1080/00288330.2005.9517374

Rowden, A.A., Dower, J.F., Schlacher, T.A., Consalvey, M., Clark, M.R., 2010a. Paradigms in seamount ecology: fact, fiction and future: Paradigms in seamount ecology. Marine Ecology, a 31, 226–241. https://doi.org/10.1111/j.1439-0485.2010.00400.x

Rowden, A.A., Schlacher, T.A., Williams, A., Clark, M.R., Stewart, R., Althaus, F., Bowden, D.A., Consalvey, M., Robinson, W., Dowdney, J., 2010b. A test of the seamount oasis hypothesis: seamounts support higher epibenthic megafaunal biomass than adjacent slopes: A test of the seamount oasis hypothesis. Marine Ecology, b 31, 95–106. https://doi.org/10.1111/j.1439-0485.2010.00369.x

Rubio, F., Rolán, E., 2022. New species of Vitrinellidae (Gastropoda: Truncatelloidea) from the Indo-Pacific. The genus Circulus Jeffreys, 1865. Museo National de Historia Natural, Universidad de Santiago de Compostela, 1-422.

Sahlmann, C., Chan, T.-Y., Chan, B.K.K., 2011. Feeding modes of deep-sea lobsters (Crustacea: Decapoda: Nephropidae and Palinuridae) in Northwest Pacific waters: Functional morphology of mouthparts, feeding behaviour and gut content analysis. Zoologischer Anzeiger - A Journal of Comparative Zoology 250, 55–66. https://doi.org/10.1016/j.jcz.2010.11.003

Samadi, S., Bottan, L., Macpherson, E., De Forges, B.R., Boisselier, M.-C., 2006. Seamount endemism questioned by the geographic distribution and population genetic structure of marine invertebrates. Marine Biology 149, 1463–1475. https://doi.org/10.1007/s00227-006-0306-4

Sautya, S., Ingole, B., Ray, D., Stöhr, S., Samudrala, K., Raju, K.A.K., Mudholkar, A., 2011. Megafaunal Community Structure of Andaman Seamounts Including the Back-Arc Basin – A Quantitative Exploration from the Indian Ocean. PLoS ONE 6, e16162. https://doi.org/10.1371/journal.pone.0016162

Schlacher, T.A., Baco, A.R., Rowden, A.A., O'Hara, T.D., Clark, M.R., Kelley, C., Dower, J.F., 2014. Seamount benthos in a cobalt-rich crust region of the central Pacific: conservation challenges for future seabed mining. Diversity and Distributions 20, 491–502. https://doi.org/10.1111/ddi.12142

Shaun Walbridge, Noah Slocum, Marjean Pobuda, Dawn Wright, 2018. Unified Geomorphological Analysis Workflows with Benthic Terrain Modeler. Geosciences 8, 94. https://doi.org/10.3390/geosciences8030094

Shen, C., Lu, B., Li, Z., Zhang, R., Chen, W., Xu, P., Yao, H., Chen, Z., Pang, J., Wang, C., Zhang, D., 2021. Community structure of benthic megafauna on a seamount with cobalt-rich ferromanganese crusts in the northwestern Pacific Ocean. Deep Sea Research Part I: Oceanographic Research Papers 178, 103661. https://doi.org/10.1016/j.dsr.2021.103661

Staudigel, H., Clague, D.A., 2010. The Geological History of Deep-Sea Volcanoes: Biosphere, Hydrosphere, and Lithosphere Interactions. Oceanography 23, 58–71. https://doi.org/10.5670/oceanog.2010.62

Tapia-Guerra, J.M., Mecho, A., Easton, E.E., Gallardo, M. de los Á., Gorny, M., Sellanes, J., 2021. First description of deep benthic habitats and communities of oceanic islands and seamounts of the Nazca Desventuradas Marine Park, Chile. Sci Rep 11, 6209. https://doi.org/10.1038/s41598-021-85516-8

Taylor, J.D., Glover, E.A., 2018. Hanging on — lucinid bivalve survivors from the Paleocene and Eocene in the western Indian Ocean (Bivalvia: Lucinidae). Zoosystema 40, 123. https://doi.org/10.5252/zoosystema2018v40a7

Tew-Kai, E., Marsac, F., 2009. Patterns of variability of sea surface chlorophyll in the Mozambique Channel: A quantitative approach. Journal of Marine Systems 77, 77–88. https://doi.org/10.1016/j.jmarsys.2008.11.007

Thistle, D., 2003. The deep-sea floor: An overview 34.

Thomassin, B., 1977. BENTHEDI I cruise, RV Le Suroît. https://doi.org/10.17600/77003111

Turnewitsch, R., Dumont, M., Kiriakoulakis, K., Legg, S., Mohn, C., Peine, F., Wolff, G., 2016. Tidal influence on particulate organic carbon export fluxes around a tall seamount. Progress in Oceanography 149, 189–213. https://doi.org/10.1016/j.pocean.2016.10.009

Victorero, L., Robert, K., Robinson, L.F., Taylor, M.L., Huvenne, V.A.I., 2018. Species replacement dominates megabenthos beta diversity in a remote seamount setting. Scientific Reports 8. https://doi.org/10.1038/s41598-018-22296-8

Vilhena, D.A., Antonelli, A., 2015. A network approach for identifying and delimiting biogeographical regions. Nat Commun 6, 6848. https://doi.org/10.1038/ncomms7848

White, M., Bashmachnikov, I., Arístegui, J., Martins, A., 2007. Physical processes and seamount productivity, in: Pitcher, T.J., Morato, T., Hart, P.J.B., Clark, M.R., Haggan, N., Santos, R.S. (Eds.), Seamounts: Ecology, Conservation and Management, Fish and Aquatic Resources. Blackwell, Oxford, UK, pp. 65–84.

Wickham, H., Chang, W., Wickham, M.H., 2016. Package 'ggplot2'. Create elegant data visualisations using the grammar of graphics. Version, 2(1), 1-189.

Williams, A., Althaus, F., Clark, M.R., Gowlett-Holmes, K., 2011. Composition and distribution of deep-sea benthic invertebrate megafauna on the Lord Howe Rise and Norfolk Ridge, southwest Pacific Ocean. Deep Sea Research Part II: Topical Studies in Oceanography 58, 948–958. https://doi.org/10.1016/j.dsr2.2010.10.050

Wilson, M.F.J., O'Connell, B., Brown, C., Guinan, J.C., Grehan, A.J., 2007. Multiscale Terrain Analysis of Multibeam Bathymetry Data for Habitat Mapping on the Continental Slope. Marine Geodesy 30, 3–35. https://doi.org/10.1080/01490410701295962

II.7 Supplementary materials

Supplementary material II.1 : List of the taxonomic composition of the dataset

Cnidaria	**Porifera**	**Decapoda**	**Actinopterygii**	**Asteroidea**	**Echinoidea**	**Echinodermata (others)**	**Mollusca**	**Other taxa**
Actiniaria	Demospongiae	*Acanthephyra*	Anguilliformes	Asterinidae	*Araeosoma*	Comatulida	Bivalvia	Annelida
Alcyonacea	Hexactinellida	*Agononida*	Aulopiformes	Asteroidea sp.	*Aspidodiadema*	Holothuroidea	Gastropoda	Brachiopoda
Antipatharia		*Aristaeopsis edwardsiana* sp. inc.	Beryciformes	Astropectinidae	*Caenopedina pulchella* sp. inc.	Ophiuroidea	Xenophoridae	
Bathyalcyon		*Aristeus*	*Chlorophthalmus*	Brisingida	*Caenopedina* sp.	Peduncled Crinoidea		
Enallopsammia		*Aristeus mabahissae*	Gadiformes	*Cheiraster*	*Echinolampas*			
Hydrozoa		*Benthesicymus*	Lophiiformes	*Coronaster*	*Heterobrissus*			
Javania		*Cyrtomaia*	*Malthopsis*	Echinasteridae	Laganidae			
Pennatulacea		Epialtidae	Myctophiformes	Goniasteridae	*Micropyga* sp1			
Primnoidae		*Eumunida*	Ophidiiformes	Myxasteridae	*Micropyga* sp2			
Scleractinia (solitary)		*Glyphocrangon*	Perciformes	*Nepanthia*	*Pourtalesia*			
Scleractinia (colonial)		Goneplacoidea	Peristediidae	Ophidiasteridae Fam. inc.	*Spatangus*			
Stylasteridae incertae		*Haliporoides*	Pleuronectiformes	*Pteraster* sp.	*Stereocidaris*			
Umbellula		*Hemipenaeus*	*Poecilopsetta*	Solasteridae	*Stylocidaris*			
Zoantharia		*Heterocarpus*	*Polymixia*	*Tremaster mirabilis*				
Zoanthidae		Homolidae	Scorpaeniformes					
		Hymenodora	Squaliformes					
		Leucosiidae	Stomiiformes					
		Mathildellidae	Synodontidae					
		Munida						
		Nematocarcinus						
		Oxypleurodon						
		Paguroidea						
		Parthenopidae						
		Penaeopsis						
		Plesionika						
		Puerulus carinatus						
		Sympagurus sp1						
		Sympagurus sp2						

Supplementary material II.2 : Oxygen, temperature and salinity depth profiles for each camera transect

Available online at:

https://docs.google.com/document/d/19C86UmVLcmwVFtrugKCh85crXO_uJjHKJVQ7kKeS4VA/edit?usp=sharing

Supplementary material II.3 : Geomorphological classes catalog

Carbonates (slab) Bright, flat, smooth	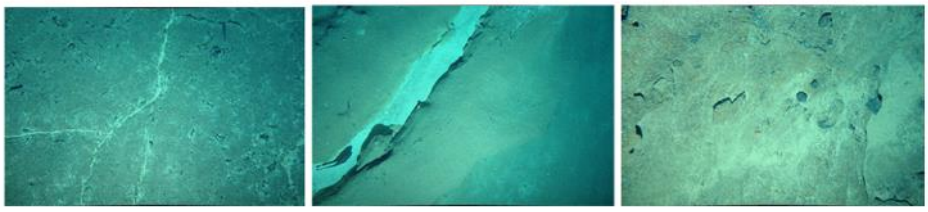
Volcanics (lava flow) Dark, rugged relief, vacuolar	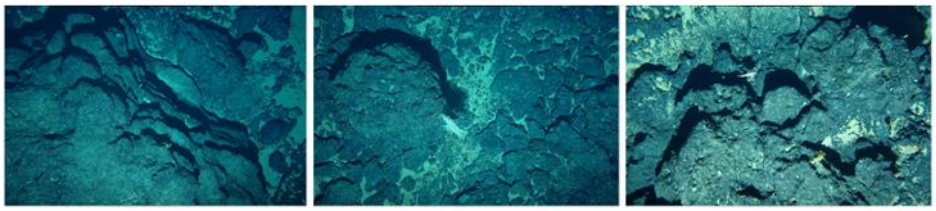
Mixed Carbonate + sand + volcanic	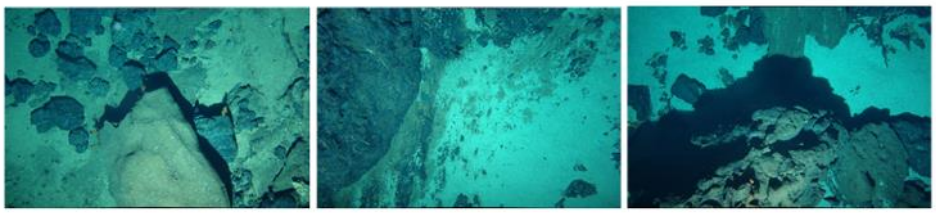
Sedimentary Elongated ridges, smooth, domal	

Supplementary material II.4 : Substrate categories catalog **(1)** = primary substrate, and **(2)** = secondary substrate

Soft (1)	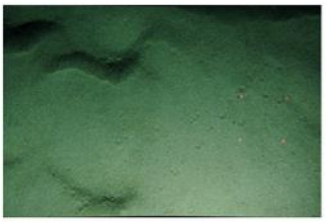
Gravels (1)	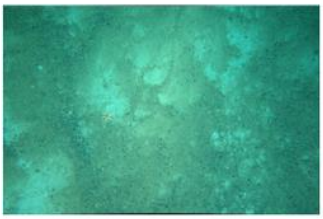
Biogenic (1)	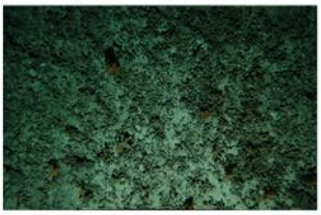 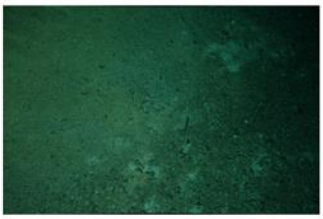
Soft (1) / Carbonate rock (2)	

Soft (1) / Volcanic rock (2)	
Mixed volcanic-sediment	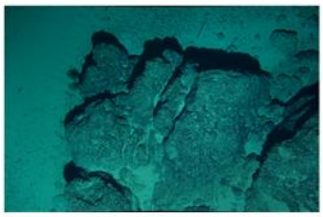 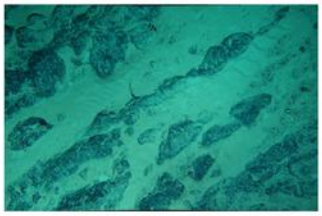
Mixed carbonate-sediment	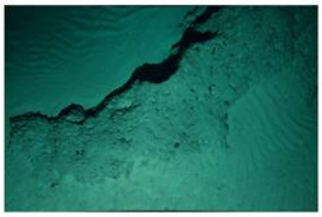
Volcanic rock (1)/ soft (2)	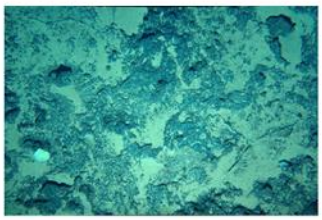

Carbonate rock (1)/ soft (2)	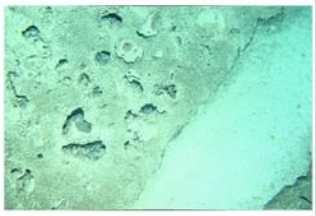
Volcanic rock (1)	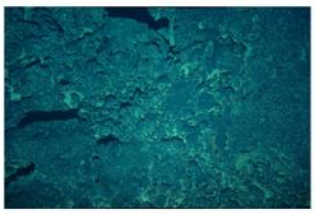
Carbonate rock (1)	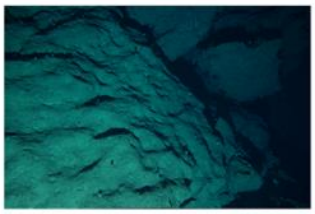 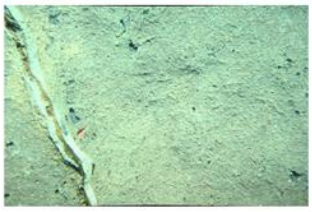

Mixed rock (volcanic, carbonate)	 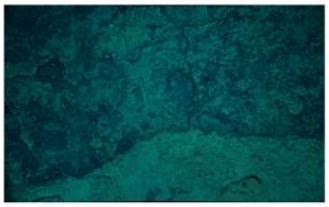
Mixed (volcanic, carbonate, soft)	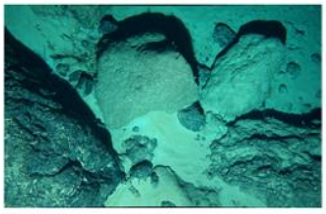
Gravels (1) /carbonate (2)	
Mixed biogenic/gravels	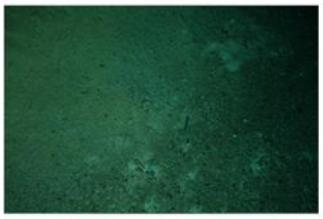
Carbonate rock (1) /biogenic (2)	

Supplementary material II.5 : Histogram of relative frequencies of cnidarian orders

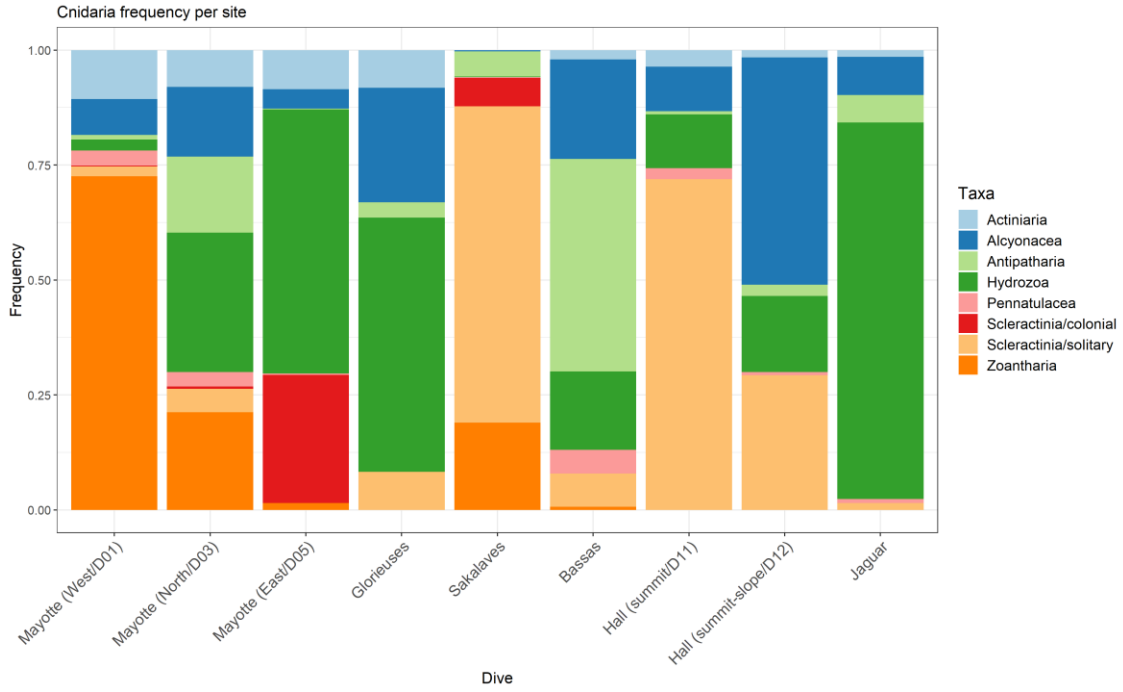

Supplementary material II.6 : Summary of the taxon densities per site

Available online at:

https://docs.google.com/spreadsheets/d/1-3eq-s_EPY8TkkaizuLBMs7kCGbAPkJctNAkhaRDNXg/edit?usp=sharing

Supplementary material II.7 : Taxonomic composition of the assemblages along the Mozambique Channel, and for each taxon, indication of its relative frequency of occurrence within the assemblage (Fidelity), its relative abundance (Specificity), and its indicator value of contribution to the assemblage (IndVal)

Assemblages	Taxa	Fidelity (%)	Specificity (%)	IndVal (%)
A1	Demospongiae	91.5	77.8	71.1
	Brachiopoda	80.9	56.4	45.6
	Micropyga sp2	33.3	29.7	9.9
	Tremaster mirabilis	1.4	39.1	0.6
	Pourtalesia	0.7	100.0	0.7
A2	*Chlorophthalmus*	95.6	30.9	29.6
	Pleuronectiformes	41.6	27.2	11.3
	Anguilliformes	26.7	4.5	1.2
	Puerulus carinatus	17.1	24.4	4.2
	Poecilopsetta	15.2	41.0	6.2
	Araeosoma	8.5	16.0	1.4
	Cheiraster	5.8	16.2	0.9
	Peristediidae	8.3	22.5	1.9
	Pteraster sp	2.5	13.3	0.3
	Penaeopsis	0.8	100.0	0.8
A3	Hexactinellida	99.6	15.9	15.8
	Enallopsammia	5.5	73.0	4.0
	Heterocarpus	3.4	6.3	0.2
	Acanthephyra	0.4	100.0	0.4
	Eumunida	0.4	100.0	0.4
	Benthesicymus	0.4	100.0	0.4
A4	Gastropoda	98.4	34.5	33.9
	Paguroidea	39.5	24.7	9.8
	Caenopedina sp.CODE.	4.8	41.5	2.0
	Stomiiformes	2.4	72.2	1.8
	Aristeus mabahissae	0.8	53.9	0.4
	Bathyalcyon	0.8	100.0	0.8
	Sympagurus sp2	0.8	100.0	0.8
	Echinolampas	0.8	100.0	0.8
A5	Stylasteridae incertae	100.0	63.4	63.4
	Epialtidae	2.9	100.0	2.9
A6	Scleractinia solitary	100.0	44.5	44.5
	Scleractinia colonial	14.9	83.5	12.4
	Heterobrissus	7.4	60.6	4.5
	Oxypleurodon	1.1	100.0	1.1
A7	Zoanthidae	100.0	95.3	95.3
A8	Alcyonacea	87.9	24.5	21.6
	Comatulida	48.5	23.2	11.3
	Hydrozoa	1.5	27.9	0.4
A9	Ophiuroidea	100.0	75.0	75.0
A10	Antipatharia	80.0	37.2	29.7
	Annelida	38.3	34.8	13.4
	Javania sp.	30.0	42.4	12.7
	Solasteridae	3.3	75.3	2.5
A11	*Micropyga* sp1	77.8	32.4	25.2
	Goniasteridae	41.7	24.1	10.0
	Parthenopidae	11.1	19.6	2.2

A12	Lophiiformes	75.0	41.7	31.3
	Scorpaeniformes	75.0	53.3	40.0
A13	Actiniaria	97.1	22.2	21.6
	Squaliformes	5.7	5.5	0.3
	Synodontidae	14.3	33.4	4.8
	Myctophiformes	5.7	49.3	2.8
A14	*Stereocidaris*	91.3	37.0	33.8
	Bivalvia	30.4	22.4	6.8
A15	Beryciformes	100.0	83.9	83.9
A16	Holothuroidea	100.0	24.1	24.1
	Hymenodora	3.6	100.0	3.6
A17	*Aspidodiadema*	100.0	97.2	97.2
A18	Pennatulacea	100.0	36.2	36.2
A19	Ophidiiformes	69.2	57.1	39.6
	Goneplacoidea	46.2	52.6	24.3
	Mathildellidae	7.7	22.8	1.8
	Ophidiasteridae Fam. incertae	7.7	100.0	7.7
A20	*Stylocidaris*	100.0	45.1	45.1
A21	*Munida*	100.0	66.5	66.5
A22	Perciformes	100.0	47.7	47.7
	Myxasteridae	10.0	88.0	8.8
A23	Zoantharia	100.0	84.1	84.1
	Homolidae	9.1	71.7	6.5
A24	*Glyphocrangon*	100.0	49.5	49.5
A25	Xenophoridae	100.0	76.0	76.0
A26	*Polymixia*	100.0	88.0	88.0
A27	*Nepanthia*	100.0	85.4	85.4
	Asterinidae	20.0	85.2	17.0
A28	Peduncled Crinoidea	70.0	82.1	57.5
	Aulopiformes	60.0	80.7	48.4
	Umbellula	20.0	65.1	13.0
	Laganidae	10.0	87.0	8.7
A29	*Agononida*	100.0	70.7	70.7
A30	Gadiformes	100.0	88.3	88.3
	Cyrtomaia	22.2	100.0	22.2
A31	*Caenopedina pulchella* sp. incertae	100.0	78.1	78.1
A32	*Sympagurus* sp1	100.0	87.8	87.8
A33	Echinasteridae	100.0	75.1	75.1
	Astropectinidae	33.3	75.6	25.2
A34	*Aristeus*	83.3	70.8	59.0
	Haliporoides	33.3	93.8	31.3
A35	*Plesionika*	100.0	97.3	97.3
A36	*Aristaeopsis edwardsiana* sp. incertae	100.0	92.5	92.5
A37	Primnoidae	100.0	70.3	70.3
A38	*Nematocarcinus*	100.0	85.2	85.2
A39	Brisingida	100.0	94.2	94.2
A40	Asteroidea sp	100.0	100.0	100.0
A41	*Coronaster*	100.0	95.1	95.1
A42	*Spatangus*	100.0	98.2	98.2
A43	*Hemipenaeus*	100.0	100.0	100.0
A44	*Malthopsis*	100.0	98.2	98.2
A45	Leucosiidae	100.0	99.1	99.1

Supplementary material II.8 : Summary of the environmental variables descriptive statistics

Available online at:

https://docs.google.com/spreadsheets/d/1zdcdGFpvbOs-XefR3-Vv6pVE82V5I4KFSh7mmsWk2GI/edit?usp=sharing

Supplementary material II.9 : Comparative environmental conditions of sites using maps of the transects

Geomorphology

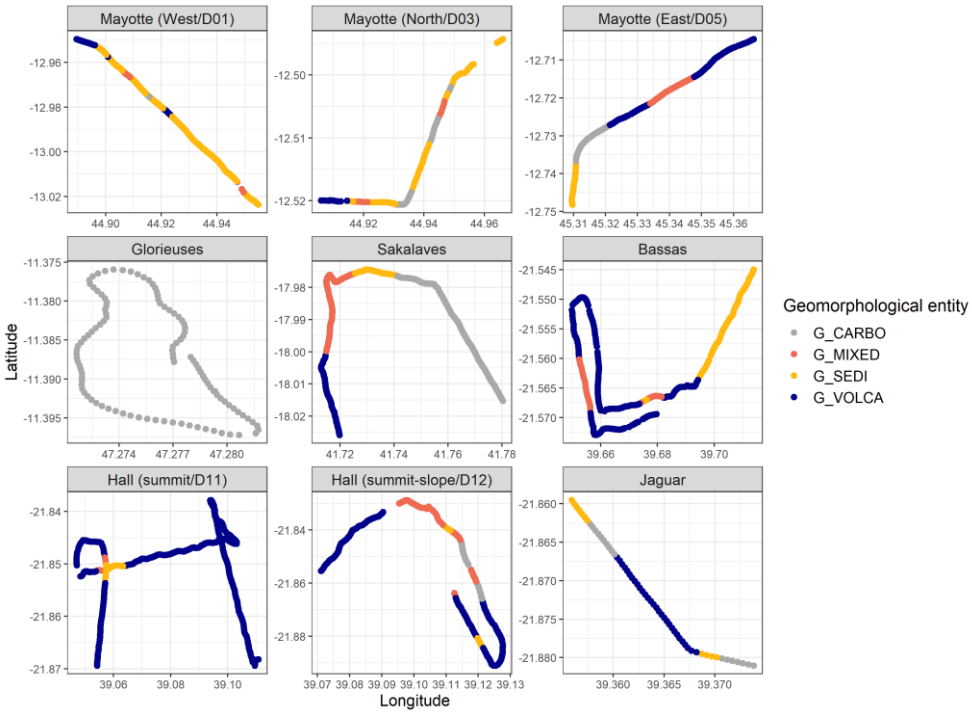

Bathymetry

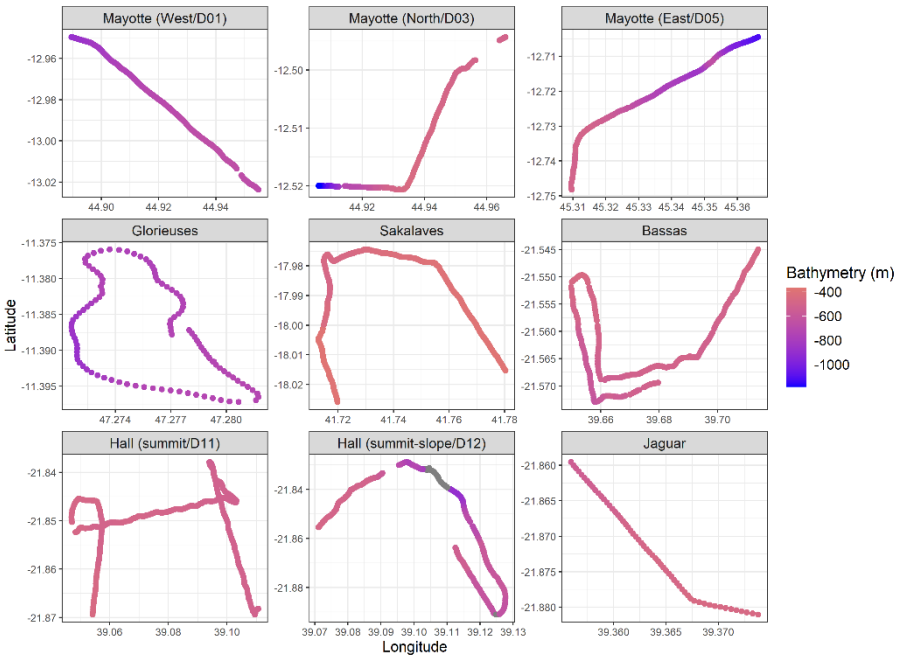

Slope

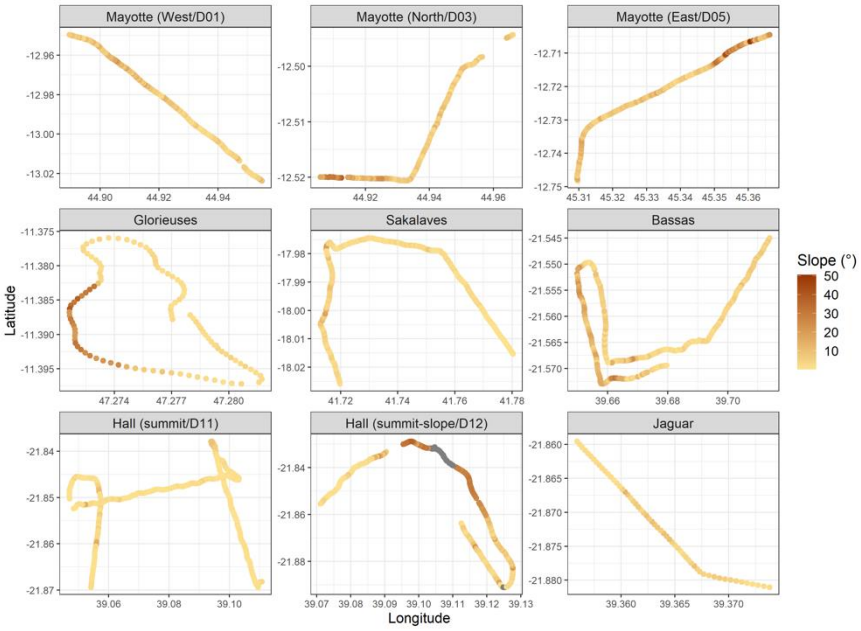

Rugosity

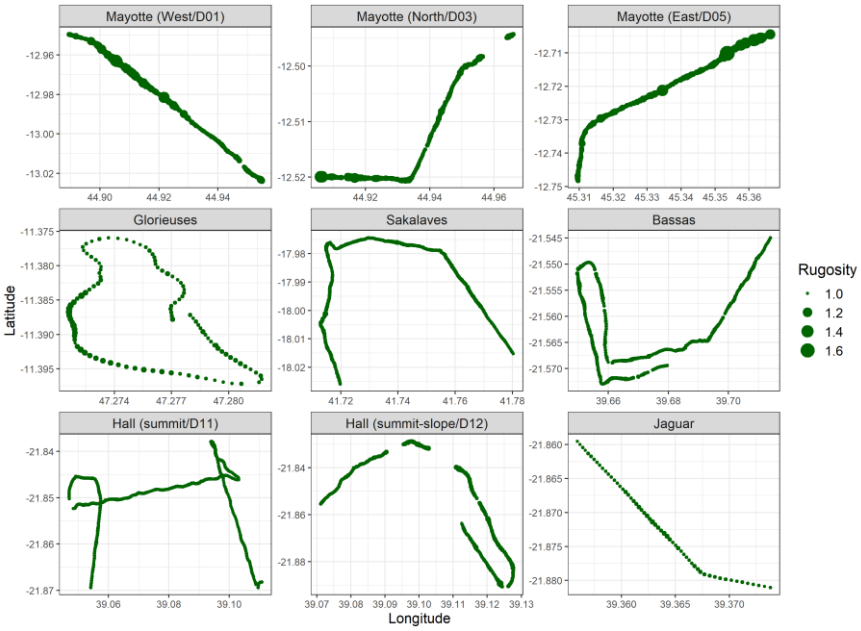

Eastness

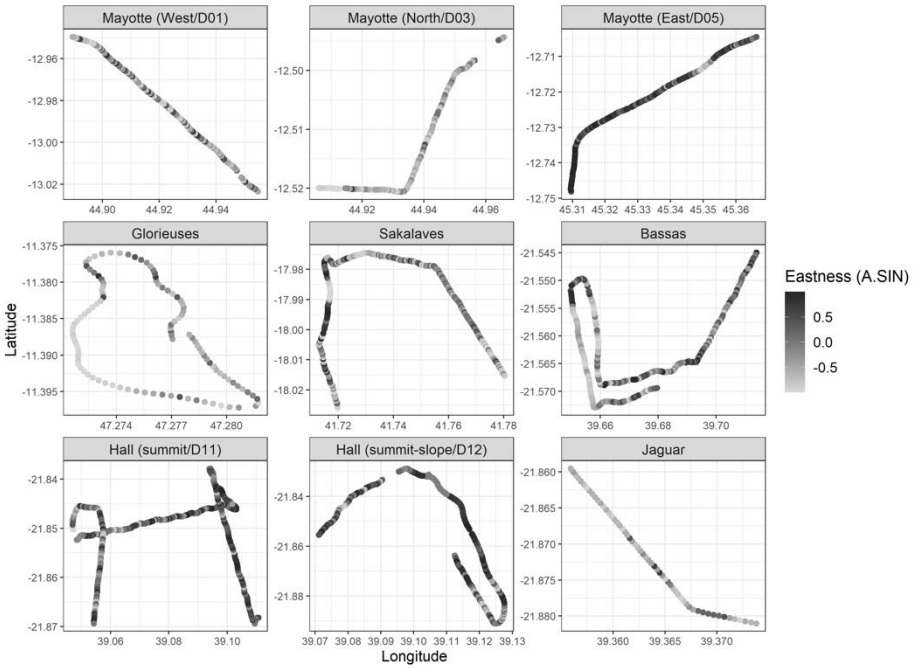

Northness

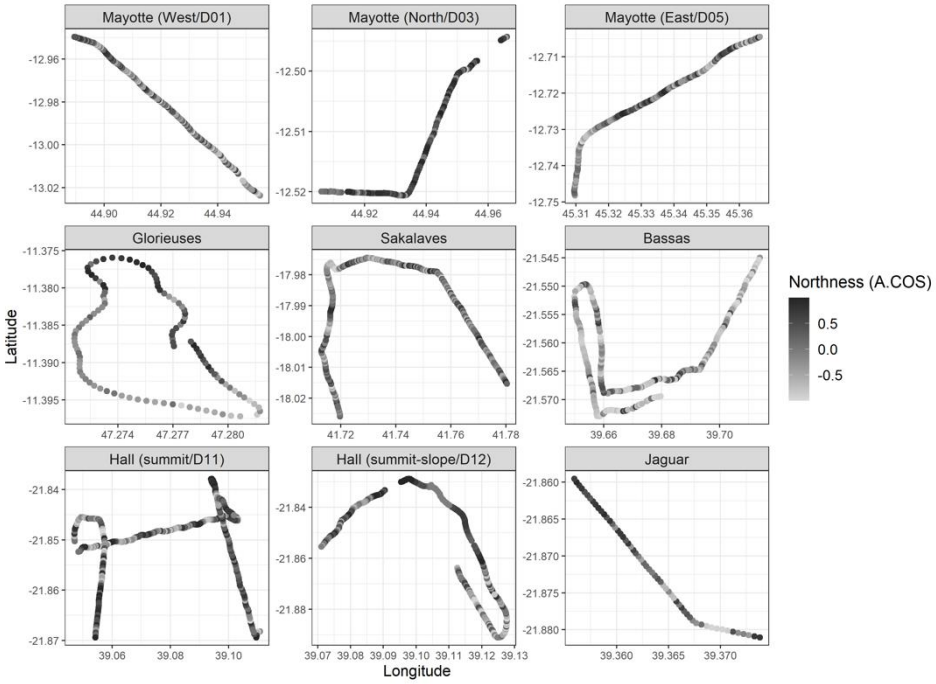

BPI 60 m

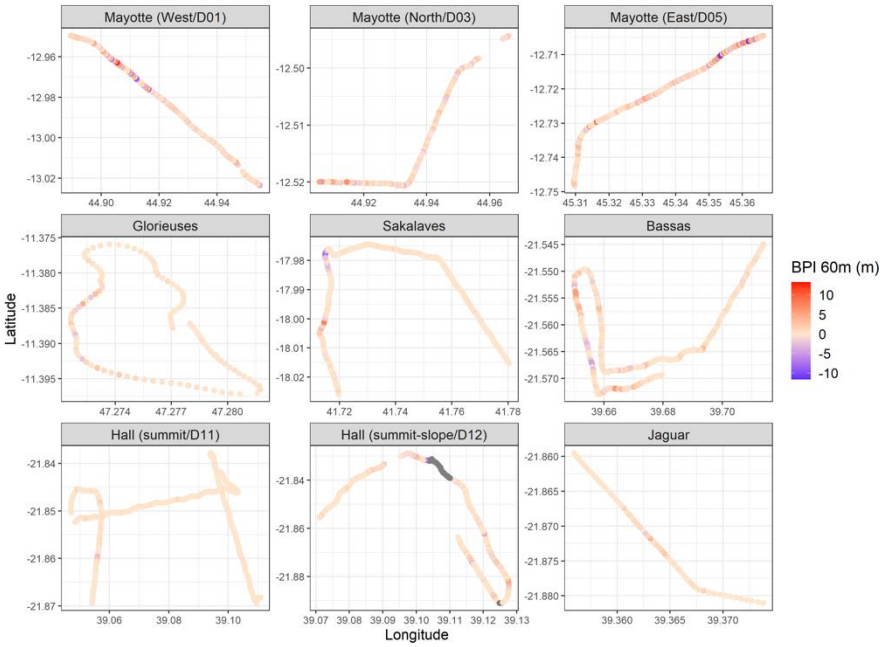

BPI 120 m

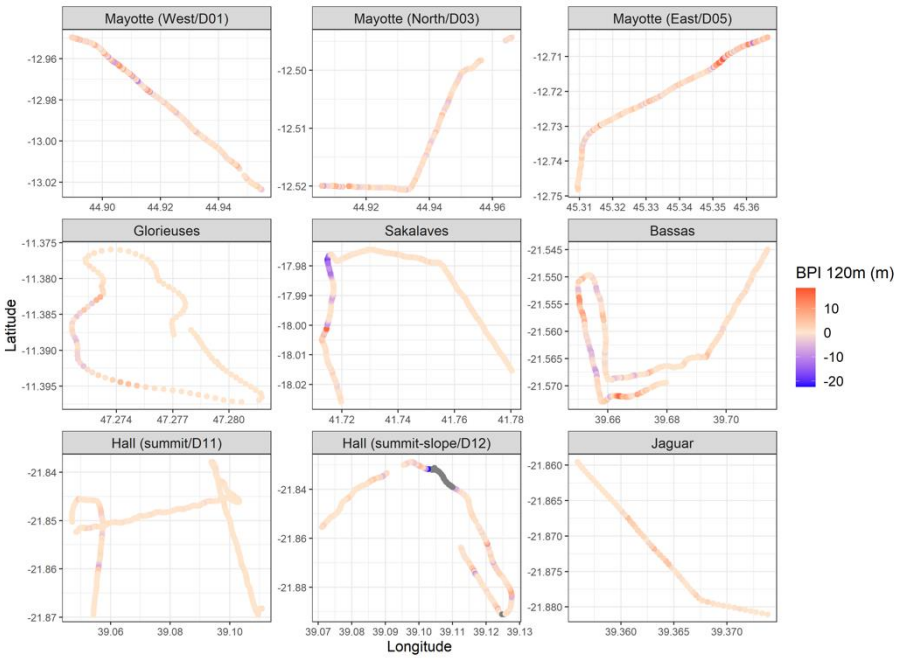

BPI 500 m

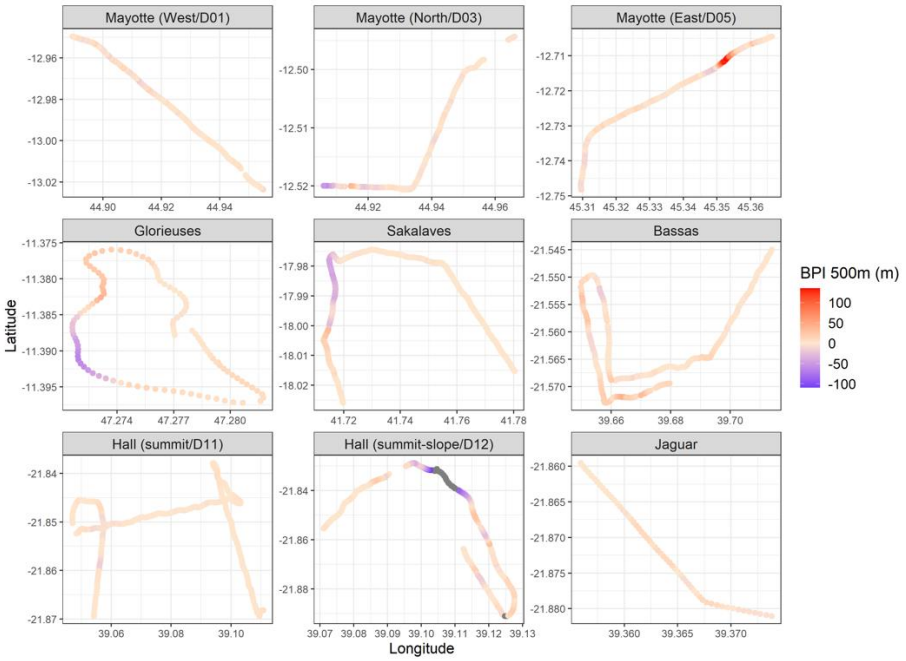

Temperature

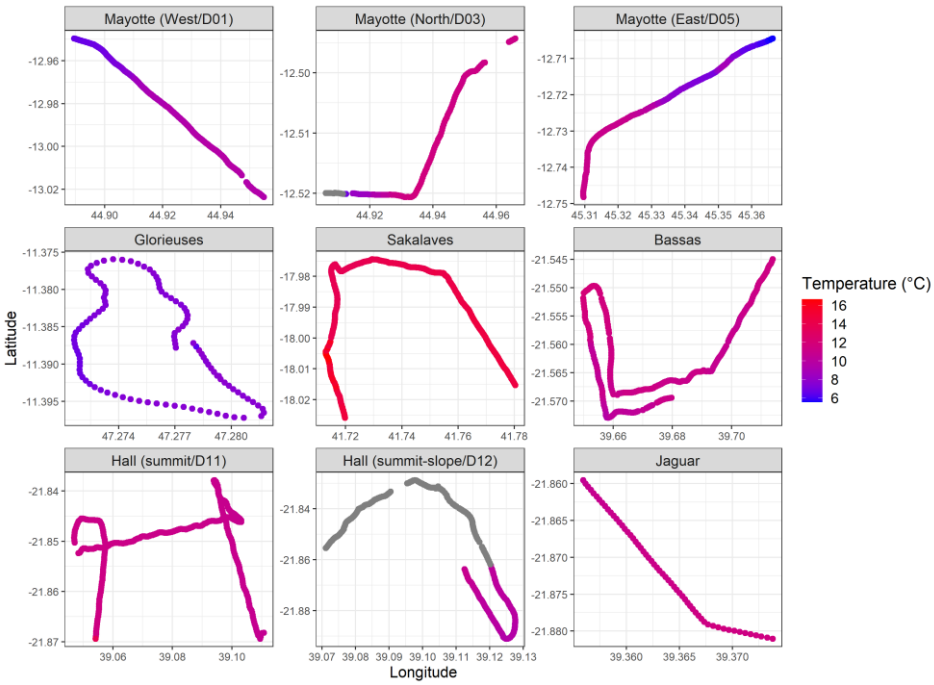

Oxygen

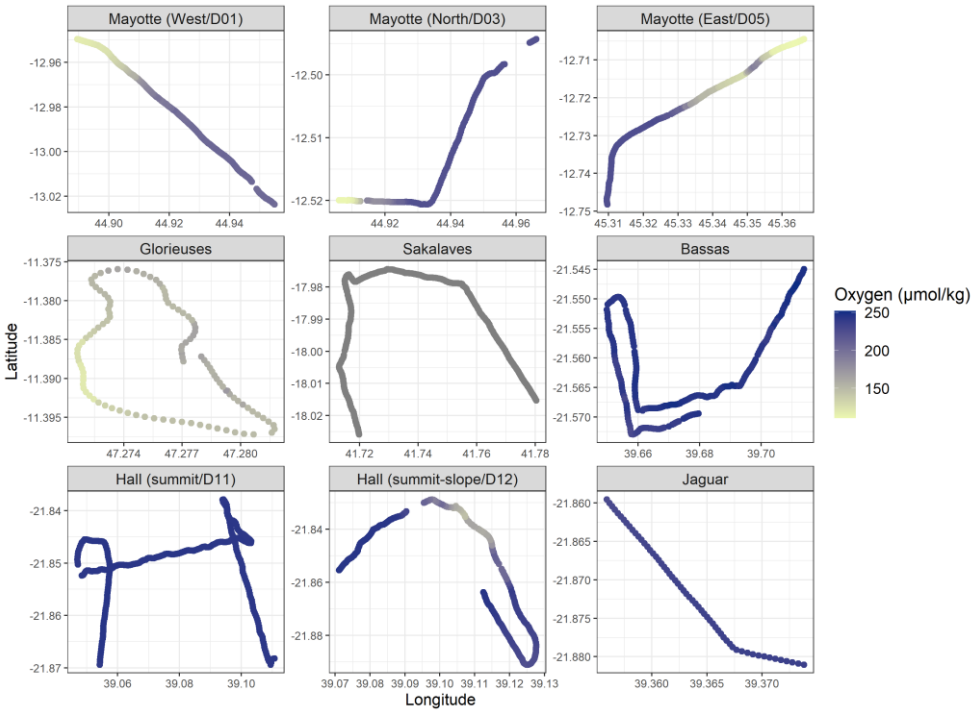

Substrate diversity

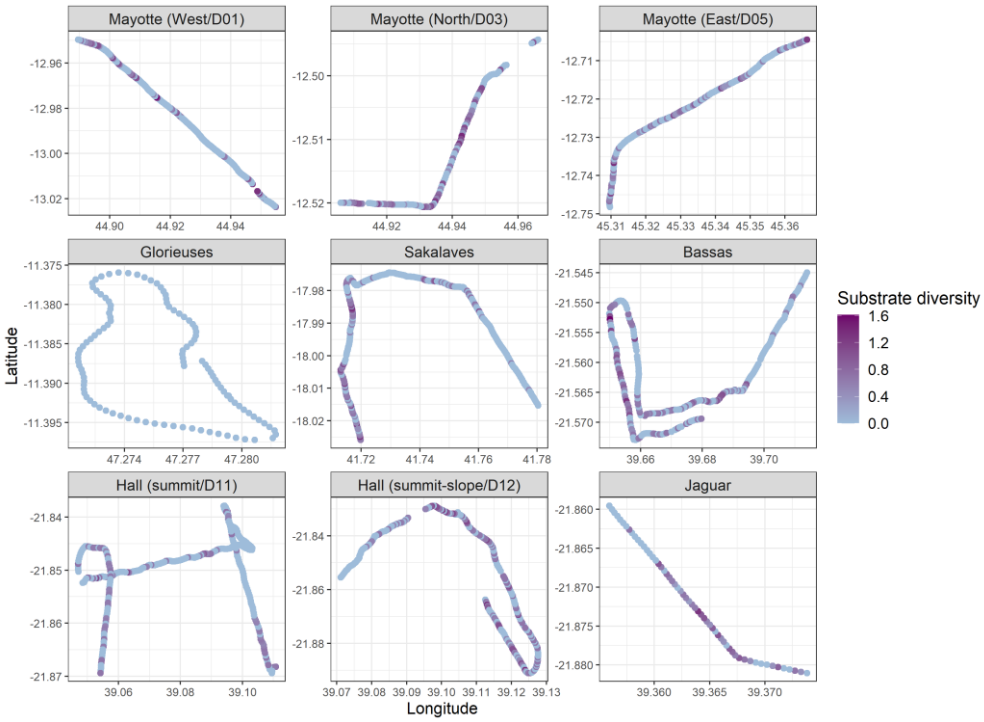

Hardness

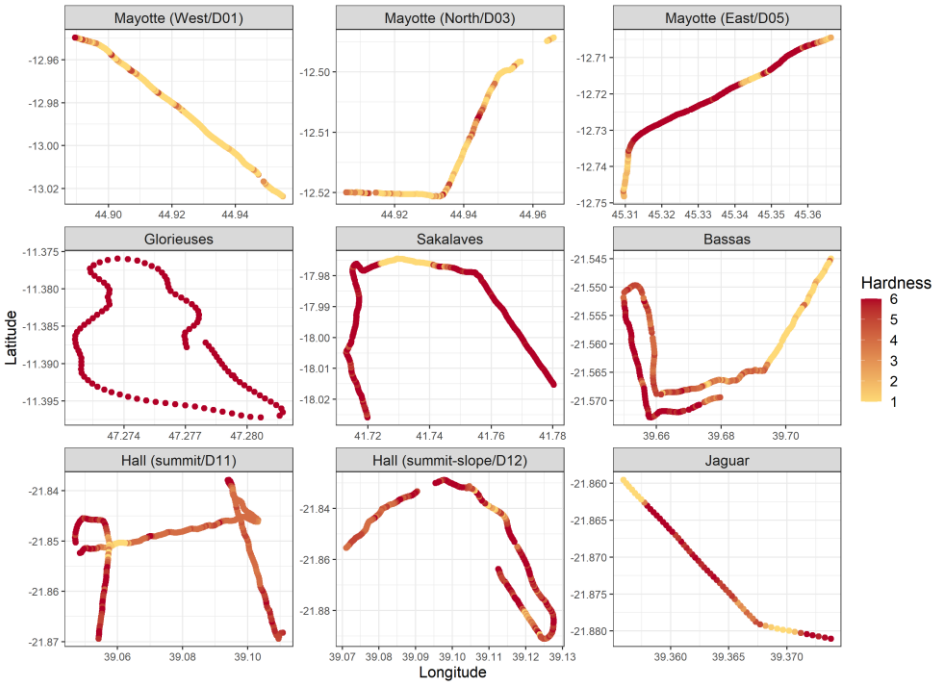
Mayotte (West/D01)
Mayotte (North/D03)
Mayotte (East/D05)
Glorieuses
Sakalaves
Bassas
Hall (summit/D11)
Hall (summit-slope/D12)
Jaguar
Latitude
Longitude
Hardness
6
5
4
3
2
1

Supplementary material II.10 : Maps of the significant large, medium and fine scale spatial patterns along the island slopes of Mayotte and Bassas da India

Mayotte West slope

Broad

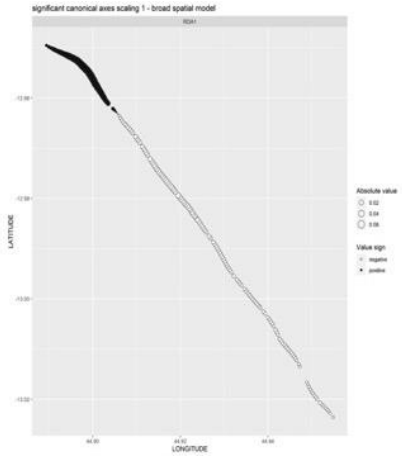

Medium

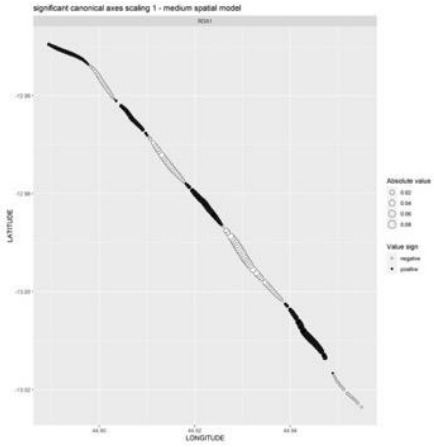

Fine

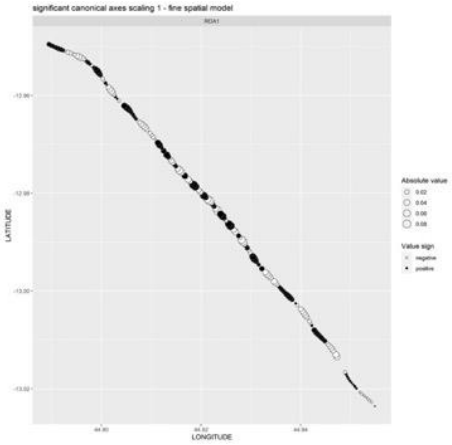

Mayotte North slope

Broad

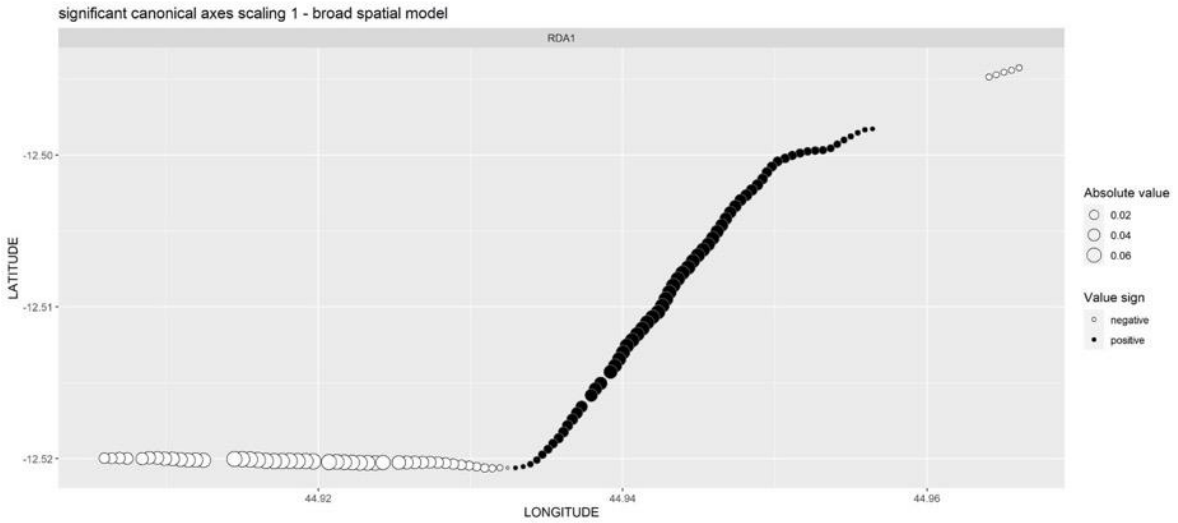

Medium

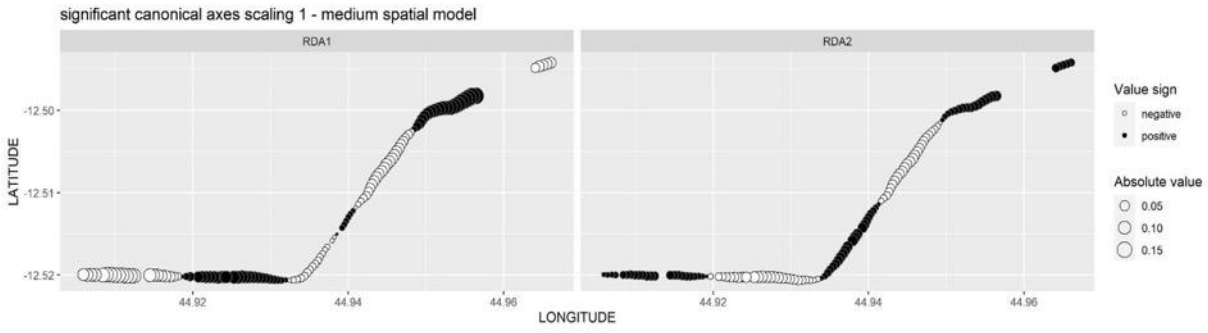

Mayotte East slope

Broad

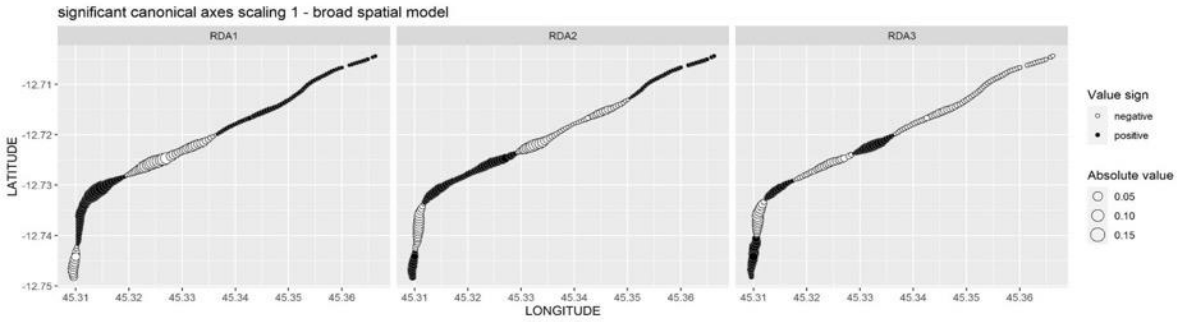

Medium

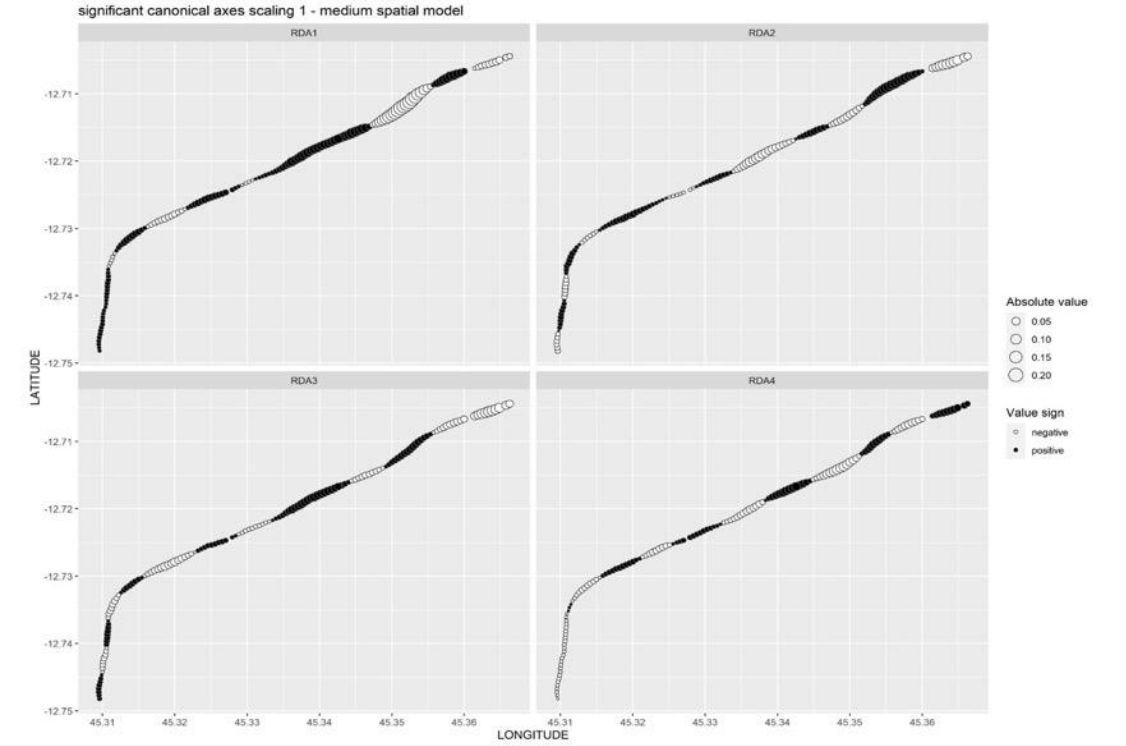

Fine

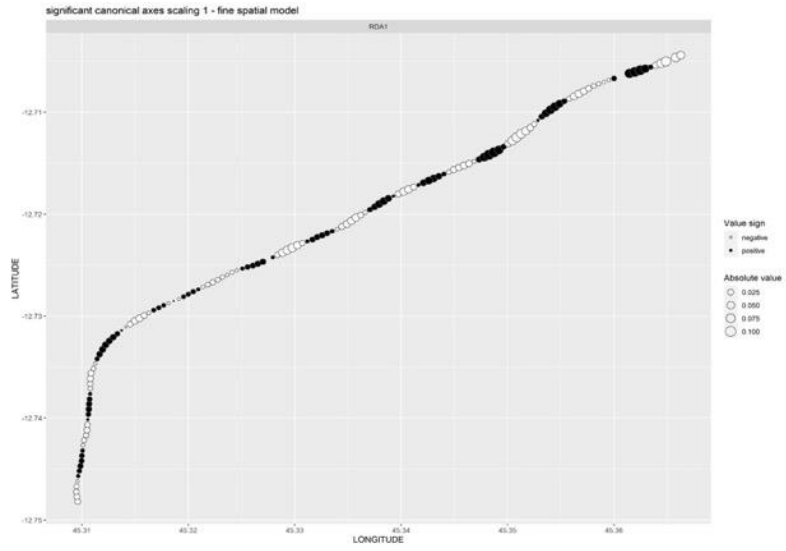

Bassas da India

Broad

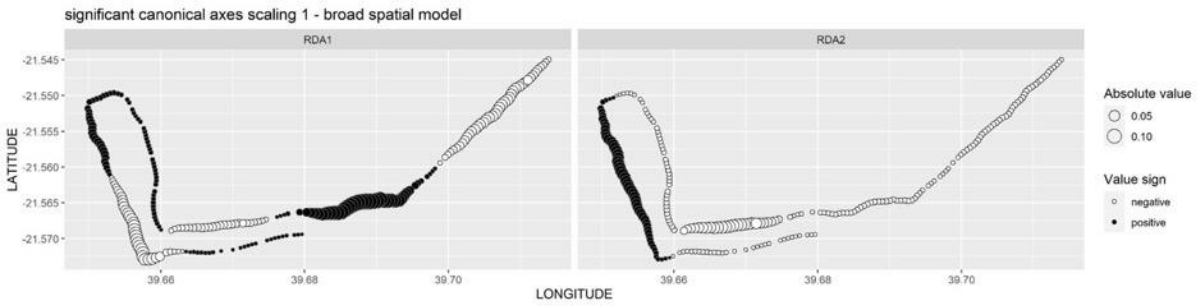

Medium

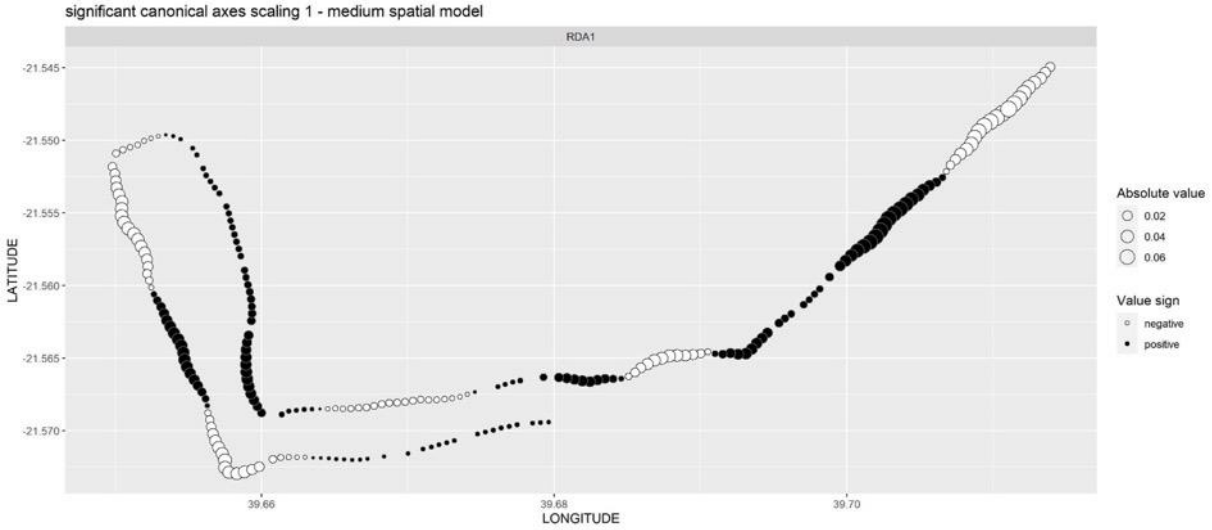

Fine

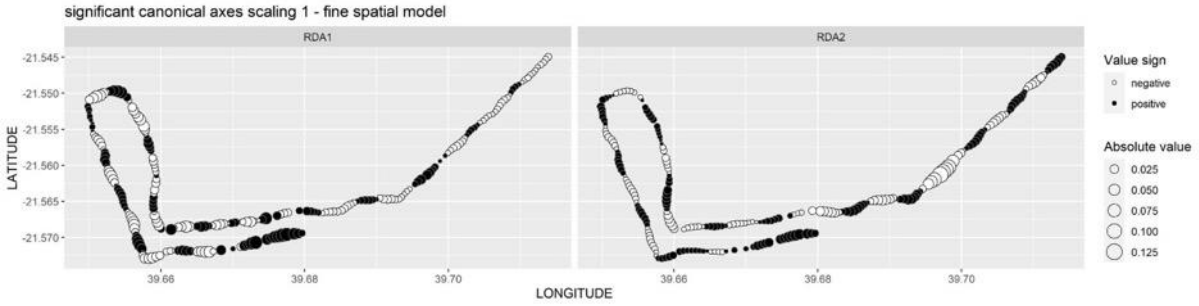

III. Caractérisation morpho-fonctionnelle des cnidaires et porifères à partir d'images *in situ* en milieux profonds

Les cnidaires (Cnidaria) et les porifères (Porifera) sont des phylums clés du fonctionnement des écosystèmes marins, par exemple en fournissant un abri, une nurserie et une source de nourriture ou en offrant des niches écologiques supplémentaires aux espèces associées. Ce sont également des taxons à croissance lente et à longue durée de vie, ce qui les rend peu résilients aux perturbations anthropiques, et sont donc utilisés comme des taxons indicateurs d'écosystèmes marins vulnérables. L'évaluation de la distribution spatiale et de la diversité de ces taxons constructeurs d'habitats repose sur des images *in situ* du fond marin, mais l'identification à partir d'images des cnidaires et des éponges au-delà des rangs classe/ordre est particulièrement difficile. En effet, ces groupes présentent une plasticité morphologique intraspécifique et une convergence de forme entre les taxons, qui sont sources de confusion taxonomique. Leur identification aux rangs taxonomiques inférieurs nécessite l'observation de caractères diagnostiques microscopiques (par exemple, les sclérites pour les coraux, les spicules pour les éponges) ou l'utilisation de marqueurs moléculaires qui ne sont pas visibles sur les images. De plus, l'identification taxonomique aux rangs supérieurs ne reflète pas leur diversité fonctionnelle. Pour surmonter ces problèmes, nous avons appliqué ici (1) une classification de ces groupes, à partir des images, qui s'appuie sur une approche multi-traits macro-morphologiques, visant à caractériser leur diversité fonctionnelle plutôt que leur diversité taxonomique. Puis nous avons construit (2) une trame d'analyse pour définir statistiquement des groupes morpho-fonctionnels basés sur ces traits. Ces groupes morpho-fonctionnels ont ensuite été utilisés comme entités (variable réponse) dans les analyses écologiques, à la place des taxons.

Nous avons appliqué cette méthodologie aux monts sous-marins et aux pentes des îles dans le canal du Mozambique, une région peu échantillonnée où la question de l'identification

taxonomique est particulièrement critique. Les données ont été analysées pour caractériser : (a) la diversité et la distribution des spongiaires et des cnidaires à différentes échelles spatiales, (b) leurs réponses aux contraintes/gradients environnementaux, (c) leurs rôles structurants sur les communautés de mégafaune associées.

Nous avons identifié 37 et 34 groupes morpho-fonctionnels (GMFs) de spongiaires et de cnidaires respectivement ; avec quatre morphologies dominantes de spongiaires, et cinq morphologies dominantes de cnidaires, qui diffèrent en densité entre les sites étudiés. Les patrons de richesse des GMFs de spongiaires et de cnidaires diffèrent entre les monts sous-marins et avec les pentes des îles. A l'exception des plateformes Glorieuses et Sakalaves pour lesquelles la diversité bêta est faible, tous les sites présentent une diversité bêta des assemblages de GMFs d'éponges intermédiaires. Dans le nord du canal, la diversité bêta des GMFs de cnidaires est élevée le long des pentes insulaires de Mayotte, alors qu'elle est faible en comparaison sur Glorieuses. Au sein de chaque mont sous-marin et pente insulaire, nous avons observé une variabilité de l'habitat biogénique à des échelles spatiales allant de 0,06 km à 3 km. Cette hétérogénéité est créée par quelques GMFs ayant une plus grande abondance, particulièrement au niveau des faciès géomorphologiques volcaniques et des zones pentues. L'hydrologie (courant, chlorophylle a), explique 26% de la structure spatiale des GMFs d'éponges le long du canal ; cependant, la topographie et le substrat sont parmi les principaux facteurs de cette structure dans la partie nord du canal (18-23%). Notre approche nous a permis de révéler une co-structuration entre certains GMFs d'éponges et de cnidaires avec les autres taxons méga-benthiques.

L'application des groupes morpho-fonctionnels à la caractérisation de la structure des communautés de spongiaires et de cnidaires le long du canal du Mozambique a souligné l'intérêt de cette approche méthodologique flexible, en particulier pour les spongiaires. Cette méthode permet explicitement de quantifier les variations morphologiques des spongiaires et des cnidaires à partir de l'imagerie en utilisant des traits qualitatifs, et d'identifier les facteurs environnementaux qui déterminent la distribution spatiale de ces traits, ainsi que de caractériser l'habitat biogénique potentiel qu'ils fournissent à d'autres organismes méga-benthiques.

Mots clés : Classification morpho-fonctionnelle, Cnidaria, Porifera, habitats biogéniques, écosystèmes marins vulnérables, traits morphologiques, analyses spatiales, analyses d'images

Ce manuscrit est en cours de préparation pour une soumission avec les auteurs suivants :

Mélissa Hanafi-Portier, Karine Olu, Paco Cardenas, Eric Pante, Sarah Samadi

A morpho-functional approach to palliate poor taxonomic resolution of cnidarians and sponges from deep-sea images: case studies from poorly sampled areas

Abstract

Cnidaria and Porifera are key phyla of marine ecosystem functioning, for example by providing shelter, nursery, and food source or by offering additional ecological niches to associated species. They are also slow-growing and long-lived taxa, making them poorly resilient to human disturbances and are therefore used as indicator taxa of Vulnerable Marine Ecosystems. Assessing the spatial and diversity patterns of these habitat-forming taxa relies on seafloor images but identification from images of cnidarians and sponges beyond class/order ranks is particularly challenging. Indeed, both morphological plasticity within species and convergence among taxa are sources of taxonomic confusion. Their identification at lower taxonomic ranks requires the observation of microscopic diagnostic characters (e.g., sclerites for corals, spicules for sponges) or the use of molecular markers that are not visible on images. Moreover, taxonomic identification at higher ranks does not reflect their functional diversity. To overcome these issues, we here applied (1) an image-based classification relying on a multiple macro-morphological traits approach aiming at characterising their functional diversity rather than their taxonomic diversity. Then we built (2) a framework for defining statistically morphological groups based on these traits. These morpho-functional groups were then used as entities (response variable) in ecological analyses, instead of taxa.

We applied this methodology to seamounts and island slopes in the Mozambique Channel, a poorly sampled region where the taxonomic identification issue is particularly critical. The data were analysed to characterise: (a) sponges and cnidarians diversity and distribution patterns at various spatial scales, (b) their responses to environmental constraints/gradients, (c) their structuring roles on associated megafaunal communities.

We identified 37 and 34 morpho-functional groups (MFGs) of sponges and cnidarians respectively; with four dominant sponge morphologies, and five dominant cnidarians

morphologies, which differ in densities between the surveyed sites. Patterns of sponges and cnidarian MFGs richness differ between seamounts and with island slopes. Intermediate beta diversity of sponge MFG assemblages characterised all the site except for Glorieuses and Sakalaves platforms for which the beta diversity is low. In the northern channel, the beta diversity of cnidarian MFGs was high along Mayotte island slopes, while low in comparison at Glorieuses archipelago. Within each seamount and island slope, we observed variability of the biogenic habitat at small (0.06 km) to large (~3 km) spatial scales. This heterogeneity is created by a few MFGs displaying higher abundance particularly over volcanic geomorphological features and sloping areas. Hydrology (current, chlorophyll a), explains 26% of the sponge MFGs spatial structure along the channel; however, topography and substrate are among the main drivers of this structure in the northern part of the channel (18-23%). Our approach allowed us to reveal co-structuring between some sponge and cnidarian MFGs with the other megabenthic taxa.

Application of morpho-functional groups to characterised sponges and cnidarians community structure along the Mozambique Channel outlined the interest of this flexible methodological approach, particularly for sponges. This method explicitly allows quantification of the sponges and cnidarians morphological variations from imagery using qualitative traits, to identify the environmental drivers shaping the spatial distribution of these traits, and also to characterised the potential biogenic habitat they provide for other megabenthic organisms.

Keywords: Morpho-functional classification, Cnidaria, Porifera, habitat-forming taxa, vulnerable marine ecosystems, morphological traits, spatial analyses, image analyses

III.1 Introduction

In marine benthic environments, sessile, filter-feeding organisms may form large aggregations in which are found a flock of associated species. These structures are described as animal forest because they are functionally similar to the terrestrial forests (Rossi and Bramanti, 2020).

Among such benthic organisms, poriferans and cnidarians can form large structures (> 3 m), which provide shelter space, nurseries for other species but also contribute in regulating biogeochemical/nutrient cycles or providing medicine molecules (Bell, 2008; Rossi et al., 2017). Furthermore, through their three-dimensional structure, these habitat-forming taxa contribute to increase the degree of habitat complexity, which supports high levels of diversity of the associated community (Beazley et al., 2013; Bell, 2008; Hawkes et al., 2019; Quattrini et al., 2012; Rogers et al., 2014). Their 3D structure also interacts with currents and locally modulates the current regime, creating turbulence and resuspension retaining food particles or preys for associated fauna (Buhl-Mortensen et al., 2010).

Despite the recognized functional importance of the marine animal forests, there is still a gap in knowledge of their biodiversity pattern, and of the environmental drivers shaping their spatial structure notably in the deep sea, mainly due to the difficulty of exploration at such depth.

In deep-sea environments, seamounts are places where coral gardens and sponges grounds are found. These seamounts are also areas for industrial fishing and deep-sea mining of the rare metals (e.g., cobalt-rich crust) that cover their surface (Hein et al., 2010). Such activities can have adverse consequences – razing activities, smothering – on the benthic suspension feeder communities that commonly occur over these topographic features (Baco et al., 2020; Morgan and Baco, 2021). Sponges and cnidarians living in the deep sea are slow-growing and long-lived taxa, making them poorly resilient to human disturbances and are therefore defined as indicator taxa of Vulnerable Marine Ecosystems (VME) (FAO, 2009; Watling and Auster, 2021; Williams et al., 2020a). However, few is known regarding the factors that explain VME distribution and how they structure the diversity of the associated fauna. The analysis of their role in the structure of deep-sea communities requires deployment of submarine imaging

systems but a major source of difficulty remains the taxonomic identification of these taxa from images.

Indeed, identification of cnidarians and sponges from bottom images is hardly achievable beyond the class level, because the diagnostic criteria can be assessed mainly at the microscopic level (e.g., sclerites for cnidarians, spicules for sponges) (Barnes and Bell, 2002; Pante et al., 2012b). Given this limitation, many studies in image-based ecology use any observable features on images (such as colour or global shape) to define morphotypes outside the formal framework of taxonomy. Such approaches make it difficult to compare data between regions and studies. Other studies (cf. chapitre 2) tentatively identified these taxa at higher ranks (e.g., class or order), but these identifications do not reflect the three-dimensional complexity observable on images.

For these taxa, morphology is highly variable both at high taxonomic levels and at the intraspecific one, and both at macro and microscopic scales (Bell, 2007; Todd, 2008). This variability leads to intraspecific polymorphism (explained notably by phenotypic plasticity) and to morphological convergences among distant species. Consequently, the use of morphotypes to approximate taxonomic diversity is questionable (Krell, 2004). While some studies revealed a positive correlation between morphological and taxonomic diversity (Bell and Barnes, 2001; Hadi et al., 2015), there is no consensus regarding these relations (Bell, 2007). Therefore, taxonomic identification of these groups from images is a limiting and poorly robust approach to study the functional role of sponges and cnidarians in benthic communities.

Thus, to study the functional role of these habitat-forming taxa in benthic communities, many authors suggested to analyse directly the morphologies to determine how it varies in response to the environmental factors (Buhl-Mortensen et al., 2010; Denis et al., 2017; Mary George et al., 2018; Schönberg, 2021; Zawada et al., 2019b, 2019a) and how their variabilities explain the structure of the associated fauna.

Studies have notably revealed variability of the morphology of these sessile fauna in response to a range of environmental parameters, including light and sedimentation (Chappell, 1980), hydrodynamic (Barnes and Bell, 2002; Bell and Barnes, 2000; Chappell, 1980; McDonald et al.,

2002; Pronzato et al., 1998), depth (Barnes and Bell, 2002; Bell and Barnes, 2000), or substrate (Barnes and Bell, 2002).

In addition, these taxa play many structuring roles on benthic communities through their size, flexibility and 3D structure that are positively correlated to the diversity of associated species and influence, directly or indirectly, the fitness of the communities they support, by offering a variety of local environmental conditions (supply and storage of organic matter in interstices, shelter from currents, breeding area, attachment support, etc.) (Buhl-Mortensen et al., 2010).

To assess how their architectural structure plays a role in the structure of associated fauna, Buhl-Mortensen et al. (2010) suggested the use of descriptors such as size, complexity (surface/volume), branching patterns or flexibility of biotic structures.

Such approaches, based on multiple traits quantifying the morphological diversity and structural complexity of coral habitats, were for example recently used to understand how coral reefs respond to anthropogenic activity (Zawada et al., 2019b) and to a bleaching event (Denis et al., 2017). Furthermore, owing to the difficulty in identifying sponges in the images and the need to characterise the structure of these communities, Schönberg (2021) has recently developed a standard classification to characterise sponges based on their functional morphologies rather than their taxonomic identities, adapted in particular to the use of images. This classification uses the CATAMI standards (Althaus et al., 2015), which is another classification scheme proposing a mix between morphological and taxonomic classification to identify morphotypes for different taxonomic groups (e.g., cnidarians). In addition, Untiedt et al. (2021) conducted a comparative study on the spatial diversity patterns of antipatharians and octocorals using five classifications based on taxonomy, morphology, and at varying resolutions.

We recently used image data from towed camera transects to characterise the spatial variability of the whole megafauna community from the summits and upper slopes of four seamounts and island slopes of Mayotte and Bassas da India in the Mozambique Channel (Hanafi-Portier et al. in prep.). The levels of identification reached for porifera and cnidaria in this study were respectively the class and the order levels. These levels of identification revealed patterns of variability at various spatial scales that were partly explained by environmental factors. Given the morphological variability observed at these taxonomic

ranks, we hypothesise that this analysis does not fully address the functional response of these groups to the high environmental heterogeneity evidenced in the studied area nor their structuring role on other organisms for which they create a habitat. We therefore used the same dataset of images to characterise the morphological variability of these organisms in order to analyse firstly, how it responds to environmental factors and secondly, how it contributes to explain the structure of the communities of other organisms.

Here, we intended to propose a classification of sponges adapted to our dataset, based on existing classification (Althaus et al., 2015; Schönberg, 2021), less hierarchical and using additional traits. We also created one for the cnidarians observed on images using a multi-traits approach, and integrating additional features (size, accessory structures, polyp size, etc.). Both for sponges and cnidarians, our method does integrate any taxonomic identification.

Our approach is to **(1)** define morphotypes based on unique combination of traits' modalities as a primary step, **(2)** group them into morpho-functional units (Tsakalos et al., 2019) and **(3)** apply community analysis on these morpho-functional units instead of taxonomic entities.

By using this methodology, we aimed to assess **(1)** sponges and cnidarians diversity from qualitative morpho-traits descriptors and distribution patterns at multiple spatial scales, **(2)** their responses to environmental constraints, **(3)** their structuring roles on the associated megafaunal communities.

Using this renewed approach, our study thus aims at exploring how abiotic factors drive the morphological diversity and density of sponge and cnidarians assemblages and how the communities of this habitat-forming animals structure the associated megafauna in the western Indian Ocean, where only one study suggests that substrate and current regime heterogeneity are key determinants of morphological diversity in sponge assemblages (Barnes and Bell, 2002).

III.2 Materials and methods

III.2.1 Study area and field acquisition

The data were obtained in the scope of the PAMELA project (Bourillet et al., 2013) during the campaigns PAMELA MOZ01 (Olu, 2014) on board the research vessel (R/V) *L'Atalante* and

PAMELA MOZ04 (Jouet and Deville, 2015) on board the R/V *Le pourquoi Pas ?.* These cruises allowed the exploration of four seamounts (Glorieuses, Sakalaves platform, Jaguar and Hall Banks) and the terrace of an island slope of Bassas da India (**Figure III.1**).

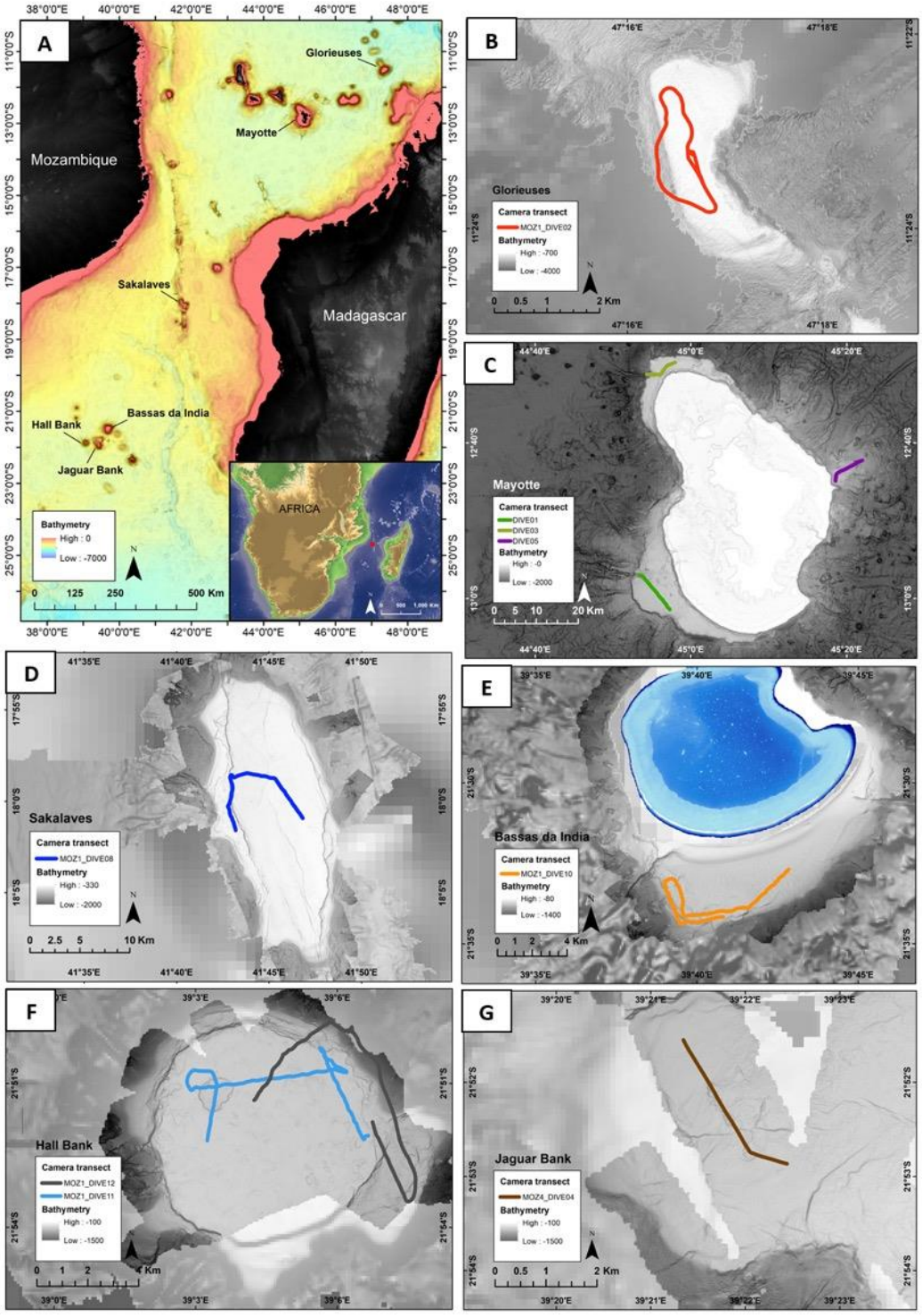

Figure III.1 : (A) Map of the Mozambique Channel locating the different seamounts and islands explored, and specific map of each towed camera transect on seamounts and island slopes: (B) Glorieuses, (C) Mayotte Island slopes, (D) Sakalaves platform, (E) Bassas da India, (F) Hall Bank, (G) Jaguar Bank

The data were also obtained on three outer slopes (East, North, and West) of Mayotte Island, during the BIOMAGLO campaign (Corbari et al., 2017) on board the R/V *L'Antea* (**Figure III.1**).

Images were captured at each site from transects of a towed camera (SCAMPI, French IFREMER fleet), in a vertical position at intervals of 30 s (except for Glorieuses, about 15 s), at 2.5-3 m altitudes and a speed of 0.5 m/s with a NIKON D700 HD camera (focal length 18 mm, resolution 4 256 × 2 832 pixels).

A total of nine camera transects were processed for this study (**Table III.1**). For cnidarians classification, we considered only images dataset from Glorieuses and the three outer slopes of Mayotte (four transects), while for sponges, we considered all the nine transects. The images were georeferenced via the vessel positioning system processed with the ADELIE application (French oceanographic fleet) developed at IFREMER and implemented using ArcGiS V10.3 software.

Table III.1 : Summary of sampling effort, location and depth for the nine towed camera transects

Cruise	Site	Morphology	Camera transect code	Depth (m) (min-max)	Number of images	Distance covered (km)	Latitude (start-end transect)	Longitude (start-end transect)
Biomaglo	Mayotte, West slope	Island slope (terrace)	DIVE01	654-888	900	11	-13.02/-12.95	44.95/44.89
	Mayotte, North slope	Island slope (terrace)	DIVE03	449-1183	1101	8	-12.49/-12.52	44.97/44.90
	Mayotte, East slope	Island slope	DIVE05	492-1117	938	8.5	-12.75/-12.70	45.30/45.37
Pamela moz01	Glorieuses	Carbonate platform	MOZ1 DIVE02	724-883	1155	6	-11.39/-11.38	47.28/42.28
	Sakalaves platform	Platform and escarpment	MOZ1 DIVE08	368-482	1251	15	-18.02/-18.01	41.72/41.78
	Bassas da India	Island slope (terrace and upper slope)	MOZ1 DIVE10	453-623	1123	14	-21.54/-21.57	39.71/39.68
	Hall (summit)	Bank summit	MOZ1 DIVE11	456-540	1170	16	-21.87/-21.85	39.05/39.07
	Hall (summit-slope)	Bank summit, terrace upper slope	MOZ1 DIVE12	480-903	1050	16	-21.86/-21.86	39.11/39.07
Pamela moz04	Jaguar	Bank summit	MOZ4 DIVE04	456-549	926	3	-21.88/-21.86	39.37/39.36

High resolution bathymetry and acoustic reflectivity data were acquired with a multibeam echosounder (Kongsberg EM122 for the deepest areas and EM710 for the shallowest areas) (Audru et al., 2006; Courgeon et al., 2016). In addition, CTD (Temperature, Salinity) and oxygen data were acquired during the SCAMPI dives from CTD and optode (microcat) sensors mounted on the camera frame.

More specifics on the study area and field acquisition are available in the Materials and Methods section in Hanafi-Portier et al., in prep. (cf. chapitre 2).

III.2.2 Image and environmental data processing

III.2.2.1 Megabenthic community dataset

We annotated and identified a total of 99 taxa on a total of 9614 images, using BIIGLE 2.0, a web-based image annotation platform (Langenkämper et al., 2017).

Details of the method for identifying megafauna in images are described in Hanafi-Portier et al. (2021) (cf. chapitre 1), and details of the conserved identification ranks and the final megabenthic community dataset are described in the Materials and Methods section in Hanafi-Portier et al., in prep. (cf. chapitre 2). The final dataset comprise different identification ranks according to the taxonomic group, from high rank (phylum, class, order; e.g., brachiopods, gastropods, annelids, sponges, cnidarians, fishes) to final taxonomic ranks (genus, morphospecies/species) for echinoids, decapods, asteroids, and some fishes.

Fauna densities were standardised in 200 m^2 (~60 m linear) sample units, to capture sufficient fauna density while conserving scale of habitat heterogeneity.

III.2.2.2 Morphotype annotation

We used the set of images in which cnidarians and sponges have been identified, to the best identification rank achievable from images. We then classified the sponges and cnidarians into morphotypes, according to criteria observable in the images: general shape, shared structure (e.g., long spicule giving a hairy appearance), and color. Each morphotype was then assigned to a size category (small, medium, large). In some cases, the morphotypes corresponded to taxa identified at lower taxonomic ranks (e.g., genera, *Umbellula*, *Bathyalcyon*, *Enallopsammia* for cnidarians; *Aphrocallistes* for sponges; families, Primnoidae for cnidarians; Euplectellidae, Hyalonematidae for sponges). For these taxa, the identification at low rank was indeed possible because they correspond to unique morphologies, easily recognizable from images. Conversely, most of the taxonomic identifications, achieved at the order (cnidarians) and class (sponges) ranks, were divided into several morphotypes.

The classification of the morphotypes was facilitated by the use of the BIIGLE *Largo tool*, which allows us to visualise the already classified morphotypes in the form of an image catalogue.

We therefore referred to this catalogue to classify the remaining images. Unclassifiable morphologies and too blurry images were discarded from the analyses.

III.2.2.3 Environmental dataset

Specifics on the environmental data processing and dataset are available in the Materials and Methods section in Hanafi-Portier et al., in prep. (cf. chapitre 2). We considered hydrological parameters (current over three depth layer, Chlorophyll a concentration); high resolution bathymetry (Digital Terrain Model – DTM, 10 m for the PAMELA project (Charline Guérin, IFREMER engineer); 20 m for Mayotte (Audru et al., 2006; SHOM data) from which we calculated seafloor variables (topography) (i.e., Bottom position index – BPI at fine (30, 60, 90 m) and large (120, 250, 500 m) scales; longitudinal, transverse and total curvature; aspect converted to eastness and northness (bounded between -1 and 1) from the cosine and sine of the aspect angle; bottom roughness using an Arc Chord method; slope. We also classified four geomorphological classes (volcanic, carbonate, sedimentary, mixed) and quantified substrate composition, diversity and hardness (ranging from 1 to 6) (**Table III.2**).

Environmental variables were aggregated in 200 m^2 sampling units (polygon) using R.

III.2.3 Morphological traits selection and definition

The morphotypes were then described through a set of morphological traits. For the cnidarians, our selection of traits is notably based on the classification scheme for scoring marine biota and substrata in underwater imagery (CATAMI), by Althaus et al. (2014). This catalogue proposes a morphological classification of cnidarians using a combination of high identification ranks (e.g., Scleractiniaria, Octocorals and Antipatharia) with morphological categories, and is particularly relevant to characterise elements such as robustness (Fleshy/Hard), complexity (single or multiple axis) and to standardise different morphological categories with a unique CAAB – Codes for Australian Aquatic Biota – number. We have declined some of the proposed morphological categories into unique traits. For example, in the CATAMI, the category “CAAB 11 168906” corresponds to Black & Octocorals > Branching (3D) > Non-fleshy > Bottle-brush > Simple (axe). Here, we declined a unique pathway into a set of different combination of traits: e.g., morphological trait (e.g., bottle-brush), the presence of branches (in the CATAMI “Branching (3D)”), the dimension (2D/3D), the skeleton flexibility (in the CATAMI Fleshy/Non-fleshy that here we declined in four sub-categories

Fleshy/Semi-fleshy/Semi-rigid/Rigid), and the number of axes (in the CATAMI, Single/Complex, that we declined into Single/Multiple/No main axis).

Table III.2 : Summary of the environmental variables originally used for the analyses. Variables in bold are those conserved for the analyses after removal of collinearities. All the variables were averaged in 200 m^2 polygons

Parameters	Variables	Abbreviation for the variables conserved after removal of collinearities	Resolution and description
Current	Current velocity 0-50 m Current velocity 50-200 m **Current velocity 350-650 m**	/ / **SP 350.650**	Average current velocity form daily output over 1993-2014 at 4.4 x 4.4 km resolution
	Current variability 0-50 m Current variability 50-200 m **Current variability 350-650 m**	**STD 0.50** / **STD 350.650**	Standard deviation of current velocity from daily output over 1993-2014 at 4.4 x 4.4 km resolution
Chlorophyll a concentration (Chla)	**Winter Chla** Summer Chla Minimum Chla Maximum Chla **Inter-annual Chla variability** Intra-annual Chla variability	**CHLA.WIN** / / / **CHLA.y.sd** /	Monthly satellite data of daily mean surface Chla at 4 x 4 km resolution
Water parameters	Temperature Salinity Oxygen	/ / /	Bottom temperature, salinity and oxygen captured along dive transect (optode, CTD)
Spatial	**Latitude** **Longitude**	**LAT** **LONG**	/
	Distance to Madagascar coast Distance to Madagascar coast Distance to the closest shore	DIST.MAL DIST.MOZ DIST.SHORT	/
Bathymetry	**Bathymetry**	**BATHY**	Bathymetry calculated from digital terrain model at 10 m resolution (Glorieuses, Sakalaves, Jaguar, Hall, Bassas) and at 20 m resolution (Mayotte)
Seafloor variables	Bottom position index (BPI) at: **60 m** 90 m **120 m** 250 m **500 m**	 **BPI60** / **BPI120** / **BPI500**	BPI is an indicator of the relative position of a cell to the surrounding seafloor (positive, negative relief), calculated from depth at 10 m resolution (Glorieuses, Sakalaves, Jaguar, Hall, Bassas) and at 20 m resolution (Mayotte).
	Longitudinal (profile) curvature **Transverse (plan) curvature** Total curvature	**CURV.L** **CURV.T** /	Indication of deceleration/acceleration and convergence/divergence processes of the current. Longitudinal curvature is parallel to slope, transverse curvature is perpendicular to slope. Calculated from 3 x 3 grid cells from 10 m or 20 m grid resolution (DTM).
	Aspect northness **Aspect eastness**	**A.COS** **A.SIN**	Indication of the degree of exposure of a surface to water movement. Conversion of the aspect (°) into unitless values between 1 (north or east) and -1 (south or west). Calculated from 3 x 3 grid cells from 10 m or 20 m grid resolution (DTM).

	Rugosity	**RUG**	Indicator of terrain variability. Calculated from 3 x 3 grid cells from 10 m or 20 m grid resolution (DTM), using Arc Chord ratio. Flat surface = 1; > 1 (surface variation).
	Slope	**SLOPE**	First derivative of depth, calculated from 3 x 3 grid cells from 10 m or 20 m grid resolution (DTM).
Geomorphology	**Volcanic geomorphology** **Carbonate geomorphology** **Mixed geomorphology** **Sedimentary geomorphology**	**G.VOLCA** **G.CARBO** **G.MIX** **G.SEDI**	Classification of geomorphological class from overlapping layers of depth, slope and backscatter data using GIS. (> km)
Substrate	**Substrate diversity**	**SUB.div**	Diversity of substrate per sampling unit (polygon, ~60 m linear), measured using the Exponential component of Shannon-Weaver index applied on substrate frequency.
	Substrate composition (nine facies): Sediment **Gravels** **Biogenic** **Carbonate rock** **Volcanic rock** **Mixed (sediment + rock)** **Mixed carbonate-sediment** **Mixed volcanic-sediment** **Mixed rock**	 / **GRAV** **BIOG** **RC** **RV** **MIX** **MIX.RC.S** **MIX.RV.S** **MIX.R**	Frequency of each substrate per sampling unit (polygon, ~60 m linear), as the sum of images where the substrate is present/total images of the polygon.
	Hardness	**HARD**	Level of substrate hardness (bounded between 1 to 6) per sampling unit (polygon, ~60 m linear), calculated from hardness score applied for each 17 substrate frequency.

We integrated additional traits that we considered relevant with respect to their ecological function, particularly sociability, anchoring mode to the substratum, relative polyp(s) size, relative cnidarian body size, space between the branches (compact, aerial), inclination of the structure to the current, as well as provision of an internal volume for other organisms (**Table III.3**).

For sponges, our selection of traits was partly based on the work of Schönberg (2021). This catalogue proposes a standardised classification scheme of sponge growth forms based on their ecological function. The morphological classes also have a unique CAAB number (Althaus et al., 2015). The catalogue follows a hierarchical structure, and allows scoring at different levels of resolution (ranging from 4 to 21 functional morphologies) according to the scientific purpose. In the case of assessing environmental conditions of sponges, at least 14 morphologies are needed to be scored.

Table III.3 : Morpho-functional traits used for the classification of cnidarians in morpho-functional groups

Traits	Modalities	Description	Ecological/functional relevance
Dimension	2D	Structure in a two-dimensional plane ("flattenable" structure).	Complexity of forms, habitat niche creation for other species.
	3D	Three-dimensional (a volume).	
Sociability	Colonial	Single polyp within the same skeleton (one individual).	Evolutionary process ?
	Solitary	Several polyps within the same skeleton.	
Anchoring	Calcified disc	A calcified disc attached to rock bottom.	Link with energy flow, productivity in the ecosystem.
	Pedal disc	Surface opposite the mouth allowing anchoring to rock bottom.	
	Peduncle	Lower part of the Pennatulacea, a stalk-like structure, embedded in the sediment (Bayer, 1983).	
	Rhizoids	Root-like features extending from the base of the colony (Bayer, 1983) (e.g., *Acanella*).	
Skeleton flexibility	Fleshy	No calcified skeleton (e.g., Actiniaria).	Resistance to disturbance, related to energy flow (Chappell, 1980). Effect on epibionts (Buhl-Mortensen et al., 2010).
	Semi-fleshy	No calcified skeleton but rigidifying parts (e.g., some Zoantharia).	
	Semi-rigid	Rigid axis, and the remaining parts are more flexible (e.g., some Zoantharia, Pennatulacea, Antipatharia, Alcyonaria), on images can be observed some bent parts by the effect of the currents.	
	Rigid	Almost completely calcified skeleton (e.g., Stylasteridae, Scleractiniaria), thick rigid appearance on images.	
Polyp size	Small	Not visible on the images.	
	Medium	Quite visible on the images (one can guess a small cap or a star shape – polyp –).	
	Large	Discernible on the images with clearly visible tentacles.	
Body size	Small	~2-5 cm	Link with energy flow, productivity in the ecosystem and habitat niche for others species.
	Medium to large	> 5- ~15 cm	
	Very large	>> 15 cm	
Spacing between branches	Branching compact	Branches in clusters or tufts, dense appearance, few space between branches (adapted from Veron, 2000).	Link with food particles trapping, and space for other species (e.g., ophiuroids, etc.) (McKinney, 1981).
	Branching opened	Branches of similar length given off at similar angles, open space between branches (adapted from Veron, 2000), "holes" clearly visible between the branches.	
	No branches	e.g., solitary polyp, Pennatulacea (leaf).	
Number of axes	Single	A single central inner rigidified supporting structure, bearing lateral branches, leaves or polyps.	
	Multiple	Multiple inner rigidified supporting structure.	
	No main axis	All forms carried by a pedal disc (e.g., Actiniaria) or solitary scleractinians.	
Polyp location	From a central axis, or leaf	Polyp arrangement from the central axis directly, or form leaf extending from the central axis.	
	On lateral branches (secondary axes)	Arrangement of the polyp from the lateral (secondary) branches.	
	On a basal support	Arrangement of the polyp on top of a large pedal disc or basal support (calcified disc) (e.g., Actiniaria or solitary scleractinians).	
Internal space/volume	0/1	Presence of a semi-enclosed internal space/cavity (e.g., *Acanella*, *Chrysogorgia*, colonising Actiniaria on hermit crab).	Refuge for other species, trap of food particles.
Orientation toward current	Erect	Structure facing the current, right.	Resistance to water flow, feeding strategy efficiency/prey capture.
	Curved	Inclined structure, which is subject to the current.	
Fan (Pinnate)	0/1	A single or multiple central axis with parallel side branches in a single plane (Althaus et al., 2014). Branched colonies in which the branching pattern is feather-like, with the branchlets in one plane (Bayer, 1983).	
Quill	0/1	Single stem with polyp leaves, base bulbous. Stem never branched (Althaus et al., 2014).	

Arborescent	0/1	Tree-like structure, networks of branches with multiple axes (2D or 3D), rigid or flexible, regularly organised or not.
Bushy	0/1	Dense, with many short branches, and compact and fluffy appearance (Althaus et al., 2014).
Polyp (anchoring small/not visible)	0/1	Only the polyp is visible, on/near the bottom.
Polyp (anchoring large and visible)	0/1	Polyp(s) with visible large pedal disc or calcified stem and disc.
Bottle-brush	0/1	3D column with a bushy appearance, short branches radiating from the main axis (Althaus et al., 2014).
Whip	0/1	A long thin single stem/axis, sometimes twists around itself, with very short lateral branches around the axis or axial polyps directly (Althaus et al., 2014).
Tulip-like	0/1	e.g., *Umbellula*, *Bathyalcyon*. A calyx at the end of a long stem/pedal disc.

We followed this classification, enabling us to score 16 morphological categories, however, in the cup-like category (CAAB 10 000909), we differentiate a new category “vase” as an intermediate form between complete wide cups (CAAB 10 000919), narrow cups (tubes and chimneys) (“CAAB 10 000911”) and barrels (CAAB 10 000907). We also considered traits identified in the literature as adaptation to deep-sea environments, notably for Hexactinellida (Tabachnick, 1991), or as potential effect on the community. Some traits in relation to processes such as filtration efficiency, productivity in the ecosystem, and provision of additional niche for associated fauna appeared to be relevant. We thus added the sponge’s size, the osculum(s) size (at least their visibility in the images), the level of compactness of the sponges, the presence/absence of internal cavities, and of outgrowths and long apparent spicules (hispidity) (**Table III.4**).

Table III.4 : Morpho-functional traits used for classification of the sponges in morpho-functional groups

Traits	Modalities	Description	Ecological/functional relevance
Sieve plates	0/1	Presence of sieves plates perforated by atrial cavities that cover the osculum.	Osculum protection, preventing sediment from clogging the oscules. The pores are also sometimes sieved, but are usually smaller than the oscules, and therefore less visible from images.
Large spicules (Hispidity)	0/1	Large visible spicules that cover the body of the sponge giving a hairy appearance (e.g., *Pheronema*).	Prevent other macro-organisms from attaching to the sponge and retain sediment and debris (Schönberg, 2015).
Internal cavities	0/1	Presence of cavities (large holes, gaps, spaces between or hole within branches-like features) as potential refuge for associated species.	Shelter space for other mobile organisms.
Branches/outgrowths	0/1	Structures with outgrowths reminiscent of branches.	Increases the amount of pore surface for filtration. Shelter for other organisms and/or allowing to trap food particles (particulate organic matter, dissolved organic carbon).
Compactness	Aerial	Delicate, thin, "fragile" structure, more contact surface.	Resistance to turbulent flow.
	Intermediate	Some openings in the structure.	
	Compact	A compact and homogeneous volume, with little or no airspace/opening.	

Osculum visibility	Large and visible	A large opening on the top of the sponge (exhalant opening), ≥ 50% of the sponge body.	Link to the current regime.
	Small and visible	Single or multiple little opening across the sponge body.	
	Not visible	Either too small to be observed on images, or closed according to water stream conditions, or unfavourable viewing angle.	
Body size	Small	~2-5 cm	Link with energy flow, productivity in the ecosystem, predictor of pumping rate (McMurray et al., 2014).
	Medium to large	> 5- ~15 cm	
	Very large	>> 15 cm	
Thinly encrusted (Crust) (CAAB 10 000923)	0/1	Forming a thin crust (flat sheet) over a hard substrate (very low profile) (Schönberg, 2021)	Lowest profile with large anchoring surface, making it very resistant to strong current/damaging hydrodynamics (Schönberg, 2021).
Thickly encrusted (Crust) (CAAB 10 000924)	0/1	Forming a thick crust (few mm to ~1 cm), slightly elevated from the hard substrate (low profile) (Schönberg, 2021).	
Creeping (Crust) (CAAB 10 000917)	0/1	Growth following the substrate (repent sponge), slightly thick in width, and elevated from the substrate. Some morphologies can be curved (incomplete vase shape, not closed).	Can adjust to different environmental conditions (less predictable) and substrate type (Schönberg, 2021).
Ball (Massive) (CAAB 10 000905)	0/1	Globular/ball shaped sponges: can be small or large, compact or with a fragile appearance.	Growth form that can tolerate a wide range of environmental conditions (Schönberg, 2021).
Amorphous simple (Massive) (CAAB 10 000904)	0/1	Irregularly shaped sponges, with no particular morphology or detectable structures (e.g., branches), generally quite large.	Growth forms adapted to low level of sedimentation, with rocky bottoms on which settle and medium to strong and predictable current (Schönberg, 2021).
Amorphous composite (Massive) (CAAB 10 000925)	0/1	Irregularly-shaped sponges, composed of merged sub-unit (Schönberg, 2021).	They function similarly to simple-massive sponges, but would tend to accumulate more sediment (Schönberg, 2021).
Fistular/Cryptic (Erect) (CAAB 10 000908)	0/1	The sponge is partly buried in the sediment, with only siphons emerging from the substrate.	Well suited to high sedimentation rate, and support burial in sediment through their erect oscule reducing the risk of clogging the aquiferous system (Schönberg, 2021).
Columnar (Erect) (CAAB 10 00916)	0/1	Simple erect sponge, higher than wide, not branched, solid in cross-section (Schönberg, 2021).	Do not tolerate a high energy environment and as it extends into the water column, it should occur in limited nutrient conditions (Schönberg, 2021).
Laminar (Erect) (CAAB 10 000913)	0/1	Erect growth form with flattened body, can have a small stalk (have a low anchoring area) (include fans, blades and spatulas) (Schönberg, 2021).	Commonly flexible, can bend when strong currents occur, and optimise their nutrient intake by standing right facing to the prevailing directional flow (Schönberg, 2021; Schönberg and Fromont, 2012).
Stalked (Erect) (CAAB 10 000906)	0/1	Include all erect forms, standing up from the substrate from a stalk, small or high. Upper part can be cup, ball, branching-shaped, etc., but the stem is inactive, meaning it do not have oscules/ostiae (Schönberg, 2021).	Suited to different substrate types, and from the stalk it can avoid damaging effects of sediment (Schönberg., 2021; Tabachnick, 1991). Growth forms in poor nutrient conditions.
Bushy/arborescent (Erect) (CAAB 10 000915)	0/1	Dense 3D structure, forming a little bush/tree and narrow interstice between extended structures (e.g., "branches"). Oscules/ostia scattered across the sponges (Schönberg, 2021)	Growth forms in reduced water mixing, and poor nutrient availability. Not suited to strong and turbulent current (fragile morphology) (Schönberg, 2021).
Amphoras (Narrow cup-like) (CAAB 10 000927)	0/1	Hollow with a narrow opening (Schönberg, 2021).	Well suited to moderate sedimentation rate (Schönberg, 2021).
Tube (Narrow cup-like) (CAAB 10 000911)	0/1	Hollow along most of their body. Apical opening of similar diameter as the body (Schönberg, 2021).	Well suited to moderate sedimentation rate. Do not accumulate sediment in their “lumen” (Schönberg, 2021).
Vase-shaped (~Wide cup-like)	0/1	Deep and wide-opened osculum, body hollowed in cross-section with apical part having the largest diameter.	
Cup (Wide cup-like) (CAAB 10 000919)	0/1	Complete wide cup, concave with apical part having the largest diameter (Schönberg, 2021).	Not well suited to high level of sedimentation rate (sediment accumulation at the top of the cup) (Schönberg, 2021).

Incomplete cup (Cup-like) (CAAB 10 000918)	0/1	Intermediate forms between erect-laminar sponges, cups and tables. Semi-closed (Schönberg, 2021).	Function like wide cup but sediment can be washed away (not completely closed) (Schönberg, 2021).

III.2.4 From morphotypes to morpho-functional groups (MFGs)

Each morphotype was annotated according to the set of traits (**Table III.3**, **Table III.4**), scoring 1 or 0 according to the presence or absence of the trait for the morphotype considered, to obtain a binary matrix of "morphotypes x presence/absence of traits" (**Figure III.2 - step (1)**). A total of 24 835 annotations of sponges and 4005 annotations of cnidarians were considered for the traits scoring.

Morpho-functional groups (MFGs) were then obtained using hierarchical ascendant classification (HAC) with Unweighted Pair Group Method with Arithmetic Mean (UPGMA) with *hclust()* function ('stats' package, R Core Team, 2021) on the Gower distance matrix of sponges and cnidarians morphotype traits respectively, calculated from *daisy()* function, using 'vegan' package (Oksanen et al., 2020). UPGMA was selected after testing different classification methods – (Ward, complete and simple linkage, Weighted Pair Group Method with Arithmetic Mean (WPGMA), Weighted Pair Group Method with Centroid (WPGMC), Unweighted Pair Group Method with Centroid (UPGMC)) – based on the best cophenetic correlation value (Borcard et al., 2018). We selected the best partition according to the analysis of the last high inertia gap (Borcard et al., 2018). For sponge morphotypes classification, we removed the 'sieve plates' trait of the matrix because of the lack of consistency in the annotation of this trait (hardly visible on the images). This numerical classification approach provides a simplified group number depending on the cutting threshold of the tree, from a more complex multiple traits matrix (Tsakalos et al., 2019) (**Figure III.2 - step (2)**).

From the export file of cnidarian and sponge morphotype annotation data in BIIGLE, we summed the abundances of morphotypes corresponding to the same MFG (i.e., clusters obtained from the HAC), and those for each set of morphotypes belonging to the same MFG. (**Figure III.2 - step (3)**). Thus, we obtain a new matrix "images x MFG abundances". From this matrix, we calculated and standardised the MFG densities per polygon of 200 m^2 (~60 m linear) sample unit, from the navigation of the camera and its speed, using ADELIE software (internal dev. IFREMER; ArcGIS 10.7 plugin) (**Figure III.2 - step (4)**).

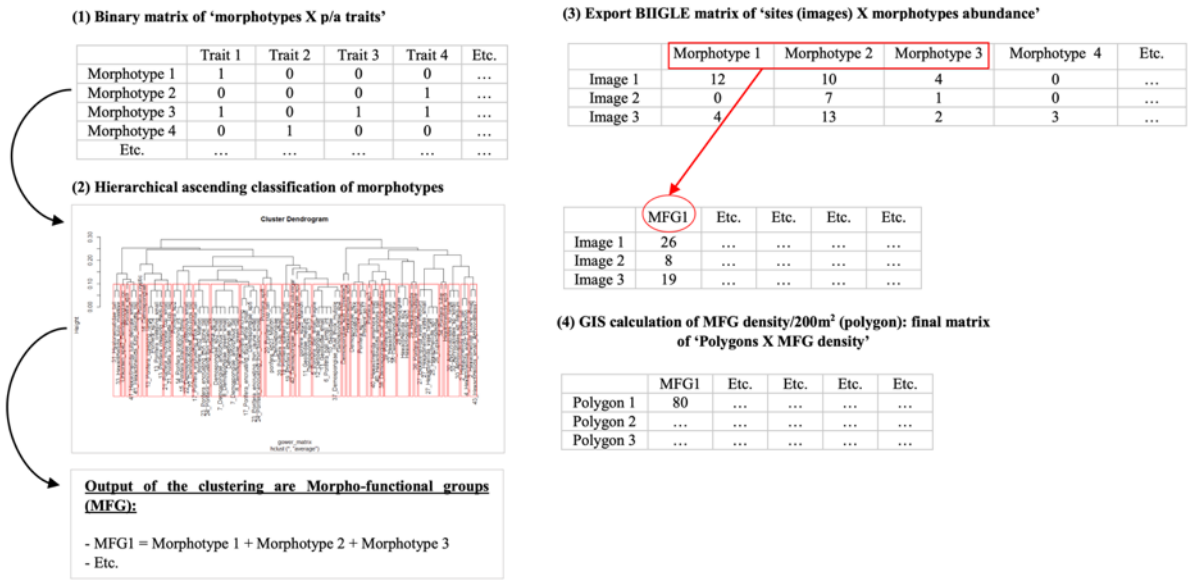

	Trait 1	Trait 2	Trait 3	Trait 4	Etc.
Morphotype 1	1	0	0	0	…
Morphotype 2	0	0	0	1	…
Morphotype 3	1	0	1	1	…
Morphotype 4	0	1	0	0	…
Etc.	…	…	…	…	…

	Morphotype 1	Morphotype 2	Morphotype 3	Morphotype 4	Etc.
Image 1	12	10	4	0	…
Image 2	0	7	1	0	…
Image 3	4	13	2	3	…

	MFG1	Etc.	Etc.	Etc.	Etc.
Image 1	26	…	…	…	…
Image 2	8	…	…	…	…
Image 3	19	…	…	…	…

	MFG1	Etc.	Etc.	Etc.	Etc.
Polygon 1	80	…	…	…	…
Polygon 2	…	…	…	…	…
Polygon 3	…	…	…	…	…

Figure III.2 : Analytical scheme to obtain morpho-functional groups from the classification of morphotypes with a multi-traits approach

III.2.5 Statistical analyses

All analyses were performed using the R environment (V4.1.2) (R Core Team, 2021).

III.2.5.1 Morpho-functional group structures (richness, diversity, composition)

Comparison of MFGs richness between seamounts and island slopes were assessed from sample-based rarefaction curves (on polygons), using *specaccum()* function of 'vegan' package, with "exact" method.

We characterised MFGs composition among sites using Principal Component Analysis (PCA) with *dudi.pca()* function ('ade4' package, Dray and Dufour, 2007) based on Hellinger-transformed MFG densities, obtained from *decostand()* function ('vegan' package).

Beta diversity (BD) (here referring to the degree of MFGs differentiation within site) was quantified for each transect using *beta.div()* function ('adespatial' package, Dray et al. (2022)) from Hellinger distance, as well as derived LCBD (Local Contribution to Beta Diversity) and SCBD (Species contribution to beta diversity) index. LCBD value reflect the uniqueness of sampling units in terms of their composition in MFGs (characteristic sites), while SCBD value reflect the level of variation of each MFG within the considered transect (MFGs with high SCBD coefficient have strong contribution in generating variability within transect) (Legendre and De Cáceres, 2013).

III.2.5.2 Morpho-functional group responses to environmental constraints and structuring role on associated megafaunal communities

We tested the role of environmental drivers in shaping MFGs composition within and between sites from redundancy analysis (RDA) and partial redundancy analysis (pRDA) (on Hellinger-transformed MFG densities) for the latter, considering different covariables: latitude and longitude, as well as quantification of current and chlorophyll a concentration (Chla) contribution independently. We first removed collinear variables using Spearman's pairwise correlations (removal when Spearman's $r > 0.85$). RDA and pRDA were performed using *rda()* function and we tested the significance of the RDA models, axes and environmental variables with *anova.cca()* by a permutation test of the F-statistic (999 permutations, $p < 0.05$). Selection of parsimonious models were possible from forward selections of the explanatory variables with the *ordiR2step()* function ('vegan' package), using the adjusted R^2 selection criterion (Borcard et al., 2018). Contribution of the environmental variables and their interrelationships were quantified from variation partitioning analyses using *varpart()* function ('vegan' package) for the following set of factors: hydrology comprising current and Chla, topography variables and substrate as well as geomorphology. Fractions explained were tested with a permutation test (*anova.cca()* function, n = 999 permutations, p-value < 0.05) and were represented from Venn diagrams.

We also tested the structuring role of MFGs on the associated megafaunal communities; here by considering MFGs as explanatory variables using RDA. Using pRDA, we also quantified and adjusted the RDA model by considering spatial variables (latitude, longitude) and also to determine the structuring role of sponge MFGs when cnidarians remain in the community and when they are removed, and vice versa for cnidarian MFGs.

All the graphical representations were made using the 'ggplot' package (Wickham et al., 2016).

III.3 Results

III.3.1 Patterns of Cnidaria and Porifera morpho-functional groups (diversity, spatial distribution)

III.3.1.1 Composition of Cnidaria and Porifera morpho-functional groups

From the 75 morphotypes of cnidarians and 70 morphotypes of sponges (84 entities for cnidarians and sponges respectively considering the size class of the morphotypes), we obtained 34 MFGs for cnidarians and 37 MFGs for sponges from the hierarchical ascendant classification (**Table III.5**, **Table III.6**, **Supplementary material III.1**). Trait annotation matrices are available in **Supplementary material III.2**.

Table III.5 : Cnidarian morpho-functional groups obtained from the hierarchical ascendent classification

MFG code	Number of morphotypes within the MFG	Description	Identification associated to the morphotypes regrouped in the MFG
C1	2 (one with two sizes)	Semi-rigid, pedal disc, medium polyps attached to dead sponge stalk or hermit crab	Zoantharia, *Epizoanthus*
C2	3	Semi-fleshy, pedal disc, large polyps	Alcyoniidae, *Anthomastus*
C3	4	Small solitary, calcified disc, mix flexibility (rigid, semi-fleshy), with large polyp	Scleractinia, Anthozoa, Ceriantharia incertae
C4	2	Medium to large solitary, calcified disc, rigid, with large polyp	*Javania*, Scleractinia (solitary)
C5	7	Solitary fleshy, large polyp (near bottom: pedal disc not visible/small)	Actiniaria
C6	4	Large solitary fleshy, large polyp (carried by a large pedal disc)	Actiniaria
C7	1	Small solitary fleshy, medium polyp, within bushy sponge hosts	Actiniaria
C8	2	Small solitary fleshy, large polyp attached on biological host (over Paguroidea)	Actiniaria
C9	1	Pinnate, large, semi-rigid, medium polyps, with compact branching, multiple axes	Antipatharia
C10	1 (two sizes)	Pinnate, small & medium, semi-rigid, medium polyps, with compact branching, single axe	Antipatharia
C11	3	Arborescent, medium to large, semi-rigid, small polyps, with compact branching	Antipatharia, Alcyonacea, Scleraxonia
C12	5	Arborescent, large, semi-rigid to rigid, small polyps, with compact branching	Scleractinia (colonial), *Enallopsammia*, *Corallium*, Primnoidae, Anthozoa (colonial)
C13	7	Arborescent, medium to large, semi-rigid, small to medium polyps, with opened branching	Alcyonacea, Primnoidae, Anthozoa (colonial), Holaxonia, Isididae
C14	1	Arborescent, small, rigid, small polyps, with opened branching	Stylasteridae incertae
C15	1	Arborescent, small, semi-rigid, small polyps, with opened branching, inclined to the current	Alcyonacea
C16	2	Bushy, large, semi-rigid, medium polyps, with compact branching, inclined or not to the current and provide internal volume	Anthozoa (colonial), Isididae
C17	1 (two sizes)	Bushy, semi-rigid, medium polyps, with compact branching	Zoanthidae
C18	1 (two sizes)	Bushy, semi-rigid to rigid, small polyps, with compact branching	Anthozoa colonial
C19	1	Bottle-brush, small, semi-rigid, small polyps, with compact branching	Anthozoa colonial

C20	1	Bottle-brush, medium to large, semi-rigid, small polyps, with compact branching	Anthozoa colonial
C21	1	Bottle-brush, with rhizoids, medium to large, semi-rigid, medium polyps, with compact branching and provide internal volume	*Acanella*
C22	1 (two sizes)	Bottle-brush, semi-rigid, small polyps, with compact branching and provide internal volume	Antipatharia
C23	3 (one with two sizes)	Bottle-brush, semi-rigid, medium polyps, with compact branching and provide internal volume	Alcyonacea, Chrysogorgiidae
C24	1	Medium to large, pedal disc, semi-fleshy, small polyps, with opened pseudo-branching,	Alcyonacea
C25	1	Medium to large, pedal disc, semi-fleshy, small polyps, no branches	Alcyonacea
C26	1	Tulip-shaped, medium to large, semi-fleshy, pedal disc, small polyps	*Bathyalcyon*
C27	1 (two sizes)	Tulip-shaped, fleshy, large polyps on top of a long stem, inclined to the current	Hydrozoa
C28	1 (two sizes)	Tulip-shaped, peduncled, semi-rigid, large polyps, inclined to the current	*Umbellula*
C29	1	Whip, large, semi-rigid, small polyps, with opened pseudo-branching, inclined to the current	Isididae
C30	3	Whip, large, semi-rigid, medium polyps, no branches, inclined to the current	Anthozoa, Isididae
C31	1 (two sizes)	Whip, small & medium, semi-rigid, medium polyps, no branches, inclined to the current	Anthozoa
C32	1	« Pseudo-quill », medium to large, semi-rigid, simple axe with lateral large polyps	Alcyonacea
C33	3	Quill, peduncled, large, semi-rigid, medium polyps, ~3D	Pennatulacea
C34	6	Quill, peduncled, small to medium, semi-rigid, medium polyps, 2D	Pennatulacea

Table III.6 : Sponge morpho-functional groups obtained from the hierarchical ascendent classification

MFG code	Number of morphotypes within the MFG	Description	Identification associated to the morphotypes regrouped in the MFG
P1	2	Stalked, large, aerial	Hyalonematidae, Hexactinellida
P2	1	Stalked with a laminar upper part, small, aerial	Porifera (Silicea)
P3	1	Stalked with a ball upper part, small, aerial, medium to large osculum	Hexactinellida
P4	1 (two sizes)	Stalked with a ball upper part, aerial	Hexactinellida
P5	1	Cryptic, small, intermediate, with excrescences	Porifera
P6	1	Amorphous composite, large, intermediate with internal cavity	Demospongiae
P7	2 (one with three sizes)	Creeping, intermediate	Porifera
P8	1 (two sizes)	Creeping forming incomplete cup, intermediate, with internal cavity	Porifera
P9	3	Amorphous composite, medium to large, compact, with excrescences	Porifera
P10	1 (two sizes)	Ball, compact, with excrescences and long spicules	Demospongiae
P11	4	Crust, medium to large, compact	Porifera
P12	5 (two with two sizes)	Amorphous simple, small & medium, compact	Demospongiae, Porifera
P13	5	Crust, small, compact	Porifera
P14	1	Cup, medium to large, intermediate, with internal cavity	Porifera
P15	3 (one with two sizes)	Cup, small & medium, compact, with internal cavity	Porifera, Demospongiae
P16	1	Stalked, small, intermediate, small visible osculum	Porifera
P17	1	Columnar (with basal crust), medium to large, compact, small visible osculum	Demospongiae
P18	1	Amorphous simple, large, compact, small visible osculum	Demospongiae
P19	2	Ball, medium to large, compact, small visible osculum	Geodiidae, Demospongiae
P20	7	Ball, small, compact, small visible osculum	Geodiidae, Demospongiae
P21	1	Cup, large, intermediate, with internal cavity, small visible osculum	Demospongiae
P22	1	Cup, medium to large, aerial, with internal cavity, small visible osculum	Hexactinellida
P23	2	Amphora, large, compact, medium to large osculum	Demospongiae, Porifera

P24	1 (two sizes)	Amphora, small & medium, compact, medium to large osculum	Porifera
P25	1	Amphora, small, intermediate, medium to large osculum	Porifera
P26	1 (two sizes)	Amphora, aerial, medium to large osculum	Hexactinellida
P27	1	Thick crust, small, compact, medium to large osculum, with internal cavity	Demospongiae
P28	3	Tube, small, mixed compactness (compact/aerial/intermediate), medium to large osculum, with internal cavity	Hexactinellida
P29	3	Cup-like (Amphora & cup), large, intermediate, medium to large osculum, with internal cavity, long spicules	Demospongiae, Hexactinellida
P30	1	Tube, medium to large, intermediate, medium to large osculum, visible sieve plates	Hexactinellida
P31	1	Creeping, medium to large, intermediate, multiple visible medium to large osculums, with internal cavity	Porifera
P32	3 (one with three sizes)	Vase, aerial, medium to large osculum, with internal cavity, visible sieve plates	Hexactinellida, Euplectellidae
P33	1	Vase, small, aerial	Porifera
P34	1	Vase, medium to large, aerial	Hexactinellida
P35	1 (three sizes)	Stalked with a cup upper part with excrescences, aerial, medium to large osculum, with internal cavity, sieve plates	*Aphrocallistes*
P36	2	Bushy (excrescences), medium to large, aerial, medium to large osculum, with internal cavity	Hexactinellida
P37	2	Bushy (excrescences), small, aerial, medium to large osculum, with internal cavity	Hexactinellida

For cnidarians, 12 MFGs out of 34 represent a single morphotype while for sponges, 20 MFGs/37 constitute a single morphotype, and for both groups, which can be composed of different sizes. Sponges and cnidarians identified at finer taxonomic resolution with particular morphologies are mostly attributed to a single morphotype, sole representative of an MFG (e.g., *Aphrocallistes*, *Bathyalcyon*) (**Table III.5**, **Table III.6**).

For cnidarians whose taxonomic identification is finer than sponges, we observed some traits are specific to a particular taxonomic group, such as quill morphology, and peduncled anchoring mode, specific to Pennatulacea. However, the pennatulids alone group nine morphotypes, divided into two MFGs (**Table III.4**). The same is observed for Actiniaria. Other MFGs gathered different taxa, however all belonging to the Alcyonacea order (e.g., C13; Alcyonacea, Primnoidae, Holaxonia, Isididae) and an unidentified colonial anthozoan.

The composition and relative frequencies of cnidarian and sponge MFGs (and shared morphologies) varies among surveyed sites (**Figure III.3**, **Supplementary material III.3**).

There are four main sponge morphologies within the channel – dominant at one or several sites – which differ in occurrence and relative frequency between sites; comprising bushy aerial, stalked aerial, simple amorphous (compact) and cup forms (**Figure III.3A**).

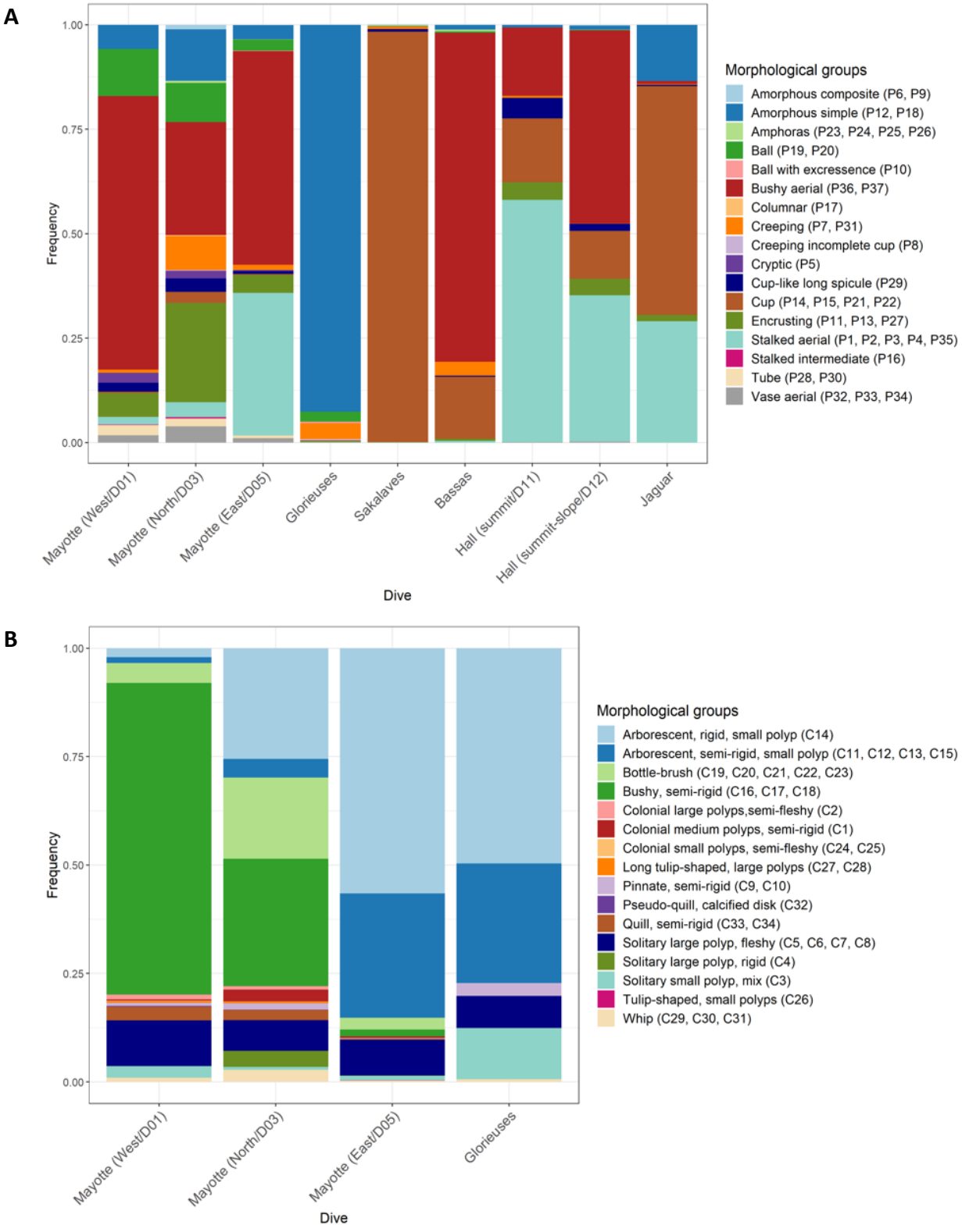

Figure III.3 : Morphological composition between seamounts and island slopes, **(A)** for sponges between the nine camera transects along the Mozambique Channel, **(B)** for cnidarians between Mayotte island slopes and Glorieuses. The morpho-functional groups are grouped manually into a lower number of categories according to their shared morphologies

Bushy aerial forms were observed on all sites, except Glorieuses, with higher relative frequency on the island slopes of Mayotte (P37, P36) and Bassas; as well as on Hall bank (P36), particularly for the slope transect (dive 12). Stalked aerial forms were observed on all sites with higher relative frequency on Hall bank (P2, notably the summit, and Jaguar; but also on the eastern slope of Mayotte island. We observed that cup forms have higher densities in the south of the channel, and dominate on Sakalaves terrace, as well as on Jaguar bank, while ball, and tube forms have higher densities in the North, on the slopes of Mayotte, and also on the Glorieuses terrace, more specifically tube forms were absent of the southern sites.

Vase aerial forms have higher relative frequency along the slope of Mayotte, but were also observed in lower relative frequency on Glorieuses, and Hall Bank.

The encrusting forms are particularly abundant on the northern slope of Mayotte. Creeping forms were observed with low relative frequency on the northern slope of Mayotte as well as on Glorieuses and Bassas external slope. Finally, cryptic morphologies were restricted to the island slopes of Mayotte.

The terrace of Glorieuses is composed of six dominant MFGs that constitute compact sponge forms – amorphous morphology (P12), small cup (P15), the latter also dominant on the Sakalaves terrace (**Figure III.4B**), and ball morphologies (P19, P10) –, as well as intermediate compactness forms (creeping forms (P7) and incomplete cup (P8)) (**Figure III.4A**). Other compact sponges were observed particularly along the northern slopes of Mayotte island, in the form of encrusting sponges such as P13 and P11 (**Figure III.4A**), the latter also dominant on Hall Bank (**Figure III.4**). These compact forms (mainly Demospongiae) differ from the aerial ones observed along the eastern slope of Mayotte, comprising amphoras (P26), and bushy morphologies (P37, P36) also abundant on Bassas island slopes and the slope of Hall Bank (P36); as well as stalked morphologies (P35, i.e., *Aphrocallistes* and P4), also present along the northern and western slopes (P1). P2 (a small stalked aerial form with a laminar upper part) was observed only in the central and southern site, as well as P21 (large cup with small visible osculum) restricted to Bassas and that dominate on Jaguar (**Figure III.4B**).

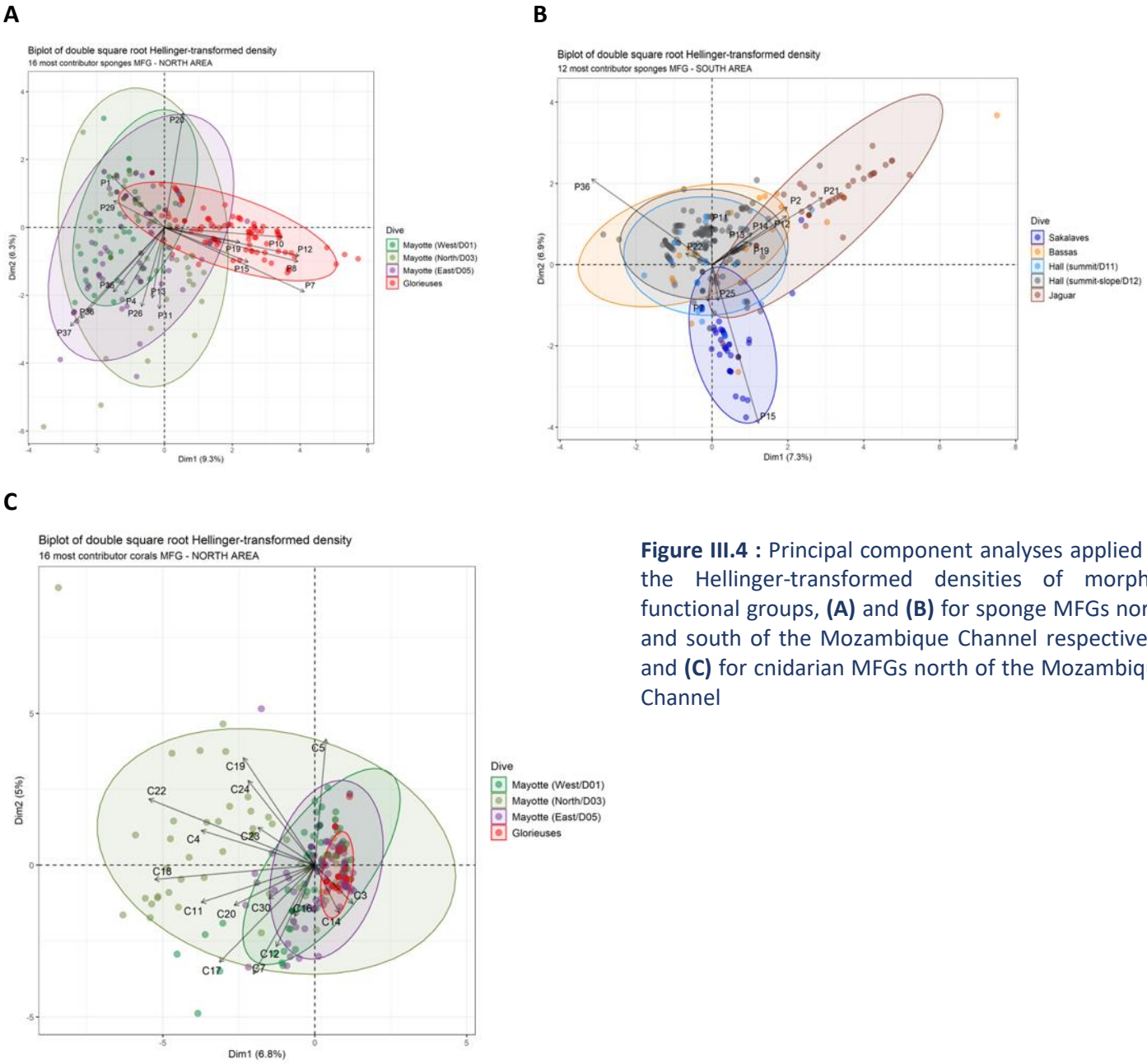

Figure III.4 : Principal component analyses applied to the Hellinger-transformed densities of morpho-functional groups, **(A)** and **(B)** for sponge MFGs north and south of the Mozambique Channel respectively, and **(C)** for cnidarian MFGs north of the Mozambique Channel

Regarding cnidarians assessed in the north area, we observed five abundant morphologies along Mayotte island slopes and on Glorieuses comprising rigid and semi-rigid arborescent forms, both with small polyps, as well as bushy and bottle-brush forms, and fleshy solitary forms with a large polyp (**Figure III.3B**).

Semi-rigid bushy forms are dominant on the northern and western slopes of Mayotte (Zoanthidae and other colonial anthozoans) while semi-rigid to rigid arborescent forms with small polyps are dominant on the eastern slope of Mayotte and Glorieuses. Other morphologies were restricted to Mayotte island slopes, such as quill (representative of Pennatulacea), bottle-brush or colonial forms with medium polyps (representative of

Zoantharia), but differences in abundance were observed between the three slopes. For instance, bottle-brush morphologies, and colonial forms with medium polyps were more abundant along the northern slopes as for whip ones.

Finally, solitary forms with small polyp but mixed rigidity were observed on the island slopes of Mayotte and on Glorieuses, but in higher relative frequency along the western slope of Mayotte and Glorieuses than on the other slopes of Mayotte. Solitary rigid forms with large polyp (*Javania* sp. and other solitary scleractinians) were restricted along the northern and eastern slope of Mayotte, and differ in abundance between the two slopes, with higher abundance along the northern one.

PCA on the cnidarian MFG densities mainly dissociate the bottle-brush shapes – abundant along the northern Mayotte island slope (C22, C19) and for C23 also along the northern slope – on the upper left part of the plot, from the bushy ones – observed along the northern slopes (e.g., C18) and western one also (C17, i.e., Zoanthidae) – and the medium to large arborescent morphologies – along the Mayotte eastern slope (e.g., C12), northern and western as well (C11) – on the lower left part (**Figure III.4C**). The Glorieuses sites form a compact cluster nested within the cluster of sites on the Mayotte island slopes, meaning Glorieuses has a poor number of cnidarians MFGs, mainly of small morphologies, such as C3 (solitary forms with large polyp) and C14 (small arborescent morphology, i.e., Stylasteridae incertae), observed in higher densities along the northern and western slopes of Mayotte island.

III.3.1.2 Richness of Porifera and Cnidaria morpho-functional groups

At equal sampling effort (n = 58 polygons), the highest sponge MFGs richness is observed on the northern slope of Mayotte (19 MFGs) and the eastern slope (16 MFGs). MFGs richness is intermediate on Glorieuses (14 MFGs), the western slope of Mayotte (13 MFGs), and the summit-slope of Hall and Jaguar (12 MFGs) (**Figure III.5A**, **Table III.7**). The lowest MFGs richness is observed on Sakalaves, Bassas and the Hall summit (7 to 8 MFGs).

For cnidarians, at equal sampling effort in the North area (n = 106 polygons), the highest MFGs richness is observed on the northern slope of Mayotte (28 MFGs) as for sponges, intermediate MFGs richness and few differences were observed along the eastern and western slopes (20-22 MFGS), while the richness was very low on Glorieuses (7 MFGs) (**Figure III.5B**, **Table III.7**).

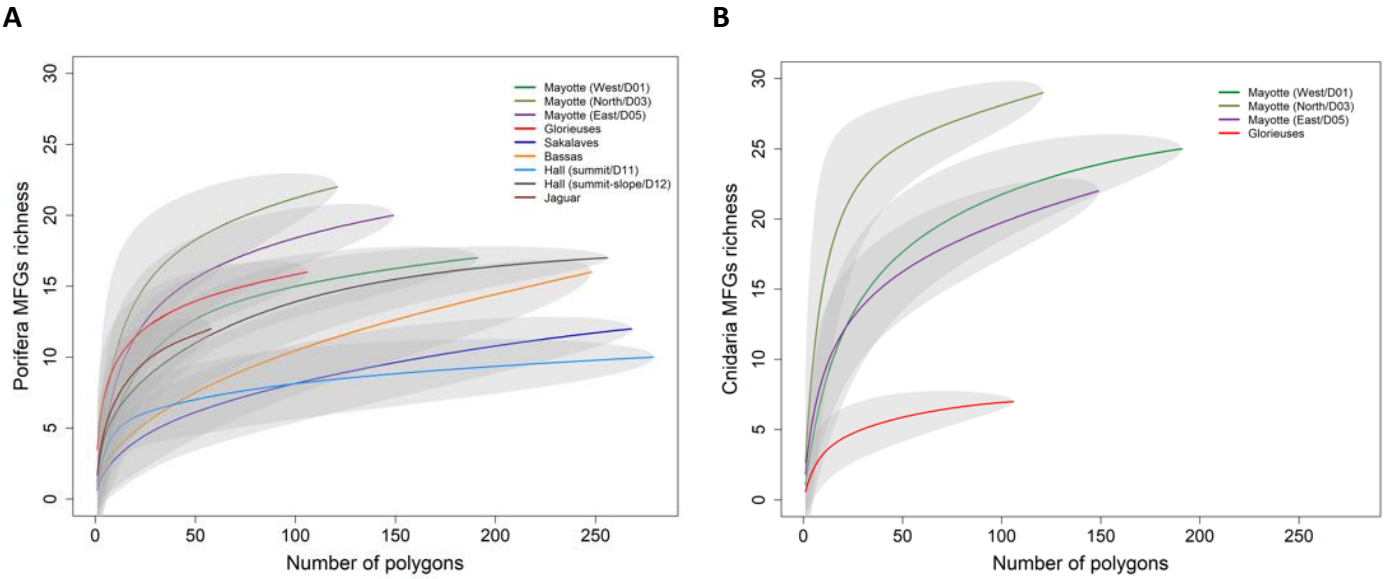

Figure III.5 : Sample-based rarefaction curves for **(A)** sponge morpho-functional groups for the nine camera transects along the Mozambique Channel, and **(B)** cnidarian morpho-functional groups for the four camera transects along Mayotte island slopes and Glorieuses

Table III.7 : Summary of diversity metrics comprising MFGs richness (from rarefaction curves, **Figure III.5**) between sites (camera transects), and MFGs beta diversity, i.e., values of within-transect variability in MFG assemblages (from beta diversity analyses with Hellinger distance), for the morpho-functional groups of sponges and cnidarians. "_" = no data

	Cnidaria		**Porifera**	
Sites	MFG richness (n = 106 polygons)	MFG Beta diversity	MFG richness (n = 58 polygons)	MFG Beta diversity
Mayotte West slope	22	0.54	13	0.46
Mayotte North slope	28	0.61	19	0.46
Mayotte East slope	20	0.60	16	0.54
Glorieuses	7	0.39	14	0.33
Sakalaves	_	_	7	0.34
Bassas	_	_	8	0.39
Hall summit	_	_	7	0.48
Hall summit-slope	_	_	12	0.51
Jaguar	_	_	12	0.44

III.3.1.3 Variability of morpho-functional group assemblages within and among surveyed sites

The variability of MFG assemblages (beta diversity) differs between sites. Firstly, for sponges, the beta diversity (BD) of MFGs are the highest along the eastern slope of Mayotte and the summit-slope of Hall Bank (0.54 and 0.51 respectively). Intermediate BD are observed for the northern and western slopes of Mayotte, as well as on Hall summit and Jaguar (0.44 to 0.48). The lowest BD are observed along Bassas external slope, Sakalaves and Glorieuses platforms (0.33 to 0.39) (**Table III.7**). Secondly, for cnidarians, examined only in the northern part of the

Mozambique Channel, the MFGs BD are the highest along the northern and western slope of Mayotte (0.60-0.61 out of 1). The MFGs BD are lower along the eastern slope than along the two other ones, with intermediate value (0.54) while the MFGs BD are the lowest along the Glorieuses transect (0.39) (**Table III.7**).

Sponge MFGs generating more variability than average (with high SCBD coefficient), are more numerous in the northern Mozambique Channel than in the central and southern part, where no more than four MFGs have been identified as generating variability (**Figure III.6A**). This pattern is mirrored in the lower number of unique polygons (LCBD) observed along the central/southern sites (**Figure III.6B**).

P20 (small compact balls) has among the top SCBD indexes along Mayotte island slopes and Glorieuses ranging from 16.9% contribution along the northern slope of Mayotte to 31.8% contribution along the western one. In the central and southern channel – except on Jaguar – P22 (medium to large aerial cups) is identified as highly contributing to beta diversity ranging from 13% to 25.9% contribution (**Figure III.6A**).

Other sponge MFGs with high SCBDs are shared in the north and south of the channel for some sites, such as P36 (medium to large aerial bushy forms) on the island slope of Bassas and eastern slope of Mayotte, and Hall Bank, with up to 55% contribution on Bassas. The analogue MFG (same morphotype but of smaller size; P37) was only identified as having high SCBD along the Mayotte island slopes, especially the western slope (up to 16.4% contribution). Shared MFGs with high SCBD is also true for P12 (small to medium simple amorphous compact forms), on the north area sites and Jaguar, with up to 22.1% contribution on this site.

Some sponge MFGs with high SCBD values are site specific, such as P15 (small to medium compact cup) on Sakalaves (66%), P21 (large cup with intermediate compactness) on Jaguar (23.8%) or P7 (creeping forms with intermediate compactness) on Glorieuses.

In addition, significant LCBDs (unique polygons in the composition of sponge MFGs) vary in number and in distribution between sites. They are particularly numerous along the Mayotte island slopes, distributed all along the transects but particularly abundant in volcanic areas, but also on other predominantly carbonate bottoms and locally in sedimentary areas (where blocks of hard substrate are sparsely distributed) (**Figure III.6D**). Conversely, on the Glorieuses and the seamounts of the central/southern Mozambique Channel, we have identified less

significant LCBDs, more or less localised in specific areas such as volcanic areas (Sakalaves, Bassas, Hall), in transition areas between geomorphological facies (all sites), and locally sediment dominated areas (**Figure III.6C**).

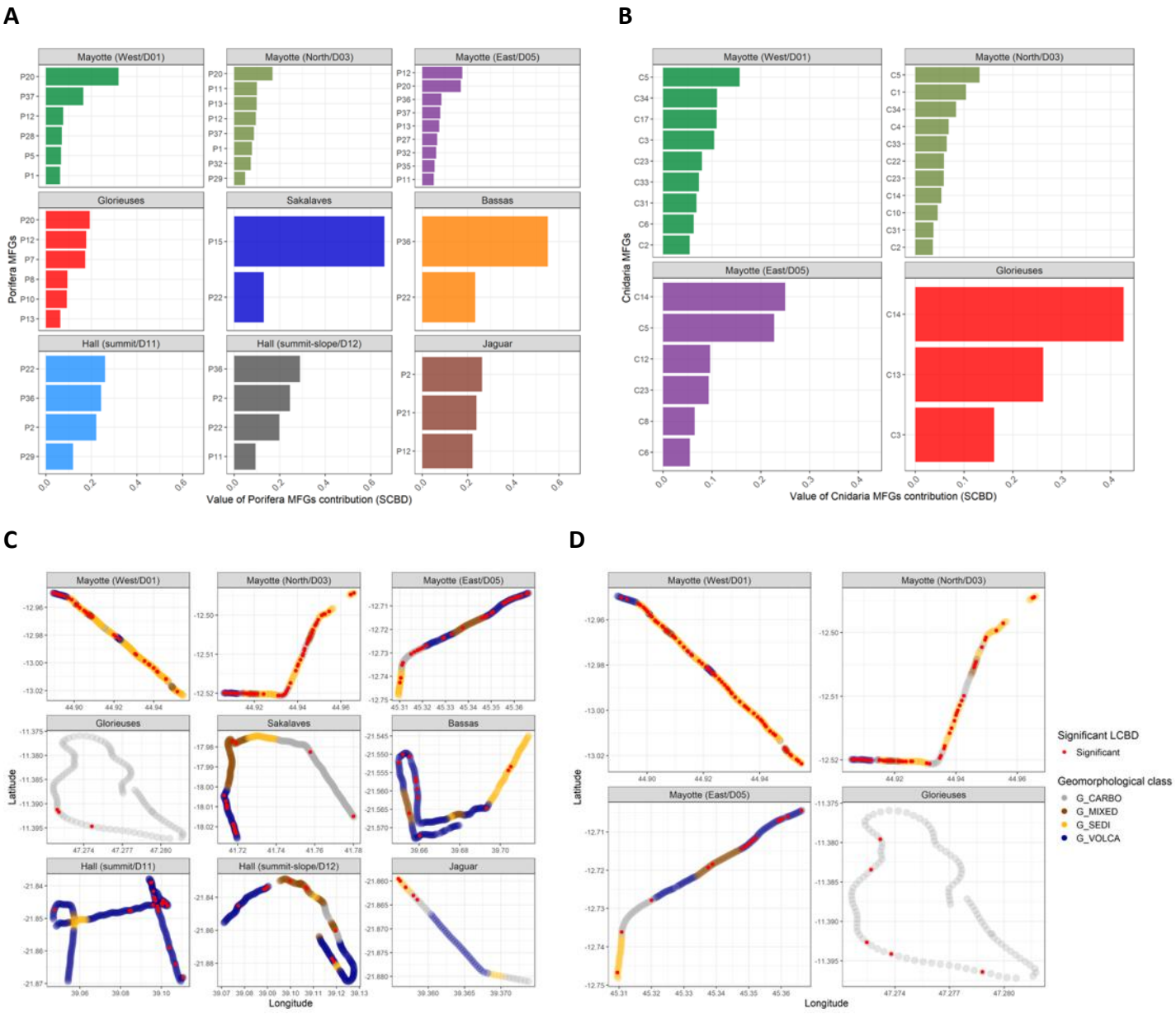

Figure III.6 : (A) and **(B)**, histograms representing respectively the morpho-functional groups of sponges and cnidarians, whose contributions to the variability within each transect – "beta diversity" – are higher than the transect average (i.e., Species Contribution to Beta Diversity, SCBD). Panels **(C)** and **(D)** are maps representing, for sponges and cnidarians respectively, polygons with a significant LCBD (Local Contribution to Beta Diversity) value (999 permutations, $p < 0.05$) (red dot), i.e., with a unique morpho-functional group composition, for each transect

Regarding the cnidarian MFGs, we identified a higher number of cnidarian MFGs with high SCBD along the Mayotte island slope, especially the northern and western slopes compared to Glorieuses (**Figure III.6B**).

C5 (solitary fleshy forms with large polyp, i.e., Actiniaria, with no visible anchoring features) is among the top MFG contributing to the beta diversity (SCBD) identified only along the Mayotte island slopes (up to 22.7% contribution). Some MFGs with high SCBD were identified only along the northern and western slope such as C34 (small to medium peduncled quills, i.e., pennatulids) and C33 (large peduncled quills) (6.5 up to 11% contribution) where sedimentary facies are abundant. Other MFGs with high SCBD on Mayotte were shared with Glorieuses, such as C14 (small rigid arborescent form, i.e., Stylasteridae incertae) for the eastern slope of Mayotte (25-42.6% contribution), or C3 (small solitary form with large polyp and mixed rigidity) for the western slope of Mayotte (10.4-16.2% contribution). Finally, some cnidarian MFGs with high SCBD were site-specific such as C1 (semi-rigid medium polyp attached to dead sponge stem, i.e., Zoantharia) on the northern Mayotte island slope (10.4%); C17 (bushy semi-rigid forms, i.e., Zoanthidae) along the western slope (11%); C12 (large semi-rigid arborescent forms with compact branching) along the eastern slope or C13 (medium to large semi-rigid arborescent forms with open branching) on Glorieuses.

The distribution of sites contributing to the beta diversity (LCBD) of cnidarian MFGs shows, as for sponges, variability between sites with extremely high number of contributing sites regularly distributed along the western slope of Mayotte, revealing small scale structure, while the eastern one displays lower significant LCBD distributed spatially over larger distance suggesting structuring at larger scale (**Figure III.6D**). Along this slope, significant sites are concentrated at geomorphological facies interface and in the volcanic dominated area. In comparison, very few sites have been identified on the Glorieuses terrace, localised either on the summit or sloping area.

III.3.2 Environmental drivers of Porifera and Cnidaria morpho-functional groups

Partial redundancy analyses highlight the spatial structure of cnidarian and sponge MFGs in relation to different environmental drivers.

Along the Mozambique Channel, numerous (18%) significant environmental variables explain 19.9% of the sponge MFGs spatial structure while spatial variables (latitude, longitude) explain 16.8%, considering six significant axes.

Current variability (STD 0.50 m and 350.650 m), inter-annual chlorophyll a concentration (CHLA.y.sd), slope, bathymetry, carbonate geomorphology (G.CARBO), carbonate rock percentage (RC) and hardness (HARD) are among the most contributors (**Figure III.7A**). Four sponge MFGs are well represented along the factorial plan (P15, P36, P12 & P2). The MFG P15 groups several morphotypes (small to medium compact cups) and correlates to high current variability at 0-50 m (STD0.50), hardness and carbonate geomorphology (and so carbonate rock) and is present mainly on Sakalaves platform, Hall Bank and Glorieuses. The MFG P36 groups medium to large aerial bushy forms and correlates to high inter-annual variability in Chla and to several variables characterising the volcanic dominant areas found deeper, with higher slope, rugosity, BPI at 120 and 500 m although these three last variables have low contribution to RDA axes. P12 that groups small simple amorphous compact forms and P2 grouping a small stalked form with upper laminar part correlate to high deep current variability at 350-650 m (STD350.650), as well as deep current speed in lesser extent (SP350-650). One can notice that RDA axis 1 separates carbonate areas with higher current speed and variability (mainly found on seamounts summits) from volcanic or those mixed with sediment, with higher chlorophyll levels, found both along island slopes and summits or upper slopes of seamounts. Axis 2 contributes to isolate steeper and rougher areas.

Partial RDA on sponge MFGs focussing on the northern area only do not reveal any pattern between the three Mayotte island slopes and the Glorieuses terrace but specify habitat preferences of other MFGs (**Figure III.7B**). Environment explains 16.4% of sponge MFGs structure, while spatial variables explain 12.7%. The second RDA dimension separates mainly MFGs with compact and intermediate compactness (e.g., P12, P13, P11) in the lower left part from the MFGs grouping aerial and/or stalked forms in the upper RDA plot part (e.g., P37, P36, P35, P32). MFGs grouping compact small to large crusts (P13, P11), and simple amorphous forms (P12), and creeping forms with intermediate compactness (P7) are correlated to more or less carbonate geomorphology and carbonate rock coverage, and winter Chla, while inversely correlated to bathymetry. The P37 and P36 MFGs grouping small to large aerial bushy forms, as well as P35 – a stalked aerial forms with excrescences (i.e., *Aphrocallistes*) –

and P32 – grouping medium to large aerial vases (e.g., Euplectellidae) – are mostly correlated to BPI 500 m; volcanic rock (RV) and mixed volcanic rock with sediment substrate (MIX.RV.S) as well as slope. The MFG P1, a large stalked aerial form (i.e., Hyalonematidae) is also correlated to intermediate bathymetry and surface current variability à 0-50 m (STD0.50). P20, grouping small compact ball forms, although well represented along the first dimension and highly abundant on Glorieuses site, are poorly correlated to explanatory variables.

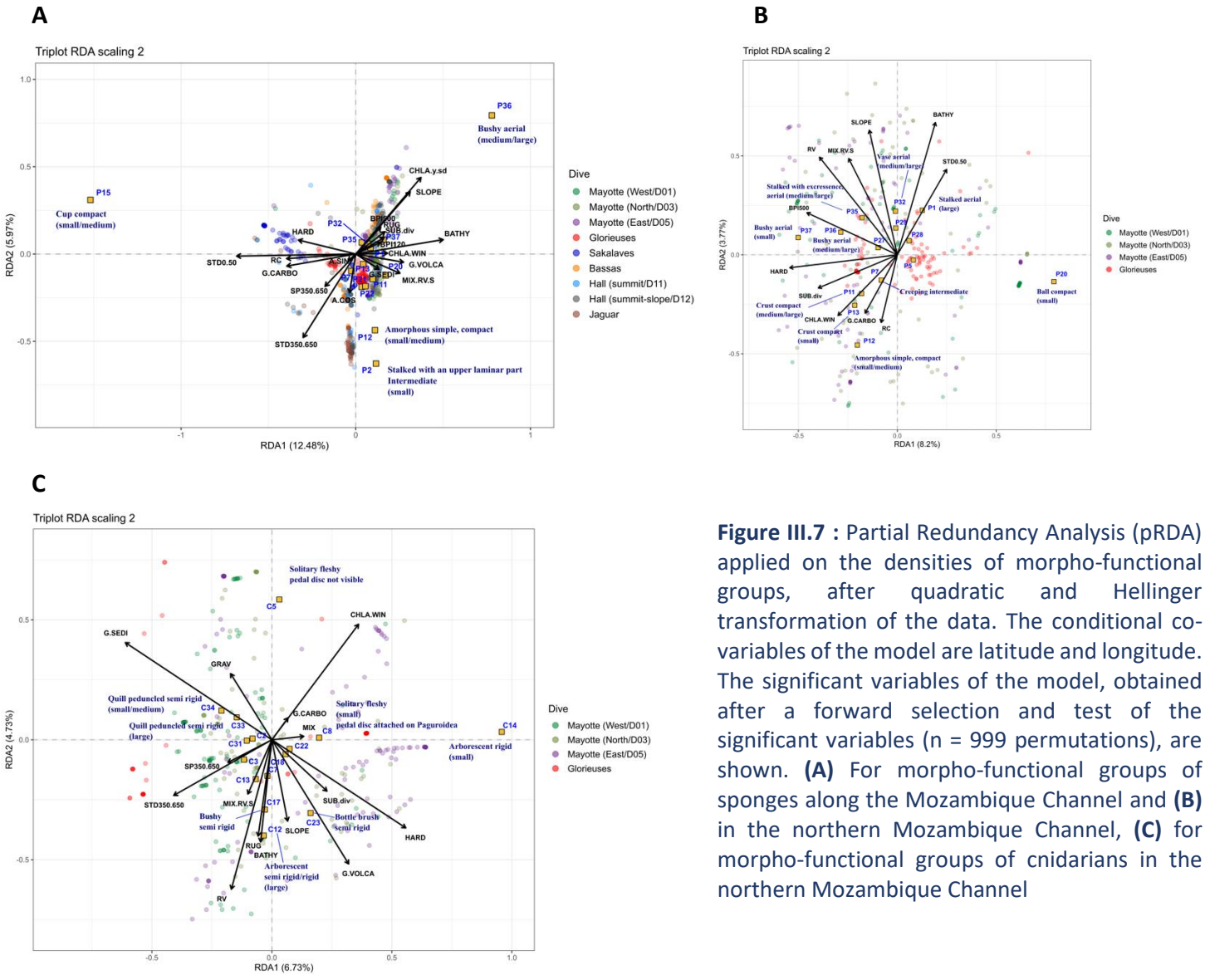

Figure III.7 : Partial Redundancy Analysis (pRDA) applied on the densities of morpho-functional groups, after quadratic and Hellinger transformation of the data. The conditional co-variables of the model are latitude and longitude. The significant variables of the model, obtained after a forward selection and test of the significant variables (n = 999 permutations), are shown. **(A)** For morpho-functional groups of sponges along the Mozambique Channel and **(B)** in the northern Mozambique Channel, **(C)** for morpho-functional groups of cnidarians in the northern Mozambique Channel

When considering the whole Mozambique Channel explored areas, hydrological variables (current and Chla) is the main contributor of sponge MFGs variance (26.4%) followed by the topography and substrate variables explaining 22.5%. Pure contribution of hydrology is quite high (8%) (**Figure III.8A**) but the main part is shared with topography/substrate variables,

geomorphology ones, or combined with spatial variables. Considering only the northern Mozambique Channel (**Figure III.8B**), hydrology contribution is almost two-fold lower, however, topography/substrate contribution remains as high as in the whole channel (~23%) and geomorphology is also of the same order of magnitude than at larger scale (~12%).

A

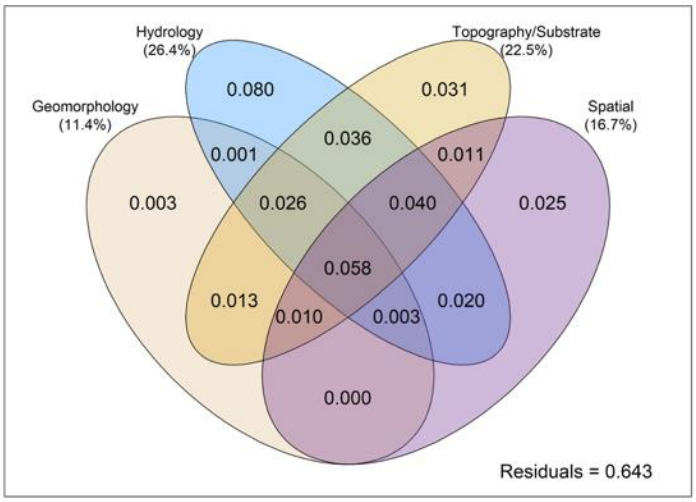

B

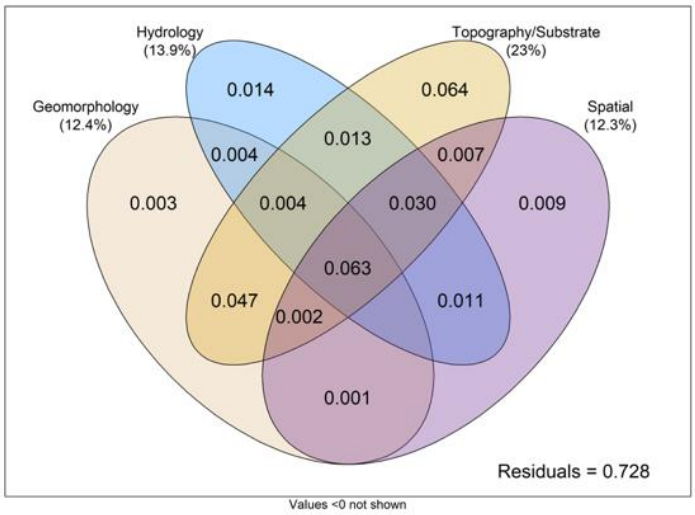

C

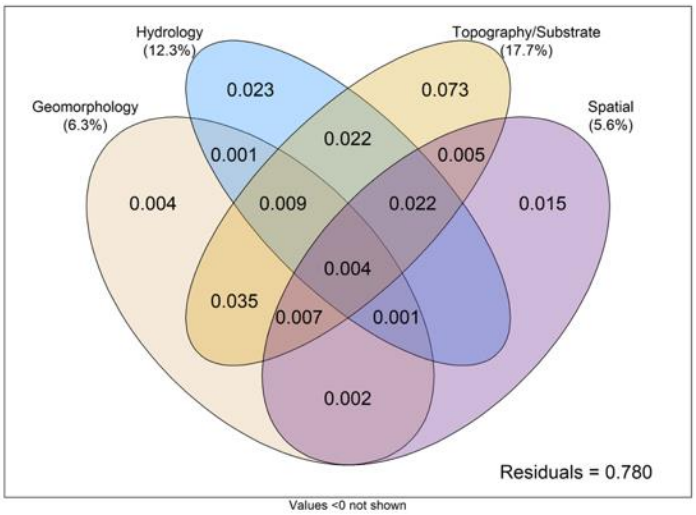

Figure III.8 : Venn diagrams representing the contributions of the different sets of explanatory variables, resulting from a variation partitioning analysis **(A)** for morpho-functional groups of sponges along the Mozambique Channel and **(B)** in the northern Mozambique Channel, **(C)** for morpho-functional groups of cnidarians in the northern Mozambique Channel. Numbers indicate the fractions of variation explained by each set of environmental variables. Contributions < 1% are not shown

RDA run on cnidarians of the northern Mozambique Channel sites, Glorieuses and Mayotte, highlighted 15 significant environmental variables, explaining 19.1% of cnidarian MFGs variance, while spatial variables explained 5.9%, by considering six significant axes (**Figure III.7C**). Sedimentary and volcanic geomorphologies, hardness, volcanic rock, as well as winter Chla and bottom current speed are among the best contributors of the two first axes.

The MFG C5, grouping solitary fleshy form with large polyp and no visible anchoring feature (i.e., Actiniaria) correlates to high winter Chla concentration, as well as sedimentary

geomorphology (G.SEDI) and gravels (GRAV) areas. C33 and C34 – small to large quills (i.e., Pennatulacea) – are also correlated to sedimentary geomorphology. MFGs C13 and C12, grouping medium to large semi-rigid to rigid arborescent forms and C17, a MFG grouping a bushy semi-rigid form with medium polyps (i.e., Zoanthidae) are correlated to high coverage of volcanic rock, bathymetry and rugosity, as well as slope. The MFG C23, grouping bottle-brush forms (e.g., Chrysogorgidae) is also correlated to high slope inclination, and high volcanic geomorphology coverage and so hardness. Other bottle-brush (C22, i.e., Antipatharia) and bushy forms, the latter semi-rigid to rigid with medium polyps (C18) are not well represented on the RDA plan and poorly correlated to explanatory variables. The MFG C14, a small rigid arborescent form (i.e., Sylasteridae incertae) is isolated on the right first dimension part, mostly correlated to hardness, but also areas of variable substrate (mixed substrate, high substrate diversity) and winter Chla. Finally, deep current variability and in lower extent speed at 350-650 m (STD350.650, SP350.3650) contribute also to the dispersion of sites along the two axes and are correlated to the MFG C3 (grouping small solitary forms with large polyp close to the bottom; i.e., scleractinians, anthozoans or cerianthids) and the MFG C31 (small to medium whip, semi-rigid) (**Figure III.7C**).

Topography/substrate are the main factors explaining the variance in cnidarian MFGs in the northern Mozambique Channel (17.7%) (**Figure III.8C**), of which 7.3% correspond to a pure contribution independently of the other variables and also quite high shared contribution with the other sets of explanatory variables, especially geomorphology (3.5%). Hydrology also has a high contribution, with 12.3%, of which 2.3% pure variance explanation, and as much shared contribution with topography/substrate and spatial structure (2.2%).

III.3.3 Structuring role of Porifera and Cnidaria morpho-functional groups on associated megabenthic communities

Redundancy analyses revealed spatial co-structuring between MFGs and the remaining megabenthic community for some taxa (**Figure III.9**).

Along the Mozambique Channel, many sponge MFGs (n = 22) correlate significantly with other megabenthic taxa. The 22 significant sponge MFGs explain 16.6% of the associated megabenthic spatial structure and of which 7.7% representing pure spatial structure (from variation partitioning analysis, not shown).

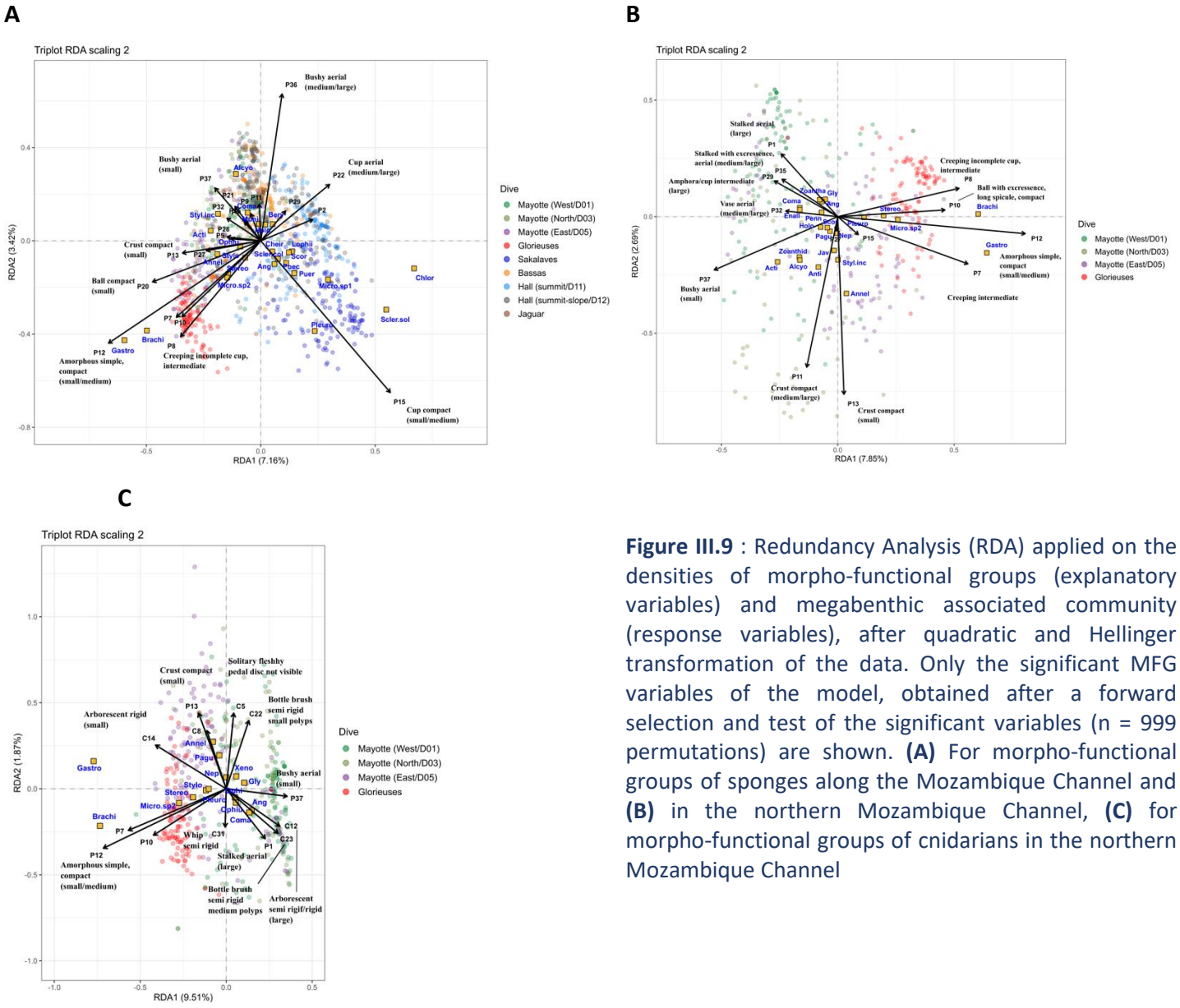

Figure III.9 : Redundancy Analysis (RDA) applied on the densities of morpho-functional groups (explanatory variables) and megabenthic associated community (response variables), after quadratic and Hellinger transformation of the data. Only the significant MFG variables of the model, obtained after a forward selection and test of the significant variables (n = 999 permutations) are shown. **(A)** For morpho-functional groups of sponges along the Mozambique Channel and **(B)** in the northern Mozambique Channel, **(C)** for morpho-functional groups of cnidarians in the northern Mozambique Channel

Among the 22 significant MFGs, only seven have a high contribution to site dispersion along the first two dimensions. High relative abundance of fish (e.g., *Chlorophthalmus*, Pleuronectiformes, *Poecilopsetta*, Scorpaeniformes) and *Micropyga* sp1 sea urchins correlate with P15 (small to medium compact sponges) on the Sakalaves platform (**Figure III.9A**). Other urchins (e.g., *Micropyga* sp2, *Stereocidaris*), although poorly represented along the factorial plan because of their lower abundance, correlate with high relative abundance of intermediate to compact sponges (creeping, ball-shaped, amorphous) (e.g., P8, P10, P12). However, RDA restricted to the northern Mozambique Channel revealed clearer correlation

(**Figure III.9B**). Brachiopoda and Gastropoda, more abundant, also show correlation with these same sponge MFGs, on the Glorieuses terrace.

In the northern Mozambique Channel, 10 out of the 13 significant sponge MFGs highly contribute in site dispersion along the two first dimensions. We observed correlation between high relative abundance of Annelida with sponge encrusting forms (P11, P13) along the northern slope of Mayotte (**Figure III.9B**). Zoanthidae, Alcyonacea and Actiniaria correlate with P37 (grouping aerial bushy morphologies), observed along Mayotte island slopes. Comatulida, Zoantharia and the large colonial scleractinia *Enallopsammia* sp. correlate with MFGs grouping large aerial stalked morphologies – P1 and P35, i.e., *Aphrocallistes* – or other large sponge morphologies (e.g., aerial vases, P32; amphoras and cups, P29), evidencing shared habitat.

Redundancy analyses combining both sponge and cnidarian MFGs as explanatory variables revealed that Ophiuroidea (even poorly represented) and Anguilliformes as well, are also correlated to P1, grouping large sponges stalked morphologies, as well as C23, grouping bottle-brush cnidarian forms (e.g., Chrysogorgidae) and C12 grouping large arborescent semi-rigid to rigid cnidarian forms with compact branching (**Figure III.9C**).

Other taxa, such as *Nepanthia* (asteroid), Paguroidea, Holothuroidea, Anguilliformes, although poorly represented on the graph, appear to have some correlation/co-structure with sponge MFGs (**Figure III.9B**). Among the 15.2% of variance explained by the sponge MFGs, 10.5% represents spatial structure only. The same is observed when combining sponge and cnidarian MFGs, with 15.7% of explained variance and 9.1% representing spatial structure (deduced from pRDAs with spatial variables as covariates).

III.4 Discussion

III.4.1 Spatial distribution of sponge and cnidarian morpho-functional groups

Morpho-functional groups (MFGs) richness differs between seamounts and island slopes. Sponge MFGs richness are higher along the northern and western slopes of Mayotte than in the other sites. A previous study on sponge morphological diversity in the Western Indian Ocean revealed a major influence of substratum nature and heterogeneity in explaining sponge morphological diversity (Bell and Barnes, 2001). It is likely that the high to

intermediate level of substrate diversity quantified along these slopes (Hanafi-Portier et al., in prep.) partly explained their higher sponge MFGs. Compared to the slopes of Mayotte island, the richness of sponge MFGs is almost 2.7 lower on the Sakalaves platform and Hall Bank summit where two dominant compact morphologies were present (small cup and medium to large crust, respectively). A decrease in sponges' morphological diversity in response to increasing current regime was observed in Barnes and Bell (2002), because of the removal of more fragile forms. The high to intermediate current speed and turbulence crossing Sakalaves and Hall may select for a small range of sponge morphologies able to support such hydrodynamics. Despite the strong current speed that crosses Glorieuses platform, this seamount is composed of a diversity of sponge MFGs, whose some are densely covering the summit and able to form large structures (e.g., ball, creeping forms). However, these morphologies have large contact surfaces with seafloor and are generally favored in strong hydrodynamic conditions (Bell and Barnes, 2000; Schönberg, 2021). Conversely, the comparison of cnidarian MFGs richness on the northern Mozambique Channel, reveal that along Mayotte island slopes, cnidarian MFGs richness is three to four-fold higher than on Glorieuses. It is possible that the high sponge densities over this platform generate competition for space or food with cnidarians, which are mostly solitary and small-sized on this site.

We quantified intermediate sponge MFGs beta diversity values for most of the sites (~0.40-0.48), however higher along the eastern slope of Mayotte, and the sloping transect of Hall, while lower on the Glorieuses and Sakalaves platform. Several factors can explain these differences, such as the substrate diversity (which is high along the terrace-upper slope of Hall bank) and the large bathymetric gradient along the eastern slope of Mayotte. Both are much lower on Glorieuses. The discrepancy observed at Glorieuses between a relatively high sponge MFGs richness and low beta diversity one, suggests that the various sponge communities formed on Glorieuses vary only marginally with a lot of rare MFGs (one MFG largely dominate the community) with community changes at the boundary between the summit and the upper slope (LCBD) (**Figure III.6C**), and that these various MFGs reflect the same response to the strong but stable current conditions that flow through the platform. Richness and beta diversity of cnidarian MFGs are much lower on this seamount than along the Mayotte slopes. Along the eastern slope, we quantified MFGs beta diversity comparable to the one obtained

when considering taxonomic composition of the whole megabenthic community (Hanafi-Portier et al., in prep.). It would therefore be mainly the cnidarian communities that generate variability along this slope.

The scale of variability of the cnidarian and sponge MFG assemblages and therefore of the habitats created by these groups highly differ from one site to another (**Figure III.6C-D**). Small scale variability of sponge and cnidarian MFGs composition, evidenced by the number and distribution of the Local Contribution of Beta Diversity – i.e., site with particular MFGs composition – characterise the Mayotte island slopes, especially the northern and western ones while lower variability occurring over larger scale is observed for the other seamounts and both for sponge and cnidarian MFGs. The LCBD along the northern and western slope of Mayotte, were localised on volcanic areas and interface between different substrate types/geomorphologies. The northern and western slopes of Mayotte have high to intermediate substrate diversity, comprising volcanic areas and carbonate bottoms as well as large sedimentary areas interspersed with blocks and rocky bottoms sparsely distributed along the slopes. The substrate heterogeneity over small spatial scales may therefore potentially explain the MFGs richness along these slopes. The spatial variability within each seamount and island slope are generated by few MFGs displaying higher abundance at sites likely displaying their optimal niche.

More generally at the channel scale, MFGs composition and densities differ among sites, even when considering only their shared morphology. We identified four dominant sponge morphologies along the Mozambique Channel whose densities differ among sites. Some sites are highly dominated by one morphology (and one MFG). Aerial bushy forms dominate island external slopes (Mayotte and Bassas), as well as the upper slope of Hall Bank, cup morphologies dominate on seamount summit of Jaguar and Sakalaves (> 90% of the sponges), amorphous simple dominate on Glorieuses terrace (> 90%) and stalked aerial forms dominate Hall summit and are also abundant on its upper slope, and parts of the Mayotte slope and Sakalaves mound. We also identified five dominant cnidarian morphologies in the northern area whose densities differ among sites and comprising rigid and semi-rigid arborescent forms, bushy, bottle-brush and solitary fleshy forms with large polyp.

These differences in MFGs composition were explained by various environmental drivers.

III.4.2 Drivers of the spatial distribution of sponge and cnidarian morpho-functional groups

We highlighted the important role of hydrology, gathering current speed and variability, as well as chlorophyll a concentration (26%) in shaping sponge MFGs composition along the Mozambique Channel, and secondly of substrate and topography variables (23%). Geomorphology also contributes to the spatial patterns with 11.4%. Among the hydrological parameters, we identified surface and deep current variability and speed as significant drivers of sponge MFGs composition. Hydrodynamics is a key parameter for the survival of sponges which, through their pumping activity, will oxygenate themselves, feed on suspended food particles, exchange sexual products and clean their waste while being prevent from detrimental smothering from high sedimentation (Schönberg, 2021). More specifically, currents were correlated to compact sponge forms such as small cups on Sakalaves or small amorphous forms on Glorieuses. Amorphous sponges act as simple massives whose morphologies are not suited to stagnant water and are at risk of being clogged by sedimentation, so prefer intermediate to high and predictable current velocity (Schönberg, 2021). Such water current conditions are encountered on Glorieuses platform. Furthermore, although cup-like sponges appear not to be well suited to strong and variable hydrodynamics, these morphologies could occur in oxygen-reduced environments (Schönberg, 2021), and could explain the high abundance of these forms on the oxygen-poor Sakalaves platform (Hanafi-Portier et al., in prep.). Compact forms, such as crust, creeping and amorphous forms were also correlated to carbonate geomorphology coverage, and carbonate rock as well. It is likely that the high contact surface of these morphologies favours the homogeneous bottom provided by carbonate slab as more robust anchoring and that the high rocky (carbonate) coverage highlight associated low sedimentary rate favouring growth forms poorly resistant to sedimentation pressure (e.g., crust) (Schönberg, 2021). A small compact ball morphology (P20), abundantly observed over Glorieuses especially, and over Mayotte island slopes, was poorly correlated to environmental drivers. These ball morphologies could tolerate a wider range of abiotic conditions than other sponge morphologies; including both high sedimentation/low water flow and turbulent water (Schönberg, 2021). It is possible that the contrasted environmental conditions observed along Glorieuses compared to the Mayotte island slope, explained the poor environmental matching.

Delicate sponge morphologies, with aerial compactness, such as bushy, stalked and vase morphologies were mostly correlated to topography (slope, depth, rugosity, BPI) and substrate comprising volcanic rock coverage or mixed with sediment while were weakly correlated to current variability. These growth forms commonly develop in nutrient depleted environments, with poor water and nutrient mixing (Schönberg, 2021).

Topography and substrate play a predominant structuring role in shaping cnidarian MFGs community (~18%), followed by hydrological parameters (current and Chla concentration) (12.3%), and the same pattern was observed for sponge when only considering the northern Mozambique Channel, for the latter probably due to the lower contribution of the hydrographic processes (mesoscale eddies) that take place in the center and south of the channel and therefore driving part of the variability at this scale. Nevertheless in the northern part, deep current variability and velocity were identified as significant drivers of cnidarian MFGs composition, as well as winter Chla concentration.

Substrate preferences of the cnidarians depending on their anchoring mode can explain differences in MFGs composition between and within sites. Areas composed of gravels and fine sediment were positively correlated to the high relative abundance of actinians with no visible anchoring features (e.g., C5), as for quill morphologies (pennatulids) on the northern and western slope of Mayotte. Pennatulids have a peduncled anchoring mode, embedded in the sediment (Bayer, 1983). Conversely, medium to large arborescent forms, and bottle-brush forms (e.g., Chrysogorgiidae alcyonaceans) or bushy one (e.g., Zoanthidae) with a calcified disc as attachment mode, were correlated to volcanic rock (or volcanic geomorphology), but also to rugosity, that characterised roughness provided by volcanic reliefs, and that benefit to settlement of these stalked morphologies. These medium to large stalked colonial morphologies were also correlated to slope. It is established that suspension feeder corals favor sloping areas where rectified flow and current acceleration enhance food particle resuspension and so food fluxes (Genin et al., 1986).

Finally, both for sponge and cnidarian MFGs, the hydrology displays high shared contribution with topography, substrate and geomorphology in explaining MFGs variance in composition, revealing the complex interaction prevailing between the seamounts topography, rectified current flow and resulting processes in food fluxes and larvae recruitment.

The high spatial structure detected may include environmental variables spatially structured but not measured, or not identified by analyses (part of the variability is linked to individual taxa forming the MFGs); or biological processes (population dynamics, interactions between taxa, neutral processes) which could be detected for morpho-functional groups gathering one or a few taxa.

III.4.3 Structuring role of sponge and cnidarian morpho-functional groups on the associated megabenthic communities

Our study highlights spatial co-structuring between some sponge and cnidarian morpho-functional groups (MFGs) with other megabenthic taxa observed on seafloor images.

Although only part of the spatial structure of the megafauna community is explained by the occurrence of MFGs, the study evidenced some correlations between mobile, or sessile taxa and these biological structures whose size, flexibility, and architectural complexity – some of the characters we used to define the groups – are related to species diversity (Buhl-Mortensen et al., 2010). On Mozambique Channel seamounts and island slopes, comatulids and ophiuroids have been observed positively correlated with large stalked sponge forms or arborescent cnidarians. These large structures allow the associated taxa to rise into the bottom boundary layer – a zone with a strong gradient of energy and chemical and organic components – which is conducive to the provision of food for these taxa. Depending on the feeding mode of the taxa associated with these structures (e.g., deposit feeders, filter feeders), large arborescent forms would both provide a platform for passive particle filtration (e.g., for crinoids) or benefit from particles agglomerated on the mucus secreted by cnidarians (e.g., for ophiuroids) (Patton, 1972). Zoantharia were also correlated to large stalked sponge (e.g., Hyalonematidae) while never observed on hard bottom or sediment. It is likely that these Zoantharia colonies would benefit from the elevated position provided by the sponge stem to enhance their filtering activity.

We also observed a correlation between small actinians (C5) and bushy aerial sponges. This association was observed from the images, in which the small actinians were located in the interstitial space provided by the excrescences of bushy sponges. In this way, actinians could benefit from a sheltered environment and of the water flow and food fluxes crossing the sponge interstices.

Annelids display co-structure with encrusting sponges but here, reflecting more the co-occurrence of tubicole annelids and encrusting sponges over rocky surface.

Furthermore, a high proportion of echinoids (*Mircopyga*, *Stereocidaris*, *Stylocidaris* genera) were related to the densities of compact sponges such as creeping, ball-shaped and amorphous sponges. Cidaroid echinoids were reported as feeding on sponges (Bo et al., 2012) and would explain the spatial co-structuring between the sponge MFGs and echinoids observed in our study.

However, many other associations are not visible as we only considered megafauna in the images while sponge and coral association with macrofauna and meiofauna commonly occur (e.g., copepod, amphipod, polychaete) (Buhl-Mortensen et al., 2010; Wulff, 2006).

Those are interesting insights into biological interaction/association but should be interpreted with caution, as the observed co-structures cannot be dissociated from a potential co-response to the same environmental factors not considered in the RDA analyses, but influencing the spatial pattern of megabenthic communities. Besides, when considering partial RDA, with sponge and cnidarian MFGs location as covariates, we revealed high variation explained only by the spatial structure. This spatial structure includes the environmental drivers, themselves spatially structured, and playing a role in shaping megabenthic community structure, but also potential biogeographic patterns. On a smaller scale, it includes the effect of community dynamics that comprises biological interactions such as association with cryptic species, macrofauna and other small-sized organisms not accessible from images and so not considered in the analyses.

Complementary analyses of the correlation between the richness and beta diversity of cnidarian and sponge habitats and the richness and beta diversity of the associated megafauna would make it possible to test the effect of these biogenic structures on the associated diversity, in particular by comparing their structuring effect in sedimentary and rocky areas. De la Torriente et al. (2018) indeed revealed over seamount a greater structuring effect of habitat-forming taxa in soft and mixed bottom compared to rocky one, as a result of higher effect of structural complexity in more homogeneous habitat.

III.4.4 Benefits and limitations of the morpho-functional groups approach

Our results using morpho-functional groups provide further details on spatial structure of sponge and cnidarian communities over seamounts and island slopes explored in the Mozambique Channel. Our previous study was based on high ranking identification (mainly order for cnidarians, class for sponges) (Hanafi-Portier et al., in prep.) and identified Hexactinellida and Demospongiae (sponges), as for several cnidarian orders (e.g., Antipatharia, Alcyonacea, Scleractinia) as strong contributors of the high beta diversity quantified over the channel seamounts and island slopes. These taxa displayed patchy distribution forming locally habitats of more or less high abundance. Here, the morpho-functional group approach on the same dataset reveals patterns of spatial variability of different growth/morphological strategies, occurring even on a small scale (e.g., Mayotte island slopes).

However, the morpho-functional group classification seems to be of greater interest to study more precisely the spatial structuring of sponge assemblages in response to environmental factors than for cnidarians. For sponges, compared to the identifications mostly limited to class rank, we observed a multitude of morphologies and combinations of possible traits (e.g., compactness, size) sometimes observable in both hexactinellids and demosponges. For cnidarians, the morpho-functional groups identified as contributors to beta diversity mainly reflect orders identified at higher rank (e.g., quill with peduncle means Pennatulacea, solitary fleshy means Actiniaria, or solitary semi-fleshy means Alcyoniidae). Comparing morphological categories (using CATAMI) and photo-taxa; Untiedt et al. (2021) find also similar patterns of assemblage composition for cnidarians, between the two classifications, although the latter performs better in detecting dominant and scarce but locally abundant coral entities.

However, a few morphologies gather several taxa, at the order, or finer levels (e.g., bottle-brush for Antipatharia and Alcyonacea – Chrysogorgiidae or *Acanella* –). Similarly for Porifera, with for example cup morphology that exist both within the Hexactinellida and the Demospongiae classes, however one additional trait may be specific to one taxa (e.g., compactness addition allows splitting between Hexactinellida (cup aerial) and Demospongiae (cup compact).

Furthermore, the cnidarian MFGs identified as contributors to beta diversity within each site (SCBD) mainly reflect the orders identified as having high SCBD for each site in Hanafi-Portier et al., in prep. (cf. chapitre 2). The morpho-functional group approach with sponges is therefore of more interest in this context. Furthermore, the RDAs with environmental factors do not highlight other responses than those already identified with the cnidarian orders (Hanafi-Portier et al., in prep.).

Some traits used in our classification are subjective (e.g., spacing between branches) and should be clarified, based on measurements on the images; others require the taxonomic knowledge of the taxa (e.g., root system of the genus *Acanella* or level of rigidity for cnidarians) to score the different morphotypes.

Owing to the close relationship between some morphologies and their taxonomic assignment, this approach raises the following question: are we describing a functional response of these sponge and cnidarian groups to the habitat or is this an expression of their taxonomy?

To answer the question, it would be interesting to apply this morpho-functional approach to image data of sponges and cnidarians calibrated by physical samples (e.g., using ROV). Therefore, the photo-taxa in the images could be identified at a finer identification rank, allowing to assess whether the classified morpho-groups gather different taxa, or on the contrary the same taxonomic group (family, genus). In the latter case, the morpho-groups would reflect a phylogenetic signal rather than a functional response to the habitat.

The use of MFGs classification also enables us to assess the structuring role of habitat-forming taxa, by linking indirectly – via the morpho-functional groups – different traits characterising MFGs (e.g., size, stalk) with the associated fauna. Other analytical angles of this dataset (functional analyses) using biological trait approach (BTA) (Beauchard et al., 2017; Bremner et al., 2006; Dray et al., 2014; Dray and Legendre, 2008; Kleyer et al., 2012) through fourth-corner method would allow a better assessment of the correlation between response traits and environmental conditions, and also the effect traits have on the associated fauna. For example, response of size classes to abiotic drivers (e.g., Chla) or effect on richness of associated fauna could be tested that way, as size classes were sometimes hiden/mixed within the same MFG. Nonetheless, the advantage of the morpho-functional group classification approach is that it provides a less complex dataset than a matrix of multiple traits and allows

otherwise applied analyses to be performed on taxa community. However, the high number of classified morpho-functional groups (up to 37) may have made the interpretation more difficult. It would be interesting to define a higher cut-off point within the hierarchical ascendant classification in order to find a compromise between accuracy in the analysis description (level of description of community and spatial structures) and the ease of interpretation. Furthermore, we identified some intra-morphotype variability regarding some traits (e.g., inclination towards the current) according to the observed image sets. Fuzzy coding of the traits matrix would be an optimal analytical option to consider trait variance within morphotype, a method proposed initially to test intraspecific trait variability (Beauchard et al., 2017).

In the absence of possible accurate identification of sponge and cnidarian groups, a common problem encountered from images, a morpho-functional approach is a reliable and less time-consuming method, enabling a more detailed study of the structuring patterns of the sponge assemblages. This method also provides additional information not obtained using the taxonomic entity, by enabling assessment of the structuring role of habitat-forming taxa on associated communities. Annotation using a multi-traits approach may take a little longer than annotation of morphotypes alone, however the use of machine learning could advance the first stage of morphology classification.

To our knowledge, this is the first study applying beta diversity analysis as well as “taxa” (SCBD) or sites (LCBD) contributors to beta diversity, to morpho-functional groups. Such metrics and framework would enable the identification of vulnerable habitats (from SCBD metrics) and spatial scales of variability (from LCBD metrics) performing different functional roles and responding differently to disturbance according to their morpho-functional groups composition.

III.5 Conclusion

The main results of the case study of cnidarian and sponge community structure in the Mozambique Channel using a morpho-functional approach are:

- No consistent pattern of sponge morpho-functional groups (MFGs) richness differences occurs in the northern Mozambique Channel, neither among seamount and island slopes (Glorieuses and Mayotte) nor among the island slopes of Mayotte. In

the southern Mozambique Channel, there is a weak MFGs richness difference (~ factor 1.5) for Hall (summit-slope) and Jaguar compared to the summit of Hall and Sakalaves, and with island slope of Bassas. However, the pattern of sponge MFGs richness differs between some of the northern and southern seamounts, as well as between Mayotte and Bassas da India island slopes (factor of 2-3). For cnidarians in the northern part of the Mozambique Channel, MFGs richness differ by factor 3 to 4 when comparing Mayotte island slopes with Glorieuses seamounts; while no differences occur between Mayotte island slopes.

- Beta diversity of sponge MFG assemblages is intermediate (0.44-0.54) both on seamounts and island slopes, except at Glorieuses and Sakalaves seamounts, where we estimated low values (< 0.40). Cnidarian MFGs beta diversities are high on Mayotte slopes (up to 0.61), while lower on Glorieuses seamounts (0.39).

- The scale of variability of the cnidarian and sponge MFG assemblages' composition highly differ among sites, over small spatial scale (0.06 km) (eastern and northern slope of Mayotte) to larger scale on the other sites.

- Therefore, the diversity of biogenic habitats provided by these MFG assemblages, as well as their spatial distribution differ among seamounts and island slopes.

- Volcanic geomorphological seafloor, and interface areas (substrate type, sloping topography) are characterised by unique combinations of MFG assemblages.

- MFG assemblages differ between sites in composition and densities.

- Hydrology is the main driver of sponge MFGs distribution (26% contribution) along the channel followed by substrate and topography (23%) and geomorphology (11.4%). Topography and substrate are the predominant drivers of cnidarian MFGs in the northern part of the channel (~18%), followed by hydrology (12.3%) while geomorphology plays a lower role (~6%). Hydrology has a high shared contribution with topography, substrate and geomorphology, both for sponges and cnidarians, highlighting the role that the complex interaction between seamount morphology and currents plays in the structure of sponge and cnidarian MFGs.

- We identified correlation between some MFGs with other megabenthic taxa (e.g., Zoantharia with large sponge stalked forms; ophiuroids with large arborescent cnidarian morphologies; echinoids with amorphous or creeping sponges); revealing the structuring role sponge and cnidarian MFGs play on associated benthic megafauna.

The main methodological results of this study are:

- Highlighting the interest of a morpho-functional approach, particularly for sponges, to analyse more finely the structure of sponge communities in response to environmental constraints.

- It also allows a primary evaluation of the structuring role of biogenic habitats on the associated community (e.g., sponges/urchins, Actiniaria and Zoantharia/sponges; ophiuroids/large arborescent cnidarians), using qualitative traits to characterise the micro-habitats these groups provide.

- The method adaptability: in terms of annotation and combination of possible traits (no single path); of classification method and choice of cut-off point. The method is also repeatable and evolves with the knowledge acquired.

- Further perspectives include correlating taxonomic diversity of cnidarians and sponges, with diversity in MFG (diversity of function?), and taxonomic traits with morphological traits (habitat function? or phylogenetic signal?).

- The provision of an explicit method to describe the morphological variation of sponges and cnidarians that can be measured from images, focusing on the traits that characterise how they create habitat. This allows us to identify the factors that explain the spatial distribution of these traits and to investigate how they explain the distribution of organisms for which they are potentially a habitat.

III.6 References

Althaus, F., Hill, N., Edwards, L., Ferrari, R., 2014. CATAMI Classification Scheme for scoring marine biota and substrata in underwater imagery 102.

Althaus, F., Hill, N., Ferrari, R., Edwards, L., Przeslawski, R., Schönberg, C.H.L., Stuart-Smith, R., Barrett, N., Edgar, G., Colquhoun, J., Tran, M., Jordan, A., Rees, T., Gowlett-Holmes, K., 2015. A Standardised Vocabulary for Identifying Benthic Biota and Substrata from Underwater Imagery: The CATAMI Classification Scheme. PLOS ONE 10, e0141039. https://doi.org/10.1371/journal.pone.0141039

Audru, J.-C., Guennoc, P., Thinon, I., Abellard, O., 2006. Bathymay : la structure sous-marine de Mayotte révélée par l'imagerie multifaisceaux. Comptes Rendus Geoscience 338, 1240–1249. https://doi.org/10.1016/j.crte.2006.07.010

Baco, A.R., Morgan, N.B., Roark, E.B., 2020. Observations of vulnerable marine ecosystems and significant adverse impacts on high seas seamounts of the northwestern Hawaiian Ridge and Emperor Seamount Chain. Marine Policy 115, 103834. https://doi.org/10.1016/j.marpol.2020.103834

Barnes, D.K.A., Bell, J.J., 2002. Coastal sponge communities of the West Indian Ocean: morphological richness and diversity. African J Ecol 40, 350–359. https://doi.org/10.1046/j.1365-2028.2002.00388.x

Bayer, F.M. (Ed.), 1983. Illustrated trilingual glossary of morphological and anatomical terms applied to octocorallia. Brill, Leiden.

Beauchard, O., Veríssimo, H., Queirós, A.M., Herman, P.M.J., 2017. The use of multiple biological traits in marine community ecology and its potential in ecological indicator development. Ecological Indicators 76, 81–96. https://doi.org/10.1016/j.ecolind.2017.01.011

Beazley, L.I., Kenchington, E.L., Murillo, F.J., Sacau, M. del M., 2013. Deep-sea sponge grounds enhance diversity and abundance of epibenthic megafauna in the Northwest Atlantic. ICES Journal of Marine Science 70, 1471–1490. https://doi.org/10.1093/icesjms/fst124

Bell, J., 2007. Contrasting patterns of species and functional composition of coral reef sponge assemblages. Mar. Ecol. Prog. Ser. 339, 73–81. https://doi.org/10.3354/meps339073

Bell, J.J., 2008. The functional roles of marine sponges. Estuarine, Coastal and Shelf Science 79, 341–353. https://doi.org/10.1016/j.ecss.2008.05.002

Bell, J.J., Barnes, D.K.A., 2001. Sponge morphological diversity: a qualitative predictor of species diversity? Aquatic Conserv: Mar. Freshw. Ecosyst. 11, 109–121. https://doi.org/10.1002/aqc.436

Bell, J.J., Barnes, D.K.A., 2000. The influences of bathymetry and flow regime upon the morphology of sublittoral sponge communities. J. Mar. Biol. Ass. 80, 707–718. https://doi.org/10.1017/S0025315400002538

Bo, M., Bertolino, M., Bavestrello, G., Canese, S., Giusti, M., Angiolillo, M., Pansini, M., Taviani, M., 2012. Role of deep sponge grounds in the Mediterranean Sea: a case study in southern Italy. Hydrobiologia 687, 163–177. https://doi.org/10.1007/s10750-011-0964-1

Borcard, D., Gillet, F., Legendre, P., 2018. Numerical Ecology with R, Use R! Springer International Publishing, Cham. https://doi.org/10.1007/978-3-319-71404-2

Bourillet, J.-F., Ferry, J.-N., Bourges, P., 2013. PAMELA : Passive Margins Exploration Laboratories. https://doi.org/10.18142/236

Bremner, J., Rogers, S., Frid, C., 2006. Methods for describing ecological functioning of marine benthic assemblages using biological traits analysis (BTA). Ecological Indicators 6, 609–622. https://doi.org/10.1016/j.ecolind.2005.08.026

Buhl-Mortensen, L., Vanreusel, A., Gooday, A.J., Levin, L.A., Priede, I.G., Buhl-Mortensen, P., Gheerardyn, H., King, N.J., Raes, M., 2010. Biological structures as a source of habitat heterogeneity and biodiversity on the deep ocean margins: Biological structures and biodiversity. Marine Ecology 31, 21–50. https://doi.org/10.1111/j.1439-0485.2010.00359.x

Chappell, J., 1980. Coral morphology, diversity and reef growth. Nature 286, 249–252. https://doi.org/10.1038/286249a0

Corbari, L., Samadi, S., Olu, K., 2017. BIOMAGLO cruise, RV Antea. https://doi.org/10.17600/17004000

Courgeon, S., Jorry, S.J., Camoin, G.F., BouDagher-Fadel, M.K., Jouet, G., Révillon, S., Bachèlery, P., Pelleter, E., Borgomano, J., Poli, E., Droxler, A.W., 2016. Growth and demise of Cenozoic isolated carbonate platforms: New insights from the Mozambique Channel seamounts (SW Indian Ocean). Marine Geology 380, 90–105. https://doi.org/10.1016/j.margeo.2016.07.006

de la Torriente, A., Serrano, A., Fernández-Salas, L.M., García, M., Aguilar, R., 2018. Identifying epibenthic habitats on the Seco de los Olivos Seamount: Species assemblages and environmental characteristics. Deep Sea Research Part I: Oceanographic Research Papers 135, 9–22. https://doi.org/10.1016/j.dsr.2018.03.015

Denis, V., Ribas-Deulofeu, L., Sturaro, N., Kuo, C.-Y., Chen, C.A., 2017. A functional approach to the structural complexity of coral assemblages based on colony morphological features. Scientific Reports 7. https://doi.org/10.1038/s41598-017-10334-w

Dray, S., Bauman, D., Blanchet, F.G., Borcard, D., Clappe, S., Guenard, G., Jombart, T., Larocque, G., Legendre, P., Madi, N., Wagner, H., 2022. adespatial: Multivariate Multiscale Spatial Analysis. R package version 0.3-16.

Dray, S., Choler, P., Dolédec, S., Peres-Neto, P.R., Thuiller, W., Pavoine, S., ter Braak, C.J.F., 2014. Combining the fourth-corner and the RLQ methods for assessing trait responses to environmental variation. Ecology 95, 14–21. https://doi.org/10.1890/13-0196.1

Dray, S., Dufour, A.-B., 2007. The ade4 Package: Implementing the Duality Diagram for Ecologists. J. Stat. Soft. 22. https://doi.org/10.18637/jss.v022.i04

Dray, S., Legendre, P., 2008. Testing the species traits–environment relationships: the fourth-corner problem revisited. Ecology 89, 3400–3412. https://doi.org/10.1890/08-0349.1

FAO (Ed.), 2009. International guidelines for the management of deep-sea fisheries in the high seas: = Directives internationales sur la gestion de la pêche profonde en haute mer. Food and Agriculture Organization of the United Nations, Rome.

Genin, A., Dayton, P.K., Lonsdale, P.F., Spiess, F.N., 1986. Corals on seamount peaks provide evidence of current acceleration over deep-sea topography. Nature 322, 59–61. https://doi.org/10.1038/322059a0

Hadi, T.A., Budiyanto, A., Wentao, N., 2015. The morphological and species diversity of sponges in coral reef ecosystem in the Lembeh Strait, Bitung 13.

Hanafi-Portier, M., Samadi, S., Corbari, L., Chan, T.-Y., Chen, W.-J., Chen, J.-N., Lee, M.-Y., Mah, C., Saucède, T., Borremans, C., Olu, K., 2021. When Imagery and Physical Sampling Work Together: Toward an Integrative Methodology of Deep-Sea Image-Based Megafauna Identification. Front. Mar. Sci. 8, 749078. https://doi.org/10.3389/fmars.2021.749078

Hawkes, N., Korabik, M., Beazley, L., Rapp, H., Xavier, J., Kenchington, E., 2019. Glass sponge grounds on the Scotian Shelf and their associated biodiversity. Mar. Ecol. Prog. Ser. 614, 91–109. https://doi.org/10.3354/meps12903

Hein, J.R., Conrad, T.A., Staudigel, H., 2010. Seamount mineral deposits, a source of rare metals for high-technology industries. Oceanography 23, 184–189.

Jouet, G., Deville, E., 2015. PAMELA-MOZ04 cruise, RV Pourquoi pas ?,. https://doi.org/10.17600/15000700

Kleyer, M., Dray, S., Bello, F., Lepš, J., Pakeman, R.J., Strauss, B., Thuiller, W., Lavorel, S., 2012. Assessing species and community functional responses to environmental gradients: which multivariate methods? Journal of Vegetation Science 23, 805–821. https://doi.org/10.1111/j.1654-1103.2012.01402.x

Krell, F.-T., 2004. Parataxonomy vs. taxonomy in biodiversity studies – pitfalls and applicability of 'morphospecies' sorting. Biodiversity and Conservation 13, 795–812. https://doi.org/10.1023/B:BIOC.0000011727.53780.63

Langenkämper, D., Zurowietz, M., Schoening, T., Nattkemper, T.W., 2017. BIIGLE 2.0 - Browsing and Annotating Large Marine Image Collections. Frontiers in Marine Science 4. https://doi.org/10.3389/fmars.2017.00083

Legendre, P., De Cáceres, M., 2013. Beta diversity as the variance of community data: dissimilarity coefficients and partitioning. Ecology Letters 16, 951–963. https://doi.org/10.1111/ele.12141

Mary George, A., Brodie, J., Daniell, J., Capper, A., Jonker, M., 2018. Can sponge morphologies act as environmental proxies to biophysical factors in the Great Barrier Reef, Australia? Ecological Indicators 93, 1152–1162. https://doi.org/10.1016/j.ecolind.2018.06.016

McDonald, J.I., Hooper, J.N.A., McGuinness, K.A., 2002. Environmentally influenced variability in the morphology of Cinachyrella australiensis (Carter 1886) (Porifera : Spirophorida : Tetillidae). Mar. Freshwater Res. 53, 79–84. https://doi.org/10.1071/mf00153

McKinney, F.K., 1981. Planar branch systems in colonial suspension feeders. Paleobiology 7, 344–354. https://doi.org/10.1017/S0094837300004656

McMurray, S., Pawlik, J., Finelli, C., 2014. Trait-mediated ecosystem impacts: how morphology and size affect pumping rates of the Caribbean giant barrel sponge. Aquat. Biol. 23, 1–13. https://doi.org/10.3354/ab00612

Morgan, N.B., Baco, A.R., 2021. Recent fishing footprint of the high-seas bottom trawl fisheries on the Northwestern Hawaiian Ridge and Emperor Seamount Chain: A finer-scale approach to a large-scale issue. Ecological Indicators 121, 107051. https://doi.org/10.1016/j.ecolind.2020.107051

Oksanen, J., Blanchet, F.G., Friendly, M., Kindt, R., Legendre, P., McGlinn, D., Minchin, P.R., O'Hara, R.B., Gavin, L.S., Peter, S., H. Stevens, M. henry, Szoecs, E., Wagner, H., 2020. vegan: Community Ecology Package. R package version 2.5-7.

Olu, K., 2014. PAMELA-MOZ01 cruise, RV L'Atalante,. https://doi.org/10.17600/14001000

Pante, E., France, S.C., Couloux, A., Cruaud, C., McFadden, C.S., Samadi, S., Watling, L., 2012. Deep-Sea Origin and In-Situ Diversification of Chrysogorgiid Octocorals. PLoS ONE 7, e38357. https://doi.org/10.1371/journal.pone.0038357

Patton, W.K., 1972. Studies on the animal symbionts of the gorgonian coral, leptogorgia virgulata (lamarck). Bulletin of Marine Science 22, 419–431.

Pronzato, R., Bavestrello, G., Cerrano, C., 1998. Morpho-functional adaptations of three species of spongia (porifera, demospongiae) from a mediterranean vertical cliff. Bulletin of Marine Science 63, 12.

Quattrini, A.M., Ross, S.W., Carlson, M.C.T., Nizinski, M.S., 2012. Megafaunal-habitat associations at a deep-sea coral mound off North Carolina, USA. Mar Biol 159, 1079–1094. https://doi.org/10.1007/s00227-012-1888-7

R Core Team, 2021. R: A language and environment for statistical computing. Vienna: R Foundation for Statistical Computing.

Rogers, A., Blanchard, J.L., Mumby, P.J., 2014. Vulnerability of Coral Reef Fisheries to a Loss of Structural Complexity. Current Biology 24, 1000–1005. https://doi.org/10.1016/j.cub.2014.03.026

Rossi, S., Bramanti, L. (Eds.), 2020. Perspectives on the Marine Animal Forests of the World. Springer International Publishing, Cham. https://doi.org/10.1007/978-3-030-57054-5

Rossi, S., Bramanti, L., Gori, A., Orejas, C. (Eds.), 2017. Marine Animal Forests: The Ecology of Benthic Biodiversity Hotspots. Springer International Publishing, Cham. https://doi.org/10.1007/978-3-319-21012-4

Schönberg, C.H.L., 2021. No taxonomy needed: Sponge functional morphologies inform about environmental conditions. Ecological Indicators 129. https://doi.org/https:DDdoi.orgD10.101BDj.ecolind.2021.107A0B

Schönberg, C.H.L., 2015. Self-cleaning surfaces in sponges. Mar Biodiv 45, 623–624. https://doi.org/10.1007/s12526-014-0302-8

Schönberg, C.H.L., Fromont, J., 2014. (PDF) Sponge functional growth forms as a means for classifying sponges without taxonomy [WWW Document]. ResearchGate. URL https://www.researchgate.net/publication/278627643_Sponge_functional_growth_forms_as_a_means_for_classifying_sponges_without_taxonomy (accessed 6.22.20).

Tabachnick, K.R., 1991. Adaptation of the Hexactinelid Sponges to Deep-Sea Life 9.

Todd, P.A., 2008. Morphological plasticity in scleractinian corals. Biological Reviews 83, 315–337. https://doi.org/10.1111/j.1469-185X.2008.00045.x

Tsakalos, J.L., Renton, M., Riviera, F., Veneklaas, E.J., Dobrowolski, M.P., Mucina, L., 2019. Trait-based formal definition of plant functional types and functional communities in the multi-species and multi-traits context. Ecological Complexity 40, 100787. https://doi.org/10.1016/j.ecocom.2019.100787

Untiedt, C.B., Williams, A., Althaus, F., Alderslade, P., Clark, M.R., 2021. Identifying Black Corals and Octocorals From Deep-Sea Imagery for Ecological Assessments: Trade-Offs Between Morphology and Taxonomy. Front. Mar. Sci. 8, 722839. https://doi.org/10.3389/fmars.2021.722839

Watling, L., Auster, P.J., 2021. Vulnerable Marine Ecosystems, Communities, and Indicator Species: Confusing Concepts for Conservation of Seamounts. Front. Mar. Sci. 8, 622586. https://doi.org/10.3389/fmars.2021.622586

Wickham, H., Chang, W., Wickham, M.H., 2016. Package 'ggplot2'. Create elegant data visualisations using the grammar of graphics. Version, 2(1), 1-189.

Williams, A., Althaus, F., Green, M., Maguire, K., Untiedt, C., Mortimer, N., Jackett, C.J., Clark, M., Bax, N., Pitcher, R., Schlacher, T., 2020. True Size Matters for Conservation: A Robust Method to Determine the Size of Deep-Sea Coral Reefs Shows They Are Typically Small on Seamounts in the Southwest Pacific Ocean. Front. Mar. Sci., a 7, 187. https://doi.org/10.3389/fmars.2020.00187

Wulff, J.L., 2006. Resistance vs recovery: morphological strategies of coral reef sponges. Funct Ecology 20, 699–708. https://doi.org/10.1111/j.1365-2435.2006.01143.x

Zawada, K.J.A., Dornelas, M., Madin, J.S., 2019a. Quantifying coral morphology. Coral Reefs 38, 1281–1292. https://doi.org/10.1007/s00338-019-01842-4

Zawada, K.J.A., Madin, J.S., Baird, A.H., Bridge, T.C.L., Dornelas, M., 2019b. Morphological traits can track coral reef responses to the Anthropocene. Functional Ecology. https://doi.org/10.1111/1365-2435.13358

III.7 Supplementary materials

Supplementary material III.1 : Illustrative images of (A) cnidarian morpho-functional groups and (B) sponge morpho-functional groups.

Corresponding taxa for Figure 3A: 1 – *Epizoanthus*; 2 – *Zoantharia* colonizing sponge stem; 3,5 – Alcyoniidae, 4 – *Anthomastus*; 6,8 – Scleractinia (solitary); 7 – Ceriantharia; 9 – *Javania*; 10 – Scleractinia (solitary); 11,18 – Actiniaria; 19,20 – Actiniaria within bushy sponges; 21 – Actiniaria on Paguroidea; 23,26 – Antipatharia; 27 – Alcyonacea; 28 – Antipatharia; 29 – Scleraxonia; 30 – Anthozoa (colonial); 31 – *Corallium* incertae; 32 – *Enallopsammia*; 33 – Primnoidae; 34 – Scleractinia (colonial); 35, 36 – Anthozoa colonial; 37 – Holaxonia; 38 – Isididae; 39 – Primnoidae; 40,41 – Stylasteridae incertae; 42 – Alcyonacea; 43 – Anthozoa (colonial); 44 – Isididae; 45,46 – Zoanthidae; 47,52; Anthozoa (colonial); 53,54 – *Acanella*; 55,56 – Antipatharia; 57 – *Chrysogorgia*; 58 – Chrysogorgiidae; 59, 60 – Alcyonacea; 61 – *Bathyalcyon*; 62,63 – Hydrozoa; 64 – *Umbellula*; 65 – Isididae; 66,67 – Anthozoa (colonial); 68 – Isididae; 69,70 – Anthozoa (colonial); 71,72 – Alcyonacea; 73,79 – Pennatulacea.

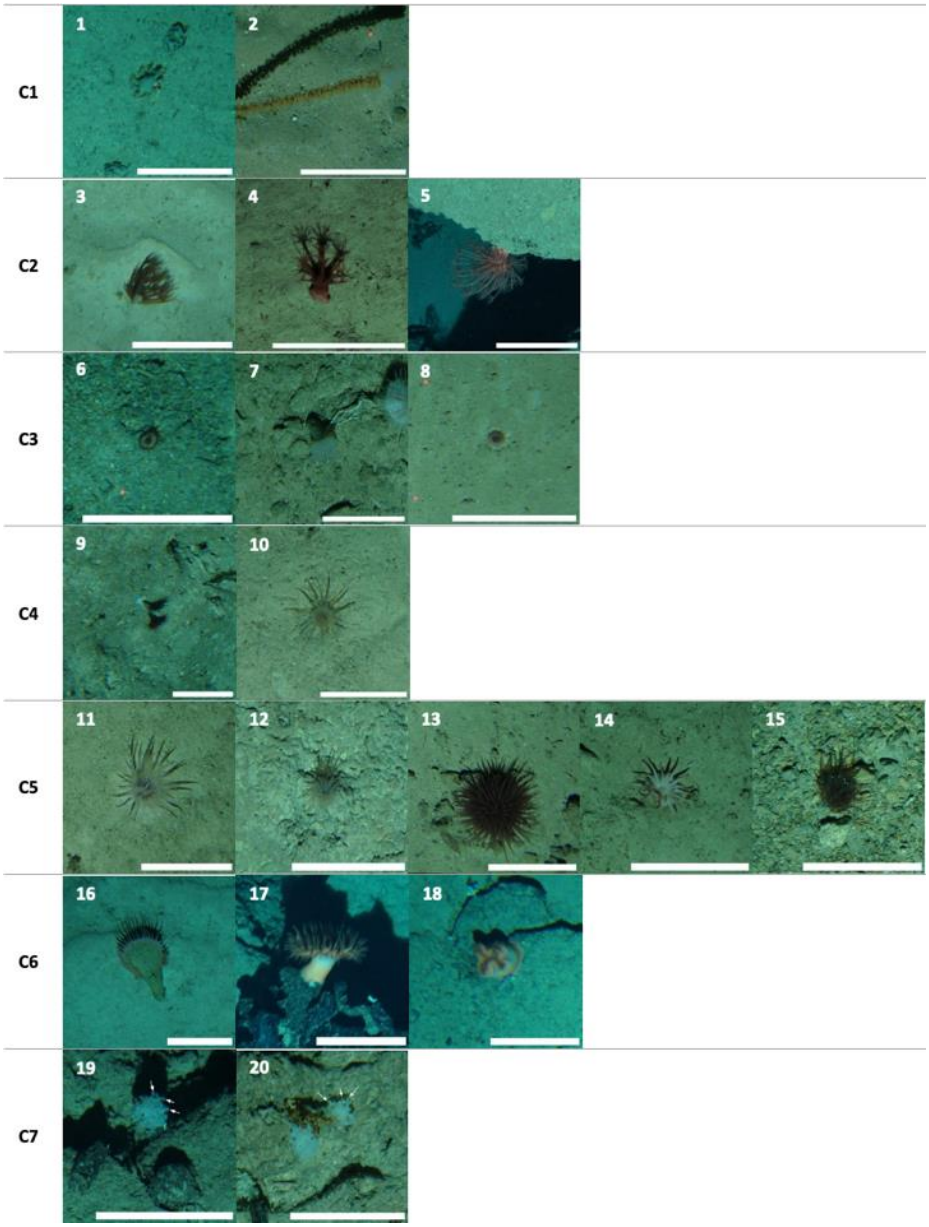

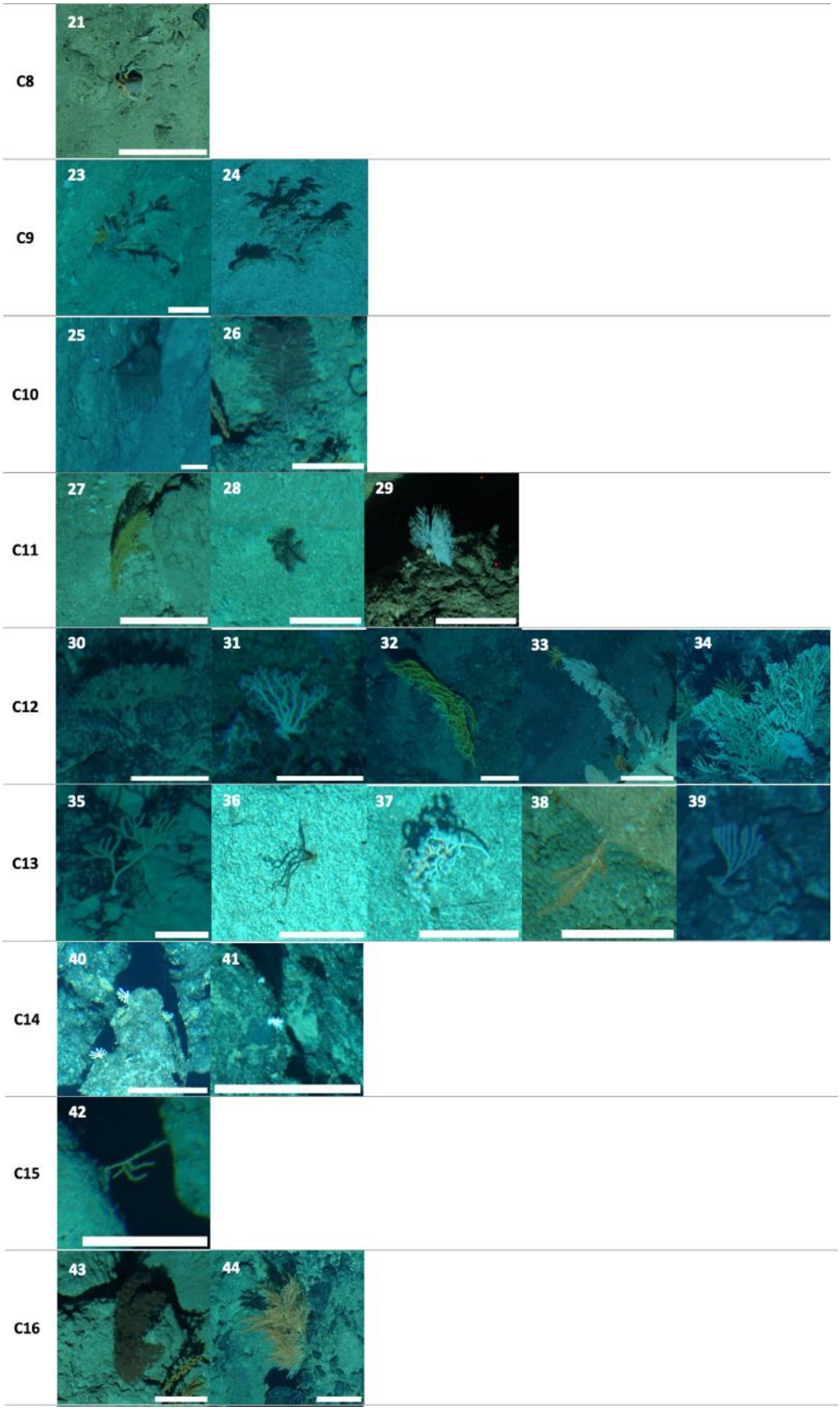
C8
21
C9
23
24
C10
25
26
C11
27
28
29
C12
30
31
32
33
34
C13
35
36
37
38
39
C14
40
41
C15
42
C16
43
44

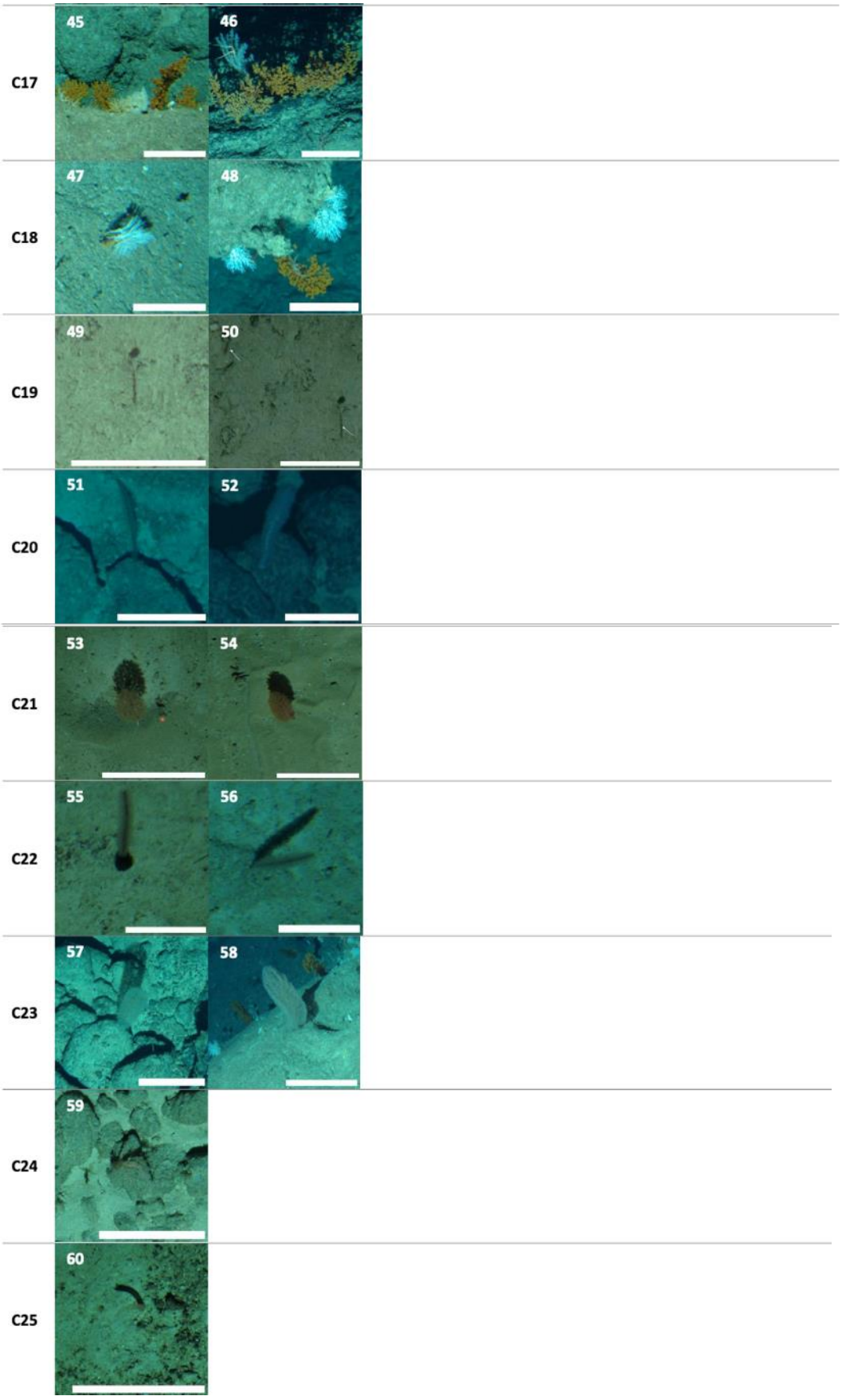
C17
45
46
C18
47
48
C19
49
50
C20
51
52
C21
53
54
C22
55
56
C23
57
58
C24
59
C25
60

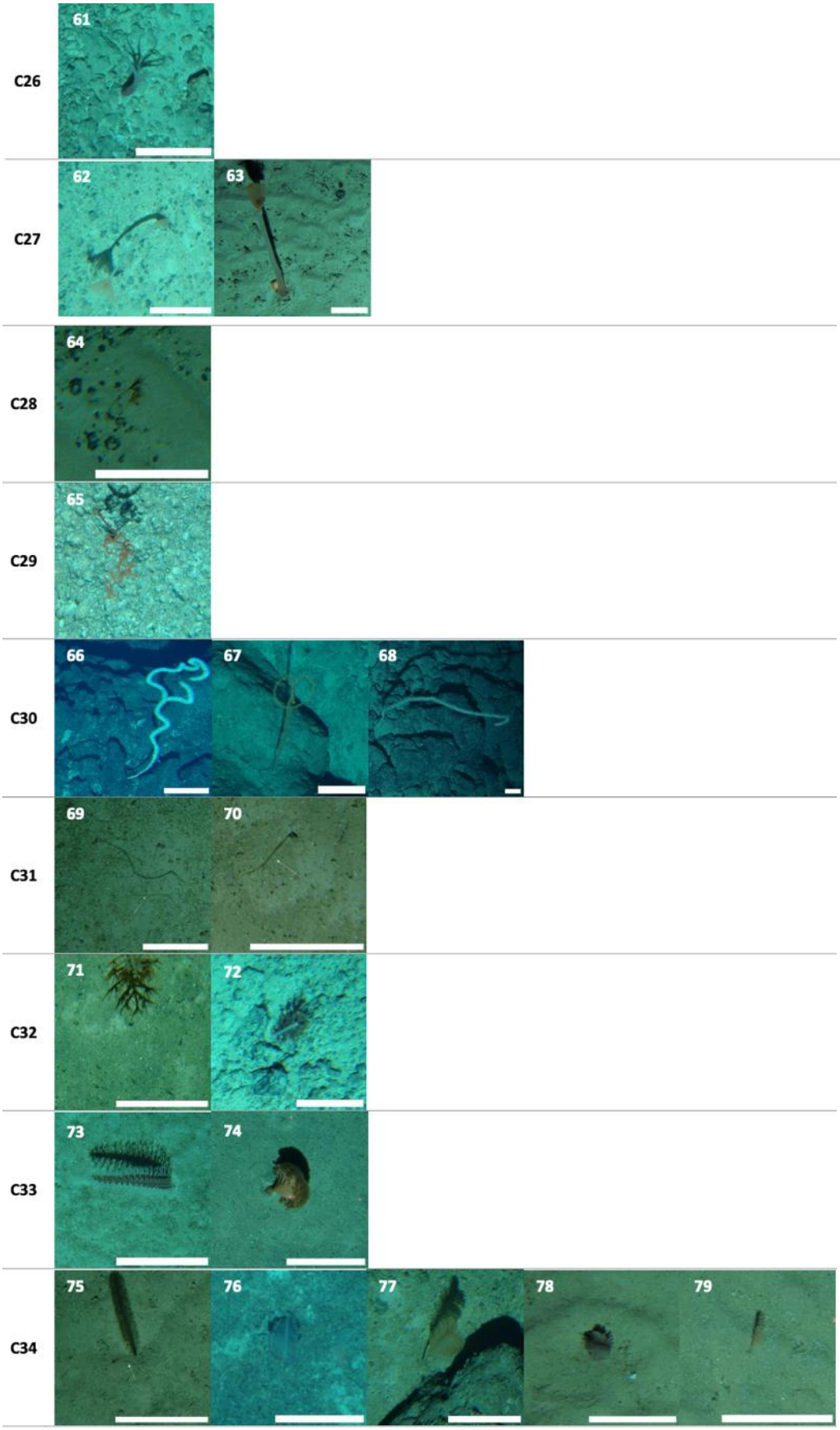
C26
61
C27
62
63
C28
64
C29
65
C30
66
67
68
C31
69
70
C32
71
72
C33
73
74
C34
75
76
77
78
79

Corresponding taxa identified to family/genus level for Figure 3B: 2 – Hyalonematidae; 40 – Geodiidae; 75, 76, 77 – *Aphrocallistes*

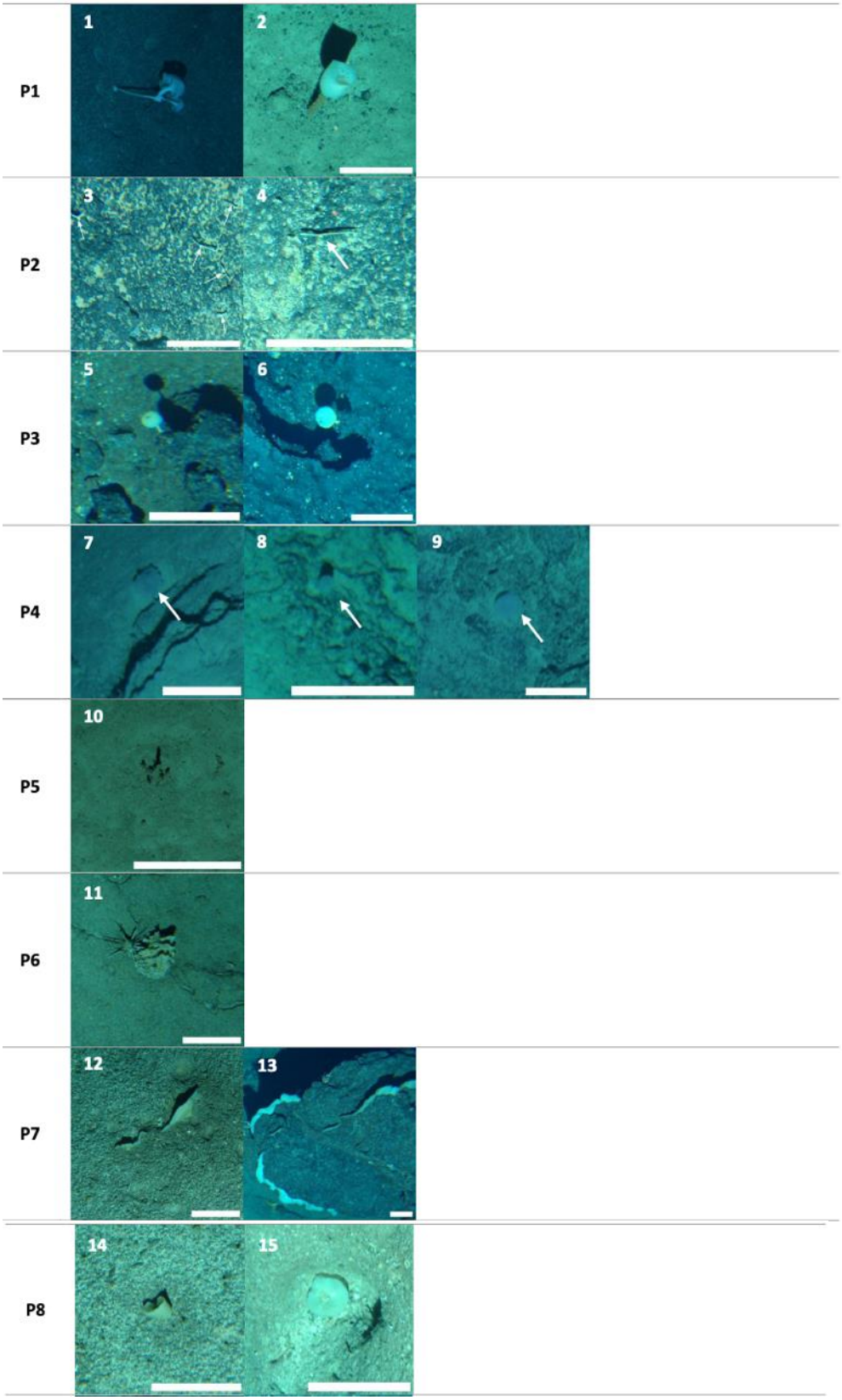

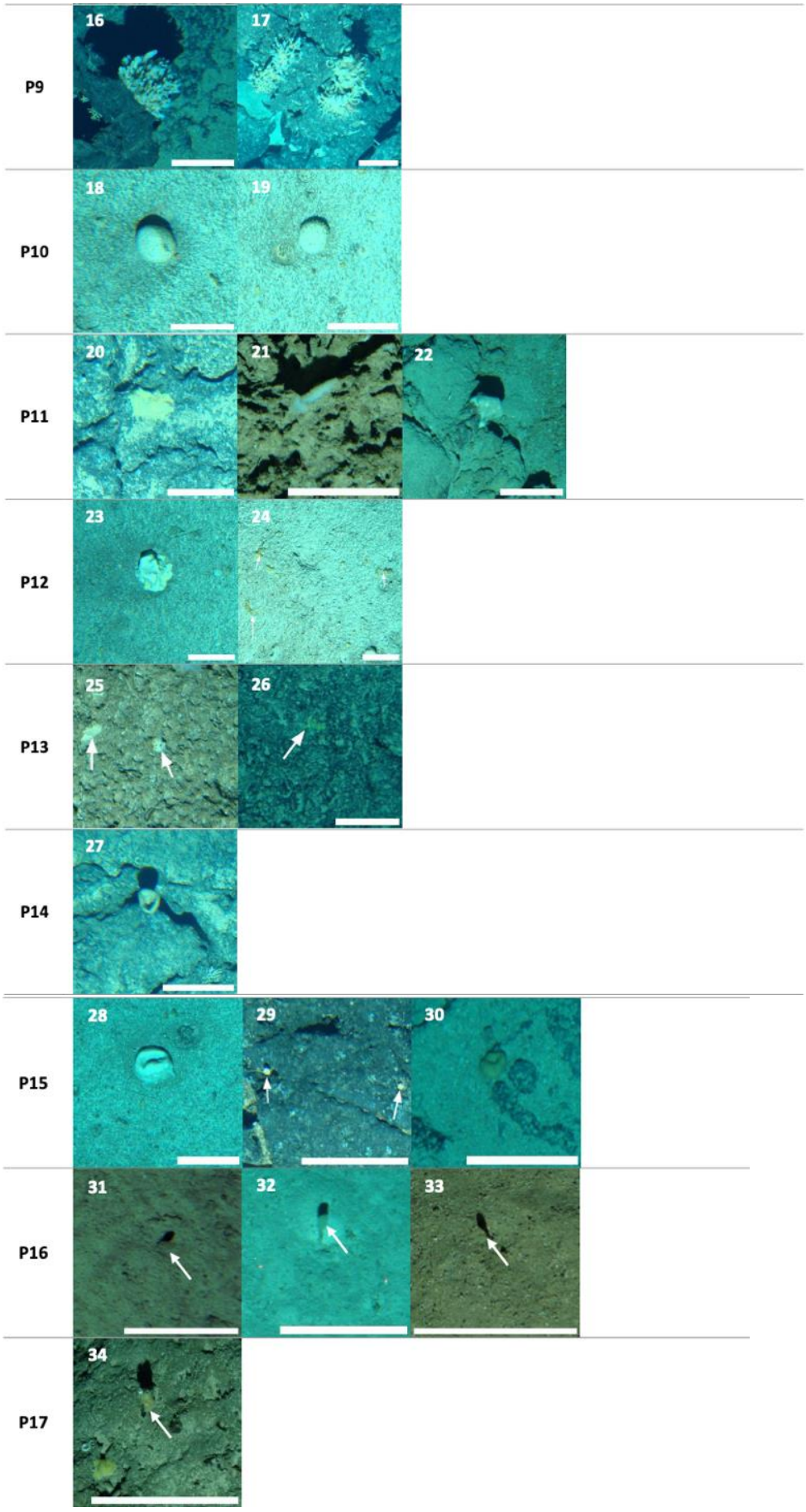
P9
16
17
P10
18
19
P11
20
21
22
P12
23
24
P13
25
26
P14
27
P15
28
29
30
P16
31
32
33
P17
34

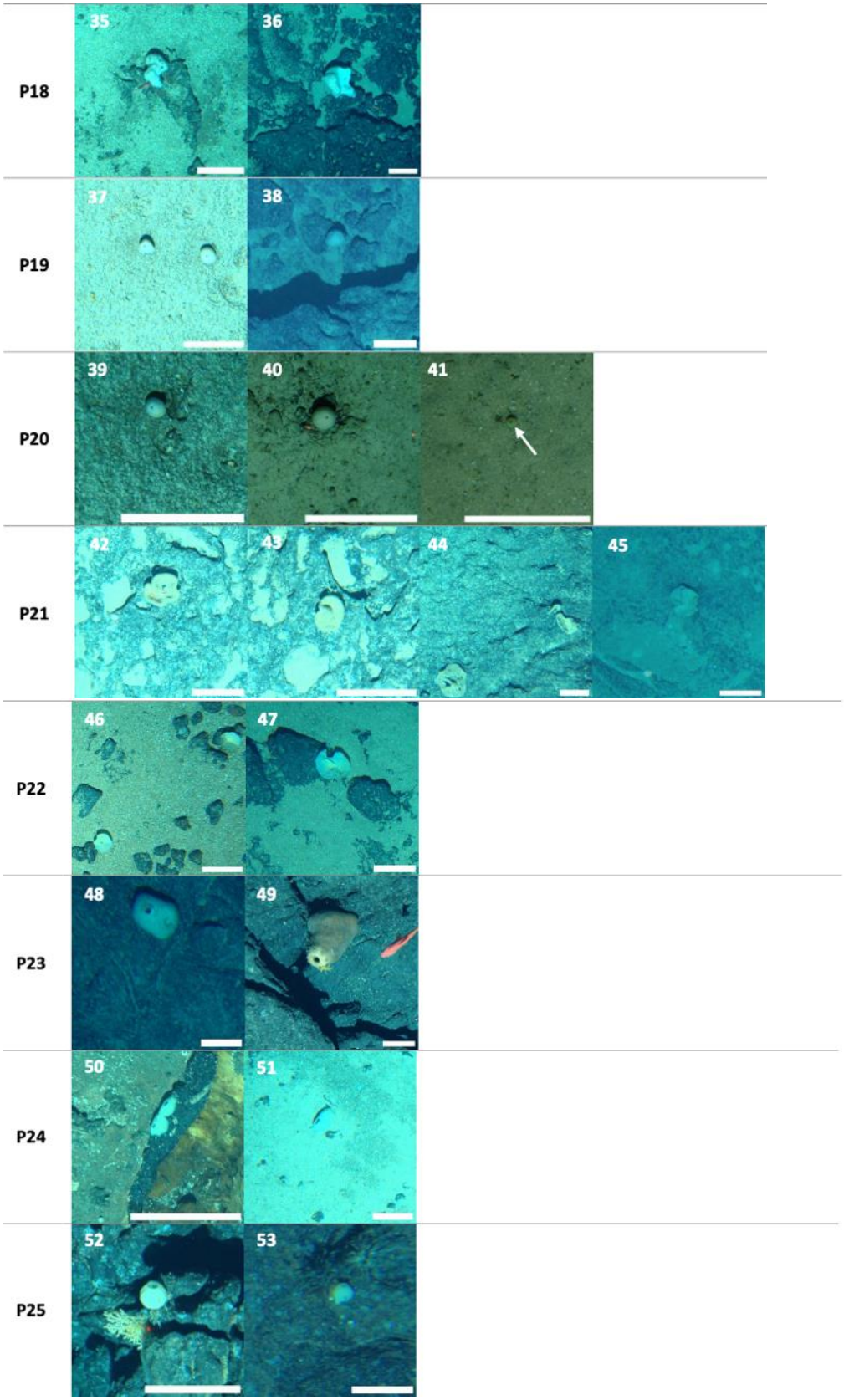
P18
35
36
P19
37
38
P20
39
40
41
P21
42
43
44
45
P22
46
47
P23
48
49
P24
50
51
P25
52
53

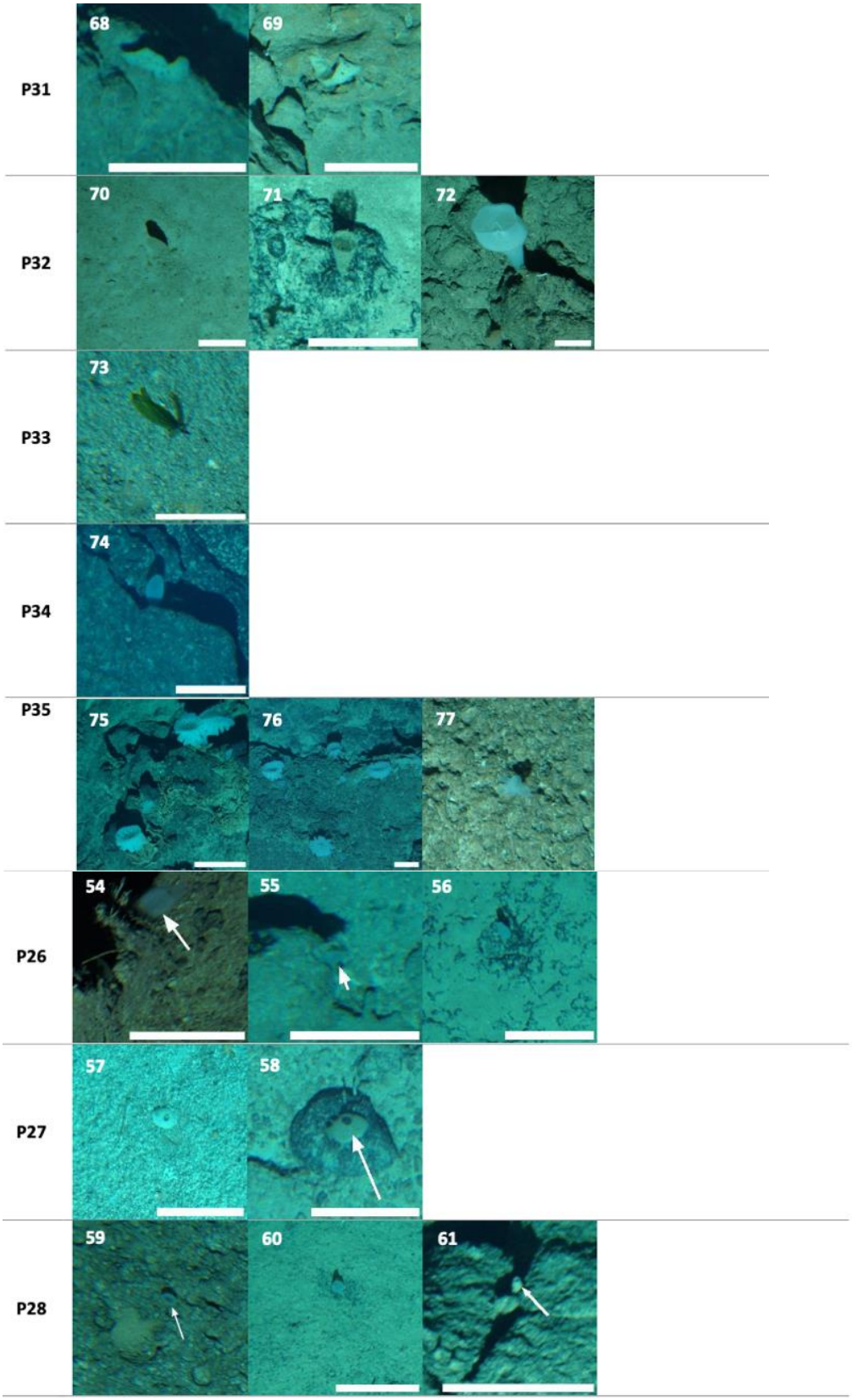
P31
68
69
P32
70
71
72
P33
73
P34
74
P35
75
76
77
P26
54
55
56
P27
57
58
P28
59
60
61

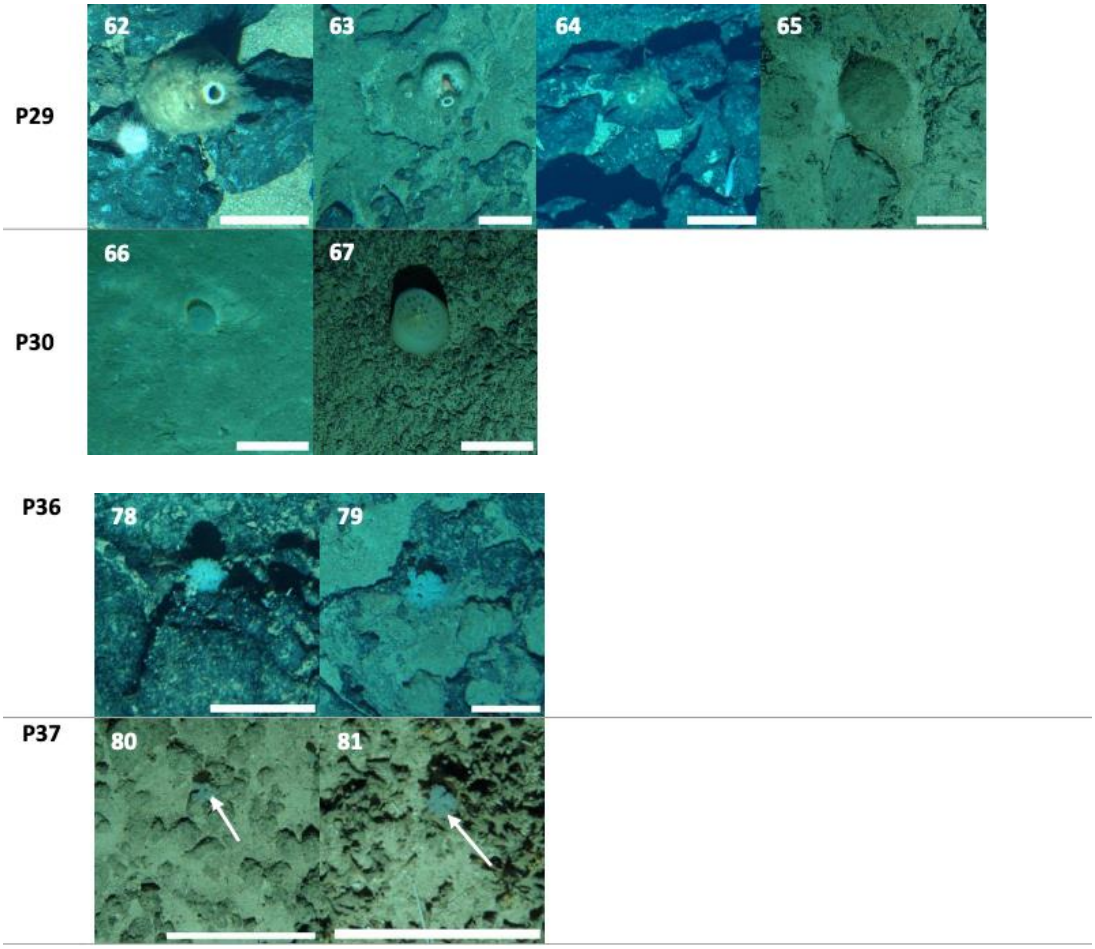
P29
62
63
64
65
P30
66
67
P36
78
79
P37
80
81

Supplementary material III.2 : Matrices of trait annotations for (A) cnidarian morphotypes and (B) sponge morphotypes

Available online at:

(A) https://docs.google.com/spreadsheets/d/1EAJ3mT-VAatEkkF4CliKTvLNodHk0ev8wYH5s0pG5hc/edit?usp=sharing

(B) https://docs.google.com/spreadsheets/d/1zwTuusuKRX8t4Y0cHIWYjJRdlVKvdrEQwXwlOrKIcqk/edit?usp=sharing

Supplementary material III.3 : Summary of densities per site of the morpho-functional groups and shared morphologies (MFG's grouping), **(A)** for cnidarians and **(B)** for sponges

Available online at:

(A) https://docs.google.com/spreadsheets/d/1OrfuYyEc0rcy4DNqM7yph9cAqj2CpuUD4dtB-lqYV5Q/edit?usp=sharing

(B) https://docs.google.com/spreadsheets/d/1iUD56xOhqGhYMACO4yb6BnhwEydxPXdKejCDG9-s3q8/edit?usp=sharing

IV. Conclusions et perspectives

Ce projet de thèse apporte des résultats nouveaux sur la diversité et la structure spatiale des communautés méga-benthiques des monts sous-marins et pentes insulaires situés dans le canal du Mozambique – région où aucune donnée n'existait sur la structure des communautés en zone bathyale – à partir d'une approche intégrative à multi-échelles ; et il a permis de caractériser les facteurs abiotiques structurant ces communautés aux échelles régionale et locale. De plus, ce projet a permis de mener une réflexion sur les limites inhérentes à l'utilisation de l'imagerie *in situ* pour identifier et caractériser des organismes en eaux profondes. Cette étude contribue donc à cette problématique en proposant de nouvelles méthodes et recommandations afin d'obtenir des données plus robustes sur les communautés de mégafaune benthique à partir d'images.

Les principales conclusions, recommandations et perspectives issues des différentes études menées au cours de ce projet sont résumées ci-dessous.

IV.1 Développement d'une méthodologie intégrative pour améliorer l'identification de la mégafaune benthique à partir d'images

Le premier axe de travail de ce projet a été de développer une méthode intégrative d'identification de la mégafaune à partir d'images, combinant des données de collectes physiques d'organismes à des données d'imagerie, afin d'obtenir un jeu de données plus robuste sur lequel reposerait les analyses spatiales des communautés. Pour cela, une analyse comparative des patrons de biodiversité évalués à partir des images et de la collecte physique d'organismes a été effectuée dans divers habitats benthiques, caractérisés par différentes natures et différents niveaux d'hétérogénéité des fonds marins (pente continentale meuble avec bois coulés, canyon ou suintements froids, pentes insulaires volcaniques à substrat dur dominant).

Cette comparaison a révélé des vues différentielles et tronquées de la biodiversité pour chacune des méthodes d'échantillonnage (images et collectes) et selon les habitats benthiques explorés.

Les deux méthodes d'échantillonnage sont sélectives. D'une part, les collectes physiques échantillonnent mal les organismes fortement fixés au substrat (ex : cnidaires, éponges), très mobiles (ex : poissons), ou fragiles (ex : échinides), et du fait de l'hétérogénéité de l'environnement (topographie abrupte et rocheuse mal échantillonnées). D'autre part, les images ne permettent pas de visualiser les organismes de petite taille, et certains organismes selon leur mode de vie (ceux enfouis ne sont pas visibles) et leur mobilité (images floues). Ces différences n'ont pas les mêmes conséquences pour tous les grands groupes zoologiques présents dans ces environnements. Ainsi, les niveaux d'identification qu'il est possible d'atteindre sur les images varient selon ces taxons.

Les échinides, astérides, décapodes et poissons sont détectés comme de bons candidats pour l'identification taxonomique à partir d'images, car ces taxons présentent des caractères d'identification qui sont évaluables à partir des images. De plus, dans les régions concernées par notre étude, l'inventaire faunistique de ces taxons était plus complet que pour d'autres taxons, bien que loin d'être exhaustif. Enfin, les taxonomistes de ces groupes étaient suffisamment impliqués dans le projet pour permettre l'identification des spécimens collectés, et sur les images. Les rangs d'identification varient pour ces quatre taxons, allant du rang ordre/famille pour les poissons, genre pour les échinides et astérides, et jusqu'au rang espèce/morpho-espèce pour les crustacés.

Dans les habitats à fond dur et hétérogène, les patrons de richesse taxonomique sont mieux évalués à partir des images qu'à partir des collectes, pour ces quatre taxons et aux rangs identifiés. Les engins d'échantillonnage physique (dragues, chaluts) sont faiblement performants dans les habitats hétérogènes, où la présence de reliefs abrupts, durs ou de structures biogéniques peut casser et obstruer les engins, limitant ainsi la collecte d'organismes. De même, les patrons de diversité régionale des crustacés et des poissons sont mieux estimés à partir des images que des collectes dans ces environnements, pour les mêmes raisons, tandis qu'aucune différence n'est observée pour le groupe des échinodermes. Dans les habitats à fond meuble, l'échantillonnage physique tend à fournir des niveaux de richesse taxonomique plus élevés qu'à partir des images pour les crustacés, et astérides, cependant, ces différences entre les méthodes d'échantillonnage varient selon le rang taxonomique considéré. De même, la diversité régionale ("gamma") est mieux évaluée à partir des collectes

que par les images pour les poissons et crustacés, cependant, aucune différence notoire n'est observée pour les échinodermes.

Cette comparaison met également en évidence la complémentarité des images et des collectes, et soulève l'importance d'établir au préalable un inventaire détaillé de la faune présente dans la région étudiée. En effet, les images ne permettent le plus souvent pas d'observer les caractères diagnostiques permettant de définir les taxons ou de les reconnaître avec la même précision que quand on les a physiquement entre les mains. Un inventaire taxonomique détaillé d'une région permet de choisir d'autres caractères, visibles sur les images, permettant d'attribuer les individus aux taxons connus de cette région et ainsi de construire des clés d'identification adaptées aux images acquises dans cette région. Par exemple, un caractère tel que la couleur peut ne pas être un caractère diagnostique dans la classification d'un taxon donné, cependant, ce caractère peut devenir informatif pour l'identification sur les images si nous savons que dans ce groupe taxonomique, seule une espèce – connue – a une couleur particulière et qui correspond au pattern observé sur l'image. Seule une connaissance poussée des taxons présents dans la région étudiée permet de réaliser ces comparaisons relatives.

Notre étude concerne une zone où l'inventaire est loin d'être complet et nous avons formalisé, dans ce contexte, les étapes de travail pour une identification taxonomique de la mégafaune la plus fine possible, à partir d'images, aux vues des connaissances disponibles. Notre approche tient compte explicitement de l'état de l'art de l'inventaire taxonomique en s'appuyant notamment sur les avis des experts, la littérature taxonomique et les inventaires des espèces collectées. Elle soulève également la collaboration nécessaire avec les taxonomistes pour identifier les caractères permettant de reconnaître au plus fin niveau taxonomique possible les organismes sur les images. Ces caractères peuvent être morphologiques mais aussi contextuels (par exemple l'habitat, les associations biologiques, etc.) et toujours relatifs à la connaissance des espèces présentes dans la région. Cette étude a également mis en évidence que pour certains taxons, l'état des connaissances, les caractéristiques morphologiques intrinsèques mais aussi le faible nombre de taxonomistes disponibles pour collaborer étaient des facteurs limitant les possibilités d'utiliser les images pour étudier les patrons de diversité taxonomique.

La compilation des différents caractères utilisés pour l'identification des taxons sur les images a abouti au développement des premières clés d'identification adaptées à des images en environnements profonds pour la région du canal du Mozambique, grâce à la collaboration de spécialistes de trois différents groupes zoologiques ciblés : Dr. Thomas Saucède (échinides), Dr. Christopher Mah (astérides), le Pr. Tin-Yam Chan et le Dr. Laure Corbari (décapodes). En retour, ce travail collaboratif a fourni aux taxonomistes, via les images, des informations complémentaires sur le milieu de vie des espèces, tel que leur substrat préférentiel, leur comportement (ex : nage, position par rapport au fond, prédation et source de nourriture), et les associations d'espèces – qui sont des connaissances qui contribuent également au développement des clés dédiées aux images.

Ces clés sont adaptées à l'identification de la mégafaune pour la région du canal du Mozambique, et sont préliminaires, relativement à l'état d'avancement de l'inventaire taxonomique dans la région.

Cette méthodologie et ces clés d'identification permettent de :

- Fiabiliser l'identification d'organismes à partir d'images en proposant des critères d'identification formels. Ces clés fournissent un cadre d'identification de taxons et de délimitation de morpho-espèces qui tient compte de la connaissance des espèces dans la région.

- Fournir un guide de référence pour aider un non-expert à identifier de manière reproductible des organismes sur les images, et ainsi d'assurer la pertinence des comparaisons des communautés biologiques entre différentes études. Ces guides permettent de compléter l'approche d'identification basée seulement sur des catalogues photos et garantissent d'obtenir des données reproductibles (et donc plus robustes) pour les analyses sur la structure des communautés méga-benthiques.

Cette étude propose les recommandations suivantes :

- Prendre en considération dans les études de suivi des communautés les différences de patrons de biodiversité obtenues à partir des images et des collectes. Dans des habitats homogènes ou à fonds meubles, les dragues et les chaluts semblent être des options plus appropriées que l'utilisation de caméra remorquée. Dans ces environnements,

l'acquisition d'images est une approche complémentaire pour vérifier l'absence de structures plus complexes formées par des espèces ingénieures (ex : éponges, cnidaires, polychètes Siboglinidae ou moulières dans le cas des émissions de fluides). Dans ces habitats à fonds plus hétérogènes, et notamment dans le cas d'habitats biogéniques fragiles (coraux, éponges), l'imagerie doit être privilégiée et complétée par un effort d'échantillonnage physique ciblé. Cependant, il est nécessaire de déployer au préalable un effort d'échantillonnage dans la région étudiée, afin d'apporter des connaissances suffisantes et nécessaires pour permettre une identification pertinente des organismes sur les images. Par ailleurs, des angles de vue inclinés par rapport au fond sont à considérer lors des campagnes d'acquisition des données, car ces vues sont complémentaires (ex : décapodes) voire indispensables pour l'identification de certains taxons (ex : poissons).

- Concentrer les efforts d'identification sur des taxons pertinents pour l'identification à partir d'images, c'est-à-dire qui remplissent les conditions suivantes : **(1)** pour lesquels un échantillonnage physique des spécimens dans la région et des identifications dans les collections par les taxonomistes sont disponibles (littérature taxonomique, base de données), **(2)** et pour lesquels les caractères morphologiques dont le polymorphisme visibles sur les images permettent de reconnaître les espèces connues localement.

- Fixer un rang seuil d'identification, au-delà duquel le niveau de confiance dans l'identification est faible ou diminue. Ces seuils varient selon les taxons considérés et dépendent : de la récurrence d'observation d'un taxon sur les images (augmente les possibilités de visualiser différents angles de vue), de la littérature disponible, de l'implication et de la disponibilité des taxonomistes dans l'identification des spécimens tant à partir des images que des échantillons collectés, ainsi que de la possibilité d'évaluer un nombre suffisant de caractères diagnostiques à partir d'images.

- Pour les taxons qui ne remplissent pas les conditions ci-dessus notamment pour lesquels les caractères morphologiques ne sont pas visibles (éponges/cnidaires notamment, ophiures, etc.), il est nécessaire d'identifier à un rang élevé (ex : classes pour les ophiures) ou de rechercher une autre méthode de classification des organismes (cf. chapitre 3).

Perspectives pour améliorer l'identification de la faune à partir d'images :

Pour obtenir des données plus robustes sur l'identification des taxons sur les images, il est nécessaire de mener un échantillonnage ciblé – pour des taxons considérés comme bons candidats – lorsque cela est possible (ex : avec un ROV) afin de construire un catalogue d'identification de référence. Lors de campagnes océanographiques, la prise systématique de photos des organismes frais récoltés à bord, afin d'en documenter la couleur et la forme, contribue notamment à construire ce type de catalogue. Cependant, pour certains taxons (ex : cnidaires, éponges), la forme des organismes *in situ* ne ressemble pas toujours à celle des organismes récoltés à bord (structure flétrie). De plus, même un ROV peut poser des limites pour l'identification de certains groupes abondants sur les monts sous-marins (ex : poissons, cnidaires tels que des gorgones) du fait de l'angle de vue ou du positionnement des caméras. En effet, l'appareil photo OTUS du ROV Victor génère des angles de vue du dessus seulement, et la caméra vidéo 4K est positionnée trop haut sur l'engin. Suite à une campagne océanographique – KANADEEP 2 – à laquelle j'ai participé, nous avons proposé une modification de la configuration pour la modernisation du Victor (appareil photo numérique en position basse et orientable en fonction du type de faune/habitats et de l'inclinaison du fond). Il faudra cependant adapter la suite logicielle pour estimer les surfaces couvertes en fonction de l'inclinaison de la caméra (on pourra s'inspirer de ce qui est fait par l'équipe du CSIRO (Shortis et al., 2008 ; Williams et al., 2015). Les clés d'identification développées au cours de cette étude pourraient être améliorées, d'une part à l'issue d'un effort d'échantillonnage plus complet des espèces de la région du canal du Mozambique, et par l'acquisition de données images de meilleure résolution, afin de compléter les clés **(1)** par des caractères d'identification permettant d'affiner les rangs d'identification et **(2)** par des taxons additionnels.

D'autre part, en proposant des clés multi-entrées pour les décapodes et les astérides, comme cela a été fait pour les échinides. Ce type de clé est plus flexible et adapté à l'identification à partir d'images car les caractères en entrée d'une clé dichotomique ne sont pas toujours visibles depuis une image, stoppant le cheminement de l'identification (Walter et Winterton, 2007). De plus, les clés multi-entrées permettent plus facilement d'intégrer des poids dans les critères d'identification, ainsi que des caractères contextuels relatifs à l'habitat (ex : type de

substrat, profondeur), et leur format numérique peut être mis à jour suivant l'état des connaissances (Saucède et al., 2020 ; Walter et Winterton, 2007).

IV.2 Diversité, densité, distribution spatiale et facteurs structurants des communautés méga-benthiques des monts sous-marins et pentes insulaires (Mayotte, Bassas da India) le long du canal du Mozambique

L'application de cette méthodologie d'identification aux images acquises sur quatre monts sous-marins (Banc du Jaguar, Banc de Hall, Monts Sakalaves et terrasses des Glorieuses) et sur les pentes insulaires de Mayotte, et Bassas da India, le long du canal du Mozambique, a permis d'obtenir un jeu de données robuste sur les communautés méga-benthiques, afin d'évaluer leurs structurations spatiales et les facteurs de l'environnement structurants aux échelles régionale et locale.

La comparaison des métriques de communauté (densité, richesse taxonomique et diversité bêta) entre les monts sous-marins et pentes insulaires a révélé des différences contrastées entre les sites étudiés. **Par exemple, les densités peuvent varier d'un facteur 10 entre les monts sous-marins ; et sont supérieures d'un facteur 4 à 10 sur les monts comparés aux pentes insulaires**, lorsque l'on compare les sites aux mêmes latitudes. **Les diversités bêta des monts et pentes insulaires explorés sont élevées (0.60 à 0.80 sur un total de 1), excepté sur la terrasse de l'archipel des Glorieuses** qui présente une structure des communautés plus homogène (BD = 0.28), en lien avec la présence d'un substrat unique de dalle carbonatée, et des courants forts et plutôt constants.

L'évaluation des facteurs structurant les différences de métriques des communautés entre les monts et pentes insulaires a en effet mis en évidence l'**influence de la géomorphologie** (c'est-à-dire de la nature du substrat dominant et relief associé) **et des vitesses de courant sur les différences de densité.** Par ailleurs, la quantification précise de la diversité et de la dureté du substrat a permis de mettre en évidence une **influence positive de la diversité du substrat sur la diversité bêta ;** l'hétérogénéité des fonds (proportion de substrat dur et différentes natures de roches dures carbonatées et volcaniques) favorise l'établissement de communautés plus diversifiées.

Cette étude a révélé également une distribution spatiale et une composition des assemblages méga-benthiques très hétérogènes, à la fois entre les monts et pentes

insulaires, distants de 4 km à 1400 km, mais également au sein d'un seul mont sous-marin ou pente insulaire sur des échelles de 0,06 km à 2 km. Cette hétérogénéité est expliquée par de multiples forçages environnementaux.

Le long du canal du Mozambique**, ces facteurs incluent l'hydrologie** (courant et productivité primaire), qui est un facteur structurant identifié comme majeur (jusqu'à ~ 15% de contribution). L'importance de ce facteur dans la structure des communautés reflète la forte dynamique hydrologique du canal du Mozambique (ex : tourbillons à méso-échelle, remontées d'eau et courant nord-est de Madagascar). **L'hydrologie présente une interaction avec d'autres facteurs ayant une contribution élevée à différentes échelles spatiales : géomorphologie (6,5% ; > km), topographie (7,9% ; 60-500 m), et le substrat (i.e. composition, dureté, diversité) (9,5% ; 60 m).** De plus, nous avons mis en évidence un **rôle structurant des différences de nature rocheuse (volcanique vs. carbonatée)** avec notamment certains taxons qui préfèrent les dalles carbonatées (ex : demosponges, brachiopodes), alors que d'autres taxons préfèrent les zones de reliefs volcaniques plus rugueuses.

Il en résulte les recommandations suivantes pour les études futures ou en termes de gestion :

- La multiplicité des facteurs environnementaux révélés structurants appuie la nécessité de mener des études incluant le maximum de facteurs abiotiques, et notamment l'importance d'intégrer des données hydrologiques/hydrodynamiques comme les courants jusqu'ici encore peu testés.

- Il est également nécessaire de poursuivre les efforts de caractérisation et quantification de la nature des substrats, notamment des différences de nature rocheuse. Par exemple, les roches carbonatées et volcaniques se caractérisent par des rugosités/microreliefs différents, ce qui contribue probablement à leur rôle structurant sur les communautés.

- Les différences de structure de communautés observées entres les monts, mais également au sein même d'un mont, et l'hétérogénéité environnementale des différents monts sous-marins et pentes insulaires explorés appuie la nécessité d'études intégratives, ciblant à la fois des structures topographiques aux

caractéristiques environnementales hétérogènes, et des analyses ciblées localement sur un mont (ciblant différentes structures topographiques au sein d'un mont : sommet, pente, différentes orientations de pente).

- L'échelle de l'hétérogénéité de l'habitat, les métriques et structures des communautés (densité, richesse, diversité et composition) sont contrastées entre les pentes insulaires de Mayotte et la plateforme des Glorieuses. Ce sont des éléments importants à considérer pour la gestion des zones de Mayotte et des Glorieuses, qui font partie intégrante d'aires marines protégées.

L'évaluation de la structure spatiale des communautés méga-benthiques **le long des pentes insulaires de Mayotte et Bassas da India révèle une structuration plutôt à moyenne échelle en lien avec des facteurs tels que la topographie, le substrat, la profondeur, la pente et l'hydrologie.** Nous n'avons pas pu mettre en évidence de facteurs de l'environnement expliquant une structure des communautés à plus petite échelle, visible sur les pentes Est et Ouest de Mayotte, ce qui reflète probablement une faible correspondance entre l'échelle des données environnementales et la structure à fine échelle des communautés.

Sur cette base, nous recommandons pour les études ultérieures :

- **L'intégration de données environnementales à plus fine résolution, par exemple, à partir de modèle numérique de terrain (bathymétrie) à haute résolution (< 10-20 m) et de l'analyse d'images, est donc nécessaire pour comprendre le rôle que joue l'environnement sur la structuration à petite échelle des communautés.** De nouvelles techniques d'analyse 3D, par exemple issues de reconstruction de mosaïque en 3D des fonds marins, permettraient également une analyse quantitative plus fine (rugosité, substrat) des fonds. Les transects de la caméra tractée n'ont cependant pas permis ces reconstructions plus aisées avec des images ROV dont l'altitude au-dessus du fond est plus stable.

- Les densités faibles par taxon (du fait des faibles densités et de la diversité taxonomique) ont nécessité d'augmenter la taille des échantillons (polygones dans lesquels sont sommées les observations) et donc de la plus petite échelle d'analyse des structures spatiales (60 m). Dans ce cas, **une augmentation de l'effort**

d'échantillonnage par imagerie (actuellement 1 image/30 sec) permettrait de diminuer la surface de ces unités d'échantillonnage. Un compromis sera cependant à rechercher afin de ne pas trop augmenter le temps consacré à l'annotation (ou recherche de méthodes d'annotation automatisées pour certaines phases, voir p. 285).

Enfin, les **taxons potentiellement constructeurs d'habitats (éponges et cnidaires) sont ceux qui contribuent le plus à la diversité bêta** des pentes et monts explorés. Ceci a pu être mis en évidence **malgré la faible résolution de leur identification taxonomique** (classes pour les éponges, et ordres pour les cnidaires). Par ailleurs, l**es taxons mobiles plus finement identifiés contribuent également à la diversité bêta**, et aux différences entre monts.

Il en résulte les recommandations suivantes :

Ce résultat conforte notre choix méthodologique d'intégration de différents rangs taxonomiques dans notre jeu de données, associant aussi bien des taxons identifiés à haut rang que des taxons cibles identifiés plus finement.

Il souligne également l'intérêt de fixer des rangs seuils d'identification pour certains taxons, mais aussi de pousser les efforts d'identification pour d'autres lorsque cela est possible. Les identifications de haut rang indiquent principalement des différences d'abondance, en particulier pour les taxons potentiellement constructeurs d'habitats (éponges, cnidaires), tandis que les identifications plus finement résolues fournissent des informations plus qualitatives sur la diversité taxonomique et de potentiels patterns biogéographiques. La faible résolution taxonomique de certains taxons ne permet cependant pas de bien caractériser la diversité fonctionnelle ni le rôle des interactions biologiques (facteurs biotiques) dans la structuration des communautés. C'est pourquoi dans le chapitre suivant nous avons développé une approche fondée sur les morphologies fonctionnelles des taxons constructeurs d'habitats plutôt que sur leur identification taxonomique pour évaluer le rôle structurant des habitats biogéniques sur la mégafaune associée (cf. chapitre 3).

Perspectives d'approfondissement des analyses sur la structure des communautés dans le canal du Mozambique :

Au cours de ce projet de thèse, une base de données de traits fonctionnels a été développée et renseignée en collaboration avec de nombreux taxonomistes : Dr. Thomas Saucède (échinides), Pr. Nadia Améziane (crinoïdes), Dr. Daniela Pica (Stylasteridae), Pr. Wei-Jen Chen and Dr. Mao-Ying Lee (poissons), Pr. Tin-Yam Chan and Dr. Laure Corbari (décapodes), Dr. Enrique Macpherson (galathées), Dr. Paco Cardenas (éponges), Dr. Éric Pante (alcyonaires) Dr. Nicolas Puillandre (gastéropodes). Ce jeu de données n'a pas pu être analysé, cependant, il serait intéressant de croiser les résultats issus de l'analyse sur l'écologie des communautés (taxonomique) avec une analyse sur l'écologie fonctionnelle des communautés méga-benthiques du canal du Mozambique. De plus, cette base de données fournit une trame qui sera applicable, par exemple, pour des données acquises sur d'autres monts sous-marins.

Les résultats de l'analyse écologique des communautés méga-benthiques du canal du Mozambique ont révélé une distribution restreinte de certains genres de décapodes (ex : *Glyphocrangon*), d'astérides (ex : *Pteraster*) et d'échinides (ex : *Heterobrissus*, *Pourtalesia*), à certains sites. Ces données issues des images doivent être comparées aux données d'occurrences des spécimens récoltés à l'échelle de la région, au même rang d'identification (genre) pour mettre en évidence un éventuel endémisme. Il serait intéressant d'appliquer une analyse de réseau biogéographique (Vilhena et Antonelli, 2015) sur les individus identifiés au genre le long des transects caméra, ainsi que sur les données issues des collectes physiques à l'échelle régionale, afin d'évaluer si les mêmes patterns de distribution spatiale sont présents dans les deux jeux de données, révélant ainsi un signal biogéographique dans les données.

IV.3 Développement méthodologique et apport d'une approche morpho-fonctionnelle à la caractérisation des peuplements d'éponges et cnidaires à partir d'images en eaux profondes

Les limites d'identification des cnidaires et éponges mises en évidence dans le chapitre 1, les fortes contributions de ces taxons à l'hétérogénéité de l'habitat révélées dans le chapitre 2, ainsi que leur importance dans la définition des Écosystèmes Marins Vulnérables (VMEs), ont renforcé le besoin de proposer une approche alternative pour évaluer plus finement la

structure spatiale de leur peuplement et de leur rôle structurant sur d'autres organismes pour lesquels ils constituent potentiellement un habitat.

À partir d'un cas d'étude sur les éponges et cnidaires observés sur les monts et pentes insulaires du canal du Mozambique – caractérisés précédemment à haut rang taxonomique – , l'objectif était de caractériser ces groupes à partir de traits morphologiques afin d'en évaluer une potentielle réponse fonctionnelle aux contraintes abiotiques, ainsi que leur rôle structurant sur des organismes associés.

Les annotations de cnidaires et éponges, identifiés précédemment à haut rang taxonomique, ont été classées de façon préliminaire en morphotypes suivant des critères observables sur les images tels que la forme générale, la couleur et la présence de structures partagées (ex : des excroissances, de longs spicules). Ces morphotypes ont ensuite été scorés suivant une liste de traits morphologiques. Ces traits ont été choisis sur la base de classifications existantes pour les éponges (Schönberg, 2021), et également pour les cnidaires (Althaus et al., 2015) pour quelques traits morphologiques. D'autres traits ont été proposés à partir de littérature relative à l'étude de la réponse morpho-fonctionnelle de ces taxons à l'environnement (études expérimentales) et sur avis d'experts de ces groupes (Dr. Éric Pante pour les cnidaires et Dr. Paco Cardenas pour les porifères).

La différence de cette classification avec les deux classifications précédemment énoncées est que ce système d'annotation n'est pas uni-catégoriel (donc il est multi-traits), et il est non hiérarchique (pas de chemin unique). À partir de la matrice morphotypes/traits ainsi constituée, des classifications ascendantes hiérarchiques appliquées aux morphotypes ont permis d'obtenir des groupes morpho-fonctionnels (GMFs) sur la base de leurs traits partagés. Ces GMFs ont ensuite été utilisés comme une variable réponse dans des analyses sur l'écologie des communautés généralement appliquées à des taxons (diversité bêta, richesse, structure spatiale).

Les résultats obtenus sur **les groupes morpho-fonctionnels d'éponges et de cnidaires** dans le canal du Mozambique révèlent **des différences de richesse et de densité entre les monts sous-marins et pentes insulaires explorés.** Au sein des groupes morpho-fonctionnels identifiés, quatre morphologies d'éponges et cinq morphologies de cnidaires dominent le long du canal.

La composition des assemblages de groupes morpho-fonctionnels d'éponges et de cnidaires varie à différentes échelles ; allant d'une petite échelle spatiale, notamment sur les pentes Nord et Est de Mayotte (~ 0.06 km), à de plus grandes échelles de variation, par exemple sur la terrasse des Glorieuses.

Cette étude apporte des résultats complémentaires à l'étude des communautés benthiques du chapitre 2, notamment pour les éponges, révélant, par exemple, une diversité de groupes morpho-fonctionnels relativement plus élevée sur Glorieuses comparativement aux autres sites, alors que la richesse taxonomique intégrée au niveau de la communauté y était très faible, avec les porifères dominés majoritairement par des demosponges non identifiables au-delà de ce rang. La diversité bêta de ces groupes morpho-fonctionnels y est cependant faible, ce qui révèle une faible structuration spatiale de la diversité fonctionnelle de ce groupe, qui semble répondre de manière similaire aux conditions plutôt homogènes de l'habitat sur cette plateforme carbonatée (dalle de carbonate et courants constants).

Cette approche permet donc de mettre en évidence une plus ou moins grande diversité de l'habitat biogénique fourni par ces assemblages de groupes morpho-fonctionnels, ainsi que de leur distribution spatiale.

L'hydrologie (notamment les courants) apparaît comme un facteur majeur structurant les groupes morpho-fonctionnels d'éponges à l'échelle du canal ; tandis que la topographie et le substrat sont des facteurs structurants majeurs des groupes morpho-fonctionnels de cnidaires, mais aussi des éponges lorsqu'on n'intègre que le nord du canal. Par ailleurs, les paramètres hydrologiques présentent de fortes contributions partagées avec la topographie, le substrat et la géomorphologie, soulignant l'interaction complexe entre la morphologie des monts et les courants dans la structure des groupes morpho-fonctionnels d'éponges et des cnidaires.

Enfin, la caractérisation des cnidaires et des éponges par une approche morpho-fonctionnelle nous a permis d'identifier des **corrélations entre certains groupes morpho-fonctionnels et d'autres taxons méga-benthiques** ; ce qui révèle indirectement le rôle de certains traits morphologiques des organismes constructeurs dans la distribution spatiale des autres organismes de ces communautés.

Cette étude propose donc un cadre original d'analyse, associant des analyses spatiales des communautés biologiques appliquées à des groupes morpho-fonctionnels définis au préalable, au lieu d'entités taxonomiques.

L'apport d'une approche morpho-fonctionnelle suivant ce cadre d'analyse est résumé dans les points suivants :

- C'est une méthode explicite qui permet une double évaluation, à la fois de la structure spatiale des habitats biogéniques et de leur réponse à l'environnement, et aussi de leur rôle structurant sur la communauté associée. Ceci à partir de la caractérisation de traits morphologiques, mesurables à partir d'images.

- La méthode est adaptable et flexible : elle peut évoluer, avec l'état des connaissances acquises, dans le choix des traits et dans la méthode de classification, et le système d'annotation est non hiérarchique, ce qui apporte une flexibilité d'annotation et de combinaison de traits possibles. Cette méthode est aussi applicable sans connaissance taxonomique approfondie de ces taxons, dont les identifications sont généralement limitées à un haut rang taxonomique, et permet donc de fournir un jeu de données plus détaillé des peuplements d'éponges et de cnidaires.

- Cette méthode fournit des métriques pour caractériser des habitats vulnérables, ainsi que leur échelle de distribution spatiale, de par l'application d'indices de diversité bêta à ces groupes morpho-fonctionnels – usuellement appliqués à des taxons – remplissant des rôles fonctionnels différents et répondant différemment aux contraintes de l'habitat selon leur composition.

IV.4 Application des méthodes et travaux menés au cours de ce projet à de nouvelles campagnes d'acquisition de données

IV.4.1 Application à des données acquises le long de monts sous-marins dans la région Pacifique Sud (ZEE de Nouvelle-Calédonie)

Les principales limites du jeu de données à disposition pour la thèse étaient le manque de connaissances faunistiques du fait de l'échantillonnage encore incomplet de la faune dans les régions étudiées – notamment dans le canal du Mozambique –, ceci couplé à l'utilisation d'une

caméra tractée, qui génère des contraintes en termes d'acquisition des images (ex : altitude variable, résolution des images) et qui ne permet pas de prélever des organismes associés aux images. Ces contraintes ont rendu difficile l'identification des organismes sur les images et limité l'établissement de clés d'identification.

Cependant, les réflexions et travaux menés au cours de ce projet de thèse ont guidé la réflexion sur la stratégie d'exploration d'une nouvelle campagne – KANADEEP 2 (Samadi et Olu, 2019) – menée en septembre 2019 au large de la Nouvelle-Calédonie, et à laquelle j'ai pu participer. L'état des connaissances faunistiques dans cette région était plus avancé, et pour cette campagne, nous disposions d'un ROV (Remotely Operated Vehicle).

Cette campagne avait pour objectif d'apporter de nouvelles données sur les habitats profonds encore peu explorés au sein du parc marin de Nouvelle-Calédonie. Le premier leg de la mission avait plus spécifiquement pour objectif de compléter l'exploration de trois monts sous-marins – Mont D, Munida et Stylaster – à partir du ROV Victor 6000. L'utilisation du ROV permet d'obtenir des données images de haute résolution sur les sommets et sur un large gradient bathymétrique le long des pentes de ces structures, mais aussi d'échantillonner la faune des pentes qui sont difficiles à échantillonner avec les engins traînants.

Le choix des monts sous-marins reposait sur la connaissance acquise sur ces sites par des campagnes d'échantillonnage passées dans le cadre du programme Tropical Deep Sea Benthos menées par le MNHN et l'IRD depuis la fin des années 1970, ainsi que des connaissances acquises sur la géologie des fonds. L'état des connaissances faunistiques dans la région a guidé le choix de ces trois monts. Le choix du mont D était guidé par la difficulté d'échantillonnage des monts de cette zone qui sont assez profonds et dont les sommets très durs rendent difficile l'exploration par des engins traînants. Le choix des deux autres monts sous-marins visait à comparer deux assemblages biologiques distincts mais proches géographiquement et dans une même gamme bathymétrique, avec d'une part le mont Munida, peuplé de denses habitats d'éponges, et d'autre part le mont Stylaster, peuplé de denses communautés de Stylasteridae. Ces deux monts présentent des gammes de profondeurs comparables et une proximité avec la côte calédonienne, avec cependant des contextes géologiques distincts.

Pour explorer l'hétérogénéité des habitats, une stratégie d'acquisition d'images sur chaque sommet et d'exploration de trois orientations de pente sur chaque mont sous-marin a été menée. Cette stratégie visait à évaluer l'hétérogénéité des fonds et des communautés benthiques au sein et entre ces deux monts. Contrairement à la zone du canal du Mozambique qui a fait l'objet de cette thèse, les monts sous-marins et les pentes insulaires de Nouvelle-Calédonie ont été intensivement échantillonnés depuis le début des années 1980. L'inventaire faunistique, bien que non encore saturé, est nettement plus avancé dans cette région. Pour les trois monts explorés, les données faunistiques concernent principalement les sommets. Un échantillonnage de la mégafaune visible sur les images du ROV a été réalisé, afin de calibrer les identifications sur les images et de construire un catalogue photo de référence.

La réflexion sur le choix des taxons à cibler pour l'échantillonnage reposait sur l'état des connaissances faunistiques dans la région, révélant l'intérêt de cibler des taxons tels que les crinoïdes, les ophiures et parmi les décapodes, le groupe des galathées, ainsi que sur les avis d'experts. En effet, de nombreux taxonomistes ont embarqué sur cette campagne – spécialistes de divers taxons – afin d'élargir le spectre des taxons à cibler pour l'échantillonnage, notamment des spécialistes des éponges et des cnidaires, qui ont fait l'objet d'une attention particulière de par les habitats biogéniques qu'ils forment sur ces monts.

À bord, les équipes et l'organisation des quarts de travail ont été pensés afin d'optimiser l'identification des organismes sur les images. Au moins deux taxonomistes étaient présents par quart, afin de renseigner dans un cahier de quart toute information pertinente sur les organismes observés sur les images. Les taxonomistes pouvaient, par exemple, préciser si des zooms sur des taxons particuliers étaient pertinents, ou mentionner le besoin de collecter des organismes selon l'état des connaissances.

La stratégie de bancarisation et de traçabilité des données associe les pratiques de l'équipe Ifremer (conforment à la bancarisation des données de campagnes par le SISMER) et le système d'inventaire des spécimens, en lien avec les référentiels géographiques des campagnes à la mer, intégrés aux collections du MNHN. L'acquisition des données d'images en lien avec l'échantillonnage des organismes a été pensée en amont et ajustée au cours de la campagne, en vue de constituer des catalogues photos de référence. Chaque événement de prélèvement (date, engin, coordonnées géographiques, profondeur) est codé de façon unique et constitue un événement de collecte dans le référentiel géographique de la

campagne. L'image de chaque organisme prélevé lors de ces événements était référencée avec ce code. Une fois à bord, une étiquette avec un code de référence (code de collection MNHN) associée à une étiquette comportant le code de l'événement d'échantillonnage, étaient attribuées au spécimen physique. Une photo du spécimen récolté était prise à bord, avec l'étiquette MNHN visible, afin d'en documenter la couleur et la forme. Lors de la bancarisation des données, les codes de prélèvement et codes MNHN sont associés, permettant par la suite de faire le lien entre les identifications des spécimens récoltés et les photos à bord, avec leurs images *in situ*.

Les données acquises sur les monts sous-marins de Nouvelle-Calédonie et la stratégie de calibration des identifications sur les images, employée au cours de cette campagne, ouvrent de nouvelles perspectives de développement de clés d'identification pour cette région. Des clés pourront être développées pour les mêmes taxons identifiés comme bons candidats à l'identification à partir d'images (décapodes, astérides et échinides), ainsi que pour de nouveaux taxons identifiés comme bons candidats : crinoïdes, galathées, et, potentiellement, les poissons. La calibration des images *in situ* des cnidaires et des éponges permettra notamment de préciser les identifications au-delà du rang ordre ou classe, au moins aux rangs famille et genre pour certains taxons dont les caractères diagnostiques applicables sur les images permettent leur identification à ces rangs (ex : Euplectellidae pour les éponges).

Il serait également intéressant de contribuer à l'effort international de standardisation et de centralisation des catalogues d'identification taxonomique par région, en proposant, par exemple, des catalogues par secteur géographique, aussi bien pour la zone de l'océan Indien que pour le Pacifique (Howell et al., 2019). Ma participation au groupe de travail sur l'imagerie dans le cadre du projet Challenger 150 (Howell et al., 2020) va dans ce sens. Le développement d'un catalogue image des identifications réalisées sur les images du canal du Mozambique est un projet en cours d'élaboration au sein de l'UMR BEEP. Pour les images acquises sur les monts sous-marins de Nouvelle-Calédonie, parallèlement à leur annotation, il faut que les taxonomistes fournissent les identifications des spécimens récoltés par le ROV. Ces identifications associées aux images prises *in situ* de ces mêmes spécimens contribueront à la constitution d'un catalogue de référence qui permettra ensuite d'identifier les organismes annotés sur les autres images. Une collaboration avec les équipes du CSIRO (Australie) qui s'intéressent aux peuplements des monts sous-marins de la ZEE australienne, à partir

d'imageries couplées à des échantillonnages (Williams et al., 2015) et à des méthodes d'identification couplant identification taxonomique et par morphotypes (Untiedt et al., 2021), est en cours notamment pour standardiser nos méthodes d'acquisition, annotation, analyse et bancarisation d'images sous-marines.

De plus, ces données ont fait l'objet d'analyses exploratoires aux cours d'un stage en 2021 que j'ai co-encadré (Saint Germain, 2021). Ce stage avait pour objectif de caractériser la structure des peuplements d'éponges et de cnidaires dominants sur les monts Munida et Stylaster respectivement, à partir de la même approche morpho-fonctionnelle appliquée aux communautés d'éponges et cnidaires dans le canal du Mozambique. Par ailleurs, ce stage a permis de mûrir la réflexion sur la méthodologie d'analyse des données morpho-fonctionnelles acquises en parallèle sur les monts du canal du Mozambique, notamment par le test de plusieurs méthodes de classification (classification ascendante hiérarchique et K-means) des morphotypes d'éponges.

De plus, les résultats du chapitre 3 de ce projet de thèse ont mis en évidence une correspondance étroite entre certains traits morphologiques et certains taxons (ex : forme solitaire et charnue pour les actinies, présence d'un pédoncule chez les pennatules). Cette correspondance souligne un potentiel signal phylogénétique – tendance qu'ont des espèces apparentées à présenter des traits similaires (Kamilar et Cooper, 2013) – dans les données des groupes morpho-fonctionnels. Il serait intéressant d'explorer cette hypothèse avec le jeu de données acquis sur les monts Munida et Stylaster (Nouvelle-Calédonie), pour lesquels les identifications sur les images pourront être plus poussées en raison de la stratégie de calibration des identifications et de l'effort d'échantillonnage porté sur les cnidaires et éponges lors de la campagne d'acquisition des données. Une comparaison des groupes morpho-fonctionnels obtenus à l'issue d'une analyse de regroupement avec leur composition taxonomique (par exemple au rang famille ou genre) permettra d'évaluer si un signal phylogénétique est présent dans le jeu de données (forte correspondance entre les taxons qui constituent un groupe morpho-fonctionnel).

IV.4.2 Application à un cas d'étude d'impact d'une éruption volcanique sur les communautés benthiques, au large de l'île de Mayotte

En 2018, une éruption volcanique à eu lieu à 50 km à l'est de l'île de Mayotte, créant un édifice volcanique à 3600 m de fond, d'une hauteur de 820 m (5 km^3). Des émissions de fluide, avec des anomalies en méthane, hydrogène, mais également pH (acide) ont été enregistrées dans la colonne d'eau au niveau d'une zone d'essaim (Fer à cheval) (Feuillet et al., 2021). La zone du Fer à cheval se situe à une distance de 4 à 8 km de la pente insulaire Est de Mayotte, explorée en 2017 lors de la campagne BIOMAGLO (Corbari et al., 2017), et dont la structure des communautés benthiques a été analysée au cours de ce projet de thèse.

Dans ce contexte, le projet ScinObs « Science, Innovations et Observatoires sous-marins » a pour objectif de déployer un système d'observatoire sous-marin au large de l'île de Mayotte, comme support de surveillance des activités sismiques et volcaniques de la région, et de ses conséquences sur l'évolution des écosystèmes marins. Cet observatoire sera principalement basé sur des systèmes d'observation fixes (stations benthiques, mouillages), mais également par des transects d'exploration réguliers.

La pente externe Est de Mayotte était composée dans sa partie basse de denses communautés de scléractiniaires coloniaux (*Enallopsammia*) et d'éponges hexactinellides (*Aphrocallistes*), qui sont des organismes suspensivores, à squelette calcaire et siliceux respectivement, et qui seraient potentiellement impactés par les perturbations des conditions hydrologiques de la colonne d'eau liées à ces émissions de fluides. Pour vérifier cette hypothèse, de nouveaux transects de caméra tractée ou ROV, effectués perpendiculairement à la pente Est, répétant le transect de la caméra tractée effectué en 2017 et à des distances variables entre ce transect et la zone de l'essaim permettraient d'effectuer une comparaison des communautés à T0 (2017) et T1 (2018), ainsi que d'évaluer l'effet de la distance de l'essaim sur la structure des communautés et notamment sur les taxons structurant l'habitat potentiellement sensibles aux variations de pH.

IV.5 Travaux et contraintes liés au traitement d'images

Les données acquises au cours de ce projet sont issues d'un travail conséquent de traitement des images. Ces images impliquent un travail pluridisciplinaire, en collaboration avec divers spécialistes, notamment des taxonomistes, pour obtenir des données biologiques sur

l'identité des taxons ; mais aussi des informaticiens et ingénieurs en traitement d'images, en vue de développer des algorithmes de reconnaissance/classification automatique d'objets à détecter dans les images (ex : substrat) pour réduire le temps d'acquisition des données. De plus, pour obtenir des données sur la géomorphologie et les substrats, il est nécessaire d'interagir avec des géologues impliqués, pour interpréter au mieux les structures et les substrats observés sur les images. L'échange avec des géomaticiens a également été nécessaire pour s'initier à l'intégration et à la quantification de données, par exemple sur la nature du fond et sur la géomorphologie, à partir de modèle numérique de terrain. Par ailleurs, le volume d'images soulève un problème de manque de place pour enregistrer les images et ses données dérivées sur les réseaux informatiques. Ceci soulève un dernier point relatif à la difficulté de mettre à disposition simplement et rapidement des images pour des travaux collaboratifs.

IV.6 Contribution au développement d'outils informatiques pour le traitement et l'analyse des données d'imagerie

Ce projet de thèse a également soulevé des besoins de développements méthodologiques annexes, en lien avec les outils requis pour l'acquisition et le traitement des données images. Ce projet est le premier à traiter des données images avec la plateforme d'annotation BIIGLE puis l'application ADELIE associée au logiciel SIG ArcGIS pour les analyses quantitatives et spatiales. Cette dernière étape avait été adaptée uniquement aux données vidéo, principalement analysées au sein de l'UMR BEEP (Biologie et Écologie des Écosystèmes Marins Profonds). De ce fait, les outils de traitement de l'IFREMER manquaient de compatibilité pour l'analyse et le géo référencement des annotations issues de données images. Ainsi, des outils tels que ADELIE SIG (logiciel IFREMER de traitement des données, basé sur le système d'informations géographiques ArcView) n'étaient pas adaptés au traitement d'images, notamment au traitement des exports de faune et de substrat issus de la récente plateforme en ligne d'annotation d'images BIIGLE (Langenkämper et al., 2017) et utilisée au cours de ce projet. Face aux besoins soulevés et aux difficultés rencontrées pendant mes travaux de thèse, une interface BIIGLE locale au sein de l'IFREMER, et surtout une chaîne de traitement simplifiée entre l'interface d'annotation BIIGLE et le logiciel de post-traitement ADELIE SIG ont pu être développées et de nouvelles modalités sont en cours de développement. Des échanges réguliers ont donc été nécessaires avec l'équipe de l'université de Bienfield (logiciel

d'annotation d'image BIIGLE) pour participer à l'évolution du logiciel, et en interne IFREMER avec Olivier Soubigou (responsable ADELIE). Ce travail a montré l'intérêt de coupler les deux logiciels et de les faire évoluer conjointement. Un projet d'ANR bilatérale franco-allemande a été déposé entre les deux instituts à l'appel d'offre 2022 (projet TIAMAT).

Enfin, deux projets de développement d'algorithmes de classification semi-automatique d'images ont été menés avec l'ISEN de Brest (école d'ingénieurs), en lien étroit avec le besoin de réduire le temps d'acquisition des données par rapport aux volumes de données images à traiter. Deux projets de stage, en collaboration avec le Dr. Thibault Napoléon, ont abouti au développement, d'une part, d'un algorithme de classification automatique permettant d'obtenir des données quantitatives sur la nature des substrats sur les monts sous-marins et pentes insulaires explorés dans le canal du Mozambique (Dugard et Carcopino, 2020). Bien que les données quantifiées sur la nature du substrat par image extraites de l'algorithme de classification automatique des substrats n'aient pas pu être analysées directement (taux d'erreur de 15%), ces données ont permis de fournir une classification primaire des substrats qui a été ensuite complétée manuellement. Il serait intéressant d'améliorer l'algorithme avec un jeu de données d'entraînement plus conséquent, pour ensuite le généraliser à d'autres jeux de données et permettre une quantification automatique et robuste de la couverture des natures de substrat. Ceci est prévu dans le cadre du jeu de données sur les monts sous-marins de Nouvelle-Calédonie.

D'autre part, un algorithme de classification automatique de morphologies d'éponges (Doudet et Thomas, 2021) a été développé en vue d'obtenir des données préliminaires accélérant les premières étapes d'annotations des morphotypes dominants d'éponges, à partir des images acquises sur les monts de Nouvelle-Calédonie. Ces données issues de l'algorithme de classification automatique des morphotypes d'éponges n'ont pas pu être utilisées en raison d'un manque de compatibilité entre l'interface d'annotation BIIGLE et les annotations extraites à part depuis l'interface de l'algorithme. Cependant, l'algorithme est performant et pourrait être utilisé via un développement informatique permettant l'import des annotations automatiques extraites de l'interface de l'algorithme vers BIIGLE. Le jeu de données d'entraînement de l'algorithme pourra être élargi (complété par de nouvelles images de morphotypes). D'autres tests ont été réalisés avec le logiciel de reconnaissance automatique MAIA associé à BIIGLE (Zurowietz et al., 2018) sur quelques morphotypes

d'éponges des sites de Glorieuses et Mayotte dans le cadre d'un stage que j'ai co-encadré (Gourdon, 2020). Les résultats montrent que le jeu d'entraînement doit être conséquent (au moins 200 images par morphotype) et que de nombreux faux positifs sont détectés du fait de l'hétérogénéité du substrat. Cependant, même avec la phase de validation manuelle des résultats issus de l'algorithme, nous avons estimé un gain de temps égal à la moitié de celui passé pour l'annotation manuelle, rendant cette approche intéressante pour la phase d'annotation "non-experte".

Plus généralement, l'évolution des outils développés spécifiquement dans le cadre de ce projet permettrait d'élargir leur utilisation à d'autres jeux de données, et de pérenniser ces outils informatiques.

Enfin, de nouvelles techniques de reconstruction 3D sous forme de mosaïques des habitats benthiques à partir des images offrent la possibilité d'obtenir des données à fine résolution (~ cm), par exemple sur la rugosité du terrain et la topographie. De telles reconstructions ont été initiées à partir des images des monts sous-marins du canal du Mozambique, issues d'une caméra tractée. Cependant, les capacités de calcul du logiciel utilisé pour effectuer ces mosaïques (MATISSE 3D, développement par Aurélien Arnaubec) relativement aux longues portions de transect images à traiter (> 7 km) ont rendu difficile voire impossible l'utilisation de cette méthode. Pour l'analyse des images de la campagne KANADEEP 2, nous prévoyons des reconstructions de plus petites portions de transect images en vue d'en extraire des données sur le terrain (ex : rugosité, analyse et quantification des substrats). Cette méthode est facilitée par de plus grandes capacités de calcul récemment accessibles au laboratoire. La plus grande stabilité du ROV par rapport à la caméra tractée favorise aussi la réalisation de mosaïques.

V. Bibliographie

Agnarsson, I., Kuntner, M., 2007. Taxonomy in a Changing World: Seeking Solutions for a Science in Crisis. Systematic Biology 56, 531–539. https://doi.org/10.1080/10635150701424546

Althaus, F., Hill, N., Edwards, L., Ferrari, R., 2014. CATAMI Classification Scheme for scoring marine biota and substrata in underwater imagery 102.

Althaus, F., Hill, N., Ferrari, R., Edwards, L., Przeslawski, R., Schönberg, C.H.L., Stuart-Smith, R., Barrett, N., Edgar, G., Colquhoun, J., Tran, M., Jordan, A., Rees, T., Gowlett-Holmes, K., 2015. A Standardised Vocabulary for Identifying Benthic Biota and Substrata from Underwater Imagery: The CATAMI Classification Scheme. PLOS ONE 10, e0141039. https://doi.org/10.1371/journal.pone.0141039

Althaus, F., Williams, A., Schlacher, T., Kloser, R., Green, M., Barker, B., Bax, N., Brodie, P., Hoenlinger-Schlacher, M., 2009. Impacts of bottom trawling on deep-coral ecosystems of seamounts are long-lasting. Marine Ecology Progress Series 397, 279–294. https://doi.org/10.3354/meps08248

Anastasopoulou, A., Kapiris, K., 2008. Feeding ecology of the shortnose greeneye Chlorophthalmus agassizi Bonaparte, 1840 (Pisces: Chlorophthalmidae) in the eastern Ionian Sea (eastern Mediterranean). J Appl Ichthyol 24, 170–179. https://doi.org/10.1111/j.1439-0426.2007.01028.x

Ângelo Adolfo Langa, A., 2021. Seasonal and Spatial Variability of Primary Production in the Mozambique Channel. WROS 10, 61. https://doi.org/10.11648/j.wros.20211003.14

Audru, J.-C., Guennoc, P., Thinon, I., Abellard, O., 2006. Bathymay : la structure sous-marine de Mayotte révélée par l'imagerie multifaisceaux. Comptes Rendus Geoscience 338, 1240–1249. https://doi.org/10.1016/j.crte.2006.07.010

Auscavitch, S.R., Deere, M.C., Keller, A.G., Rotjan, R.D., Shank, T.M., Cordes, E.E., 2020a. Oceanographic Drivers of Deep-Sea Coral Species Distribution and Community Assembly on Seamounts, Islands, Atolls, and Reefs Within the Phoenix Islands Protected Area. Front. Mar. Sci., a 7, 42. https://doi.org/10.3389/fmars.2020.00042

Auscavitch, S.R., Lunden, J.J., Barkman, A., Quattrini, A.M., Demopoulos, A.W.J., Cordes, E.E., 2020b. Distribution of deep-water scleractinian and stylasterid corals across abiotic environmental gradients on three seamounts in the Anegada Passage. PeerJ, b 8, e9523. https://doi.org/10.7717/peerj.9523

Baco, A.R., Morgan, N.B., Roark, E.B., 2020. Observations of vulnerable marine ecosystems and significant adverse impacts on high seas seamounts of the northwestern Hawaiian Ridge and Emperor Seamount Chain. Marine Policy 115, 103834. https://doi.org/10.1016/j.marpol.2020.103834

Barberousse, A., Bary, S., 2019. Marine Biodiversity Databanks, in: Casetta, E., Marques da Silva, J., Vecchi, D. (Eds.), From Assessing to Conserving Biodiversity: Conceptual and Practical Challenges, History, Philosophy and Theory of the Life Sciences. Springer International Publishing, p. 23.

Barnes, D.K.A., Bell, J.J., 2002. Coastal sponge communities of the West Indian Ocean: morphological richness and diversity. African J Ecol 40, 350–359. https://doi.org/10.1046/j.1365-2028.2002.00388.x

Bayer, F.M. (Ed.), 1983. Illustrated trilingual glossary of morphological and anatomical terms applied to octocorallia. Brill, Leiden.

Beauchard, O., Veríssimo, H., Queirós, A.M., Herman, P.M.J., 2017. The use of multiple biological traits in marine community ecology and its potential in ecological indicator development. Ecological Indicators 76, 81–96. https://doi.org/10.1016/j.ecolind.2017.01.011

Beazley, L.I., Kenchington, E.L., Murillo, F.J., Sacau, M. del M., 2013. Deep-sea sponge grounds enhance diversity and abundance of epibenthic megafauna in the Northwest Atlantic. ICES Journal of Marine Science 70, 1471–1490. https://doi.org/10.1093/icesjms/fst124

Beisiegel, K., Darr, A., Gogina, M., Zettler, M.L., 2017. Benefits and shortcomings of non-destructive benthic imagery for monitoring hard-bottom habitats. Marine Pollution Bulletin 121, 5–15. https://doi.org/10.1016/j.marpolbul.2017.04.009

Bell, J., 2007. Contrasting patterns of species and functional composition of coral reef sponge assemblages. Mar. Ecol. Prog. Ser. 339, 73–81. https://doi.org/10.3354/meps339073

Bell, J.B., Alt, C.H.S., Jones, D.O.B., 2016. Benthic megafauna on steep slopes at the Northern Mid-Atlantic Ridge. Marine Ecology 37, 1290–1302. https://doi.org/10.1111/maec.12319

Bell, J.J., 2008. The functional roles of marine sponges. Estuarine, Coastal and Shelf Science 79, 341–353. https://doi.org/10.1016/j.ecss.2008.05.002

Bell, J.J., Barnes, D.K.A., 2001. Sponge morphological diversity: a qualitative predictor of species diversity? Aquatic Conserv: Mar. Freshw. Ecosyst. 11, 109–121. https://doi.org/10.1002/aqc.436

Bell, J.J., Barnes, D.K.A., 2000. The influences of bathymetry and flow regime upon the morphology of sublittoral sponge communities. J. Mar. Biol. Ass. 80, 707–718. https://doi.org/10.1017/S0025315400002538

Bell, K.L.C., Chow, J.S., Hope, A., Quinzin, M.C., Cantner, K.A., Amon, D.J., Cramp, J.E., Rotjan, R.D., Kamalu, L., de Vos, A., Talma, S., Buglass, S., Wade, V., Filander, Z., Noyes, K., Lynch, M., Knight, A., Lourenço, N., Girguis, P.R., de Sousa, J.B., Blake, C., Kennedy, B.R.C., Noyes, T.J., McClain, C.R., 2022. Low-Cost, Deep-Sea Imaging and Analysis Tools for Deep-Sea Exploration: A Collaborative Design Study. Front. Mar. Sci. 9, 873700. https://doi.org/10.3389/fmars.2022.873700

Bo, M., Bertolino, M., Bavestrello, G., Canese, S., Giusti, M., Angiolillo, M., Pansini, M., Taviani, M., 2012. Role of deep sponge grounds in the Mediterranean Sea: a case study in southern Italy. Hydrobiologia 687, 163–177. https://doi.org/10.1007/s10750-011-0964-1

Bo, M., Bertolino, M., Borghini, M., Castellano, M., Covazzi Harriague, A., Di Camillo, C.G., Gasparini, G., Misic, C., Povero, P., Pusceddu, A., Schroeder, K., Bavestrello, G., 2011. Characteristics of the Mesophotic Megabenthic Assemblages of the Vercelli Seamount (North Tyrrhenian Sea). PLoS ONE 6, e16357. https://doi.org/10.1371/journal.pone.0016357

Bo, M., Coppari, M., Betti, F., Massa, F., Gay, G., Cattaneo-Vietti, R., Bavestrello, G., 2020. Unveiling the deep biodiversity of the Janua Seamount (Ligurian Sea): first Mediterranean sighting of the rare Atlantic bamboo coral Chelidonisis aurantiaca Studer, 1890. Deep Sea Research Part I: Oceanographic Research Papers 156, 103186. https://doi.org/10.1016/j.dsr.2019.103186

Borcard, D., Gillet, F., Legendre, P., 2018. Numerical Ecology with R, Use R! Springer International Publishing, Cham. https://doi.org/10.1007/978-3-319-71404-2

Boschen, R., Rowden, A., Clark, M., Barton, S., Pallentin, A., Gardner, J., 2015. Megabenthic assemblage structure on three New Zealand seamounts: implications for seafloor massive sulfide mining. Marine Ecology Progress Series 523, 1–14. https://doi.org/10.3354/meps11239

Bouchet, P., 2009. MIRIKY Cruise, RV MIRIKY [WWW Document]. URL https://expeditions.mnhn.fr/campaign/miriky?lang=en_US

Bouchet, P., Perez, T., Le Gall, L., 2010. ATIMO VATAE cruise, RV Antea. https://doi.org/10.17600/10110040

Bouchet, P., Ramos, A., 2009. MAINBAZA Cruise, RV Vizcondede Eza [WWW Document]. URL https://expeditions.mnhn.fr/campaign/mainbaza?lang=en_US

Bourillet, J.-F., Ferry, J.-N., Bourges, P., 2013. PAMELA : Passive Margins Exploration Laboratories. https://doi.org/10.18142/236

Bowden, D.A., Rowden, A.A., Chin, C.C., Hempel, S., Wood, B.A., Hart, A.C., Clark, M.R., Fisheries New Zealand (Government agency), 2020. Best practice in seabed image analysis for determining taxa, habitat, or substrata distributions.

Bowden, D.A., Rowden, A.A., Leduc, D., Beaumont, J., Clark, M.R., 2016. Deep-sea seabed habitats: Do they support distinct mega-epifaunal communities that have different vulnerabilities to anthropogenic disturbance? Deep Sea Research Part I: Oceanographic Research Papers 107, 31–47. https://doi.org/10.1016/j.dsr.2015.10.011

Braga-Henriques, A., Porteiro, F.M., Ribeiro, P.A., de Matos, V., Sampaio, I., Ocaña, O., Santos, R.S., 2013. Diversity, distribution and spatial structure of the cold-water coral fauna of the Azores (NE Atlantic). Biogeosciences 10, 4009–4036. https://doi.org/10.5194/bg-10-4009-2013

Brault, S., Stuart, C.T., Wagstaff, M.C., McClain, C.R., Allen, J.A., Rex, M.A., 2013. Contrasting patterns of α- and β-diversity in deep-sea bivalves of the eastern and western North Atlantic. Deep Sea Research Part II: Topical Studies in Oceanography 92, 157–164. https://doi.org/10.1016/j.dsr2.2013.01.018

Bremner, J., Rogers, S., Frid, C., 2006. Methods for describing ecological functioning of marine benthic assemblages using biological traits analysis (BTA). Ecological Indicators 6, 609–622. https://doi.org/10.1016/j.ecolind.2005.08.026

Brewin, P.E., Stocks, K.I., Menezes, G., 2007. A history of seamount research, in: Pitcher, T.J., Morato, T., Hart, P.J.B., Clark, M.R., Haggan, N., Santos, R.S. (Eds.), Seamounts: Ecology, Fisheries & Conservation. Blackwell Publishing Ltd, Oxford, UK, pp. 41–61. https://doi.org/10.1002/9780470691953.ch3

Bridges, A.E.H., Barnes, D.K.A., Bell, J.B., Ross, R.E., Howell, K.L., 2022. Depth and latitudinal gradients of diversity in seamount benthic communities. Journal of Biogeography jbi.14355. https://doi.org/10.1111/jbi.14355

Bridges, A.E.H., Barnes, D.K.A., Bell, J.B., Ross, R.E., Howell, K.L., 2021. Benthic Assemblage Composition of South Atlantic Seamounts. Front. Mar. Sci. 8, 660648. https://doi.org/10.3389/fmars.2021.660648

Buhl-Mortensen, L., Vanreusel, A., Gooday, A.J., Levin, L.A., Priede, I.G., Buhl-Mortensen, P., Gheerardyn, H., King, N.J., Raes, M., 2010. Biological structures as a source of habitat heterogeneity and biodiversity on the deep ocean margins: Biological structures and biodiversity. Marine Ecology 31, 21–50. https://doi.org/10.1111/j.1439-0485.2010.00359.x

Buhl-Mortensen, P., Buhl-Mortensen, L., Purser, A., 2016. Trophic Ecology and Habitat Provision in Cold-Water Coral Ecosystems, in: Rossi, S., Bramanti, L., Gori, A., Orejas, C. (Eds.), Marine Animal Forests. Springer International Publishing, Cham, pp. 1–26. https://doi.org/10.1007/978-3-319-17001-5_20-1

Burukovsky, R.N., 2013. Shrimps of the family Nematocarcinidae Smith, 1884 (Crustacea, Decapoda, Caridea) from Taiwan and the Philippines collected by the TAIWAN, PANGLAO 2005 and AURORA expeditions in the western Pacific, in: Ahyong, S.T., Chan, T.-Y., Corbari, L., P. K. L., N. (Eds.), Tropical Deep-Sea Benthos 27 Mémoires Du Muséum National d'Histoire Naturelle (1993). pp. 154–189.

Burukovsky, R.N., 2011. Geographic distribution of nematocarcinidae shrimps (Crustacea, Decapoda). Zoologicheskii Zhurnal 90, 293–301.

Cárdenas, P., Pérez, T., Boury-Esnault, N., 2012. Sponge Systematics Facing New Challenges, in: Becerro, M.A., Uriz, M.J., Maldonado, M., Turon, X. (Eds.), Advances in Marine Biology. Elsevier, pp. 79–209. https://doi.org/10.1016/B978-0-12-387787-1.00010-6

Castelin, M., Delavenne, J., Brisset, J., Chambart, C., Corbari, L., Keszler, L., Lozouet, P., Olu, K., Poncet, L., Puillandre, N., Samadi, S., 2017. Exploration et étude de la biodiversité benthique profonde de Mayotte et des îles éparses (Rapport final de la convention MNHN-TAAF dans le cadre du Xème FED régional « Gestion durable du patrimoine naturel de Mayotte et des îles Eparses ».).

Chappell, J., 1980. Coral morphology, diversity and reef growth. Nature 286, 249–252. https://doi.org/10.1038/286249a0

Charles, C., Pelleter, E., Révillon, S., Nonnotte, P., Jorry, S.J., Kluska, J.-M., 2020. Intermediate and deep ocean current circulation in the Mozambique Channel: New insights from ferromanganese crust Nd isotopes. Marine Geology 430, 106356. https://doi.org/10.1016/j.margeo.2020.106356

Clark, M.R., Bowden, D.A., 2015. Seamount biodiversity: high variability both within and between seamounts in the Ross Sea region of Antarctica. Hydrobiologia 761, 161–180. https://doi.org/10.1007/s10750-015-2327-9

Clark, M.R., Bowden, D.A., Rowden, A.A., Stewart, R., 2019. Little Evidence of Benthic Community Resilience to Bottom Trawling on Seamounts After 15 Years. Front. Mar. Sci. 6, 63. https://doi.org/10.3389/fmars.2019.00063

Clark, M.R., Consalvey, M., Rowden, A.A. (Eds.), 2016. Biological Sampling in the Deep Sea, Wiley-Blackwell. ed.

Clark, M.R., Rowden, A.A., Schlacher, T., Williams, A., Consalvey, M., Stocks, K.I., Rogers, A.D., O'Hara, T.D., White, M., Shank, T.M., Hall-Spencer, J.M., 2010. The Ecology of Seamounts: Structure, Function, and Human Impacts. Annual Review of Marine Science 2, 253–278. https://doi.org/10.1146/annurev-marine-120308-081109

Clark, M.R., Schlacher, T.A., Rowden, A.A., Stocks, K.I., Consalvey, M., 2012. Science Priorities for Seamounts: Research Links to Conservation and Management. PLoS ONE 7, e29232. https://doi.org/10.1371/journal.pone.0029232

Collins, C., Hermes, J.C., Roman, R.E., Reason, C.J.C., 2016. First dedicated hydrographic survey of the Comoros Basin. Journal of Geophysical Research: Oceans 121, 1291–1305. https://doi.org/10.1002/2015JC011418

Collins, P., Kennedy, R., Van Dover, C., 2012. A biological survey method applied to seafloor massive sulphides (SMS) with contagiously distributed hydrothermal-vent fauna. Mar. Ecol. Prog. Ser. 452, 89–107. https://doi.org/10.3354/meps09646

Corbari, L., Olu, K., Samadi, S., 2014. MADEEP cruise, RV Alis. https://doi.org/10.17600/14004000

Corbari, L., Samadi, S., Olu, K., 2017. BIOMAGLO cruise, RV Antea. https://doi.org/10.17600/17004000

Courgeon, S., Bachèlery, P., Jouet, G., Jorry, S.J., Bou, E., BouDagher-Fadel, M.K., Révillon, S., Camoin, G., Poli, E., 2018. The offshore east African rift system: new insights from the Sakalaves seamounts (Davie Ridge, SW Indian Ocean). Terra Nova 30, 380–388. https://doi.org/10.1111/ter.12353

Courgeon, S., Jorry, S.J., Camoin, G.F., BouDagher-Fadel, M.K., Jouet, G., Révillon, S., Bachèlery, P., Pelleter, E., Borgomano, J., Poli, E., Droxler, A.W., 2016. Growth and demise of Cenozoic isolated carbonate platforms: New insights from the Mozambique Channel seamounts (SW Indian Ocean). Marine Geology 380, 90–105. https://doi.org/10.1016/j.margeo.2016.07.006

Courgeon, S., Jorry, S.J., Jouet, G., Camoin, G., BouDagher-Fadel, M.K., Bachèlery, P., Caline, B., Boichard, R., Révillon, S., Thomas, Y., Thereau, E., Guérin, C., 2017. Impact of tectonic and volcanism on the Neogene evolution of isolated carbonate platforms (SW Indian Ocean). Sedimentary Geology 355, 114–131. https://doi.org/10.1016/j.sedgeo.2017.04.008

Cunha, M.R., Hilário, A., Santos, R.S., 2017. Advances in deep-sea biology: biodiversity, ecosystem functioning and conservation. An introduction and overview. Deep Sea Research Part II: Topical Studies in Oceanography 137, 1–5. https://doi.org/10.1016/j.dsr2.2017.02.003

d'Hondt, M.J., d'Hondt, J.L., 2019. Note sur quelques espèces d'Anthomastus et autres Anthomastinae (Octocoralliaires, Alcyoniidae) ; description de Pseudoanthomastus gloriosus n. sp. Bulletin de la Société Linnéenne de Bordeaux 154(1/2), nouvelle série n°47 103–108.

Da Ros, Z., Dell'Anno, A., Morato, T., Sweetman, A.K., Carreiro-Silva, M., Smith, C.J., Papadopoulou, N., Corinaldesi, C., Bianchelli, S., Gambi, C., Cimino, R., Snelgrove, P., Van Dover, C.L., Danovaro, R., 2019. The deep sea: The new frontier for ecological restoration. Marine Policy 108, 103642. https://doi.org/10.1016/j.marpol.2019.103642

Danovaro, R., Corinaldesi, C., Dell'Anno, A., Snelgrove, P.V.R., 2017. The deep-sea under global change. Current Biology 27, R461–R465. https://doi.org/10.1016/j.cub.2017.02.046

Danovaro, R., Snelgrove, P.V.R., Tyler, P., 2014. Challenging the paradigms of deep-sea ecology. Trends in Ecology & Evolution 29, 465–475. https://doi.org/10.1016/j.tree.2014.06.002

Davies, J.S., Stewart, H.A., Narayanaswamy, B.E., Jacobs, C., Spicer, J., Golding, N., Howell, K.L., 2015. Benthic Assemblages of the Anton Dohrn Seamount (NE Atlantic): Defining Deep-Sea Biotopes to Support Habitat Mapping and Management Efforts with a Focus on Vulnerable Marine Ecosystems. PLoS ONE 10, e0124815. https://doi.org/10.1371/journal.pone.0124815

de la Torriente, A., Aguilar, R., González-Irusta, J.M., Blanco, M., Serrano, A., 2020. Habitat forming species explain taxonomic and functional diversities in a Mediterranean seamount. Ecological Indicators 118, 106747. https://doi.org/10.1016/j.ecolind.2020.106747

de la Torriente, A., Serrano, A., Fernández-Salas, L.M., García, M., Aguilar, R., 2018. Identifying epibenthic habitats on the Seco de los Olivos Seamount: Species assemblages and environmental characteristics. Deep Sea Research Part I: Oceanographic Research Papers 135, 9–22. https://doi.org/10.1016/j.dsr.2018.03.015

de Mendonça, S.N., Metaxas, A., 2021. Comparing the Performance of a Remotely Operated Vehicle, a Drop Camera, and a Trawl in Capturing Deep-Sea Epifaunal Abundance and Diversity. Front. Mar. Sci. 8, 631354. https://doi.org/10.3389/fmars.2021.631354

de Ruijter, W.P.M., Aken, H.M. van, Beier, E.J., Lutjeharms, J.R.E., Matano, R.P., Schouten, M.W., 2004. Eddies and dipoles around South Madagascar: formation, pathways and large-scale impact. Deep Sea Research Part I: Oceanographic Research Papers 51, 383–400. https://doi.org/10.1016/j.dsr.2003.10.011

de Ruijter, W.P.M., Ridderinkhof, H., Lutjeharms, J.R.E., Schouten, M.W., Veth, C., 2002. Observations of the flow in the Mozambique Channel. Geophysical Research Letters 29, 140-1-140–3. https://doi.org/10.1029/2001GL013714

DeBiasse, M.B., Hellberg, M.E., 2015. Discordance between morphological and molecular species boundaries among Caribbean species of the reef sponge *Callyspongia*. Ecol Evol 5, 663–675. https://doi.org/10.1002/ece3.1381

Denis, V., Ribas-Deulofeu, L., Sturaro, N., Kuo, C.-Y., Chen, C.A., 2017. A functional approach to the structural complexity of coral assemblages based on colony morphological features. Scientific Reports 7. https://doi.org/10.1038/s41598-017-10334-w

Dijkstra, J.A., Mello, K., Sowers, D., Malik, M., Watling, L., Mayer, L.A., 2021. Fine-scale mapping of deep-sea habitat-forming species densities reveals taxonomic specific environmental drivers. Global Ecol Biogeogr 30, 1286–1298. https://doi.org/10.1111/geb.13285

Doudet, M., Thomas, A., 2021. Classification automatique d'éponges marines profondes par imagerie (Rapport de stage (M1)). Institut Supérieur de l'Électronique et du Numérique (ISEN) - Institut français de recherche pour l'exploitation de la mer (Ifremer).

Dray, S., Bauman, D., Blanchet, F.G., Borcard, D., Clappe, S., Guenard, G., Jombart, T., Larocque, G., Legendre, P., Madi, N., Wagner, H., 2022. adespatial: Multivariate Multiscale Spatial Analysis. R package version 0.3-16.

Dray, S., Choler, P., Dolédec, S., Peres-Neto, P.R., Thuiller, W., Pavoine, S., ter Braak, C.J.F., 2014. Combining the fourth-corner and the RLQ methods for assessing trait responses to environmental variation. Ecology 95, 14–21. https://doi.org/10.1890/13-0196.1

Dray, S., Dufour, A.-B., 2007. The ade4 Package: Implementing the Duality Diagram for Ecologists. J. Stat. Soft. 22. https://doi.org/10.18637/jss.v022.i04

Dray, S., Legendre, P., 2008. Testing the species traits–environment relationships: the fourth-corner problem revisited. Ecology 89, 3400–3412. https://doi.org/10.1890/08-0349.1

Du Preez, C., Curtis, J.M.R., Clarke, M.E., 2016. The Structure and Distribution of Benthic Communities on a Shallow Seamount (Cobb Seamount, Northeast Pacific Ocean). PLoS ONE 11, e0165513. https://doi.org/10.1371/journal.pone.0165513

Du Preez, C., Swan, K.D., Curtis, J.M.R., 2020. Cold-Water Corals and Other Vulnerable Biological Structures on a North Pacific Seamount After Half a Century of Fishing. Front. Mar. Sci. 7, 17. https://doi.org/10.3389/fmars.2020.00017

Dufrêne, M., Legendre, P., 1997. Species assemblages and indicator species: the need for a flexible asymmetrical approach. Ecological Monographs 67, 22.

Dugard, C., Carcopino, C., 2020. Classification des habitats marins par imagerie (Ifremer) (Rapport de stage (M1)). Institut Supérieur de l'Électronique et du Numérique (ISEN) - Institut français de recherche pour l'exploitation de la mer (Ifremer).

Durden, J.M., Bett, B., Schoening, T., Morris, K., Nattkemper, T., Ruhl, H., 2016a. Comparison of image annotation data generated by multiple investigators for benthic ecology. Marine Ecology Progress Series 552, 61–70. https://doi.org/10.3354/meps11775

Durden, J.M., Schoening, T., Althaus, F., Friedman, A., Garcia, R., Glover, A.G., Greinert, J., Jacobsen-Stout, N., Jones, D.O.B., Jordt, A., Kaeli, J., Koser, K., Kuhnz, L., Lindsay, D., Morris, K., Nattkemper, T.W., Osterloff, J., Ruhl, H., Singh, H., Tran, M., Bett, B.J., 2016b. Perspectives in visual imaging for marine biology and ecology: from acquisition to understanding. Oceanography and Marine Biology An Annual Review, Oceanography and Marine Biology - An Annual Review 54, 1–72. https://doi.org/10.1201/9781315368597

Elliott, J., 2016. Morphological plasticity allows coral to actively overgrow the aggressive sponge Terpios hoshinota (Mauritius, Southwestern Indian Ocean) 5.

Faivre, L., Teichert, N., Valade, P., Monnier, O., Couprie, S., 2020. Evaluation des conditions de référence des cours d'eau de Mayotte - Projet REZORD -MAY - Volet 1 : Caractérisation des pressions s'exerçant sur les populations de poissons et de macro- crustacés amphihalins de Mayotte. Rapport final OCE, MNHN, OFB.

FAO (Ed.), 2009. International guidelines for the management of deep-sea fisheries in the high seas: = Directives internationales sur la gestion de la pêche profonde en haute mer. Food and Agriculture Organization of the United Nations, Rome.

Feng, J.-C., Liang, J., Cai, Y., Zhang, S., Xue, J., Yang, Z., 2022. Deep-sea organisms research oriented by deep-sea technologies development. https://doi.org/10.1016/j.scib.2022.07.016

Feuillet, N., Jorry, S., Crawford, W.C., Deplus, C., Thinon, I., Jacques, E., Saurel, J.M., Lemoine, A., Paquet, F., Satriano, C., Aiken, C., Foix, O., Kowalski, P., Laurent, A., Rinnert, E., Cathalot, C., Donval, J.-P., Guyader, V., Gaillot, A., Scalabrin, C., Moreira, M., Peltier, A., Beauducel, F., Grandin, R., Ballu, V., Daniel, R., Pelleau, P., Gomez, J., Besançon, S., Geli, L., Bernard, P., Bachelery, P., Fouquet, Y., Bertil, D., Lemarchand, A., Van der Woerd, J., 2021. Birth of a large volcanic edifice offshore Mayotte via lithosphere-scale dyke intrusion. Nat. Geosci. 14, 787–795. https://doi.org/10.1038/s41561-021-00809-x

Fischer, W., Bianchi, G. (Eds.), 1984. FAO Species Identification Sheets for Fishery Purposes. Western Indian Ocean (Fishing Area 51), Prepared and Printed with the Support of the Danish International Development Agency (DANIDA). ed. FAO, Rome.

Fontaine, B., Perrard, A., Bouchet, P., 2012. 21 years of shelf life between discovery and description of new species. Current Biology 22, R943–R944. https://doi.org/10.1016/j.cub.2012.10.029

Genin, A., Dayton, P.K., Lonsdale, P.F., Spiess, F.N., 1986. Corals on seamount peaks provide evidence of current acceleration over deep-sea topography. Nature 322, 59–61. https://doi.org/10.1038/322059a0

Glover, A.G., Wiklund, H., Chen, C., Dahlgren, T.G., 2018. Managing a sustainable deep-sea 'blue economy' requires knowledge of what actually lives there. eLife 7, e41319. https://doi.org/10.7554/eLife.41319

Gollner, S., Kaiser, S., Menzel, L., Jones, D.O.B., Brown, A., Mestre, N.C., van Oevelen, D., Menot, L., Colaço, A., Canals, M., Cuvelier, D., Durden, J.M., Gebruk, A., Egho, G.A., Haeckel, M., Marcon, Y., Mevenkamp, L., Morato, T., Pham, C.K., Purser, A., Sanchez-Vidal, A., Vanreusel, A., Vink, A., Martinez Arbizu, P., 2017. Resilience of benthic deep-sea fauna to mining activities. Marine Environmental Research 129, 76–101. https://doi.org/10.1016/j.marenvres.2017.04.010

Goode, S.L., Rowden, A.A., Bowden, D.A., Clark, M.R., Stephenson, F., 2021. Fine-Scale Mapping of Mega-Epibenthic Communities and Their Patch Characteristics on Two New Zealand Seamounts. Front. Mar. Sci. 8, 765407. https://doi.org/10.3389/fmars.2021.765407

Gourdon, S., 2020. Approches méthodologiques pour la caractérisation de la mégafaune à partir de l'analyse d'images de monts sous-marins : Cas d'étude sur les éponges peuplant les fonds durs dans le canal du Mozambique et en Nouvelle-Calédonie (Rapport de stage (L2)). Université de Bretagne-Occidentale - IUT Brest - Institut français de recherche pour l'exploitation de la mer (Ifremer).

Grassle, J.F., Sanders, H.L., Hessler, R.R., Rowe, G.T., McLellan, T., 1975. Pattern and zonation: a study of the bathyal megafauna using the research submersible Alvin. Deep Sea Research and Oceanographic Abstracts 22, 457–481. https://doi.org/10.1016/0011-7471(75)90020-0

Hadi, T.A., Budiyanto, A., Wentao, N., 2015. The morphological and species diversity of sponges in coral reef ecosystem in the Lembeh Strait, Bitung 13.

Hagedorn, G., Rambold, G., Martellos, S., 2010. Types of identification keys 6.

Hall-Spencer, J., Rogers, A., Davies, J., Foggo, A., 2007. Deep-sea coral distribution on seamounts, oceanic islands, and continental slopes in the Northeast Atlantic 13.

Hanafi-Portier, M., Samadi, S., Corbari, L., Chan, T.-Y., Chen, W.-J., Chen, J.-N., Lee, M.-Y., Mah, C., Saucède, T., Borremans, C., Olu, K., 2021. When Imagery and Physical Sampling Work Together: Toward an Integrative Methodology of Deep-Sea Image-Based Megafauna Identification. Front. Mar. Sci. 8, 749078. https://doi.org/10.3389/fmars.2021.749078

Hawkes, N., Korabik, M., Beazley, L., Rapp, H., Xavier, J., Kenchington, E., 2019. Glass sponge grounds on the Scotian Shelf and their associated biodiversity. Mar. Ecol. Prog. Ser. 614, 91–109. https://doi.org/10.3354/meps12903

Hein, J.R., Conrad, T.A., Staudigel, H., 2010. Seamount mineral deposits, a source of rare metals for high-technology industries. Oceanography 23, 184–189.

Henry, L.-A., Roberts, J.M., 2014. Recommendations for best practice in deep-sea habitat classification: Bullimore et al. as a case study. ICES Journal of Marine Science 71, 895–898. https://doi.org/10.1093/icesjms/fst175

Henry, L.-A., Vad, J., Findlay, H.S., Murillo, J., Milligan, R., Roberts, J.M., 2015. Environmental variability and biodiversity of megabenthos on the Hebrides Terrace Seamount (Northeast Atlantic). Scientific Reports 4. https://doi.org/10.1038/srep05589

Hoff, G.R., Stevens, B., 2005. Faunal assemblage structure on the Patton Seamount (Gulf of Alaska, USA) 13.

Horton, T., Marsh, L., Bett, B.J., Gates, A.R., Jones, D.O.B., Benoist, N.M.A., Pfeifer, S., Simon-Lledó, E., Durden, J.M., Vandepitte, L., Appeltans, W., 2021. Recommendations for the Standardisation of Open Taxonomic Nomenclature for Image-Based Identifications. Front. Mar. Sci. 8, 620702. https://doi.org/10.3389/fmars.2021.620702

Howell, K.L., Bullimore, R.D., Foster, N.L., 2014. Quality assurance in the identification of deep-sea taxa from video and image analysis: response to Henry and Roberts. ICES Journal of Marine Science 71, 899–906. https://doi.org/10.1093/icesjms/fsu052

Howell, K.L., Davies, J.S., Allcock, A.L., Braga-Henriques, A., Buhl-Mortensen, P., Carreiro-Silva, M., Dominguez-Carrió, C., Durden, J.M., Foster, N.L., Game, C.A., Hitchin, B., Horton, T., Hosking, B., Jones, D.O.B., Mah, C., Laguionie Marchais, C., Menot, L., Morato, T., Pearman, T.R.R., Piechaud, N., Ross, R.E., Ruhl, H.A., Saeedi, H., Stefanoudis, P.V., Taranto, G.H., Thompson, M.B., Taylor, J.R., Tyler, P., Vad, J., Victorero, L., Vieira, R.P., Woodall, L.C., Xavier, J.R., Wagner, D., 2019. A framework for the development of a global standardised marine taxon reference image database (SMarTaR-ID) to support image-based analyses. PLOS ONE 14, e0218904. https://doi.org/10.1371/journal.pone.0218904

Howell, K.L., Hilário, A., Allcock, A.L., Bailey, D.M., Baker, M., Clark, M.R., Colaço, A., Copley, J., Cordes, E.E., Danovaro, R., Dissanayake, A., Escobar, E., Esquete, P., Gallagher, A.J., Gates, A.R., Gaudron, S.M., German, C.R., Gjerde, K.M., Higgs, N.D., Le Bris, N., Levin, L.A., Manea, E., McClain, C., Menot, L., Mestre, N.C., Metaxas, A., Milligan, R.J., Muthumbi, A.W.N., Narayanaswamy, B.E., Ramalho, S.P., Ramirez-Llodra, E., Robson, L.M., Rogers, A.D., Sellanes, J., Sigwart, J.D., Sink, K., Snelgrove, P.V.R., Stefanoudis, P.V., Sumida, P.Y., Taylor, M.L., Thurber, A.R., Vieira, R.P., Watanabe, H.K., Woodall, L.C., Xavier, J.R., 2020. A Blueprint for an Inclusive, Global Deep-Sea Ocean Decade Field Program. Front. Mar. Sci. 7, 584861. https://doi.org/10.3389/fmars.2020.584861

Howell, K.L., Mowles, S.L., Foggo, A., 2010. Mounting evidence: near-slope seamounts are faunally indistinct from an adjacent bank: Seamounts are not faunally distinct. Marine Ecology 31, 52–62. https://doi.org/10.1111/j.1439-0485.2010.00368.x

Hoyoux, C., Zbinden, M., Samadi, S., Gaill, F., Compère, P., 2012. Diet and gut microorganisms of *Munidopsis* squat lobsters associated with natural woods and mesh-enclosed substrates in the deep South Pacific. Marine Biology Research 8, 28–47. https://doi.org/10.1080/17451000.2011.605144

Hsieh, T.C., Ma, K.H., Chao, A., 2020. iNEXT: iNterpolation and EXTrapolation for species diversity. R package version 2.0.20.

Hubbs, C.L., 1959. Initial discoveries of fish faunas on seamounts and offshore banks in the eastern Pacific. Pacific Science 12, 311–316.

Jorry, S., 2014. PTOLEMEE cruise, RV L'Atalante. https://doi.org/10.17600/14000900

Jouet, G., Deville, E., 2015. PAMELA-MOZ04 cruise, RV Pourquoi pas ?. https://doi.org/10.17600/15000700

Kamilar, J.M., Cooper, N., 2013. Phylogenetic signal in primate behaviour, ecology and life history. Phil. Trans. R. Soc. B 368, rstb.2012.0341, 20120341. https://doi.org/10.1098/rstb.2012.0341

Katzschmann, R.K., DelPreto, J., MacCurdy, R., Rus, D., 2018. Exploration of underwater life with an acoustically controlled soft robotic fish. Sci. Robot. 3, eaar3449. https://doi.org/10.1126/scirobotics.aar3449

Kaufmann, R.S., Wakefield, W.W., Genin, A., 1989. Distribution of epibenthic megafauna and lebensspuren on two central North Pacific seamounts. Deep Sea Research Part A. Oceanographic Research Papers 36, 1863–1896. https://doi.org/10.1016/0198-0149(89)90116-7

Kleyer, M., Dray, S., Bello, F., Lepš, J., Pakeman, R.J., Strauss, B., Thuiller, W., Lavorel, S., 2012. Assessing species and community functional responses to environmental gradients: which multivariate methods? Journal of Vegetation Science 23, 805–821. https://doi.org/10.1111/j.1654-1103.2012.01402.x

Komai, T., Chan, T.-Y., 2013. New records of Glyphocrangon A. Milne-Edwards, 1881 (Crustacea, Decapoda, Caridea, Glyphocrangonidae) from recent French expeditions off the Mozambique Channel and Papua New Guinea, with description of one new species. Mémoires du Muséum national d'Histoire naturelle (1993).

Krell, F.-T., 2004. Parataxonomy vs. taxonomy in biodiversity studies – pitfalls and applicability of 'morphospecies' sorting. Biodiversity and Conservation 13, 795–812. https://doi.org/10.1023/B:BIOC.0000011727.53780.63

Kroh, A., Smith, A.B., 2010. The phylogeny and classification of post-Palaeozoic echinoids. Journal of Systematic Palaeontology 8, 147–212. https://doi.org/10.1080/14772011003603556

Kvile, K.Ø., Taranto, G.H., Pitcher, T.J., Morato, T., 2014. A global assessment of seamount ecosystems knowledge using an ecosystem evaluation framework. Biological Conservation 173, 108–120. https://doi.org/10.1016/j.biocon.2013.10.002

Langenkämper, D., Zurowietz, M., Schoening, T., Nattkemper, T.W., 2017. BIIGLE 2.0 - Browsing and Annotating Large Marine Image Collections. Frontiers in Marine Science 4. https://doi.org/10.3389/fmars.2017.00083

Lapointe, A.E., Watling, L., France, S.C., Auster, P.J., 2020. Megabenthic assemblages in the lower bathyal (700–3000 m) on the New England and Corner Rise Seamounts, Northwest Atlantic. Deep Sea Research Part I: Oceanographic Research Papers 165, 103366. https://doi.org/10.1016/j.dsr.2020.103366

Laschi, C., Calisti, M., 2021. Soft robot reached the deepest part of the ocean. Nature 591, 35–36. https://doi.org/10.1038/d41586-021-00297-4

Lavelle, J.W., Mohn, C., 2010. Motion, commotion and biophysical connections at deepocean seamounts. Oceanography 23, 90–103.

Lawrence, J.M., Jangoux, M., 2020. Chapter 21: Cidaroids, in: Lawrence, J.M. (Ed.), Sea Urchins: Biology and Ecology.

Legendre, P., 2014. Interpreting the replacement and richness difference components of beta diversity: Replacement and richness difference components. Global Ecology and Biogeography 23, 1324–1334. https://doi.org/10.1111/geb.12207

Legendre, P., De Cáceres, M., 2013. Beta diversity as the variance of community data: dissimilarity coefficients and partitioning. Ecology Letters 16, 951–963. https://doi.org/10.1111/ele.12141

Legendre, P., Gallagher, E.D., 2001. Ecologically meaningful transformations for ordination of species data. Oecologia 129, 271–280. https://doi.org/10.1007/s004420100716

Legendre, P., Legendre, L.F., 2012. Numerical ecology, 3rd ed. Elsevier.

Leroy, B., 2022. biogeonetworks: Biogeographical Network Manipulation And Analysis. R package version 0.1.2.

Levin, L.A., 2005. Ecology of cold seep sediments: interactions of fauna with flow, chemistry and microbes 46.

Levin, L.A., Le Bris, N., 2015. The deep ocean under climate change. Science 350, 766–768. https://doi.org/10.1126/science.aad0126

Levin, L.A., Sibuet, M., 2012. Understanding Continental Margin Biodiversity: A New Imperative. Annual Review of Marine Science 4, 79–112. https://doi.org/10.1146/annurev-marine-120709-142714

Lévy, M., Klein, P., Treguier, A.-M., 2001. Impact of sub-mesoscale physics on production and subduction of phytoplankton in an oligotrophic regime. Journal of Marine Research 59, 535–565. https://doi.org/10.1357/002224001762842181

Long, D.J., Baco, A.R., 2014. Rapid change with depth in megabenthic structure-forming communities of the Makapu'u deep-sea coral bed. Deep Sea Research Part II: Topical Studies in Oceanography 99, 158–168. https://doi.org/10.1016/j.dsr2.2013.05.032

Łukowiak, M., 2020. Utilizing sponge spicules in taxonomic, ecological and environmental reconstructions: a review. PeerJ 8, e10601. https://doi.org/10.7717/peerj.10601

Lundsten, L., Barry, J., Cailliet, G., Clague, D., DeVogelaere, A., Geller, J., 2009. Benthic invertebrate communities on three seamounts off southern and central California, USA. Mar. Ecol. Prog. Ser. 374, 23–32. https://doi.org/10.3354/meps07745

Mah, C., 2007. Phylogeny of the Zoroasteridae (Zorocallina; Forcipulatida): evolutionary events in deep-sea Asteroidea displaying Palaeozoic features. Zoological Journal of the Linnean Society 150, 177–210. https://doi.org/10.1111/j.1096-3642.2007.00291.x

Mah, C.L., 2020. New species, occurrence records and observations of predation by deep-sea Asteroidea (Echinodermata) from the North Atlantic by NOAA ship Okeanos Explorer. Zootaxa 4766, 201–260. https://doi.org/10.11646/zootaxa.4766.2.1

Malauene, B.S., Shillington, F.A., Roberts, M.J., Moloney, C.L., 2014. Cool, elevated chlorophyll-a waters off northern Mozambique. Deep Sea Research Part II: Topical Studies in Oceanography 100, 68–78. https://doi.org/10.1016/j.dsr2.2013.10.017

Marsac, F., Barlow, R., Ternon, J.F., Ménard, F., Roberts, M., 2014. Ecosystem functioning in the Mozambique Channel: Synthesis and future research. Deep Sea Research Part II: Topical Studies in Oceanography 100, 212–220. https://doi.org/10.1016/j.dsr2.2013.10.028

Mary George, A., Brodie, J., Daniell, J., Capper, A., Jonker, M., 2018. Can sponge morphologies act as environmental proxies to biophysical factors in the Great Barrier Reef, Australia? Ecological Indicators 93, 1152–1162. https://doi.org/10.1016/j.ecolind.2018.06.016

McClain, C.R., Lundsten, L., 2015. Assemblage structure is related to slope and depth on a deep offshore Pacific seamount chain. Marine Ecology 36, 210–220. https://doi.org/10.1111/maec.12136

McClain, C.R., Lundsten, L., Barry, J., DeVogelaere, A., 2010. Assemblage structure, but not diversity or density, change with depth on a northeast Pacific seamount: Bathymetric patterns in diversity, abundance and assemblage structure. Marine Ecology 31, 14–25. https://doi.org/10.1111/j.1439-0485.2010.00367.x

McClain, C.R., Lundsten, L., Ream, M., Barry, J., DeVogelaere, A., 2009. Endemicity, Biogeography, Composition, and Community Structure On a Northeast Pacific Seamount. PLoS ONE 4, e4141. https://doi.org/10.1371/journal.pone.0004141

McClain, C.R., Schlacher, T.A., 2015. On some hypotheses of diversity of animal life at great depths on the sea floor. Mar Ecol 36, 849–872. https://doi.org/10.1111/maec.12288

McDonald, J.I., Hooper, J.N.A., McGuinness, K.A., 2002. Environmentally influenced variability in the morphology of Cinachyrella australiensis (Carter 1886) (Porifera : Spirophorida : Tetillidae). Mar. Freshwater Res. 53, 79–84. https://doi.org/10.1071/mf00153

McKinney, F.K., 1981. Planar branch systems in colonial suspension feeders. Paleobiology 7, 344–354. https://doi.org/10.1017/S0094837300004656

McMurray, S., Pawlik, J., Finelli, C., 2014. Trait-mediated ecosystem impacts: how morphology and size affect pumping rates of the Caribbean giant barrel sponge. Aquat. Biol. 23, 1–13. https://doi.org/10.3354/ab00612

Miramontes, E., Jorry, S.J., Jouet, G., Counts, J.W., Courgeon, S., Le Roy, P., Guerin, C., Hernández-Molina, F.J., 2019a. Deep-water dunes on drowned isolated carbonate terraces (Mozambique Channel, south-west Indian Ocean). Sedimentology 66, 1222–1242. https://doi.org/10.1111/sed.12572

Miramontes, E., Penven, P., Fierens, R., Droz, L., Toucanne, S., Jorry, S.J., Jouet, G., Pastor, L., Silva Jacinto, R., Gaillot, A., Giraudeau, J., Raisson, F., 2019b. The influence of bottom currents on the Zambezi Valley morphology (Mozambique Channel, SW Indian Ocean): In situ current observations and hydrodynamic modelling. Marine Geology 410, 42–55. https://doi.org/10.1016/j.margeo.2019.01.002

Morato, T., Clark, M.R., 2007. Seamount fishes: ecology and life histories, in: Pitcher, T.J., Morato, T., Paul, J.B.H., Clark, M.R., Nigel, H., Ricardo, S.S. (Eds.), Seamounts: Ecology, Fisheries & Conservation. John Wiley & Sons, Ltd, pp. 170–188. https://doi.org/10.1002/9780470691953.ch9

Morato, T., Hoyle, S.D., Allain, V., Nicol, S.J., 2010. Seamounts are hotspots of pelagic biodiversity in the open ocean. Proc. Natl. Acad. Sci. U.S.A. 107, 9707–9711. https://doi.org/10.1073/pnas.0910290107

Morato, T., Varkey, D., Damaso, C., Machete, M., Santos, M., Prieto, R., Pitcher, T., Santos, R., 2008. Evidence of a seamount effect on aggregating visitors. Mar. Ecol. Prog. Ser. 357, 23–32. https://doi.org/10.3354/meps07269

Morgan, N.B., Baco, A.R., 2021. Recent fishing footprint of the high-seas bottom trawl fisheries on the Northwestern Hawaiian Ridge and Emperor Seamount Chain: A finer-scale approach to a large-scale issue. Ecological Indicators 121, 107051. https://doi.org/10.1016/j.ecolind.2020.107051

Morgan, N.B., Cairns, S., Reiswig, H., Baco, A.R., 2015. Benthic megafaunal community structure of cobalt-rich manganese crusts on Necker Ridge. Deep Sea Research Part I: Oceanographic Research Papers 104, 92–105. https://doi.org/10.1016/j.dsr.2015.07.003

Morgan, N.B., Goode, S., Roark, E.B., Baco, A.R., 2019. Fine Scale Assemblage Structure of Benthic Invertebrate Megafauna on the North Pacific Seamount Mokumanamana. Front. Mar. Sci. 6, 715. https://doi.org/10.3389/fmars.2019.00715

Narayanaswamy, B.E., Hughes, D.J., Howell, K.L., Davies, J., Jacobs, C., 2013. First observations of megafaunal communities inhabiting George Bligh Bank, Northeast Atlantic. Deep Sea Research Part II: Topical Studies in Oceanography 92, 79–86. https://doi.org/10.1016/j.dsr2.2013.03.004

Nybakken, J., Craig, S., Smith-Beasley, L., Moreno, G., Summers, A., Weetman, L., 1998. Distribution density and relative abundance of benthic invertebrate megafauna from three sites at the base of the continental slope off central California as determined by camera sled and beam trawl. Deep Sea Research Part II: Topical Studies in Oceanography 45, 1753–1780. https://doi.org/10.1016/S0967-0645(98)80016-7

Obura, D., 2012. The Diversity and Biogeography of Western Indian Ocean Reef-Building Corals. PLoS ONE 7, e45013. https://doi.org/10.1371/journal.pone.0045013

Obura, D., Church, J., Gabrié, C., Macharia, D., 2012. Assessing Marine World Heritage from an Ecosystem Perspective: The Western Indian Ocean 125.

O'Hara, T.D., 2007. Seamounts: centres of endemism or species richness for ophiuroids? Global Ecology and Biogeography 16, 720–732. https://doi.org/10.1111/j.1466-8238.2007.00329.x

O'Hara, T.D., Consalvey, M., Lavrado, H.P., Stocks, K.I., 2010. Environmental predictors and turnover of biota along a seamount chain: Assemblage composition along a seamount chain. Marine Ecology 31, 84–94. https://doi.org/10.1111/j.1439-0485.2010.00379.x

O'Hara, T.D., Hugall, G., Andrew F., Woolley, S.N.C., Bribiesca-Contreras, G., Bax, N.J., 2019. Contrasting processes drive ophiuroid phylodiversity across shallow and deep seafloors 18.

O'Hara, T.D., Tittensor, D.P., 2010. Environmental drivers of ophiuroid species richness on seamounts: Ophiuroid seamount species richness. Marine Ecology 31, 26–38. https://doi.org/10.1111/j.1439-0485.2010.00373.x

O'Hara, T.D., Williams, A., Woolley, S.N.C., Nau, A.W., Bax, N.J., 2020. Deep-sea temperate-tropical faunal transition across uniform environmental gradients. Deep Sea Research Part I: Oceanographic Research Papers 161, 103283. https://doi.org/10.1016/j.dsr.2020.103283

Oksanen, J., Blanchet, F.G., Friendly, M., Kindt, R., Legendre, P., McGlinn, D., Minchin, P.R., O'Hara, R.B., Gavin, L.S., Peter, S., H. Stevens, M. henry, Szoecs, E., Wagner, H., 2020. vegan: Community Ecology Package. R package version 2.5-7.

Oksanen, J., Blanchet, F.G., Friendly, M.K., Legendre, P., McGlinn, D., 2019. vegan: Community Ecology Package. R package version 2.5-6.

Olu, K., 2014. PAMELA-MOZ01 cruise, RV L'Atalante. https://doi.org/10.17600/14001000

Pante, E., Corbari, L., Thubaut, J., Chan, T.-Y., Mana, R., Boisselier, M.-C., Bouchet, P., Samadi, S., 2012a. Exploration of the Deep-Sea Fauna of Papua New Guinea. Oceanography 25. https://doi.org/10.5670/oceanog.2012.65

Pante, E., France, S.C., Couloux, A., Cruaud, C., McFadden, C.S., Samadi, S., Watling, L., 2012b. Deep-Sea Origin and In-Situ Diversification of Chrysogorgiid Octocorals. PLoS ONE 7, e38357. https://doi.org/10.1371/journal.pone.0038357

Pante, E., France, S.C., Gey, D., Cruaud, C., Samadi, S., 2015. An inter-ocean comparison of coral endemism on seamounts: the case of *Chrysogorgia*. Journal of Biogeography 42, 1907–1918. https://doi.org/10.1111/jbi.12564

Pante, E., Watling, L., 2012. *Chrysogorgia* from the New England and Corner Seamounts: Atlantic–Pacific connections. Journal of the Marine Biological Association of the United Kingdom 92, 911–927. https://doi.org/10.1017/S0025315411001354

Patton, W.K., 1972. Studies on the animal symbionts of the gorgonian coral, leptogorgia virgulata (lamarck). Bulletin of Marine Science 22, 419–431.

Payri, C., Archambault, P., Samadi, S., 2012. MADANG 2012 cruise, RV Alis. https://doi.org/10.17600/18000841

Peres-Neto, P.R., Legendre, P., 2010. Estimating and controlling for spatial structure in the study of ecological communities. Global Ecology and Biogeography 19, 174–184. https://doi.org/10.1111/j.1466-8238.2009.00506.x

Petersen, S., Krätschell, A., Augustin, N., Jamieson, J., Hein, J.R., Hannington, M.D., 2016. News from the seabed – Geological characteristics and resource potential of deep-sea mineral resources. Marine Policy 13.

Pierrejean, M., Grant, C., Neves, B. de M., Chaillou, G., Edinger, E., Blanchet, F.G., Maps, F., Nozais, C., Archambault, P., 2020. Influence of Deep-Water Corals and Sponge Gardens on Infaunal Community Composition and Ecosystem Functioning in the Eastern Canadian Arctic. Front. Mar. Sci. 7, 495. https://doi.org/10.3389/fmars.2020.00495

Pomponi, S.A., 2016. Emerging Technologies for Biological Sampling in the Ocean. National Ocean Exploration Forum 2016.

Probert, P.K., Christiansen, S., Gjerde, K.M., Gubbay, S., Santos, R.S., 2007. Management and conservation of seamounts, in: Pitcher, T.J., Morato, T., Hart, P.J.B., Clark, M.R., Haggan, N., Santos, R.S. (Eds.), Seamounts: Ecology, Fisheries & Conservation. Blackwell Publishing Ltd, Oxford, UK, pp. 442–475. https://doi.org/10.1002/9780470691953.ch20

Pronzato, R., Bavestrello, G., Cerrano, C., 1998. Morpho-functional adaptations of three species of spongia (porifera, demospongiae) from a mediterranean vertical cliff. Bulletin of Marine Science 63, 12.

Quattrini, A.M., Ross, S.W., Carlson, M.C.T., Nizinski, M.S., 2012. Megafaunal-habitat associations at a deep-sea coral mound off North Carolina, USA. Mar Biol 159, 1079–1094. https://doi.org/10.1007/s00227-012-1888-7

R Core Team, 2021. R: A language and environment for statistical computing. Vienna: R Foundation for Statistical Computing.

R Core Team, 2020. R: A language and environment for statistical computing. Vienna: R Foundation for Statistical Computing.

Ramirez-Llodra, E., Tyler, P.A., Baker, M.C., Bergstad, O.A., Clark, M.R., Escobar, E., Levin, L.A., Menot, L., Rowden, A.A., Smith, C.R., Van Dover, C.L., 2011. Man and the Last Great Wilderness: Human Impact on the Deep Sea. PLoS ONE 6, e22588. https://doi.org/10.1371/journal.pone.0022588

Ramiro-Sánchez, B., González-Irusta, J.M., Henry, L.-A., Cleland, J., Yeo, I., Xavier, J.R., Carreiro-Silva, M., Sampaio, Í., Spearman, J., Victorero, L., Messing, C.G., Kazanidis, G., Roberts, J.M., Murton, B., 2019. Characterization and Mapping of a Deep-Sea Sponge Ground on the Tropic Seamount (Northeast Tropical Atlantic): Implications for Spatial Management in the High Seas. Front. Mar. Sci. 6, 278. https://doi.org/10.3389/fmars.2019.00278

Ramos, M., Bertocci, I., Tempera, F., Calado, G., Albuquerque, M., Duarte, P., 2016. Patterns in megabenthic assemblages on a seamount summit (Ormonde Peak, Gorringe Bank, Northeast Atlantic). Marine Ecology 37, 1057–1072. https://doi.org/10.1111/maec.12353

Rice, A., Aldred, R., Darlington, E., Wild, R., 1982. The quantitative estimation of the deep-sea megabenthos - a new approach to an old problem. Oceanologica Acta 5, 63–72.

Richer de Forges, B., Koslow, J.A., Poore, G.C.B., 2000. Diversity and endemism of the benthic seamount fauna in the southwest Pacific. Nature 405, 944–947. https://doi.org/10.1038/35016066

Robert, K., Jones, D., Huvenne, V., 2014. Megafaunal distribution and biodiversity in a heterogeneous landscape: the iceberg-scoured Rockall Bank, NE Atlantic. Marine Ecology Progress Series 501, 67–88. https://doi.org/10.3354/meps10677

Roberts, D.W., 2019. labdsv: Ordination and Multivariate Analysis for Ecology. R package version 2.0-1.

Rogers, A., Blanchard, J.L., Mumby, P.J., 2014. Vulnerability of Coral Reef Fisheries to a Loss of Structural Complexity. Current Biology 24, 1000–1005. https://doi.org/10.1016/j.cub.2014.03.026

Rogers, A.D., 2019. Threats to Seamount Ecosystems and Their Management, in: Sheppard, C. (Ed.), World Seas: An Environmental Evaluation. Elsevier, pp. 427–451. https://doi.org/10.1016/B978-0-12-805052-1.00018-8

Rogers, A.D., 2018. The Biology of Seamounts: 25 Years on, in: Advances in Marine Biology. Elsevier, pp. 137–224. https://doi.org/10.1016/bs.amb.2018.06.001

Rossi, S., Bramanti, L. (Eds.), 2020. Perspectives on the Marine Animal Forests of the World. Springer International Publishing, Cham. https://doi.org/10.1007/978-3-030-57054-5

Rossi, S., Bramanti, L., Gori, A., Orejas, C. (Eds.), 2017. Marine Animal Forests: The Ecology of Benthic Biodiversity Hotspots. Springer International Publishing, Cham. https://doi.org/10.1007/978-3-319-21012-4

Rowden, A.A., Clark, M.R., Wright, I.C., 2005. Physical characterisation and a biologically focused classification of "seamounts" in the New Zealand region. New Zealand Journal of Marine and Freshwater Research 39, 1039–1059. https://doi.org/10.1080/00288330.2005.9517374

Rowden, A.A., Dower, J.F., Schlacher, T.A., Consalvey, M., Clark, M.R., 2010a. Paradigms in seamount ecology: fact, fiction and future: Paradigms in seamount ecology. Marine Ecology, a 31, 226–241. https://doi.org/10.1111/j.1439-0485.2010.00400.x

Rowden, A.A., Schlacher, T.A., Williams, A., Clark, M.R., Stewart, R., Althaus, F., Bowden, D.A., Consalvey, M., Robinson, W., Dowdney, J., 2010b. A test of the seamount oasis hypothesis: seamounts support higher epibenthic megafaunal biomass than adjacent slopes: A test of the seamount oasis hypothesis. Marine Ecology, b 31, 95–106. https://doi.org/10.1111/j.1439-0485.2010.00369.x

Rubio, F., Rolán, E., 2022. New species of Vitrinellidae (Gastropoda: Truncatelloidea) from the Indo-Pacific. The genus Circulus Jeffreys, 1865. Museo National de Historia Natural, Universidad de Santiago de Compostela, 1-422.

Sahlmann, C., Chan, T.-Y., Chan, B.K.K., 2011. Feeding modes of deep-sea lobsters (Crustacea: Decapoda: Nephropidae and Palinuridae) in Northwest Pacific waters: Functional morphology of mouthparts, feeding behaviour and gut content analysis. Zoologischer Anzeiger - A Journal of Comparative Zoology 250, 55–66. https://doi.org/10.1016/j.jcz.2010.11.003

Saint Germain, A., 2021. Peuplements benthiques sur les monts sous-marins : caractérisation de la megafaune et des peuplements d'éponges le long d'une pente et sur le sommet du mont Munida (Rapport de stage (M1)). Université de Pau et des Pays de l'Adour - Institut français de recherche pour l'exploitation de la mer (Ifremer).

Salinas-de-León, P., Martí-Puig, P., Buglass, S., Arnés-Urgellés, C., Rastoin-Laplane, E., Creemers, M., Cairns, S., Fisher, C., O'Hara, T., Ott, B., Raineault, N.A., Reiswig, H., Rouse, G., Rowley, S., Shank, T.M., Suarez, J., Watling, L., Wicksten, M.K., Marsh, L., 2020. Characterization of deep-sea benthic invertebrate megafauna of the Galapagos Islands. Sci Rep 10, 13894. https://doi.org/10.1038/s41598-020-70744-1

Samadi, S., Bottan, L., Macpherson, E., De Forges, B.R., Boisselier, M.-C., 2006. Seamount endemism questioned by the geographic distribution and population genetic structure of marine invertebrates. Marine Biology 149, 1463–1475. https://doi.org/10.1007/s00227-006-0306-4

Samadi, S., Corbari, L., 2010. BIOPAPUA cruise, RV Alis. https://doi.org/10.17600/10100040

Samadi, S., Olu, K., 2019. KANADEEP 2 cruise, RV L'Atalante. https://doi.org/10.17600/18000883

Samadi, S., Puillandre, N., Pante, E., Boisselier, M.-C., Corbari, L., Chen, W.-J., Maestrati, P., Mana, R., Thubaut, J., Zuccon, D., Hourdez, S., 2015. Patchiness of deep-sea communities in Papua New Guinea and potential susceptibility to anthropogenic disturbances illustrated by seep organisms. Marine Ecology 36, 109–132. https://doi.org/10.1111/maec.12204

Saucède, T., Eléaume, M., Jossart, Q., Moreau, C., Downey, R., Bax, N., Sands, C., Mercado, B., Gallut, C., Vignes-Lebbe, R., 2020. Taxonomy 2.0: computer-aided identification tools to assist Antarctic biologists in the field and in the laboratory. Antarctic Science 1–13. https://doi.org/10.1017/S0954102020000462

Sautya, S., Ingole, B., Ray, D., Stöhr, S., Samudrala, K., Raju, K.A.K., Mudholkar, A., 2011. Megafaunal Community Structure of Andaman Seamounts Including the Back-Arc Basin – A Quantitative Exploration from the Indian Ocean. PLoS ONE 6, e16162. https://doi.org/10.1371/journal.pone.0016162

Schlacher, T.A., Baco, A.R., Rowden, A.A., O'Hara, T.D., Clark, M.R., Kelley, C., Dower, J.F., 2014. Seamount benthos in a cobalt-rich crust region of the central Pacific: conservation challenges for future seabed mining. Diversity and Distributions 20, 491–502. https://doi.org/10.1111/ddi.12142

Schlacher, T.A., Williams, A., Althaus, F., Schlacher-Hoenlinger, M.A., 2010. High-resolution seabed imagery as a tool for biodiversity conservation planning on continental margins: Submarine canyon megabenthos and conservation planning. Marine Ecology 31, 200–221. https://doi.org/10.1111/j.1439-0485.2009.00286.x

Schoening, T., Durden, J.M., Faber, C., Felden, J., Heger, K., Hoving, H.-J.T., Kiko, R., Köser, K., Krämmer, C., Kwasnitschka, T., Möller, K.O., Nakath, D., Naß, A., Nattkemper, T.W., Purser, A., Zurowietz, M., 2022. Making marine image data FAIR. Sci Data 9, 414. https://doi.org/10.1038/s41597-022-01491-3

Schönberg, C.H.L., 2021. No taxonomy needed: Sponge functional morphologies inform about environmental conditions. Ecological Indicators 129. https://doi.org/https:DDdoi.orgD10.101BDj.ecolind.2021.107A0B

Schönberg, C.H.L., 2015. Self-cleaning surfaces in sponges. Mar Biodiv 45, 623–624. https://doi.org/10.1007/s12526-014-0302-8

Schönberg, C.H.L., Fromont, J., 2014. (PDF) Sponge functional growth forms as a means for classifying sponges without taxonomy [WWW Document]. ResearchGate. URL https://www.researchgate.net/publication/278627643_Sponge_functional_growth_forms_as_a_means_for_classifying_sponges_without_taxonomy (accessed 6.22.20).

Serrano, A., González-Irusta, J.M., Punzón, A., García-Alegre, A., Lourido, A., Ríos, P., Blanco, M., Gómez-Ballesteros, M., Druet, M., Cristobo, J., Cartes, J.E., 2017. Deep-sea benthic habitats modeling and mapping in a NE Atlantic seamount (Galicia Bank). Deep Sea Research Part I: Oceanographic Research Papers 126, 115–127. https://doi.org/10.1016/j.dsr.2017.06.003

Shank, T.M., 2010. Seamounts: deep-ocean laboratories of faunal connectivity, evolution, and endemism. Oceanography 23, 108–122.

Shaun Walbridge, Noah Slocum, Marjean Pobuda, Dawn Wright, 2018. Unified Geomorphological Analysis Workflows with Benthic Terrain Modeler. Geosciences 8, 94. https://doi.org/10.3390/geosciences8030094

Shen, C., Lu, B., Li, Z., Zhang, R., Chen, W., Xu, P., Yao, H., Chen, Z., Pang, J., Wang, C., Zhang, D., 2021. Community structure of benthic megafauna on a seamount with cobalt-rich ferromanganese crusts in the northwestern Pacific Ocean. Deep Sea Research Part I: Oceanographic Research Papers 178, 103661. https://doi.org/10.1016/j.dsr.2021.103661

Shortis, M.R., Seager, J.W., Williams, A., Barker, B.A., Sherlock, M., 2008. Using Stereo-Video for Deep Water Benthic Habitat Surveys. Marine Technology Society Journal 42, 28–37. https://doi.org/10.4031/002533208787157624

Sibuet, M., Olu, K., 1998. Biogeography, biodiversity and fluid dependence of deep-sea cold-seep communities at active and passive margins. Deep Sea Research Part II: Topical Studies in Oceanography 45, 517–567. https://doi.org/10.1016/S0967-0645(97)00074-X

Sigovini, M., Keppel, E., Tagliapietra, D., 2016. Open Nomenclature in the biodiversity era. Methods Ecol Evol 7, 1217–1225. https://doi.org/10.1111/2041-210X.12594

Staudigel, H., Clague, D.A., 2010. The Geological History of Deep-Sea Volcanoes: Biosphere, Hydrosphere, and Lithosphere Interactions. Oceanography 23, 58–71. https://doi.org/10.5670/oceanog.2010.62

Stocks, K.I., Clark, M.R., Rowden, A.A., Consalvey, M., Schlacher, T.A., 2012. CenSeam, an International Program on Seamounts within the Census of Marine Life: Achievements and Lessons Learned. PLoS ONE 7, e32031. https://doi.org/10.1371/journal.pone.0032031

Sweetman, A.K., Thurber, A.R., Smith, C.R., Levin, L.A., Mora, C., Wei, C.-L., Gooday, A.J., Jones, D.O.B., Rex, M., Yasuhara, M., Ingels, J., Ruhl, H.A., Frieder, C.A., Danovaro, R., Würzberg, L., Baco, A., Grupe, B.M., Pasulka, A., Meyer, K.S., Dunlop, K.M., Henry, L.-A., Roberts, J.M., 2017. Major impacts of climate change on deep-sea benthic ecosystems. Elementa: Science of the Anthropocene 5, 4. https://doi.org/10.1525/elementa.203

Tabachnick, K.R., 1991. Adaptation of the Hexactinelid Sponges to Deep-Sea Life 9.

Tapia-Guerra, J.M., Mecho, A., Easton, E.E., Gallardo, M. de los Á., Gorny, M., Sellanes, J., 2021. First description of deep benthic habitats and communities of oceanic islands and seamounts of the Nazca Desventuradas Marine Park, Chile. Sci Rep 11, 6209. https://doi.org/10.1038/s41598-021-85516-8

Tappin, D.R., Watts, P., McMurtry, G.M., Lafoy, Y., Matsumoto, T., 2001. The Sissano, Papua New Guinea tsunami of July 1998 – offshore evidence on the source mechanism. Marine Geology 23.

Taylor, J.D., Glover, E.A., 2018. Hanging on — lucinid bivalve survivors from the Paleocene and Eocene in the western Indian Ocean (Bivalvia: Lucinidae). Zoosystema 40, 123. https://doi.org/10.5252/zoosystema2018v40a7

Tew-Kai, E., Marsac, F., 2009. Patterns of variability of sea surface chlorophyll in the Mozambique Channel: A quantitative approach. Journal of Marine Systems 77, 77–88. https://doi.org/10.1016/j.jmarsys.2008.11.007

Thistle, D., 2003. The deep-sea floor: An overview 34.

Thomassin, B., 1977. BENTHEDI I cruise, RV Le Suroît. https://doi.org/10.17600/77003111

Thomson, S.A., Pyle, R.L., Ahyong, S.T., Alonso-Zarazaga, M., Ammirati, J., Araya, J.F., Ascher, J.S., Audisio, T.L., Azevedo-Santos, V.M., Bailly, N., Baker, W.J., Balke, M., Barclay, M.V.L., Barrett, R.L., Benine, R.C., Bickerstaff, J.R.M., Bouchard, P., Bour, R., Bourgoin, T., Boyko, C.B., Breure, A.S.H., Brothers, D.J., Byng, J.W., Campbell, D., Ceríaco, L.M.P., Cernák, I., Cerretti, P., Chang, C.-H., Cho, S., Copus, J.M., Costello, M.J., Cseh, A., Csuzdi, C., Culham, A., D'Elía, G., d'Udekem d'Acoz, C., Daneliya, M.E., Dekker, R., Dickinson, E.C., Dickinson, T.A., van Dijk, P.P., Dijkstra, K.-D.B., Dima, B., Dmitriev, D.A., Duistermaat, L., Dumbacher, J.P., Eiserhardt, W.L., Ekrem, T., Evenhuis, N.L., Faille, A., Fernández-Triana, J.L., Fiesler, E., Fishbein, M., Fordham, B.G., Freitas, A.V.L., Friol, N.R., Fritz, U., Frøslev, T., Funk, V.A., Gaimari, S.D., Garbino, G.S.T., Garraffoni, A.R.S., Geml, J., Gill, A.C., Gray, A., Grazziotin, F.G., Greenslade, P., Gutiérrez, E.E., Harvey, M.S., Hazevoet, C.J., He, K., He, X., Helfer, S., Helgen, K.M., van Heteren, A.H., Hita Garcia, F., Holstein, N., Horváth, M.K., Hovenkamp, P.H., Hwang, W.S., Hyvönen, J., Islam, M.B., Iverson, J.B., Ivie, M.A., Jaafar, Z., Jackson, M.D., Jayat, J.P., Johnson, N.F., Kaiser, H., Klitgård, B.B., Knapp, D.G., Kojima, J., Kõljalg, U., Kontschán, J., Krell, F.-T., Krisai-Greilhuber, I., Kullander, S., Latella, L., Lattke, J.E., Lencioni, V., Lewis, G.P., Lhano, M.G., Lujan, N.K., Luksenburg, J.A., Mariaux, J., Marinho-Filho, J., Marshall, C.J., Mate, J.F., McDonough, M.M., Michel, E., Miranda, V.F.O., Mitroiu, M.-D., Molinari, J., Monks, S., Moore, A.J., Moratelli, R., Murányi, D., Nakano, T., Nikolaeva, S., Noyes, J., Ohl, M., Oleas, N.H., Orrell, T., Páll-Gergely, B., Pape, T., Papp, V., Parenti, L.R., Patterson, D., Pavlinov, I.Ya., Pine, R.H., Poczai, P., Prado, J., Prathapan, D., Rabeler, R.K., Randall, J.E., Rheindt, F.E., Rhodin, A.G.J., Rodríguez, S.M., Rogers, D.C., Roque, F. de O., Rowe, K.C., Ruedas, L.A., Salazar-Bravo, J., Salvador, R.B., Sangster, G., Sarmiento, C.E., Schigel, D.S., Schmidt, S., Schueler, F.W., Segers, H., Snow, N., Souza-Dias, P.G.B., Stals, R., Stenroos, S., Stone, R.D., Sturm, C.F., Štys, P., Teta, P., Thomas, D.C., Timm, R.M., Tindall, B.J., Todd, J.A., Triebel, D., Valdecasas, A.G., Vizzini, A., Vorontsova, M.S., de Vos, J.M., Wagner, P., Watling, L., Weakley, A., Welter-Schultes, F., Whitmore, D., Wilding, N., Will, K., Williams, J., Wilson, K., Winston, J.E., Wüster, W., Yanega, D., Yeates, D.K., Zaher, H., Zhang, G., Zhang, Z.-Q., Zhou, H.-Z., 2018. Taxonomy based on science is necessary for global conservation. PLoS Biol 16, e2005075. https://doi.org/10.1371/journal.pbio.2005075

Thresher, R., Althaus, F., Adkins, J., Gowlett-Holmes, K., Alderslade, P., Dowdney, J., Cho, W., Gagnon, A., Staples, D., McEnnulty, F., Williams, A., 2014. Strong Depth-Related Zonation of Megabenthos on a Rocky Continental Margin (~700–4000 m) off Southern Tasmania, Australia. PLoS ONE 9, e85872. https://doi.org/10.1371/journal.pone.0085872

Thresher, R.E., Adkins, J., Fallon, S.J., Gowlett-Holmes, K., Althaus, F., Williams, A., 2011. Extraordinarily high biomass benthic community on Southern Ocean seamounts. Sci Rep 1, 119. https://doi.org/10.1038/srep00119

Thurber, A.R., Sweetman, A.K., Narayanaswamy, B.E., Jones, D.O.B., Ingels, J., Hansman, R.L., 2014. Ecosystem function and services provided by the deep sea. Biogeosciences 11, 3941–3963. https://doi.org/10.5194/bg-11-3941-2014

Todd, P.A., 2008. Morphological plasticity in scleractinian corals. Biological Reviews 83, 315–337. https://doi.org/10.1111/j.1469-185X.2008.00045.x

Tregoning, P., McQueen, H., Lambeck, K., Jackson, R., Little, R., Saunders, S., Rosa, R., 2000. Present-day crustal motion in Papua New Guinea. Earth Planet Sp 52, 727–730. https://doi.org/10.1186/BF03352272

Tsakalos, J.L., Renton, M., Riviera, F., Veneklaas, E.J., Dobrowolski, M.P., Mucina, L., 2019. Trait-based formal definition of plant functional types and functional communities in the multi-species and multi-traits context. Ecological Complexity 40, 100787. https://doi.org/10.1016/j.ecocom.2019.100787

Turnewitsch, R., Dumont, M., Kiriakoulakis, K., Legg, S., Mohn, C., Peine, F., Wolff, G., 2016. Tidal influence on particulate organic carbon export fluxes around a tall seamount. Progress in Oceanography 149, 189–213. https://doi.org/10.1016/j.pocean.2016.10.009

Tyler, P., Baker, M.C., Ramirez-Llodra, E., 2016. Deep-Sea Benthic Habitats: Clark/Biological Sampling in the Deep Sea. https://doi.org/10.1002/9781118332535.ch1.

Tyler, P.A. (Ed.), 2003. Ecosystems of the Deep Oceans. Elsevier.

Untiedt, C.B., Williams, A., Althaus, F., Alderslade, P., Clark, M.R., 2021. Identifying Black Corals and Octocorals From Deep-Sea Imagery for Ecological Assessments: Trade-Offs Between Morphology and Taxonomy. Front. Mar. Sci. 8, 722839. https://doi.org/10.3389/fmars.2021.722839

Van Dover, C., 2012. Hydrothermal Vent Ecosystems and Conservation. oceanog 25, 313–316. https://doi.org/10.5670/oceanog.2012.36

Veron, J.E.N., Devantier, L.M., Turak, E., Green, A.L., Kininmonth, S., Stafford-Smith, M., Peterson, N., 2009. Delineating the Coral Triangle. Galaxea, Journal of Coral Reef Studies 11, 91–100. https://doi.org/10.3755/galaxea.11.91

Victorero, L., Robert, K., Robinson, L.F., Taylor, M.L., Huvenne, V.A.I., 2018. Species replacement dominates megabenthos beta diversity in a remote seamount setting. Scientific Reports 8. https://doi.org/10.1038/s41598-018-22296-8

Vieira, P.E., Lavrador, A.S., Parente, M.I., Parretti, P., Costa, A.C., Costa, F.O., Duarte, S., 2021. Gaps in DNA sequence libraries for Macaronesian marine macroinvertebrates imply decades till completion and robust monitoring. Divers Distrib 27, 2003–2015. https://doi.org/10.1111/ddi.13305

Vilhena, D.A., Antonelli, A., 2015. A network approach for identifying and delimiting biogeographical regions. Nat Commun 6, 6848. https://doi.org/10.1038/ncomms7848

Walter, D.E., Winterton, S., 2007. Keys and the Crisis in Taxonomy: Extinction or Reinvention? Annual Review of Entomology 52, 193–208. https://doi.org/10.1146/annurev.ento.51.110104.151054

Warnes, R.G., Bolker, B., Bonebakker, L., Gentleman, R., Huber, Liaw, A., 2020. gplots: Various R Programming Tools for Plotting Data. R package version 3.1.0.

Watling, L., Auster, P.J., 2021. Vulnerable Marine Ecosystems, Communities, and Indicator Species: Confusing Concepts for Conservation of Seamounts. Front. Mar. Sci. 8, 622586. https://doi.org/10.3389/fmars.2021.622586

White, M., Bashmachnikov, I., Arístegui, J., Martins, A., 2007. Physical processes and seamount productivity, in: Pitcher, T.J., Morato, T., Hart, P.J.B., Clark, M.R., Haggan, N., Santos, R.S. (Eds.), Seamounts: Ecology, Conservation and Management, Fish and Aquatic Resources. Blackwell, Oxford, UK, pp. 65–84.

Wickham, H., Chang, W., Wickham, M.H., 2016. Package 'ggplot2'. Create elegant data visualisations using the grammar of graphics. Version, 2(1), 1-189.

Wilkinson, M.D., Dumontier, M., Aalbersberg, Ij.J., Appleton, G., Axton, M., Baak, A., Blomberg, N., Boiten, J.-W., da Silva Santos, L.B., Bourne, P.E., Bouwman, J., Brookes, A.J., Clark, T., Crosas, M., Dillo, I., Dumon, O., Edmunds, S., Evelo, C.T., Finkers, R., Gonzalez-Beltran, A., Gray, A.J.G., Groth, P., Goble, C., Grethe, J.S., Heringa, J., 't Hoen, P.A.C., Hooft, R., Kuhn, T., Kok, R., Kok, J., Lusher, S.J., Martone, M.E., Mons, A., Packer, A.L., Persson, B., Rocca-Serra, P., Roos, M., van Schaik, R., Sansone, S.-A., Schultes, E., Sengstag, T., Slater, T., Strawn, G., Swertz, M.A., Thompson, M., van der Lei, J., van Mulligen, E., Velterop, J., Waagmeester, A., Wittenburg, P., Wolstencroft, K., Zhao, J., Mons, B., 2016. The FAIR Guiding Principles for scientific data management and stewardship. Sci Data 3, 160018. https://doi.org/10.1038/sdata.2016.18

Williams, A., Althaus, F., Clark, M.R., Gowlett-Holmes, K., 2011. Composition and distribution of deep-sea benthic invertebrate megafauna on the Lord Howe Rise and Norfolk Ridge, southwest Pacific Ocean. Deep Sea Research Part II: Topical Studies in Oceanography 58, 948–958. https://doi.org/10.1016/j.dsr2.2010.10.050

Williams, A., Althaus, F., Green, M., Maguire, K., Untiedt, C., Mortimer, N., Jackett, C.J., Clark, M., Bax, N., Pitcher, R., Schlacher, T., 2020a. True Size Matters for Conservation: A Robust Method to Determine the Size of Deep-Sea Coral Reefs Shows They Are Typically Small on Seamounts in the Southwest Pacific Ocean. Front. Mar. Sci., a 7, 187. https://doi.org/10.3389/fmars.2020.00187

Williams, A., Althaus, F., Maguire, K., Green, M., Untiedt, C., Alderslade, P., Clark, M.R., Bax, N., Schlacher, T.A., 2020b. The Fate of Deep-Sea Coral Reefs on Seamounts in a Fishery-Seascape: What Are the Impacts, What Remains, and What Is Protected? Front. Mar. Sci., b 7, 567002. https://doi.org/10.3389/fmars.2020.567002

Williams, A., Althaus, F., Schlacher, T.A., 2015. Towed camera imagery and benthic sled catches provide different views of seamount benthic diversity: Gear selectivity for seamount benthos. Limnology and Oceanography: Methods 13, e10007. https://doi.org/10.1002/lom3.10007

Wilson, M.F.J., O'Connell, B., Brown, C., Guinan, J.C., Grehan, A.J., 2007. Multiscale Terrain Analysis of Multibeam Bathymetry Data for Habitat Mapping on the Continental Slope. Marine Geodesy 30, 3–35. https://doi.org/10.1080/01490410701295962

Wilson, R.R., Kaufmann, R., 1987. Seamount Biota and Biogeography. Washington DC American Geophysical Union Geophysical Monograph Series 43, 355–377. https://doi.org/10.1029/GM043p0355

Woodstock, M.S., Zhang, Y., 2022. Towards ecosystem modeling in the deep sea: A review of past efforts and primer for the future. Deep Sea Research Part I: Oceanographic Research Papers 188. https://doi.org/10.1016/j.dsr.2022.103851

Wudrick, A., Beazley, L., Culwick, T., Goodwin, C., Cárdenas, P., Xavier, J., Kenchington, E., 2020. A pictorial guide to the epibenthic megafauna of Orphan Knoll (northwest Atlantic) identified from in situ benthic video footage 161.

Wulff, J.L., 2006. Resistance vs recovery: morphological strategies of coral reef sponges. Funct Ecology 20, 699–708. https://doi.org/10.1111/j.1365-2435.2006.01143.x

Yesson, C., Clark, M.R., Taylor, M.L., Rogers, A.D., 2011. The global distribution of seamounts based on 30 arc seconds bathymetry data. Deep Sea Research Part I: Oceanographic Research Papers 58, 442–453. https://doi.org/10.1016/j.dsr.2011.02.004

Zawada, K.J.A., Dornelas, M., Madin, J.S., 2019a. Quantifying coral morphology. Coral Reefs 38, 1281–1292. https://doi.org/10.1007/s00338-019-01842-4

Zawada, K.J.A., Madin, J.S., Baird, A.H., Bridge, T.C.L., Dornelas, M., 2019b. Morphological traits can track coral reef responses to the Anthropocene. Functional Ecology. https://doi.org/10.1111/1365-2435.13358

Zurowietz, M., Langenkämper, D., Hosking, B., Ruhl, H.A., Nattkemper, T.W., 2018. MAIA—A machine learning assisted image annotation method for environmental monitoring and exploration. PLOS ONE 13, e0207498. https://doi.org/10.1371/journal.pone.0207498

VI. Annexe

frontiers in Marine Science

ORIGINAL RESEARCH
published: 19 November 2021
doi: 10.3389/fmars.2021.749078

When Imagery and Physical Sampling Work Together: Toward an Integrative Methodology of Deep-Sea Image-Based Megafauna Identification

Mélissa Hanafi-Portier[1,2], Sarah Samadi[2†], Laure Corbari[2†], Tin-Yam Chan[3], Wei-Jen Chen[4], Jhen-Nien Chen[4], Mao-Ying Lee[5], Christopher Mah[6], Thomas Saucède[7], Catherine Borremans[1] and Karine Olu[1†]*

[1] Laboratoire Environnement Profond, IFREMER, REM/EEP, Centre de Bretagne, Plouzané, France, [2] UMR 7205 ISYEB, Équipe "Explorations, Espèces et Spéciations", Muséum National d'Histoire Naturelle, Paris, France, [3] Institute of Marine Biology and Center of Excellence for the Oceans, National Taiwan Ocean University, Keelung, Taiwan, [4] Institute of Oceanography, National Taiwan University, Taipei, Taiwan, [5] Marine Fisheries Division, Fisheries Research Institute, Council of Agriculture, Keelung, Taiwan, [6] Department of Invertebrate Zoology, National Museum of Natural History, Smithsonian Institution, Washington, DC, United States, [7] Biogéosciences, UMR 6282, CNRS, Université Bourgogne Franche-Comté, Dijon, France

OPEN ACCESS

Edited by:
Ashley Alun Rowden, National Institute of Water and Atmospheric Research (NIWA), New Zealand

Reviewed by:
Franziska Althaus, Commonwealth Scientific and Industrial Research Organisation (CSIRO), Australia
Damianos Chatzievangelou, Jacobs University Bremen, Germany

***Correspondence:**
Mélissa Hanafi-Portier
Melissa.Hanafi.Portier@ifremer.fr;
hanafimelissa@gmail.com

[†] These authors have contributed equally to this work

Specialty section:
This article was submitted to Deep-Sea Environments and Ecology, a section of the journal Frontiers in Marine Science

Received: *28 July 2021*
Accepted: *11 October 2021*
Published: *19 November 2021*

Citation:
Hanafi-Portier M, Samadi S, Corbari L, Chan T-Y, Chen W-J, Chen J-N, Lee M-Y, Mah C, Saucède T, Borremans C and Olu K (2021) When Imagery and Physical Sampling Work Together: Toward an Integrative Methodology of Deep-Sea Image-Based Megafauna Identification. Front. Mar. Sci. 8:749078. doi: 10.3389/fmars.2021.749078

Imagery has become a key tool for assessing deep-sea megafaunal biodiversity, historically based on physical sampling using fishing gears. Image datasets provide quantitative and repeatable estimates, small-scale spatial patterns and habitat descriptions. However, taxon identification from images is challenging and often relies on morphotypes without considering a taxonomic framework. Taxon identification is particularly challenging in regions where the fauna is poorly known and/or highly diverse. Furthermore, the efficiency of imagery and physical sampling may vary among habitat types. Here, we compared biodiversity metrics (alpha and gamma diversity, composition) based on physical sampling (dredging and trawling) and towed-camera still images (1) along the upper continental slope of Papua New Guinea (sedimented slope with wood-falls, a canyon and cold seeps), and (2) on the outer slopes of the volcanic islands of Mayotte, dominated by hard bottoms. The comparison was done on selected taxa (Pisces, Crustacea, Echinoidea, and Asteroidea), which are good candidates for identification from images. Taxonomic identification ranks obtained for the images varied among these taxa (e.g., family/order for fishes, genus for echinoderms). At these ranks, imagery provided a higher taxonomic richness for hard-bottom and complex habitats, partially explained by the poor performance of trawling on these rough substrates. For the same reason, the gamma diversity of Pisces and Crustacea was also higher from images, but no difference was observed for echinoderms. On soft bottoms, physical sampling provided higher alpha and gamma diversity for fishes and crustaceans, but these differences tended to decrease for crustaceans identified to the species/morphospecies level from images. Physical sampling and imagery were selective against some taxa (e.g., according to size or behavior), therefore providing different facets of biodiversity. In addition, specimens collected at a larger scale facilitated megafauna identification from images. Based on this complementary

approach, we propose a robust methodology for image-based faunal identification relying on a taxonomic framework, from collaborative work with taxonomists. An original outcome of this collaborative work is the creation of identification keys dedicated specifically to *in situ* images and which take into account the state of the taxonomic knowledge for the explored sites.

Keywords: deep-sea megafauna, image-based identification, biodiversity assessment, identification keys, integrative methodology, towed camera, physical sampling

INTRODUCTION

The deep ocean (depths below 200 m) faces increasing threats, ranging from climate change to direct anthropogenic activities, such as fisheries, mining and physical/chemical pollution (Ramirez-Llodra et al., 2011; Levin and Sibuet, 2012; Levin and Le Bris, 2015). Continental margin habitats (e.g., upper sedimentary slopes, seeps and wood-fall-related environments, cold-water corals, canyons, seamounts) are especially at risk to be affected by human activities (Levin and Sibuet, 2012). Such habitats, especially those of the bathyal zone, often display biological or energy/mineral resources; their proximity to the coast and relatively shallow depth compared to abyssal ones, makes them vulnerable to terrestrial pollution and human activities. However, despite the acceleration of technological developments to prospect deep-sea resources through fisheries and mining, their impact on benthic communities is still poorly documented (Bowden et al., 2016). It is therefore urgent to develop conservation and restoration planning for marine biodiversity and habitats, first with an understanding of natural ecosystem variability, at regional and local scales (Da Ros et al., 2019).

Megafauna, which is usually defined as fauna of sufficient size to be seen by eyes from the images (Grassle et al., 1975) or that can be caught by fishing gears such as sledges, dredges and trawls (Clark et al., 2016), plays many key roles in deep-sea habitats. For instance, they can add structural complexity to the habitat, thereby promoting the diversity of associated fauna (Buhl-Mortensen et al., 2010) and/or, through their activity, modify the local environment of other species (Levin, 2005).

However, reliable assessment of the megafauna biodiversity in the deep sea and of the factors contributing to its spatial structuring is challenging. Historically, the megafauna from the deep sea were explored using fishing gears such as sledges, trawls, or dredges. Paradigms depicting the deep ocean as a species-poor and homogeneous environment have been progressively revised with technological developments (Tyler, 2003), revealing multi-scale heterogeneity of the deep-sea floor (Ramirez-Llodra et al., 2011; Danovaro et al., 2014).

Physical sampling is indeed needed for assessing the biodiversity of the fauna because accurate taxonomic identification can only be carried out upon morphological and/or molecular examination of the collected specimens. Biodiversity surveys from image data do not need the collection of physical samples; however, taxonomic identification from images still relies on the current state of knowledge, which is based on physical sampling. The same situation is encountered for biodiversity surveys based on environmental DNA/metabarcoding approach that also requires well-documented genetic reference libraries based on voucher specimens to be fully interpreted (Vieira et al., 2021). Studies comparing diversity metrics obtained via images and collected samples have shown that the latter provide a higher estimation of species richness (Williams et al., 2015; Beisiegel et al., 2017).

Furthermore, occurrence data derived from the identification of physical samples enable large-scale analyses of community structure and have revealed, for example, a temperate-tropical water transition of megafaunal assemblages along a uniform horizontal abiotic gradient (O'Hara et al., 2020) or significant geographical structure of coral species assemblages with longitude and along bathymetric gradients at the scale of the Azores Exclusive Economic Zone (Braga-Henriques et al., 2013). These data also help to answer phylogenetic (Mah, 2007; Kroh and Smith, 2010; O'Hara et al., 2019) and biogeographic studies (McClain et al., 2009) and subsequent conservation questions.

However, finer scale (meter) characterization of species distribution patterns, and structuring factors such as substrate heterogeneity, cannot be straightforward prospected with classical sampling, and require *in situ* habitat observation. In complex topographic habitats particularly, fishing gears alone provide mainly qualitative data and only poor quantitative estimates as reported by Williams et al. (2015) from epibenthic sled and also by Nybakken et al. (1998) in the context of soft bottoms from trawling operations. Moreover, fishing gear performance or capture efficiency can vary according to the type of organism, bottom, or fishing gear (e.g., trawl vs. dredge) and therefore therefore also only provide estimates of true abundance. Although endofauna is well captured by trawling in soft bottoms, fishing gears have been shown to be selective against species attached to hard substrates, such as corals or sponges from an epibenthic sled (Williams et al., 2015) or against some attached soft-bottom cnidarians, such as pennatulids or cerianthids from a trawl (Nybakken et al., 1998) or from an epibenthic sledge (Rice et al., 1982). Recently, a comparative study between imagery tools (ROV and towed camera) and trawling in soft bottoms, also highlighted a selectivity of trawling against some small-sized pennatulids, as well as a higher capture efficiency of mobile fauna, due to the light avoidance of mobile forms toward camera systems (de Mendonça and Metaxas, 2021). In addition, all these fishing gears can be less effective if their nets become clogged by sediment or biogenic debris before the end of the transect (Rice et al., 1982; Williams et al., 2015).

Since the end of the 1970s and with the advent of submersibles, the growing use of imagery has made it possible to document the biological and abiotic components of the seafloor quantitatively and *in situ* (Durden et al., 2016b). Although imagery only allows the observation of epifauna of sufficient size to be detected from images (Rice et al., 1982; Nybakken et al., 1998; Williams et al., 2015; Beisiegel et al., 2017), it has become a common scientific tool used for documenting seafloor heterogeneity, diversity and spatial patterns of benthic megafauna communities, even at sub-meter scales (Danovaro et al., 2014). Image-based studies in various environments have revealed that benthic communities are spatially heterogeneous, especially through the presence of habitat-building species that promote beta diversity (variation in species composition among sites, Legendre, 2014). For instance, in cold-water coral gardens (Buhl-Mortensen et al., 2010), or in deep-sea sponge grounds (Beazley et al., 2013). The spatial heterogeneity of benthic communities can also be related to substrate heterogeneity assessed at the scale of meters using sediment size characterization from images (Robert et al., 2014). In the case of marine protected areas, or vulnerable ecosystems—as well as for long-term temporal monitoring—imagery is desirable as a minimal disturbance approach (Beisiegel et al., 2017). However, this study also pointed out the necessity of having good prior knowledge of the species composition in the region by collecting the organisms to be identified from images. This is particularly necessary in poorly explored environments for which knowledge of the fauna is very poor.

The examination of morphological characters that allows accurate taxonomic identification of organisms is often limited from images, especially if the aim is to identify organisms at the species level (Henry and Roberts, 2014; Howell et al., 2014). A common approach used in ecology is to delineate morphospecies (or parataxonomic units) to define community assemblages and approximate taxonomic diversity (Krell, 2004). This morphospecies delineation consists in dividing the organisms into biological units based on external morphology without assigning them to scientific names that requires the observation of diagnostic characters generally not visible from images. In poorly known environments, this morphospecies approach may be biased due to an erroneous interpretation of the significance of any morphological polymorphism (i.e., undetected sexual dimorphism, intraspecific polymorphism, ontogenetic change, cryptic species, etc.). Therefore, this approach likely leads to a biased approximation of taxonomic diversity (Krell, 2004).

The taxonomic literature alone hardly allows the identification of organisms from images because illustrative *in situ* images of organisms are lacking and, when taxonomic-identification keys are available, the diagnostic characters used are often not observable from images. Image-based identification thus requires the use of other resources such as the often sparse literature on the species biology/ecology which give complementary information (depth range, associated species, etc.), or handbooks dedicated to some specific environments (e.g., deep-sea hydrothermal vent fauna) or online catalogs (e.g., NOAA, Atlantic Deep Sea Catalog). However, these resources do not provide taxonomic identification keys applicable for images, and accurate identification remains at relatively high taxonomic level. The construction of identification keys dedicated to image-based identification relies on having a detailed knowledge of the organisms present in the targeted areas. Such taxonomic identification guides have only been recently developed for example for the Antarctic area (Saucède et al., 2020), or for the Northwest Atlantic (Wudrick et al., 2020), two areas where the environment and fauna are well explored.

Deep-sea habitat explorations remain disparate, and have mainly been focused on the Northern Hemisphere while the Southern Hemisphere has remained underexplored (Cunha et al., 2017). Papua New Guinea and Mayotte (northern Mozambique Channel) are two southern regions where high faunal diversity has been reported (Obura, 2012; Pante et al., 2012). However, to date, the diversity of the deep-sea fauna is still poorly documented. An exploration program, Tropical Deep-Sea Benthos (TDSB), led by the French National Natural History Museum (*Muséum national d'Histoire naturelle*; MNHN) and the French National Research Institute for Sustainable Development (*Institut de Recherche pour le Développement;* IRD) established a geographically and taxonomically non-exhaustive inventory in progress, of benthic species in these areas. In 2014, images have been acquired to provide additional information on deep-sea habitats and the structure of biodiversity at small spatial scales. The challenge is therefore to propose an integrative method relying on robust taxonomic data to analyze the structure of communities at local scales in little-known areas with high faunal diversity.

In this context, we first compared the patterns of biodiversity for the megafauna obtained from physical sampling (dredges and trawls) with those based on still images taken by a towed camera, in various bathyal environments: along the sedimentary continental slopes of Papua New Guinea including a cold-seep area and a bay with wood-falls and a canyon, as well as along the outer slopes of Mayotte dominated by a hard-bottom substrate. We addressed the following questions: (1) What is the lowest taxonomic rank of identification reached for different taxa from images? (2) What biodiversity metrics (alpha and "gamma" diversities, faunistic composition) do these two approaches provide? (3) How physical sampling improve image-based identification, especially in areas where the fauna is poorly known and how to use it to formalize photo-taxa identification from images?

MATERIALS AND METHODS

Study Areas and Field Collection

Papua New Guinea: Upper Sedimented Slopes and Cold Seeps

Papua New Guinea (PNG) lies in the Coral Triangle in the southwest Pacific Ocean, and shows exceptional biological diversity, especially of zooxanthellate coral, accounting for up to 76% of the species known worldwide (Veron et al., 2009). The region is characterized by geological complexity and dynamics (Tregoning et al., 2000), which have resulted in a diversity of habitats, such as vents (Collins et al., 2012; Van Dover, 2012),

seeps (Tappin et al., 2001), seamounts, canyons, sedimentary plains, wood-falls and other plant remains (Pante et al., 2012; Samadi et al., 2015).

Several expeditions, as part of the TDSB program (MNHN/IRD; 2010–2014), explored and discovered new environments in this area, down to about 1,000 m depth. Two of these expeditions [BioPapua (Samadi and Corbari, 2010); Papua Niugini (Payri et al., 2012)] revealed in particular two chemosynthetic habitats linked to cold seeps off the Sepik River mouth and in the Basamuk Canyon where impact of nickel factory release was evidenced (Pante et al., 2012; Samadi et al., 2015). High abundance of wood-falls and other plant debris in Astrolabe Bay were revealed as well from samples. The physical sampling of the benthic fauna provided a first glimpse of the species occurring in these areas.

All dredging and trawling operations undertaken respectively in Astrolabe Bay and in the Sepik area during the BioPapua and Papua Niugini expeditions were integrated in this study to help with the taxonomic identification from images by providing a baseline of species occurring in the whole Astrolabe Bay or Sepik area. These samples are referred to as surrounding area samples (called "Cl-around"). A total of 25 sites were sampled (**Table 1**). We use the term "sedimented slopes habitats" to refer to the habitats explored in PNG area.

Image acquisition was undertaken during the Madeep expedition (Corbari et al., 2014), on board the R/V *Alis* on 05 May 2014. Images were acquired along a selection of dredge and trawl transects carried out during past TDSB expeditions (BioPapua, Papua Niugini). Two sites were visited by camera. The first site is Astrolabe Bay, covering an area of about 514 km^2, and showing topographic gradients from the upper slope (∼300 m depth) down to ∼1,000 m depth. The bay is divided by a canyon, which is 100–600 m deeper than the adjacent slope. A total of eight camera transects (called "Dives") were carried out in Astrolabe Bay along previous trawl or dredge transects (called "Cl-dives") and three were selected for this study: Dive18, Dive16 and Dive13 because they are representative of each habitat (upper slope, intermediate slope and canyon) (**Figure 1** and **Table 1**). Each transect was about 4 km. From image observations, Dive18 and Dive16 were mainly composed of soft sediment and wood-falls or plant debris, and Dive13 showed a mix between soft sediment and the presence of large cobbles. The second site is Broken Bay, off the Sepik River mouth, where cold-seep fauna, Bathymodiolinae mussels and Siboglinidae tubeworms had previously been sampled at 450 m depth (Samadi et al., 2015). Here, we call this area the Sepik area. Dive06 was located along two trawl transects in this area (**Figure 1** and **Table 1**).

Mayotte: Volcanic Island Outer Slopes Dominated by Hard Bottoms

Mayotte is located in the northern Mozambique Channel, between Madagascar and the Mozambique coast in the West Indian Ocean. It is part of the Comoros archipelago, and is surrounded by a barrier reef that hosts a large lagoon (1,100 km^2) (Audru et al., 2006), which is part of the Mayotte Marine Natural Park.

Mayotte islands are crisscrossed by numerous faults, due to post-eruptive volcanic activities (Audru et al., 2006). The outer slopes range from 4 to 20° in inclination (up to 88° on some western flanks) and extend to 1,000 m depth from the barrier reef in the north and east and connect to the abyssal plain through two plateaus in the south and west. The slopes are characterized by geomorphological and substrate complexity, composed of a network of canyons surrounding the all islands, plateaus, cliffs, volcanic cones and of rugged areas (Audru et al., 2006) and provide a supplementary interesting study case for our comparison.

The northern part of the Mozambique Channel is also considered as a hotspot of biodiversity, after the Coral Triangle in the southwest Pacific Ocean, from its exceptional coral reef diversity (Obura et al., 2012). However, little is known regarding the non-reef environments, especially the deep-sea habitats.

Past expeditions of the TDSB program have provided knowledge of the species occurring in the region, with sampling carried out along the Mozambique Coast (MAINBAZA, Bouchet and Ramos, 2009), the Northwest and South Madagascar coast (MIRIKY, Bouchet, 2009 and ATIMO VATAE, Bouchet et al., 2010, respectively). IFREMER expeditions provided additional data on the central part of the Mozambique Channel (PAMELA-MOZ01, Olu, 2014; PAMELA-MOZ04, Jouet and Deville, 2015). However, biodiversity data on the Comoros archipelago are scarce, with only one dedicated expedition in this area (BENTHEDI, Thomassin, 1977) and with sampling gears deployed down to 3,700 m. Details of the MNHN and BENTHEDI expeditions can be found on BaseExp database (Muséum national d'Histoire naturelle, 2019)[1].

Images were acquired during the BioMaGlo expedition (Corbari et al., 2017), on board the R/V *Antea* on 21 January 2017 in the Mayotte-Gloriosos area. Three slope orientations were explored by camera: (1) the northwestern slopes characterized by a plateau at 600 m depth and covering 100 km^2 then surrounded by deeper crater-like or volcanoes network features; (2) the southwestern slopes with a deeper and larger plateau at 750 m covering 250 km^2 and (3) the eastern slopes, extending continuously down to 1,000 m depth and characterized by shallower volcanic cones (Audru et al., 2006).

A total of five camera transects were carried out and three were selected for this study (Dive01, Dive03, Dive05) (**Figure 2**), as they provide similar sampling and image acquisition effort, and include a substrate gradient from dive01 (soft bottom) to dive05 (hard and heterogeneous bottom), to assess the influence of bottom type.

Dive01 and Dive03 cross a relatively homogeneous bathymetric gradient around 600–700 m and 450–500 m depth, respectively, along the plateaus, and both ending at the mouth of a deeper channel (880 and 1,100 m respectively). Dive01 is mainly composed of soft substrate with sparse blocks or peaks and Dive03 shows an intermediate area of soft sediment and others with large rocky blocks (∼1 m size). Dive05 presents a larger and continuous bathymetric gradient from 500 m down to 1,130 m depth, ending with a passage on a volcanic cone. The area is mainly composed of carbonate and volcanic hard bottoms and is characterized by a very heterogeneous seafloor (gravel, pebbles, cobbles, boulders, blocks, and rugged areas, etc.).

[1]https://expeditions.mnhn.fr/?lang=en_US

TABLE 1 | Summary of image acquisition and physical sampling efforts with sites information for the dive, sampling along dive (cl-dive) and in the surrounding area (cl-around) in the Astrolabe Bay and Sepik River area (Papua New Guinea).

Area	Dive	Dive transect length analyzed (m)	Images total area (m^2)	Number of analyzed images	Depth (m)
Sepik/cold seeps	Dive06	1,697	2,244	490	431–581
Astrolabe/canyon	Dive13	1,649	1,951	426	931–940
Astrolabe/lower slopes	Dive16	4,187	4,538	991	795–820
Astrolabe/upper slopes	Dive18	3,780	4,534	990	546–587
Area	**Sampling along dive (CL-DIVE)**	**Corresponding dive**	**Sampling transect length (m)**	**Sampling total area (m^2)**	**Depth (m)**
Sepik/cold seeps	CP4040 CP4042	Dive06	3,497	13,989	468–779
Astrolabe/canyon	CP4022	Dive13	2,802	11,207	926–941
Astrolabe/lower sedimented slopes	CP4027	Dive16	3,629	14,514	793–820
Astrolabe/upper sedimented slopes	CP4025	Dive18	2,814	11,258	549–578
Area	**Surrounding area sampling (CL-AROUND)**	**Sampling transect length (m)**	**Sampling total area (m^2)**		
Astrolabe Bay	14 CP	49,063	196,254		
Sepik Bay	11 CP	32,996	131,984		
Total	25 CP	82,059	328,238		

Sampling operations refer to beam trawl (CP). Image acquisition was carried out in April 2014 and sampling operations in September/October 2010 (Biopapua expedition) and December 2012 (Papua Niugini expedition).

Images were acquired before undertaking co-located dredge and trawl transects (Cl-dives). Each dive included more than one co-located sampling; thus, the different dredge and trawl transects undertaken along each of the three camera transect positions were pooled for comparisons of diversity. A total of three dives and 10 dredge/trawl transects were analyzed (**Table 2**). Each transect was about 9 km long. Similar to the PNG area, all the 73 sampling catches undertaken during the BioMaGlo expedition (i.e., all around Mayotte area and the other explored Comoros islands including Gloriosos islands, Moheli, Geyzer Bank) were included in the comparison and referred to as surrounding area samples (Cl-around) (**Table 2**). These samplings helped the identification from images by providing a baseline of species occurring in the area. Moreover, we also used species baseline knowledge provided by past expeditions undertaken along the Mozambique Channel to help with the identification.

Physical Sampling Gears and Towed Camera

Physical sampling was carried out along 1–2 km transects using a Warén dredge of 1 m width with a fine 3–5 mm mesh size and a large and more robust 20–50 mm mesh size, deployed for hard substrate; and using a beam trawl of 4 m width, with a fine mesh (15–12 mm) deployed for soft sediment. On board, the sampling strategy aimed to maximize the number of taxa sampled. These two fishing gears have different selectivity for the different fauna components (for example, mobile and epibenthic fauna are generally better sampled with trawls than dredges). However, the topography does not always allow deploying both sampling gears.

Camera transects were carried out with a towed camera (SCAMPI, French Oceanographic Fleet), at 2.5–3 m above seafloor at 0.5 m/s. Images were acquired at 10 s intervals (PNG) and 30 s intervals (Mayotte) with an HD Camera (NIXON D700, focal length 18 mm, resolution 4,256 × 2,832 pixels) and geo-referenced using the ship positioning system processed with Adelie tools (French Oceanographic Fleet) developed at IFREMER and implemented using ArcGiS software V10.3.

The detection of organisms either from the observation in images or from capture by the fishing gears, reflects the respective efficiency of the cameras and the gears rather than the exact occurrence of the organisms at a given place. Indeed, some organisms may have been missed because the images are not overlapping. Similarly the probability of capture by the fishing gears may vary according to the topography and/or the nature of the substrate.

Taxonomic Processing

Specimen Identification

On board, all dredge and trawl catches were sorted at high taxonomic level and some taxa were photographed to record color patterns before being preserved in ethanol. Photographs were also obtained of preserved specimens stored in the MNHN collections[2]. These photos were used to build catalogs of taxa sampled in the area. Faunal samples were sent to an international network of taxonomists for processing and taxon identification. Taxon identification workshop sessions organized with taxonomists to study these collections stimulated discussions to determine the limits of identification from images for each taxonomic group.

[2]https://science.mnhn.fr/institution/mnhn/item/search/form?expedition=BIOMAGLO&image=on&lang=en_US

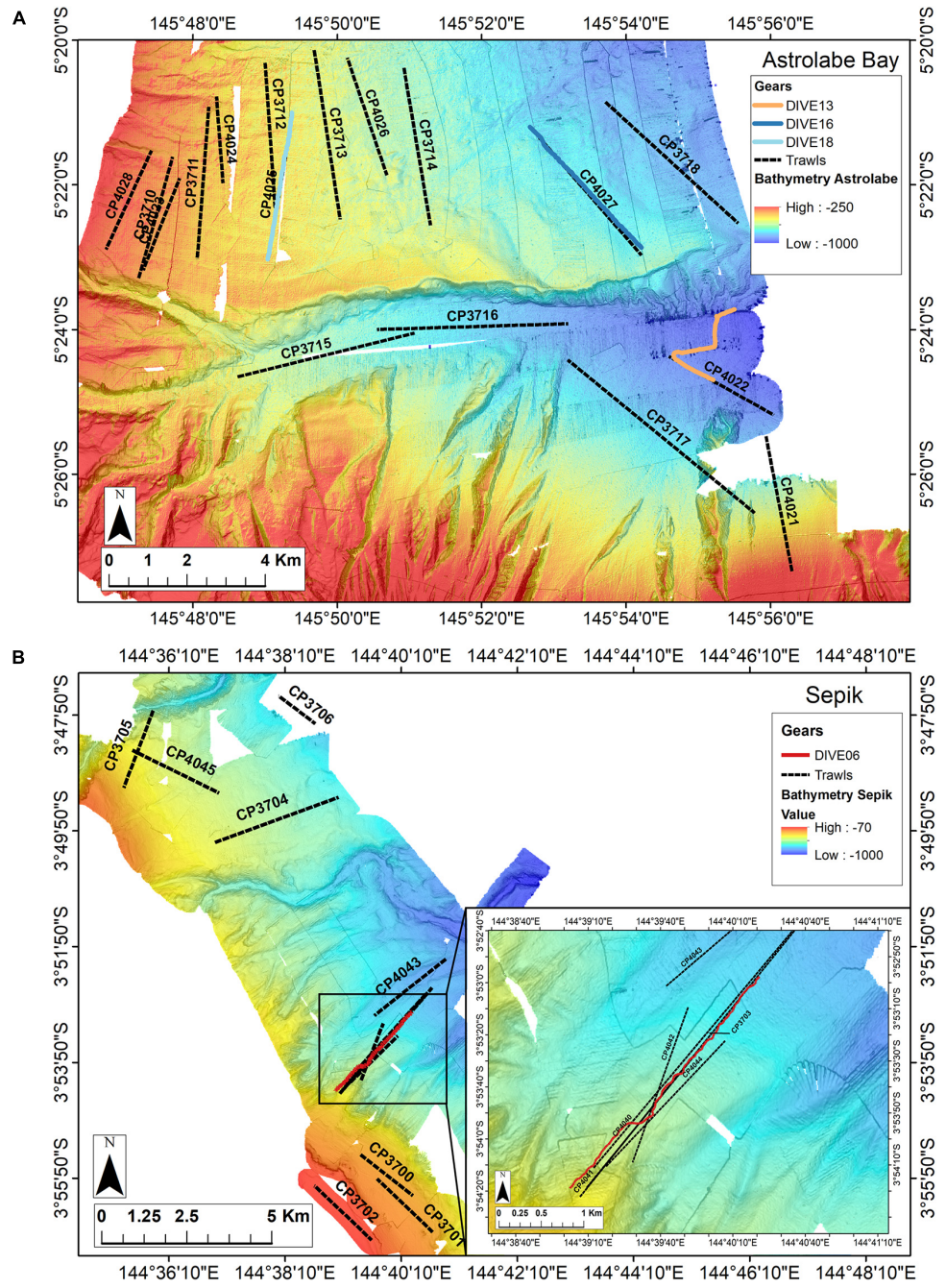

FIGURE 1 | Locationof the camera transects and dredge/trawl transects operations (dive, sampling along dive and in the surrounding area): Panel **(A)** in the Astrolabe Bay and panel **(B)** in the Sepik River area (Broken Water Bay). Colored lines represent camera transects, black dotted lines represent dredging (DW) and trawling (CP) operations.

Identifications From Images

A total of 7,674 images were analyzed and annotated (i.e., organism delineation in images and labeling of taxonomic ranks) using the web platform BIIGLE 2.0 (Benthic Image Indexing and Graphical Labelling Environment) (Langenkämper et al., 2017). BIIGLE 2.0 was chosen because it provides effective methods (1) allowing collaborative and interactive work with taxonomists who can actively contribute to the identification of organisms from images and (2) allowing easy comparisons and revisions of annotations with the *LARGO* tool. The platform allows the export

of a database with observation records of each faunal annotation. We then summed up these observations to obtain an abundance matrix for each georeferenced image.

Megafaunal identification from images consisted of five steps divided into three main processes that involve different levels of expertise: non-expert annotation, objective identification and contextual identification, the last two performed in collaboration with taxonomists (**Figure 3** and corresponding details on the working steps in **Supplementary Material 1**). Finally, identification keys adapted to images were produced for Decapoda, Asteroidea (**Supplementary Materials 2**, **3**) and Echinoidea[3].

Final Dataset Processing

After exporting the matrix of specimen observations from each georeferenced image of the BIIGLE platform, hierarchical taxonomic labels were homogenized between physical sample and image datasets according to the taxonomic hierarchy provided by the Worlds Register of Marine Species (WoRMS) database. Contrary to physical sampling, images can provide abundance data. Thus, to compare biodiversity patterns between images and physical samples along dives and in the surrounding area, we transformed the abundance data from image analysis into presence/absence data for each image. For easier naming convention, we will refer to the term Pisces for Osteichthyes/Chondrichthyes groups.

Diversity metrics were used: alpha diversity corresponding to the intra-transect diversity that was analyzed at the different levels of identification reached in the images, which were generally not the species level. Thus, for images, alpha diversity generally does not represent the species diversity and is represented by taxonomic richness. Beta diversity cannot be compared between images and physical samples because we could not assess this diversity from trawls or dredges (data integrated across the whole transect). For the sedimented slopes area, the regional scale ("gamma" diversity) corresponds to the pooling of the four dives and the four co-located trawl transects, respectively, of Astrolabe Bay and the Sepik area. For the Mayotte slopes area, the "gamma" diversity corresponds to the pooling of the three dives and the 10 co-located dredge/trawl transects, respectively.

Statistical Analyses

All analyses were performed using the R environment (V3.6.3) (R Core Team, 2020). Taxonomic richness comparison between camera transects and co-located sampling was assessed at different taxonomic levels using sample-based rarefaction curves with 999 random permutations on presence/absence data using the vegan package (*speceaccum* function) (Oksanen et al., 2019).

Differences in assemblage composition between camera transects and co-located sampling were assessed using principal component analysis (PCA) on Hellinger-transformed presence/absence data with the ade4 package (*dudi.pca* function) (Dray and Dufour, 2007). This transformation allows the species presence/absence dataset to be represented in a Euclidean space (Legendre and Gallagher, 2001). For crustaceans, PCA and Venn analyses were performed at the genus rank only, to consider comparative taxonomic names between image and sampling datasets (i.e., at a specific rank of comparison, morphospecies names in the image dataset do not match the species name in the sampling dataset).

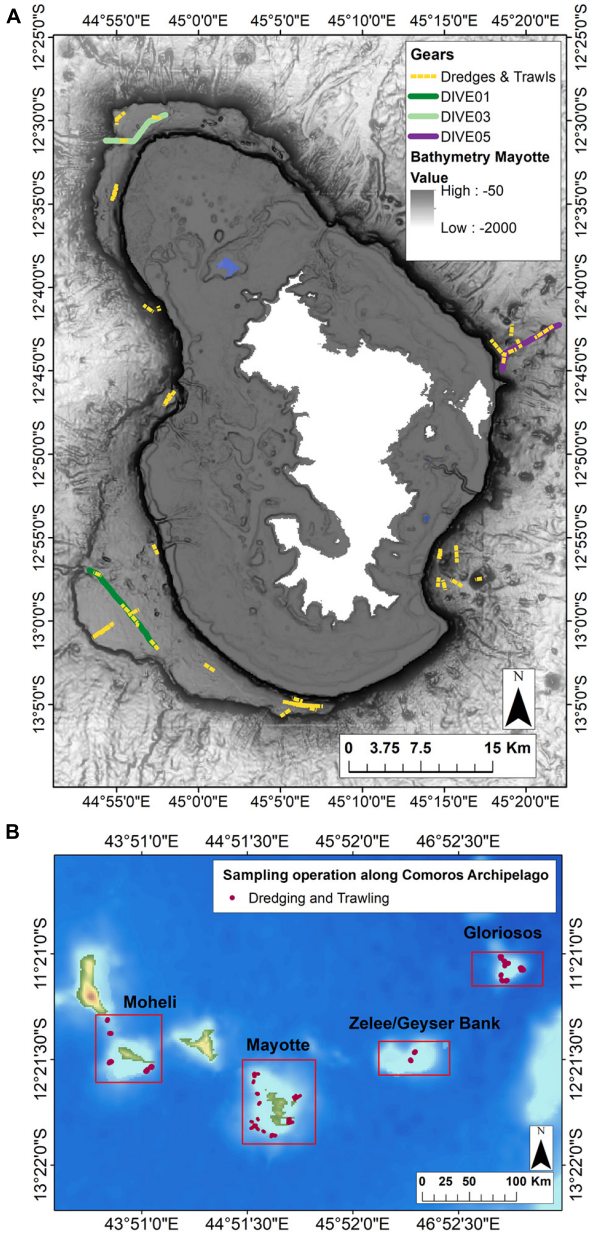

FIGURE 2 | (A) Location of the camera transects and dredge/trawl transects operations (dive, sampling along dive and in the surrounding area) undertaken along the outer slopes of Mayotte. **(B)** Location of the sampling in the surrounding area undertaken in the Comores Archipelago (Moheli, Geyzer Bank, Gloriosos). Solid lines represent camera transects and yellow dotted lines represent dredging (DW) and trawling (CP) operations.

[3]https://mozechinoids-deepsea-scampi.identificationkey.org

TABLE 2 | Summary of image acquisition and physical sampling efforts with sites information for the dive, sampling along dive (cl-dive) and in the surrounding area (cl-around) along volcanic island slopes of Mayotte.

Area	Dive	Dive transect length analyzed (m)	Images total area (m^2)	Number of analyzed images	Depth (m)
Southwest slope/soft-bottom area	Dive01	10,456	4,122	900	545–900
Northwest slopes/mix substrate	Dive03	7,408	5,043	1,101	433–1,200
East slopes/hard-bottom area	Dive05	8,125	4,296	938	460–1,100
Area	**Sampling along dive (CL-DIVE)**	**Corresponding dive**	**Sampling transect length (m)**	**Sampling total area (m^2)**	**Depth (m)**
Southwest slope/soft-bottom area	**CL-DIVE01** (DW4850 CP4852 DW4851 DW4853 CP4858)	Dive01	5,063	10,495	664–864
Northwest slopes/mix substrate	**CL-DIVE03** (DW4860 DW4861)	Dive03	1,928	1,928	486–646
East slopes/hard-bottom area	**CL-DIVE05** (DW4871 DW4872 DW4873)	Dive05	4,467	4,467	486–795
Area	**Surrounding area sampling (CL-AROUND)**	**Sampling transect length (m)**	**Sampling total area (m^2)**		
Around Mayotte island	11 CP/21 DW	44,995	110,481		
Others Comoros Islands	5 CP/36 DW	54,335	88,897		

Sampling operations refer to Warén dredge (DW) and beam trawl (CP). Image and sampling acquisition were carried out in late January/early February 2017.

Similarities and dissimilarities in taxonomic composition between images and physical samples and according to the image acquisition and physical sampling efforts (camera transects, co-located dredge/trawl transects and surrounding area transects) were represented in Venn diagram using the gplots package (*venn* function) (Warnes et al., 2020).

RESULTS

Biodiversity Pattern Compared Between Images and Physical Samples

Taxonomic Levels and Community Composition

For sedimented slopes we were able to reach an identification level above class for both images and physical samples mainly for Pisces (Chordata) and Crustacea (Arthropoda). The taxonomic ranks we reached ranged from order to family for fishes, and from genus to species/morphospecies for crustaceans (**Table 3A**). These two taxonomic groups were also well represented both in the images and physical samples along volcanic island slopes, at the same taxonomic ranks respectively (**Table 3B**). The high proportion of Annelida (93%) and Mollusca (49%) we identified to the family level in the images of the Sepik cold-seep area reflect respectively the dominance of Siboglinidae and Bathymodiolinae. Along the volcanic island slopes, the proportion of mollusks we identified to the class level (97%) reflects the dominance of Gastropoda, abundantly observed in images. However, the small individual size did not allow us to identify them beyond the rank of class from images, whereas we identified the collected specimens to the genus rank (27%). Animalia cetera identifications, fauna observed in images that were unclassifiable into phyla, represent 17% (1669 ind.) of the total fauna in the PNG area and 5% (783 ind.) in Mayotte.

On the sedimented slopes, we abundantly observed cnidarians (mainly composed of actinids, cerianthids and pennatulids) in images; however, our identifications remained limited to the class level (40%) and never exceeded the order (39%). In the physical samples, we collected few cnidarian individuals, mainly identified as pennatulids. In the time of this study we were only able to identify them to the order (**Table 3A**).

Along the volcanic island slopes, we observed many cnidarians and poriferans in images. However, we reached identification only to high taxonomic ranks (i.e., phylum and class for Porifera and order for Cnidaria). The diversity of these two groups was thus underestimated. For individuals sampled using dredges or trawls the specialists involved in the study generally identified them to the genus rank. Consequently, compared with images, diversity appeared higher for physical captures (**Table 3B**). For these taxonomic groups, the morphological characters required for identification are mainly microscopic and therefore cannot be observed from images.

We observed few asteroids along the sedimented slopes habitat, and the total of 2,417 observed Echinodermata individuals reflected the dominance of only one morphotype of semi-burying spatangoid echinoid, considering most of them were visible (**Table 3A**). Along the volcanic island slopes, we identified a higher number of echinoderm taxa either from specimens observed in images or from specimens collected by the sampling gears. For asteroids and echinoids identification from images, we reached the genus rank for most individuals (**Table 3C**).

For comparing the level of diversity estimated from images and from physical samples, in sedimented slopes and volcanic island slopes datasets, we selected the order and family ranks

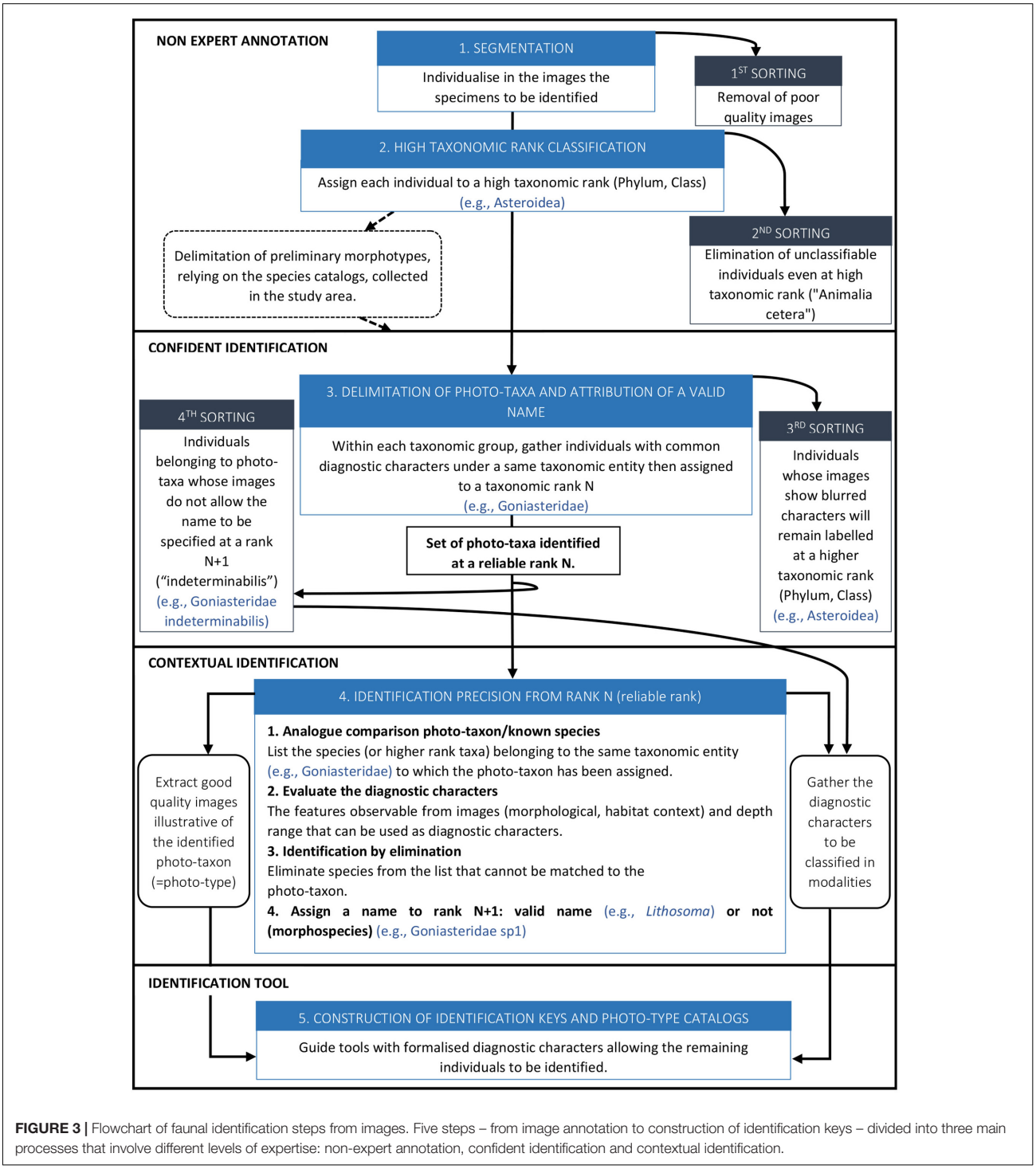

FIGURE 3 | Flowchart of faunal identification steps from images. Five steps – from image annotation to construction of identification keys – divided into three main processes that involve different levels of expertise: non-expert annotation, confident identification and contextual identification.

for fishes, and the genus and species/morphospecies ranks for crustaceans. We made the comparisons at the genus rank in hard-bottom environments for asteroids and echinoids, because we generally reached these levels of identification both for specimens observed in images and for specimens collected by the sampling gears. The inventory for each targeted taxon and taxonomic level, in the images and physical samples, are listed in **Supplementary Material 4** and raw databases used for analyses are available in **Supplementary Materials 5** (PNG) and **6** (Mayotte). For each percentage of individuals in **Table 3**, the corresponding

TABLE 3 | Percentages of individuals identified by taxonomic rank and by method (images = dive, sampling along dive = cl-dive), **(A)** along sedimented slopes (PNG) and **(B)** along volcanic island slopes dominated by hard bottom (Mayotte) with **(C)** a focus on echinoids and asteroids.

(A) Sedimented slopes (PNG)

TAXA	ANNELIDA		ARTHROPODA		CHORDATA		CNIDARIA		ECHINODERMATA		MOLLUSCA	
Taxonomic rank	**DIVE**	**CL-DIVE**	**DIVE**	**CL-DIVE**	**DIVE**	**CL-DIVE**	**DIVE**	**CL-DIVE**	**DIVE**	**CL-DIVE**	**DIVE**	**CL-DIVE**
Phylum	7	–	–	–	2	–	21	–	–	–	2	–
Class	–	–	70	1	32	–	40	–	86	–	41	–
Order	–	–	7	–	18	–	39	100	14	–	8	–
Family	93	70	2	10	48	3	–	–	–	–	49	10
Genus	–	30	20	15	–	27	–	–	–	–	–	76
Species	–	–	1	74	–	70	–	–	–	–	–	14
Morphospecies	20	–	12	–	–	3	–	–	–	–	–	–
Total individuals (n)	289	471	4,677	242	432	30	677	8	2,417	–	925	351

(B) Volcanic island slopes (Mayotte)

TAXA	ARTHROPODA		CHORDATA		CNIDARIA		ECHINODERMATA		MOLLUSCA		PORIFERA	
Taxonomic rank	**DIVE**	**CL-DIVE**	**DIVE**	**CL-DIVE**	**DIVE**	**CL-DIVE**	**DIVE**	**CL-DIVE**	**DIVE**	**CL-DIVE**	**DIVE**	**CL-DIVE**
Phylum	–	–	–	13	34	–	–	–	–	–	51	59
Class	5	11	52	–	–	4	38	7	97	–	39	8
Order	49	5	24	6	45	–	14	–	–	–	–	–
Family	18	33	19	–	13	36	7	7	3	71	1	–
Genus	23	14	4	50	7	52	41	37	–	27	2	25
Species	5	37	1	31	1	8	<<1	49	–	2	7	8
Morphospecies	13	–	13	6	–	–	4	–	2	–	1	–
Total individuals (n)	535	116	688	16	6,004	25	1,070	57	3,501	59	2,773	12

(C) Volcanic island slopes (focus on echinoderms)

ECHINODERMATA	ECHINOIDEA		ASTEROIDEA	
Taxonomic rank	**DIVE**	**CL-DIVE**	**DIVE**	**CL-DIVE**
Class	4	10	55	–
Order	1	–	7	–
Family	7	–	18	7
Genus	88	28	17	72
Species	–	62	3	21
Morphospecies	7	–	4	
Total individuals (n)	452	40	243	14

Morphospecies proportion is not included in the total proportion summed from phylum to species as it cannot be referred to any specific level.

number of taxa identified at each taxonomic rank are available in **Supplementary Material 7**.

Pisces

We evaluated the richness of Pisces orders in the sedimented slopes habitats of PNG, as two-fold higher in images than in physical samples while we estimated it as equivalent at the family level (**Figure 4A**). Conversely, for the canyon site (Dive13), we estimated that the richness of orders and families was lower from images than from physical samples.

In volcanic island habitats of Mayotte, we estimated the Pisces order richness at least two-fold higher in images than in physical samples for both families and orders levels (**Figure 4B**).

In the sedimented slopes habitats, we found the compositions of fish families in the physical samples and in the images similar for two sites (Dive06, Dive16), but unalike for the two others (**Figure 5A**), with some families only sampled by trawls within the canyon and sedimented slope sites (Cl-dive13, Cl-dive18).

On the contrary, in volcanic island areas, the dredges and trawls sampled a few families not, or poorly observed in images (Macrouridae) (**Figure 5B**). In the case of Bembridae and Ostracoberycidae (Perciformes), identification of specimens observed in images was possible only to the order level. However, images allowed us to observe many families that were not sampled by the fishing gears.

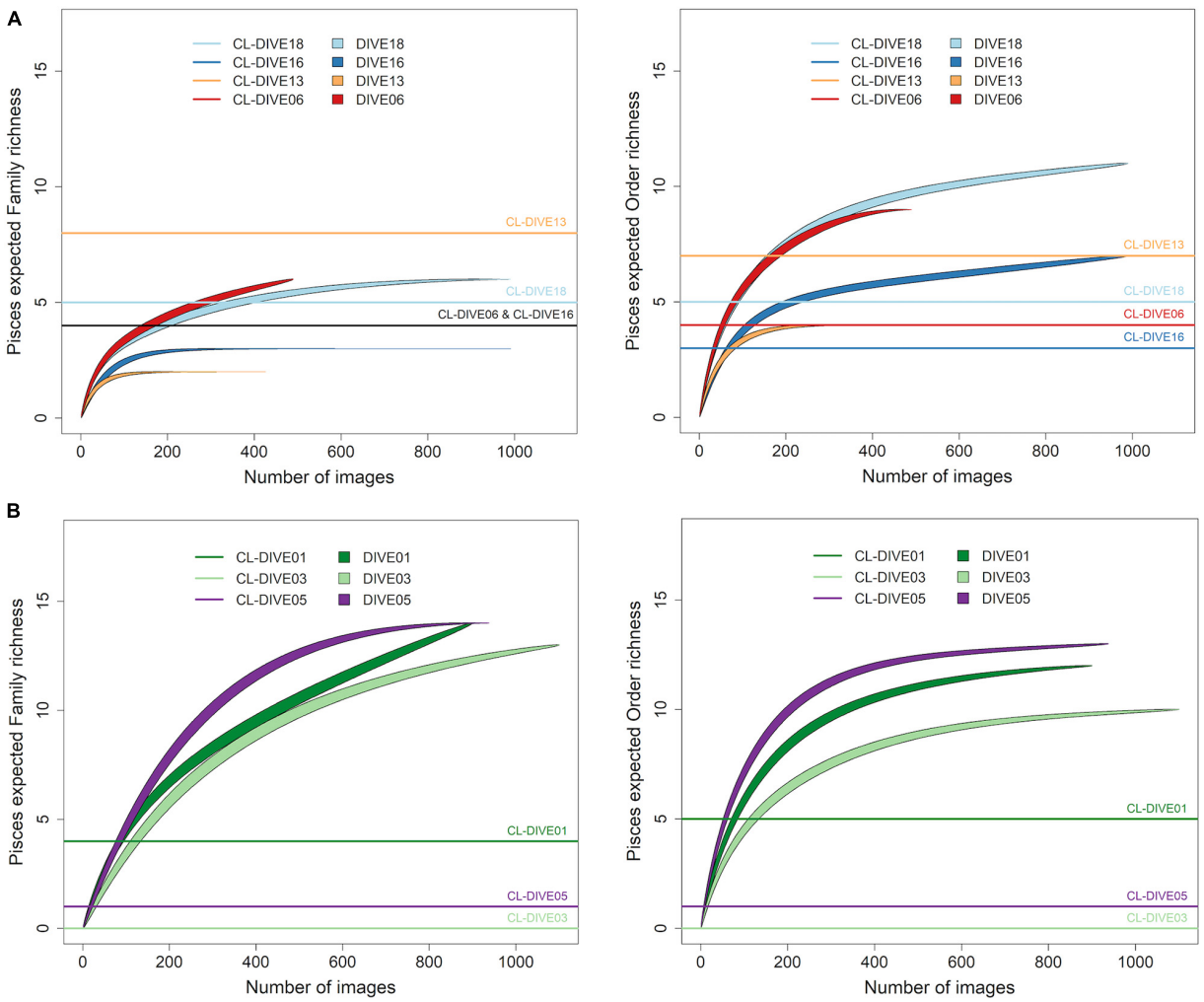

FIGURE 4 | Expected richness from rarefaction curves for Pisces at order and family ranks (exact method, n = 999 permutations), along **(A)** sedimented slope habitats (PNG) and **(B)** volcanic island slopes (Mayotte). Comparison between imagery (dive) and sampling along dive (cl-dive).

In sedimented slopes habitats, by pooling the four camera transects (dives) and the four trawl transects (cl-dives) respectively, we confirmed that the estimated diversity of fish families was higher from physical sampling than from observation in images (**Figure 6A**). Moreover, taking into account the surrounding area samples (cl-around) we considerably increased the family richness, and also added a few orders. These samples helped us to identify one additional order and two families from the images, which were not collected in the co-located samples. Inversely, on volcanic island slopes, the family diversity and the order diversity, estimated from the observations in images pooled from the camera transects was higher than from the pool of specimens from the trawl transects (**Figure 6B**). The benefit of the surrounding area samples for taxon identification using images was more pronounced on volcanic island slopes, with 13 additional families and 6 additional orders identified from images (**Figure 6B**).

Crustacea

In the sedimented slopes habitats of PNG, we estimated the genus richness of crustaceans higher in physical sampling than in images (Dive18, Dive13) or equivalent (Dive06, Dive16). At the species level (including morphospecies), we estimated the same richness patterns except for two sites (Dive18, Dive06), where we estimated the richness higher from images than sampling (**Figure 7A**). In volcanic island habitats of Mayotte, we estimated the genus richness as higher in the physical sampling than in the images and the species richness as equivalent, in the soft-bottom-dominated site (Dive01). Inversely, in the two hard-bottom-dominated sites (Dive03, dive05) and at both taxonomic levels, we estimated the richness higher from images (**Figure 7B**).

Small-sized and endogenous crustacean genera were captured more easily with trawls than observed in images (e.g., *Ethusa*, *Lepas*, *Bathycheles*, *Stereomastis*) along the sedimented slopes of

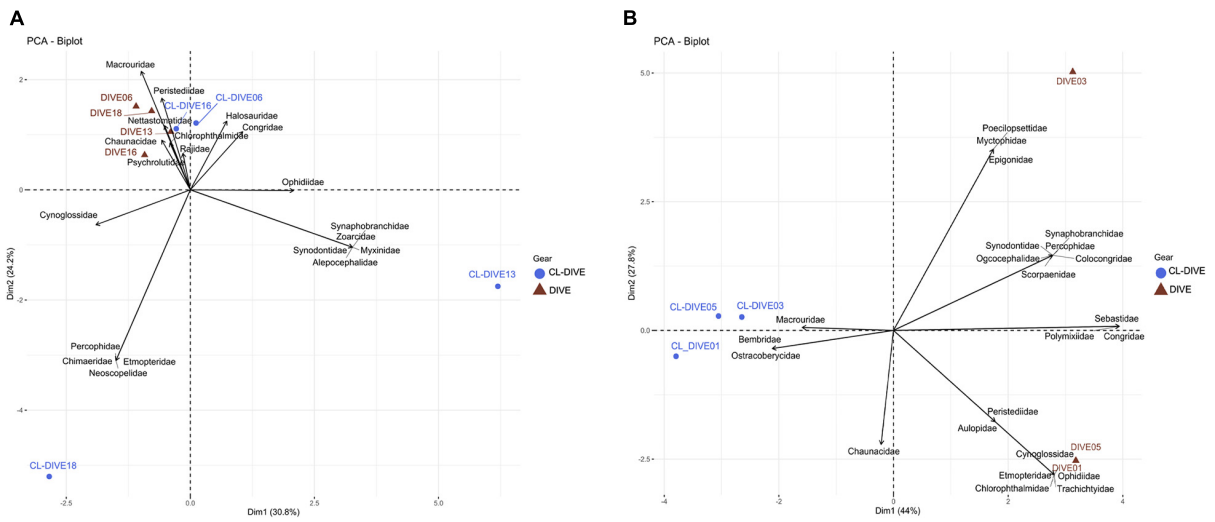

FIGURE 5 | Comparison of fish assemblages between imagery (dive) and sampling along dive (cl-dive) along **(A)** sedimented slope habitats (PNG) (55% of variance on first two PCs) and **(B)** volcanic island slopes (Mayotte) (71.8% of variance on first two PCs). Principal Component Analysis (PCA) of Hellinger-transformed presence/absence fish data at family rank.

PNG (**Figure 8A**). Inversely, we repeatedly observed four genera in images that were poorly sampled with trawls (e.g., *Xylocheles*, *Haliporoides*, *Agononida*, *Galacantha*) (**Figure 8A**). We observed common genera in images (*Nematocarcinus*, *Glyphocrangon*, *Haliporoides*, *Hymenopenaeus*), whereas we identified a higher diversity of genera from trawl samples. Selectivity appeared more pronounced between the camera and trawl transects along the volcanic island slopes of Mayotte (**Figure 8B**). We identified galatheids of small-size or associated with biogenic habitat and woods exclusively from specimens captured by trawls (*Uroptychus*, *Munidopsis*, *Paramunida*), whereas we identified large-sized crabs (*Brachyura*) exclusively from observation of the images from the Dive03 (e.g., *Beuroisia*, *Cyrtomaia*, *Gornodopsis*). The images allowed us to identify more genera while dredge/trawl transects showed more similar genus compositions (**Figure 8B**). Therefore, we estimated a higher gamma diversity of crustacean genera from physical samples than from observation in images on sedimented slopes habitats, and conversely in hard-bottom habitats.

The sampling from the surrounding area (cl-around) allowed us to identify 49 additional genera in both habitats (**Figures 6C,D**); supplementing the regional diversity inventory, insufficiently described with the camera transect and co-located sampling. These surrounding samples enabled the identification of three and five additional crustacean genera in images respectively on soft sediment slopes and volcanic island slopes.

Echinoidea

We estimated the Echinoid genus richness (from rarefaction curves not shown) as equivalent from images and physical sampling in the soft-bottom-dominated site (Dive01) but higher from images than from physical sampling in the two hard-bottom-dominated sites (Dive03, dive05).

Some genera were well sampled in physical samples, particularly the small-sized echinoids (*Echinocyamus* and *Podocidaris*) and some cidarid genera (*Stereocidaris*, *Goniocidaris*, *Histocidaris*). In contrast, we better observed and identified from images spatangoid echinoids (*Spatangus* and *Echinolampas*) and the very fragile, regular echinoid *Aspidodiadema*. We estimated a higher diversity of Cidaridae genera from physical sampling than from observation in images (**Figure 9**), but we observed the genera *Stereocidaris* and *Stylocidaris* (Cidaridae) only from images.

From the pooled camera transect (dives) and the pooled co-located sampling (cl-dives), respectively, we observed equal values of genus diversity between the two methods (9 genera) (**Figure 6E**). The surrounding area sampling allowed us to identify four additional genera (**Figure 6E**) that in turn allowed the identification of two additional genera from images (*Stylocidaris*, *Aspidodiadema*).

Asteroidea

As for echinoids, we estimated (from rarefaction curves not shown) a higher richness of asteroid genera from physical sampling than from observation in images in the soft-bottom-dominated site (Dive01) and conversely in the two hard-bottom-dominated sites. Besides, no asteroid was recovered from the sampling operations along the Dive03.

Asteroids genus composition between images and physical samples were different. We identified six genera exclusively from observation in images (*Lithosoma*, *Paranepanthia*, *Tremaster*, *Anthenoides*, *Sphaeriodiscus*, *Astroceramus*), and five genera exclusively in the physical samples (*Allostichaster*, *Tamaria*, *Mediaster*, *Persephonaster* and *Tritonaster*). However, we observed a more similar genus composition between images and physical samples in the soft-bottom-dominated

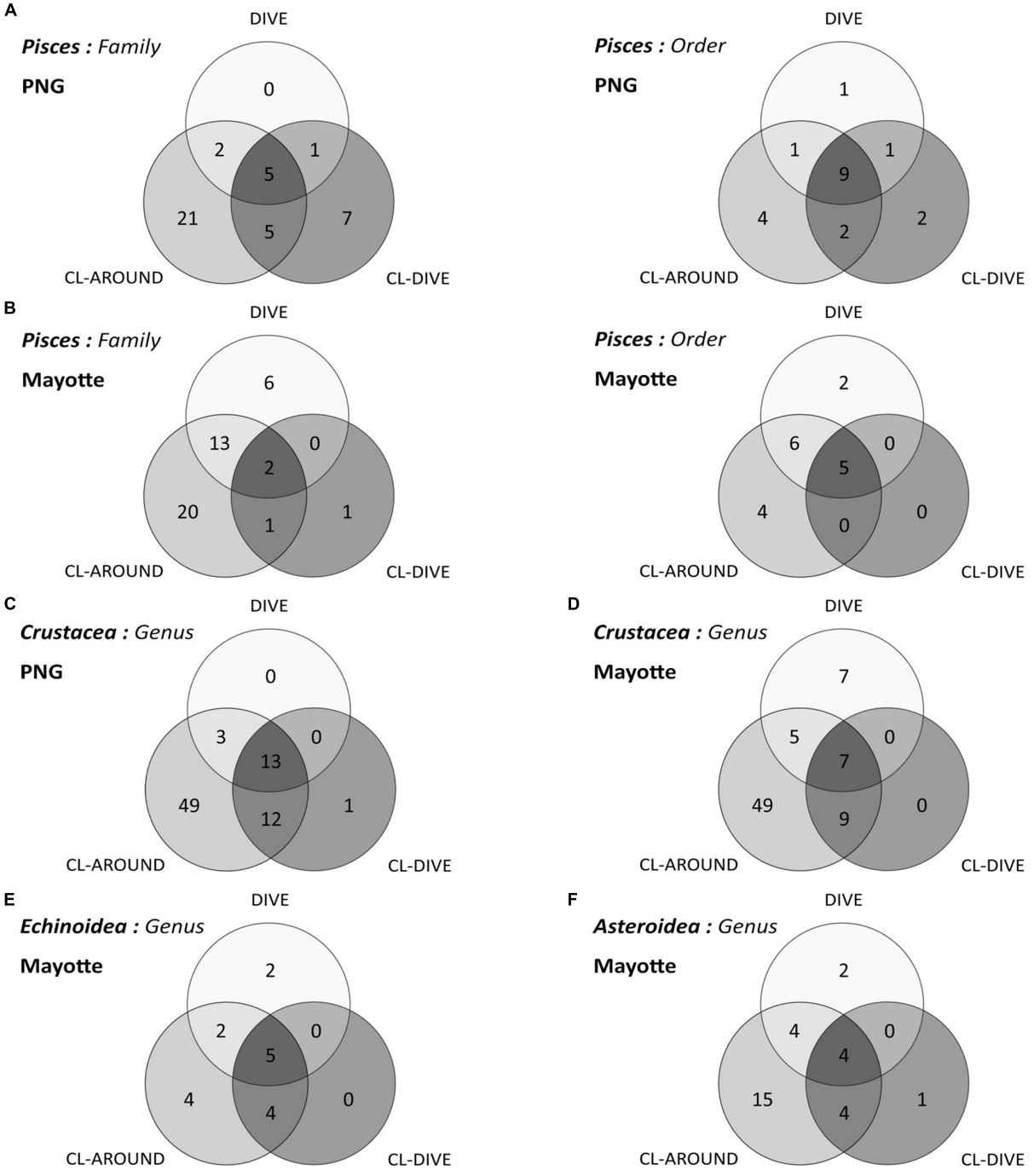

FIGURE 6 | Venn diagrams of taxonomic richness captured and identified from images (dive), sampling along dive (cl-dive) and in the surrounding area (cl-around): **(A)** Pisces at order and family ranks along sedimented slope habitats (PNG) and **(B)** along volcanic island slopes (Mayotte); **(C)** Crustacea at genus rank in PNG and **(D)** in Mayotte; **(E)** Echinoidea at genus rank in Mayotte; **(F)** Asteroidea at genus rank in Mayotte. In each circle the sum of numbers represents a taxonomic rank captured (e.g., number of order or family, etc.).

slope (Dive01) (i.e., *Plinthaster*, *Henricia*, *Cheiraster*) than for the other two hard-bottom-dominated volcanic slopes (**Figure 10**). Furthermore, we also observed *Henricia* and *Cheiraster* in images of the Dive03 and Dive05, but these genera were not captured in their co-located sampling operations (Cl-dive03 and Cl-dive05).

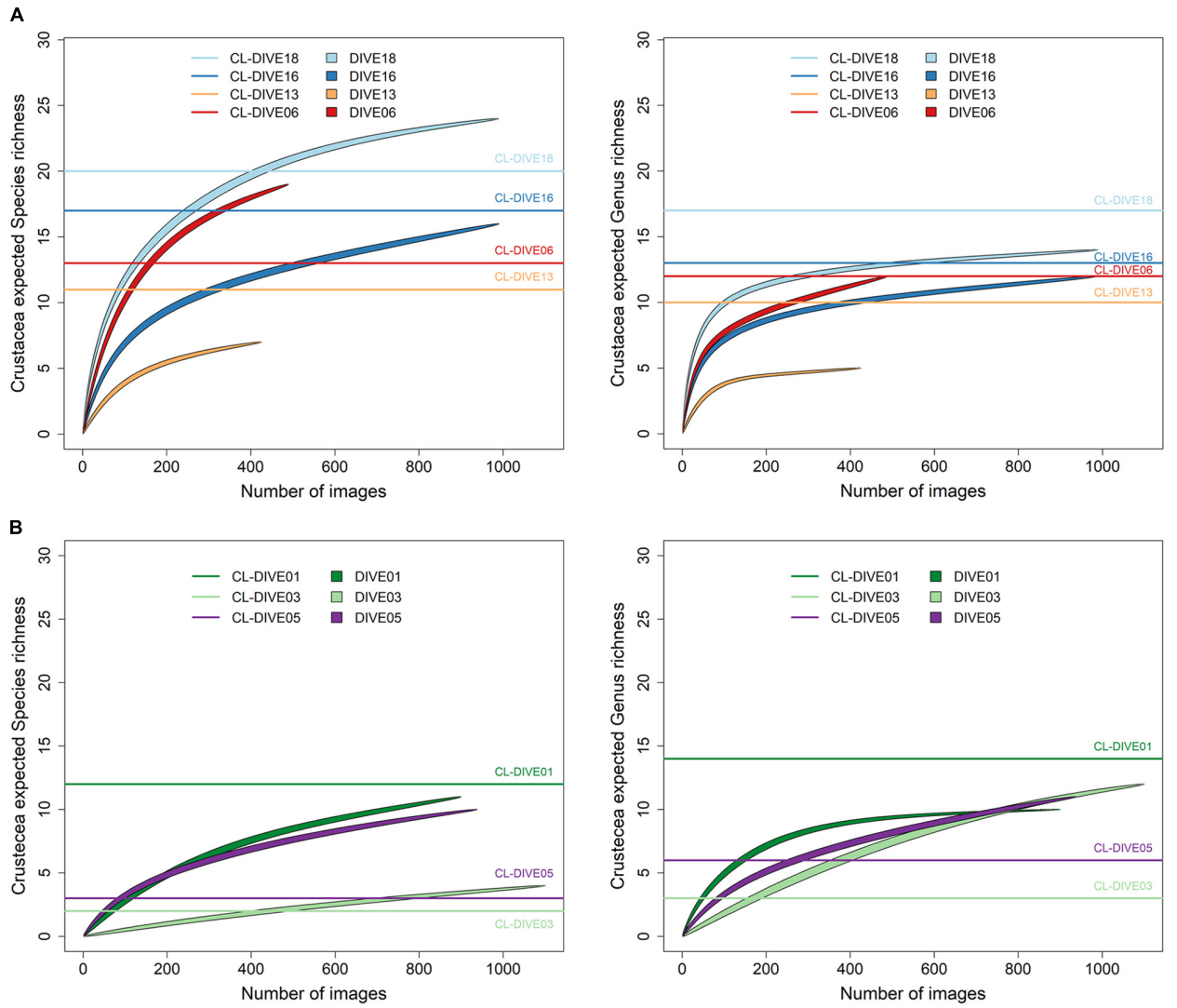

FIGURE 7 | Expected richness from rarefaction curves on Crustacea at genus and species ranks (exact method, *n* = 999 permutations), along **(A)** sedimented slope habitats (PNG) and **(B)** volcanic island slopes (Mayotte). Comparison between imagery (dive) and sampling along dive (cl-dive).

When pooling respectively camera transects (dives) and dredge/trawls transects (cl-dives), we estimated an equivalent diversity at the genus rank from observation in images and from identification of specimens from physical samples (**Figure 6F**). However, we identified two families only from images (Myxasteridae and Solastereidae), but because of the lack of diagnostic characters visible in images we were not able to identify them at the genus level. Consequently we underestimated the genus diversity from images. The surrounding area sampling (cl-around) allowed us to identify 15 supplementary genera, that in turn allowed the identification of four additional genera from images.

Ilustration of the Proposed Integrative Methodology for the Photo-Taxa Identification of Crustaceans (Caridea and Galatheoidea): Construction of Photo-Type Catalogs and Identification Keys

Specimens collected in the co-located sampling and in the surrounding area in Astrolabe Bay and the Sepik area (PNG), and in the Comoros archipelago (for Mayotte), provide additional knowledge of the species occurring in these areas, and directly aid the identification of photo-taxa. Here we use the Caridea, observed on three dives along Mayotte volcanic island slopes,

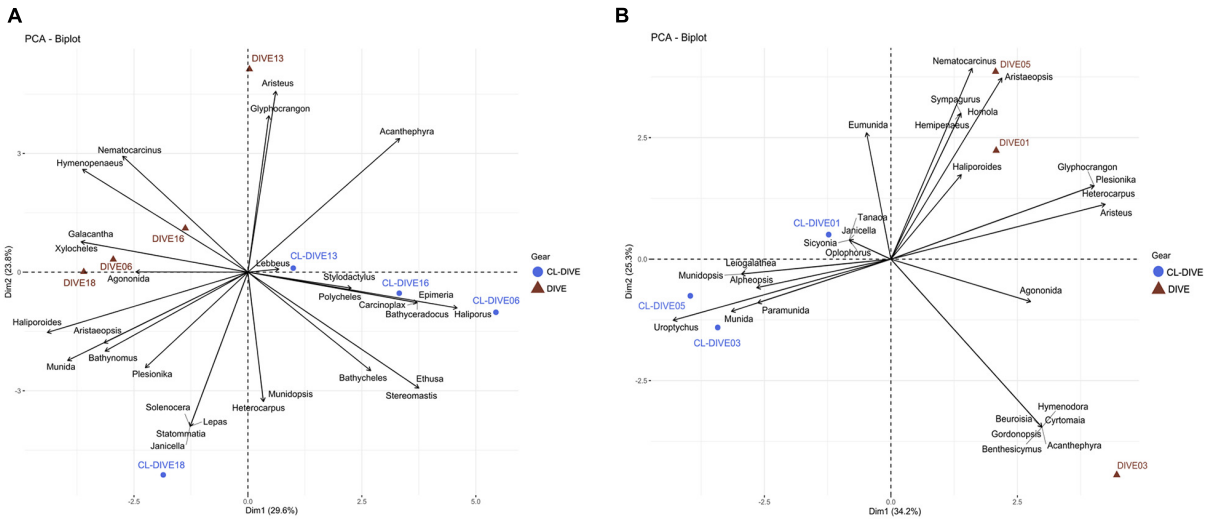

FIGURE 8 | Comparison of crustacean assemblages between imagery (dive) and sampling along dive (cl-dive) along **(A)** sedimented slope habitats (PNG) (53.4% of variance on first two PCs) and **(B)** volcanic island slopes (Mayotte) (59.5% of variance on first two PCs). Principal Component Analysis (PCA) of Hellinger-transformed presence/absence crustacean data at genus rank.

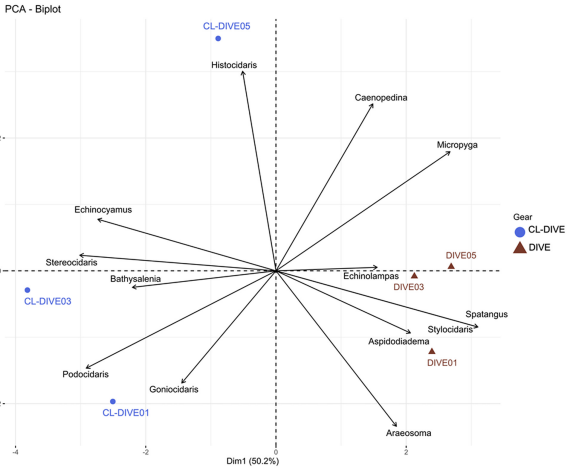

FIGURE 9 | Comparison of echinoid assemblages between imagery (dive) and sampling along dive (cl-dive) along volcanic island slopes (Mayotte) (72.9% of variance on first two PCs). Principal Component Analysis (PCA) of Hellinger-transformed presence/absence echinoid data at genus rank.

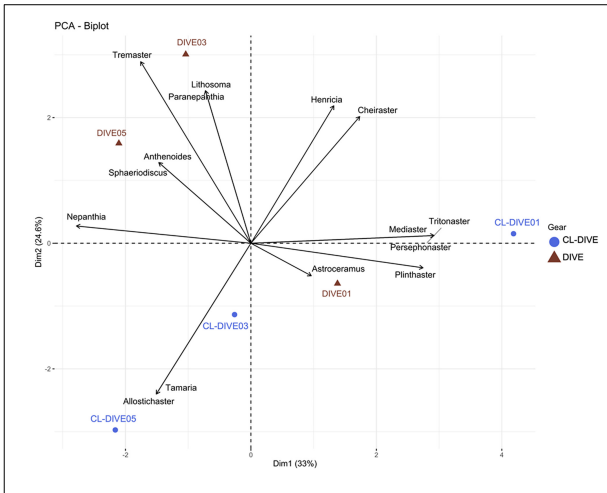

FIGURE 10 | Comparison of asteroid assemblages between imagery (dive) and sampling along dive (cl-dive) along volcanic island slopes (Mayotte) (57.6% of variance on first two PCs). Principal Component Analysis (PCA) of Hellinger-transformed presence/absence asteroid data at genus rank.

to illustrate our method of identification from images. This example illustrates the identification steps, from the photo-taxon identification to the construction of the identification key. We provide another illustration of the methodology in **Supplementary Material 8** for galatheid identification at the morphospecies level along the four PNG sedimented slopes.

We considered four groups of Caridea specimens observed in images as belonging to different genera and thus delimited them into four different photo-taxa attributed to a reliable genus rank. We identified these four genera primarily based on observable morphological characters from images. In the physical samples (data from the BioMaGlo expeditions as well as from previous expeditions), we identified species attributed to these four genera that thus constitute a pool of species potentially present in the analyzed images (**Table 4**). For each of these four genera, we compared the morphological characters observable on the photo-taxa by using the characters of potential species. From this comparison, we were able to determine the individuals to the species or morphospecies ranks, whereas for some photo-taxa, identification did not go beyond the genus rank.

TABLE 4 | Examples of Caridea photo-taxa identified from images in relation with Caridea species collected either from sampling along dive, or from sampling in the surrounding area from Mayotte, Moheli, Geyzer Bank and Gloriosos (BioMaGlo expedition), or from regional sampling from past expeditions undertaken along the Mozambique Channel.

Photo-taxon (identified at a reliable rank N)	Dive	Sampled species belonging to the rank attributed to the photo-taxon	Spatial scale of sampling	Photo-taxon (contextual identification)
Heterocarpus	DIVE01 DIVE03 DIVE05	*Heterocarpus laevigatus* Bate, 1888	Along dive /Around	*Heterocarpus laevigatus*
		Heterocarpus ensifer A. Milne-Edwards, 1881	Around/Regional	*Heterocarpus* indeterminabilis
		Heterocarpus lepidus de Man, 1917	Along dive /Around/Regional	
		Heterocarpus dorsalis Bate, 1888	Around	
		Heterocarpus calmani Crosnier, 1988 *Heterocarpus gibbosus* Bate, 1888	Regional	
Plesionika	DIVE01 DIVE03 DIVE05	*Plesionika semilaevis Bate, 1888*	Along dive/Around/Regional	*Plesionika* indeterminabilis
		Plesionika ensis (A. Milne-Edwards, 1881) *Plesionika crosnieri* Chan & Yu, 1991 *Plesionika spinensis* Chace, 1985 *Plesionika martia* (A. Milne-Edwards, 1883) *Plesionika bifurca* Alcock & Anderson, 1894	Around	
		Plesionika neon Komai & Chan, 2010 *Plesionika alcocki* (Anderson, 1896)	Regional	
		Plesionika nesisi (Burukovsky, 1986) *Plesionika spinidorsalis* (Rathbun, 1906) *Plesionika edwardsii* (Brandt, 1851) *Plesionika crosnieri* Chan & Yu, 1991 *Plesionika indica* de Man, 1917	Around/Regional	
Nematocarcinus	DIVE01 DIVE05	*Nematocarcinus parvus* Burukovsky, 2000	Around/Regional	*Nematocarcinus* sp1 *Nematocarcinus* sp2
		Nematocarcinus tenuirostris Bate, 1888 *Nematocarcinus productus* Bate, 1888 *Nematocarcinus nudirostris* Burukovsky, 1991 *Nematocarcinus tenuipes* Bate, 1888	Regional	
Glyphocrangon	DIVE01 DIVE03 DIVE05	*Glyphocrangon amblytes* Komai, 2004 *Glyphocrangon pulchra* Komai & Chan, 2003 *Glyphocrangon ferox* Komai, 2004 *Glyphocrangon brevis* Komai, 2006 *Glyphocrangon dentata* Komai, 2004 *Glyphocrangon indonesiensis* Komai, 2004 *Glyphocrangon musorstomia* Komai, 2006	Regional	*Glyphocrangon amblytes*
		Glyphocrangon crosnieri Komai, 2004	Along dive /Around/Regional	*Glyphocrangon crosnieri*

For the photo-taxon assigned to the genus *Heterocarpus*, comparisons made it possible to differentiate individuals belonging to this photo-taxon with morphological characters attributed to the species *Heterocapus laevigatus* (i.e., dorsal rostrum without tooth in most length, no dorsal spine on the abdomen, with a body red to orange, with red vertical stripes on abdomen between somites). Thus, for these individuals, we delimited a new photo-taxon assigned to the species *H. laevigatus*. For the other *Heterocarpus* individuals, the quality of the images was insufficient to establish a difference at the species rank. Thus, these individuals remained assigned to the genus *Heterocarpus* with the qualifier status "indeterminabilis".

For the photo-taxon assigned to the genus *Plesionika*, although several potential species corresponding to this genus were collected and are known in the study area, the quality of the images and the observable characters were insufficient to differentiate several subsets at the species level. Many of these observable characters (e.g., white spots on the abdomen) are shared between several species, or highly variable within species (e.g., specimens color variation according to the background substrates). Therefore, we limited our identification to the genus level with the qualifier status "indeterminabilis".

For the photo-taxon assigned to the genus *Nematocarcinus*, five species are known in the area (Burukovsky, 2011). However, the characters observable from images were not sufficient to identify them at the species rank with a valid species name. Nevertheless, we were able to differentiate two groups of individuals within this photo-taxon: individuals with a banded

abdomen and individuals with homogeneous orange abdomen. These two patterns indubitably correspond to at least two different species, as the eight species of *Nematocarcinus* have their colorations illustrated in Burukovsky (2013) all lacking bands on the abdomen. We thus assigned them to two distinct morphospecies.

Finally, for the photo-taxon assigned to the genus *Glyphocrangon,* we distinguished two potential species on a distinct morphological character (i.e., post-antennal spines widely directed outward or not from the front carapace). Using the list of the eight *Glyphocrangon* species present in the region, the state of this observable character from images allowed us to assign each of these two groups of individuals respectively to *Glyphocrangon amblytes* or *Glyphocrangon crosnieri* [also according to their white body coloration with black eyes and orange bands on the abdomen amongst the species reported in the region (Komai and Chan, 2013)].

After having delimited Caridea photo-taxa and attributed each one to at least a genus rank (taxonomic rank illustrated for this example), we selected the best-quality images to compile the photo-type catalogs for use in identifying the remaining photo-taxa. We then compiled all the diagnostic characters we identified as relevant for the identification of these photo-taxa.

Therefore, resulting from this methodology of identification, we developed identification keys for three target taxa based respectively on the expertise of Pr. Tin-Yam Chan and Dr. Laure Corbari for Crustacea (mainly Dendrobranchiata and Caridea), Dr. Thomas Saucède for Echinoidea and Dr. Christopher Mah for Asteroidea. The keys for shrimps and asteroids are dichotomous while the key for echinoids is an online multiple-entry interactive key. We built these keys based on the identification of specimens observed in the images from the Mayotte volcanic island slopes, and from other seamounts in the Mozambique Channel. The taxonomic rank reached in these keys represents the identification rank achieved from the images. Therefore, these keys are yet incomplete. First, for some taxonomic group the characters needed to differentiate the taxa at lower level might be not observable in images. Second, we do not have images of all the species known in the Mozambique Channel. These keys must thus be completed with additional data.

DISCUSSION

Efficiency of Images and Physical Samples in Different Habitat Types

Taxonomic Coverage and Resolution

We reached a level of identification lower than the class level for Pisces (order/family), Asteroidea and Echinoidea (down to genus) and Crustacea (down to species/morphospecies). Assignment to these taxonomic ranks reflects both their recurrence on the images, the available literature and the involvement and availability of taxonomy experts in the identification of specimens both from images and from collected samples. Furthermore, for these groups, a sufficient number of diagnostic characters can be examined from images (e.g., test shape and spine thickness for echinoids, antennular length and color or rostral teeth for shrimps).

Identification of other phyla in images is of lower resolution, from phyla/class for Porifera, order for Cnidaria, and class to family for Mollusca. It is worth noting that the mollusks, as well as the annelids identified at the family level were specialized fauna associated with cold seeps where the low diversity and the large size of individuals (e.g., Sibuet and Olu, 1998) make the identification of these groups easier. On the contrary, in other habitats, annelids and bivalves are usually of small-size and inconspicuous (i.e., buried in the sediments or hidden in habitat-forming organisms such as corals or sponges). For instance, we observed a high proportion of gastropods along the Mayotte island volcanic slopes but whose identification from images of the shells only never exceeded the class rank. We expected such limitation, which was previously observed on hard bottoms (Williams et al., 2015; Beisiegel et al., 2017).

We also obtained incomplete identification from physical samples for mollusks and annelids and for other groups as well (e.g., actinids and echinoderms from the upper PNG sedimented slopes area). This reflects the time-consuming practice of taxonomy (e.g., fieldwork, species delimitation, description and naming, curation of collections, etc.). Moreover, this scientific field suffers from poor funding, decreasing numbers of experts and lack of employment opportunities (Agnarsson and Kuntner, 2007). These hindrances further increase the time between the discovery and the description of new species (Fontaine et al., 2012). Furthermore, in areas where the fauna is poorly known and very diversified such as in PNG—where more than 300 new species have been described by the TDSB Program—and in the north Mozambique Channel—with 85 species described from one expedition (Benthedi)—the identification effort needed from taxonomists is all the more important.

Lastly, from images, we annotated many cnidarians and poriferans, whose identification beyond the class or order ranks was difficult and uncertain. These taxonomic groups have complex taxonomy and show high morphological plasticity or convergence from the high to intraspecific levels (Barnes and Bell, 2002; Todd, 2008). Moreover, diagnostic characters required for identification at the species rank are mainly microscopic or internal (e.g., *Chrysogorgia* species) (Pante and Watling, 2012), and thus cannot be observed from images. In addition, we observed that the erect 3D structure of these habitat-forming species was not efficiently captured in dredges and trawls on the hard bottoms of the Mayotte volcanic island slopes; similarly for penatulids and actinarians which have been observed only in images along sedimented slopes of PNG. This fishing gear selectivity has already been mentioned for hard bottoms (Williams et al., 2015) and for soft bottoms (e.g., pennatulids, actinids) (Rice et al., 1982; Nybakken et al., 1998; de Mendonça and Metaxas, 2021). However, cnidarians and poriferans represent key groups in the benthic ecosystem functioning, because they can host a large diversity of associated fauna (Buhl-Mortensen et al., 2010; Beazley et al., 2013). They are also highly vulnerable to anthropogenic impacts due to their low resilience (Schlacher et al., 2010) and thus provide a good vulnerable marine ecosystem (VME) indicator

(Food and Agriculture Organization of the United Nations [FAO], 2009). For these groups, the use of ROVs can help identification by coupling high-resolution imagery with the collection of targeted specimens and establish a robust baseline catalog. However, the cost by using ROVs is much higher than using the towed cameras, and have still their limitation to survey the whole diversity. This underlines the necessity for developing alternative approaches to assess the diversity of habitat-forming taxa, which is an ongoing work of M. Hanafi-Portier' Ph.D. by developing a classification of observable characters based on their morphology and their function (e.g., size, 3D structure) independently of their taxonomy. Such characters have been reported to be good proxies for the role of these habitat-forming species on associated fauna and how they could respond to abiotic constraints (Schonberg and Fromont, 2014; Denis et al., 2017; Zawada et al., 2019; Schonberg, 2021).

Our study underlines the need to put the research efforts on targeted taxonomic groups that fulfill at least three conditions: (1) an extensive record of both physical specimens and identifications in collections, (2) the ability to identify diagnostic morphological characters from images and (3) the availability and active involvement of taxonomists to identify them from images. For those unidentifiable from images and/or not efficiently collected, biodiversity quantification must then be assessed using other approaches (e.g., morpho-functional).

Biodiversity Metrics for the Targeted Taxonomic Groups

For each targeted taxonomic group, we have compared the diversity and composition metrics at the taxonomic rank reached for images. For a given sampling area, these metrics differ when estimated based on physical samples or from observations made in images.

In areas dominated by hard bottoms or showing high habitat heterogeneity such as cold seeps, we observed higher taxonomic richness in images than in physical samples, for all the targeted taxa in this study, and at variable taxonomic ranks of comparison. This reflects mainly the difficulties for the dredges in these environments, with for example, large boulders (∼1 m in size) along the Mayotte slopes. In the cold-seep area, abundant large siboglinid tubeworm bushes and mussel beds clogging the trawl nets seems to have limited the sampling of other taxa.

In areas dominated by soft sediment, including the sedimented slopes of Astrolabe Bay in PNG and the soft-bottom areas of the Mayotte island slopes (Dive01), we expected a better sampling efficiency than in hard bottoms. However, at the transect scale we did not detect consistent differences in taxonomic richness estimated from observation from images and from identification of physical samples. This low richness of the very mobile fauna in fishing gears—as observed for Pisces—highlight the need to widen the sampling area. The physical sampling alone captured only part of the faunal diversity, probably because of gear selectivity and insufficient sampling effort with respect to the diversity of the different groups in the studied regions. Assessment by environmental DNA/metabarcoding approach could be an interesting complement to improve the biodiversity exploration at the local scale. However, this approach requires DNA-barcoding reference databases which are yet far from completed for the deep-sea fauna. Crustaceans are better sampled by fishing gears if comparing the metrics at the genus rank. However, when considering the identification of morphospecies in images and the identification of species for physical samples, we obtained similar metrics. The metrics estimated at the species level for images might have overestimated the real richness. Indeed, several morphospecies can represent a single species with intraspecific polymorphism. Such issues can be solved only when DNA barcoding analysis is conducted on the collected specimens. Nevertheless, underestimation of diversity is also possible, because one morphospecies can potentially gather several species (Williams et al., 2015). This could explain the lower richness observed in images compared to physical samples in this study (190 species identified from sleds, vs 57 photo-taxa) which contrasts with our results. The use of taxonomic levels, or thresholds, defined for each taxonomic group, could be a more cautious and robust way to assess the biodiversity from image datasets, even if these levels are heterogeneous.

Images alone give a partial estimation of the diversity notably due to identification limitations, particularly for the mobile species that appeared blurry in images (e.g., Malacostraca indeterminabilis dominated in the canyon site) or for small-sized taxa (e.g., genus *Echinocyamus* for echinoids, genus *Lepas* for crustaceans). In soft bottoms, endogenous fauna cannot be detected in images (Rice et al., 1982); this also applies to some crustacean genera (e.g., *Stereomastis*) and burrowing fish families which camouflage themselves (Synodontidae, Myxinidae). Also, some diagnostic characters cannot be observed in images for some taxa (e.g., the Myxasteridae family for Asteroidea, the Perciformes order for Pisces). For echinoids the diversity of some families was better represented from sampling (e.g., Cidaridae) mainly due to the difficulty in identifying characters from images. Thus, imagery tends to smooth the gamma diversity for this family.

Nevertheless, selectivity of fishing gears was also deduced from this comparison, especially in complex seabed habitats for very mobile taxa, but also due to the living habits or fragility of some species. For instance, the fragile genus *Aspidodiadema* (Echinoidea), which lives with its test raised above the seafloor by its long spines, was not collected. Interestingly, images revealed the occurrence of this genus in hard-bottom areas making evident the misconceptions about the soft-bottom living habits of the genus. Similarly, the half-buried spatangoid genera and the burrowing ones (e.g., *Eupatagus*) were identified in images but not in samples, likely because of their fragility.

In summary, we conclude that neither imagery nor physical sampling at the transect scale can give a complete view of megafauna diversity and composition. Imagery is advantageous in hard-bottom and heterogeneous habitats, where the topography and the nature of the substrate limit the efficiency of fishing gears. In contrast, in soft-bottom habitats, the benefit of physical sampling is more pronounced, because endogenous and small-sized fauna cannot be detected in images. Gamma diversity is better estimated from sampling in soft-bottom habitats. The use of imagery in these environments

can provide complementary information on habitats (e.g., wood distribution, cold seeps) at the transect scale, or among transects, revealing their potential role in structuring megafauna biodiversity. In hard-bottom environments, due to sampling difficulties, sampling effort should cover a larger spatial scale to catch the regional species pool and allow identification from images.

Increase the Robustness of Photo-Taxa Identification by an Integrative Methodology

The sampling undertaken in the surrounding areas (up to 400 km) contributed to a significant increase in the knowledge of species occurring in the area. In return, this knowledge helped the identification of individuals from images. For Pisces, the contribution of the knowledge of the surrounding fauna is the highest for the volcanic island slopes, with an increase up to nine-fold of family richness. For echinoids, specimens sampled in the surrounding areas increased the genus richness to a lesser extent than for the very mobile fauna ($\sim$1.7$\times$), probably because of a higher probability of capture and a lower gamma diversity, leading to capture much of the diversity from the "local" samples along the dives. It seems that the contribution increases with fauna mobility and with gamma diversity.

The case study of decapods illustrates the methodological approach we developed based on a taxonomic framework. It shows in particular that photo-taxon identification relies on observation of morphological characters relative to one or several potential analogous species/taxa collected in the area. If morphological characters cannot be sufficiently differentiated between or within one photo-taxon to proceed to a lower identification level, we suggest identification at the lowest robustly determined taxonomic rank.

Although morphological characters cannot be sufficiently observed to assign a species name to a specimen in images, we suggest morphospecies delimitation from knowledge of the taxa occurring in the area at regional and also local scales (specimens exclusively sampled along dive). This approach can be applied to any rank higher than genus (e.g., morphospecies delimited at the family level) according to the lowest resolved identification level. However, when the distinction between morphological characters does not allow the clear delimitation between individuals, identification remains at the lowest robustly resolved taxonomic rank designated with an identification status qualifier "indeterminabilis" (e.g., *Plesionika* indeterminabilis).

In some cases, species-level identification is possible, as illustrated with *H. laevigatus*, because this species was the only one of the *Heterocarpus* genus collected in the surrounding area that showed diagnostic characters corresponding to those observed in the photo-taxon.

We also tried to supplement and enhance the robustness in identification with an integrative approach, by also considering the species habitat, feeding preferences, substrate, living habits or position relative to seafloor. Habitat context was not an informative diagnostic character for the identification of decapods, because most specimens observed in images belonged to genera characteristic of soft- or mixed-bottom types and with a wide depth range. However, for some other taxa, habitat provided useful information. For instance, the knowledge of the preference of some *Munidopsis* species for sunken wood (Hoyoux et al., 2012) that were sampled in the area was a helping criterion to increase confidence in the identification of this genus from images. Similarly, the knowledge of feeding preference of some asteroid species belonging to the genus *Henricia,* that predate on sponges (Mah, 2020), increased confidence in image-based identification of this genus. At the species/morphospecies rank of identification, to weight potentially diagnostic features and increase confidence in the distinction among the potential species, it may be useful to add additional criteria relative to the environment, as discussed above for genus-level identification.

Finally, we developed photo-type catalogs to help in the identification of the remaining photo-taxa to be identified. However, catalogs alone are subject to interpretation according to observers and can lead to erroneous identifications or variable identifications between observers (Henry and Roberts, 2014; Howell et al., 2014; Durden et al., 2016a). Therefore, catalogs of marine taxa need to be fed by formalized diagnostic criteria required for consistent and robust identification.

Formalization of Image-Based Taxonomic Identification From Keys Adapted for Imagery

We observed that images and physical samples provide differential and complementary views of the structure of the benthic megafauna, and uncovered the need for and the contribution of physical sampling at local scales and beyond to help in the identification of photo-taxa. Our formalization of the process of identification of the organisms observed in images gives a taxonomic framework to photo-taxon identification, to refine the taxonomic rank of determination, and for morphospecies delimitation.

From this complementarity, and for three target taxa (Echinoidea, Asteroidea, Decapoda), the diagnostic characters observed in images, the satisfactory level of identification, the collaboration and involvement of taxonomists all enabled the development of identification keys adapted to the images acquired from the Mayotte slopes, and by extension adapted to the Mozambique Channel area. This is a first step for these keys, which can be adapted to other areas in the future (Indo-West Pacific area).

We tested the identification keys for asteroid and decapod identification on a set of four naive observers, as recommended in Walter and Winterton (2007). Results indicated some limitations for the two dichotomous keys, including misinterpretation or low image resolution leading to inefficient or inadequate observation of diagnostic characters. Obviously, the identification of photo-taxa using keys is easier for specialists than for non-experts. We then integrated photo-type images and illustrations of characters to make the keys more user-friendly. However, inherent to their structure, dichotomous keys can be difficult to use due to pathway problems. Misinterpretation or unanswerable couplets

of characters can lead to a dead-end, and thus require going back to the starting entry points (Walter and Winterton, 2007; Hagedorn et al., 2010). Unanswerable couplets can be particularly limiting in the case of image analyses (characters not visible from image), leading us to focus on the development of a multiple-access key such that the user can choose any character according its availability (observable from images) or familiarity (doubt regarding some characters), and also recommended by Howell et al. (2019) in the case of image-based identification.

This type of key is available for echinoid identification at the genus rank. It can be easily updated and quickly provides the information sought to end-users on a web platform. It also facilitates the documentation of environmental settings and of main abiotic and biotic elements of habitats along with their implementation in datasets (e.g., taxon depth range, substrate type, associated living communities, etc.).

The development of image-based keys for fish identification holds promise, but the limited image resolution and top-view acquisition were not suitable to build such keys. Indeed, the morphological characters observable in the images, especially when images were taken with a towed camera, are poorly informative for taxonomic identification. We consequently recommend to systematically supplement top views with a profile view, especially for the identification of Pisces (e.g., number of dorsal fins, profile shape, etc.) and Decapoda (e.g., rostrum shape and armature, abdominal armature etc.), or to use stereo cameras which can provide 3D views. Video sequences can provide informative supplementary diagnostic characters, allowing observation of behavior, flexibility and movement. Advances in biomimicking robotics such as fish-like robots could help encompassing such limitations by offering side-view observations and the exploration of behaviors (Katzschmann et al., 2018; Laschi and Calisti, 2021).

Furthermore, from a non-expert point of view, we noticed different complex methodological choices and questions in terms of photo-taxon identification and morphospecies delimitation. For instance, regarding the choice of whether or not to delimit different morphospecies for a given photo-taxon, the confidence we placed in the species identification level or the choice to maintain the taxon at an indeterminabilis level of identification. We combined these questions in an integrative scheme, considering in particular new recommendations for a standardized, open nomenclature for image-based identification (Horton et al., 2021; **Figure 11**).

Open nomenclature (ON) provides a set of terms and their abbreviation (signs) to inform on the provisional uncertainty status of an identification (Sigovini et al., 2016).

However, the use of Sigovini et al. (2016) ON adapted to physical specimens, as recommended by Horton et al. for image identifications, requires the sampling of the specimens observed in images, which is possible using ROV but not using a towed camera. We can only make hypotheses of known analogous species to link the photo-taxa observed from images with the pool of species collected in the area and sharing similar diagnostic morphological or other characters. Although systematic collection by ROV of specimens observed in images is hardly feasible in highly diverse areas, and onerous, targeted sampling appears to be an efficient option to calibrate photo-taxa identification from images.

Furthermore, as mentioned by Horton et al. (2021), the choice of which ON signs to use will depend on the intended application (analyses, taxon catalogs, etc.) and in the case of community matrix/ecological analyses, that a taxonomic roll-up (merge taxa to higher taxonomic rank) to the most confident identification should be processed. We therefore recommend setting, for each taxonomic group to be analyzed, a threshold taxonomic identification rank enabling to avoid the use of "incertae" ON signs. Using such threshold for the identification rank, the community structure analyses can be robustly conducted. The robustness of this community analysis will rest on the consistency of the taxonomic rank reached within a given taxonomic group. The selection of this threshold depends on the taxonomic group considered, the level of knowledge of the taxa occurring in the area and on the morphological criteria detectable from images. The morphospecies rank can be considered in these analyses if they are confidently delimited and validated by a taxonomy expert.

However, in some cases, we determined the photo-taxa to the species rank, and based on affinities to collected specimens, we assigned them to a species name using "cf" or "aff" ON signs for the analogous species. We corrected the use of these ON signs for "sp incertae" following recommendation of Horton et al. (2021). For analysis, the lack of distinction between uncertainty in the identifications at a given rank and uncertainty of the species name at the species rank can lead to a loss of information if roll-up every photo-taxon assigned to "incertae" ON sign. Therefore, these species, despite uncertain identification, can be included in species rank analyses.

Finally, the keys help mainly for identification at the family or the genus levels. Sometimes morphospecies level delimitations are suggested or, at least, a set of observable morphological characters of the morphospecies are listed in the key. Such indications should help the delimitation of morphospecies in future studies. However, the naming convention for certain morphospecies in this study will certainly not be the same in another study. There is a need for future studies to develop identification keys in other oceanic regions, systematically accompanied by a morphospecies catalog—if morphospecies are delimited—and by listing the corresponding, potentially analogous known species in the area. The identification keys and the morphospecies catalog should both relied on the standardized database of marine taxa image catalog developed by Howell et al. (2019) in the Atlantic region, and using a Darwin Core format.

CONCLUSION

Imagery and physical sampling have benefits and biases that influence the estimated patterns of biodiversity. The taxonomic level of identification, the studied taxonomic groups and habitat type are important elements to be considered. Each of these choices needs to be carefully considered according to the questions addressed by the study but also by the costs and the environmental issues.

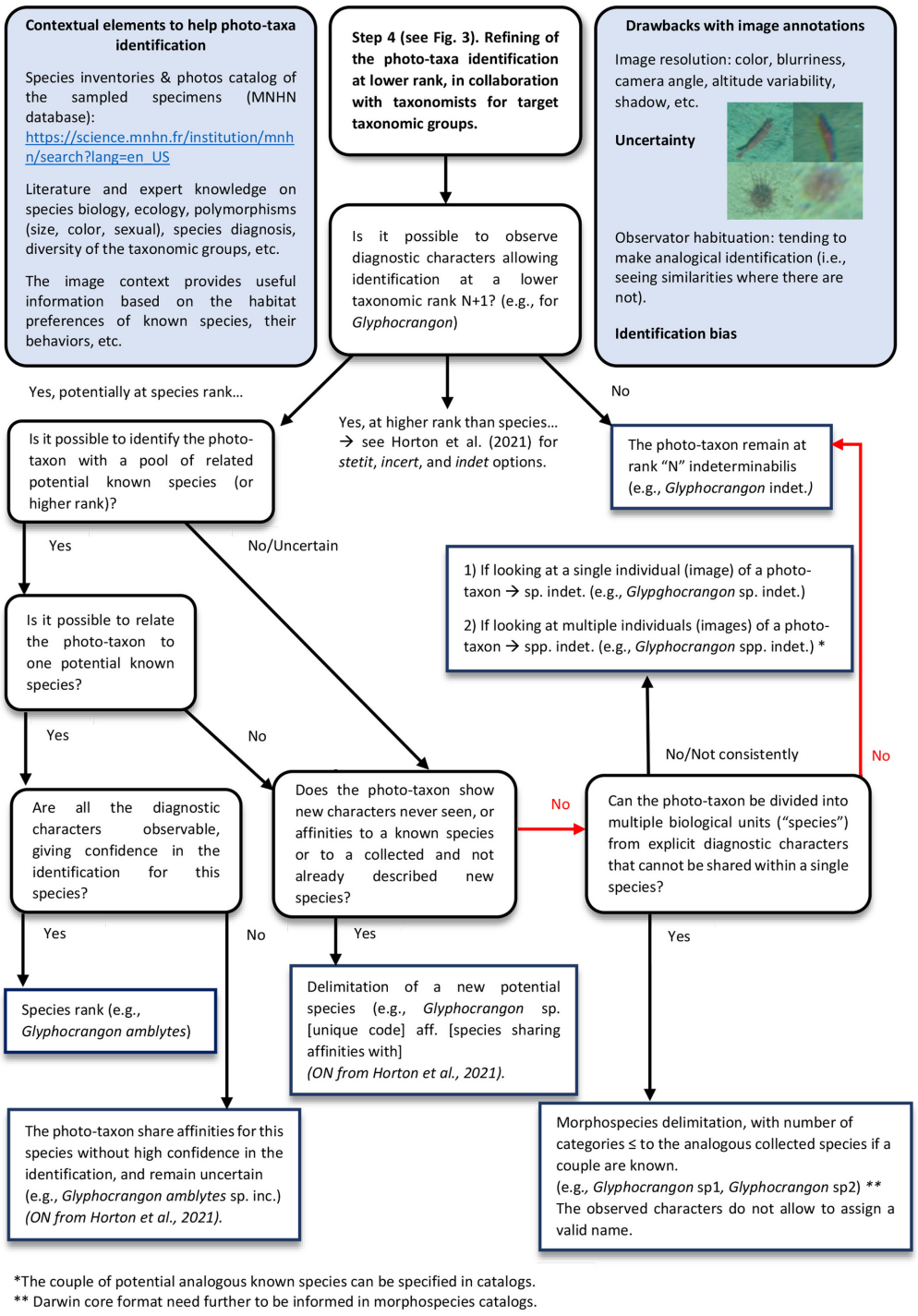

FIGURE 11 | Integrative scheme for photo-taxa identification and nomenclature from images.

In poorly explored areas with poorly known fauna, processing taxon identification from images is very difficult and could lead to potential important misidentifications. Our study shows that deploying imagery-based studies require prior extensive physical sampling to establish a baseline knowledge of the species occurences in the area. To assess the pattern of benthic megafauna communities, in homogeneous or soft-bottom habitats, dredges and trawls seem to be more suitable

options than towed camera. In such environments, image acquisition is a supplementary approach to check for the absence of more complex structures formed by engineer species. In more heterogeneous habitats, such as cold seeps or hard-substrate environments composed of fragile biotic habitats (corals, sponges), imagery should be favored and supplemented with limited physical sampling effort. Ideally, targeted sampling by ROV should be preferred, including new robotic hands or "needle-biopsy" samplers for a minimally invasive sampling (Pomponi, 2016), but this recommendation cannot be generalized due to its implementation cost.

Imagery and physical sampling are complementary methods and using both together will improve assessments of benthic megafauna community patterns. These elements are important to consider for establishing policy management in environments increasingly threatened by anthropic activities, such as Astrolabe Bay, where the Ramu refinery activity could lead to potentially destructive impacts (Samadi et al., 2015) or in the context of the Mayotte Natural Marine Park. From these complementary methods, we propose an integrative methodological approach to process faunal identification from images, based on contextual tools and supported by a taxonomical framework.

Above all, the difficulty of carrying out identification from images raises the necessity of collaborative work with taxonomists. Their expertise is essential for assessing the quality and the validity of the identification, at the lowest taxonomic level possible. This complexity reveals the need to focus on specific taxonomic groups that present observable morphological characters from images and the need to set a reasonable and robust level of identification. Such considerations require the involvement in the study of taxonomists to identify collected specimens and photo-taxa (specimens in images). This methodology has led to the development of identification keys adapted for imagery data, for target taxonomic groups (echinoids, asteroids and shrimps). Improvement of image resolution and different camera angles could offer interesting perspective to improve megafauna' identification from images, and for instance, to develop identification keys for fish. The combination of image acquisition with targeted sampling is also a crucial way for the calibration of the identification. Finally, these identification keys were developed from the Mozambique Channel seamount fauna dataset and could be extended to other areas of the Indo-West Pacific region, through further international collaborative effort.

DATA AVAILABILITY STATEMENT

The original contributions presented in the study are included in the article/**Supplementary Material**, further inquiries can be directed to the corresponding author/s.

AUTHOR CONTRIBUTIONS

KO, LC, and SS designed the sampling and led the data acquisition. MH-P, KO, and LC analyzed the data. MH-P, KO, and CB processed the images. T-YC, LC, TS, W-JC, M-YL, J-NC, CM, and MH-P identified taxa in the images and constructed the identification keys. MH-P, KO, and SS wrote the manuscript. KO, SS, LC, T-YC, TS, W-JC, and M-YL contributed to the critical revision of the manuscript. KO and SS are Ph.D. supervisors. All authors contributed to the article and approved the submitted version.

FUNDING

The BioMaGlo cruise and project was supported by funding from the Xth European Development Fund (*Fonds Européen de Développement*; FED) "sustainable management of the natural heritage of Mayotte and the Eparses Islands" program led by the French Southern and Antarctic Lands (*Terres australes et antarctiques françaises*; TAAF) with the support of the Mayotte Departmental Council (*Conseil Départemental de Mayotte*), the French Development Agency (*Agence Française de Développement*; AFD) and the European Union. Collaboration with Taiwan was supported by funding from the Ministry of Science and Technology, Taiwan (MOST 102-2923-B-002-001-MY3, MOST 107-2611-M-002-007- and MOST 108-2611-M-002-012-MY2 to W-JC) and the French National Research Agency (ANR 12-ISV7-0005-01 to SS) and the Center of Excellence for the Oceans, National Taiwan Ocean University to T-YC. The thesis of MH-P is co-funded by TOTAL and IFREMER as part of the PAMELA (Passive Margin Exploration Laboratories) scientific project.

ACKNOWLEDGMENTS

We would like to thank the officers and crews of RV's *ANTEA* and *ALIS* as well as the SCAMPI towed-camera team for their contribution and assistance with data acquisition. We are grateful to the chief scientists of the Madeep, BioMaGlo, BioPapua, and Papua Niugini cruises as well as the entire scientific team. Moreover, we would like to thank J. Tourolle for the helping and assisting in the analysis of GIS data, EJ. Pernet for the processing of the fauna samples, L. Keszler for the primary annotation of the BioMaGlo campaign images. We are grateful to T. Nattkemper and D. Langenkämper for allowing the loading of the image data and their annotation with Biigle 2.0 and for their technical support. We are particularly grateful to all the taxonomists who have contributed to the identification of the fauna in the images and in the collections: N. Puillandre (gastropods), P. Maestratti (bivalves), E. Pante and D. Pica (cnidarians), P. Cardenas and C. Debitus (poriferans), P. Giannassi (fishes), E. Macpherson (galatheids). This paper has been professionally edited for the English language by C. Engel-Gautier (CHRYSALIDE). Finally, we would like to thank the two reviewers for their critical comments that have contributed to improve the manuscript quality.

SUPPLEMENTARY MATERIAL

The Supplementary Material for this article can be found online at: https://www.frontiersin.org/articles/10.3389/fmars.2021.749078/full#supplementary-material

Supplementary Material 1 | Details of the working steps followed in the process of fauna identification from images.

Supplementary Material 2 | Decapoda identification key adapted for deep-sea images.

Supplementary Material 3 | Asteroidea identification key adapted for deep-sea images.

Supplementary Material 4 | Inventory of photo-taxa identified from images (dive) and of species collected along dive according to the target taxa and taxonomic rank: **(A)** along the PNG sedimented slopes and **(B)** along Mayotte volcanic outer slopes.

Supplementary Material 5 | Datasets of sampled (from fishing gears) versus observed (from images) specimens in Papua New Guinea areas.

Supplementary Material 6 | Datasets of sampled (from fishing gears) versus observed (from images) specimens in Mayotte areas.

Supplementary Material 7 | Number of distinct taxa remained identified at each taxonomic rank according to the method (images = dive, sampling along dive = cl-dive), **(A)** along sedimented slopes (PNG) and **(B)** along volcanic island slopes dominated by hard bottom (Mayotte) with **(C)** a focus on echinoids and asteroids.

Supplementary Material 8 | Illustration of the integrative methodology for the galatheids identification from images at morphospecies rank, along the upper sedimented slopes of the Papua New Guinea.

REFERENCES

Agnarsson, I., and Kuntner, M. (2007). Taxonomy in a Changing World: seeking Solutions for a Science in Crisis. *Syst. Biol.* 56, 531–539. doi: 10.1080/10635150701424546

Althaus, F., Williams, A., Schlacher, T., Kloser, R., Green, M., Barker, B., et al. (2009). Impacts of bottom trawling on deep-coral ecosystems of seamounts are long-lasting. *Mar. Ecol. Prog. Ser.* 397, 279–294. doi: 10.3354/meps08248

Audru, J.-C., Guennoc, P., Thinon, I., and Abellard, O. (2006). Bathymay?: la structure sous-marine de Mayotte révélée par l'imagerie multifaisceaux. *C. R. Geosci.* 338, 1240–1249. doi: 10.1016/j.crte.2006.07.010

Barnes, D. K. A., and Bell, J. J. (2002). Coastal sponge communities of the West Indian Ocean: morphological richness and diversity. *Afr. J. Ecol.* 40, 350–359. doi: 10.1046/j.1365-2028.2002.00388.x

Beazley, L. I., Kenchington, E. L., Murillo, F. J., Sacau, M., and del, M. (2013). Deep-sea sponge grounds enhance diversity and abundance of epibenthic megafauna in the Northwest Atlantic. *ICES J. Mar. Sci.* 70, 1471–1490. doi: 10.1093/icesjms/fst124

Beisiegel, K., Darr, A., Gogina, M., and Zettler, M. L. (2017). Benefits and shortcomings of non-destructive benthic imagery for monitoring hard-bottom habitats. *Mar. Pollut. Bull.* 121, 5–15. doi: 10.1016/j.marpolbul.2017.04.009

Bouchet, P. (2009). *MIRIKY Cruise, RV MIRIKY*. Available online at: https://expeditions.mnhn.fr/campaign/miriky?lang=en_US (accessed October 19, 2021).

Bouchet, P., and Ramos, A. (2009). *MAINBAZA Cruise, RV Vizcondede Eza.* Available online at: https://expeditions.mnhn.fr/campaign/mainbaza?lang=en_US (accessed October 19, 2021).

Bouchet, P., Perez, T., and Le Gall, L. (2010). *ATIMO VATAE cruise, RV Antea.* doi: 10.17600/10110040

Bowden, D. A., Rowden, A. A., Leduc, D., Beaumont, J., and Clark, M. R. (2016). Deep-sea seabed habitats: do they support distinct mega-epifaunal communities that have different vulnerabilities to anthropogenic disturbance?. *Deep Sea Res. I Oceanogr. Res. Pap.* 107, 31–47. doi: 10.1016/j.dsr.2015.10.011

Braga-Henriques, A., Porteiro, F. M., Ribeiro, P. A., de Matos, V., Sampaio, I., Ocaña, O., et al. (2013). Diversity, distribution and spatial structure of the cold-water coral fauna of the Azores (NE Atlantic). *Biogeosciences* 10, 4009–4036. doi: 10.5194/bg-10-4009-2013

Buhl-Mortensen, L., Vanreusel, A., Gooday, A. J., Levin, L. A., Priede, I. G., Buhl-Mortensen, P., et al. (2010). Biological structures as a source of habitat heterogeneity and biodiversity on the deep ocean margins: biological structures and biodiversity. *Mar. Ecol.* 31, 21–50. doi: 10.1111/j.1439-0485.2010.00359.x

Burukovsky, R. N. (2011). Geographic distribution of nematocarcinidae shrimps (*Crustacea. Decapoda*). *Zool. Zh.* 90, 293–301.

Burukovsky, R. N. (2013). "Shrimps of the family Nematocarcinidae Smith, 1884 (Crustacea, Decapoda, Caridea) from Taiwan and the Philippines collected by the TAIWAN, PANGLAO 2005 and AURORA expeditions in the western Pacific," in *Tropical Deep-Sea Benthos 27*, eds S. T. Ahyong, T.-Y. Chan, L. Corbari, and P. K. L. Ng (New York: Mémoires du Muséum national d'Histoire naturelle), 154–189.

Clark, M. R., Consalvey, M., and Rowden, A. A. (eds) (2016). *Biological Sampling In The Deep Sea*. New Jersey: Wiley-Blackwell.

Collins, P., Kennedy, R., and Van Dover, C. (2012). A biological survey method applied to seafloor massive sulphides (SMS) with contagiously distributed hydrothermal-vent fauna. *Mar. Ecol. Prog. Ser.* 452, 89–107. doi: 10.3354/meps09646

Corbari, L., Olu, K., and Samadi, S. (2014). *MADEEP cruise, RV Alis*. doi: 10.17600/14004000

Corbari, L., Samadi, S., and Olu, K. (2017). *BIOMAGLO cruise, RV Antea*. doi: 10.17600/17004000

R Core Team (2020). *R: A language and environment for statistical computing*. Vienna: R Foundation for Statistical Computing.

Cunha, M. R., Hilário, A., and Santos, R. S. (2017). Advances in deep-sea biology: biodiversity, ecosystem functioning and conservation. An introduction and overview. *Deep Sea Res. II Top. Stud. Oceanogr.* 137, 1–5. doi: 10.1016/j.dsr2.2017.02.003

Da Ros, Z., Dell'Anno, A., Morato, T., Sweetman, A. K., Carreiro-Silva, M., Smith, C. J., et al. (2019). The deep sea: the new frontier for ecological restoration. *Mar. Policy* 108:103642. doi: 10.1016/j.marpol.2019.103642

Danovaro, R., Snelgrove, P. V. R., and Tyler, P. (2014). Challenging the paradigms of deep-sea ecology. *Trends Ecol. Evol.* 29, 465–475. doi: 10.1016/j.tree.2014.06.002

de Mendonça, S. N., and Metaxas, A. (2021). Comparing the Performance of a Remotely Operated Vehicle, a Drop Camera, and a Trawl in Capturing Deep-Sea Epifaunal Abundance and Diversity. *Front. Mar. Sci.* 8:631354. doi: 10.3389/fmars.2021.631354

Denis, V., Ribas-Deulofeu, L., Sturaro, N., Kuo, C.-Y., and Chen, C. A. (2017). A functional approach to the structural complexity of coral assemblages based on colony morphological features. *Sci. Rep.* 7:9849. doi: 10.1038/s41598-017-10334-w

Dray, S., and Dufour, A. (2007). The ade4 Package: implementing the Duality Diagram for Ecologists. *J. Stat. Softw.* 22, 1–20. doi: 10.18637/jss.v022.i04

Durden, J. M., Schoening, T., Althaus, F., Friedman, A., Garcia, R., Glover, A. G., et al. (2016b). Perspectives in visual imaging for marine biology and ecology: from acquisition to understanding. *Oceanogr. Mar. Biol.* 54, 1–72. doi: 10.1201/9781315368597

Durden, J. M., Bett, B., Schoening, T., Morris, K., Nattkemper, T., and Ruhl, H. (2016a). Comparison of image annotation data generated by multiple investigators for benthic ecology. *Mar. Ecol. Prog. Ser.* 552, 61–70. doi: 10.3354/meps11775

Fontaine, B., Perrard, A., and Bouchet, P. (2012). 21 years of shelf life between discovery and description of new species. *Curr. Biol.* 22, R943–R944. doi: 10.1016/j.cub.2012.10.029

Food and Agriculture Organization of the United Nations [FAO] (2009). *International guidelines for the management of deep-sea fisheries in the high seas: Directives internationales sur la gestion de la pêche profonde en haute mer*. Rome: Food and Agriculture Organization of the United Nations.

Grassle, J. F., Sanders, H. L., Hessler, R. R., Rowe, G. T., and McLellan, T. (1975). Pattern and zonation: a study of the bathyal megafauna using the research

submersible Alvin. *Deep Sea Res. Oceanogr. Abstr.* 22, 457–481. doi: 10.1016/0011-7471(75)90020-0

Hagedorn, G., Rambold, G., and Martellos, S. (2010). "Types of identification keys," in *Proceedings of Bioidentify eu: Tools for Identifying Biodiversity: Progress and Problems*, eds P. L. Nimis and R. Vignes Lebbe (Trieste: Edizioni Università di Trieste), 59–64.

Henry, L.-A., and Roberts, J. M. (2014). Recommendations for best practice in deep-sea habitat classification: Bullimore et al. as a case study. *ICES J. Mar. Sci.* 71, 895–898. doi: 10.1093/icesjms/fst175

Horton, T., Marsh, L., Bett, B. J., Gates, A. R., Jones, D. O. B., Benoist, N. M. A., et al. (2021). Recommendations for the Standardisation of Open Taxonomic Nomenclature for Image-Based Identifications. *Front. Mar. Sci.* 8:620702. doi: 10.3389/fmars.2021.620702

Howell, K. L., Bullimore, R. D., and Foster, N. L. (2014). Quality assurance in the identification of deep-sea taxa from video and image analysis: response to Henry and Roberts. *ICES J. Mar. Sci.* 71, 899–906. doi: 10.1093/icesjms/fsu052

Howell, K. L., Davies, J. S., Allcock, A. L., Braga-Henriques, A., Buhl-Mortensen, P., Carreiro-Silva, M., et al. (2019). A framework for the development of a global standardised marine taxon reference image database (SMarTaR-ID) to support image-based analyses. *PLoS One* 14:e0218904. doi: 10.1371/journal.pone.0218904

Hoyoux, C., Zbinden, M., Samadi, S., Gaill, F., and Compère, P. (2012). Diet and gut microorganisms of *Munidopsis* squat lobsters associated with natural woods and mesh-enclosed substrates in the deep South Pacific. *Mar. Biol. Res.* 8, 28–47. doi: 10.1080/17451000.2011.605144

Jouet, G., and Deville, E. (2015). *PAMELA-MOZ04 cruise, RV Pourquoi pas ?*. doi: 10.17600/15000700

Katzschmann, R. K., DelPreto, J., MacCurdy, R., and Rus, D. (2018). Exploration of underwater life with an acoustically controlled soft robotic fish. *Sci. Robot.* 3:eaar3449. doi: 10.1126/scirobotics.aar3449

Komai, T., and Chan, T.-Y. (2013). "New records of Glyphocrangon A. Milne-Edwards, 1881 (Crustacea, Decapoda, Caridea, Glyphocrangonidae) from recent French expeditions off the Mozambique Channel and Papua New Guinea, with description of one new species," in *Tropical Deep-Sea Benthos 27*, eds S. T. AHYONG, T.-Y. CHAN, L. CORBARI, and P. K. L. NG (New York: Mémoires du Muséum national d'Histoire naturelle), 107–128.

Krell, F.-T. (2004). Parataxonomy vs. taxonomy in biodiversity studies – pitfalls and applicability of 'morphospecies' sorting. *Biodivers. Conserv.* 13, 795–812. doi: 10.1023/B:BIOC.0000011727.53780.63

Kroh, A., and Smith, A. B. (2010). The phylogeny and classification of post-Palaeozoic echinoids. *J. Syst. Palaeontol.* 8, 147–212. doi: 10.1080/14772011003603556

Langenkämper, D., Zurowietz, M., Schoening, T., and Nattkemper, T. W. (2017). BIIGLE 2.0 - Browsing and Annotating Large Marine Image Collections. *Front. Mar. Sci.* 4:83. doi: 10.3389/fmars.2017.00083

Laschi, C., and Calisti, M. (2021). Soft robot reached the deepest part of the ocean. *Nature* 591, 35–36. doi: 10.1038/d41586-021-00297-4

Legendre, P. (2014). Interpreting the replacement and richness difference components of beta diversity: replacement and richness difference components. *Glob. Ecol. Biogeogr.* 23, 1324–1334. doi: 10.1111/geb.12207

Legendre, P., and Gallagher, E. D. (2001). Ecologically meaningful transformations for ordination of species data. *Oecologia* 129, 271–280. doi: 10.1007/s004420100716

Levin, L. A. (2005). Ecology of cold seep sediments: interactions of fauna with flow, chemistry and microbes. *Oceanogr. Mar. Biol. Annu. Rev.* 43, 1–46.

Levin, L. A., and Le Bris, N. (2015). The deep ocean under climate change. *Science* 350, 766–768. doi: 10.1126/science.aad0126

Levin, L. A., and Sibuet, M. (2012). Understanding Continental Margin Biodiversity: a New Imperative. *Annu. Rev. Mar. Sci.* 4, 79–112. doi: 10.1146/annurev-marine-120709-142714

Mah, C. L. (2007). Phylogeny of the Zoroasteridae (Zorocallina; Forcipulatida): evolutionary events in deep-sea Asteroidea displaying Palaeozoic features. *Zool. J. Linn. Soc.* 150, 177–210. doi: 10.1111/j.1096-3642.2007.00291.x

Mah, C. L. (2020). New species, occurrence records and observations of predation by deep-sea Asteroidea (Echinodermata) from the North Atlantic by NOAA ship Okeanos Explorer. *Zootaxa* 4766, 201–260. doi: 10.11646/zootaxa.4766.2.1

McClain, C. R., Lundsten, L., Ream, M., Barry, J., and DeVogelaere, A. (2009). Endemicity, Biogeography, Composition, and Community Structure On a Northeast Pacific Seamount. *PLoS One* 4:e4141. doi: 10.1371/journal.pone.0004141

Muséum national d'Histoire naturelle (2019). *Repository of collection surveys*. Available online at: http://expeditions.mnhn.fr. - V 2.22.0 (accessed April 15, 2021).

Nybakken, J., Craig, S., Smith-Beasley, L., Moreno, G., Summers, A., and Weetman, L. (1998). Distribution density and relative abundance of benthic invertebrate megafauna from three sites at the base of the continental slope off central California as determined by camera sled and beam trawl. *Deep Sea Res. II Top. Stud. Oceanogr.* 45, 1753–1780. doi: 10.1016/S0967-0645(98)80016-7

Obura, D. (2012). The Diversity and Biogeography of Western Indian Ocean Reef-Building Corals. *PLoS One* 7:e45013. doi: 10.1371/journal.pone.0045013

Obura, D., Church, J., Gabrié, C., and Macharia, D. (2012). *Assessing Marine World Heritage from an Ecosystem Perspective: the Western Indian Ocean*. Paris: United Nations Education, Science and Cultural Organization (UNESCO), 125.

O'Hara, T. D., Hugall, G., Andrew, F., Woolley, S. N. C., Bribiesca-Contreras, G., and Bax, N. J. (2019). Contrasting processes drive ophiuroid phylodiversity across shallow and deep seafloors. *Nature* 565, 636–639.

O'Hara, T. D., Williams, A., Woolley, S. N. C., Nau, A. W., and Bax, N. J. (2020). Deep-sea temperate-tropical faunal transition across uniform environmental gradients. *Deep Sea Res. I Oceanogr. Res. Pap.* 161:103283. doi: 10.1016/j.dsr.2020.103283

Oksanen, J., Blanchet, F. G., Friendly, M., Kindt, R., Legendre, P., and McGlinn, D. (2019). *vegan: Community Ecology Package. R package version 2.5-6*.

Olu, K. (2014). *PAMELA-MOZ01 cruise, RV L'Atalante*. doi: 10.17600/14000100

Pante, E., Corbari, L., Thubaut, J., Chan, T.-Y., Mana, R., Boisselier, M.-C., et al. (2012). Exploration of the Deep-Sea Fauna of Papua New Guinea. *Oceanography* 25, 214–225. doi: 10.5670/oceanog.2012.65

Pante, E., and Watling, L. (2012). *Chrysogorgia* from the New England and Corner Seamounts: atlantic–pacific connections. *J. Mar. Biol. Assoc. U. K.* 92, 911–927. doi: 10.1017/S0025315411001354

Payri, C., Archambault, P., and Samadi, S. (2012). *MADANG 2012 cruise, RV Alis*. doi: 10.17600/18000841

Pomponi, A. S. (2016). *Emerging Technologies for Biological Sampling in the Ocean. National Ocean Exploration Forum 2016*. Available online at: https://oceanexplorer.noaa.gov/national-forum/media/noef-2016-pomponi.pdf (accessed September 30, 2021).

Ramirez-Llodra, E., Tyler, P. A., Baker, M. C., Bergstad, O. A., Clark, M. R., Escobar, E., et al. (2011). Man and the Last Great Wilderness: human Impact on the Deep Sea. *PLoS One* 6:e22588. doi: 10.1371/journal.pone.0022588

Rice, A., Aldred, R., Darlington, E., and Wild, R. (1982). The quantitative estimation of the deep-sea megabenthos - a new approach to an old problem. *Oceanol. Acta* 5, 63–72.

Robert, K., Jones, D., and Huvenne, V. (2014). Megafaunal distribution and biodiversity in a heterogeneous landscape: the iceberg-scoured Rockall Bank, NE Atlantic. *Mar. Ecol. Prog. Ser.* 501, 67–88. doi: 10.3354/meps10677

Samadi, S., and Corbari, L. (2010). *BIOPAPUA cruise, RV Alis*. doi: 10.17600/10100040

Samadi, S., Puillandre, N., Pante, E., Boisselier, M.-C., Corbari, L., Chen, W.-J., et al. (2015). Patchiness of deep-sea communities in Papua New Guinea and potential susceptibility to anthropogenic disturbances illustrated by seep organisms. *Mar. Ecol.* 36, 109–132. doi: 10.1111/maec.12204

Saucède, T., Eléaume, M., Jossart, Q., Moreau, C., Downey, R., Bax, N., et al. (2020). Taxonomy 2.0: computer-aided identification tools to assist Antarctic biologists in the field and in the laboratory. *Antarct. Sci.* 33, 39–51. doi: 10.1017/S0954102020000462

Schlacher, T. A., Williams, A., Althaus, F., and Schlacher-Hoenlinger, M. A. (2010). High-resolution seabed imagery as a tool for biodiversity conservation planning on continental margins: submarine canyon megabenthos and conservation planning. *Mar. Ecol.* 31, 200–221. doi: 10.1111/j.1439-0485.2009.00286.x

Schonberg, C. H. L. (2021). No taxonomy needed: sponge functional morphologies inform about environmental conditions. *Ecol. Indic.* 129:107806. doi: 10.1016/j.ecolind.2021.107806

Schonberg, C. H. L., and Fromont, J. (2014). *Sponge functional growth forms as a means for classifying sponges without taxonomy*. Available online at: https://www.researchgate.net/publication/278627643_Sponge_functional_growth_forms_as_a_means_for_classifying_sponges_without_taxonomy (accessed June 22, 2020).

Sibuet, M., and Olu, K. (1998). Biogeography, biodiversity and fluid dependence of deep-sea cold-seep communities at active and passive margins. *Deep Sea Res. II Top. Stud. Oceanogr.* 45, 517–567. doi: 10.1016/S0967-0645(97)00074-X

Sigovini, M., Keppel, E., and Tagliapietra, D. (2016). Open Nomenclature in the biodiversity era. *Methods Ecol. Evol.* 7, 1217–1225. doi: 10.1111/2041-210X.12594

Tappin, D. R., Watts, P., McMurtry, G. M., Lafoy, Y., and Matsumoto, T. (2001). The Sissano, Papua New Guinea tsunami of July 1998 — offshore evidence on the source mechanism. *Mar. Geol.* 175, 1–23.

Thomassin, B. (1977). *BENTHEDI I cruise, RV Le Suroît*. doi: 10.17600/7700 3111

Todd, P. A. (2008). Morphological plasticity in scleractinian corals. *Biol. Rev.* 83, 315–337. doi: 10.1111/j.1469-185X.2008.00045.x

Tregoning, P., McQueen, H., Lambeck, K., Jackson, R., Little, R., Saunders, S., et al. (2000). Present-day crustal motion in Papua New Guinea. *Earth Planet Sp.* 52, 727–730. doi: 10.1186/BF03352272

Tyler, P. A. (2003). "Introduction: Ecosystems of the world," in *Ecosystems of the Deep Oceans*, ed. P. A. Tyler (Amsterdam: Elsevier), 1–5.

Van Dover, C. (2012). Hydrothermal Vent Ecosystems and Conservation. *Oceanog* 25, 313–316. doi: 10.5670/oceanog.2012.36

Veron, J. E. N., Devantier, L. M., Turak, E., Green, A. L., Kininmonth, S., Stafford-Smith, M., et al. (2009). Delineating the Coral Triangle. Galaxea. *J. Coral Reef Stud.* 11, 91–100. doi: 10.3755/galaxea.11.91

Vieira, P. E., Lavrador, A. S., Parente, M. I., Parretti, P., Costa, A. C., Costa, F. O., et al. (2021). Gaps in DNA sequence libraries for Macaronesian marine macroinvertebrates imply decades till completion and robust monitoring. *Divers. Distrib.* 27, 2003–2015. doi: 10.1111/ddi.13305

Walter, D. E., and Winterton, S. (2007). Keys and the Crisis in Taxonomy: extinction or Reinvention? *Annu. Rev. Entomol.* 52, 193–208. doi: 10.1146/annurev.ento.51.110104.151054

Warnes, R. G., Bolker, B., Bonebakker, L., Gentleman, R., Huber, W., and Liaw, A. (2020). *gplots: Various R Programming Tools for Plotting Data. R package version 3.1.0*.

Williams, A., Althaus, F., and Schlacher, T. A. (2015). Towed camera imagery and benthic sled catches provide different views of seamount benthic diversity: gear selectivity for seamount benthos. *Limnol. Oceanogr. Methods* 13:e10007. doi: 10.1002/lom3.10007

Wudrick, A., Beazley, L., Culwick, T., Goodwin, C., Cárdenas, P., Xavier, J., et al. (2020). A pictorial guide to the epibenthic megafauna of Orphan Knoll (northwest Atlantic) identified from in situ benthic video footage. *Can. Tech. Rep. Fish. Aquat. Sci.* 3375:154.

Zawada, K. J. A., Madin, J. S., Baird, A. H., Bridge, T. C. L., and Dornelas, M. (2019). Morphological traits can track coral reef responses to the Anthropocene. *Funct. Ecol.* 33, 962–975. doi: 10.1111/1365-2435.13358

Conflict of Interest: The authors declare that the research was conducted in the absence of any commercial or financial relationships that could be construed as a potential conflict of interest.

Publisher's Note: All claims expressed in this article are solely those of the authors and do not necessarily represent those of their affiliated organizations, or those of the publisher, the editors and the reviewers. Any product that may be evaluated in this article, or claim that may be made by its manufacturer, is not guaranteed or endorsed by the publisher.

DOCTORAT SCIENCES BRETAGNE DE LA MER LOIRE ET DU LITTORAL

UBO Université de Bretagne Occidentale

Titre : Structure spatiale à multi-échelles de la biodiversité benthique des monts sous-marins et pentes insulaires à partir de l'analyse d'images : approches méthodologiques et rôle de l'habitat

Mots clés : Monts sous-marins, mégafaune benthique, structure des communautés, analyses spatiales multi-échelles, analyses d'images, développements méthodologiques

Résumé : Les monts sous-marins présentent une forte hétérogénéité d'habitats. Cependant, la structure spatiale à multi-échelles de leurs communautés et les facteurs de l'environnement qui l'expliquent sont peu documentés. Dans un contexte où ces habitats sont soumis à de nombreuses pressions anthropiques (ex : pêche industrielle, exploitation minière), il est urgent de combler ces déficits de connaissances. Cela implique d'utiliser des méthodes d'imagerie sous-marine et un plan d'échantillonnage multi-échelles. Or, la faune des milieux profonds reste très méconnue et une des difficultés majeures est d'identifier de façon robuste les organismes visibles sur les images. Cette thèse a donc pour objectifs d'améliorer les méthodes de caractérisation de la faune visible sur des images et d'utiliser ces méthodes pour décrire la structure spatiale des communautés méga-benthiques des monts sous-marins et pentes insulaires du canal du Mozambique (Océan Indien), et enfin, d'identifier les facteurs environnementaux qui expliquent cette structure aux échelles régionales et locales. La comparaison des données de biodiversité évaluées à partir de dragues/chaluts et d'images *in situ* dans divers habitats benthiques montre des différences selon la méthode (image/collecte), les habitats (fond meuble/rocheux) et les taxons. Ces méthodes sont complémentaires et nous proposons des recommandations pour améliorer l'identification de la faune sur les images, avec notamment des clés d'identification adaptées aux images. L'identification des éponges et des cnidaires sur les images n'excède pas le rang de l'ordre ou classe. Pour ces organismes constructeurs, nous proposons de caractériser la diversité par une approche morpho-fonctionnelle. Ces méthodes ont été déployées sur des transects de caméra tractée sur les sommets et haut de pente de quatre monts sous-marins et les pentes de deux îles du canal du Mozambique et associées à des données environnementales quantitatives. Les densités peuvent varier d'un facteur 10 entre les sites, favorisées par les courants forts. De fortes diversités bêta sont expliquées par la diversité du substrat, y compris différentes natures de roches. Les communautés sont très hétérogènes à l'échelle d'un site (mont/pente insulaire) et entre sites, distants de 4 à 1400 km. Les facteurs qui contribuent à expliquer cette variabilité sont l'hydrologie (courant, production primaire) (15% ; > km), la géomorphologie (6,5% ; > km), la topographie (7,9% ; 60-500 m) et le substrat (9,5% ; 60 m). L'approche morpho-fonctionnelle sur les cnidaires et les éponges a permis d'évaluer la structure spatiale de leur diversité morphologique, sa réponse à l'environnement, et son rôle sur la structure des communautés d'organismes associés. Cette méthode fournit des indicateurs de la structure des habitats vulnérables.
Ce travail fournit des premiers résultats sur les communautés des monts sous-marins dans le canal du Mozambique, et pourra servir à la mise en place de stratégies de gestion, notamment dans le cadre des aires marines protégées de Mayotte et de l'archipel des Glorieuses.

Title: Multiscale spatial patterns of benthic biodiversity on seamounts and island slopes from image analysis: methodological approaches and role of habitat

Keywords: Seamounts, benthic megafauna, community structure, multiscale spatial analyses, image analyses, methodological developments

Abstract: Seamounts display high habitat heterogeneity. However, the multiscale spatial structure of their community and the environmental factors that explain it are poorly documented. In a context where these habitats are subject to various anthropogenic pressures (e.g., industrial fishing, mining of rare metals), it is urgent to fill these knowledge gaps. This implies using underwater imaging methods and a multiscale sampling plan. However, the deep-sea fauna remains largely unknown and one of the major difficulties is to robustly identify the organisms visible on the images.The objectives of this thesis are to improve the methods for characterising the visible fauna on bottom images and to use these methods to describe the spatial structure of the megabenthic communities of seamounts and island slopes of the Mozambique Channel (Indian Ocean), and finally, to identify the environmental factors that explain this structure at regional and local scales.The comparison of biodiversity data assessed from dredges/trawls and *in situ* images in various benthic habitats shows differences according to the method (image/physical sampling), the habitats (soft/rocky bottom) and the taxa. These methods are complementary and we propose recommendations to improve the identification of fauna on images, notably with identification keys adapted to the images. The taxonomic identification of sponges and cnidarians on images does not exceed the rank of the order or class. For these habitat-forming organisms, we propose to characterize diversity using a morpho-functional approach. These methods were deployed on towed camera transects on the summits and upper slopes of four seamounts and the slopes of two islands in the Mozambique Channel and combined with quantitative environmental data. Densities can vary by a factor of 10 between sites, favoured by strong currents. High levels of beta diversity are explained by the diversity of the substrate, and of different rock types. The communities are very heterogeneous within sites (a mount or an island slope) and between sites which are 4 to 1400 km apart. The factors that contribute to explain this heterogeneity are hydrology (current, primary production) (15%; > km), geomorphology (6.5%; > km), topography (7.9%; 60-500 m), and substrate (9.5%; 60 m). The morpho-functional approach on cnidarians and sponges allowed the assessment of the spatial structure of their morphological diversity and how it responds to the environment, as well as its role on the structure of communities of associated organisms. This method provides indicators of the structure of vulnerable habitats.
This work provides initial results on seamount communities in the Mozambique Channel, and could be used to implement management strategies, particularly in the context of the marine protected areas of Mayotte and the Glorieuses archipelago.